RHEOLOGICAL STUDIES ON IDENTIFICATION OF NEW RUTTING PARAMETERS FOR UNMODIFIED BITUMEN

Submitted in partial fulfilment of the requirements

for the award of the degree of

Doctor of Philosophy

by

SYED MUBASHIRHUSSAIN

701303

DEPARTMENT OF CIVIL ENGINEERING

NATIONAL INSTITUTE OF TECHNOLOGY, WARANGAL

MARCH 2020

RHEOLOGICAL STUDIES ON IDENTIFICATION OF NEW RUTTING PARAMETERS FOR UNMODIFIED BITUMEN

Submitted in partial fulfilment of the requirements

for the award of the degree of

Doctor of Philosophy

by

SYED MUBASHIRHUSSAIN

701303

Supervisor

Dr. Venkaiah Chowdary

DEPARTMENT OF CIVIL ENGINEERING

NATIONAL INSTITUTE OF TECHNOLOGY, WARANGAL

MARCH 2020

NATIONAL INSTITUTE OF TECHNOLOGY

WARANGAL

CERTIFICATE

This is to certify that the thesis entitled **"RHEOLOGICAL STUDIES ON IDENTIFICATION OF NEW RUTTING PARAMETERS FOR UNMODIFIED BITUMEN"** being submitted by **Mr. SYED MUBASHIRHUSSAIN** for the award of the degree of **DOCTOR OF PHILOSOPHY** to the **Department of Civil Engineering** of **NATIONAL INSTITUTE OF TECHNOLOGY, WARANGAL** is a record of bonafide research work carried out by him under my supervision and it has not been submitted elsewhere for award of any degree.

Dr. VENKAIAH CHOWDARY

Thesis Supervisor
Associate Professor
Department of Civil Engineering
National Institute of Technology, Warangal
Telangana, India

APPROVAL SHEET

This Thesis entitled **"RHEOLOGICAL STUDIES ON IDENTIFICATION OF NEW RUTTING PARAMETERS FOR UNMODIFIED BITUMEN"** by **Mr. SYED MUBASHIRHUSSAIN** is approved for the degree of Doctor of Philosophy.

Examiners

_____

_____

_____

Supervisor

_____

Chairman

_____

Date: _____

DECLARATION

This is to certify that the work presented in the thesis entitled **"RHEOLOGICAL STUDIES ON IDENTIFICATION OF NEW RUTTING PARAMETERS FOR UNMODIFIED BITUMEN"**, is a bonafide work done by me under the supervision of **Dr. Venkaiah Chowdary**, Associate Professor, Department of Civil Engineering, NIT, Warangal, Telangana, India and was not submitted elsewhere for the award of any degree. I hereby declare that this thesis comprises of my ideas written in my own words. I have adequately cited and referenced the original sources where others ideas or words have been included. I also declare that I have adhered to all principles of academic honesty and integrity and have not misrepresented or fabricated or falsified any idea /data/ fact/source in my submission. I understand that any violation of the above will be cause for disciplinary action by the institute and can also evoke penal action from the sources which have thus not been properly cited or from whom proper permission has not been taken when needed.

_____

Syed Mubashirhussain

Roll No. 701303

Date:

To

My Father, Mother and Wife

ACKNOWLEDGEMENTS

The acknowledgement section is the only one in a doctoral thesis where the author tries to connect on a human level. And also, I know that I am not going to write many more books. Therefore, I will take this opportunity to try and acknowledge each and every one who has, knowingly or unknowingly, helped me in completing my doctoral research.

Firstly, I express my heartfelt gratitude to my thesis guide, **Dr. Venkaiah Chowdary** for accepting me as his first Ph.D student and nurturing me throughout my thesis work. By guiding me throughout my research period, he has invested a lot of his physical, mental and emotional energy. He is the solid foundation on which my thesis rests. Thank you, Sir.

Secondly, I am truly grateful to **Dr. C.S.R.K. Prasad** for taking a leap of faith by enrolling me in the Ph.D program in December, 2012 when he was the then Head of the Civil Engineering department. I cannot thank him enough for his support in carrying out my research tenure. He is truly a source of inspiration.

I wish to express my gratitude to the Head of Civil Engineering Department **Prof. M. Chandrasekhar** and the former heads of the Civil Engineering Department**, Prof. Deva Pratap, Prof. D. Rama Seshu and Prof. G. Rajesh Kumar** for the support provided in completing my doctoral research. Also, I truly appreciate the support and suggestions provided to me by my Doctoral Committee members **Dr. C.S.R.K. Prasad**, Professor, Department of Civil Engineering, **Dr. A. Venu Gopal**, Professor, Department of Mechanical Engineering and **Dr. V. Ramana Murthy**, Professor, Department of Civil Engineering.

I express my sincere thanks to **Dr. K.V.R. Ravi Shankar, Dr. S. Shankar** and **Dr. Arpan Mehar** Assistant Professors, Transportation Division, Department of Civil Engineering, National Institute of Technology, Warangal and **Dr. P. Sasanka Bhushan**, former faculty at National Institute of Technology, Warangal and currently working as an Associate Professor at VIT University, for their valuable support.

I am grateful to **Prof. N.V. Ramana Rao,** Director, National Institute of Technology, Warangal and also the former directors for extending every possible help during my research tenure.

I truly appreciate the help provided **by Md. Abdul Gafar**, **K. Ramesh**, **K**.**Purushotham** and especially **Mr. Amjad Pasha** in completing my laboratory experimental work.

A big thanks to all my current and former research colleagues. In particular, I thank **Dr. M. Anil**, **Dr. S. Srikanth**, **K.M. Peera** and **Dr. D. Harinder** for their timely support. A special thanks to **Dr. D. Abhigna** and **K. Srikanth** for helping me in my Ph. D thesis.

To **Utsav Vishal** and **T. Arjun Kumar**, I appreciate your immense help in completing my experimental work. Without you, it would have been a bit more difficult in completing my research.

I would like to gratefully acknowledge **Prof. J. Murali Krishnan**, Department of Civil Engineering, Indian Institute of Technology Madras (IITM) for his valuable suggestions and also allowing to conduct my experiments in the Pavement Engineering Laboratory and Asphalt Laboratory at IITM. I would also like to thank him for providing two different grades of unmodified bitumen for this research work.

I also thank all the teaching and non-teaching staff of all the departments and in particular the Civil Engineering Department for their cooperation during the research period. I would like to thank all my teachers and friends.

Finally, I reserve my special thanks to my parents **Syed Manzoor Hussain** and **Noorunnisa**, I surely would not have completed my doctoral research without the awesome support provided by my father and mother. I thank my brothers **Syed Mudassir Hussain** and **Syed Mutahir Hussain** for their constant support and bickering. There is a saying called "Patience is a Virtue". I thank my wife **Mumtaz Jahan** for being super-duper patient with me. And most importantly, to my children, thanks for your understanding.

SYED MUBASHIRHUSSAIN

ABSTRACT

Permanent deformation in bituminous pavements is considered to be the most critical distress phenomena and is generally associated with high temperatures. Bituminous mixture performance tests are mostly conducted at the Performance Grade (PG) temperatures or at 60 °C. However, rutting also occur at temperatures lower than the PG pass/fail temperature. This rutting performance of bituminous mixtures is highly dependent upon the response characteristics of a bitumen binder subjected to shear. Therefore, it is important to measure viscosity of bitumen at different temperatures. Bitumen can exhibit non-Newtonian behaviour at pavement temperatures lower than the PG pass/fail temperature. This non-Newtonian behaviour can become prominent with aging of bitumen. Zero Shear Viscosity (ZSV) is a property of bitumen corresponding to the Newtonian plateau observed at shear rates approaching zero. However, there are issues with the measurement of ZSV, wherein, ZSV measured from different methods and models is different. Moreover, the creep test to measure ZSV is time consuming. Thus, the main research aim is to characterise the non-Newtonian response of bitumen at typical pavement temperatures. This non-Newtonian response of the bitumen binders is studied by adopting a Linear Shear Rate Sweep (LSRS) test protocol and a Step-wise Steady Shear Rate Sweep (SWSSRS) test protocol. The LSRS test protocol is a linear sweep protocol wherein the rate of change of shear rate is constant. On the other hand, SWSSRS test is a step-wise steady shear test conducted at very low shear rates. Further, wheel tracking tests are widely used to measure the rutting resistance of bituminous mixtures in the laboratory where a loaded solid rubber wheel moves at a particular speed over a specimen prepared with bituminous mixtures and rut depth is measured at a particular temperature. As the loaded rubber wheel moves over the specimen, deformation is measured and rut depth is computed. The accumulated permanent deformation with repeated application of wheel passes is termed as rutting in bituminous mixtures.

The main aim of the LSRS test was to capture the classical response of viscosity as a function of the shear rate. However, it was observed that the resultant response of the binder was quite different. For most cases, both Newtonian as well as a non-Newtonian response was observed. At very low shear rates, an initial plateau region was observed which was followed by a shear thickening region. This shear thickening region was subsequently followed by two shear thinning regions for most cases. The initial plateau was able to give a direct measure of ZSV denoted as $\eta_{0(\mathrm{L})}$. Moreover, from the shear thickening region the peak transient viscosity (η_{TV}) is selected and is proposed as a non-Newtonian rutting parameter, respectively. The non-

Newtonian response in the SWSSRS test was characterized by the appearance of a stress overshoot. A steady state was observed after this stress overshoot at time, 't_s'. It was observed that the bitumen response was independent of shear rate, time and shear history. Since, the adopted shear rates in the SWSSRS test were very low and is within the region where ZSV is typically measured, the viscosity at 't_s' in the first forward sweep was considered as an alternate ZSV and is denoted as $\eta_{0(S)}$. $\eta_{0(S)}$ is also proposed as a rutting parameter. $|G^*|/\sin\delta$, $|G^*|/(1-(1/\tan\delta\sin\delta))$ and J_{nr} were also measured by following the standard test procedures.

From the wheel tracking tests it was observed that there is considerable scatter in the rut data measured along the loaded wheel traverse. A probabilistic approach was chosen to analyse the scatter in the rut data. It was observed that the Weibull and lognormal distributions were able to represent the scatter in the rut data comparatively better than the normal distribution. Using the Weibull and lognormal forms, probability curves were determined at 50, 80, 90, and 99% reliability levels. However, it was further observed that the lognormal distribution tend to over-estimate the probabilistic rut data. With an increase in reliability, there was an increase in rut depths. Comparative analysis of the probabilistic rut data showed that the Dense graded Bituminous Macadam (DBM) mixture was comparatively better at resisting permanent deformation than the Bituminous Concrete (BC) mixtures. Effect of bitumen aging was observed wherein, the long-term aged mixtures had greater resistance towards rutting than the short-term aged mixtures. Moreover, three rutting rates were determined.

In order to determine the efficacy of the proposed bitumen parameters to be used as alternative to the existing rutting parameters, correlation of the bitumen parameters with the mixture rut depth and mixture rut rate were identified. It was observed that all the six binder parameters determined in this research showed a strong correlation with mixture performance. This strong correlation was observed with both the rut depth as well as the rut rate. These correlations were observed to be indpedent of wheel passes and percentage reliability.

However, from the overall correlations a clear hierarchy was observed, wherein, $\eta_{0(S)}$ had the better coefficient of correlation followed by J_{nr}. Thus, the non-Newtonian characterisation of the unmodified bitumen binders helped to identify two bitumen parameters, a Newtonian parameter, $\eta_{0(S)}$ and a non-Newtonian parameter, $\eta_{0(L)}$ which were corraborated through the wheel tracking tests.

Keywords – Aging, bitumen, Newtonian, non-Newtonian, permanent deformation, rheological study, reliability, rutting parameter, shear thickening, steady-state, stress overshoot.

CONTENTS

List of Figures

List of Tables

ABBREVIATIONS

AASHTO	American Association of State Highway and Transportation Officials
AGPT	Guide to Pavement Technology – Austoroads
ALF	Accelerated Loading Facility
APA	Asphalt Pavement Analyzer
AST	Amplitude Sweep Test
ASTM	American Society of Testing and Materials
BC	Bituminous Concrete
BIS	Bureau of Indian Standards
CDOT	Colorado Department of Transportation
C-M	Cannon-Manning
DBM	Dense graded Bituminous Macadam
DOT	Department of Transportation
DSR	Dynamic Shear Rheometer
EPDM	Ethylene Propylene-Diene Monomer
FDO	Forced Draft Oven
FDOA	Forced Draft Oven Aging
FHWA	Federal Highway Administration
FN	Flow Number
FRT	French Rut Tester
HMA	Hot Mix Asphalt
HWTD	Hamburg Wheel Tracking Device
HWTT	Hamburg Wheel Tracking Test
IIT KGP	Indian Institute of Technology Kharagpur
IRC	Indian Roads Congress
IS	Indian Standard
K-S	Kolmogorov–Smirnov
LSRS	Linear Shear Rate Sweep
LSV	Low Shear Viscosity
LTA	Long term Aged
LVE	Linear Visco-elastic
MAPE	Mean Absolute Percentage Error
MoRTH	Ministry of Road Transport and Highways

ABBREVIATIONS

MSCR	Multi Stress Creep and Recovery
NRR	Normalized Rutting Rate
PAV	Pressure Aging Vessel
PG	Performance Grade
PMB	Polymer Modified Bitumen
RAP	Reclaimed Asphalt Pavement
RMSE	Root Mean Square Error
RPM	Rotations Per Minute
RR	Rutting Rate
RTFO	Rolling Thin-Film Oven
RV	Rotational Viscometer
SBS	Styrene Butadiene-Styrene
SHRP	Strategic Highway Research Program
SMA	Stone Matrix Asphalt
STA	Short-term Aged
SWSSRS	Step-wise Steady Shear Rate Sweep
TA	Total Average
TFO	Thin Film Oven
TI	Thixotropic Index
TxDOT	Texas Department of Transportation
UDOT	Utah Department of Transportation
US	United States
UV	Ultra Violet
VDO	Vacuum Degassing oven
VG	Viscosity Grade
WMA	Warm Mix Additive
WTD	Wheel Tracking Device
ZSV	Zero Shear Viscosity

NOTATIONS

G_{mb}	Bulk specific gravity
$\mathbf{R}^2$	Coefficient of correlation
G^*	Complex modulus
°C	Degree centigrade
°	Degrees
W_c	Dissipated energy
$\|G^*\|$	Dynamic shear modulus
J''	Loss compliance
G''	loss modulus
τ_{max}	Maxium shear stress
J_{nr}	Non-recovarable creep compliance
γ_{max}	Maximum shear strain
η_{TV}	Peak transient viscosity
δ	Phase angle
Mr	Resilient Modulus
Rr	Rutting rate
Rr_M	Rutting rate Morea
Rr_P	Rutting rate primary
Rr_T	Rutting rate Terminal
$\dot{\gamma}$	Shear rate
t_s	steady-state time
G'	Storage modulus
G_{mm}	Theoretical maximum specific gravity
$\tau_{hyst\%}$	Thixotropic index
η	Viscosity
η_0	ZSV
$\eta_{0(L)}$	ZSV from LSRS tests
$\eta_{0(S)}$	ZSV from SWSSRS tests

CHAPTER-1

INTRODUCTION

1.1 BACKGROUND

Almost 94% of the paved roads in the US are flexible pavements (WAPA, 2019) whereas, in Europe, more than 90% of the paved roads and highways are flexible pavements (NAPA and EAPA, 2011). A similar scenario exists in India wherein more than 90% of the highway network comprises of flexible pavements (IAT, 2000; CRRI, 2019). Flexible pavements are generally preferred because they offer better ride quality, have a comparatively better skid resistance and generate low tire-pavement noise (Boodihal et al., 2014). Flexible pavement is a combination of different layers superimposed over a stable subgrade. The top two courses are bituminous layers whereas the subsequent layers are either granular or stabilized layers. The cross-section of a conventional flexible pavement is shown in Figure 1.1. A bituminous layer is generally composed of coarse and fine aggregates mixed with bitumen acting as a binding agent. Here, the bitumen binder is a viscoelastic material. This viscoelastic nature of bitumen binder, in turn, makes the bituminous mixture viscoelastic. In the flexible pavements, the stresses due to the vehicular loads are transferred through the grain-to-grain contact in the aggregate matrix (Hussain et al., 2013; Abo-Qudais, 2004) whereas the flexibility of the bituminous pavements is due to the viscoelastic nature of bitumen binder.

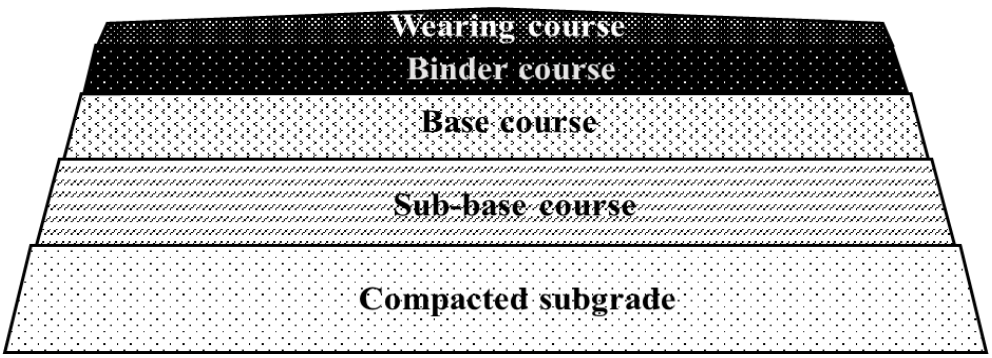

Fig. 1.1 Cross-section of a conventional flexible pavement

In order to design a workable pavement cross-section, almost all the design methodologies around the world consider minimizing rutting and fatigue cracking in flexible pavements. However, rutting is the most critical distress among the two flexible pavement

distresses. Rutting can be easily observed after a rain when the depressions are filled with water, thereby causing hydroplaning. Rutting results in loss of serviceability of pavement and is also hazardous as the rut tends to pull the vehicle towards itself when the vehicle is steered across the rut. Therefore, rutting can be classified as a structural failure as well as a functional failure. These problems result in early failure of flexible pavements. The importance of rutting can be assessed based upon the results of a survey of the pavement industry, wherein the pavement industry rates rutting as the most important distress phenomena followed by fatigue and thermal cracking respectively (Witczak et al., 2002). In India, flexible pavements are designed based on IRC: 37-2018 (IRC, 2018) where the vertical compressive strain on top of the subgrade is considered as the sole parameter to control rutting and no separate criteria are included in these guidelines with respect to granular layers and bituminous layers. Even though the same guidelines (IRC: 37-2018) highlight the fact that bituminous layers can undergo permanent deformation by contributing towards the incidence of rutting especially at higher pavement temperatures, the guidelines also state that such rutting can be controlled by selecting sufficiently stiffer bituminous mixtures with binders that are less susceptible to permanent deformation at higher pavement temperatures and higher wheel load stresses. This shows that the binder characteristics play an important role in the onset of rutting, particularly in upper bituminous layers. But it has been observed that all the layers of bituminous pavement, over the course of time, undergo rutting (Garba, 2002) and most importantly, it has been reported that most of the rutting occurs in the top layers i.e., bituminous layers (Brown and Cross, 1989).

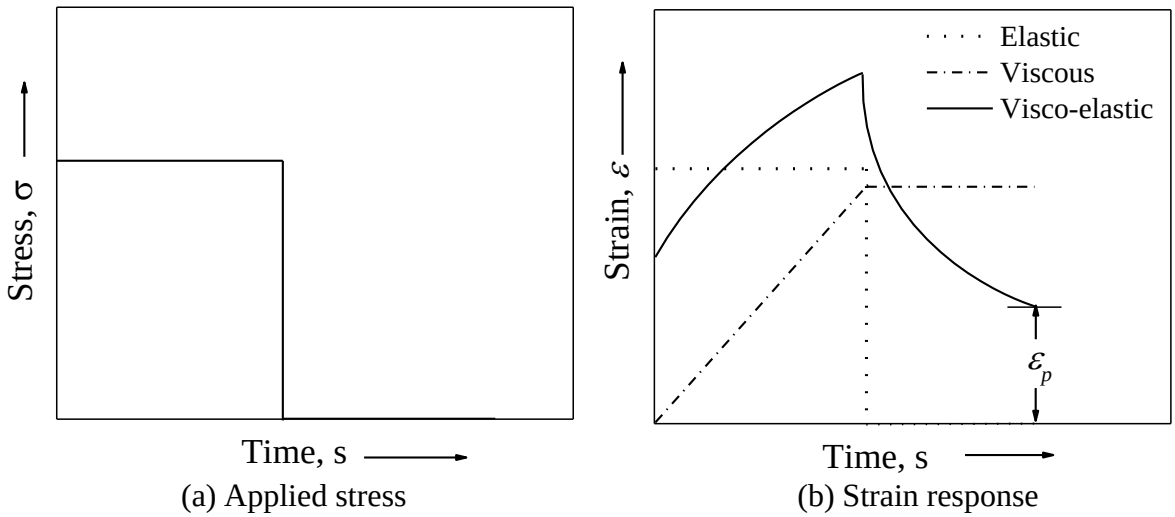

(a) Applied stress (b) Strain response

Fig. 1.2 Response of different materials under constant stress

The mechanism of rutting in bituminous layers can be easily understood by conducting a creep and recovery test on elastic, viscous and viscoelastic materials as shown in Figure 1.2.

It can be seen that on removing the stress, elastic materials exhibit complete strain recovery and the viscous materials show no recovery, whereas the viscoelastic materials show partial recovery and the strain may or may not become zero depending on the time of application of the next load cycle. This residual strain or the unrecovered strain is termed as the permanent strain per cycle. Since a bituminous layer is a viscoelastic entity, it exhibits a residual strain for every passage of a wheel load. The accumulation of this permanent strain due to repeated passes of wheel loads is known as permanent deformation. Permanent deformation manifests as surface depressions along the wheel path with/without pavement uplift.

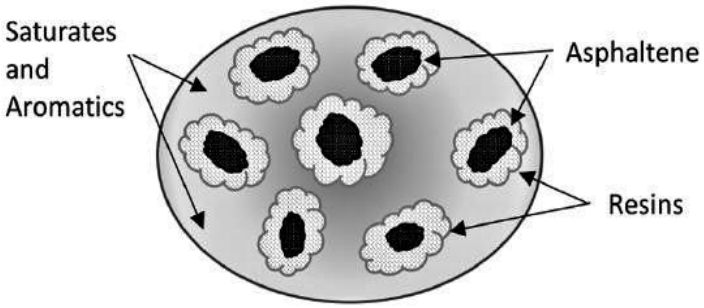

Fig. 1.3 Colloidal structure of bitumen (NCAT, 2018)

Characterizing rutting in bituminous mixtures is highly complex as it depends upon many factors including the characteristics of the aggregates (Fernando et al., 1997; Kandhal and Cooley, 2002; Pan et al., 2006), temperature (Weidong et al., 2006; Li et al., 2011), axle load (Salama et al., 2006; Behiry et al., 2012), mixture gradation (Yang et al. 2006, Sefidmazgi et al., 2012), volumetric characteristics (Brown and Cross, 1989; Archilla and Diaz, 2011; Grebenschikov and Prozzi, 2011; Xu and Huang, 2012), tyre pressure (Tielking and Roberts, 1987; Kim et al., 1989; Douglas 1997; Owende et al. 2001), speed (Chen et al., 2004; Ali et al., 2009), presence of water (Wong et al., 2004). However, bitumen should be considered as the principal component because it is the one that binds the aggregates to form a stable mixture. Bitumen is a residue obtained from the fractional distillation of crude oil (Sorensen and Wichert, 2012). It is a hydrocarbon refined to form a stable substance which is semi-solid at room temperature and is viscoelastic in nature. Bitumen has been extensively used in the construction of the pavements (Krishnan and Rajagopal, 2003). Bitumen, as shown in Figure 1.3, has a colloidal structure made up of asphaltenes, saturates, aromatics and resins (NCAT, 2018). Bitumen is a material whose rheological properties are highly dependent upon time, temperature, the applied shearing forc, and shear history. These rheological properties are being used as indicators of the performance of bitumen binders in terms of their ability to resist permanent deformation in bituminous mixtures. Therefore, in

this research, the central focus is on characterizing the rheological response of the unmodified bitumen binders and also the characterization of the permanent deformation in bituminous mixtures. In the subsequent sections, rheology of bitumen, bitumen aging and the permanent deformation in bituminous mixtures are discussed.

1.2 RHEOLOGY OF BITUMEN

Rheology is known as the study of *"flow"* of materials. In the case of bitumen, it is the determination of the inherent properties of bitumen when the bitumen flows upon an application of shear. It is a known fact that bitumen is a highly temperature susceptible material wherein the response characteristics of the bitumen binders vary drastically from a solid-like behavior to a fluid-like behavior with the rise in temperature. In general, in the case of laboratory experiments, the flow in bitumen is induced through oscillatory shear or rotational shear. This flow in the bitumen binders is due to deformation of the material or the rearrangement of the particles in the material or the breaking of the bonds in the material (Anderson et al., 2002; Viola and Baird, 1986). Bitumen response to the applied shear is either Newtonian or non-Newtonian depending upon the temperature, bitumen composition, presence of additives and bitumen aging. Aging of bitumen is the increase in stiffness of bitumen binders due to volatilization and oxidation (Yin et al., 2017). Aging of bitumen occurs in two distinct phases. In the first phase, aging of bitumen is due to loss of volatiles during mixing, laying and compaction operations of bituminous mixtures in the field which is termed as short-term aging of bitumen (Sirin et al., 2018). Thereafter, aging of bitumen is due to oxidation of compacted mixture during its service life which is termed as long-term aging of bitumen (Sirin et al., 2018). A comprehensive explanation of the various aspects involved with the aging of bitumen binders has been discussed by Krishnan and Rajagopal (2003) and the mechanism will be discussed in Chapter 2. Since, bitumen is known as a material that is highly susceptible to temperature, wherein its response characteristics vary drastically from a solid-like behavior to a fluid-like behavior with the rise in temperature (Poulikakos et al., 2014), bitumen binders behave as Newtonian materials at high temperatures and behave as non-Newtonian materials at lower temperatures. Even at 60 °C, bitumen binders exhibit non-Newtonian response where the viscosity depends also on the applied shear rate (Chowdary et al., 2007). Moreover, a soft binder which exhibits Newtonian response at a particular temperature can exhibit predominantly non-Newtonian response due to the aging of bitumen (Poulikakos et al., 2014; Sirin et al., 2018). Thus, the response characteristics of the bitumen used in the upper bituminous layers significantly affect the performance of the flexible

pavement especially in terms of rutting. This resulted in the introduction of performance based binder specifications. To define it in simple terms, a Newtonian material is one whose viscosity, at a particular temperature, does not change with a change in the shear rate whereas a non-Newtonian material is one whose viscosity, at a particular temperature, changes with a change in the applied shear rate. The Newtonian and non-Newtonian responses can be seen in Figure 1.4. Further, the non-Newtonian materials can again be classified as time independent non-Newtonian (shear thinning and shear thickening) and time dependent non-Newtonian materials (thixotropic and anti-thixotropic).

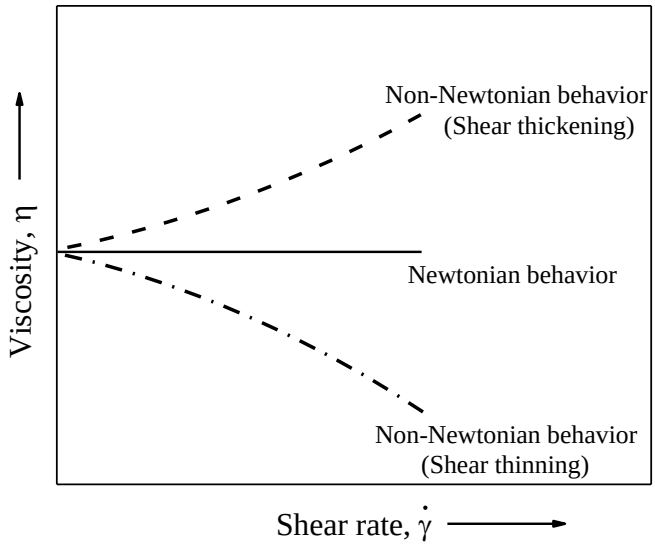

Fig. 1.4 Variation of viscosity for the Newtonian and non-Newtonian materials

The popular instruments used to carry out rheological investigations on bitumen binders are Rotational Viscometer (RV) and Dynamic Shear Rheometer (DSR). In a RV, the flow in bitumen binders is induced through rotational shear in coaxial cylinders, whereas in a DSR, flow is induced using either rotational or oscillatory shear between two parallel plates. In the RV, the bitumen sample placed in a cylinder is sheared using a cylindrical spindle. Here, the cylinder is stationary and the spindle is rotated which causes the bitumen sample in the cylinder to flow. In the DSR, shearing is induced using a circular parallel plate geometry, wherein, the bitumen sample is sandwiched between two parallel plates. Here, the bottom plate is stationary whereas the upper plate (test geometry) either rotates or oscillates depending upon the test protocol thereby causing flow in the bitumen sample. The flow induced in the bitumen binders using the RV and the DSR generates a resultant torque which is the actual response of the material to the applied shear. Here, the torque is the measured value and the various rheological properties are calculated values. These rheological

properties are calculated based upon the applied shear, the torque generated, the volume of sample sheared and the dimensions of the shearing spindle or the test geometry.

1.3 PERMANENT DEFORMATION IN BITUMINOUS MIXTURES

The manifestation of rutting in bituminous mixtures can be generally categorized into two stages. The first stage is the *'densification stage'* and the second stage is the *'shear deformation stage'* (Xu and Huang, 2012). The densification stage of rutting is due to a reduction in air voids when the flexible pavement is subjected to repeated passage of wheel loads. Rutting occurring in flexible pavements due to a reduction in air voids is shown in Figure 1.5 (a). The second stage of rutting is the shear deformation stage in which the pavement material moves away from the wheel path and causes an upheaval on the sides of the wheel path. This stage is also known as *'plastic deformation'*. A typical pavement with shear upheaval on the sides of the wheel path is shown in Figure 1.5 (b). This is the primary cause of rutting in well-compacted bituminous mixtures. Shear deformation occurs when the binder is weak in shear strength and when the binder coating on the aggregate particle is thicker which allows easier movement of aggregate particles.

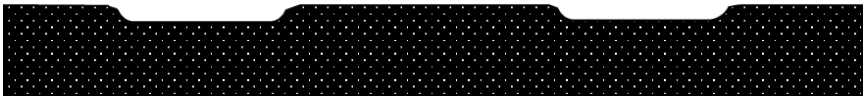

(a) Deformation due to a reduction in air voids

(b) Deformation with shear upheaval

Fig. 1.5 Manifestation of rutting

The relationship between permanent deformation and the number of load applications in laboratory and in accelerated pavement testing has been found to include three distinct stages including the primary stage, the secondary stage and the tertiary stage (Zhou et al., 2004), as shown in Figure 1.6. During the primary stage, densification occurs and the accumulated permanent deformation increases rapidly. Here, the permanent deformation per load cycle tends to decrease with an increase in a number of passes and reaches a constant value which denotes the start of the secondary stage (Zhou et al., 2004). As the densification increases with time, the mixture stability improves due to rearrangement of the aggregate

matrix, the improved interlock between aggregate particles and the hardening of the binder. In this stage, the void content decreases to a very low value known as the 'refusal air void content'. The secondary stage is a transition zone between the densification and shear deformation stage wherein, the permanent deformation increases at a constant rate. Thereafter, the permanent deformation per load cycle starts increasing rapidly and the permanent deformation increases again. This is the onset of the tertiary stage. The tertiary stage shows the start of the second mechanism of permanent deformation where the shear deformation starts and permanent deformation increases rapidly.

It is important to note here that, apart from permanent deformation, bituminous mixtures also undergo aging over the service life of the pavement. Aging of the bitumen in the bituminous mixtures has also shown to increase the dynamic modulus of the bituminous mixtures. (Morian et al. 2011, Tarbox and Daniel, 2012.). This increase in dynamic modulus results in increased resistance to permanent deformation. Research has also shown that it is important to quantify the effect of long term aging on permanent deformation so that its effect can be incorporated in the mix design (Azari and Mohseni, 2013). When the bituminous mixture is layed, it is compacted to a density of 92 to 94% of maximum specific gravity of the mixture i.e., there would be 6 to 8% of air voids present in the compacted mixture. However, as the pavement (bituminous mixture) ages, there would be a gradual reduction in the air voids of the bituminous layer due to vehicular loading. This reduction in the air voids makes the bituminous layer denser thereby offering more resistance to permanent deformation. An increase in resistance to rutting by 7 to 63% can be achieved when there is a decrease in air voids by 1% (Tran et al., 2016).

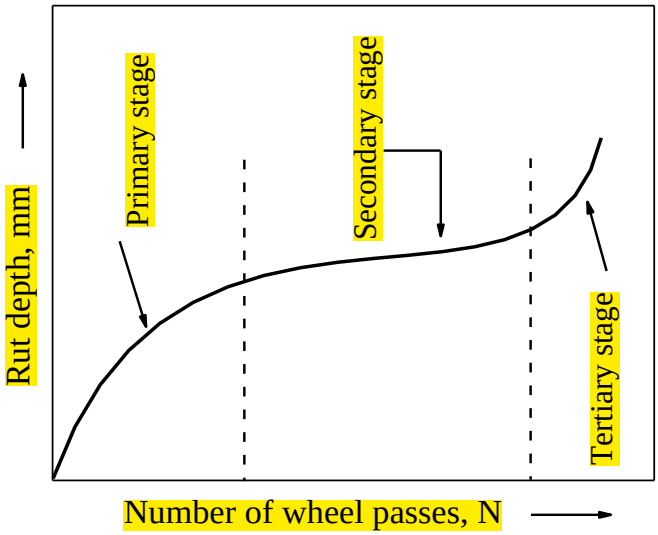

Fig.1.6 Three stage permanent deformation curve

Wheel tracking tests are widely used to measure rutting resistance of bituminous mixtures in the laboratory using a Wheel Tracking Device (WTD). These are simulation tests used to characterize the permanent deformation in bituminous mixtures. Some of the major loaded WTDs are the Georgia Loaded Wheel Tester, Asphalt Pavement Analyser (APA), Hamburg Wheel Tracking Device (HWTD), LCPC French Rut tester (FRT), Purdue University Laboratory Wheel Tracking Device, Model Mobile Load Simulator, Evaluator of Rutting and Stripping equipment. In the wheel tracking tests, the specimen is subjected to a 'to and fro' motion of a loaded wheel moving at a particular speed and permanent deformation is measured at a particular temperature. The deformation in the bituminous mixtures is recorded by a linear variable differential transducer. As the loaded rubber wheel moves over the specimen, the permanent deformation is captured along the wheel traverse.

The stability of the aggregate matrix in the bituminous mixture is essentially due to bitumen holding it together. Therefore, bitumen also plays a vital role in resisting permanent deformation in bituminous mixtures (Garba, 2002). The bitumen property $|G^*|/\sin\delta$ was proposed as the first rutting parameter (Andersen and Kennedy, 1993). Thereafter, parameters like $|G^*|/(1-(1/\tan\delta\sin\delta))$, ZSV and J_{nr} have been proposed as parameters to evaluate the permanent deformation in bituminous mixtures. These parameters will be reviewed in detail in Chapter 2.

1.4 OBJECTIVES OF THE RESEARCH

The objectives of the research are as follows.

1. To identify rheological parameters from the Newtonian and non-Newtonian responses.
2. To develop reliability-based representative rutting curves by taking into account the variability observed along the wheel traverse
3. To correlate the rheological parameters with permanent deformation in bituminous mixtures.

1.5 ORGANISATION OF THE RESEARCH

The thesis is organized into seven chapters. The first chapter, i.e., the introduction chapter deals with an introduction of rutting/permanent deformation. In this chapter, an introduction on the aging of bitumen is presented apart from the rheological characterization of bitumen binders.

In Chapter 2, the review of the literature is presented, wherein, research concerned with the existing rutting parameters is reviewed.

In Chapter 3, the detailed methodology adopted to achieve the set objectives is discussed. Here, the test protocols adopted to characterize the Newtonian and non-Newtonian response characteristics of the bitumen binders are presented. Also, the test procedure to characterize the permanent deformation characteristics of bituminous mixtures is detailed.

In Chapter 4, the results obtained from the rheological study on the unaged and short term aged bitumen binders using the RV are discussed. Further, the results obtained from the Newtonian and non-Newtonian characterization of the unaged and aged bitumen binders using the DSR are discussed.

In Chapter 5, the results from the wheel tracking tests are discussed. The methodology adopted to utilize the wheel tracking data is discussed in detail.

In Chapter 6, correlations of the rutting parameters with the permanent deformation data are discussed in detail.

In Chapter 7, the apart from the summary, the conclusions drawn from the current study are presented along with the limitations of the study and the scope for further research.

CHAPTER 2

LITERATURE REVIEW

2.1 GENERAL

Initially, bitumen was graded and labeled as hard or soft by chewing a small amount of the material. This process of grading the bitumen as hard or soft was highly subjective because the response of material as being hard or soft upon chewing depends upon the perception of a person grading the bitumen and this perception changes from person to person. Later, at the start of the 20th century, penetration grading of bitumen was developed by the American Society of Testing and Materials (ASTM) by forming a committee known as ASTM D04 (ASTM, 2003). The performance of a bitumen binder predicted based upon empirical parameters such as penetration, softening point, ductility did not match the field performance (Anderson et al. 1991). These inconsistencies then forced the researchers to identify the intrinsic rheological properties of bitumen binders which could show a better correlation with the permanent deformation occurring in the bituminous mixtures. Therefore, it is important to analyze the effect of the rheological properties on the performance of bitumen binders and also the effect of aging on the rheological properties of bitumen binders. Therefore, the following three sections deal with the review of existing rutting parameters, the effect of aging on the rheological properties of bitumen binders, the aging on bituminous mixtures and finally a summary of the literature review.

2.2 RUTTING PARAMETERS

2.2.1 SHRP Rutting Parameter – $|G^*|/\sin\delta$

The SHRP rutting parameter, $|G^*|/\sin\delta$, is based upon the concept of rheology and dissipated energy (W_c) (Petersen et al., 1994). Non-recoverable deformation of bitumen binders was considered as a critical parameter in order to characterize the rutting resistance of bitumen binders. Initially, the viscous component of stiffness at 0.1 s of loading time was selected as a critical specification criterion for rutting resistance of bitumen binders. However, correlation of the viscous component of stiffness with the mixture data showed that it did not give

sufficient weightage to the elastic portion of the response. Therefore, the inverse of loss compliance ($1/J''$) was then adopted as the criterion for rutting resistance of bitumen binders. The inverse of loss compliance ($1/J''$) is equal to dynamic shear modulus ($|G^*|$) divided by the sine of the phase angle ($\sin\delta$) i.e., $|G^*|/\sin\delta$ (Andersen and Kennedy, 1993). The SHRP rutting parameter is determined in the linear viscoelastic (LVE) region (the range of strain wherein the response of the material is linear).

$$W_c = \pi \tau_{max} \gamma_{max} sin\delta, \tag{2.1}$$

$$W_c = \pi \frac{\tau_{max}^2}{\left(\frac{|G^*|}{sin\delta}\right)}, \tag{2.2}$$

where,

W_c = energy dissipated per cycle,

τ_{max} = maximum shear stress,

γ_{max} = maximum shear strain,

δ = phase angle, and

$|G^*|$ = dynamic shear modulus

Moreover, for each cycle of loading, the work done in the deformation of bitumen binders is recovered partially by the elastic component of strain and partially dissipated by the viscous flow component of strain and the associated generation of heat. The energy dissipated per cycle from a single application of a loading cycle is shown in Equation (2.1). And since modulus is equal to stress divided by strain ($|G^*| = \tau / \gamma$), the Equation (2.1) is modified as Equation (2.2). The term $|G^*|/\sin\delta$ was proposed as the rutting parameter. Higher the binder $|G^*|/\sin\delta$, lower is the dissipated energy and consequently a higher resistance against permanent deformation. Since, bitumen is a viscoelastic material, in the term $|G^*|/\sin\delta$, $|G^*|$ represents the dynamic shear modulus of the viscoelastic material which in turn captures the resistance towards permanent deformation, whereas, the term $\sin\delta$ represents the relative amount of energy dissipated per loading cycle. The binder $|G^*|/\sin\delta$ is determined at a frequency of 10 rad/s corresponding to a vehicular speed of 80 kmph.

In order to validate the SHRP rutting parameter, $|G^*|/\sin\delta$, Hicks et al (1993) conducted a study, wherein, the $|G^*|/\sin\delta$ was determined for 16 short-term aged binders. Moreover, wheel tracking tests were conducted on bituminous mixtures with two aggregate types at a target air void content of 4% and at a temperature of 40 °C for 5000 passes. From the wheel tracking tests, two parameters were identified namely the total rut depth (RD, *mm*) and the normalized rutting rate (NRR, *mm/MPa/hr*). The results showed a poor correlation of $|G^*|/\sin\delta$ with both the RD and NRR with an R^2 of 0.30 and 0.18 respectively. However, this poor correlation was attributed to the lower test precision encountered with the WTD used in the study. Also, it was opined that the test temperature of 40 °C was not high enough for the viscous characteristics to affect the rutting response of the bituminous mixtures.

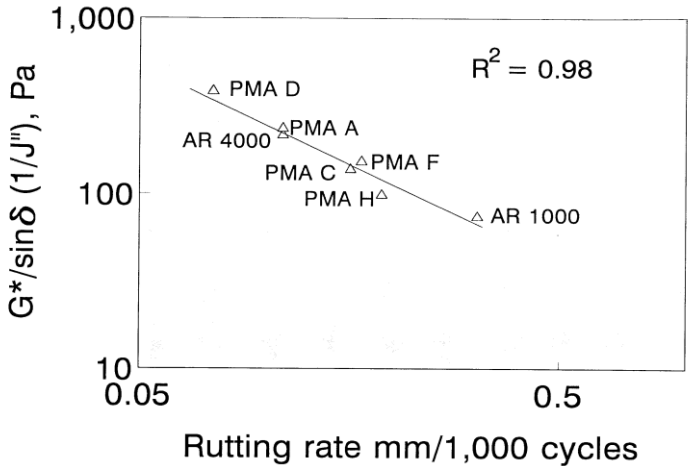

Fig. 2.1 Relationship between $|G^*|/\sin\delta$, and RR (Petersen, et al., 1994)

Later on, $|G^*|/\sin\delta$ had a favorable outcome, wherein, the $|G^*|/\sin\delta$ of the unmodified and the modified bitumen binders had a good correlation (R^2 = 0.98) with the rutting rate (Rr, mm/1000 cycles) determined through the wheel tracking tests (Petersen et al., 1994). These results are shown in Figure 2.1. Similar results were obtained, wherein, the relationship between the $|G^*|/\sin\delta$ of elastomer modified, plastomer modified and air blown bitumen binders and the field rutting from an experimental section on a four-lane arterial highway in Pennsylvania showed a good degree of correlation (Planche et al., 1996). Further, Chen and Lin (2000) conducted amplitude sweep tests on two unmodified and two modified bitumen binders to determine $|G^*|/\sin\delta$ and also determined the rutting performance by testing a 4 km test section for a period of 3 years. In addition, wheel tracking tests were also conducted on slab samples at 60 °C using a WTD similar to HWTD. The authors reported a strong correlation between the Rr (0.01 mm/day) and $|G^*|/\sin\delta$. These results provided support to the SHRP Superpave™ specification parameter $|G^*|/\sin\delta$.

Stuart et al. (2000) reported that the angular frequency based upon the loading time of 0.1 s should be 62.8 rad/s instead of 10 rad/s. The authors also conducted tests at a frequency of 2.25 rad/s. The authors reported that, even though the binder $|G^*|/\sin\delta$ was different at different frequencies, the rankings of the different binders when tested at different frequencies was same.

Bahia et al. (2001) were of the opinion that the loading mode (linear) and the small number of cycles involved in determining $|G^*|/\sin\delta$ is not enough to estimate the contribution of binder, especially the modified binder, towards rutting. For this, they carried out the rheological characterization of modified binders to evaluate the performance of bituminous mixtures in terms of bitumen $|G^*|/\sin\delta$ and also evaluated the permanent deformation in the bituminous mixtures by conducting a repeated shear at constant height test. The authors conducted repeated creep and recovery tests on the bitumen binders, wherein, the bitumen binders were subjected to a creep loading (shear stress) of 300 Pa for a duration of 1 s which was followed by a recovery duration of 9 *s* (rest period) for a total of 100 cycles, and proposed a new rutting parameter, G_v. Here, G_v represents the viscous component of the creep stiffness of the bitumen binders. They observed a poor correlation with an R^2 of 0.24 between $|G^*|/\sin\delta$ and the accumulated strain rate, whereas, the correlation between G_v and the permanent deformation in bituminous mixtures showed a relative improvement with an R^2 of 0.68. The main drawback of the proposed rutting parameter, G_v, was that its correlation with the rutting resistance in bituminous mixtures was highly subjective to the aggregate type used in the bituminous mixtures.

Radhakrishnan et al. (2018) also evaluated the ability of $|G^*|/\sin\delta$ in terms of rutting resistance. The authors conducted oscillatory tests on unmodified and modified bitumen binders at 60 °C and determined the $|G^*|/\sin\delta$ at 2, 10 and 20 rad/s. The results indicated a good correlation of the $|G^*|/\sin\delta$ with the rut depth (mm) from the wheel tracking tests for the unmodified binders at all levels of frequency, whereas the modified binders had a poor correlation between $|G^*|/\sin\delta$ and the rut depth (mm). This poor correlation of $|G^*|/\sin\delta$ of modified binders with rutting observed in bituminous mixtures was also seen with the binder modified with Warm Mix Additive (WMA), where, Zhao et al. (2012) reported a poor correlation between the $G^*/\sin\delta$ of both the extracted and blended WMA modified binders with the rutting results obtained from the APA.

2.2.2 Shenoy's Rutting Parameter – $|G^*|/(1-(1/\tan\delta\sin\delta))$

Shenoy (2001) used the concept of Bahia et al. (2001), as discussed previously, and proposed a new rutting parameter as an improvement over the SHRP rutting parameter, $|G^*|/\sin\delta$. The proposed new rutting parameter is represented as $|G^*|/(1-(1/\tan\delta\sin\delta))$. The author suggested that the proposed new rutting parameter was able to consider the effect of delayed elastic strain characteristics of viscoelastic systems, whereby, an accurate representation of the unrecovered strain is supposedly made by $|G^*|/(1-(1/\tan\delta\sin\delta))$. Higher the $|G^*|/(1-(1/\tan\delta\sin\delta))$, higher would be the rutting resistance. $|G^*|/(1-(1/\tan\delta\sin\delta))$ was supposed to be able to provide an improvement over $G^*/\sin\delta$ for both the unmodified and modified bitumen binders. Shenoy's rutting parameter is to be determined in the LVE region.

Shenoy (2004) described an alternative approach in using the parameter, $|G^*|/(1-(1/\tan\delta\sin\delta))$ to determine the high-temperature Performance Grade (PG) of the bitumen binders. Here, the temperature corresponding to the high range of the performance grading (PG) system was determined as shown in Equation (2.3). The author argued that the modified approach for using the term $|G^*|/(1-(1/\tan\delta\sin\delta))$ was more efficient than the $|G^*|/\sin\delta$ as a high-temperature performance grading parameter for bitumen binders.

$$T_{HS,}\ ℃ = \frac{T_e}{\left(1-\left(\frac{1}{tan\delta sin\delta}\right)\right)}, \tag{2.3}$$

where,

T_e = Equi-stiffness temperature (temperature where the $|G^*|$ is 1 kPa and 2.2 kPa for unaged and short-term aged bitumen binders at a frequency of 10 rad/s)

Wang and Zhang (2014) conducted rheological studies on the unmodified and Styrene Butadiene Styrene (SBS) modified binders and determined $|G^*|/\sin\delta$ and $|G^*|/(1-(1/\tan\delta\sin\delta))$ from the oscillatory tests and the J_{nr} from the MSCR test. The rutting parameter J_{nr} will be reviewed in the subsequent section. The correlations of $|G^*|/\sin\delta$ and $|G^*|/(1-(1/\tan\delta\sin\delta))$ with the J_{nr} of the binders were drawn, with the R^2 values being of 0.861 and 0.997 respectively. These results indicated that the $|G^*|/(1-(1/\tan\delta\sin\delta))$ had a relatively stronger correlation with the binder J_{nr} than $|G^*|/\sin\delta$. This result shows that the $|G^*|/(1-(1/\tan\delta\sin\delta))$ is able to capture the unrecovered strain, when the binders are in the recovery stage, in a far better manner than $|G^*|/\sin\delta$ as suggested by Shenoy (2001).

However, Dongre and D'Angelo (2003) conducted frequency sweep tests on unmodified and modified binders and determined the binder $|G^*|/(1-(1/\tan\delta\sin\delta))$. Rut data from the accelerated loading facility (ALF) of the Federal Highway Association (FHWA) and the Nevada I-80 test sections with the same binders was correlated with the binder $|G^*|/(1-(1/\tan\delta\sin\delta))$. The correlations indicated a poor relationship. The authors reported the correlation as poor because the phase angle was less than 52°. Similarly, Radhakrishnan et al. (2018) reported that, even though there was a good correlation between $|G^*|/(1-(1/\tan\delta\sin\delta))$ and the mixture rut depth for the unmodified binders, the modified binders had a poor correlation. Here the authors determined the $|G^*|/(1-(1/\tan\delta\sin\delta))$ at frequency levels of 2, 10, 20 rad/s. The R^2 values for the unmodified binders at the above frequency levels were 0.97, 0.96 and 0.96, respectively. For the modified binders, the R^2 values were 0.70, 0.42, and 0.41, respectively. These results indicate the inefficiency of $|G^*|/(1-(1/\tan\delta\sin\delta))$ with respect to modified binders.

2.2.3 Zero Shear Viscosity

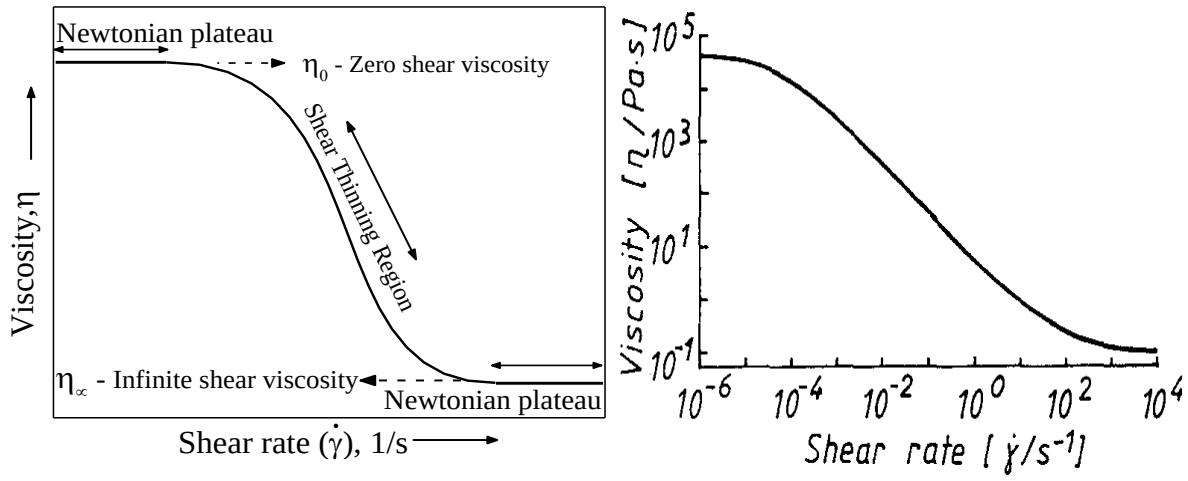

(a) (b) Sybilski, 1993

Fig. 2.2 A typical trend of viscosity versus shear rate for bitumen binders

Viscosity is one of the many rheological properties of bitumen that are important while considering its use in flexible pavements. In general, the viscosity is the inter-molecular attraction which resists deformation of a material under stress. Figure 2.2 shows the typical variation of viscosity with respect to shear rate for bituminous binders. This curve has three distinct phases, two Newtonian phases, and a shear-thinning or non-Newtonian phase. In the Newtonian phase, the viscosity of bitumen remains constant with respect to shear rate whereas in the non-Newtonian phase, the viscosity changes with a change in shear rate. The

viscosity measured in the Newtonian region corresponding to very low shear rates is termed as Zero Shear Viscosity (ZSV) and is represented as η_0 whereas viscosity measured in the Newtonian region corresponding to very high shear rates is termed as infinite shear viscosity and is represented as η_∞.

Sybilski (1993) conducted rheological tests on the polyethylene (PE), ethylene-propylene-diene monomer (EPDM) and SBS modified bitumen binders using an RV at 60, 90 and 135 °C. The modified version of the Cross model, as shown in Equation (2.4), was used to fit the viscosity data and the ZSV was determined. Moreover, power-law model was also used to determine the ZSV. The results indicated that the power-law model underestimates the ZSV when compared to the Cross model. The authors were of the opinion that, since the ZSV is determined at shear rates approaching zero, the ZSV of the binders at a particular temperature corresponds to the highest viscosity in the first Newtonian region, and thus can be considered as an inherent property of non-Newtonian materials. Sybilski (1994) used a similar

$$\eta = \frac{\eta_0}{1+(k*\dot{\gamma})^m} \tag{2.4}$$

where,

η = apparent viscosity,

η_0 = ZSV,

$\dot{\gamma}$ = shear rate, and

k, m = constants

approach and determined the ZSV of EPDM and SBS modified bitumen binders using a RV at 60 °C. Further, in order to validate the use of ZSV as a performance indicator for bituminous mixtures, the author also conducted wheel tracking tests using a FRT at 45 °C. The use of ZSV, determined at 60 °C, showed a good correlation with the permanent deformation results from the FRT. The author reported that the ZSV is an objective property of viscoelastic materials and suggested that ZSV be used as a parameter to evaluate the permanent deformation in bituminous mixtures. In the subsequent research, Sybilski (1996) determined the ZSV of the Polymer Modified Binders (PMB's) and rubber modified binder using a RV. Similar to previous studies, wheel tracking tests were conducted using a FRT at

45 °C on the bituminous mixtures. A linear regression analysis using ZSV, penetration index and penetration value at 25 °C showed a good correlation with the mixture rut results.

Desmazes et al. (2000) evaluated the use of long duration creep, creep and recovery tests in order to determine the ZSV of unmodified and modified bitumen binders. The tests were conducted using a DSR at a gap setting of 1 mm using a 25 mm test plate at a temperature of 40 °C. The main aim of the authors was to propose a test protocol to get a reliable estimate of ZSV for bitumen binders. The authors proposed the waiting time for steady-state and the relaxation and retardation times to be used in the creep and recovery tests at different stress levels. The ZSV was calculated based upon the inverse of the slope of the compliance curve in the steady-state. The total test duration can vary between 6 to 8 h for unmodified binders and 24 to 36 hrs for modified binders. For highly modified binders, where the steady-state would not reach, the authors suggested either to increase the temperature to 60 or 70 °C or to increase the creep duration.

Anderson et al. (2002) conducted a rheological examination of 10 short-term aged binders consisting of both unmodified and modified variants with the main objective of comparing different methods of determining the ZSV of bitumen binders. Frequency sweep test and the creep and recovery test were conducted and the ZSV was determined using the Cross model and the inverse of the slope of the compliance curve in the steady-state respectively. The tests were conducted at temperatures ranging from 52 to 82 °C in the interval of 6 °C. The ZSV from the frequency sweep tests and the creep and recovery tests showed similar results. Moreover, the relationship between ZSV and the $|G^*|/\sin\delta$ at the Superpave™ performance grading temperature was poor. The authors reported that the use of the creep and recovery tests to determine the binder ZSV are impractical because of the longer test duration required to achieve a steady-state especially in the case of highly modified bitumen binders.

Dongre and D'Angelo (2003) evaluated ZSV of seven binders (five from FHWA and two from Nevada Department of Transportation (DOT)) by conducting single cycle creep and recovery test, multiple cycle creep and recovery test, multiple frequency sweep test and single frequency sweep test. In the single-cycle creep and recovery test, Carreau model as shown in Equation (2.5) was used to fit the steady-state viscosities at different stress levels and the ZSV was extrapolated. In the multiple cycle creep and recovery test, Burger's model was used to determine the ZSV. In the multiple frequency sweep tests, master curves were fit and the ZSV was determined using a generalized Maxwell model. In the single frequency sweep test, the

ZSV was determined using a generalized Maxwell model. The ZSV obtained were correlated with the field rutting from the ALF test section of the FHWA and the Nevada I-80 test section with the results showing a poor correlation for ZSV determined from all the tests. Since, both the creep and recovery tests were time consuming, the authors were in favor of using a single frequency sweep test to determine the ZSV.

$$\eta = \frac{\eta_0}{\{1+[\lambda(d\dot{\gamma}/dt)]^2\}^{[(1-n)/2]}} \quad (2.5)$$

where,

η = steady state viscosity,

η_o = ZSV,

λ and n = constants, and

$d\dot{\gamma}/dt$ = shear rate at steady state.

De Visscher and Vanelstraete (2004) evaluated the use of a long time creep tests, short-time creep and recovery tests and frequency sweep tests in determining the ZSV of unmodified and polymer modified bitumen binders at a temperature of 40 °C using a 25 mm parallel plate test geometry and at a gap setting of 1 mm. In the creep and recovery tests, the ZSV was determined based upon the inverse of the slope of the compliance curve in the steady-state whereas, in the frequency sweep tests, Cross model was used. Both the creep and recovery tests showed repeatability for the unmodified binders whereas repeatability was less than satisfactory for the unmodified binders. However, the results of ZSV from frequency sweep tests were repeatable. In case of the unmodified binders, both the creep and recovery tests resulted in near-identical ZSV values whereas the ZSV values from the frequency sweep tests were relatively on the lower side. For the modified binders, ZSV from the three tests was relatively different. Based on the results, the authors suggested the use of frequency sweep tests in place of the highly time consuming creep and recovery tests.

Similarly, Biro et al. (2009) compared different methods of estimating the ZSV of WMA binders in order to evaluate their performance in terms of rutting resistance. Static creep test, frequency sweep test, and the repeated creep and recovery tests were conducted. From the static creep tests, the ZSV was determined using Burger's model and Carreau model. In case of the frequency sweep tests, ZSV was estimated using Cross/Williamson's

model, Cross/Sybilski's model and Carreau model. With the repeated creep and recovery tests, the ZSV was determined using Burger's model. It was observed that the ZSV obtained from different models was the same for a particular test. However, ZSV determined using a particular model but from different tests was notably different. The authors reported that, since the determination of ZSV is highly dependent upon the test methods employed, the models, the frequency ranges, the software used, the determination of true ZSV value is almost impossible.

Zhang et al. (2009) compared the use of a single creep and recovery test method, the multiple creep and recovery test method, the frequency sweep test method in determining the ZSV of modified binders. The results indicated that the ZSV of the binders determined using the single creep and recovery tests was highly dependent upon the duration of the creep and recovery period. Higher the creep and recovery duration, higher is the ZSV. Similarly, the ZSV was highly dependent upon the stress levels employed in the multiple creep and recovery test. Moreover, it was observed that the ZSV determined from the three tests was considerably different. It was also observed that the Cross model and the Carreau model used to estimate ZSV from the frequency sweep tests showed considerably different results.

Morea et al. (2010) compared the creep tests and the frequency sweep tests in determining the ZSV of the unmodified and modified bitumen binders. ZSV was determined from compliance during the retardation period of the creep test. In case of the frequency sweep tests, the LSV was determined at a frequency of 0.001 Hz using the Cross model and was assumed as the ZSV. The ZSV from both the results were comparable. Moreover, the results were repeatable for unmodified binders and vice versa for the modified binders. It was also seen that the test duration with the creep tests was considerably longer because of the criteria involved in the attainment of the steady-state thereby making the use of frequency sweep tests as a practical approach for determining the ZSV.

Morea et al. (2011) evaluated the use of bitumen Low Shear Viscosity (LSV) as an alternative to ZSV. LSV is known as the viscosity extrapolated at a frequency of 0.001 Hz. Frequency sweep tests were conducted on the unaged conventional, multi-grade and modified bitumen binders at 50, 60, 70 and 80 °C. Cross model, as shown in Equation (2.4) was used and the LSV was extrapolated. Wheel tracking tests were conducted on similar temperatures on dense bituminous mixtures and the rutting performance was analyzed by determining the rutting rate (RR). The correlations between the binder LSV and the mixture RR was strong with an R^2 value of 0.98. A relationship between the RR and the LSV was developed and

validated with further mixture testing thereby indicating possible use of binder LSV as a rutting performance indicator.

Morea et al. (2012) continued the above research by incorporating bituminous mixtures like Stone Matrix Asphalt (SMA) and micro-asphalt along with the dense mixtures. Moreover, the LSV was also determined for the unaged as well as short-term aged bitumen binders (conventional, multi-grade and modified). Again, the relationship between the RR and the binder LSV showed strong correlations with R^2 values of 0.87 and 0.86 for unaged and short-term aged bitumen binders, respectively. Also, the authors used the Burger's model to fit the wheel tracking data and determined the viscosity parameter (η_0). It was observed that the correlation between the LSV and the η_0 was strong.

Morea et al. (2013) further expanded their study and reported that the binder LSV, the pavement temperature, and the loading conditions have an effect on the permanent deformation in the bituminous mixtures. The LSV of bitumen binders (conventional, multi-grade and modified) was determined using the Cross model. The SMA, dense and micro-asphalt bituminous mixtures were evaluated with a WTD and the rutting rate (RR) was determined. The tests were carried out at 50, 60, 70 and 80 °C. The authors developed relationships between the RR obtained from the wheel tracking test and the binder LSV, temperature and the loading levels. The proposed relationships by these authors correspond to the level of loading employed and the threshold value of LSV.

Radhakrishnan et al. (2018) determined ZSV and LSV by conducting rheological tests on unmodified and modified bitumen binders at a temperature of 60 °C using a DSR. The ZSV of the binder was determined using the Cross model whereas the LSV was determined at 0.01, 0.001, 0.0001 Hz using the Cross model. Wheel tracking tests were also carried out at 60 °C and the rut depth was measured after 20,000 passes. It was observed that there is an increase in LSV with an increase in the frequency at which LSV is calculated. Moreover, it was observed that the LSV calculated at 0.0001 Hz and the ZSV are similar. It is also reported that the binder ZSV had a good correlation with the mixture rutting.

2.2.4 J_{nr} at 3.2 kPa from the MSCR Test

The MSCR test includes the concept of applying consequent cycles of creep and recovery on the binder. The creep and recovery tests were previously used by Bahia et al. (2001). Here the samples were subjected to a stress of 300 Pa with a creep duration of 1 s followed by a rest period of 9 s for 50-100 cycles. Later, D'Angelo et al. (2007) expanded on the work done by

Bahia et al. (2001) and conducted creep and recovery tests on bitumen binders at stress levels of 0.025, 0.05, 0.1, 0.2, 0.4, 0.8, 1.6, 3.2, 6.4, 12.8 and 25.6 kPa. The creep duration was 1 s and the recovery duration was 9 s. 10 cycles of creep and recovery were applied at each stress interval. Based on the correlations with the mixture rutting, 0.1 kPa and 3.2 kPa were proposed as the stress levels at which the non-recoverable creep compliance (J_{nr}) and the percentage recovery (%R) were to be measured. Figure 2.3 shows the various terms involved in every single creep and recovery cycle of an MSCR test (De Visscher et al., 2016). Thereafter, the MSCR test was standardized by both the American Society for Testing and Materials (ASTM) as "ASTM D7405 – 15: Standard Test Method for Multiple Stress Creep and Recovery (MSCR) of Asphalt Binder Using a Dynamic Shear Rheometer" (ASTM, 2015*a*) and American Association of State Highway and Transportation Officials (AASHTO) as "AASHTO T 350: Standard Method of Test for Multiple Stress Creep Recovery (MSCR) Test of Asphalt Binder Using a Dynamic Shear Rheometer (DSR)" (AASHTO, 2014) and the J_{nr} at 3.2 kPa was proposed as a new rutting parameter. The J_{nr} at 0.1 kPa corresponds to the linear response whereas the J_{nr} at 3.2 kPa corresponds to the non-linear response of the bitumen binders.

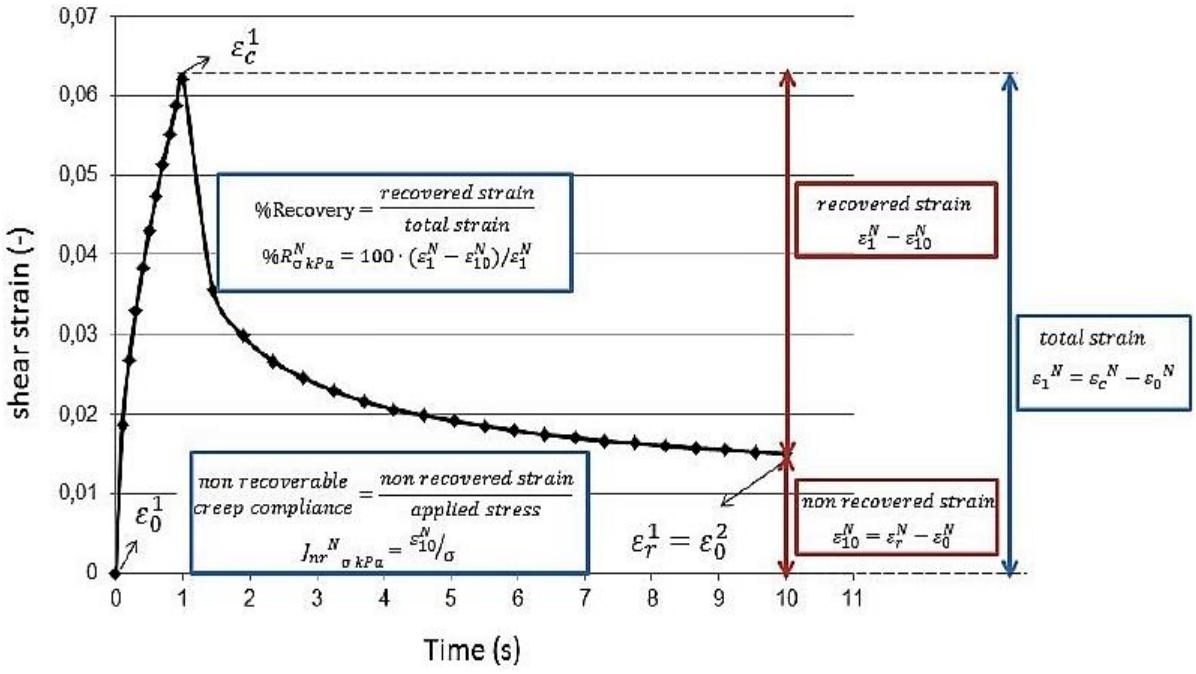

Fig. 2.3 Parameters involved in each of the creep and recovery cycle of a MSCR test (De Visscher et al., 2016)

D'Angelo et al. (2009) validated the relationship between binder J_{nr} and the mixture rutting performance by conducting binder and mixture testing on three field sections namely the MnRoad, FHWA ALF and the Mississippi DOT. In the MnRoad, three sections were

evaluated and the results indicated that there was a poor relationship between the binder $|G^*|/\sin\delta$ and the observed field rutting. On the same binders, MSCR test was conducted at stress levels ranging from 0.025 to 25.6 kPa and was seen that the J_{nr} at 12.8 kPa showed good relation with the field rut data. In order to further validate the results, the plant produced mixtures of the Minnesota DOT were compacted in the laboratory and dry wheel tracking tests were conducted using a HWTD at temperatures ranging from 58 to 70 °C. It was observed that the binder J_{nr} was able to capture the influence of binder on the mixture rutting better than the binder $|G^*|/\sin\delta$. The J_{nr} at 12.8 kPa showed the highest correlation. In the FHWA ALF, 12 sections with different polymer modified binders were field trialed at a test temperature of 64 °C with the super single tire. DSR tests on the same binder from the field sections were also conducted at 64 °C. The results showed that the binder $|G^*|/\sin\delta$ had a poor correlation (R^2 = 0.22) with the rutting observed in the 12 filed sections, whereas, the J_{nr} at 25.6 kPa showed a strong correlation (R^2 = 0.88). The stress level of 25.6 kPa was used because of the high loads and the slow-moving traffic on the FHWA ALF test sections. Similarly, field trial sections with polymer modified binders and a control unmodified binder were tested by the Mississippi DOT. The correlation of $|G^*|/\sin\delta$ with the field rutting showed a poor correlation (R^2 = 0.32). For these sections, the binder J_{nr} at 3.2 kPa showed the best correlation with the field rutting (R^2 = 0.75) which can be attributed to the typical highway traffic observed on the MSDOT trial sections. From the overall MSCR test results, the binder J_{nr} can be determined at multiple stress levels. The J_{nr} determined at stress levels closer to the observed traffic loading provides a close relationship between the binder property and the observed mixture rutting.

Golalipour (2016) studied the effect of the number of cycles and the stress levels by modifying the MSCR test. In this study, the neat and modified binders were tested at temperatures of 46, 58 and 70 °C. Results from the standard MSCR test with two stress levels of 0.1 and 3.2 kPa with 10 cycles of creep and recovery and another modified test with 30 cycles of creep and recovery at 0.1, 3.2 and 10 kPa were compared. It was observed that the application of only 10 cycles showed a transient non-steady state behavior because of the delayed elastic response after every cycle. The application of 30 cycles showed that the effect of the delayed elastic response after every cycle was decreasing and the material achieved a steady state. The analysis of variance test showed that the response of the binder due to the increase in the number of cycles from 10 to 30 was statistically significant. Further, the results from the increased stress level indicate that increased stress of 10 kPa captures the binder non-linearity and stress sensitivity better than that observed at 3.2 kPa. The J_{nr} difference between 10 kPa and 3.2 kPa was higher than the difference between 0.1 and 3.2 kPa. It was also seen

that the results at 10 kPa had high repeatability compared to results at 3.2 kPa and also there was a stable cycle to cycle response at a stress level of 10 kPa. The observed results were correlated with the mixture rutting response, wherein the binder J_{nr} was correlated with the mixture flow number (FN) obtained from the unconfined compression tests with the repeated creep and recovery loading pattern. The J_{nr} at 10 kPa after 30 cycles (average of the last 5 cycles) had the best correlation (R^2 = 0.87) when the mixtures were tested at stress levels comparable to field conditions. Following these results, the authors recommended the use of 10 kPa as the stress level and 30 cycles of creep and recovery to determine the J_{nr} (average of the last 5 cycles) from multi stress creep and recovery test.

Kakade et al. (2013) evaluated the rutting performance of modified bitumen binders. Six modified binders were tested using a DSR and the binder $|G^*|/\sin\delta$, ZSV, and the J_{nr} were determined at 60 °C. Also, the rutting resistance of Bituminous Concrete (BC) mixtures was determined using the Indian Institute of Technology Kharagpur (IIT-KGP) rut tester at 60 °C and the rut depth (mm) after 5000 cycles (10000 passes) was recorded. It was observed that the correlation between $|G^*|/\sin\delta$ and the rut depth was poor (R^2 = 0.40) followed by ZSV (R^2 = 0.60) with the J_{nr} at 3.2 kPa showing the best highest correlation (R^2 = 0.75). The J_{nr} was able to highlight the stress sensitivity of the binders.

Hafeez and Imran (2014) tested two neat and five modified binders and determined the J_{nr} from the MSCR test. Mixture testing was also carried out on dense graded mixtures with 6% air voids and the rut depth (in mm) after 20000 passes were determined. Both the binder and mixture testing were carried out at 58, 64, 70 and 76 °C temperatures. It was observed that the J_{nr} at 3.2 kPa and the mixture rut depth had a strong correlation (R^2 = 0.96) indicating the capability of the J_{nr} to evaluate the rutting performance of bitumen binders.

Saboo and Kumar (2016) evaluated the rutting characteristics of the unmodified and modified bitumen binders. The binder tests were conducted at 40, 50 and 60 °C and the binder $|G^*|/\sin\delta$ and $|G^*|/(1-(1/\tan\delta\sin\delta))$ were determined from temperature sweep tests. ZSV was determined from the frequency sweep tests using Carreau –Yasuda model and the J_{nr} was determined from the MSCR test. In their study, mixture rutting of Stone Matrix Asphalt (SMA), BC and Dense Bituminous Macadam (DBM) mixtures were evaluated at a temperature of 60 °C and the rut depth (mm) after 20000 passes were determined. The results from their study showed that all the rutting parameters ranked the binders in a similar order. Moreover, all the binder properties and the mixture rut depth were normalized and the root mean square error (RMSE) was determined. It was reported that the J_{nr} had the lowest RMSE

and thus was used to correlate with the rut depth from the wheel tracking tests. The correlation results showed a strong correlation (R^2 = 0.99 for BC and R^2 = 0.96 for DBM) between J_{nr} at 3.2 kPa and the rut depth observed in the bituminous mixtures. From the mixture point of view, the BC mixtures were relatively rut resistant than the DBM mixtures. Similarly, Singh and Kataware (2016) assessed the rutting resistance of control PMB40 binder and PMB40 binder modified with various WMA additives by determining the binder rutting parameters $|G^*|/\sin\delta$, $|G^*|/(1-(1/\tan\delta\sin\delta))$, ZSV and J_{nr} at a test temperature of 76 °C. The comparative results among the four rutting parameters showed that the binder $|G^*|/\sin\delta$ and $|G^*|/(1-(1/\tan\delta\sin\delta))$ ranked the binders similarly whereas the ranking of the binders from the binders ZSV and J_{nr} was different. The results also indicated that the binder J_{nr} was sensitive to the amount of modification. When the correlations between the rutting parameters was established, it was seen that relationship of $|G^*|/\sin\delta$ with $|G^*|/(1-(1/\tan\delta\sin\delta))$ and ZSV was strong (R^2 = 0.96 and 0.88, respectively) whereas the relationship between of $|G^*|/\sin\delta$ with J_{nr} was the lowest among the three (R^2 = 0.78). This indicates that the binder $|G^*|/\sin\delta$, $|G^*|/(1-(1/\tan\delta\sin\delta))$ and ZSV evaluate the rutting performance of the bitumen binders in a more or less similar manner. This result suggests that the binder J_{nr} is a comparatively better parameter at evaluating the rutting characteristics of bitumen binders.

Radhakrishnan et al. (2018), as discussed previously, conducted rheological tests on the unmodified and modified bitumen binders using a DSR and determined the binder $|G^*|/\sin\delta$, $|G^*|/(1-(1/\tan\delta\sin\delta))$, ZSV, LSV and J_{nr} at a temperature of 60 °C. Moreover, the ZSV of the binder was determined using the Cross model whereas the LSV was determined at 0.01, 0.001, 0.0001 Hz using the Cross model. The J_{nr} was determined at stress levels of 100, 200, 400, 800, 1600, 3200, 6400, 12800 and 256000 Pa. Wheel tracking tests were conducted on bituminous mixtures with respective binders and the rut depth (mm) after 20,000 passes was determined. The results indicated that the MSCR test parameters J_{nr} and $\%R$ were sensitive to the applied stress levels. For the unmodified binders, all the parameters had a good correlation with mixture rut depth, whereas, in the case of modified binders, only J_{nr} had good correlations whereas the other parameters had poor correlations. The effect of different stress levels involved in the MSCR test had a negligible effect on the coefficient of correlation.

2.3 EFFECT OF AGING ON RHEOLOGICAL PROPERTIES OF BITUMEN BINDERS

Lu and Isacsson (2002) studied the effect of thin-film oven (TFO) test aging and RTFO aging on the rheological properties of seven bitumen binders. The binders were subjected to the aging process at a temperature of 163 °C with the aging duration being 75 minutes and 5 hours in the RTFO and TFO tests respectively. Temperature sweep tests were conducted from -30 to 135 °C at a frequency of 1 rad/s and the frequency sweep tests from 0.1 to 100 rad/s at 25 and 60 °C. The results show that aging has a change in the temperature dependency and time dependency of the bitumen binders. The complex modulus (G^*), storage modulus (G') and loss modulus (G'') increased whereas the phase angle (δ) decreased with the aging of the binder thereby showing an increase in stiffness and the elastic component. Aging made the mechanical properties of bitumen more solid-like, however, the magnitude of increase in the solid-like response was highly dependent on the bitumen type and the condition of evaluation. Results from both the aging protocols including TFO and RTFO showed a good correlation among each other.

Liu et al. (2008) studied the effect of aging on bitumen mastics where limestone powder in varying proportions was added to the base bitumen. The bitumen mastics were subjected to RTFOT and PAV (10, 20, 30 hours) aging. The aged samples were tested using a RV at temperatures ranging from 60 to 175 °C and the viscosity was determined. Using a DSR, frequency sweep (0.1 to 100 rad/s at 20 °C) and a creep test (at a stress amplitude of 0.1 MPa using a loading time of 200 s followed by a recovery duration of 1000 s at a test temperature of 0 °C) were performed. The results from the RV tests showed that with aging the viscosity of the bitumen mastics increased at all temperatures, however, the difference between PAV aging for 20 hours and 30 hours was negligible. This was because of the reduction in the oxidation of the bitumen mastics beyond 20 hours of aging. It was also seen that there was a significant increase in $|G^*|$ and a decrease in δ with an increase in aging of the bitumen mastics which shows an increase in the elastic part of the binder, which in turn increases the rutting resistance. The results from the creep test show that there is a significant decrease in the total strain and the unrecoverable strain with an increase in the aging of the bitumen mastics.

Hossain et al. (2018) assessed the effect of bitumen aging when subjected to ultraviolet (UV) radiation, on the rheological properties of bitumen binders using a DSR. The bitumen binders were subjected to natural UV radiation for 3, 7, 28 and 45 days. Frequency sweep

tests (0.1 to 100 Hz) were conducted at temperatures ranging from 20 to 60 °C. Also, the binder $|G^*|/\sin\delta$ and aging index (Aging index = $[G^*_{\text{UV aged}} - G^*_{\text{unaged}}]*100/ G^*_{\text{unaged}}$) were also determined. The G^* and the aging index showed an incremental increase in the hardening of the binders when exposed to continuous UV radiation. The phase angle (δ) reduces gradually with little difference between results of 3 and 7 days of UV aging. The binder rutting parameter, $|G^*|/\sin\delta$, also increased gradually with the aging duration and was highest at 45 days of exposure. The authors recommended incorporating the effect of UV aging in the long-term performance of pavements.

Liu et al. (2018) studied the effect of aging on the response characteristics of neat bitumen binder and bitumen mastics with limestone filler. The neat binders and bitumen mastics were short-term aged with varying durations. Temperature sweep tests were conducted at a frequency of 10 rad/s at temperatures in the range of 46 to 70 °C at intervals of 6 °C. The observed results showed a change in the asphalt components, wherein, the aromatics change into resins and saturates change into asphaltenes leading to an increase in the stiffness of the bitumen binders and bitumen mastics. The $|G^*|$ of the binder increased rapidly with aging while there was a linear decrease in the δ. As a result, there is an increase in binder $|G^*|/\sin\delta$ and complex viscosity indicating an increased resistance towards rutting. Similar results were obtained with tests on bitumen mastics. However, with an increase in the aging in bitumen mastics, there is a deterioration in the interaction of bitumen and filler.

2.4 AGING OF BITUMINOUS MIXTURES

Bell et al. (1994) evaluated the laboratory aging procedures for bituminous mixtures wherein the mixtures were short term aged and long term aged. Forced draft oven aging (FDOA) and the extended mixing procedures were used to short-term age the loose bituminous mixtures whereas FDOA, pressure oxidation and triaxial cell testing were used to long-term age the compacted bituminous mixtures. The short-term aging using FDOA was simulated for 0, 6,15 hours at a temperature of 135 and 163 °C while the short-term aging using an extended mixing procedure was conducted using a RTFO drum at 0, 10, 120, 360 minutes at a temperature of 135 and 163 °C. The long-term aging using FDOA was conducted for a period of 0, 2 and 7 days at a temperature of 107 °C. The pressure oxidation was conducted for 0, 2 and 7 days at a pressure of 690 and 2070 kPa and at a temperature of 25 and 60 °C. In the triaxial cell, the mixtures were aged at a temperature of 25 and 60 °C at a flow rate of 0.11 m^3/h and at a pressure of 345 kPa. The results were analyzed on the basis of the resilient

modulus (M_R) ratio of the unaged, short-term aged and long-term aged bituminous mixtures. The results from the short- term aging tests showed that both the tests aged the bitumen binder significantly as there was a significant increase in the modulus of the aged bituminous mixtures. However, samples with 15 hours of aging had a low modulus because the severe aging for 15 h created problems while compacting the bituminous mixture thereby resulting in lower modulus. On the other hand, the extended aging procedure resulted in uniform aging, however, there was a loss in integrity of the samples as they were subjected to gas at high pressure. The results from the long-term aging showed that the triaxial test procedure resulted in moderate aging while there was deterioration of the samples with the pressure oxidation procedure. In case of the long term aging with the FDOA, it was seen that there was an increase in the modulus by six times after being long-term aged. Based upon the results, for short-term aging simulation in laboratories, the authors suggested the use of FDOA for a period of 4 h at a temperature of 135 °C and for long-term aging simulation, the use of FDOA and low-pressure oxidation for a period of 5 days at a temperature of 85 °C.

Morian et al. (2011) evaluated the changes in the stiffness of the mixtures when the laboratory compacted mixtures were subjected to different aging conditions. Two aggregate sources were used with unmodified and modified bitumen binders to prepare bituminous mixtures. Loose mixtures were short term aged for 4 h at 135 °C and the compacted mixtures with 7% air voids were aged for 0, 3, 6 and 9 months at a temperature of 60 °C. The dynamic modulus ($|G^*|$) was determined to study the effect of aging on the bituminous mixtures. Moreover, the recovered binder was also tested. From the $|G^*|$ master curves and the carbonyl area measurements, it was observed that the aggregate source had no significant effect on the short-term aging in bituminous mixtures and the unmodified binder aged more than the modified binder. The $|G^*|$ increases with an increase in the aging duration, however at higher test frequencies, the difference is low. For the long-term aged mixtures, the aggregate source had an effect on the oxidation of the binders because of the changes in the internal aggregate interlock for different binders. However, in case of long-term aging, both the binders aged at the same rate.

Tarbox and Daniel (2012) evaluated the effect of long-term aging on the plant produced to control and Reclaimed Asphalt Pavement (RAP) mixtures. The mixtures were compacted in the laboratory using a gyratory compactor and long-term aged for 2, 4 and 8 days at a temperature of 85 °C. The aged samples were tested using an AMPT and the dynamic modulus ($|G^*|$) and the phase angle data was determined. Moreover, Global Aging System (GAS), used by the mechanistic-empirical pavement design guide which can predict

the change in $|G^*|$ with respect to change in the aging of the bitumen binders in the bituminous mixtures was also used. The results showed that all the mixtures had an increase in the dynamic modulus and a decrease in phase angle with aging, with the 2-day aging and 4-day aging almost similar at different test frequencies but the 8-day aging was significantly different for control (0% RAP) mixtures. For the RAP mixtures the increase in aging increased the $|G^*|$, however, the increase is less than that of the control mixtures. This can be attributed to the presence of already aged bitumen binder in the RAP mixtures. The selection of 2, 4 and 8 days of aging in this study corresponds to 4, 8 and 16 years of field aging. However, the results of $|G^*|$ predicted from GAS methodology were comparatively higher than the $|G^*|$ results from the laboratory aged samples. This showed that the laboratory aging protocols did not age the samples to the required aging that happens in the field.

Azari and Mohseni (2013) evaluated the permanent deformation characteristics of unaged, short-term aged and long-term aged bituminous mixtures by conducting damage based incremental Repeated Load Permanent Deformation test at a temperature of 60 °C. The mixtures were subjected to multiple stress increments and the strain was measured at the end of each cycle. The minimum strain rate was used to prepare master curves to characterize the high-temperature performance of bituminous mixtures. The mixtures were short-term aged for 0, 1, 2, 3, 4, 5 and 6 hours. The short-term aged loose mixtures were then compacted and the specimens were long-term aged for 2, 5 and 9 days. It was observed that there was an increase in stiffness with the increase in the duration of long-term aging. It was also observed that the stiffness of the long-term aged bituminous mixtures was highly dependent upon the short-term aging duration for some mixtures and was insignificant for other bituminous mixtures. There was a significant increase in the rutting resistance with an increase in the short-term aging duration.

Yin et al. (2017) correlated the results from the laboratory long-term aging of bituminous mixtures with the results from field aging (two years after construction). Cores were taken from seven field projects from different locations in the USA during and after construction. Materials from the same projects were used to fabricate samples in the laboratory. The samples were aged in the laboratory at 60 °C for 14 days and at 85 °C for 3 and 5 days. The resilient modulus (M_R) and the HWTT were conducted on the aged samples. The results from both the M_R test and the HWTT showed that the test protocol involving 85 °C produced stiffer mixtures than the mixtures conditioned at 60 °C. It was reported that the long-term oven aging for 5 days at 85 °C produced mixtures with similar aging to the field condition (two years of aging) which is contrary to the AASHTO R30 wherein, FDOA for 5

days at 85 °C produces mixtures with an aging expected in the range of 5 to 10 years. It was also seen that the percentage increase in stiffness of WMA mixtures was higher than conventional hot mix asphalt (HMA) mixtures. Moreover, mixtures with the RAP and reclaimed asphalt shingles showed a lower increase in the mixture M_R.

2.5 WHEEL TRACKING TEST DATA

In the wheel tracking tests, as discussed in the previous section, a loaded wheel moves to and fro on the compacted bituminous mixture and the rut depth is measured using a linear variable differential transducer. The rut data is recorded at different positions along the wheel traverse. The rut data along the wheel traverse show significant scatter due to the variation in the internal distribution of air voids within the specimen and the differential aggregate interlocking along the wheel traverse and the non-uniform speed of the wheel across the bituminous mixture slab being tracked (Schram, 2014). Guo and Prozzi (2009) report that the maximum rut depth is more likely to be from among the eleven locations where the wheel tracking data is collected on the mixtures. In order to obtain a representative rut curve from among the different locations, different methodologies were proposed. The Austoroads recommends the average of the rut data from the seven locations (±37.5 mm, ±23.5 mm, ±7.5 mm and 0 mm) from the center of the sample including the center (Austoroads, 2006). The Texas Department of Transportation (TxDOT) recommends the use of the average rut depth from the three central locations of the wheel traverse (TxDOT, 2014), whereas the Colorado Department of Transportation (CDOT) recommends the use of the average rut depth from the rut data recorded at 13 locations from the central track of the wheel tracking device (CDOT, 2015). On the other hand, the Utah Department of Transportation (UDOT) considers the maximum rut depth at any location on the wheel traverse except the rut data collected 2 inches from either side (UDOT, 2015). Mohammed et al. (2017), based upon their evaluation of the HWTD's from different manufacturers and also the test protocols, recommended the average rut depth measured at the five locations (±46 mm, ±23 mm and 0 mm) from the center along the wheel traverse including the center. On the other hand, reliability-based rutting curves were obtained to take into account, the variability observed in rutting test results across the test specimens (Singh and Swamy, 2018). From above it can be understood that the measurement of a single point of rut depth, after a particular number of passes, is inconsistent.

2.6 SUMMARY

In this chapter, a detailed review of the existing rutting parameters is presented followed by implications of binder and mixture aging on rutting in bituminous mixtures. The binder $|G^*|/\sin\delta$ was proposed as a performance indicator of rutting in bituminous mixtures by the SHRP. However, it was shown that this parameter was unable to characterize the delayed elastic response of the bitumen binders and was shown to have a poor correlation with the rutting resistance, especially for the modified binders. Thereafter, Shenoy's parameter, $|G^*|/(1-(1/\tan\delta\sin\delta))$ was proposed as an improvement over the SHRP parameter because of its ability to characterize the unrecovered strain. However, its correlation with the rutting resistance of modified binders was shown to be poor. Concurrently, the ZSV was considered as an important intrinsic property of bitumen binders and was used as a parameter to predict the rutting performance of bituminous mixtures. The emergence of the MSCR test lead to the determination of the non-recoverable creep compliance (J_{nr}) of bitumen binders and J_{nr} at 3.2 kPa from MSCR test has become the most popular rutting parameter in particular for the modified binders and has shown a good relationship with rutting in bituminous mixtures. However, the stress levels of 0.1 kPa and 3.2 kPa and the recovery 10 cycles of loading were seen to be insufficient which led to the development of modified MSCR tests. The quest to further improve upon the existing rutting parameters led many researchers to look for new rheological properties which could improve the relationship with the rutting in bituminous mixtures (Dongre et al., 2004; Delgadillo et al., 2006*a*; Delgadillo et al., 2006*b*; Santagata et al., 2015). Moreover, it is known that bitumen as a material is viscoelastic in nature and behaves as Newtonian and Non-Newtonian material depending upon the test temperatures. However, the binder $|G^*|/\sin\delta$ and $|G^*|/(1-(1/\tan\delta\sin\delta))$ are determined in the linear region of the bitumen response and are determined at the PG pass-fail temperature. Even though the binder J_{nr} at 3.2 kPa from MSCR test represents the non-linear response of the bitumen binders there is still ambiguity over the number of cycles applied and the stress level used in the MSCR test. The ZSV is a Newtonian property however, there are issues related with ZSV wherein, different test methods and models give different ZSV and also the use of creep test to determine ZSV is considered to be too time-consuming and impractical.

Rutting in bituminous pavements is generally associated with high temperature and the mixture performance tests are mostly conducted at the PG temperatures or at 60 °C. However, rutting can also occur at temperatures lower than those discussed above. Therefore it is important to measure the viscosity of bitumen at different temperatures. Bitumen binders exhibit non-Newtonian behavior at pavement temperatures that are common in India. This

non-Newtonian behavior can become prominent at lower temperatures and bitumen aging adds to the complexity, whereby, the response of bitumen becomes predominantly non-Newtonian. However, consistent measurement of bitumen viscosity can be made at shear rates corresponding to the ZSV regime. Therefore, it is important to characterize this non-Newtonian response of bitumen binders at very low shear rates. Moreover, several methodologies are currently being practiced across the world to obtain a representative rut curve as a function of a number of wheel passes and there is no consensus on choosing a representative rut curve from the wheel tracking test data. Reliability-based designs are widely used in the design of flexible pavements (IRC, 2018) especially for the roads classified based on the hierarchical levels. Similarly, reliability-based rutting curves were obtained to take into account the variability observed in rutting test results across the test specimens (Singh and Swamy, 2018). Thus, the possibility of developing a reliability-based representative rut curve for a particular specimen needs to be explored. Further, the influence of aging on permanent deformation characteristics of bituminous mixes needs to be investigated. Thus the main focus of the current research is to identify the rutting parameters based on the Newtonian and non-Newtonian responses of unaged and aged bitumen binders at different temperatures. Further, there is also a need to develop reliability-based representative rutting curves by taking into account the variability observed along the wheel traverse. Finally, the identified rutting parameters need to be correlated with the permanent deformation in bituminous mixtures.

CHAPTER 3

METHODOLOGY

3.1 GENERAL

Bitumen is a viscoelastic material in its nature and is a material that is highly susceptible to temperature and stress. The performance of bituminous mixtures is highly dependent upon the response characteristics of a bitumen binder subjected to shear. It has been recognized that the rheological properties of bitumen binders have an important role to play in the performance of bituminous pavements. Thus, based upon the different shear input protocols, different rutting parameters are proposed over a period of time. The rutting parameters that gained prominence over time are $|G^*|/\sin\delta$, $|G^*|/(1-(1/\tan\delta\sin\delta))$, J_{nr} and ZSV. ZSV is a Newtonian parameter and is an intrinsic property of bitumen. Mixture performance tests are conducted at PG pass/fail temperatures. However, its measurement is complex with different results from different tests and models. It is shown that the bitumen exhibits non-Newtonian response. Thus, this research work focusses on the characterizing the non-Newtonian characteristics of bitumen binders and their ability to evaluate permanent deformation in bituminous mixtures. Two test protocols are adopted to characterize the non-Newtonian behavior of bitumen binders. One is the LSRS test protocol and the other is an SWSSRS test protocol conducted at very low shear rates. It has been observed from the literature that bitumen binders show non-Newtonian response at pavement temperatures of the order ranging from 40 to 65 °C typically observed in India.

Thus, in a nutshell, as per the proposed objectives, the current research study consists of rheological characterization of unmodified bitumen binders, identifying new rutting parameters based upon the non-Newtonian characteristics of the bitumen binders and to find a correlation between the rutting performances of bituminous mixtures with the rheological properties of the bitumen binders. Figure 3.1 represents the flow chart detailing the methodology adopted in completing the research objectives. In order to achieve the proposed objectives, the rheological characterization of the binders and the permanent deformation of the bituminous mixtures are carried out. The materials, equipment, sample preparation and test protocols employed are detailed in this chapter.

3.2 MATERIALS

3.2.1 Aggregate and Bitumen

Locally available Granite from a single source was used as the mineral aggregate. Table 3.1 enlists the properties of the mineral aggregate. The mineral aggregate satisfied all the criteria provided in "Specifications for Road and Bridge Works" by Ministry of Road Transport and Highways (MoRTH, 2013).

3.2.2 Bitumen

Viscosity graded VG20 and VG40 bitumen binders are used in this research. The binders satisfied the required specifications as per IS 73, 2013 (BIS, 2013). Table 3.2 shows the properties of the VG20 and VG40 binders.

Table 3.1 Properties of the Granite aggregates

Property	Values Obtained	Specification
Cleanliness, %	3.9	Max. 5%
Aggregate impact value, %	15.82	Max. 24%
Los Angeles abrasion value, %	21.89	Max. 30%
Combined flakiness and elongation index,%	27	Max. 35%
Specific gravity	2.626	-
Water absorption, %	0.6	Max. 2%
Retained coating of aggregates with bitumen, %	99	Min. 95%
Soundness test using sodium sulphate	1.2	Max. 12%

3.3 EQUIPMENT

The major equipments used to carry out the research work are the RV, the DSR, and the WTD. The rheological characterization of the bitumen binders is carried out using RV and DSR. The rutting characterization of the bituminous mixtures was carried out using the WTD.

3.4 AGING OF BITUMEN IN THE LABORATORY

During the mixing, compaction and the laying operations of the bituminous mixtures in the field, there will be an increase in the stiffness of the bitumen binders. This increase in the stiffness of the bitumen binders is known as 'short-term aging' whereas the stiffening of the bitumen binders during the service life of flexible pavement is known as 'long-term aging'.

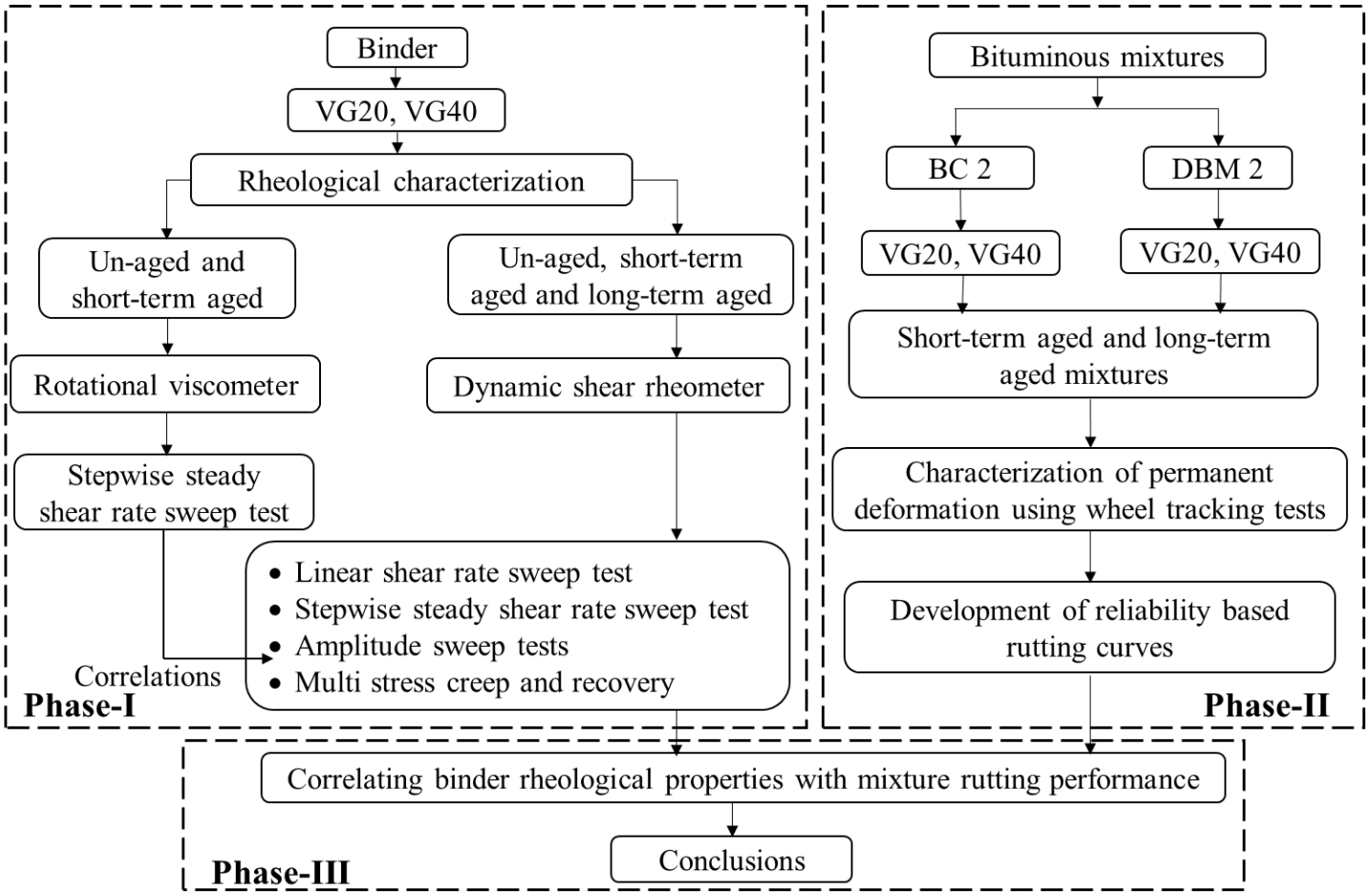

Fig. 3.1 Flow-chart representing the adopted methodology

Table 3.2 Properties of bitumen binders

Characteristics	VG20		VG40	
	Result	**Specification**	**Result**	**Specification**
Penetration at 25 °C, 100 g, 5 s, 0.1 mm	***62***	Min. 60	***36***	Min. 35
Absolute viscosity at 60 °C, Poises	***1862***	1600-2400	***4000***	3600-4800
Kinematic viscosity at 135 °C, cSt	***342***	Min. 300	***442***	Min. 400
Flash point (Cleveland open cup), °C	***315***	Min. 220	***340***	Min. 220
Solubility in trichloroethylene, %	***99***	Min. 99	***99***	Min. 99
Softening point (R&B), °C	***49***	Min. 45	***53***	Min. 50
Tests on residue from RTFO				
Viscosity ratio at 60 °C	***2.14***	Max. 4	***3.64***	Max. 4
Ductility at 25 °C, cm	***75***	Min. 50	***30***	Min. 25

The mechanism of aging in the bitumen binders is discussed in Chapter 2. As per the research methodology, the rheological properties of the bitumen binders are to be correlated with the short-term aged and the long-term aged bituminous mixtures. Therefore, it was necessary to determine the rheological properties of the unaged, short-term aged and the long-term aged bitumen binders.

Fig. 3.2 Rolling thin-film oven

3.4.1 Short-term Aging of Bitumen in the Laboratory

Short-term aging of the VG20 and the VG40 binders was simulated in the laboratory using a Rolling Thin Film Oven (RTFO) by following the procedure specified in ASTM D2872-19 (ASTM, 2019). The RTFO used for the current research is shown in Figure 3.2. The required number of glass containers of the RTFO are filled with 35 ± 0.5 g of bitumen binder and placed in the carousel. The carousel was rotated at a speed of 15 rpm in the RTFO while

subjecting the binder in the glass containers to a temperature of 163 °C for a period of 85 minutes with an airflow rate of 4 l/min. After completion of the test, the short-term aged binder obtained from all the glass containers was collected in a single container and thoroughly mixed. The short-term aged binder was utilized for further testing within the specified 72-hour duration.

(a) Pressure aging vessel (b) Vacuum degassing oven

Fig. 3.3 Equipment used for long-term aging

3.4.2 Long-term Aging of Bitumen in the Laboratory

The short-term aged bitumen binder was further subjected to long-term aging using a Pressure Aging Vessel (PAV) and a Vacuum Degassing Oven (VDO). The procedure detailed in ASTM D6521 (ASTM, 2018*a*) was followed to produce the long-term aged bitumen binders. The PAV and VDO used for the current research are shown in Figure 3.3. The short-term aged binder obtained from the RTFO was subjected to a pressure of 2.1 MPa at a temperature of 100 °C for a period of 20 hours. The aged reside obtained from the PAV was further subjected to vacuum degassing at a temperature of 170 ± 5 °C for a period of 15 ± 1 minutes in the VDO. The vacuum degassed binder was collected and utilized for further testing.

3.5 RHEOLOGICAL STUDY USING ROTATIONAL VISCO-METER

The main motive for the rheological characterization of the bitumen binders was to determine ZSV of VG20 and VG40 binders by conducting a step-wise shear rate sweep test at shear rates corresponding to the ZSV region. Brookfield DV-II+Pro RV, as shown in

Figure 3.4, was used to study the rheological behavior of VG20 and VG40 binders. The apparent viscosity of the binder was measured with the SC4-27 spindle. The diameter of the spindle is 11.76 mm and the effective length is 39.29 mm. All the samples are repeated thrice and the variation is less than 5%.

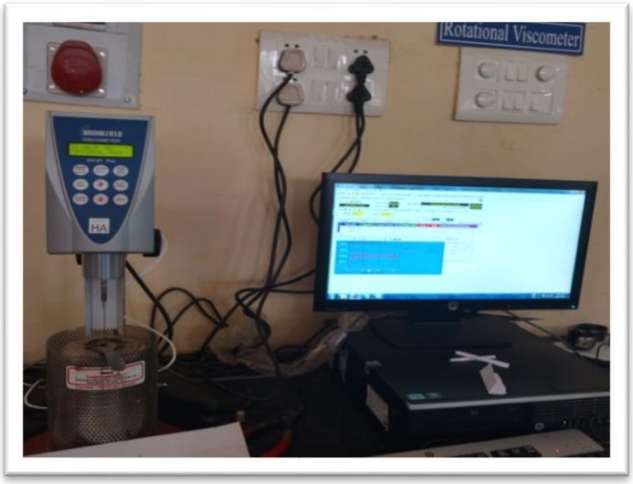

Fig. 3.4 Brookfield rotational viscometer

3.5.1 Sample Preparation

ASTM D 4402M (ASTM, 2015*b*) was followed to prepare the samples. About 10.5 ± 0.5 g of bitumen was poured into the hollow coaxial cylinder and allowed to cool for a period of 24 hours. The coaxial cylinder with the bitumen sample was placed in the thermosel which was preheated to the required test temperature. The spindle was allowed to remain at the test temperature for a period of 30 minutes such that the sample attains thermal equilibrium. Thereafter, the sample was considered to be ready for further testing.

Table 3.3 RV test temperatures

Binder	**Aging condition**	
	Unaged	**Short-term aged**
VG20	50, 55, 60, 65 °C	55, 60, 65 °C
VG40	65 °C	-

3.5.2 Test Temperatures

Both the unmodified VG20 and the VG40 bitumen binders are tested using the RV. The test temperatures are shown in Table 3.3.

3.5.3 Step-wise Steady Shear Rate Sweep Test Protocol - RV

A Step-wise Steady Shear Rate Sweep (SWSSRS) test protocol as shown in Figure 3.5 was adopted to test the bitumen binders. Here, 't_s' is the time required for the shear stress to reach a steady state. The protocol is discussed in detail in Chapter 4. Since a similar protocol is also adopted to test the bitumen binders using a DSR, the SWSSRS protocols applied using an RV and DSR are henceforth differentiated using a subscript as $SWSSRS_{RV}$ and $SWSSRS_{DSR}$.

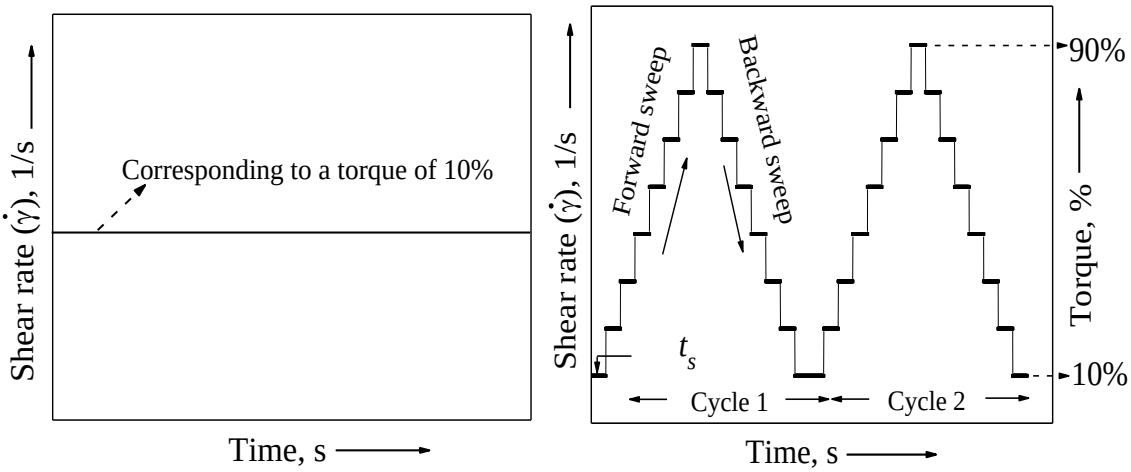

(a) Protocol to determine the 't_s' (b) $SWSSRS_{RV}$

Fig. 3.5 Test protocols using a rotational viscometer

3.5.4 Limitations of the RV to perform $SWSSRS_{RV}$ test

The limitations of the stepwise steady shear rate sweep tests using the RV are as follows:

i. The spindle could not be inserted at temperatures lower than 50 °C for unaged VG20 bitumen and 55 °C for short-term aged VG20 bitumen.

ii. Tests on long-term aged binder are not practical because of the higher viscosity of the binder.

iii. Tests on VG40 binder could be performed only on the unaged binder at 65 °C due to the higher viscosity of the binder at a temperature lower than 65 °C.

iv. Correlations of the proposed rutting parameter from the $SWSSRS_{RV}$ with the wheel tracking test data are not considered as the short-term aged VG20 could be tested at only three temperatures and moreover, tests could not be conducted on the short-term aged VG40 binder.

3.6 RHEOLOGICAL STUDIES USING DYNAMIC SHEAR RHEOMETER

To overcome the limitations encountered with the RV, the rheological characterization of the VG20 and the VG40 binders was continued with two Anton Paar DSRs which are shown in Figure 3.6. Figure 3.6 (a) shows the MCR 52 model and Figure 3.6 (b) shows the MCR 302 model. The difference between the two rheometers lies in their respective specifications and are listed in Table 3.4. All the samples are repeated thrice and the variation is less than 5%.

Table 3.4 Differences between the two dynamic shear rheometers

Specifications/Model	**MCR-52**	**MCR-302**
Bearing type	Mechanical	Air
Torque range	250 µNm to 200 mNm	0.05 µNm to 200 mNm
Torque resolution	100 mNm	0.5 mNm
Angular Frequency	Min. 10^{-3} rad/s	Min. 10^{-7} rad/s
Normal Force	-No-	0.01 to 50 N

(a) MCR-52 (b) MCR-302

Fig. 3.6 Dynamic shear rheometers

3.6.1 Specimen Preparation

The silicone mold method of sample preparation is one of the three methods described in ASTM D7175 (ASTM, 2015*c*) for testing bitumen binders using a DSR. In this study, all the

bitumen samples tested using the DSR are prepared using silicone molds. Sufficient quantity of hot bitumen binder was poured into the silicone molds. The testing was carried out only after 24 hours of specimen preparation. The specimens are kept in a refrigerator for a period of 10 minutes for a deformation free release from the molds before placing the specimens on the base plate of the rheometer as per EN 12594 (CEN, 2014). Bitumen samples in the silicone molds are shown in Figure 3.7.

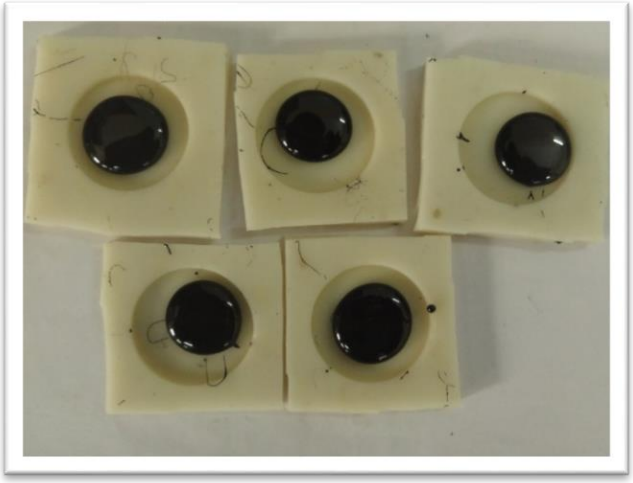

Fig. 3.7 Bitumen samples in silicone molds

3.6.2 Test Temperatures

The unaged, short-term aged and long-term aged VG20 and VG40 bitumen binders were tested using the DSR at the following temperatures: 40, 45, 50, 50, 55, 65 °C

3.6.3 Time for Thermal Equilibrium

As the samples are being kept in the refrigerator for a deformation free release, there will be a difference in the temperatures of the specimen and the base plate of the rheometer which is at the required test temperature. Therefore, it is of utmost importance to determine the time the specimen takes to reach the test temperature after being placed on the base plate of the rheometer. Determining the time for thermal equilibrium is one of the preliminary investigations on the bitumen binders before rheological properties can be determined. Appendix section X4 of ASTM D7175 (ASTM, 2015*c*) describes the procedure to determine the time it takes for a sample of bitumen to reach the thermal equilibrium. Here, the test sample was subjected to an oscillatory test at a fixed frequency of 10 rad/s using a small strain amplitude which gives a meaningful data resolution. The protocol was adopted such that the

DSR recorded the complex modulus (G^*) at every 30 seconds. As part of the research objectives, it was desired to determine the thermal equilibrium times for the unaged, short-term aged and long-term aged VG20 and VG40 binders at 40, 45, 50, 55, 60 and 65 °C. However, the testing was carried out on three temperatures as shown in Table 3.5. The thermal equilibrium times at the remaining test temperatures are determined from the linear curve fits of the data at the three test temperatures. Every test protocol was started after the bitumen samples attained the required time for thermal equilibrium at each test temperature and aging condition.

Table 3.5 Test temperatures (°C) at which thermal equilibrium times are determined

Bitumen	**Aging condition**		
	Unaged	**Short-term aged**	**Long-term aged**
VG20	40, 50, 65	40, 50, 65	40, 50, 65
VG40	40, 50, 65	40, 50, 65	50, 55, 65

3.6.4 Amplitude Sweep Tests

Amplitude sweep tests were conducted in the oscillatory mode to determine the SHRP rutting parameter – $|G^*|/\sin\delta$ and Shenoy's rutting parameter – $|G^*|/(1-(1/\tan\delta\sin\delta))$. The test protocol consisted of subjecting the bitumen binders to an increase in strain amplitudes from a lower to the higher magnitude at a constant frequency of 10 rad/s. ASTM D7175 (ASTM, 2015*c*) provides the range of strain amplitude and the target strain at which the rutting parameters are to be determined. According to ASTM D7175 (ASTM, 2015*c*), for oscillatory tests, the unaged and the short-term aged bitumen samples are to tested using a 25 mm parallel plate geometry with a gap of 1 mm whereas, the long-term aged bitumen samples are to be tested using an 8 mm parallel plate geometry with a gap of 2 mm. In the current research work, as test temperatures for the long-term aged bitumen binders are above or equal to 40 °C, the long-term aged bitumen samples could be tested using a 25 mm parallel plate geometry with a gap of 1 mm.

3.6.5 Multi Stress Creep and Recovery (MSCR) Test

The multi stress creep and recovery test is "*used to determine the presence of elastic response in an asphalt binder under shear creep and recovery at two stress levels at a specified temperature"* (ASTM, 2015*a*). The percentage recovery is intended to determine the presence of elastic response and stress dependence of polymer modified and unmodified asphalt binders (ASTM, 2015*a*). The MSCR test uses a 25 mm parallel plate geometry with 1 mm

gap setting for unaged, short-term aged as well as long-term aged bitumen binders. The binder is tested by applying constant stress of 0.1 kPa for a period of 1 s and a rest of 9 s. This procedure of creep and recovery is continued for an additional nine such cycles. Subsequently, 10 cycles of a similar creep and recovery but with a stress of 3.2 kPa are applied. In the creep phase, the stress and strain are recorded at every 0.1 s whereas in the recovery phase the stress and strain are recorded at every 0.45 s. The J_{nr} at 0.1 kPa, 3.2 kPa, and average J_{nr} is calculated following the steps provided in ASTM D7405 (ASTM, 2015*a*).

3.6.6 Linear Shear Rate Sweep (LSRS) Test

A LSRS test, as shown in Figure 3.8, was conducted on unaged, short-term aged and long-term aged bitumen binders. The test was conducted using MCR-302, shown in Figure 3.6 (b), with a 25 mm parallel plate geometry at a gap setting of 1 mm. The bitumen samples are subjected to a linear increase in shear rate and the response of the binder was measured at every second. The shear rate was increased from 0.001 to 6.001 1/s with an increment of 0.005 1/s after every second till the test sample achieves a torque of 190 mNm or up to 1200 seconds, whichever is earlier.

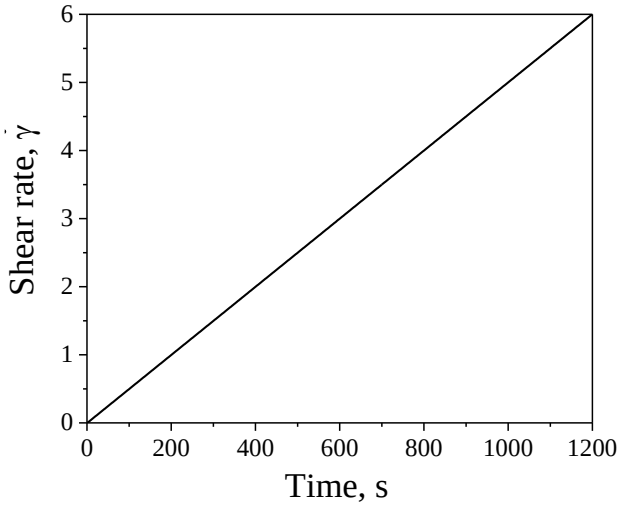

Fig. 3.8 LSRS test protocol

3.6.7 Step-wise Steady Shear Rate Sweep Test - DSR

Since there are limitations with RV (listed in Section 3.5.4), it is necessary to characterize the non-Newtonian response of the bitumen binders using a DSR. A procedure similar to $SWSSRS_{RV}$ is used. However, the protocols are modified as per the specific requirements of the DSR. The tests are conducted on the bitumen samples using a 25 mm parallel plate

geometry and at a gap of 1 mm. The $SWSSRS_{DSR}$ test protocol is shown in Figure 3.9 and is discussed in detail in Chapter 4.

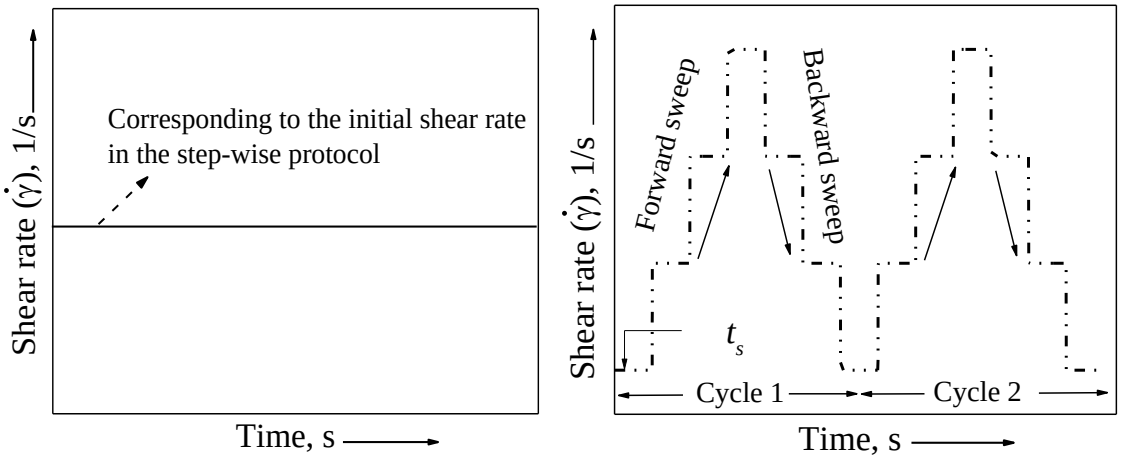

(a) Protocol to determine 't_s' (b) $SWSSRS_{DSR}$

Fig. 3.9 $SWSSRS_{DSR}$ test protocol using a dynamic shear rheometer

3.7 BITUMINOUS MIXTURE CHARACTERIZATION

BC and DBM are commonly used wearing and binder courses respectively for the flexible pavements in India. Therefore, these bituminous mixtures became the logical choice. India being a large country, there exists a lot of variation in temperatures across different geographic regions. Because of this reason, a relatively softer VG20 bitumen and a relatively stiffer VG40 bitumen are selected. In this research, both the mixtures i.e., BC and DBM correspond to grading type 2 as specified in the "Specifications for Road and Bridge Works" by MoRTH (MoRTH, 2013). Mid gradation was adopted to prepare the BC2 and DBM2 bituminous mixtures. The following sections provide a detailed description of the steps involved in evaluating the rutting performance of the BC-2 and DBM-2 mixtures.

3.7.1 Mixing and Compaction Temperatures

According to ASTM D6926-16 (ASTM, 2016*a*), the bitumen binders should have a viscosity of 0.17 ± 0.02 Pa-s at the time of mixing it with the mineral aggregate and a viscosity of 0.28 ± 0.03 Pa-s during compaction of the bituminous mixture. In order to determine the mixing and compaction temperatures, the bitumen binders were sheared in the RV at temperatures ranging from 120 to 170 °C in the increments of 10 °C and the subsequent

apparent viscosities at the above temperatures were determined. These tests are carried out in accordance with ASTM D4402 (ASTM, 2015*b*).

3.7.2 Optimum Bitumen Content (OBC)

The optimum bitumen content for the desired mixtures is determined as per the Marshall method of mix design specified in Manual Series-2 (Asphalt Institute, 2014). Specimens with varying bitumen contents are compacted using the Marshall hammer by applying 75 blows on each face of the specimen. The maximum specific gravity of the mixture (G_{mm}) and the bulk specific gravity of the mixture (G_{mb}) are determined as per ASTM D6857/D6857M-18 (ASTM, 2018*b*) and ASTM D6752/D6752M-18 (ASTM, 2018*c*) respectively using the CoreLok®. The bitumen content corresponding to 4% air voids was determined as the optimum bitumen content.

3.7.3 Preparation of Loose Bituminous Mixtures

The bituminous mixture is a combination of mineral aggregate mixed with the optimum amount of bitumen. The bitumen and the aggregates are heated separately to the required mixing temperatures and subsequently mixed together thoroughly to obtain a homogenous mixture.

Fig. 3.10 Short-term aging of bituminous mixtures

3.7.4 Short-term Aging of Bituminous Mixtures

The loose bituminous mixtures prepared in the laboratory do not stiffen the bitumen binder to such an extent that happens in the mixing plant and during the field compaction. In order to

simulate the field heating, mixing and compaction process in the laboratory, the prepared loose bituminous mixtures are short-term aged. AASHTO R30 (AASHTO, 2015) describes the procedure to simulate short-term aging of the loose bituminous mixtures in the laboratory, wherein, the loose bituminous mixtures are subjected to a temperature of 135 °C for a

Fig. 3.11 Segmented steel-wheeled roller compactor

period of 4 hours in Forced Draft Oven (FDO). The bituminous mixtures prepared at the corresponding mixing temperatures are uniformly transferred into smaller trays as shown in Figure 3.10 and subjected to short-term aging as specified in AASHTO R30. The bituminous mixture was kept in the FDO for a period of 4 hours and after every 1 hour, the bituminous mixture was thoroughly stirred to maintain uniform distribution of heat.

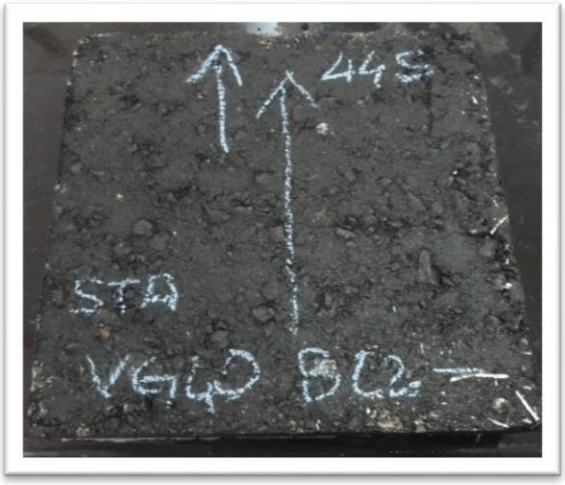

(a) BC-2 with VG40 binder

(b)) DBM-2 with VG20 binder

Fig. 3.12 Compacted bituminous mixtures

3.7.5 Short-term Aged Bituminous Mixture Slabs

The prepared loose bituminous mixture mixed at the corresponding mixing temperature was kept in a FDO maintained at a temperature of 135 °C to simulate the short term aging for a period of 4 hours as described in the previous section. After 3 and ½ hours, the temperature of the mixture was increased to the corresponding compaction temperature and the mixture was taken out of the FDO after 4 h and compacted using a segmented steel-wheeled roller compactor. The segmented steel-wheeled roller compactor is shown in Figure 3.11. The bituminous mixture slabs fabricated using the steel-wheeled roller compactor are allowed to cool to the ambient temperature and removed from the mold after a duration of 24 hours and subsequently used for testing. The compacted short-term aged bituminous slabs are shown in Figure 3.12.

3.7.6 Determination of Air Voids in the Cored Specimens

The wheel tracking tests are proposed to be conducted on the short-term aged as well as the long-term aged bituminous mixture specimens. The wearing course of a newly laid flexible pavement can have a maximum air void of 8% corresponding to 92% of G_{mm} (IRC-111, 2009) whereas, the air void content in a bituminous layer is closer to 4% after a period of

Fig. 3.13 Sample core cutting machine

5-7 years. Therefore, the short-term aged bituminous mixture specimens are prepared with an air void content of 6% and the long-term aged bituminous mixture specimens are prepared with an air void content of 4%. In order to prepare the short-term and long-term aged bituminous mixture specimens to the target air voids, cores are taken from the compacted short-term aged bituminous mixtures prepared with different air voids using a sample core cutting machine as shown in Figure 3.13 and the air voids in the cored specimens are

determined using the CoreLok®. The air void content was changed by compacting the mixtures at varying number of passes using the segmented steel-wheeled roller compactor. Cores are extracted from the compacted short-term aged slabs at different air voids and are shown in Figure 3.14. After several trials, the number of passes of the roller compactor corresponding to 6% and 4% air voids is fixed for the short-term aged and long-term aged BC2 and DBM2 mixtures prepared with VG20 and VG40 binders separately.

(a) Cored slab (b) cores corresponding to different air voids

Fig. 3.14 Coring the compacted short-term aged slabs

3.7.7 Long-term Aged Bituminous Mixture Slabs

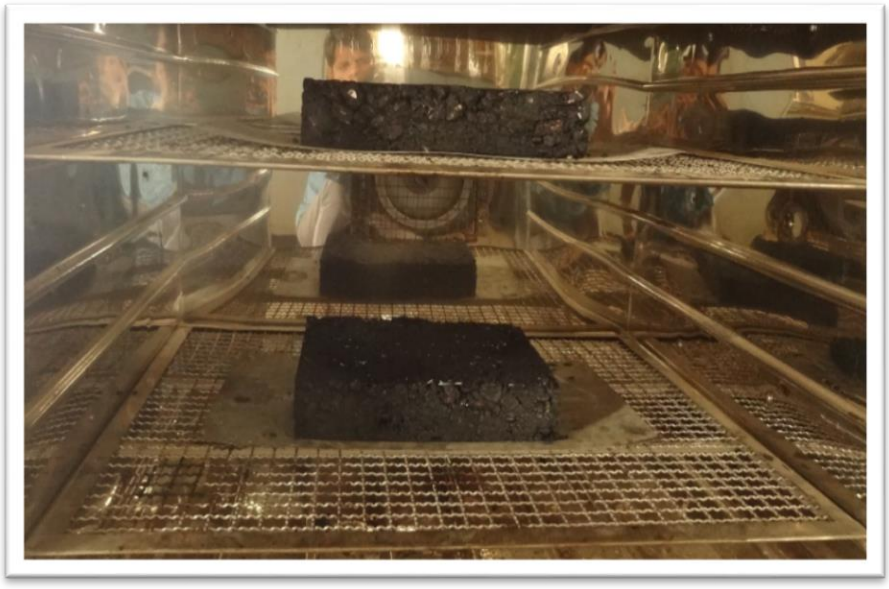

Fig. 3.15 Long-term aging of bituminous mixture slabs

The long-term aged bituminous mixture slabs are prepared in accordance with AASHTO R30 (AASHTO, 2015). The compacted short-term aged bituminous mixtures with 4% air voids are

placed in a hot air oven at a temperature of 85 ± 3 °C for a period of 120 hours to produce long-term aged bituminous mixture specimens in the laboratory as shown in Figure 3.15.

3.8 DRY WHEEL TRACKING TESTS

The permanent deformation characteristics of the short-term aged and the long-term aged BC-2 and DBM-2 bituminous mixture specimens prepared with VG20 and VG40 bitumen binders was evaluated by conducting dry wheel tracking tests using a small wheel tracking device. The wheel tracking device used in this study is shown in Figure 3.16. The test temperatures for the bituminous mixture slabs includes 40, 45, 50, 55, 60 and 65 °C.

Fig. 3.16 Small wheel tracking device

The compacted slabs are removed from the mold of the roller compactor after 24 hours and are placed in the wheel tracking machine. The slabs are conditioned at the required test temperature for a period of 6 hours before commencement of the wheel tracking test. The slabs are tested using a hard rubber wheel with an outside diameter of 200 mm at a rate of 25 cycles per minute with a load of 700 N ± 10 N. The wheel traverse on the slab was 230 +/- 5 mm. The slabs are tested in the wheel tracking machine until a rut depth of 15 mm or 200,000 passes whichever was earlier.

3.9 SUMMARY

The detailed methodology adopted to carry out various experimental works is described in detail in this chapter. The laboratory aging protocols to simulate short-term and long-term aging of bitumen is discussed. Each of the test protocol employed in this research to carry out rheological studies on the unaged, short-term aged and long-term aged bitumen are discussed in detail. Moreover, the detailed procedure involved in fabricating short-term aged and long-term aged bituminous mixture slabs to carry out wheel tracking tests is also discussed.

CHAPTER-4

RHEOLOGICAL STUDIES ON UNMODIFIED BITUMEN

4.1 INTRODUCTION

Bitumen shows non-Newtonian response at pavement temperatures of the order ranging from 50 to 65 °C typically observed in India. Researchers have been focusing on identifying bitumen properties that can be used to predict the rutting resistance of bituminous mixtures. In the past, as discussed in Section 2.2, bitumen properties have been used to estimate the performance of bituminous layers. Bitumen is highly temperature susceptible material where the response characteristics vary drastically from a solid-like behavior to a fluid-like behaviour with rise in temperature. ASTM D6373 (2016*b*) specifies measuring the viscosity of the binders at 135 °C using number 21 spindle at 20 RPM for soft binders and number 27 spindle at 20 RPM for stiffer binders. Specification of the spindle number and shear rates even at 135 °C indicates the possible non-Newtonian characteristics. However, IS:73 (BIS, 2013) specifies measuring the absolute viscosity of the bitumen using vacuum capillary viscometer at 60 °C, that is, the expected maximum pavement temperature. Bituminous binders exhibit non-Newtonian response where the viscosity depends also on the applied shear rate (Chowdary et al., 2007). The response of bitumen is time dependent as well as shear rate dependent but not at the same instant. The non-Newtonian response of bituminous binders can be quantified using a RV and a DSR. In this study, a new step-wise protocol is proposed to analyze this non-Newtonian response and to measure the viscosity of the bitumen binders in the ZSV regime. Moreover, tests like AST, MSCR test and LSRS are also conducted on the unaged, short-term aged and long-term aged bitumen binders. The subsequent sections detail the adopted test protocols and the analysis carried out. Moreover, the inter relationships between the different bitumen properties are also discussed in this chapter.

4.2 RHEOLOGICAL STUDY USING ROTATIONAL VISCOMETER

Table 4.1 Shear rates employed in the $SWSSRS_{RV}$ test

Binder	Temp., °C	Shear rates in the $SWSSRS_{RV}$
Unaged VG20	50	0.017, 0.051, 0.085, 0.119, 0.153, 0.187
	55	0.051, 0.089, 0.119, 0.153, 0.187, 0.221, 0.255, 0.289, 0.323, 0.357, 0.391
	60	0.085, 0.255, 0.425, 0.595, 0.765, 0.935
	65	0.17, 0.34, 0.51, 0.68, 0.85, 1.02, 1.19, 1.36, 1.53, 1.7, 1.87, 2.04
Short-term aged VG20	55	0.017, 0.051, 0.085, 0.119, 0.153
	60	0.017, 0.051, 0.085, 0.119, 0.153, 0.187, 0.221, 0.255, 0.289, 0.323, 0.357
	65	0.085, 0.170, 0.255, 0.340, 0.425, 0.510, 0.595, 0.680
Unaged VG40	65	0.085, 0.17, 0.255, 0.34, 0.425, 0.51

Brookfield DV-II+Pro Rotational Viscometer (RV), as shown in Figure 3.4, is used to study the non-Newtonian response of unmodified VG20 and VG40 binders. The samples are sheared with SC4-27 number spindle. The tests are carried out on the bitumen binders at temperatures and aging condition as shown in Table 3.3. All the bitumen test samples are prepared as discussed in Section 3.5.1 in accordance to ASTM D4402 (ASTM, 2015*b*). The non-Newtonian response of the bitumen binders is studied by subjecting the bitumen binders to an $SWSSRS_{RV}$ test protocol as shown in Figure 3.5. The working conditions of the RV are specific in terms of the torque produced upon rotation, wherein one has to use shear rates such that the corresponding torque is between 10 and 90%. In the current research work, all the RV tests are carried out within the specified torque limits. The shear rates corresponding to 10 and 90% torque at all the test conditions and the intermediate shear rates in the step-wise shear rate sweep are shown in Table 4.1. From Table 4.1, it can be seen that the shear rates employed in the $SWSSRS_{RV}$ correspond to the ZSV regime. This is the regime in which one can measure the viscosity of the bitumen in a consistent manner.

4.2.1 Determination of shear time corresponding to steady-state viscosity

In each step of the $SWSSRS_{RV}$ test, the bitumen binder is sheared until a steady state is observed. Before commencing the $SWSSRS_{RV}$ test, steady shear tests at a shear rate

corresponding to 10% torque are conducted as per the protocol shown in Figure 3.5(a) and the results for the VG20 bitumen are shown in Figure 4.1. From Figure 4.1, it is observed that there is an increase in viscosity with time when bitumen binder is sheared at a constant shear rate in a RV. This increase in viscosity at the beginning of shearing at a constant shear rate is known as a stress overshoot and is considered as a non-Newtonian response (Nivitha and Krishnan, 2018). This is because of the disruption in the structure and the subsequent rearrangement of the structure during the initiation of shear flow (Viola and Baird, 1986). Thereafter, the viscosity stabilizes and reaches a constant value after a specific duration

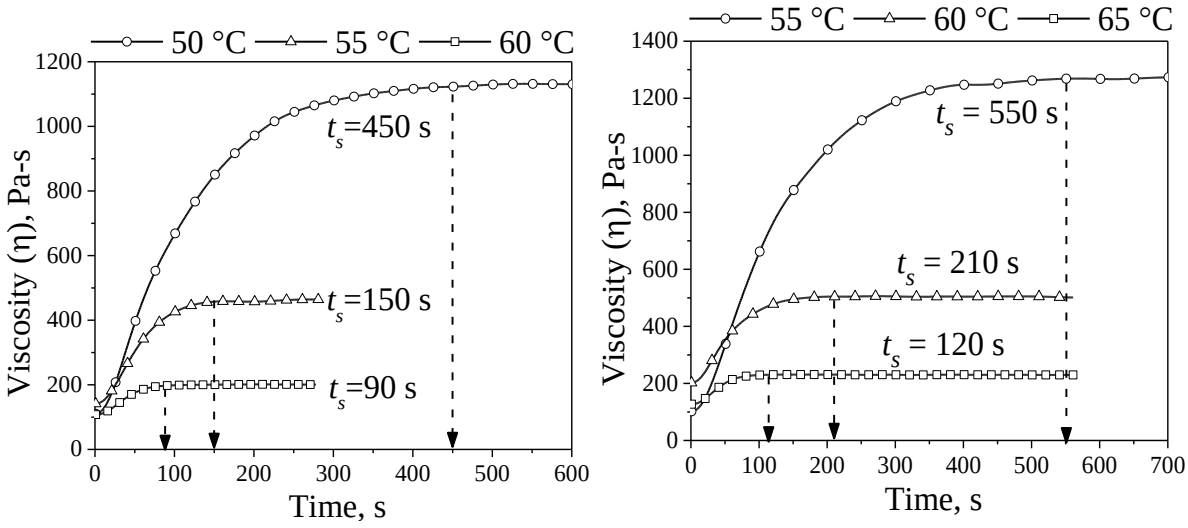

(a) Unaged (b) Short-term aged

Fig. 4.1 Viscosity as a function of time in the steady shear test at a shear rate corresponding to 10% torque for the VG20 bitumen using RV

of shearing i.e., there is an appearance of a steady-state in the response of viscosity with time when sheared at a constant shear rate. Further shearing beyond the start of this steady state showed no change in the viscosity of the samples at all the test temperatures. The appearance of a steady state viscosity means a corresponding steady response of shear stress. This time duration wherein the viscosity or the shear stress stabilizes and reaches a steady-state is denoted as 't_s' (Nivitha and Krishnan, 2018). Since, a similar study is undertaken with a DSR, the 't_s' determined with a RV and DSR are hence forth denoted as '$t_{s(RV)}$' and '$t_{s(DSR)}$', respectively . For unaged VG20 binder at 65 °C, '$t_{s(RV)}$' determined for unaged VG20 bitumen at 60 °C is used. The '$t_{s(RV)}$' for the unaged VG40 bitumen at 65 °C is shown in Appendix A (Figure A1). As the stiffness of the bitumen is different at different temperatures and the aging condition of the binder, this time interval to achieve a steady state would also be different at different temperatures. With an increase in temperature there is an increase in the mobility of the molecules and a decrease in the intermolecular attraction, thereby causing a

decrease in '$t_{s(RV)}$' (Souraki et al., 2012). However, with aging there is a loss of oily fractions resulting in a less soluble hydrocarbons leading to an increase in the viscosity and elastic stiffness (Hossain et al., 2018). Therefore, the '$t_{s(RV)}$' will be different at each temperature and aging condition as can be seen in Figure 4.1 and Table 4.2. From Table 4.2 it is observed that the '$t_{s(RV)}$' increase with a decrease in temperature. However, at a particular temperature, the '$t_{s(RV)}$' increase with bitumen aging. It is observed that there is an increase in '$t_{s(RV)}$' by 5 times when the temperature decreased from 65 to 50 °C for the unaged VG20 binder. For the short-term aged VG20 binder, there is an increase in '$t_{s(RV)}$' by 3.67, 2.33 and 1.33 times at 55, 60 and 65 °C.

Table 4.2 '$t_{s(RV)}$' determined using RV

Temp., °C	VG20		VG40
	Unaged	Short-term aged	Unaged
	s	s	s
50	450	-	-
55	150	550	-
60	90	210	-
65	90	120	280

As discussed previously, since, the viscosity at and beyond '$t_{s(RV)}$' remains constant with time, this viscosity can be considered as a Newtonian viscosity. Now, the continuous shearing of the binder gradually changed the response of the binder from a non-Newtonian response to a Newtonian response beyond the '$t_{s(RV)}$'. This Newtonian viscosity can be used as an alternative to ZSV.

4.2.2 Check for shear rate, time and shear history dependency

As this Newtonian viscosity is determined at a particular shear rate, it is important to observe the response of bitumen to a change in shear rate. Therefore, an $SWSSRS_{RV}$ test protocol with two cycles of forward and backward sweeps as shown in Figure 3.5 (b) is adopted. The first forward sweep would establish whether the binders exhibit a shear rate dependent behavior or a shear rate independent behavior. In the first backward sweep, the viscosity is measured at shear rates similar to that of the first forward sweep but at a different duration of time resulting in different shear history. Thus, the first backward sweep would establish whether the bitumen response is time dependent or time independent. The application of the second cycle of forward and a backward sweep would establish whether a previous shear history has an effect on the response of bitumen binders. As discussed earlier, at each shear rate in the

SWSSRS$_{RV}$ test, the samples are sheared at the respective '$t_{s(RV)}$' determined earlier at a particular temperature and aging condition. The same '$t_{s(RV)}$' is used at all the shear rate increments in the SWSSRS$_{RV}$ test because the '$t_{s(RV)}$' determined at a shear rate corresponding to 10% torque would hold good for shear rates corresponding to torques higher than 10%. The results of the SWSSRS$_{RV}$ test conducted on the unaged VG20 binder at 60 °C are shown in this section whereas the results of all the other test conditions are shown in Appendix A. Figures 4.2 and A2 (in Appendix A) show the observed response of the SWSSRS$_{RV}$ test wherein the variation of viscosity and shear rate as function of time is plotted. Table 4.3 shows the viscosities and the steady shear stresses at the end of each interval i.e., at '$t_{s(RV)}$' in the SWSSRS$_{RV}$ test whereas the viscosity and shear stresses at '$t_{s(RV)}$' in the SWSSRS$_{RV}$ test for all the remaining test conditions are shown in Appendix A (Table A1 and A2). From Figure 4.2 and Table 4.3 it is observed that the viscosity remains more or less similar with respected to time and shear rate.

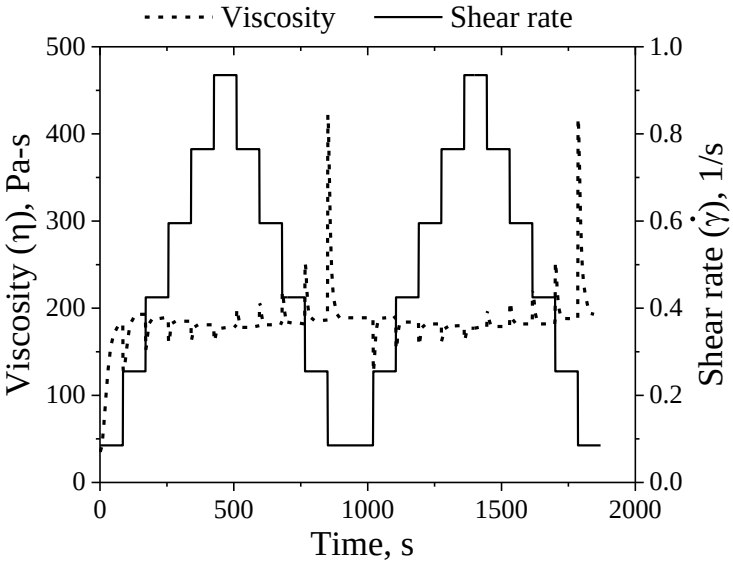

Fig. 4.2 Viscosity and shear rate as a function of time for unaged VG20 bitumen at 60 °C

As discussed earlier, at each interval in the SWSSRS$_{RV}$ test, the bitumen sample is sheared at a predetermined '$t_{s(RV)}$' corresponding to the respective test condition. Therefore, each interval in the first forward sweep of the SWSSRS$_{RV}$ test should achieve a steady state wherein a stabilized shear stress and the corresponding Newtonian viscosity should be observed. Figure 4.3 shows the shear rate input and the subsequent viscosity response of the bitumen in the first forward sweep of the SWSSRS$_{RV}$. From Figure 4.3(b), it is observed that there is an appearance of a steady state of viscosity at the end of each shearing interval. It is also observed that with an increase in shear rate, the time to achieve a steady state of viscosity decreases. As discussed earlier, these steady state viscosities can be called as

Table 4.3 Viscosity and shear stress at '$t_{s(RV)}$' in the SWSSRS$_{RV}$ test for the unaged VG20 binder at 60 °C

Shear rate, 1/s	**Cycle 1**				**Cycle 2**				**Avg. Shear stress (Pa)**	**Avg. Viscosity (Pa-s)**
	Forward Sweep		**Backward Sweep**		**Forward Sweep**		**Backward Sweep**			
	Shear stress (Pa)	Viscosity (Pa-s)	Shear stress (Pa)	Viscosity (Pa-s)	Shear stress (Pa)	Viscosity (Pa-s)	Shear stress (Pa)	Viscosity (Pa-s)		
0.085	15.43	182	16.10	189	16.10	189	16.15	190	15.94	188
0.255	48.00	193	47.00	186	47.00	191	46.00	188	47.00	184
0.425	80.13	189	77.56	182	78.02	184	77.48	182	78.30	184
0.595	109.80	185	107.96	181	108.61	183	108.56	182	108.73	183
0.765	138.18	181	136.56	179	137.40	180	137.32	179	137.36	180
0.935	165.97	178	165.97	178	165.98	178	165.98	178	165.97	178

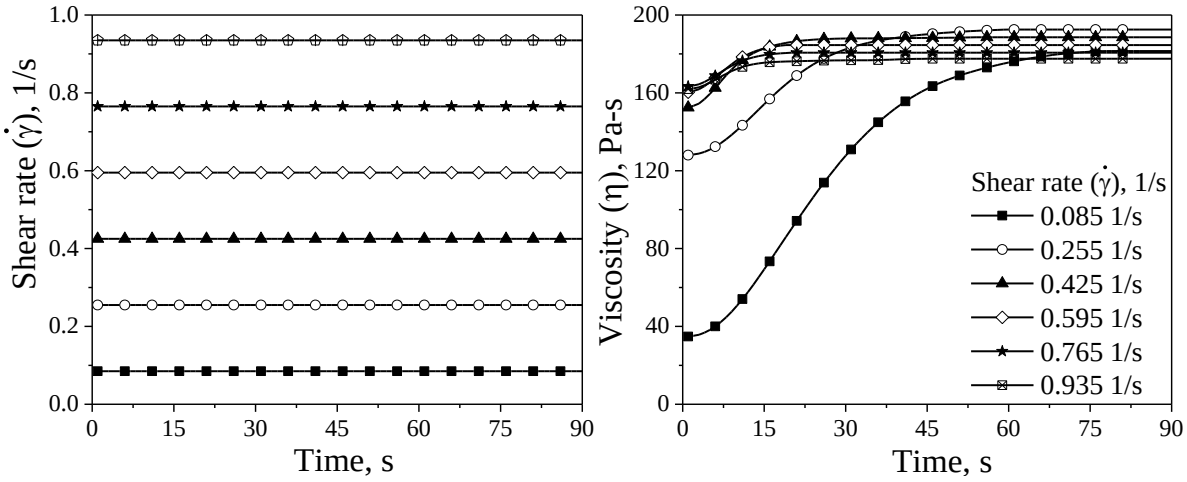

(a) Shear rate as a function of time (b) Viscosity as a function of time

Fig. 4.3 Observed response in the first forward sweep of SWSSRS$_{RV}$ test for the unaged VG20 binder at 60 °C

Newtonian viscosities and these Newtonian viscosities appear to be very close. Such response is seen at all the remaining test conditions and are shown in Appendix A (Figure A3). In order to assess the shear rate dependent behavior of the bitumen, the viscosity at '$t_{s(RV)}$' in the first forward sweep plotted as a function of shear rate at all the test conditions are shown in Figure 4.4. From figure, it is observed that the viscosity at '$t_{s(RV)}$' in the first forward sweep of the $SWSSRS_{RV}$ test remains in the ZSV regime.

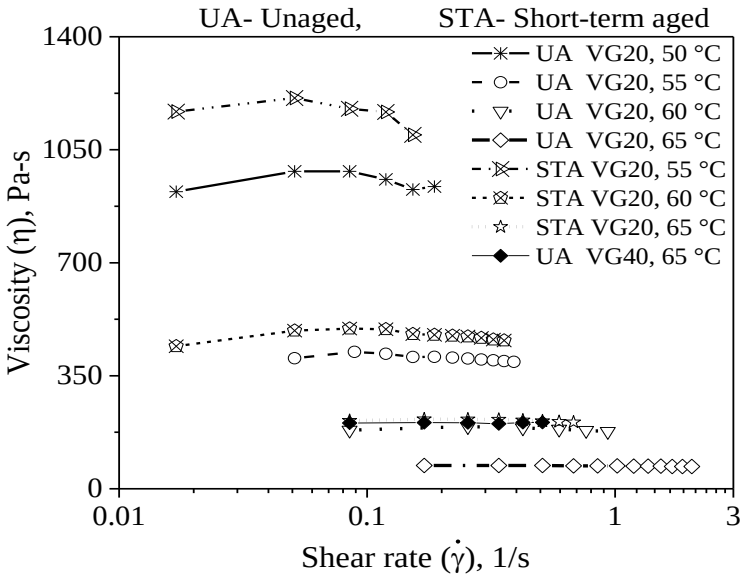

Fig. 4.4 Viscosity at '$t_{s(RV)}$' as a function of shear rate in the first forward sweep of $SWSSRS_{RV}$

In order to check the time dependency and also the effect of shear history, the response of the samples are checked for thixotropy. Figure 4.5 shows a typical thixotropic response

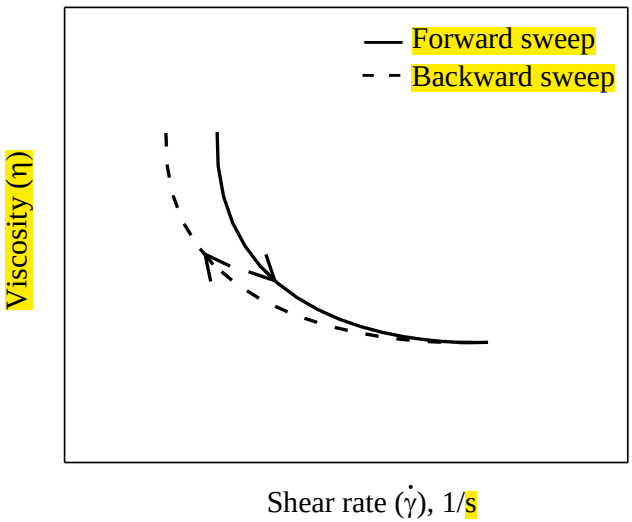

Fig. 4.5 Typical thixotropic response

(Brookfield Ametek, 2017). From Figure 4.5 it is observed that there is a decrease in viscosity of a fluid with an increase in shear rate in the forward sweep. Moreover, it is also observed that the viscosity measured at the same shear rate in the backward sweep is lower than the one measured in the forward sweep. This variation in the response of viscosity is known as a 'hysteresis loop' (Brookfield Ametek, 2017). The time dependent behaviour is analysed by calculating the thixotropic index between the forward sweep and the backward sweep of the first cycle in the $SWSSRS_{RV}$ whereas the effect of shear history is analysed by calculating the thixotropic index between the first forward sweep and the second backward sweep in the $SWSSRS_{RV}$ test. The magnitude of thixotropic behavior is quantified by determining the thixotropic index ($\tau_{hyst\%}$). The thixotropic index ($\tau_{hyst\%}$) is calculated by quantifying the relative thixotropic areas (Ghica et al., 2016) using Equation (4.1).

$$\tau_{hyst\%} = \left[\frac{S_{fwd} - S_{bwd}}{S_{fwd}} \right] x100 \tag{4.1}$$

where,

$\tau_{hyst\%}$ = Thixotropic Index,

S_{fwd} = area under the forward sweep, and

S_{bwd} = area under the backward sweep.

The thixotropic index measured to quantify the time dependent response is denoted as "$TI\text{-}1_{RV}$" whereas the thixotropic index measured to quantify the effect of shear history is denoted as "$TI\text{-}2_{RV}$. The thixotropic indices, $TI\text{-}1_{RV}$ and $TI\text{-}2_{RV}$, are shown in Table 4.4. From Table 4.4 it is observed that both the thixotropic indices are less than 5%. A thixotropic index ($\tau_{hyst\%}$) value less than 5% indicates a non-thixotropic behavior (Ghica et al., 2016). Therefore, it can be said that the response of the VG20 binder is non-thixotropic. Similarly, the $TI\text{-}1_{RV}$ and $TI\text{-}2_{RV}$ values for VG40 binder are 0.31 and 2.17%, respectively, indicating a non-thixotropic behaviour. Since the response of the VG20 and VG40 bitumen is non-thixotropic in the $SWSSRS_{RV}$ test, the response of the bitumen can be fairly assumed to be non-thixotropic. Since, all the $TI\text{-}2_{RV}$ values are less than 5%, the effect of a previous shear history is considered as negligible. As the response of the bitumen is shown to be Newtonian, the viscosity obtained at each shear rate interval can be safely considered as a Newtonian viscosity.

Table 4.4 Thixotropic index (%) for the unaged and short-term aged VG20 binder

Temp., °C	Unaged		Short-term aged	
	TI-1$_{RV}$	TI-2 $_{RV}$	TI-1 $_{RV}$	TI-2 $_{RV}$
50	2.475	0.388	-	-
55	0.683	0.632	2.988	4.556
60	1.453	1.005	0.565	0.239
65	0.322	0.709	0.361	3.197

Table 4.5 Proposed Newtonian viscosity, $\eta_{0(S\text{-}RV)}$

Temp., °C	$\eta_{0(S\text{-}RV)}$, Pa-s		
	VG20		VG40
	Unaged	Short-term aged	Unaged
50	951	-	-
55	405	1164	-
60	184	474	-
65	71	211	205

Therefore, the Newtonian viscosities in each interval of the first forward sweep are averaged and reported as single viscosity for a particular temperature and aging condition. As shown earlier, in Table 4.1, as the shear rates employed in the SWSSRS$_{RV}$ correspond to the ZSV regime, the new viscosity can be considered as an alternate ZSV. This new ZSV is denoted as $\eta_{0(S\text{-}RV)}$. Here, 'S-RV' in the subscript represents the SWSSRS$_{RV}$ test. $\eta_{0(S\text{-}RV)}$ is a Newtonian viscosity and is proposed as a rutting parameter. $\eta_{0(S\text{-}RV)}$ of the unaged and short-term aged VG20 bitumen at all the possible test temperatures and the unaged VG40 bitumen at 65 °C are shown in Table 4.5. Interestingly, it is observed that the $\eta_{0(S\text{-}RV)}$ of the short-term aged VG20 bitumen exhibited similar viscosity as that of the VG40 at 65 °C. This shows that there is a possible correspondence between the aging and temperature similar in lines as that of the time-temperature.

4.2.3 Binder Grading with $\eta_{0(S\text{-}RV)}$

In India, unmodified bitumen binders are graded as per their absolute viscosity determined at 60 °C (BIS, 2013). The absolute viscosity is to be determined using Cannon-Manning (CM) capillary U-tubes by following the protocol listed in IS: 1206 (BIS, 1978). As the original Cannon-Manning U-tubes are expensive, U-tubes which are locally manufactured and calibrated are prevalent in India because of their cost effective nature. However, it is observed that there are problems with the use of these locally calibrated U-tubes when three sources of bitumen (B-1, B-2 and B-3) corresponding to VG20 grade are tested using original Cannon-Manning U-tube and two locally manufactured and calibrated U-tubes (Tube-A and Tube-B).

The absolute viscosity results from the original and local U-tubes are shown in Table 4.6. The permissible range of absolute viscosity for VG20 binders as per IS:73 (BIS, 2013) is 1600 to 2400 Poise. Here, VG represents the viscosity grade and the index "20" represents the absolute viscosity of 2000 Poise. A tolerance of ±20% is considered in IS:73 (BIS, 2013) resulting in the corresponding absolute viscosity tolerance of ±400 Poise for VG20 bitumen and the subsequent range is 1600 to 2400 Poise. From Table 4.6, it is clear that the absolute viscosity measured using the original Cannon-Manning U-tube satisfied the VG20 grading specification. It can be seen from Table 4.6 that the absolute viscosity is highest for B-3 followed by B-2 and B-1. However, the trends observed for these three VG20 bitumen samples (B-1, B-2, and B-3) are completely different when measured using the locally manufactured U-tubes as shown in Table 4.6. If the absolute viscosities obtained using a particular tube as shown in Table 4.6 are carefully observed, it can be seen that the absolute viscosities for a particular tube are very close. This clearly shows that the locally manufactured tubes could not differentiate between the absolute viscosities obtained from the three different sources of the same grade. Further, there is no specific trends observed in absolute viscosities measured using the locally manufactured tubes as observed clearly for the original Cannon-Manning tube. It is also to be noted from Table 4.6 that there is a considerable difference in the absolute viscosities measured by both the locally manufactured U-tubes. According to IS:73 (BIS, 2013), the absolute viscosity of VG10 bitumen should be in the range of 800 to 1200 Poise, whereas the absolute viscosity of VG20 bitumen should be in the range of 1600 to 2400 Poise. Tube-B clearly satisfied the VG20 specifications whereas the Tube-A neither satisfied the specifications of VG10 bitumen nor the specifications of the VG20 bitumen. This clearly shows that it is very much essential to use original Cannon-Manning U-tubes to get the precise measurements of the absolute viscosity values. An alternative to Cannon-Manning U-tubes can be the use of RV to grade bitumen binders.

Table 4.6 Absolute viscosity of the three sources of binders

	Absolute viscosity at 60 °C, Poise		
Binder	**Original CM tube**	**Tube A**	**Tube B**
B-1	1606	1255	1785
B-2	1873	1249	1708
B-3	2026	1321	1758

In the previous section a Newtonian viscosity, $\eta_{0(\text{S-RV})}$, is proposed. Thus, this $\eta_{0(\text{S-RV})}$ is used to grade the three sources of VG20 bitumen binders so that its efficacy as a Newtonian viscosity can be verified. $\eta_{0(\text{S-RV})}$ is determined by subjecting the three sources of the VG20

bitumen to a single forward sweep of the $SWSSRS_{RV}$ test protocol at a temperature of 60 °C and the results are shown in Table 4.7. From Table 4.7 it is observed that $\eta_{0(S\text{-}RV)}$ is able to clearly differentiate between the three sources of VG20 binders. Moreover, from Table 4.7 it is observed that B-3 has the highest $\eta_{0(S\text{-}RV)}$ followed B-2 and B-1 which matches with the trend observed using the original Cannon-Manning U-tubes. This result indicates that there is a clear correspondence between the absolute viscosity obtained using original Cannon-Manning U-tube and $\eta_{0(S\text{-}RV)}$.

Table 4.7 $\eta_{0(S\text{-}RV)}$ of the three VG20 bitumen sources

Source	**$\eta_{0(S\text{-}RV)}$, Poise**
B-1	1848
B-2	2125
B-3	2473

In order to further check the correlation between the absolute viscosities obtained using the original and local U-tubes with $\eta_{0(S\text{-}RV)}$ a plot is generated as shown in Figure 4.6. Moreover, Mean Absolute Percentage Error (MAPE) between the absolute viscosities and $\eta_{0(S\text{-}RV)}$ is consolidated in Table 4.8. Ideally, if the data points shown in Figure 4.6 falls on the 45° line with same x-axis and y-axis scales, then a perfect correlation exists. From Figure 4.6, it is observed that absolute viscosity determined using the Cannon-Manning U-tube is closer to $\eta_{0(S\text{-}RV)}$ than the absolute viscosities from Tubes A and B. This correlation is further observed from Table 4.8. Thus, as shown in Figure 4.7, a relationship between absolute viscosities determined using Cannon-Manning U-tube and $\eta_{0(S\text{-}RV)}$ is developed using a linear fit and is shown in the Equation (4.2). Using Equation (4.2), if $\eta_{0(S\text{-}RV)}$ of a binder at 60 °C is determined using the rotational viscometer, the corresponding absolute viscosity can be obtained that conforms with IS:73 (BIS, 2013) specifications.

Table 4.8 MAPE between absolute viscosity and $\eta_{0(S\text{-}RV)}$

Viscometer tube	**MAPE**
Original tube	14.35
Tube-A	40.80
Tube-B	17.29

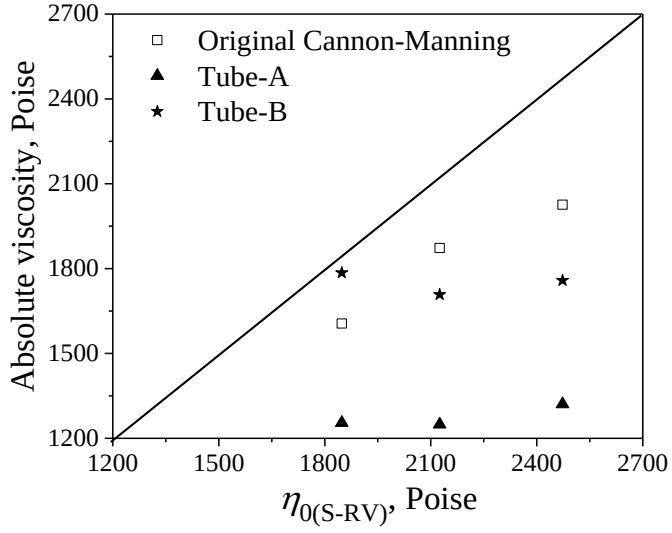

Fig. 4.6 Correlation between absolute viscosities and $\eta_{0(S\text{-}RV)}$

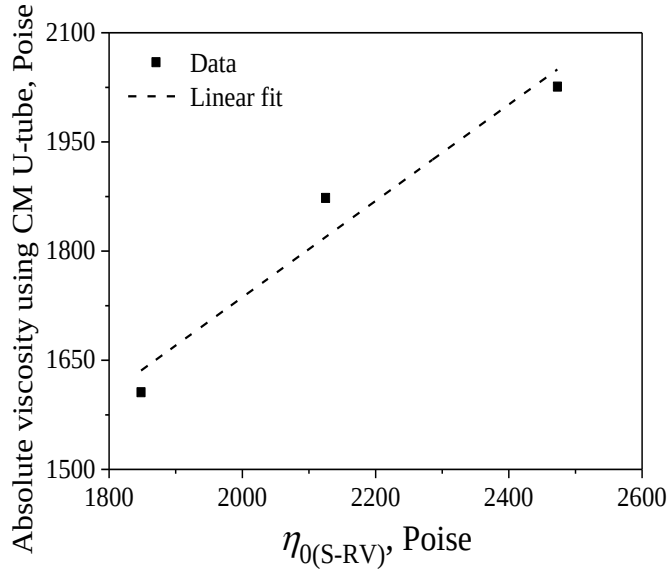

Fig. 4.7 Relationship between absolute viscosity from the Cannon-Manning U-tube and $\eta_{0(S\text{-}RV)}$

$$\text{Absolute viscosity} = 412.06 + (0.66 \times \eta_{0(S\text{-}RV)}) \quad (4.2)$$

The original Cannon-Manning U-tube grades all the three binders (B-1, B-2 and B-3) as VG20. Moreover, the original Cannon-Manning U-tube showed that there is a considerable difference in the absolute viscosity among the three binders with the binder B-3 having the highest absolute viscosity followed by B-2 and B-1 respectively. This result shows that there would be a considerable difference in the various other rheological properties of bituminous binders even though they may represent the same grade. The results obtained from the locally manufactured U-tubes, however, are completely different. Both the locally manufactured tubes are unable to differentiate between the three binders. Also, only the Tube-B is able to

grade the binders as VG20 whereas the Tube-A resulted in absolute viscosity conforming to neither VG10 nor VG20. Both these findings indicate the inability of the locally calibrated U-tubes to accurately determine the absolute viscosity of the bituminous binders. However, the latter is of utmost concern since the two tubes are manufactured and calibrated by the same manufacturer. $\eta_{0(S\text{-}RV)}$ showed results on similar terms with the results obtained from the original Cannon-Manning U-tube, wherein, the binder B-3 has a higher apparent viscosity followed by B-2 and B-1 binders respectively showing a correlation between the absolute viscosity measured using the vacuum capillary viscometer equipped with the original Cannon-Manning U-tube and $\eta_{0(S\text{-}RV)}$. This correlation is further validated where, the MAPE values from the original Cannon-Manning U-tube are the lowest among the three U-tubes. The findings of this study substantiate the fact that $\eta_{0(S\text{-}RV)}$ measured using the rotational viscometer is more reliable for grading bitumen as per IS:73 (BIS, 2013) and can successfully replace the locally calibrated U-tubes and whenever the original Cannon-Manning U-tubes are not available for grading the binder. Because of a strong underlying relationship (R^2 = 0.952) that is established between the absolute viscosity determined using the original Cannon-Manning viscometer and $\eta_{0(S\text{-}RV)}$ determined using the rotational viscometer at 60 °C, the equation proposed in this study helps the users to calculate the absolute viscosity of the binder from $\eta_{0(S\text{-}RV)}$. Thus, suitable grade of binder can be selected for the construction of roads depending upon the local climatic conditions.

4.3 RHEOLOGICAL STUDIES USING DYNAMIC SHEAR REHOMETER

DSRs, as shown in Figure 3.6, are used for conducting rheological studies on the unmodified VG20 and VG40 bitumen at all aging conditions and test temperatures as discussed in Section 3.6.2. All the tests are conducted on samples prepared as specified in Section 3.6.1.

4.3.1 Determination of Time for Thermal Equilibrium

As the field performance of bituminous roads depends highly upon the rheological properties of the bitumen used, it is paramount that the rheological properties of bitumen binders are determined accurately and at the exact temperature. As the DSR uses precise measurements to determine the rheological properties of the bitumen binders, determining the time it takes for a specimen to reach the desired test temperature before starting any rheological examination is a

crucial aspect. This time is known as the time for thermal equilibrium. In the DSR, the rheological properties of the bitumen binders are measured by shearing the required amount

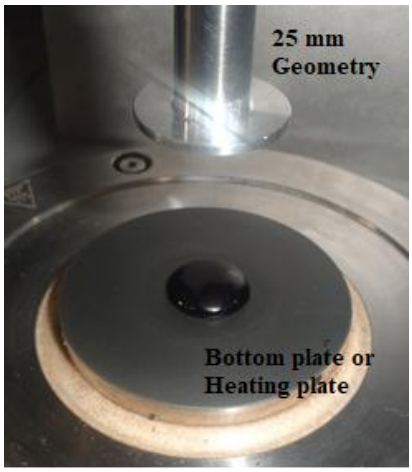

Fig. 4.8 Bitumen sample placed on the bottom heating plate of a DSR

of the bitumen sample between two parallel plates. The two parallel plate setup of a DSR is shown in Figure 4.8. The sample is placed on the bottom plate whereas the top plate applies shear which in turn induces a resultant torque through which the rheological properties are measured. The accuracy of a measurement made at the desired test temperature will be truly representative of the said temperature only if the sample has attained the said temperature. That is, the various tests conducted to determine the rheological properties of the bitumen binders can be started only after the sample has attained the thermal equilibrium. The scientific definition of thermal equilibrium (AHD, 2019) is: *"the condition under which two substances in physical contact with each other exchange no heat energy, i.e., two substances in thermal equilibrium are said to be at the same temperature"*. That is, the transfer of heat takes place from one system to another system until there is an equilibrium in the two systems. Here, the bottom plate of the DSR is connected to a heating element which heats the plate to the desired test temperature. The bitumen sample is then placed on the bottom plate as shown in Figure 4.8. The bitumen sample will be at a different temperature than the bottom plate. When the bitumen sample is placed on the bottom plate, heat from the bottom plate is gradually transferred to the bitumen sample over a period of time until both the bottom plate and the bitumen sample reaches the same temperature. The determination of the time it takes for a sample of bitumen to reach the thermal equilibrium is an essential part of the rheological investigations as it is very much important to determine the response characteristics of the bitumen binders at a precise test temperature. Further, the influence of test temperature and the aging condition of the binder on the thermal equilibrium time is not clearly established in

the literature. ASTM D7175 (ASTM, 2015*c*) provides the standard test procedure for determining the rheological properties of bitumen binders using a DSR and the protocol to determine the thermal equilibrium time is discussed in Section 3.6.3. Figure 4.9 from ASTM D7175 (ASTM, 2015*c*) gives a visual illustration for determining the time for thermal equilibrium.

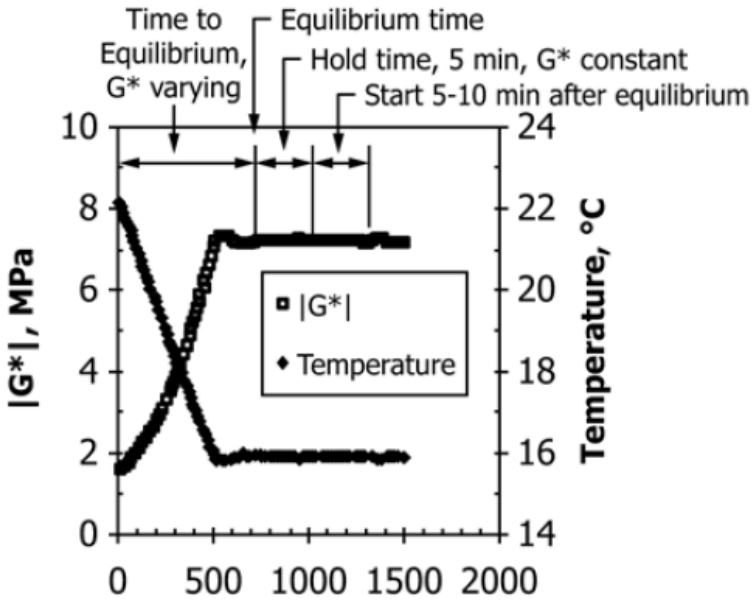

Fig. 4.9 Variation of complex modulus with time (ASTM, 2015*c*)

As per the research objectives, for the rheological characterization of VG20 and VG40 binders, it is necessary to first determine the thermal equilibrium times at all the aging conditions and test temperatures shown in Section 3.6.2. The tests are conducted using a 25 mm parallel plate geometry as the test temperatures are equal to or above 40 °C. In order to determine the thermal equilibrium times for the unaged, short-term aged and long-term aged VG20 and VG40 binders at 40, 45, 50, 55, 60 and 65 °C, the testing is however carried out only at three selected temperatures as shown in Table 4.9. From the thermal equilibrium times obtained at the three temperatures for a particular binder and aging condition as shown in Table 4.9, the thermal equilibrium times are determined for the remaining intermediate temperatures through a linear curve fit (ASTM, 2015*c*; Wineman and Rajagopal, 2000).

The DSR is set to the desired test temperature and the sample is placed on the bottom plate. The test is started after trimming the sample. Table 4.10 shows the time taken by the respective bitumen samples to spread and to trim as per the different test temperatures and the aging conditions. This time is eventually added to the thermal equilibrium time.

Table 4.9 Test temperatures used for determining thermal equilibrium time

Binder grade	Temperature, °C		
	Unaged	Short-term aged	Long-term aged
VG20	40, 50, 65	40, 50, 65	40, 50, 65
VG40	40, 50, 65	40, 50, 65	50, 55, 65

Table 4.10 Sample spread and trimming time

Temp., °C	Time, s					
	VG20			VG40		
	Unaged	Short-term aged	Long-term aged	Unaged	Short-term aged	Long-term aged
40	120	120	300	120	360	-
50	10	60	120	60	120	360
55	-	-	-	-	-	360
65	10	60	120	60	120	120

Figure 4.10 shows the variation of the complex modulus (G^*) with respect to time for the unaged VG20 and VG40 binders at 65 °C, whereas similar plots generated at all the remaining test temperatures and aging conditions are shown in Appendix A (Figure A4). The ASTM D7175 (ASTM, 2015*c*) states that "*the time to reach thermal equilibrium is the time required to reach a constant modulus. Typically, this time will be greater than the time required to reach a constant reading on the DSR thermometer*". In order to determine the

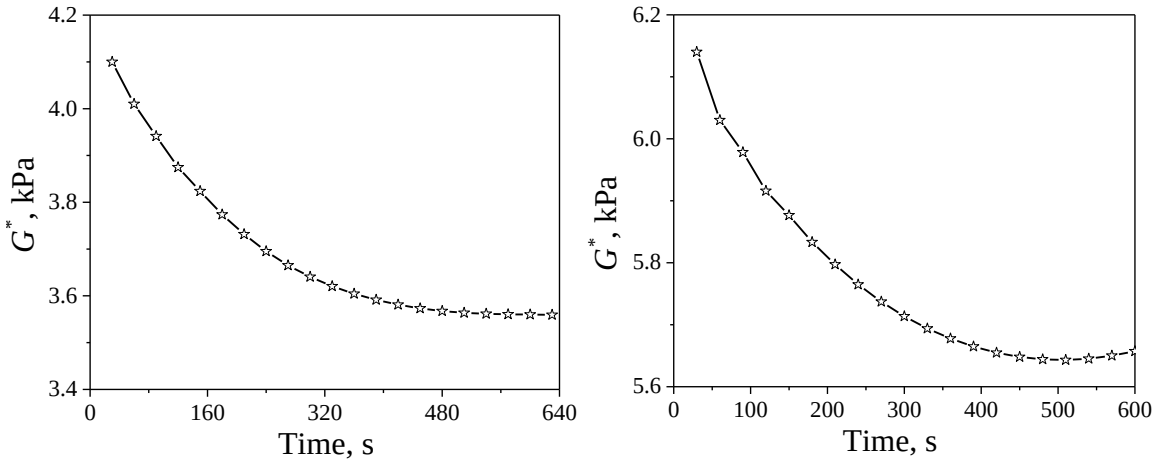

(a) Unaged VG20 binder (b) Unaged VG40 binder

Fig. 4.10 Variation of the complex modulus with time at 65 °C

time for thermal equilibrium, the variation of complex modulus with time, i.e., dG^*/dt is analyzed. The G^* obtained at 30 second intervals is smoothened using a five point moving average method. The percentage difference between the G^* at every 30 second interval is determined. The time where the percentage difference between the successive G^* decreases

below 0.5% is chosen as the thermal equilibrium time. Table 4.11 shows the time where the percentage change in G^* for the unaged, short-term aged and long-term aged VG20 and VG40 binders is less than 0.5%. It can be observed from Table 4.11 that the time when the percentage change in G^* is less than 0.5% decreases with increase in temperature, increases with the binder aging, and the time is higher for VG40 binder when compared to the VG20 binder at a given test temperature and aging condition. It is to be noted here that the times shown in Table 4.11 very much depends on the sample spread and trimming times as shown in Table 4.10. For instance, for short-term aged VG40 binder, the combined sample spread and trimming time at 40 °C is 360 s whereas this time is only 120 s at 50 °C. This resulted in a drop in the time (for the percentage change in G^* to reach less than 0.5%) to 630 s for the short-term aged VG40 binder at 40 °C when compared to 660 s for the short-term aged VG40 binder at 50 °C as can be observed from Table 4.11. Similar observation can also be made from Table 4.11 if the respective times at: (i) 50 °C for the short-term aged VG40 binder and the long-term aged VG40 binder are compared, (ii) 65 °C for the unaged VG20 binder and the unaged VG40 binder are compared.

Table 4.11 Time when the percentage change in complex modulus is less than 0.5%

Temp., °C	**Time, s**					
	VG20			**VG40**		
	Unaged	**Short-term aged**	**Long-term aged**	**Unaged**	**Short-term aged**	**Long-term aged**
40	480	600	720	600	630	-
50	450	540	660	540	660	600
55	-	-	-	-	-	480
65	330	330	420	300	420	480

As stated in the ASTM D7175 (ASTM, 2015*c*), the thermal equilibrium time determined based upon the stabilization of complex modulus will be slightly lower than the actual time for the thermal equilibrium. Therefore, an additional 300 s is added to the determined thermal equilibrium time intervals. The new thermal equilibrium times are shown in Table 4.12. Now it can be clearly observed from Table 4.12 that the thermal equilibrium time decreases with increase in temperature, increases with the binder aging as the binder becomes more stiffer, and the time is higher for VG40 binder when compared to the VG20 binder at a given test temperature and aging condition. This data is further used to generate best fits where a linear curve as shown by Equation (4.3) is found to be ideal for all the binders and aging conditions considered in this study. The linear fits to determine the thermal

equilibrium times for the unaged, short-term aged and long-term aged VG20 and VG40 binders are shown respectively in Figure 4.11. The linear fit parameters are shown in Table 4.13. The parameters obtained from the linear fit are then used to determine the time for thermal equilibrium at remaining intermediate test temperatures. Table 4.14 shows the final thermal equilibrium times for all the desired test temperatures, i.e., 40, 45, 50, 55, 60 and 65 °C for both the binders and for all the three aging conditions.

$$y = a + (b * x) \tag{4.3}$$

where,

x = independent variable (here temperature),

y = dependent variable (here G^*), and

a, b = linear fit parameters.

Table 4.12 Time for thermal equilibrium after adding the spread and trim time and an additional 300 s

Temp., °C	Time, s					
	VG20			VG40		
	Unaged	Short-term aged	Long-term aged	Unaged	Short-term aged	Long-term aged
40	900	1020	1320	1020	1290	-
50	760	900	1080	900	1080	1260
55	-	-	-	-	-	1140
65	640	690	840	660	840	900

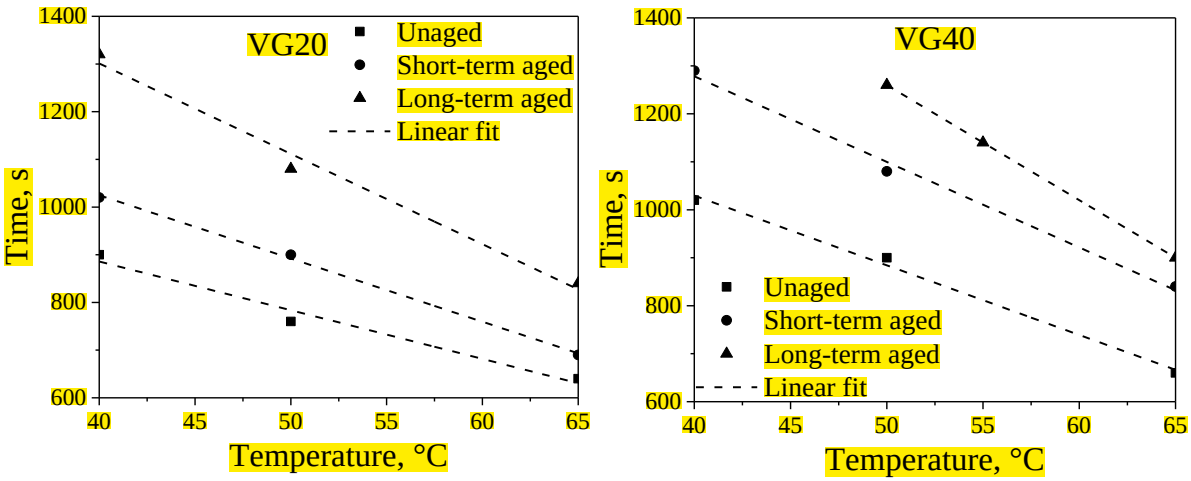

(a) (b)

Fig. 4.11 Linear fit for the (a) VG20 binder and (b) VG40 binder

Table 4.13 Parameters of the linear fit for thermal equilibrium time

Linear fit parameters	VG20			VG40		
	Unaged	Short-term aged	Long-term aged	Unaged	Short-term aged	Long-term aged
a	1312.63	1555.26	2058.95	1610.53	1991.84	2460.00
b	-10.63	-13.26	-18.95	-14.53	-17.84	-24.00

In the Appendix A (Figure A5), the plots of the thermal equilibrium times of the VG20 and the VG40 with respect to temperature, aging conditions and also the comparison across binders are shown. All the tests involving DSR are started after the samples attained thermal equilibrium. It is observed that the time for thermal equilibrium varies with the test temperature. It is observed that with an increase in test temperature, the time for thermal equilibrium decreased.

Table 4.14 Final thermal equilibrium times

Temp., °C	Time for thermal equilibrium, s					
	VG20			VG40		
	Unaged	Short-term aged	Long-term aged	Unaged	Short-term aged	Long-term aged
40	887	1025	1301	1030	1278	1500
45	834	958	1206	957	1189	1380
50	781	892	1112	884	1100	1260
55	728	826	1017	812	1011	1140
60	675	759	922	737	921	1020
65	622	693	827	666	832	900

Such trend is observed for both the VG20 and VG40 binders for different aging conditions. This clearly shows that it is very much essential to determine the thermal equilibrium time at each test temperature and also for each bitumen type. The long-term aged binder exhibited higher thermal equilibrium time followed by short-term aged binder and the unaged binder. This clearly shows that there is an increase in the time for thermal equilibrium when the binder age hardens. This kind of response is observed for both the VG20 and the VG40 binders. On comparing the two bitumen, the VG40 binder required a longer duration of time to achieve thermal equilibrium than the VG20 binder at a particular aging condition and at a specific test temperature. This clearly shows that binders with a higher viscosity require a relatively longer duration of time to achieve the desired test temperature than the soft binders.

The variation in equilibrium times is observed to be higher at lower test temperatures and the values converged at higher test temperatures for both the binder grades and for all the three aging conditions. The results clearly highlight the need to determine the time for thermal equilibrium for individual temperatures and in order to get precise characterisation of the rheological properties of the bitumen binders. When the samples are allowed to thermally equilibrate more than the required time, steric hardening in the bitumen samples could lead to undesirable results. The thermal equilibrium times determined in this study are specific to the dynamic shear rheometer used in this study. The thermal equilibrium times may vary depending upon the type of temperature controller and the size of bottom plate assembly used in the dynamic shear rheometer.

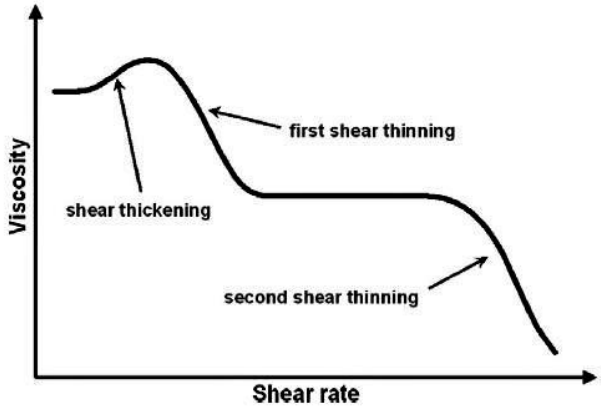

Fig. 4.12 Viscosity as a function of shear rate with a shear thickening and two shear thinning regions (Polacco et al., 2015)

4.3.2 Linear Shear Rate Sweep Test

The LSRS test is conducted on the unmodified VG20 and VG40 binder at all the aging conditions and test temperatures. The main aim of the test is to capture two Newtonian regions interceded by a shear thinning non-Newtonian region as shown in Figure 2.2. The hypothesis is that the test would lead to a direct measurement of ZSV of unmodified bitumen binders instead of using any models. The issues with the determination of ZSV have already been discussed in Section 2.2.3. However, the response of VG20 and VG40 binders to the applied test protocol is in stark contrast to the expected response and is shown in Figure 4.12. The observed response is characterized by an initial Newtonian plateau followed by a shear thickening region. The shear thickening region is followed by two shear thinning regions interceded with or without a second Newtonian plateau. Such a response is mainly observed in polymeric solutions (Annable et al., 1993) and highly modified bitumen (Polacco et al., 2015). Unmodified bitumen did not exhibit such a response when the shear rate ranged from

0.001 to 100 1/s when the temperatures ranged from 40 to 90 °C but modified bitumen exhibited a weak shear thickening followed by a shear thinning region at a similar shear rate range and temperatures (Polacco et al., 2004). Even for some polymer modified bitumen, the initial Newtonian plateau and the subsequent shear thickening is not seen when shear rate ranged from 1 to 100 1/s (Cardone et al., 2014).

The shear thickening after an initial Newtonian region is due to the clustering resulting from the interaction of particles after they move out of the layers due to hydrodynamic instability (Hoffman et al., 1998). This hydrodynamic instability causes intra and intermolecular attractions leading to an increase in shear stress and viscosity. Also, shear thickening occurs when the domain structure undergoes a rigid rearrangement, due to entanglement of the particles and chain stretching (Polacco et al., 2004; Polacco et al., 2015). The first shear thinning is due to a temporary detachment and rearrangement after shear thickening (Polacco et al., 2004) and the second shear thinning is because of disruption and the alteration in the colloidal structure of bitumen.

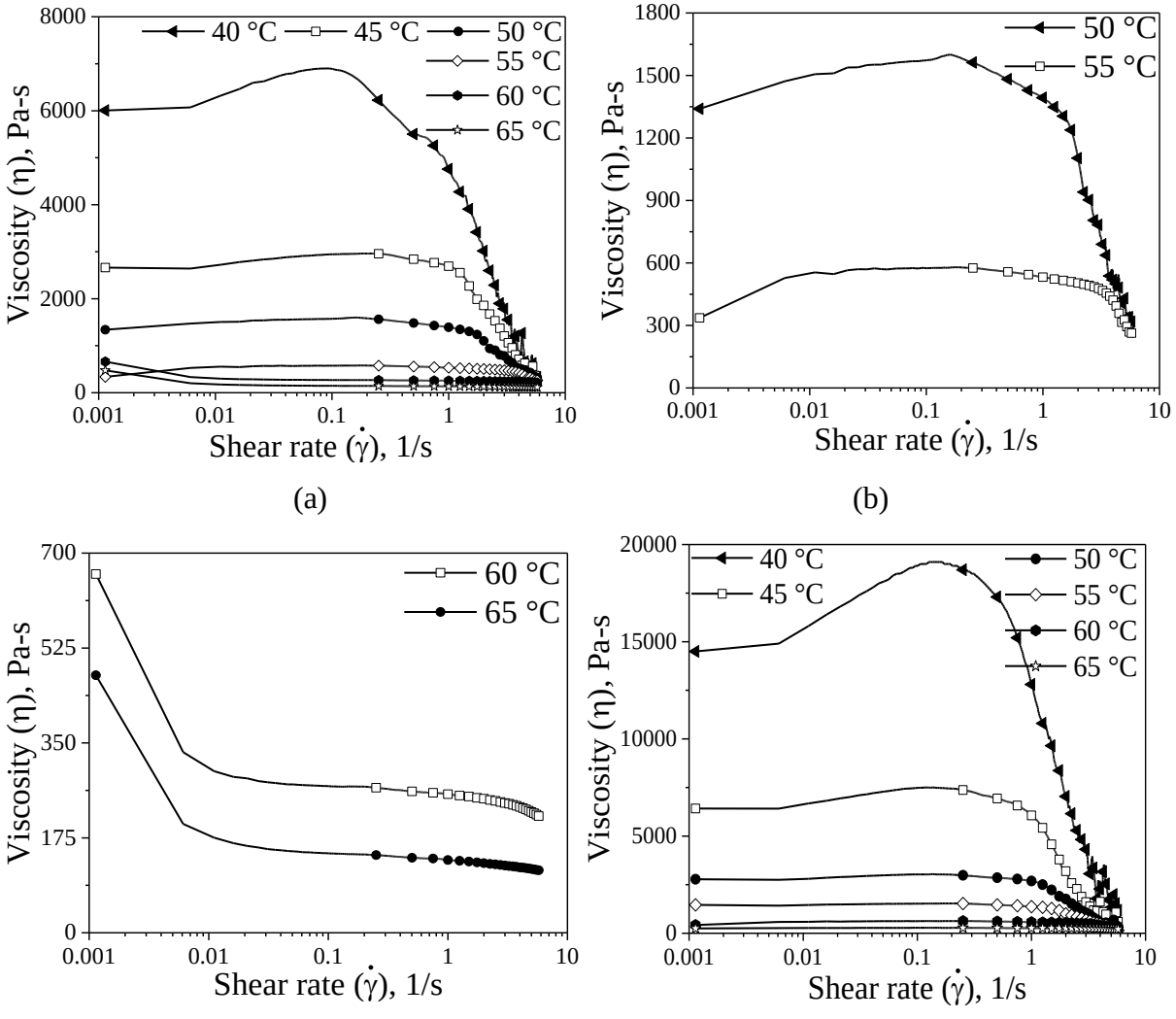

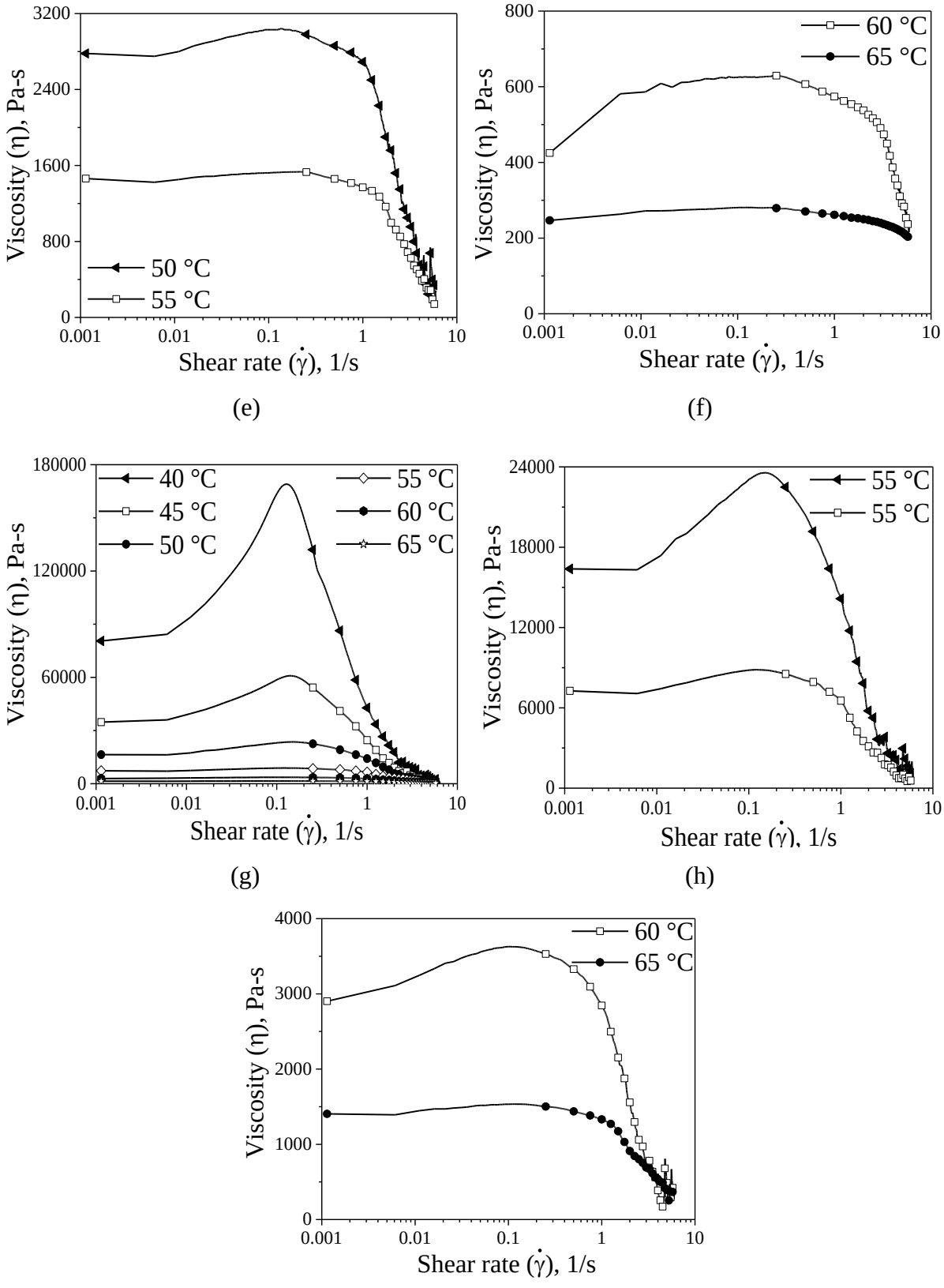

Fig. 4.13 Viscosity as a function of time from the LSRS test: (a), (b), (c) unaged VG20; (d), (e), (f) short-term aged VG20 and (g), (h), (i) long-term aged VG20

The data from the test is obtained at test conditions except for the long-term aged VG40 binder at 40 and 45 °C. For the long-term aged VG40 binder at 45 °C the test terminated before 1200 s since the torque limit is set at 190 mNM whereas for the long-term aged VG40 binder at 40 °C, even at initial shear rates the torque exceeded the limiting value. The results from the LSRS test are shown in Figures 4.13 and 4.14. From Figures 4.13 and 4.14 it is observed that, except for some cases the response of viscosity to the applied shear rate is multi-phase, wherein an initial Newtonian plateau is observed followed by a shear thickening regions subsequently followed by two shear thinning regions except for unaged VG20 bitumen at 60 and 65 °C wherein, only two shear thinning regions are observed and short-term aged VG20 bitumen at 50 and 55 °C, unaged VG40 at 65 °C wherein, shear thickening preceded two shear thinning regions without an initial Newtonian plateau. Two viscosities are chosen from the analysis of the LSRS data from the plateau region and the region where transition from shear thickening to shear thinning occurs. From the first Newtonian plateau region, the ZSV is considered and is denoted as $\eta_{0(L)}$. The 'L' in the subscript represents the ZSV obtained from the LSRS test. From the region where transition from shear thickening to shear thinning occurs, the peak transient viscosity is considered and is denoted as η_{TV}. Here, η_{TV} is defined as the highest (peak) viscosity corresponding to the shear thickening region. The viscosities, η_0 and η_{TV} are shown in Tables 4.15 and 4.16 respectively for the VG20 and VG40 bitumen and are compared in Figure 4.15. From Tables 4.15 and 4.16 it is observed that both $\eta_{0(L)}$ and η_{TV} decrease with an increase in temperature. However, at a particular temperature, the magnitude of both $\eta_{0(L)}$ and η_{TV} increases with an increase in bitumen aging. It is observed that the short-term aged and long-term aged VG20 bitumen showed an increase in $\eta_{0(L)}$ and η_{TV} respectively by 2.4 and 2.5 times and 13.1 and 18.8 times the unaged VG20 bitumen whereas the short-term aged and long-term aged VG40 bitumen showed an increase in $\eta_{0(L)}$ and η_{TV} respectively by 3.5 and 3.9 times and 19.0 and 26.0 times the unaged VG40 bitumen. From Tables 4.15 and 4.16 and Figure 4.15 it is observed that the difference between $\eta_{0(L)}$ and η_{TV} decreases with an increase in temperature. For unaged VG20 and VG40 bitumen, the percentage difference between $\eta_{0(L)}$ and η_{TV} decrease from 15 to 9.8% and 21.6 to 7.2% when the temperature increases from 40 to 55 °C and 40 to 65 °C respectively. For the short-term aged VG20 and VG40 bitumen, the percentage difference between $\eta_{0(L)}$ and η_{TV} decreases from 31.7 to 9.8% and 51.8 to 7.8% respectively when the temperature increases from 40 to 65 °C. For the long-term aged VG20 and VG40 bitumen, the percentage difference between $\eta_{0(L)}$ and η_{TV} decreases from 109.8 to 9.3% and 98.0 to 16.9% when the temperature increases from 40 to 65 °C and 45 to 65 °C, respectively.

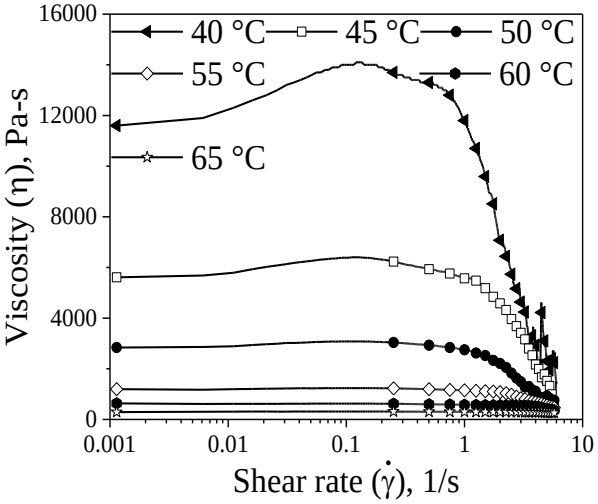
40 °C
45 °C
50 °C
55 °C
60 °C
65 °C
Viscosity (η), Pa-s
Shear rate (γ̇), 1/s

(a)

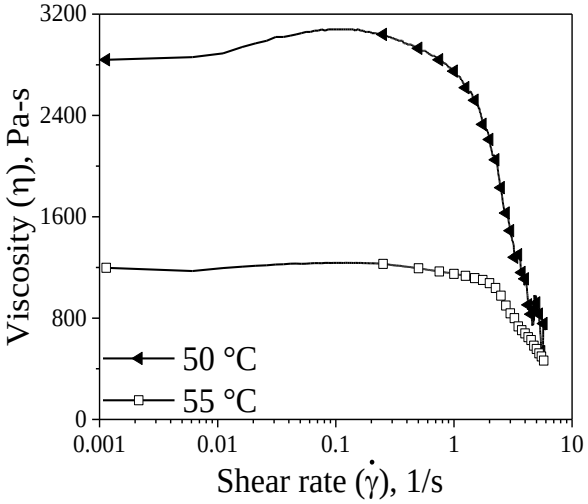
50 °C
55 °C
Viscosity (η), Pa-s
Shear rate (γ̇), 1/s

(b)

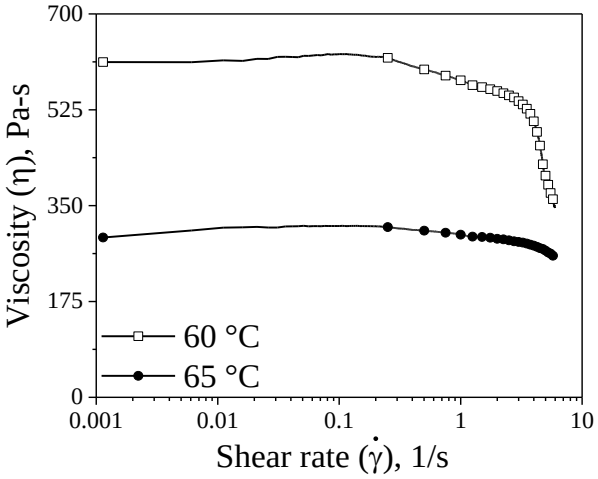
60 °C
65 °C
Viscosity (η), Pa-s
Shear rate (γ̇), 1/s

(c)

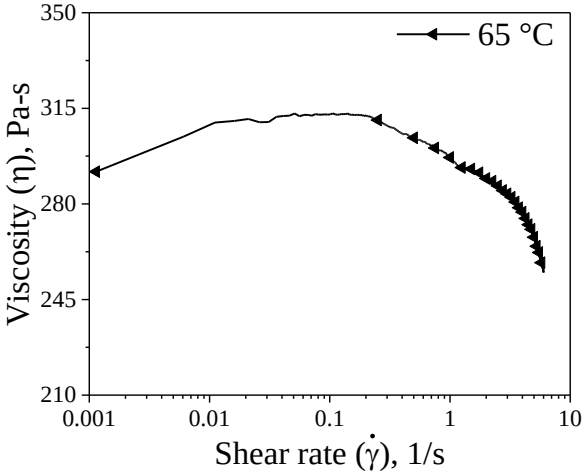
65 °C
Viscosity (η), Pa-s
Shear rate (γ̇), 1/s

(d)

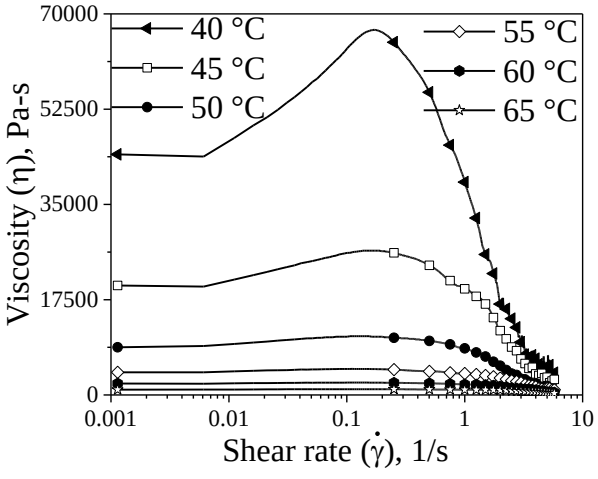
40 °C
45 °C
50 °C
55 °C
60 °C
65 °C
Viscosity (η), Pa-s
Shear rate (γ̇), 1/s

(e)

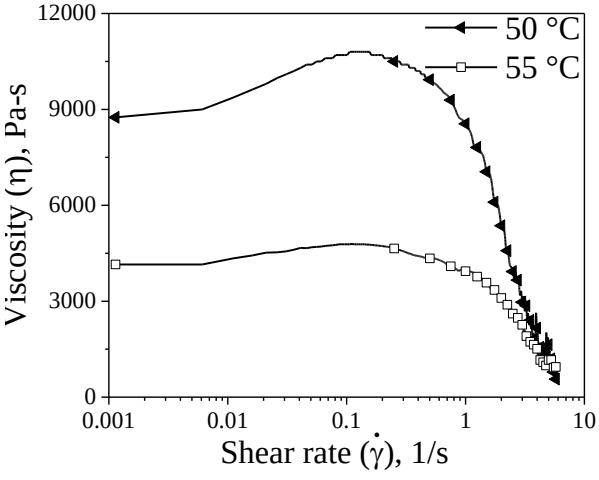
50 °C
55 °C
Viscosity (η), Pa-s
Shear rate (γ̇), 1/s

(f)

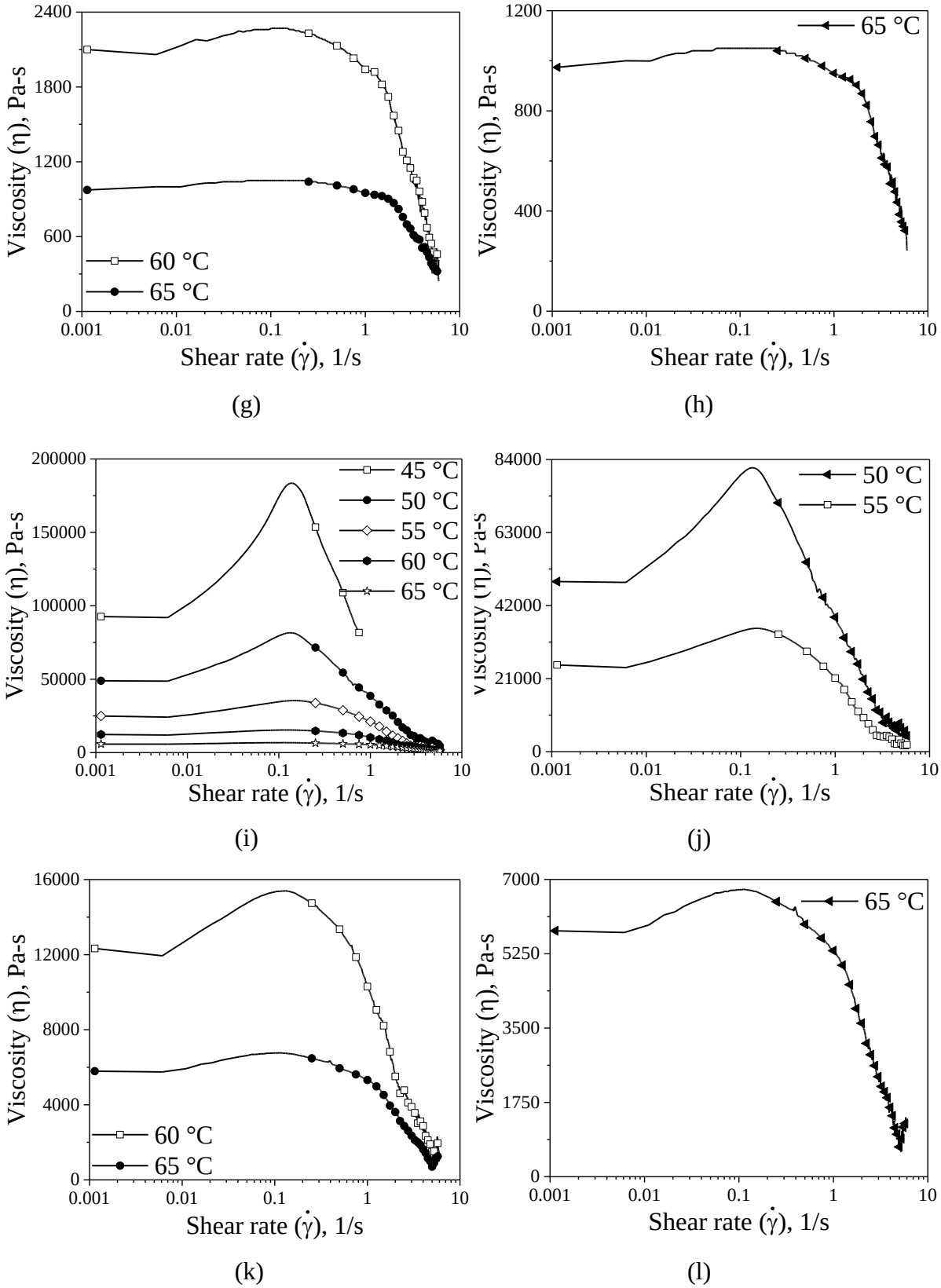

Fig. 4.14 Viscosity as a function of shear rate from LSRS test: (a), (b), (c), (d) unaged VG40; (e), (f), (g), (h) short-term aged VG40 and (i), (j), (k), (l) long-term aged VG40

Moreover, it is also observed that the percentage difference between $\eta_{0(L)}$ and η_{TV} increases with bitumen aging when compared at a particular temperature for most cases. Also

the area under the curve is shown in Table 4.17. From Table 4.17 it is observed that there is a decrease in area under the curve with an increase in temperature for all cases whereas, at a particular temperature there is an increase in area under the curve with bitumen aging for both VG20 and VG40 bitumen. The increase in $\eta_{0(L)}$, η_{TV} and area under the curve with bitumen aging is due to the increase in the high molecular components when saturates are converted to asphaltenes and the aromatics are converted to resins (Liu et al., 2018). This leads to a reduction in the less soluble hydrocarbons resulting in an increase in the elastic stiffness and the viscosity (Hossain et al., 2018). Moreover, these associations leading to an increase in the stiffness of the bitumen with an increase in aging can make the response of the bitumen binder predominantly non-Newtonian. This predominantly non-Newtonian response is observed by the increase in the percentage difference between $\eta_{0(L)}$ and η_{TV} with aging at a particular temperature for both VG20 and VG40 bitumen binders.

Table 4.15 Viscosity parameters from LSRS test for the VG20 bitumen

Temp., °C	$\eta_{0(L)}$, Pa-s			η_{TV}, Pa-s		
	Unaged	Short-term aged	Long-term aged	Unaged	Short-term aged	Long-term aged
40	6005	14500	80550	6903	19100	169000
45	2663	6420	34720	2963	7500	60910
50	1340	2780	16380	1600	3040	23560
55	528	1462	7266	580	1534	8849
60	*	425	2902	*	629	3628
65	*	247	1405	*	281	1535

$\eta_{0(L)}$ and η_{TV} as a function of temperature are shown in Figures 4.16 and 4.17 respectively. From Tables 4.15 and 4.16 and Figures 4.16 and 4.17, it is also observed that there is a decrease in $\eta_{0(L)}$ and η_{TV} with an increase in temperature at all aging conditions for both VG20 and VG40 bitumen which is on expected lines. It is observed that there is a decrease in $\eta_{0(L)}$ and η_{TV} by an average of 98.2% when the temperature increases from 40 to 65 °C at all aging conditions for both VG20 and VG40 bitumen. Moreover, it is observed that, at a particular temperature, there is an increase in $\eta_{0(L)}$ and η_{TV} with bitumen aging. It is observed that this increase in both $\eta_{0(L)}$ and η_{TV} of the short-term aged bitumen is by almost 2.4 times for the VG20 bitumen and 3.7 times for the VG40 bitumen at all test temperatures, whereas, the increase in $\eta_{0(L)}$ and η_{TV} of the long-term aged bitumen is by 13.1 and 18.8 times for the VG20 bitumen and by 18.9 and 26 times for the VG40 bitumen when compared to that of the unaged bitumen. Moreover, it is observed that the $\eta_{0(L)}$ and η_{TV} of the VG40 binder is on an average 3.12 and 3.23 times the η_0 and η_{TV} of VG20 bitumen at all temperatures and aging

conditions. These observations indicate that the aging improves the rutting performance of bitumen binders by offering an increased resistance towards permanent deformation. Also, the VG40 binder offers a higher resistance towards rutting than VG20 binder at all temperatures and aging conditions.

The shear rate corresponding to η_{TV} is shown in Table 4.18. It is seen that the shear rate corresponding to η_{TV} showed no specific trend and is more or less similar with an average value of 0.129 1/s. Since, η_{TV} is observed to be independent of shear rate, it can be considered as an integral property of the bitumen. Therefore, it is proposed to use η_{TV} as a bitumen property that could be used to predict the performance of bitumen binders in terms of their resistance to rutting in this research study. Moreover, from the Newtonian region, $\eta_{0(L)}$ is used as a rutting parameter. Thus, test two rutting parameters are determined from the LSRS test including one non-Newtonian parameter, η_{TV} and a Newtonian parameter $\eta_{0(L)}$.

Table 4.16 Viscosity parameters from LSRS test for the VG40 bitumen

Temp., °C	$\eta_{0(L)}$, Pa-s			η_{TV}, Pa-s		
	Unaged	Short-term aged	Long-term aged	Unaged	Short-term aged	Long-term aged
40	11600	44200	-	14100	67100	-
45	5610	20100	92670	6400	26500	183500
50	2840	8750	48890	3080	10800	81610
55	1197	4150	24910	1237	4780	35450
60	612	2100	12330	627	2270	15400
65	292	974	5790	313	1050	6769

Table 4.17 Area under the curve

Area under the curve, Pa						
Temp., °C	Unaged		Short-term aged		Long-term aged	
	VG20	VG40	VG20	VG40	VG20	VG40
40	14348	37275	38429	112511	146675	-
45	8535	20805	16589	60137	69707	-
50	5100	10143	8075	25740	38708	121659
55	2657	5148	4685	14505	17709	58693
60	1440	3075	2726	7363	7986	32700
65	756	1699	1436	4101	4826	17635

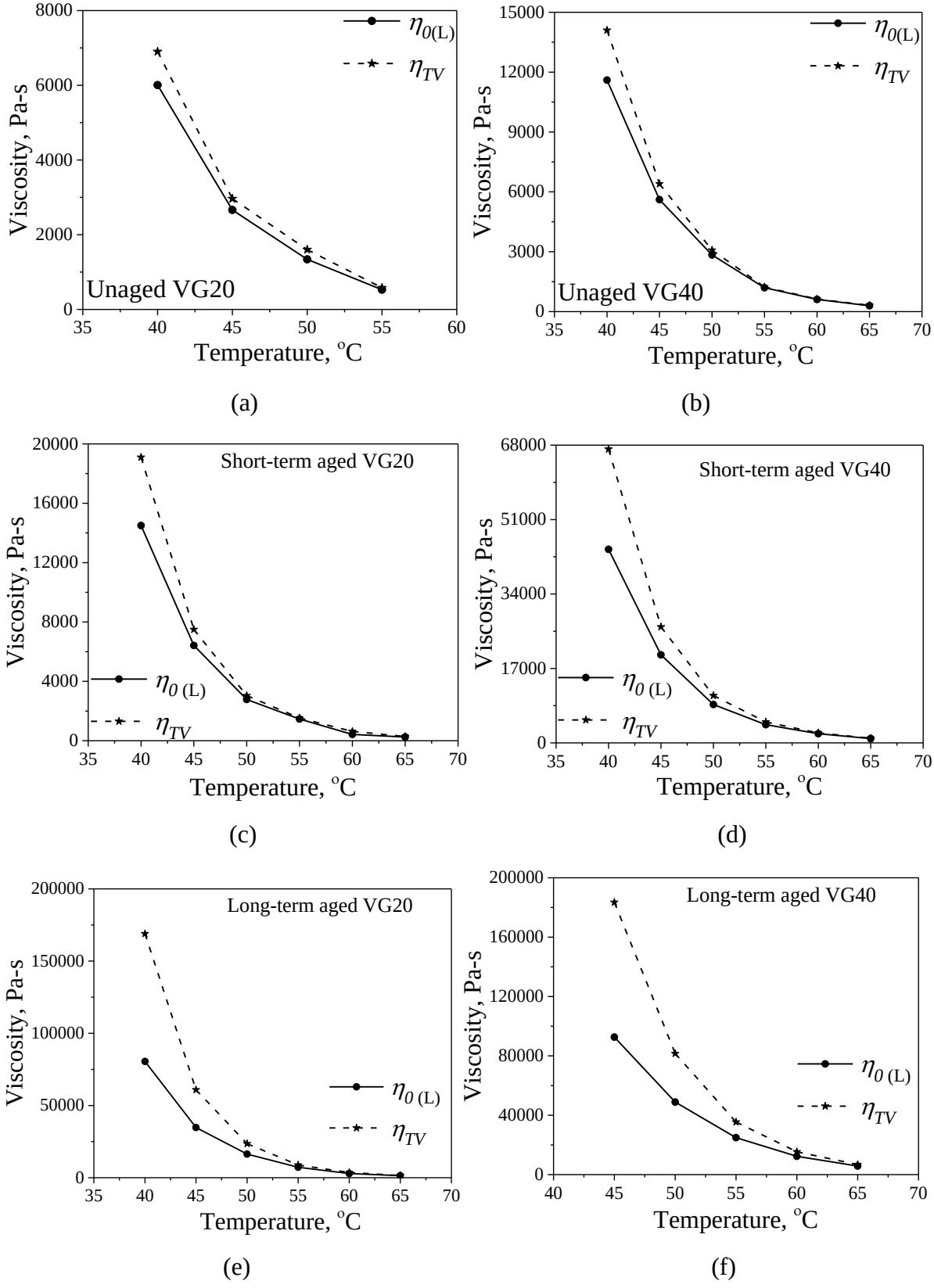

Fig. 4.15 $\eta_{0(L)}$ and η_{TV} as a function of temperature for (a), (c), (e) VG20 bitumen and (b), (d), (f) VG40 bitumen

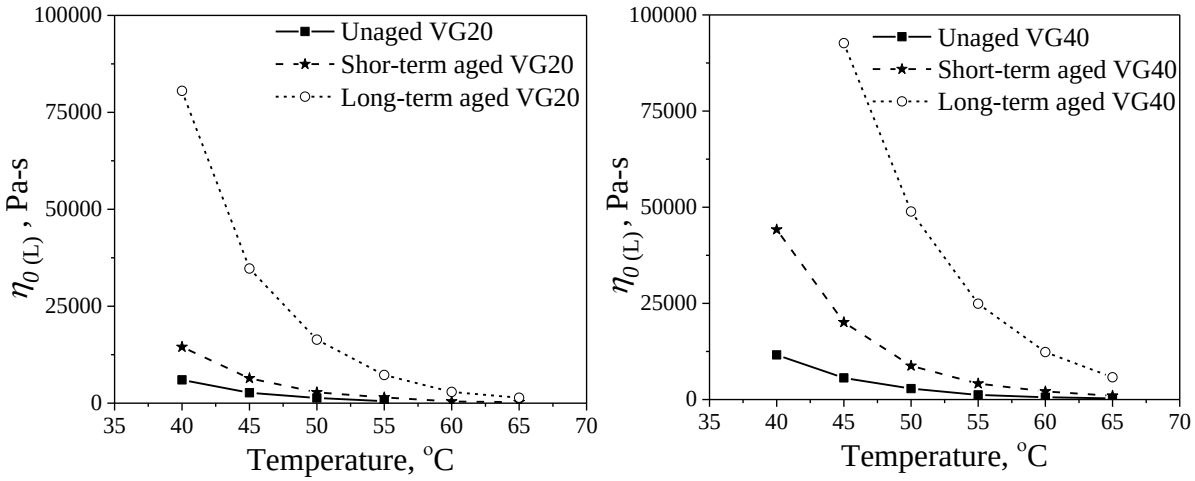

(a) VG20 (b) VG40

Fig. 4.16: $\eta_{0\,(L)}$ as a function of temperature

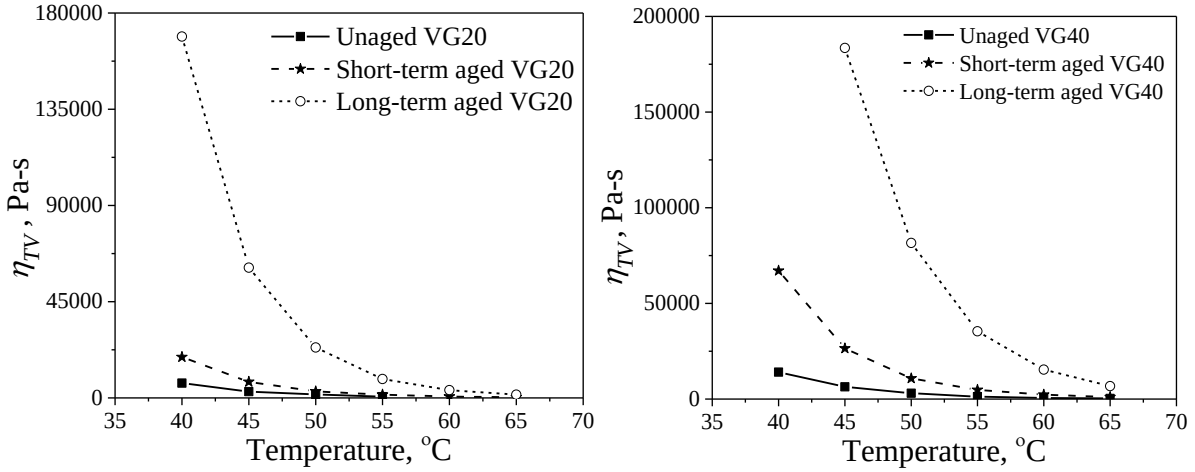

(a) VG20 (b) VG40

Fig. 4.17 η_{TV} as a function of temperature

Table 4.18 Shear rate corresponding to η_{TV}

Temp., °C	**Unaged**		**Short-term aged**		**Long-term aged**	
	VG20	**VG40**	**VG20**	**VG40**	**VG20**	**VG40**
40	0.091	0.121	0.126	0.171	0.126	-
45	0.186	0.111	0.116	0.141	0.141	0.136
50	0.161	0.076	0.131	0.103	0.146	0.146
55	0.176	0.121	0.216	0.086	0.121	0.151
60	-	0.081	0.251	0.101	0.101	0.131
65	-	0.076	0.141	0.056	0.116	0.106

4.3.3 Step-wise Steady Shear Rate Sweep Test-DSR

In order to overcome the drawbacks encountered with the RV, as discussed in Section 3.5.4, and to analyse the non-Newtonian response of VG20 and VG40 binders, a SWSSRS test protocol is adopted using a DSR. The main idea here is to evaluate the response of bitumen with respect to shearing time, effect of change in shear rate, and shear history by conducting tests similar to those carried out using a RV in Section 4.2. The shear rates corresponding to the initial and final step in the $SWSSRS_{DSR}$ test protocol are shown in Table 4.19. The selected shear rates correspond to the ZSV regime. Similar to the procedure followed in the Section 4.2, the 't_s' is initially determined at each temperature and aging condition for both the VG20 and VG40 binders. This is achieved by continously shearing the bitumen at the lowest shear rates for each condition as shown in Table 4.19. The results of the protocol to identify 't_s', the response of the bitumen binder subjected to $SWSSRS_{DSR}$ test, and the

Table 4.19 Shear rates employed in the $SWSSRS_{DSR}$ test

Temp., C	**VG20**		
	Unaged	**Shor-term aged**	**Long-term aged**
40	0.05, 0.07, 0.09, 0.11	0.03, 0.05, 0.07	0.03, 0.035, 0.04
45	0.05, 0.09, 0.12, 0.15	0.05, 0.07, 0.09	0.03, 0.035, 0.04
50	0.05, 0.09, 0.12, 0.15	0.05, 0.09, 0.12, 0.15	0.04, 0.05, 0.06
55	0.05, 0.09, 0.12, 0.15	0.05, 0.09, 0.12, 0.15	0.05, 0.07, 0.09
60	0.05, 0.12, 0.19, 0.26	0.05, 0.12, 0.19, 0.26	0.07, 0.09, 0.12
65	0.17, 0.34, 0.51, 0.68	0.17, 0.34, 0.51, 0.68	0.09, 0.12, 0.17
VG40			
40	0.05, 0.07, 0.09	0.03, 0.05, 0.07	0.03, 0.035, 0.04
45	0.05, 0.09, 0.12, 0.15	0.05, 0.07, 0.09	0.03, 0.035, 0.04
50	0.05, 0.09, 0.12, 0.15	0.05, 0.09, 0.12	0.04, 0.05, 0.06
55	0.05, 0.09, 0.12, 0.15	0.05, 0.09, 0.12, 0.15	0.05, 0.07, 0.09
60	0.05, 0.12, 0.19, 0.26	0.05, 0.12, 0.19, 0.26	0.07, 0.08, 0.09
65	0.17, 0.34, 0.51, 0.68	0.17, 0.34, 0.51, 0.68	0.09, 0.12, 0.17

analysis carried out are shown in this section for the unaged VG40 bitumen at a temperature of 50 °C whereas for all the other remaining test conditions, the results are shown in Appendix A. Figure 4.18 shows the variation of shear stress as a function of time when sheared at a minimum selected shear rate for the unaged VG40 binder at 50 °C. Similar Figures at all the remaining test conditions are shown in Appendix A (Figure A6 to A7). From Figure 4.18 it is observed that the shear stress increases with time by the appearance of a stress overshoot and gradually stabilizes and remains constant. From Figure 4.18 it is also

observed that there is an increase in shear stress followed by a gradual decrease. This phenomenon is known as stress overshoot (Rajan et al., 2008). The stress overshoot is due to the disruption in the structure of bitumen due to shear and the subsequent rearrangement (Viola and Baird, 1986). The stress overshoot represents the nonlinear response of a material upon shearing at a constant rate (Rajan et al., 2008; Jeong et al., 2017) and is characteristic of viscoelastic materials (Whittle and Dickinson, 1997). This stress overshoot can be considered as a non-Newtonian response (Nivitha and Krishnan, 2018). Due to continuous shearing of the binder for a sufficiently long duration of time at a constant shear rate, the internal structure of the bitumen breaks apart resulting in a flow that is independent of the shearing time. Here, a steady state in the response of shear stress is observed. The shearing time where the shear stress stabilizes and reaches a steady state is denoted as '$t_{s(DSR)}$' and is determined at all the test temperatures and aging conditions for both the binders as shown in Table 4.20.

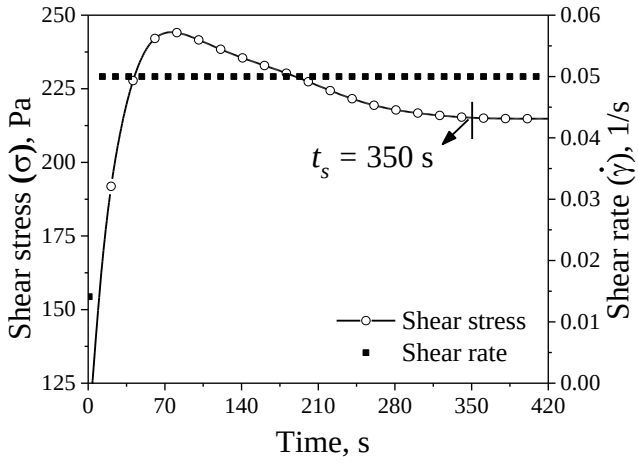

Fig. 4.18 Variation of shear stress with time for the unaged VG40 at 50 °C for an extended duration until shear stress stabilizes

During the experimental investigation, the VG20 binder is the first one to be tested, therefore, while determining $t_{s(DSR)}$ for the unaged, short-term aged and long-term aged VG20 bitumen, a buffer of 50 s is added is added to the observed '$t_{s(DSR)}$' to be on a conservative side. However, this is not the case with the VG40 binders, wherein the observed $t_{s(DSR)}$ are directly used. Therefore, the '$t_{s(DSR)}$' for both the bitumen binders appear same at almost all the temperatures and aging condition. From Table 4.20 it is observed that there is a decrease in '$t_{s(DSR)}$' with an increase in test temperature at all aging conditions. It is observed that there is a decrease in '$t_{s(DSR)}$' by 55% when the temperature decreases from 40 to 65 °C. This trend is observed for all aging conditions and for both VG20 and VG40 bitumen at all aging conditions. From Table 4.20 it is also observed that for a particular temperature there is an increase in '$t_{s(DSR)}$' with bitumen aging. For the short-term aged bitumen binders, increase in

'$t_{s(DSR)}$' ranges from 18 to 35% when temperature changes from 40 to 65 °C, whereas for the long-term aged binders, '$t_{s(DSR)}$' increases by 60% at 40 and 45 °C and by 47% at remaining temperatures. These observations indicate that '$t_{s(DSR)}$' is highly dependent upon temperature and bitumen aging.

Table 4.20 '$t_{s(DSR)}$' at different temperatures

Temp., °C	VG20			VG40		
	Unaged	Short-term aged	Long-term aged	Unaged	Short-term aged	Long-term aged
	s	s	s	s	s	s
40	450	550	1200	450	550	1200
45	400	500	900	400	500	900
50	350	450	650	350	450	650
55	300	400	550	300	400	550
60	250	350	450	250	350	450
65	200	300	350	200	300	400

From Figure 4.18 it is also observed that the shear stress at and beyond '$t_{s(DSR)}$' remains constant when sheared at a constant shear rate. Thus, the response of the binder can be considered as Newtonian and the viscosity obtained at '$t_{s(DSR)}$' can be considered as a Newtonian viscosity. This Newtonian viscosity can be used as an alternative to ZSV. However, as this Newtonian viscosity is determined at a particular shear rate, it is important to observe the response of bitumen to a change in shear rate. Therefore, an $SWSSRS_{DSR}$ test protocol is adopted.

As discussed earlier in Section 4.2, the first forward sweep would establish whether the binders exhibit a shear rate dependent behavior or a shear rate independent behavior. In the first backward sweep, the viscosity is measured at shear rates similar to that of the first forward sweep but at a different duration of time resulting in different shear history. Thus, the first backward sweep would establish whether the bitumen response is time dependent or time independent. The application of the second cycle of forward and a backward sweep would establish whether a previous shear history has an effect on the response of bitumen binders. However, for the long-term aged bitumen, at temperatures of 40 and 45 °C, only the first forward sweep of the $SWSSRS_{RV}$ is applied. This is because of the extremely high viscosity of the long-term aged bitumen at these temperatures. Figure 4.19 shows the response of the unaged VG40 binder subjected to the $SWSSRS_{DSR}$ test at a temperature of 50 °C. Similar plots for the VG20 and VG40 binders at all the test conditions are shown in Appendix A (Figures A8 and A9). Since, the binders are sheared for a particular duration corresponding to

the respective '$t_{s(DSR)}$' in each step, a Newtonian viscosity is observed at '$t_{s(DSR)}$' in every step in the $SWSSRS_{DSR}$ test,. Figure 4.20 (a) shows the input shear rate as a function of time and Figure 4.20(b) shows the variation of viscosity as a function of time at different shear rates in the first forward sweep of the $SWSSRS_{DSR}$ test. The viscosity and shear stress data at '$t_{s(DSR)}$' for all other test conditions are tabulated in Appendix A (Tables A3 to A8). From Figure 4.20(b), it is observed that a steady state of viscosity is observed at '$t_{s(DSR)}$' at all the shear rates employed in the first forward sweep. Moreover, from Figure 4.20(b), it is also observed that the viscosity at '$t_{s(DSR)}$' at different shear rates tends to converge. Similar response at all the other remaining test conditions are shown in Appendix A (Figures A10 to A15). From these Figures it is observed that for almost all the cases the viscosity at '$t_{s(DSR)}$' are very close except for the long-term aged VG20 and VG40 bitumen at 40 and 45 °C where there is a considerable drop in viscosity with an increase in shear rate. This is due to the edge failure of the sample during the test.

Figure 4.21 shows the variation of viscosity at '$t_{s(DSR)}$' as a function of shear rate in the first forward sweep of the $SWSSRS_{RV}$ test for the unaged VG40 bitumen. Similar responses at all other test conditions are shown in Appendix A (Figure A16). From Figures 4.21 and A16, it is observed that for most of the cases, the viscosity at '$t_{s(DSR)}$' remains in the ZSV regime except for the long-term aged VG20 and VG40 binders at 40 and 45 °C. The problem with the long-term aged VG20 and VG40 binder at 40 and 45 °C is the edge failure during tests because of extremely high viscoity of the bitumen. Therefore, it can be fairly concluded that the viscosity at '$t_{s(DSR)}$' in the first forward sweep of the $SWSSRS_{DSR}$ resulted in a response that is independent of shear rate.

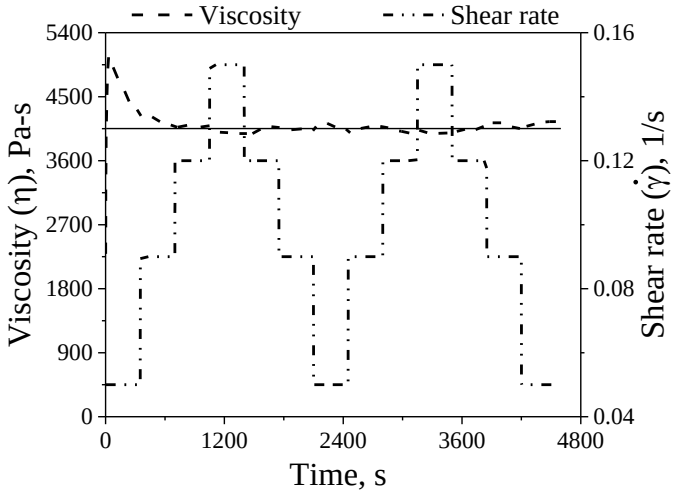

Fig. 4.19 Response of unaged VG40 bitumen at 50 °C in the $SWSSRS_{DSR}$ test protocol

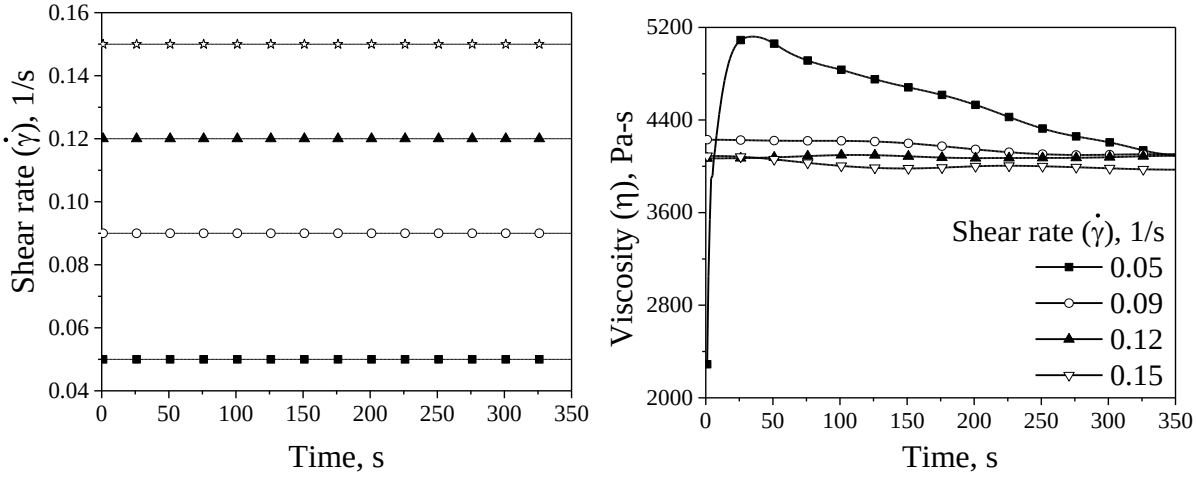

(a) Shear rate as a function of time (b) Viscosity as function of time

Fig. 4.20 Observed response in the first forward sweep of $SWSSRS_{DSR}$ test for the unaged VG40 binder at 50 °C

Further, similar to the procedure followed in Section 4.2, thixotropic index is used as a parameter to establish whether the bitumen response in the $SWSSRS_{DsR}$ is time dependent or time independent and also to check the effect of shear history. It is important to note here that for an ideal thixotropic response, the viscosity decreases with increase in shear rate in the forward sweep whereas when the shear rate is decreased in the backward sweep, the path followed by the viscosity will not be same as that of the forward sweep as shown in Figure 4.5. The thixotropic index is calculated using Equation (4.1). As discussed in Section 4.2, the time dependent behaviour is analysed by calculating the thixotropic index between the forward sweep and the backward sweep of the first cycle in the $SWSSRS_{DSR}$ and is denoted as $TI\text{-}1_{DSR}$. The effect of shear history is analysed by calculating the thixotropic index between the first forward sweep and the second backward sweep in the $SWSSRS_{DSR}$ test and is

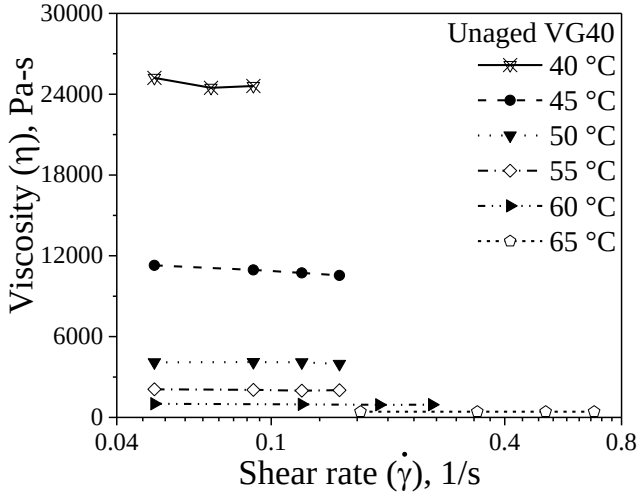

Fig. 4.21 Viscosity at '$t_{s(DSR)}$' as a function of shear rate in the first forward sweep of $SWSSRS_{DSR}$ test for the unaged VG40 bitumen

denoted as TI-2_{DSR}. The magnitudes of the thixotropic indices for the all the test conditions is shown in Table 4.21 and 4.22 for the VG20 and VG40 bitumen, respectively. The thixotropic indices, TI-1_{DSR} and TI-2_{DSR}, are observed to be less than 5% for most of the cases except for the stiffest binder, i.e., long-term aged bitumen at lower temperatures. From Tables 4.21 and 4.22 it is observed that the TI-1_{DSR} values are always less than 5% for the unaged, short-term aged and the long-term aged VG20 and VG40 binders at all the test temperatures except for the long-term aged VG40 binder at 50 °C. Overall, the above results show that both the unaged and short-term aged binders did not show a time dependent shear thinning response during the first cycle backward sweep. On the other hand, the TI-2_{DSR} values are also less than 5% for almost all the cases except at temperatures of 40, 45 and 50 °C for the short-term aged VG40 binder, at 50 °C for the long-term aged VG20 binder and at 50 and, 55 °C for the long-term aged VG40 binder. This is due to the start of edge failure at these temperatures during the final stages of the second cycle backward sweep in the stepwise shear sweep protocol. This is possibly due to the high viscosity of the short-term aged and long-term aged VG40 binders at these lower test temperatures. The TI-1_{DSR} and TI-2_{DSR} for the long-term aged VG20 and VG40 at 40 and 45 °C is not determined because at these test temperatures only the first forward sweep could be applied. Thus, from the overall observations as listed above, it can be concluded that the response of the unaged, short-term aged and long-term aged VG20 and VG40 binders is time independent in the first cycle backward sweep and also shear history has negligible effect on the response of the unaged, short-term aged and long-term aged VG20 and VG40 binders.. Thus, thus the Newtonian viscosities measured at '$t_{s(DSR)}$' at different shear rates in the first forward sweep are averaged and reported as a single viscosity. For the long-term aged VG20 and VG40 binders tested at 40 and 45 °C, the viscosity at '$t_{s(DSR)}$' before edge failure is alone considered.

Table 4.21 Thixotropic Index (%) with DSR for VG20 bitumen

Temp., °C	**Unaged**		**Short-term aged**		**Long-term aged**	
	TI-1_{DSR}	**TI-2_{DSR}**	**TI-1_{DSR}**	**TI-2_{DSR}**	**TI-1_{DSR}**	**TI-2_{DSR}**
40	0.837	0.481	2.063	4.350	-	-
45	0.233	1.278	0.567	0.169	-	-
50	2.735	3.780	0.431	0.816	4.262	12.021
55	1.699	0.033	0.046	1.241	0.675	1.938
60	1.464	0.219	0.694	0.686	0.681	0.725
65	3.574	3.118	0.157	0.303	1.068	2.728

As discussed earlier, the lower and upper limits of the shear rates in the SWSSRS test correspond to the low shear rate regime where the ZSV is generally determined. Thus the viscosity obtained from the SWSSRS test can be considered as a ZSV and is proposed as a rutting parameter. As ZSV of the bitumen binders is also measured from the $SWSSRS_{RV}$ test and LSRS test, the ZSV measured from $SWSSRS_{DSR}$ test is henceforth denoted as $\eta_{0(\text{S-DSR})}$ (here S-DSR represents the $SWSSRS_{DSR}$ test). The $\eta_{0(\text{S-DSR})}$ determined at all the test temperatures and aging conditions for the VG20 and VG40 bitumen is shown in Table 4.23 and the variation of $\eta_{0(\text{S-DSR})}$ as a function of temeprature is shown in Figure 4.22.

Table 4.22 Thixotropic Index (%) with DSR for VG40 bitumen

Temp., °C	**Unaged**		**Short-term aged**		**Long-term aged**	
	TI-1$_{DSR}$	**TI-2$_{DSR}$**	**TI-1$_{DSR}$**	**TI-2$_{DSR}$**	**TI-1$_{DSR}$**	**TI-2$_{DSR}$**
40	1.533	3.043	4.122	7.453	-	-
45	0.879	2.901	2.848	7.348	-	-
50	0.984	0.090	2.017	7.613	7.886	10.667
55	0.866	1.857	0.540	1.541	1.886	8.651
60	3.093	2.124	1.054	0.495	0.292	5.322
65	1.592	2.584	0.053	2.103	0.465	1.835

Higher the $\eta_{0(\text{S-DSR})}$, higher will be the rutting resistance. From Table 4.23 it is observed that there is a decrease in $\eta_{0(\text{S-DSR})}$ with an increase in temperature. This is attributed to the decrease in inter molecular attraction of the components of bitumen due to an increase in temperature which leads to a decrease in viscosity. It is observed that there is a decrease in $\eta_{0(\text{S-DSR})}$ by an average of 97% when the temperature increases from 40 to 65 °C at all aging conditions for both VG20 and VG40 bitumen. Moreover, it is observed that, at a particular temperature, there is an increase in $\eta_{0(\text{S-DSR})}$ with bitumen aging. The impact of aging and its mechanism has already been discussed. It is observed that there is an increase in $\eta_{0(\text{S-DSR})}$ of the short-term aged VG20 and VG40 bitumen by almost 2.1 and 2.9 times respectively at all test temperatures when compared with $\eta_{0(\text{S-DSR})}$ of unaged bitumen, whereas, the increase in $\eta_{0(\text{S-DSR})}$ of the long-term aged bitumen varies from 10.8 times at 40 °C to 17.0 times at 65 °C when compared with $\eta_{0(\text{S-DSR})}$ of unaged bitumen. Moreover, it is observed that the $\eta_{0(\text{S-DSR})}$ of the VG40 binder is on an average 3.16 times the $\eta_{0(\text{S-DSR})}$ of VG20 bitumen at all temperatures and aging conditions.

Table 4.23 $\eta_{0(\text{S-DSR})}$ (Pa-s) for VG20 and VG40 binders

Temp., °C	VG20			VG40		
	Unaged	Short-term aged	Long-term aged	Unaged	Short-term aged	Long-term aged
40	8605	28022	293500	24762	112188	1135943
45	3650	10114	128824	10878	38665	454819
50	1802	4335	28946	4065	15949	91542
55	858	2061	10435	2037	6227	31746
60	346	864	5237	964	2858	15276
65	197	374	2500	424	1190	6159

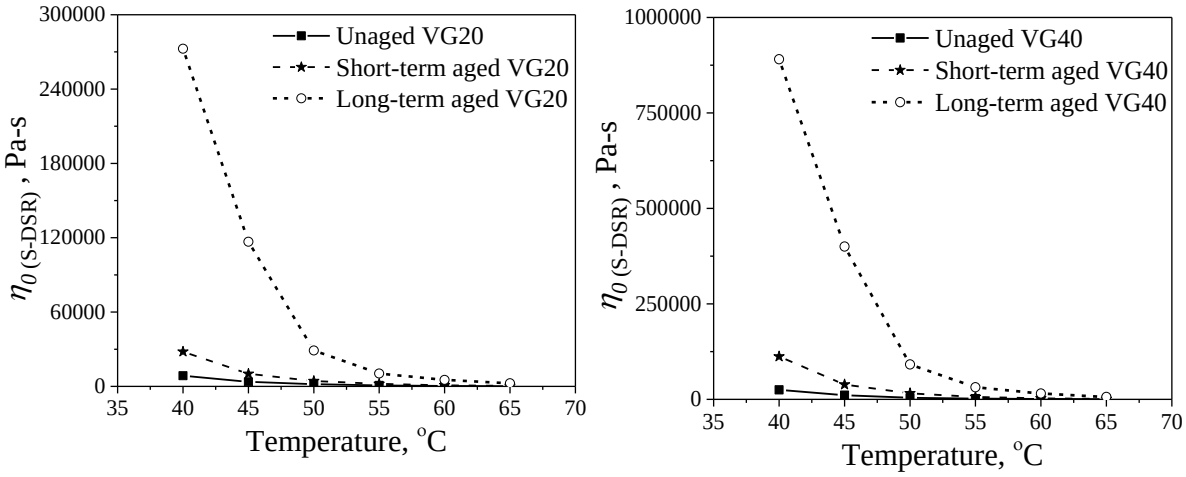

Fig. 4.22 $\eta_{0(\text{S-DSR})}$ as a function of temperature for the binders

4.3.4 Amplitude Sweep and Multi Stress Creep and Recovery Tests

In order to evaluate the newly proposed non-Newtonian viscosity, η_{TV} from LSRS test and a new Newtonian viscosity, $\eta_{0(\text{S-DSR})}$ as rutting parameters, $|G^*|/\sin\delta$, $|G^*|/(1-(1/\tan\delta\sin\delta))$ and J_{nr} at 3.2 kPa are determined. $|G^*|/\sin\delta$ and $|G^*|/(1-(1/\tan\delta\sin\delta))$ are determined by conducting amplitude sweep tests on the unaged, short-term aged and long-term aged VG20 and VG40 bitumen and the procedure of which is detailed in Section 3.6.4. The target strain levels at which $|G^*|/\sin\delta$ and $|G^*|/(1-(1/\tan\delta\sin\delta))$ are determined is provided in ASTM D7175 (ASTM, 2015*c*). For the unaged and short-term aged VG20 and VG40 bitumen, the target strain levels are 12% and 10% respectively. Since ASTM D7175 (ASTM, 2015*c*) does not provide a target strain level to determine the rutting parameter for the long-term aged bitumen, in this study $|G^*|/\sin\delta$ and $|G^*|/(1-(1/\tan\delta\sin\delta))$ of the long-term aged VG20 and VG40 bitumen are determined at 10% strain. The $|G^*|/\sin\delta$ and $|G^*|/(1-(1/\tan\delta\sin\delta))$ of the unaged, short-term aged and long-term aged VG20 and VG40 bitumen binder is shown in Tables 4.24 and 4.25, respectively, and their variation as a function of temperature is shown in Figures 4.23 and

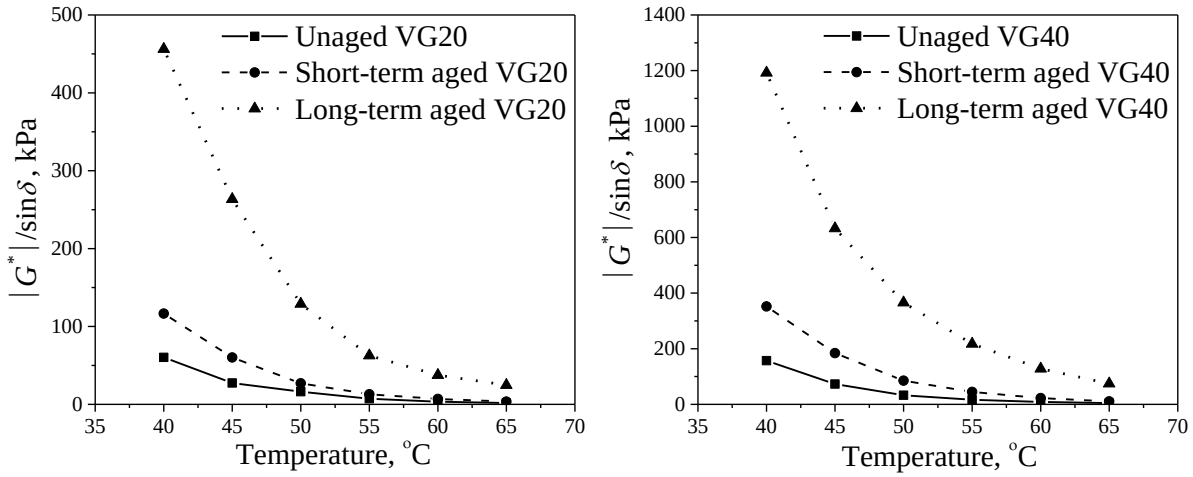

Fig. 4.23 Variation of $|G^*|/\sin\delta$ as function of temperature

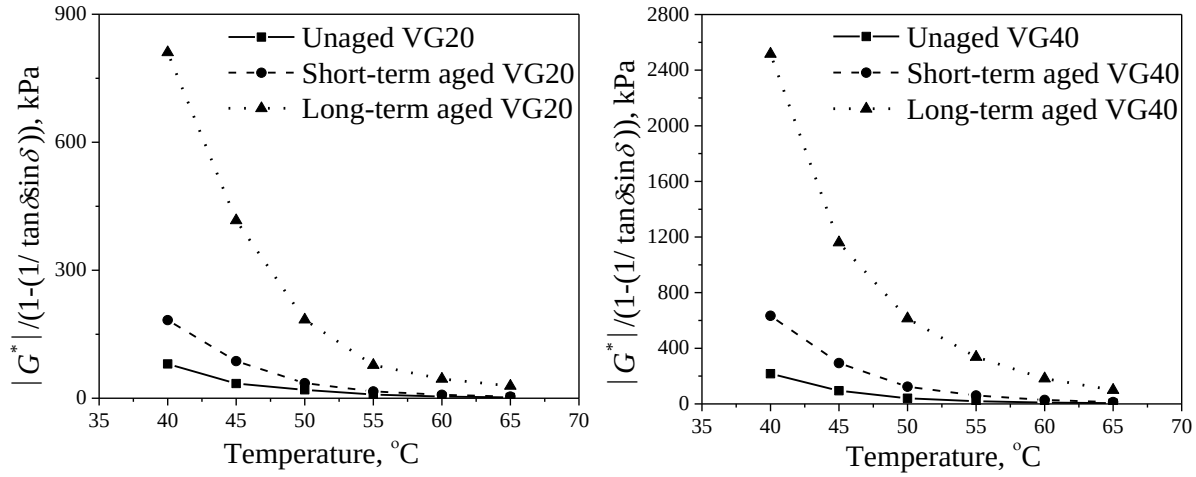

Fig. 4.24 Variation of $|G^*|/(1-(1/\tan\delta\sin\delta))$ as function of temperature

4.24, respectively. Higher the $|G^*|/\sin\delta$ and $|G^*|/(1-(1/\tan\delta\sin\delta))$, higher is the resistance towards rutting. From Tables 4.24 and 4.25 and Figures 4.23 and 4.24, it is observed that there is a decrease in $|G^*|/\sin\delta$ and $|G^*|/(1-(1/\tan\delta\sin\delta))$ with an increase in temperature which is on expected lines. It is observed that there is a decrease in $|G^*|/\sin\delta$ and $|G^*|/(1-(1/\tan\delta\sin\delta))$ by 97% when the temperature increases from 40 to 65 °C at all aging conditions for both VG20 and VG40 bitumen. Moreover, it is observed that, at a particular temperature, there is an increase in $|G^*|/\sin\delta$ and $|G^*|/(1-(1/\tan\delta\sin\delta))$ with bitumen aging. It is observed that there is an increase in $|G^*|/\sin\delta$ and $|G^*|/(1-(1/\tan\delta\sin\delta))$ of the short-term aged VG20 and VG40 bitumen by almost 2.1 and 2.7 times respectively at all test temperatures when compared with $|G^*|/\sin\delta$ and $|G^*|/(1-(1/\tan\delta\sin\delta))$ of the unaged bitumen, whereas, the increase in $|G^*|/\sin\delta$ and $|G^*|/(1-(1/\tan\delta\sin\delta))$ of the long-term aged bitumen is 7.6 times at 40 °C and gradually increases to 15.0 times at 65 °C when compared with $|G^*|/\sin\delta$ and $|G^*|/(1-(1/\tan\delta\sin\delta))$ of the unaged bitumen. Moreover, it is observed that the $|G^*|/\sin\delta$ and $|G^*|/(1-(1/\tan\delta\sin\delta))$ of the VG40 binder is on an average 2.86 and 3.16 times the $|G^*|/\sin\delta$ and $|G^*|/(1-(1/\tan\delta\sin\delta))$

respectively of VG20 bitumen at all temperatures and aging conditions. These observations indicate that the aging improves the rutting performance of bitumen binders by offering an increased resistance towards permanent deformation. Also, the VG40 binder offers a higher resistance towards rutting than VG20 binder at all temperatures and aging conditions.

Table 4.24 $|G^*|/\sin\delta$, kPa

Temp., °C	Unaged		Short-term aged		Long-term aged	
	VG20	VG40	VG20	VG40	VG20	VG40
40	60.33	156.98	116.55	352.02	456.23	1192.13
45	27.43	73.14	60.16	184.40	263.39	632.57
50	16.18	32.95	27.01	85.39	129.00	365.94
55	7.29	16.37	12.95	44.84	62.59	217.56
60	3.45	8.87	6.91	22.38	37.58	127.88
65	1.74	4.74	3.56	10.57	24.77	74.69

Table 4.25 Shenoy's rutting parameter

Temp., °C	$\|G^*\|/(1-(1/\tan\delta\sin\delta))$, kPa					
	Unaged		Short-term aged		Long-term aged	
	VG20	VG40	VG20	VG40	VG20	VG40
40	80.46	216.71	183.13	633.90	810.64	2516.52
45	34.31	94.58	86.99	293.74	416.67	1160.31
50	19.73	40.63	35.30	124.18	183.97	613.66
55	8.56	19.24	15.93	60.72	77.63	337.33
60	3.86	10.14	8.13	28.60	45.11	181.88
65	1.92	5.26	4.03	12.74	28.82	99.46

J_{nr} at 3.2 kPa is determined by conducting the MSCR test on the unaged, short-term aged and long-term aged VG20 and VG40 bitumen. The details of the MSCR test protocol are discussed in Section 3.6.5. The average of the non-recoverable creep compliance from the 10 cycles of creep and recovery at a stress level of 3.2 kPa is reported as the J_{nr} at 3.2 kPa. The J_{nr} at 3.2 kPa of the unaged, short-term aged and long-term aged VG20 and VG40 bitumen are shown in Table 4.26 and Figure 4.25. Lower the J_{nr} at 3.2 kPa higher is the resistance towards rutting. From Table 4.26 it is observed that there is an increase in J_{nr} at 3.2 kPa with an increase in temperature. It is observed that the increase in J_{nr} at 3.2 kPa when temperature increases from 40 to 65 is by 63, 112 and 237 times for the unaged, short-term aged and long-term aged condition for the VG20 and VG40 binders. This drastic increase in J_{nr} at 3.2 kPa again consolidates the fact that bitumen is a material that is highly susceptible to temperature. The increase in J_{nr} at 3.2 kPa with an increase in temperature results in a decrease in the resistance offered towards rutting. As observed previously, at a particular temperature there is

a decrease in J_{nr} at 3.2 kPa with bitumen aging which is desirable when rutting resistance is concerned. It is observed that the decrease in J_{nr} at 3.2 kPa for the short-term aged VG20 and VG40 bitumen varies from 3.83 times at 40 °C to 2.12 times at 65 °C whereas the decrease in J_{nr} at 3.2 kPa for the long-term aged VG20 and VG40 bitumen varies from 42.7 times at 40 °C to 11.3 times at 65 °C. The J_{nr} at 3.2 kPa for VG40 bitumen decreases by an average of 3.56 times to that of VG20 bitumen at all temperatures and aging conditions.

Table 4.26 J_{nr} at 3.2 kPa (1/kPa)

Temp., °C	Unaged		Short-term aged		Long-term aged	
	VG20	VG40	VG20	VG40	VG20	VG40
40	0.0918	0.0292	0.0278	0.0067	0.0021	0.0007
45	0.2645	0.0704	0.0917	0.0178	0.0080	0.0027
50	0.6177	0.1992	0.2229	0.0702	0.0276	0.0083
55	1.4881	0.4067	0.5442	0.1247	0.0875	0.0241
60	2.7113	0.9331	1.2659	0.3533	0.2504	0.0598
65	5.7606	1.8203	2.8722	0.8178	0.5338	0.1551

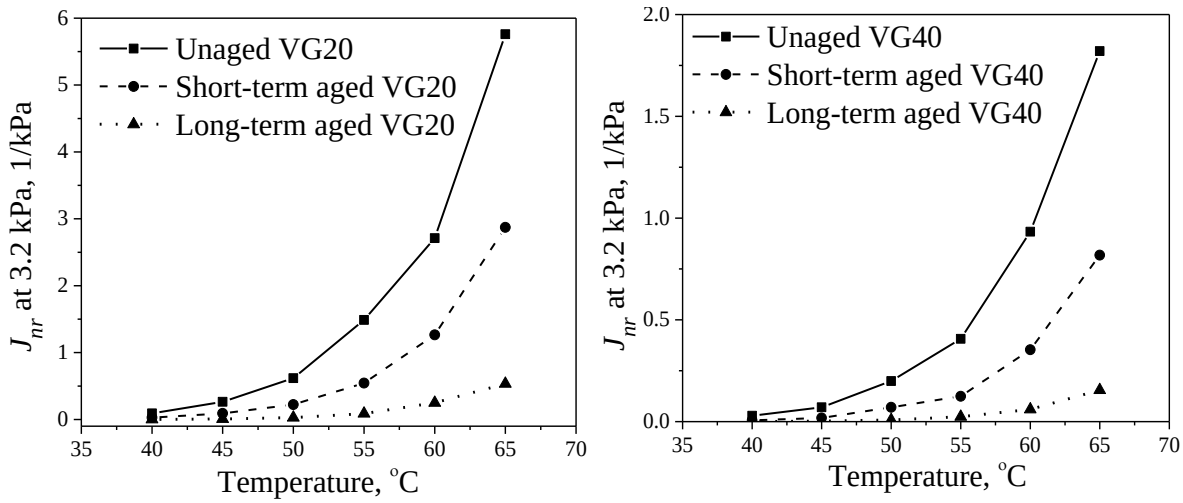

Fig. 4.25 J_{nr} at 3.2 kPa as a function of temperature

4.4 CORRELTIONS BETWEEN RUTTING PARAMETERS

A total of six rutting parameters are determined in this research study including η_{TV} and $\eta_{0(L)}$ from LSRS test, $\eta_{0(S\text{-}RV)}$ and $\eta_{0(S\text{-}DSR)}$ from $SWSSRS_{RV}$ and $SWSSRS_{DSR}$ test respectively, $|G^*|/\sin\delta$ and $|G^*|/(1-(1/\tan\delta\sin\delta))$ from amplitude sweep test and J_{nr} at 3.2 kPa from MSCR test. Relationships are developed between the new rutting parameters and the existing rutting parameters.

4.4.1 Relationship of $\eta_{0(S\text{-}RV)}$ from $SWSSRS_{RV}$ with $|G^*|/\sin\delta$, $|G^*|/(1-(1/\tan\delta\sin\delta))$ and J_{nr} at 3.2 kPa

Relationships are developed between the $\eta_{0(S\text{-}RV)}$ and the three existing rutting parameters $|G^*|/\sin\delta$, $|G^*|/(1-(1/\tan\delta\sin\delta))$ and J_{nr} at 3.2 kPa as shown in Figure 4.26. These relationships can be used to determine $|G^*|/\sin\delta$, $|G^*|/(1-(1/\tan\delta\sin\delta))$ and J_{nr} at 3.2 kPa from $\eta_{0(S\text{-}RV)}$. From Figure 4.26 it observed that the relationship of $\eta_{0(S\text{-}RV)}$ with J_{nr} at 3.2 kPa is strongest with an R^2 of 0.99 followed by $|G^*|/(1-(1/\tan\delta\sin\delta))$ and $|G^*|/\sin\delta$ respectively with an R^2 value of 0.93 and 0.93, respectively. This may be attributed to the fact that $|G^*|/\sin\delta$ and $|G^*|/(1-(1/\tan\delta\sin\delta))$ are determined in the linear regime whereas J_{nr} at 3.2 kPa and $\eta_{0(S\text{-}RV)}$ belong to the non-linear response of bitumen. It is to be noted here that $\eta_{0(S\text{-}RV)}$ is determined in the Newtonian region after the observation of a non-Newtonian response. These relationships can be used to determine $|G^*|/\sin\delta$, $|G^*|/(1-(1/\tan\delta\sin\delta))$ and J_{nr} at 3.2 kPa even in the absence of the DSR from the Equations (4.4) to (4.6). The procedure to grade bitumen binders by their performance is laid specified in ASTM D6373-16 (ASTM, 2016*b*). Performance graded bitumen binders are denoted as PGA -B, where A represents the average seven day maximum pavement temperature and B represents the minimum pavement temperature, which satisfy the minimum requirements as specified in ASTM D6373-16. $|G^*|/\sin\delta$ has a minimum specified value of 1.0 kPa and 2.2 kPa for unaged and short-term aged PG binders respectively corresponding to the maximum temperature in the PG grading system. By using the relationships established between the $\eta_{0(S\text{-}RV)}$ and $|G^*|/\sin\delta$, $\eta_{0(S\text{-}RV)}$ values corresponding to a $|G^*|/\sin\delta$ of 1.0 kPa and 2.2 kPa are 38.7 Pa-s and 101.8 Pa-s. Similarly, the $\eta_{0(S\text{-}RV)}$ values corresponding to a $|G^*|/(1-(1/\tan\delta\sin\delta))$ of 1.0 kPa and 2.2 kPa are 36.3 Pa-s and 90.9 Pa-s. By using these minimum values of $\eta_{0(S\text{-}RV)}$ one can determine the corresponding highest temperature PG grading system even in the absence of a DSR.

$$|G^*|/\sin\delta = 0.0512\ (\eta_{0(S\text{-}RV)})^{0.814} \tag{4.4}$$

$$|G^*|/(1-(1/\tan\delta\sin\delta)) = 0.0458\ (\eta_{0(S\text{-}RV)})^{0.859} \tag{4.5}$$

$$J_{nr}\text{ at 3.2 kPa} = 160.178\ (\eta_{0(S\text{-}RV)})^{-0.777} \tag{4.6}$$

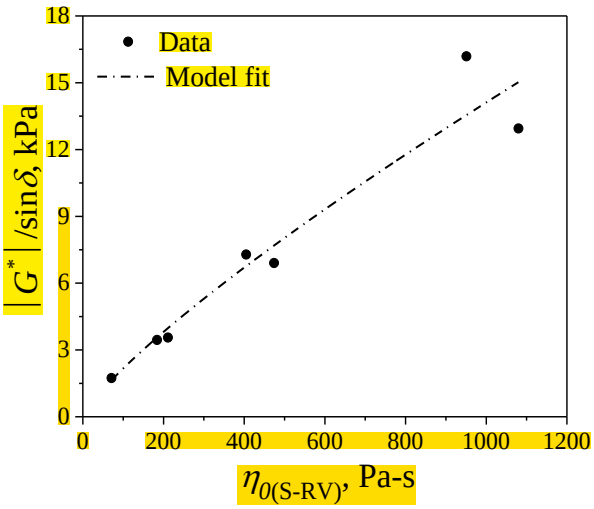

(a) $R^2 = 0.93$

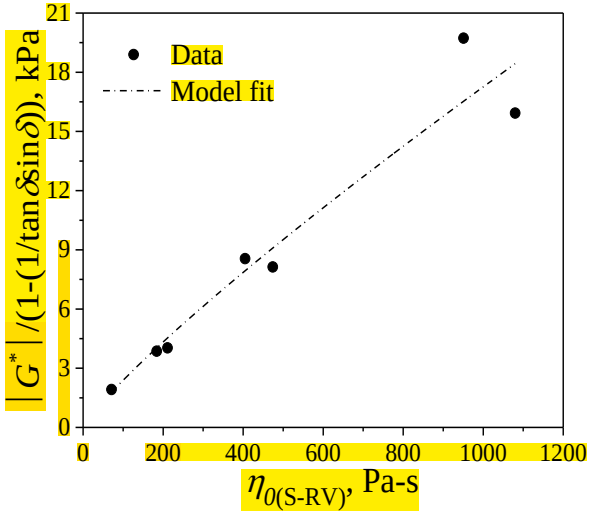

(b) $R^2 = 0.93$

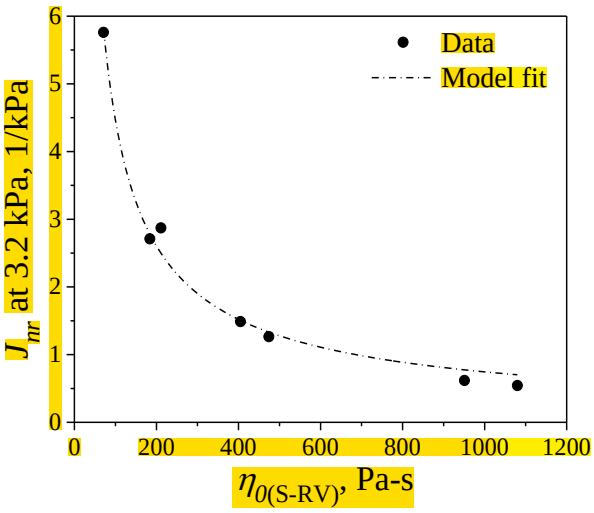

(c) $R^2 = 0.99$

Fig. 4.26 Relationship of $\eta_{0(S\text{-}RV)}$ with (a) $|G^*|/\sin\delta$, (b) $|G^*|/(1-(1/\tan\delta\sin\delta))$ and (c) J_{nr} at 3.2 kPa for the VG20 binder

4.4.2 Relationships of $\eta_{0(S\text{-}DSR)}$ from $SWSSRS_{DSR}$ and η_{TV} with other Rutting Parameters

Correlation of $\eta_{0(S\text{-}DSR)}$ from the $SWSSRS_{DSR}$ test with $|G^*|/\sin\delta$, $G^*/(1-(1/\tan\delta\sin\delta))$ and J_{nr} at 3.2 kPa are shown in Figure 4.27. From Figure 4.27 it observed that the relationship of $\eta_{0(S\text{-}DSR)}$ with J_{nr} at 3.2 kPa is strongest with an R^2 of 0.98 followed by $|G^*|/(1-(1/\tan\delta\sin\delta))$ and $|G^*|/\sin\delta$ respectively with an R^2 value of 0.96 and 0.93. Similar to the correlations in the previous section, this may be attributed to the fact that $|G^*|/\sin\delta$ and $|G^*|/(1-(1/\tan\delta\sin\delta))$ are determined in the linear regime whereas J_{nr} at 3.2 kPa and $\eta_{0(S\text{-}DSR)}$ belong to the non-linear response of bitumen.

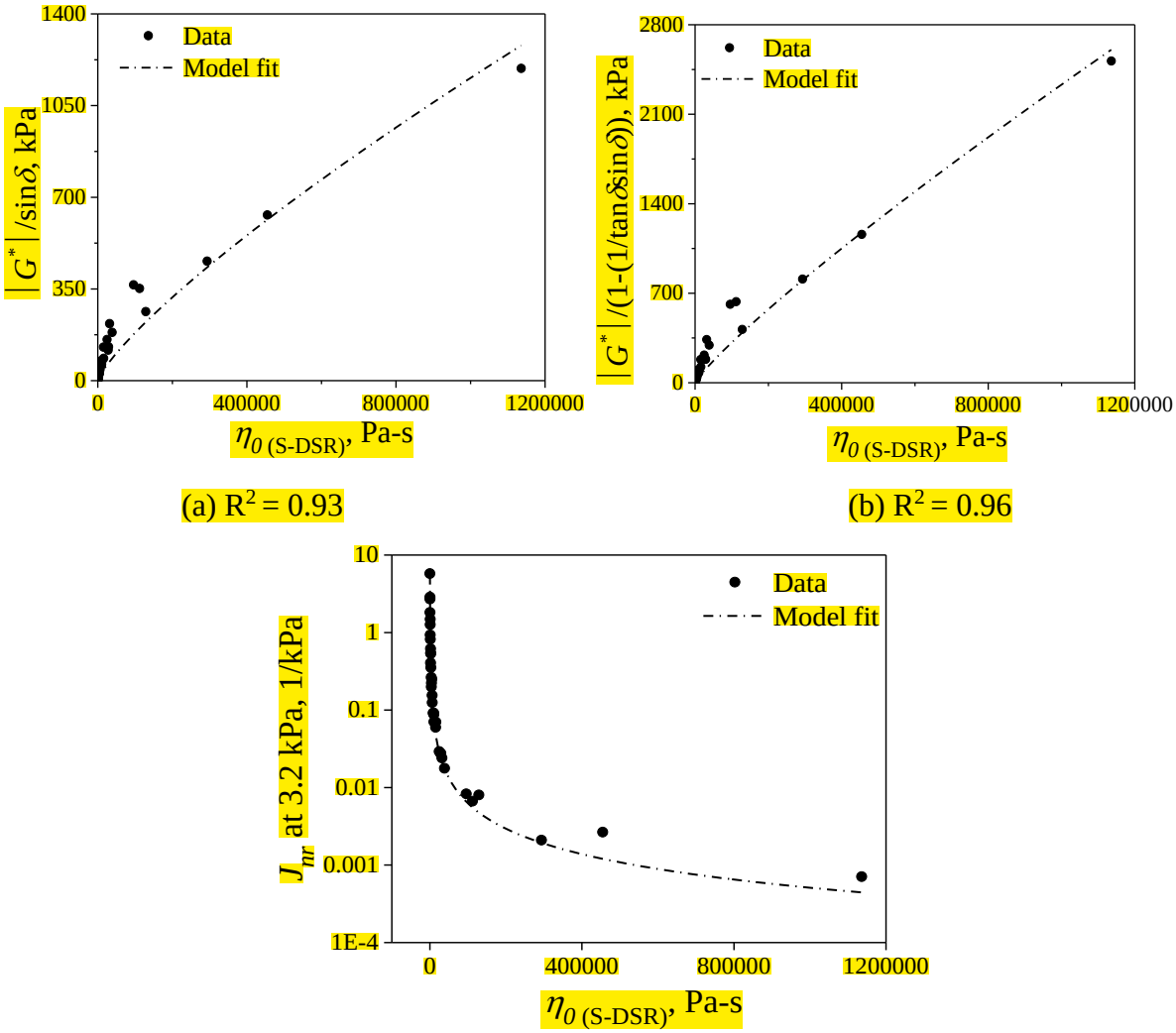

(a) $R^2 = 0.93$ (b) $R^2 = 0.96$

(c) $R^2 = 0.98$

Fig. 4.27 Relationship of $\eta_{0(S\text{-}DSR)}$ with (a) $|G^*|/\sin\delta$, (b) $|G^*|/(1-(1/\tan\delta\sin\delta))$ and (c) J_{nr} at 3.2 kPa

In the Chapter 2, the J_{nr} at 3.2 kPa is shown to be better at characterizing the unrecovered strain and subsequently the delayed elastic response in bitumen. Because of a strong relationship between $\eta_{0(S\text{-}DSR)}$ (from $SWSSRS_{DSR}$ test) and J_{nr} at 3.2 kPa, it can be inferred that the $\eta_{0(S\text{-}DSR)}$ is also capable of the same and can be considered as an improvement over the $|G^*|/\sin\delta$ and $|G^*|/(1-(1/\tan\delta\sin\delta))$. The minimum $\eta_{0(S\text{-}DSR)}$ value when the binder $|G^*|/\sin\delta$ is 1 kPa and 2.2 kPa are 136 Pa-s and 368 Pa-s, respectively. Similarly, the values of $\eta_{0(S\text{-}DSR)}$ when binder $|G^*|/(1-(1/\tan\delta\sin\delta))$ is at 1 kPa and 2.2 kPa are 125 Pa-s and 303 Pa-s, respectively.

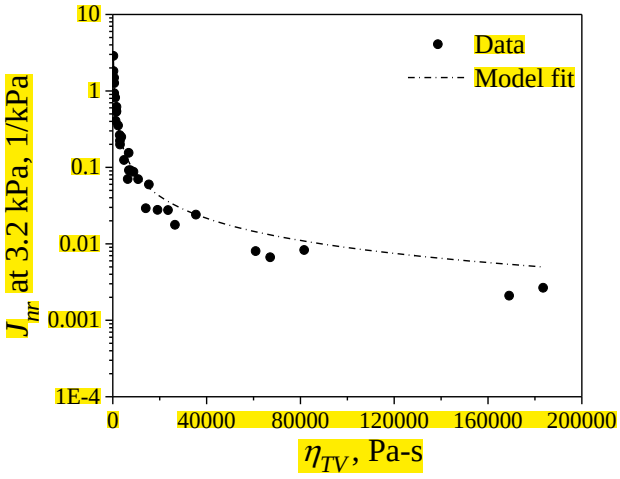

(R^2 = 0.96)

Fig. 4.28 Relationship of η_{TV} with J_{nr} at 3.2 kPa

The relationship of η_{TV} with J_{nr} at 3.2 kPa is shown in Figure 4.28. Since, η_{TV} is determined from the non-Newtonian response of the bitumen from the LSRS test, it is correlated only with the non-linear J_{nr} at 3.2 kPa. From Figure 4.28, it is observed that a strong relationship exists between η_{TV} and J_{nr} at 3.2 kPa with an R^2 of 0.98. Currently J_{nr} at 3.2 kPa is the most popular rutting parameter. In this research study, two new bitumen properties ($\eta_{0(\text{S-DSR})}$ and η_{TV}) are identified and are proposed as rutting parameters. It has been shown that there exists a strong correlation between $\eta_{0(\text{S-DSR})}$ and J_{nr} at 3.2 kPa and also between η_{TV} and J_{nr} at 3.2 kPa. This strong correlation provides an initial support to the use of $\eta_{0(\text{S-DSR})}$ and η_{TV} as possible rutting parameters.

4.5 SUMMARY

It has been seen that the response of bitumen is time dependent and shear rate dependent. In order to overcome the time dependent and shear rate dependent response of bitumen binders, in this chapter, the non-Newtonian characterization of the VG20 and the VG40 bitumen binders is carried out. Firstly, RV is used to study the non-Newtonian behaviour of the unaged VG20 and VG40 binder and the short-term aged VG20 binder by conducting a $\text{SWSSRS}_{\text{RV}}$ test protocol. The identification of 't_s' and its use in the $\text{SWSSRS}_{\text{RV}}$ is able to convert the time and shear rate dependent response to a time independent and shear rate independent response. The adopted protocol is analyzed and a new Newtonian parameter is developed which is termed as $\eta_{0(\text{S-RV})}$. Subsequently, the LSRS test protocol is adopted to capture the three phased response of viscosity as a function of shear rate. However, the response of bitumen to LSRS is in stark contrast to the expected response, wherein, a multi phased Newtonian and non-Newtonian response is observed. At very low shear rates the response is Newtonian as seen

by the appearance of a plateau region whereas with an increase in shear rate the response becomes non-Newtonian exhibiting a shear thickening response followed by a two stage shear thinning response. Even though such responses are reported in the past by some of the researchers for modified binders, such response is also characterized for unmodified unaged and aged binders in this research study. From the LSRS test, a new non-Newtonian parameter (η_{TV}) is proposed as a rutting parameter. In addition to η_{TV}, a Newtonian parameter, $\eta_{0(L)}$ is also determined from the primary Newtonian plateau.

In order to overcome the limitations encountered with the use of RV at specific aging conditions and temperatures and more so to convert the non-Newtonian response observed with the LSRS test, the non-Newtonian characterization of the unaged, short-term aged and long-term aged VG20 and VG40 binders is carried out using a DSR. A protocol similar to $SWSSRS_{RV}$ test, that is, $SWSSRS_{DSR}$ test protocol is adopted. With the identification of 't_s' and its subsequent use in the $SWSSRS_{DSR}$ test protocol, it is observed that the viscosity at 't_s' in the first forward sweep stays in the ZSV regime. Moreover, the response is shown to be independent of time and shear history. Thus, $\eta_{0(S\text{-}DSR)}$ is proposed as an alternative ZSV. In order to compare the two new rutting parameters, three existing rutting parameters namely $|G^*|/\sin\delta$, $|G^*|/(1-(1/\tan\delta\sin\delta))$ and J_{nr} at 3.2 kPa are determined by conducting parameter related standard tests.

Table 4.27 shows the comparison of viscosities from the original Cannon Manning U-tube, $\eta_{0(S\text{-}RV)}$ and $\eta_{0(S\text{-}DSR)}$ for the unaged VG20 bitumen (Barrel 1) at 60 °C. Viscosity measurement from the U-tube is based upon the flow of material whereas $\eta_{0(S\text{-}RV)}$ and $\eta_{0(S\text{-}DSR)}$ are measured after shearing the material. From Table 4.27, it is observed that viscosity from U-tube is similar to $\eta_{0(S\text{-}RV)}$, whereas $\eta_{0(S\text{-}DSR)}$ is 1.87 times $\eta_{0(S\text{-}RV)}$.

Table 4.27 Viscosities from CM U-tube, $\eta_{0(S\text{-}RV)}$ and $\eta_{0(S\text{-}DSR)}$ for the unaged VG20 bitumen

Viscosity, Poise	**C-M U-tube**	**$\eta_{0(S\text{-}RV)}$**	**$\eta_{0(S\text{-}DSR)}$**
	1606	1848	3460

CHAPTER-5

CHARACTERIZATION OF PERMANENT DEFORMATION IN DENSE BITUMINOUS MIXTURES

5.1 GENERAL

As discussed earlier, BC and DBM are the most commonly used bituminous courses in flexible pavements on Indian highways. BC is preferred in wearing (surface) courses whereas DBM is used as a binder course which is directly below the wearing course. Moreover, it has also been discussed that rutting can occur in any or all the layers of a flexible pavement (Garba, 2002) but most the rutting occurs in bituminous courses (Brown and Cross, 1989). Further, the total rutting in bituminous layers is the combined accumulated permanent deformation in the wearing (surface) course and the binder course making it important to characterize the permanent deformation in both the wearing and the binder courses. Therefore, the BC and DBM bituminous mixtures became the mixtures of choice for the laboratory characterization of permanent deformation.

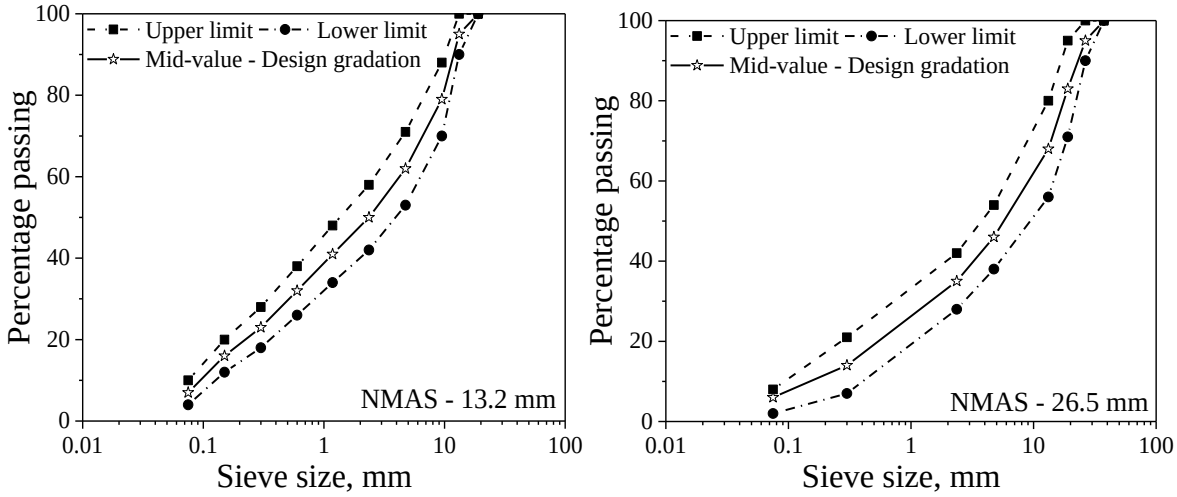

(a) (b)

Fig. 5.1 Gradation adopted for: (a) BC-2, and (b) DBM-2

For both the bituminous mixtures, type II mid gradation is adopted as the design gradation as shown in Figure 5.1. The same VG20 and VG40 binders are used along with the granite

aggregate to prepare BC2 and DBM2 bituminous mixtures. Popular methods of characterizing the rutting performance of bituminous mixtures in a laboratory include the flow number test, the dynamic modulus test, and wheel tracking tests (Azari and Mohseni, 2013). In this research study, the rutting performance of the BC2 and DBM2 bituminous mixtures prepared with VG20 and VG40 bitumen binders is conducted using a small wheel tracking device. The preliminary tests involved with the fabrication of the test specimens, the sample preparation and the analysis of the raw permanent deformation data are discussed in this chapter in the following sections.

5.2 PREPARATION OF BITUMINOUS MIXTURES

The PG pass/fail temperatures for the VG20 and VG40 bitumen are 68 and 76 °C respectively as shown in Figure B1 in Appendix B. The respective PG grade of the VG20 and VG40 bitumen is PG 64 and PG 76 respectively.

5.2.1 Mixing and Compaction Temperatures

The mixing and compaction temperatures of the VG20 and VG40 bitumen binders are determined as per the procedure specified in Section 3.7.1. The mixing temperatures of the VG20 and VG40 binders are 152 and 164 °C, respectively whereas, the compaction temperatures of the VG20 and VG40 binders are 140 and 150 °C, respectively. All the mixture samples with VG20 and VG40 binders are henceforth prepared at the respective mixing and compaction temperatures.

5.2.2 Determination of Optimum Binder Content (OBC)

The next step is to determine the OBC for the BC-2 and DBM-2 bituminous mixtures using the Marshall method of mix design which is described in Section 3.7.2. Marshall method of mix design is performed on the BC-2 and DMB-2 mixtures with VG20 binder. The OBCs for the BC-2 and DBM-2 mixtures with the VG20 binder are 5.7% and 4.5%, respectively. The other mixture parameters are shown in Table 5.1. Since, the viscosity of the both the binders will be same at their respective mixing and compaction temperatures, the binder content for the BC-2 and DBM-2 mixture with VG40 binder should remain same. In order to be on a safer side, air voids of BC-2 and DBM-2 specimens with VG40 binder prepared with a binder contents of 5.7% and 4.5%, respectively are determined using a CoreLok®. It is observed that the compacted BC-2 and DBM-2 mixtures with VG40 bitumen at a bitumen content of 5.7%

and 4.5% respectively resulted in 4% air voids. Therefore, 5.7% and 4.5% is considered as the OBC for the BC-2 and the DBM-2 mixtures with VG40 bitumen.

Table 5.1 OBC and mixture requirements

Parameter	BC-2		DBM-2	
	Measured values	**Specifications**	**Measured values**	**Specifications**
Binder Content, %	5.7	Min. 5.4	4.5	Min. 4.5
G_{mm}	2.448	-	2.479	-
G_{mb}	2.349	-	2.384	-
Air voids, %	4	3-5	4	3-5
Stability at 60 °C, kN	24.6	Min. 9	30.58	Min. 9
Flow,mm	3.05	2-4	2.49	2-4
% Voids filled with mineral aggregate (VMA)	16.21	Min. 12	13.96	Min. 11
% Voids filled with bitumen (VFB)	74.8	65-75	72.6	65-75

5.2.3 Fixing the Target Air Voids

As per the research objectives, wheel tracking tests are to be carried out on short-term aged (STA) and long-term aged (LTA) bituminous mixtures. The STA bituminous mixtures are to be prepared with 6% air voids and the LTA bituminous mixtures with 4% air voids. After following the core cutting procedure, as described in Section 3.7.6, the number of passes of the segmented steel wheeled roller compactor to fabricate BC-2 and DBM-2 mixtures with 6% and 4% air voids are (44 and 77) passes, and (90 and 180) passes, respectively. The wheel tracking tests are carried out on the specimens of STA and LTA BC-2 and DBM-2 bituminous mixtures prepared with VG20 and VG40 binders. The test temperatures are listed in Section 3.8.

5.2.4 Mixture Fabrication

The loose BC-2 and BDM-2 mixtures with the VG20 and VG40 bitumen binders are prepared at the required mixing and compaction temperatures by mixing granite aggregate with OBC. For the STA samples, the loose mixtures are conditioned in a FDO as specified in Section 3.7.5 and the slabs are compacted (as shown in Figure 3.14) after 4 hours at the target air voids of 6%. Similarly, the LTA BC-2 and DBM-2 mixture slabs are fabricated as specified in Section 3.7.7. All the slabs specimens are 300 x 300 mm in width and length with the

thickness depending upon the target density. All the slab specimens fabricated for the tests are kept in the mould for a period of 24 hours at room temperature and thereafter demoulded to perform the wheel tracking tests.

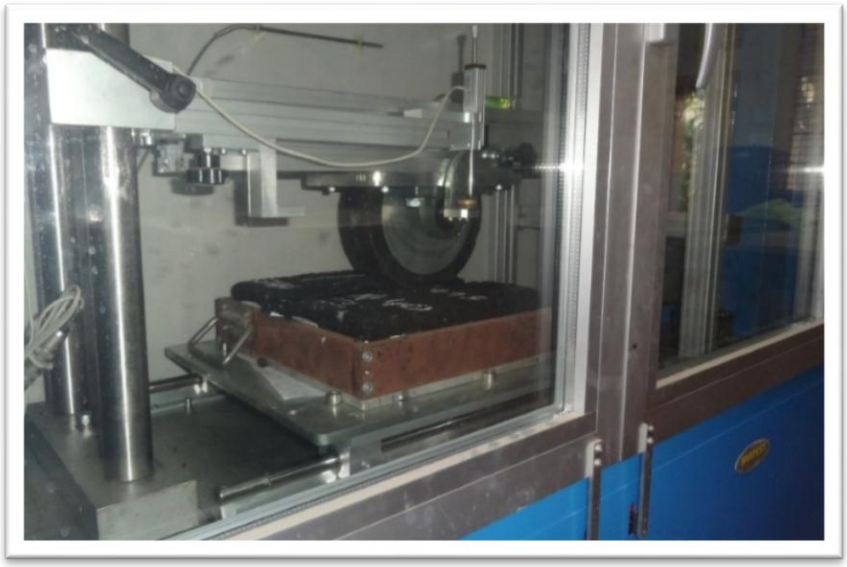

Fig. 5.2 Slab sample being tested in the wheel tracking machine

5.3 DRY WHEEL TRACKING TESTS

To evaluate the permanent deformation characteristics of the BC-2 and DBM-2 mixture slabs with VG20 and VG40 binders, a small wheel tracking machine conforming to EN 12697-22 (BS-EN, 2003) as shown in Figure 3.16 is used. The slabs are placed in the mould such that the direction of wheel tracking is same as that of the direction in which the slabs are compacted. The slabs prepared for testing are shown in Figure 3.12 and a slab being tested is shown in Figure 5.2. The specifications of the wheel tracking test are explained in the Section 3.8. The slabs are tested in the wheel tracking machine until a rut depth of 15 mm or 200,000 passes whichever is earlier.

5.3.1 Raw Permanent Deformation Data

Even though the wheel traverse on the slab is 230 ± 5 mm, the actual rut data is accumulated over a central distance of 104 mm at every 4 mm from the centre of the slab i.e., 27 rut curves are obtained along the central traverse of 104 mm on the slab. This accumulation of permanent deformation as a function of wheel passes is represented by a ‘rut curve’. Figure 5.3 shows the sample data of these 27 rut curves for the STA BC-2 mixture with VG20 binder

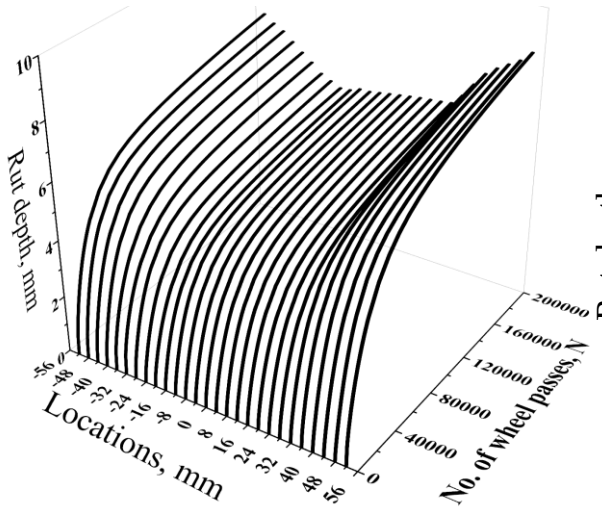

(a) 3-d View of STA BC-2 with VG20 at 40 °C

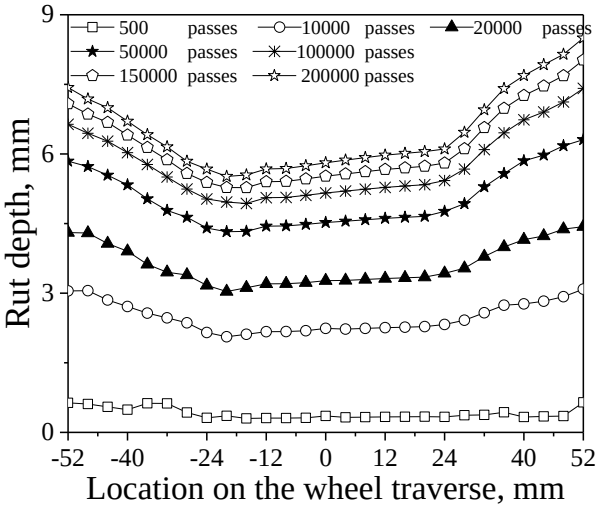

(b) Planar view of STA BC-2 with VG20 at 40 °C

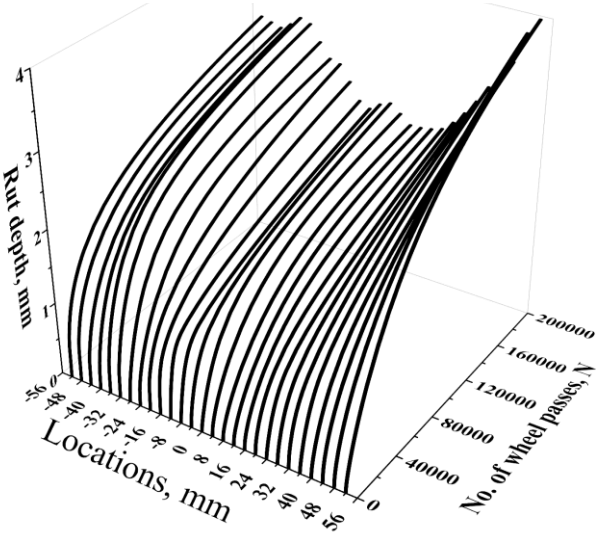

(c) 3-d View of LTA DBM2 with VG40 at 40 °C

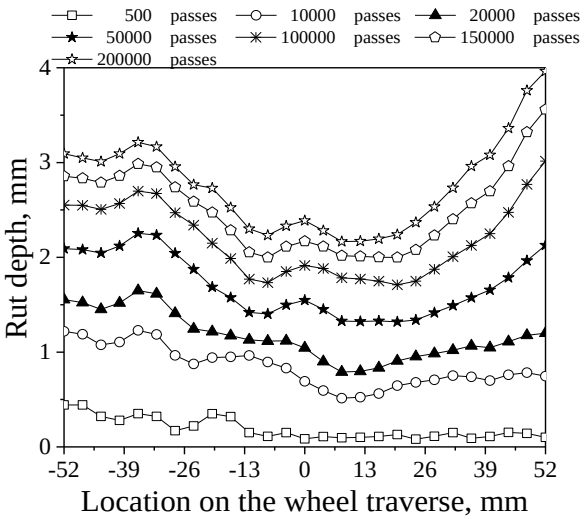

(d) Planar view of LTA DBM-2 with VG40 at 40 °C

Fig. 5.3 Variation of rut curves at 27 locations at 40 °C

and LTA DBM-2 mixture with VG40 binder at a temperature of 40 °C. The 3-d and the planar view of the rut data from Figure 5.3 clearly shows considerable scatter in the rut depth along the wheel traverse. Several methodologies are being currently practiced across the world to obtain a representative rut curve from the rut depth measured along the wheel traverse. In this research five such methodologies are compared that are as shown below:

1. Total average of all the 27 locations represented as “TA”,
2. The central location represented as “Centre”,

3. Averaging the rut data obtained from locations at -37.5, -23.5, -7.5, 0, 7.5, 23.5, 37.5 mm and represented as “AGPT” (Guide to Pavement Technology – Austoroads),
4. Averaging the rut data obtained from locations at -46, -23, 0, 23, 46 mm from Mohammed et al. (2017) and represented as “AASHTO”, and
5. The curve with highest rut depth represented as “High”

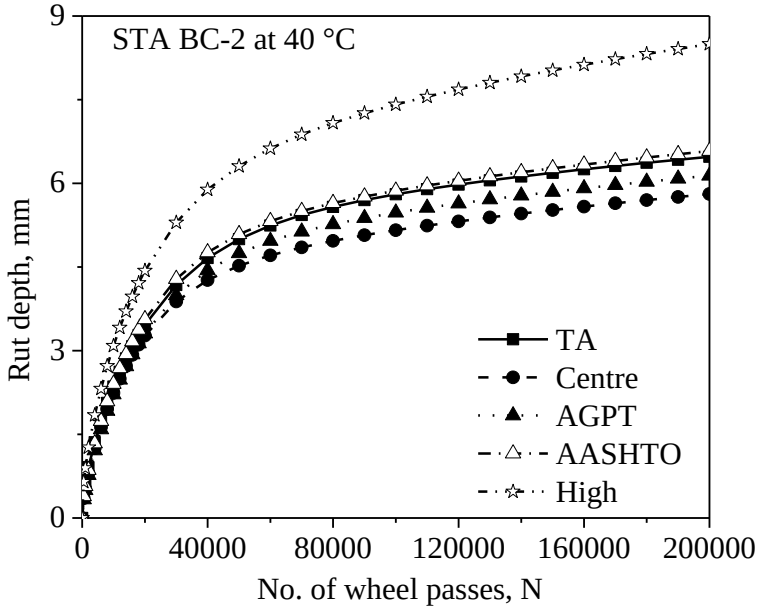

(a) VG20

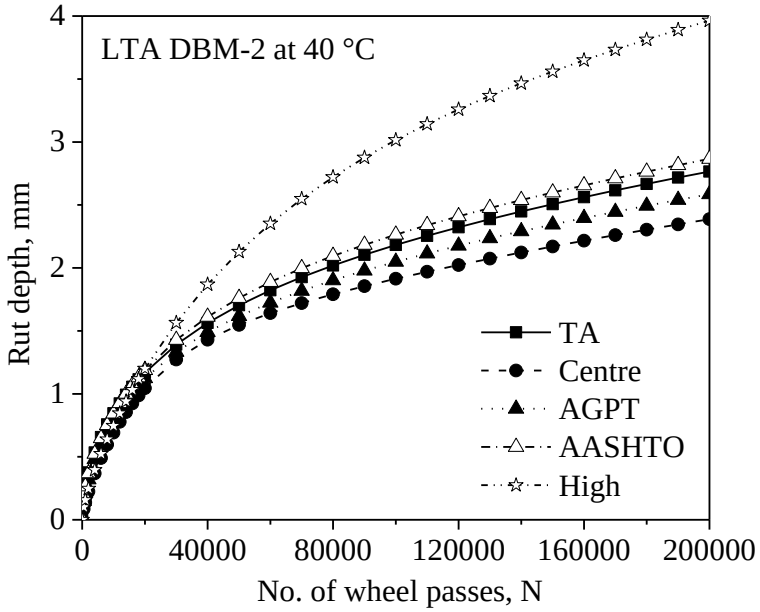

(b) VG40

Fig. 5.4 Rut curves obtained from the proposed five methodologies

A comparison of these rut curves obtained from the proposed methodologies at a test temperature of 40 °C for the STA BC-2 mixtures prepared with VG20 binder and the LTA DBM-2 mixtures prepared with VG40 binder are shown in Figure 5.4. From Figure 5.4, it is

clear that these five different methodologies again provide varying rut curves with significant scatter. Therefore, in order to have a better perspective while choosing one curve from the aforementioned five methodologies, it is necessary to analyse the data in a more comprehensive manner. For this, a procedure similar to the one adopted by Singh and Swamy (2018) is chosen and the data is analysed based upon the Model 2 of their work. Singh and Swamy (2018) analysed the rut depth scatter in identical specimens at a single temperature and developed probabilistic rutting curves at 50, 80, 90 and 99% reliability levels and then compared it with the mixture average rut depth. However, in the current study, the rut depth scatter among the 27 locations for a single sample is analysed. The analysis is done in a similar manner and probabilistic rutting curves are obtained at the four reliability levels including 50, 80, 90 and 99%. From Figure 5.4, it is observed that the AASHTO curve and the TA curve are similar. Henceforth, the TA curve is only considered hereafter. The probability curves obtained at the four reliability levels are compared with the rut curves designated as 'TA', 'Centre', 'AGPT' and 'High'.

5.3.2 Probabilistic Approach for the Analysis of Rut Data

5.3.2.1 *Statistical Analysis of the Rut Data*

The first step in analysing the scatter in the rut data at the 27 locations is to remove the noise in the rut data at all the twenty seven locations. For this, Francken model is used and smooth rut data is obtained at all locations. The Francken model form is shown in Equation (5.1). The data from all the twenty seven locations is smoothed.

$$y = a * x^b + c(e^{d*x} - 1), \tag{5.1}$$

where,

y = dependent variable, here it is the rut depth in mm,

a, b, c, and d = model coefficients,

x = independent variable, here it is the number of wheel passes, N.

The rut depths for the twenty seven locations at 500, 1000, 2000, 4000, 6000, 8000, 10000, 12000, 14000, 16000, 18000, 20000, 30000, 40000, 50000, 60000, 70000, 80000, 90000, 100000, 110000, 120000, 130000, 140000, 150000, 160000, 170000, 180000, 190000 and 200000 passes is extracted for the bituminous mixtures tested at all possible temperatures. The statistical parameters related to the rut data of the STA BC-2 mixtures prepared with

VG20 binder at 40 to 65 °C and for the specific passes are shown in Table 5.2. The statistical analysis, similar to Table 5.2, for the other remaining mixtures are shown in Appendix B (Tables B1 to B7). From Table 5.2 and Tables B 1 to B7, it is observed that the mean is always greater than the median indicating a longer right hand tail in the distribution of rut data except at a few passes where the mean value is less than the median. This right hand tailing of the data is validated by a positive skewness value. Moreover, there is an increase in the standard deviation with an increase in the number of passes indicating an increase in scatter in the rut data as the number of passes increased at almost all the cases, except at 65 °C for the STA BC-2 prepared with VG20 binder. At 65 °C for the STA BC-2 with prepared VG20 binder, the standard deviation increased with the number of passes and then decreased from 14000 passes. This is because of tertiary rutting, wherein the specimen incurred flow and thus the rut data showed a decrease in the standard deviation after 14000 passes. The analysis of kurtosis showed that most of the distributions are platykurtic while the others are leptokurtic and none are mesokurtic. The distributions are described as such based upon the excess kurtosis value. Excess kurtosis is defined as kurtosis value minus 3. Platykurtic have a negative excess kurtosis, leptokurtic have a positive excess kurtosis whereas the mesokurtic distributions have a zero excess kurtosis. The platykurtic distributions are highlighted with bold lettering and the leptokurtic distributions are highlighted as italicized in Table 5.2 and Tables B1 to B7.

5.3.2.2 *Fitting Distributions to the Rut Data*

After the statistical analysis, normal, lognormal and Weibull distributions are fitted to the rut data at the pre-specified number of passes and at all the test temperatures and for all the mixture types. These three distributions are chosen with a reference to Singh and Swamy (2018). The Kolmogorov–Smirnov (KS) test is used to determine the goodness of fit among these three distributions. Table 5.3 shows the KS test statistic of the three distributions at all the test temperatures for the STA BC-2 prepared with VG20 binder while similar Tables for the remaining mixture types are shown in Appendix B (Tables B8 to B14). A lower value of the KS test statistic indicates a better fit among the distributions. In Tables 5.3, and B8 to B14, the lowest value of the KS test statistic at each specified pass is marked with bold lettering. From Tables 5.3 and B8 to B14, it is observed that Weibull and lognormal distributions offers a better fit than the normal distribution. Weibull and lognormal distributions offering a better goodness of fit than the normal distribution is also validated from the kurtosis statistic. As discussed previously, most of the distributions are platykurtic in nature and none are mesokurtic. Weibull and lognormal distributions are a category of

platykurtic distributions whereas the normal distribution is a mesokurtic distribution, thereby supporting Weibull and lognormal distributions for offering a better fit than the normal distribution. The inability of the normal distribution to characterize the rut data distribution has been reported previously (Guo and Prozzi, 2009). Thus the data is further analysed using the lognormal and Weibull distributions. The parameters of the lognormal and the Weibull distributions for the STA BC-2 mixtures prepared with VG20 binder at all the test temperatures are shown in Table 5.4 while for the remaining mixture types, similar Tables are shown in Appendix B (Tables B15-21).

5.3.2.3 *Probability Curves at Four Reliability Levels*

Since the lognormal and Weibull distributions offered a better fit, the probability curves at 50, 80, 90, 99% reliability levels are generated using these two distributions alone for all mixture types. The probability curves are generated by back calculating the rut depths using the cumulative distribution functions of the two distributions. The forms of the cumulative distribution functions of the lognormal and Weibull distributions are shown in Equations (5.2) and (5.3), respectively. The probabilistic rut depths at each pre-specified number of passes are determined by calculating the inverse of the cumulative distribution functions. The probabilistic rut curves are determined for both the distributions at the required reliability levels using the distribution parameters. The probabilistic rut data is determined for all the STA and LTA BC-2 and DBM-2 mixtures prepared with VG20 and VG40 binders.

$$p = F(x|\,\mu,\sigma) = \frac{1}{\sigma\sqrt{2\pi}}\int_0^x \frac{e^{\frac{-\{\ln(t)-\mu\}^2}{2\sigma^2}}}{t}\,dt \tag{5.2}$$

$$p = F(x|a,b) = \int_0^x ba^{-b}t^{b-1}e^{-\left(\frac{t}{a}\right)^b} \tag{5.3}$$

where,

p = probability of occurrence at a given x,

μ = location parameter lognormal distributions,

σ = scale parameter lognormal distributions,

a = scale parameter in Weibull distribution, and

b = shape parameter in Weibull distribution.

Figure 5.5 shows the probabilistic rut data for the STA BC-2 with VG20 binder at four reliability levels for both the lognormal and Weibull distributions at a temperature of 40 °C.

Similar plots at all other remaining test conditions are shown in Appendix B (Figures B2 to B9). It is observed from these figures that, with an increase in percentage reliability there is an increase in the probabilistic rut depths at all the pre-specified passes. The rut depths from both the distributions are almost similar at 50, 80 and 90% reliability levels, whereas at the 99% reliability lognormal distribution has comparatively higher rut depths at all pre-specified passes than the Weibull distribution. Moreover, Figure 5.6 shows the comparison between the Weibull and lognormal rut curves at 99% reliability for the STA BC-2 mixture prepared with VG40 bitumen, wherein it is observed that lognormal distribution overestimates the probabilistic rut depth when compared to the Weibull distribution, particularly for cases where the difference between the smallest and the highest rut depth values among the 27 locations is too large. This may be because of the prolonged tail observed in the lognormal distribution. This overestimation with lognormal distribution can also observed from Figures B2 to B9. However, this is not observed with the Weibull distribution, wherein the probability rut depths at the four reliability levels are conservative. A similar finding is reported by Singh and Swamy (2018) where the lognormal distributions overestimated when compared to Weibull distributions whose probabilistic estimations are conservative. Based upon the comparative analysis of the probabilistic rut depths obtained at four reliability levels from the lognormal and Weibull distribution from the current analysis and also the findings from Singh and Swamy (2018), the probability curves with Weibull distribution are considered for further analysis. It is observed that there is an average decrease in rutting resistance by 56% at 40, 45 and 50 °C, by 46% at 55 and 60 °C and by 30% when the reliability is increased from 50 to 99%.

A comparison of the probabilistic rut curves with the Weibull distributions and the curves from the four selected methodologies for the STA BC-2 prepared with VG20 binder at a temperature of 40 °C are shown in Figures 5.7 while similar plots at the remaining test conditions are shown in Appendix B (Figures B10). From Figures 5.7 and B10, it is observed that the probabilistic rut curves with 50% reliability for both the distributions are closer to the TA curves at all temperatures. The AGPT curves have comparatively lower values than the curves with 50% reliability and TA curves. As the percentage reliability increases the rut depths increases. Rut curves with 80% reliability are in the middle of the “High” curve and the curve with the 50% reliability at all temperatures for both the distributions. The probabilistic curves with 90% reliability moved closer to the “High” curve and lies between the curve with 80% reliability and the “High” curve whereas the probabilistic rut curve with 99% reliability either matched the “High” curve or is slightly higher. This trend of the curves

Table 5.2(a) Statistical parameters of the rut data for the STA BC-2 mixtures prepared with VG20 binder

Passes	40 °C						45 °C						50 °C					
	Mean	Median	Mode	Standard Deviation	Skewness	Kurtosis	Mean	Median	Mode	Standard Deviation	Skewness	Kurtosis	Mean	Median	Mode	Standard Deviation	Skewness	Kurtosis
500	0.62	0.63	0.07	0.01	-0.77	*3.40*	0.68	0.69	0.16	0.03	-0.06	**1.38**	1.20	1.22	0.21	0.04	-0.25	**1.50**
1000	0.83	0.84	0.09	0.01	-0.53	**2.76**	0.96	0.98	0.20	0.04	-0.02	**1.41**	1.61	1.63	0.25	0.06	-0.21	**1.42**
2000	1.14	1.14	0.12	0.02	-0.26	**2.29**	1.42	1.44	0.25	0.06	0.14	**1.53**	2.23	2.23	0.29	0.08	-0.12	**1.34**
4000	1.63	1.59	0.18	0.03	0.05	**1.93**	2.15	2.17	0.33	0.11	0.38	**1.72**	3.14	3.12	0.34	0.12	0.05	**1.37**
6000	2.02	1.95	0.23	0.05	0.25	**1.79**	2.73	2.66	0.40	0.16	0.49	**1.80**	3.83	3.80	0.39	0.15	0.19	**1.51**
8000	2.35	2.26	0.26	0.07	0.34	**1.76**	3.21	3.07	0.46	0.21	0.54	**1.83**	4.39	4.33	0.43	0.18	0.32	**1.69**
10000	2.64	2.52	0.30	0.09	0.40	**1.75**	3.62	3.42	0.50	0.25	0.57	**1.85**	4.84	4.77	0.46	0.21	0.43	**1.88**
12000	2.90	2.75	0.33	0.11	0.45	**1.74**	3.96	3.75	0.55	0.30	0.59	**1.86**	5.21	5.13	0.49	0.24	0.51	**2.06**
14000	3.13	2.96	0.36	0.13	0.49	**1.76**	4.25	4.02	0.58	0.34	0.59	**1.85**	5.53	5.44	0.52	0.27	0.58	**2.22**
16000	3.33	3.15	0.38	0.15	0.51	**1.78**	4.49	4.26	0.61	0.38	0.60	**1.86**	5.80	5.69	0.55	0.30	0.65	**2.37**
18000	3.51	3.32	0.41	0.16	0.54	**1.79**	4.71	4.46	0.64	0.41	0.60	**1.86**	6.02	5.91	0.57	0.33	0.71	**2.50**
20000	3.68	3.49	0.43	0.18	0.56	**1.82**	4.89	4.64	0.66	0.44	0.59	**1.85**	6.22	6.10	0.59	0.35	0.75	**2.61**
30000	4.31	4.08	0.51	0.26	0.63	**1.93**	5.50	5.22	0.74	0.55	0.57	**1.82**	6.90	6.76	0.67	0.44	0.89	**2.94**
40000	4.72	4.45	0.57	0.32	0.67	**2.04**	5.84	5.54	0.78	0.61	0.55	**1.81**	7.32	7.17	0.71	0.50	0.96	*3.09*
50000	5.00	4.71	0.61	0.37	0.70	**2.13**	6.05	5.74	0.80	0.64	0.54	**1.80**	7.63	7.47	0.74	0.55	0.97	*3.13*
60000	5.21	4.90	0.64	0.41	0.72	**2.19**	6.20	5.88	0.81	0.66	0.54	**1.80**	7.88	7.71	0.76	0.58	0.99	*3.16*
70000	5.38	5.06	0.67	0.45	0.74	**2.25**	6.33	6.00	0.82	0.68	0.54	**1.80**	8.10	7.92	0.78	0.60	0.99	*3.17*
80000	5.52	5.19	0.70	0.48	0.75	**2.28**	6.43	6.10	0.83	0.69	0.55	**1.81**	8.29	8.12	0.79	0.63	0.99	*3.18*
90000	5.64	5.30	0.72	0.51	0.76	**2.29**	6.52	6.19	0.84	0.70	0.55	**1.81**	8.47	8.29	0.80	0.64	1.00	*3.20*
100000	5.74	5.40	0.74	0.54	0.76	**2.31**	6.61	6.28	0.84	0.71	0.56	**1.81**	8.63	8.45	0.81	0.66	1.00	*3.20*
110000	5.84	5.49	0.76	0.57	0.77	**2.32**	6.69	6.36	0.85	0.72	0.56	**1.82**	8.79	8.60	0.82	0.68	1.00	*3.21*
120000	5.93	5.58	0.77	0.60	0.77	**2.32**	6.76	6.43	0.85	0.73	0.57	**1.83**	8.93	8.74	0.83	0.69	1.01	*3.22*
130000	6.01	5.66	0.79	0.62	0.78	**2.33**	6.83	6.50	0.86	0.73	0.58	**1.83**	9.06	8.88	0.84	0.71	1.01	*3.23*
140000	6.09	5.74	0.81	0.65	0.78	**2.33**	6.90	6.56	0.86	0.74	0.58	**1.84**	9.19	9.00	0.85	0.72	1.02	*3.24*
150000	6.17	5.81	0.82	0.67	0.78	**2.32**	6.96	6.62	0.86	0.75	0.59	**1.84**	9.31	9.12	0.86	0.73	1.02	*3.25*
160000	6.24	5.88	0.84	0.70	0.79	**2.33**	7.02	6.68	0.87	0.75	0.59	**1.85**	9.43	9.24	0.86	0.74	1.02	*3.26*
170000	6.31	5.94	0.85	0.72	0.79	**2.32**	7.08	6.74	0.87	0.76	0.60	**1.85**	9.54	9.35	0.87	0.76	1.02	*3.27*
180000	6.37	5.99	0.86	0.75	0.79	**2.32**	7.14	6.80	0.87	0.76	0.60	**1.86**	9.65	9.45	0.88	0.77	1.03	*3.27*
190000	6.44	6.04	0.88	0.77	0.79	**2.32**	7.19	6.85	0.87	0.76	0.61	**1.87**	9.75	9.55	0.88	0.78	1.03	*3.29*
200000	6.50	6.08	0.89	0.79	0.80	**2.33**	7.24	6.90	0.88	0.77	0.61	**1.87**	9.85	9.65	0.89	0.79	1.04	*3.30*

Table 5.2(b) Statistical parameters of the rut data for the STA BC-2 mixtures prepared with VG20 binder

Passes	55 °C						60 °C						65 °C					
	Mean	Median	Mode	Standard Deviation	Skewness	Kurtosis	Mean	Median	Mode	Standard Deviation	Skewness	Kurtosis	Mean	Median	Mode	Standard Deviation	Skewness	Kurtosis
500	1.81	1.78	0.10	0.01	0.35	**2.02**	2.71	2.72	0.09	0.01	-1.27	*4.38*	3.84	3.81	0.25	0.06	0.29	**1.56**
1000	2.35	2.31	0.14	0.02	0.51	**2.19**	3.44	3.43	0.07	0.00	-1.12	*4.89*	5.15	5.14	0.29	0.08	0.33	**1.80**
2000	3.06	3.05	0.21	0.04	0.68	**2.67**	4.43	4.41	0.10	0.01	1.24	*6.10*	6.78	6.74	0.38	0.15	0.32	**1.72**
4000	4.05	4.01	0.33	0.11	0.83	*3.30*	5.74	5.69	0.19	0.04	2.61	*9.05*	8.77	8.65	0.56	0.31	0.30	**1.50**
6000	4.78	4.77	0.44	0.20	0.86	*3.54*	6.65	6.55	0.27	0.07	2.05	*6.33*	10.20	10.02	0.71	0.51	0.36	**1.54**
8000	5.38	5.35	0.54	0.29	0.86	*3.61*	7.34	7.19	0.35	0.12	1.53	*4.06*	11.41	11.16	0.83	0.69	0.40	**1.58**
10000	5.89	5.85	0.62	0.39	0.83	*3.60*	7.90	7.70	0.43	0.18	1.28	*3.03*	12.54	12.28	0.90	0.81	0.39	**1.56**
12000	6.34	6.28	0.69	0.48	0.81	*3.59*	8.36	8.11	0.51	0.26	1.20	**2.75**	13.64	13.40	0.93	0.87	0.35	**1.51**
14000	6.74	6.67	0.75	0.56	0.79	*3.57*	8.75	8.46	0.59	0.35	1.20	**2.77**	14.74	14.53	0.93	0.87	0.29	**1.43**
16000	7.10	7.02	0.80	0.63	0.78	*3.56*	9.09	8.77	0.67	0.44	1.23	**2.86**	15.84	15.69	0.91	0.84	0.22	**1.35**
18000	7.43	7.35	0.84	0.70	0.76	*3.52*	9.39	9.03	0.74	0.55	1.26	**2.96**	16.95	16.84	0.89	0.79	0.18	**1.33**
20000	7.72	7.65	0.87	0.75	0.75	*3.49*	9.67	9.27	0.81	0.65	1.28	*3.03*						
30000	8.90	8.89	0.95	0.91	0.69	*3.35*	10.73	10.20	1.06	1.11	1.36	*3.26*						
40000	9.77	9.75	0.97	0.94	0.66	*3.22*	11.52	10.91	1.20	1.43	1.38	*3.32*						
50000	10.46	10.37	0.96	0.92	0.65	*3.07*	12.15	11.49	1.27	1.62	1.37	*3.33*						
60000	11.04	10.87	0.94	0.89	0.65	**2.90**	12.68	12.01	1.32	1.73	1.35	*3.30*						
70000	11.55	11.30	0.93	0.87	0.65	**2.75**	13.15	12.47	1.34	1.80	1.33	*3.26*						
80000	12.00	11.68	0.92	0.84	0.64	**2.60**	13.57	12.89	1.36	1.84	1.31	*3.22*						
90000	12.41	12.03	0.91	0.83	0.62	**2.44**	13.95	13.27	1.37	1.87	1.29	*3.17*						
100000	12.79	12.40	0.91	0.83	0.59	**2.33**	14.30	13.62	1.38	1.90	1.26	*3.12*						
110000	13.15	12.80	0.91	0.83	0.55	**2.21**	14.63	13.95	1.39	1.92	1.24	*3.08*						
120000	13.48	13.18	0.92	0.84	0.50	**2.15**	14.93	14.26	1.39	1.94	1.21	*3.03*						
130000	13.80	13.51	0.92	0.85	0.45	**2.09**	15.22	14.55	1.40	1.96	1.19	**2.99**						
140000	14.10	13.77	0.93	0.87	0.40	**2.05**	15.49	14.82	1.41	1.98	1.17	**2.94**						
150000	14.38	14.01	0.95	0.89	0.35	**2.03**	15.75	15.08	1.41	2.00	1.15	**2.90**						
160000	14.65	14.28	0.96	0.92	0.29	**2.02**	16.00	15.33	1.42	2.02	1.13	**2.86**						
170000	14.92	14.59	0.98	0.95	0.24	**2.02**	16.23	15.57	1.43	2.04	1.11	**2.82**						
180000	15.17	14.90	0.99	0.98	0.19	**2.02**	16.46	15.80	1.44	2.06	1.09	**2.78**						
190000	15.41	15.19	1.01	1.02	0.15	**2.03**	16.68	16.02	1.44	2.08	1.08	**2.75**						
200000	15.65	15.48	1.03	1.06	0.10	**2.03**	16.89	16.23	1.45	2.10	1.06	**2.71**						

Table 5.3 K-S test statistic for the STA BC-2 mixtures prepared with VG20 binder

Passes	40 °C			45 °C			50 °C			55 °C			60 °C			65 °C		
	Normal	**Lognormal**	**Weibull**	**Normal**	**Lognormal**	**Weibull**	**Normal**	**Lognormal**	**Weibull**	**Normal**	**Lognormal**	**Weibull**	**Normal**	**Lognormal**	**Weibull**	**Normal**	**Lognormal**	**Weibull**
500	**0.143**	0.144	0.151	0.182	0.206	**0.178**	0.234	0.241	**0.187**	0.181	**0.175**	0.195	0.162	0.169	**0.070**	0.214	0.217	**0.197**
1000	0.090	0.108	**0.084**	0.209	0.226	**0.187**	0.233	0.240	**0.183**	0.203	**0.202**	0.186	**0.121**	0.125	0.121	0.209	0.211	**0.185**
2000	**0.104**	0.109	0.111	**0.191**	0.201	0.200	0.213	0.223	**0.163**	0.179	0.182	**0.143**	0.200	**0.195**	0.273	0.198	0.199	**0.179**
4000	**0.139**	0.141	0.159	0.216	**0.211**	0.212	**0.190**	0.195	0.216	**0.131**	0.134	0.144	0.335	**0.328**	0.353	0.190	0.189	**0.188**
6000	**0.138**	0.142	0.171	0.228	0.228	**0.217**	0.213	**0.207**	0.217	**0.123**	0.130	0.141	0.335	0.332	**0.320**	0.165	**0.165**	0.171
8000	0.156	**0.142**	0.178	0.226	0.227	**0.213**	0.212	**0.209**	0.209	**0.123**	0.131	0.137	0.344	0.340	**0.339**	**0.171**	0.171	0.167
10000	0.173	**0.158**	0.192	0.222	0.222	**0.209**	0.205	0.202	**0.197**	**0.123**	0.130	0.134	0.355	0.352	**0.351**	**0.168**	0.168	0.180
12000	0.185	**0.172**	0.202	0.220	0.220	**0.206**	0.199	0.196	**0.187**	**0.121**	0.129	0.137	0.364	0.360	**0.355**	0.162	**0.159**	0.173
14000	0.195	**0.183**	0.210	0.219	0.219	**0.205**	0.195	0.192	**0.182**	**0.120**	0.127	0.138	0.363	0.359	**0.355**	0.172	**0.170**	0.177
16000	0.203	**0.192**	0.216	0.217	0.217	**0.204**	0.191	0.189	**0.178**	**0.118**	0.125	0.137	0.350	**0.344**	0.353	0.179	0.178	**0.172**
18000	0.209	**0.195**	0.221	0.216	0.216	**0.203**	0.189	0.187	**0.175**	**0.116**	0.122	0.136	0.349	**0.341**	0.351	0.196	0.197	**0.193**
20000	0.214	**0.201**	0.225	0.216	0.216	**0.203**	0.187	0.185	**0.172**	**0.114**	0.120	0.134	0.348	**0.339**	0.349			
30000	0.194	**0.185**	0.204	0.221	0.221	**0.208**	0.184	**0.183**	0.186	**0.101**	0.104	0.143	0.336	**0.332**	0.334			
40000	0.201	**0.193**	0.201	0.226	0.227	**0.213**	0.184	**0.184**	0.196	0.102	**0.090**	0.136	0.334	0.330	**0.316**			
50000	0.203	**0.196**	0.201	0.230	0.231	**0.216**	**0.186**	0.186	0.201	0.120	**0.114**	*0.125*	0.329	0.324	**0.313**			
60000	0.203	**0.196**	0.200	0.232	0.233	**0.218**	**0.187**	0.188	0.202	0.153	0.151	**0.142**	0.324	0.319	**0.310**			
70000	0.202	**0.196**	0.199	0.233	0.235	**0.219**	**0.189**	0.190	0.200	0.184	0.179	**0.170**	0.320	0.314	**0.307**			
80000	0.201	**0.195**	0.197	0.234	0.235	**0.219**	**0.187**	0.187	0.198	0.189	0.184	**0.176**	0.315	0.309	**0.304**			
90000	0.199	**0.193**	0.195	0.234	0.236	**0.219**	**0.183**	0.184	0.196	0.206	0.205	**0.182**	0.311	0.305	**0.302**			
100000	0.197	**0.191**	0.193	0.234	0.236	**0.219**	0.180	**0.180**	0.194	0.204	0.203	**0.186**	0.308	0.300	**0.299**			
110000	0.196	**0.190**	0.192	0.234	0.235	**0.218**	0.178	**0.177**	0.193	0.195	0.193	**0.185**	0.304	**0.296**	0.297			
120000	0.194	**0.188**	0.193	0.233	0.235	**0.218**	0.175	**0.175**	0.191	0.212	0.208	**0.203**	0.300	**0.292**	0.295			
130000	0.196	**0.187**	0.199	0.233	0.235	**0.217**	0.173	**0.172**	0.190	0.208	0.204	**0.203**	0.297	**0.289**	0.293			
140000	0.203	**0.189**	0.204	0.232	0.234	**0.217**	0.171	**0.170**	0.189	0.184	**0.178**	0.187	0.294	**0.285**	0.291			
150000	0.209	**0.196**	0.210	0.232	0.234	**0.216**	0.168	*0.167*	0.188	0.169	**0.161**	0.186	0.291	**0.282**	0.290			
160000	0.215	**0.202**	0.214	0.231	0.233	**0.215**	0.166	*0.165*	0.187	0.172	**0.163**	0.191	0.288	**0.278**	0.288			
170000	0.221	**0.209**	0.219	0.231	0.233	**0.214**	0.164	0.163	0.186	0.149	**0.139**	0.174	0.285	**0.275**	0.286			
180000	0.222	**0.210**	0.220	0.230	0.232	**0.214**	0.163	0.161	0.188	0.126	**0.116**	0.160	0.282	**0.272**	0.285			
190000	0.221	**0.209**	0.219	0.230	0.231	**0.213**	0.161	0.162	0.190	0.116	**0.106**	0.160	0.279	**0.270**	0.283			
200000	0.220	**0.207**	0.218	0.229	0.231	**0.212**	0.160	0.162	0.191	0.124	**0.112**	0.172	0.277	**0.267**	0.282			

Table 5.4 Distribution parameters for the lognormal and Weibull distributions for the STA BC-2 mixtures prepared with VG20 binder

.Passes	40 °C				45 °C				50 °C				55 °C				60 °C				65 °C			
	Lognormal		Weibull		Lognormal		Weibull		Lognormal		Weibull		Lognormal		Weibull		Lognormal		Weibull		Lognormal		Weibull	
	μ	σ	A	B	μ	σ	A	B	μ	σ	A	B	μ	σ	A	B	μ	σ	A	B	μ	σ	A	B
0	0	0	0	0	0	0	0	0	0	0	0	0	0	0	0	0	0	0	0	0	0	0	0	0
500	-0.49	0.12	0.65	11.25	-0.42	0.25	0.74	4.92	0.17	0.18	1.29	7.05	0.60	0.05	1.86	19.78	1.00	0.03	2.74	44.70	1.34	0.06	3.96	17.05
1000	-0.20	0.12	0.87	11.34	-0.06	0.21	1.04	5.76	0.47	0.16	1.72	8.14	0.85	0.06	2.41	17.68	1.24	0.02	3.47	67.61	1.64	0.06	5.29	18.85
2000	0.13	0.11	1.20	10.96	0.34	0.18	1.52	6.55	0.79	0.13	2.35	9.48	1.12	0.07	3.16	14.55	1.49	0.02	4.48	36.39	1.91	0.06	6.96	19.14
4000	0.48	0.11	1.71	10.36	0.75	0.15	2.29	7.14	1.14	0.11	3.29	10.72	1.40	0.08	4.20	11.55	1.75	0.03	5.85	21.38	2.17	0.06	9.04	17.31
6000	0.70	0.11	2.12	10.01	0.99	0.14	2.90	7.38	1.34	0.10	4.01	11.13	1.56	0.09	4.99	10.19	1.89	0.04	6.79	19.26	2.32	0.07	10.53	15.54
8000	0.85	0.11	2.47	9.77	1.16	0.14	3.41	7.51	1.47	0.10	4.58	11.19	1.68	0.10	5.63	9.46	1.99	0.05	7.52	18.27	2.43	0.07	11.80	14.88
10000	0.97	0.11	2.78	9.61	1.28	0.14	3.84	7.60	1.57	0.09	5.05	11.12	1.77	0.10	6.18	9.04	2.07	0.05	8.11	16.93	2.53	0.07	12.97	15.11
12000	1.06	0.11	3.05	9.48	1.37	0.13	4.20	7.66	1.65	0.09	5.44	10.99	1.84	0.11	6.66	8.80	2.12	0.06	8.61	15.34	2.61	0.07	14.08	16.03
14000	1.13	0.11	3.29	9.38	1.44	0.13	4.51	7.71	1.71	0.09	5.77	10.84	1.90	0.11	7.08	8.66	2.17	0.07	9.04	13.88	2.69	0.06	15.18	17.56
16000	1.20	0.11	3.50	9.29	1.49	0.13	4.77	7.75	1.75	0.09	6.05	10.69	1.95	0.11	7.46	8.60	2.21	0.07	9.42	12.72	2.76	0.06	16.27	19.59
18000	1.25	0.11	3.70	9.21	1.54	0.13	4.99	7.78	1.79	0.09	6.29	10.55	2.00	0.11	7.81	8.60	2.24	0.08	9.76	11.82	2.83	0.05	17.37	21.73
20000	1.30	0.11	3.87	9.14	1.58	0.13	5.19	7.81	1.82	0.09	6.50	10.43	2.04	0.11	8.12	8.63	2.27	0.08	10.06	11.13				
30000	1.45	0.12	4.54	8.85	1.70	0.13	5.83	7.91	1.93	0.09	7.22	10.03	2.18	0.10	9.34	9.12	2.37	0.09	11.24	9.42				
40000	1.55	0.12	4.98	8.63	1.76	0.13	6.19	7.99	1.99	0.09	7.66	9.87	2.28	0.10	10.22	9.85	2.44	0.10	12.09	8.93				
50000	1.60	0.12	5.28	8.45	1.79	0.13	6.41	8.06	2.03	0.09	7.98	9.84	2.34	0.09	10.91	10.65	2.49	0.10	12.75	8.86				
60000	1.64	0.12	5.51	8.30	1.82	0.13	6.57	8.11	2.06	0.09	8.24	9.87	2.40	0.08	11.49	11.44	2.54	0.10	13.31	8.96				
70000	1.68	0.12	5.68	8.19	1.84	0.13	6.69	8.17	2.09	0.09	8.46	9.92	2.44	0.08	11.99	12.18	2.57	0.10	13.79	9.12				
80000	1.70	0.12	5.83	8.09	1.85	0.13	6.80	8.22	2.11	0.09	8.67	9.97	2.48	0.08	12.44	12.88	2.60	0.10	14.22	9.31				
90000	1.72	0.12	5.96	8.01	1.87	0.13	6.90	8.26	2.13	0.09	8.85	10.02	2.52	0.07	12.85	13.51	2.63	0.09	14.60	9.51				
100000	1.74	0.12	6.08	7.93	1.88	0.12	6.99	8.31	2.15	0.09	9.02	10.07	2.55	0.07	13.23	14.08	2.66	0.09	14.96	9.70				
110000	1.76	0.12	6.18	7.87	1.89	0.12	7.07	8.35	2.17	0.09	9.18	10.12	2.57	0.07	13.58	14.59	2.68	0.09	15.29	9.89				
120000	1.77	0.13	6.28	7.80	1.90	0.12	7.15	8.39	2.19	0.09	9.32	10.16	2.60	0.07	13.92	15.05	2.70	0.09	15.60	10.06				
130000	1.79	0.13	6.37	7.75	1.91	0.12	7.22	8.43	2.20	0.09	9.46	10.20	2.62	0.07	14.24	15.44	2.72	0.09	15.89	10.23				
140000	1.80	0.13	6.46	7.70	1.92	0.12	7.29	8.46	2.22	0.09	9.60	10.24	2.64	0.07	14.54	15.79	2.74	0.09	16.17	10.38				
150000	1.81	0.13	6.54	7.65	1.93	0.12	7.35	8.50	2.23	0.09	9.72	10.28	2.66	0.07	14.83	16.08	2.75	0.09	16.43	10.53				
160000	1.82	0.13	6.62	7.60	1.94	0.12	7.42	8.53	2.24	0.09	9.84	10.31	2.68	0.07	15.11	16.32	2.77	0.09	16.68	10.67				
170000	1.83	0.13	6.69	7.56	1.95	0.12	7.48	8.57	2.25	0.09	9.96	10.35	2.70	0.07	15.38	16.52	2.78	0.08	16.92	10.80				
180000	1.84	0.13	6.76	7.51	1.96	0.12	7.53	8.60	2.26	0.09	10.07	10.38	2.72	0.07	15.63	16.67	2.80	0.08	17.15	10.92				
190000	1.85	0.13	6.83	7.47	1.97	0.12	7.59	8.63	2.27	0.09	10.17	10.41	2.73	0.07	15.88	16.79	2.81	0.08	17.37	11.04				
200000	1.86	0.13	6.90	7.44	1.97	0.12	7.64	8.66	2.28	0.09	10.28	10.43	2.75	0.07	16.12	16.87	2.82	0.08	17.59	11.15				

with 90% and 99% reliability is observed for both the distributions and at all the test temperatures. Moreover, Figure 5.8 shows the comparison of the probabilistic curves at four reliability levels for the STA BC-2 prepared with VG20 binder at all test temperatures. Here, the comparison across the temperatures is made up to 200000 passes or terminal rut depth of 15 mm whichever is the earliest. It is clearly seen that as the reliability increases the rut curves move upwards and at temperatures 55, 60 and 65 °C, the terminal rut depth is reached within comparatively less number of passes.

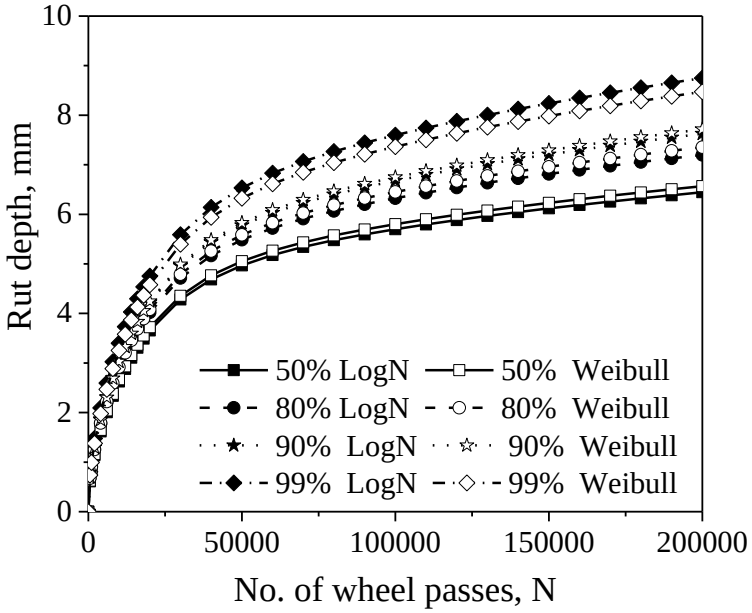

Fig. 5.5 Probabilistic rut curves for STA BC-2 prepared with VG20 bitumen at 40 °C

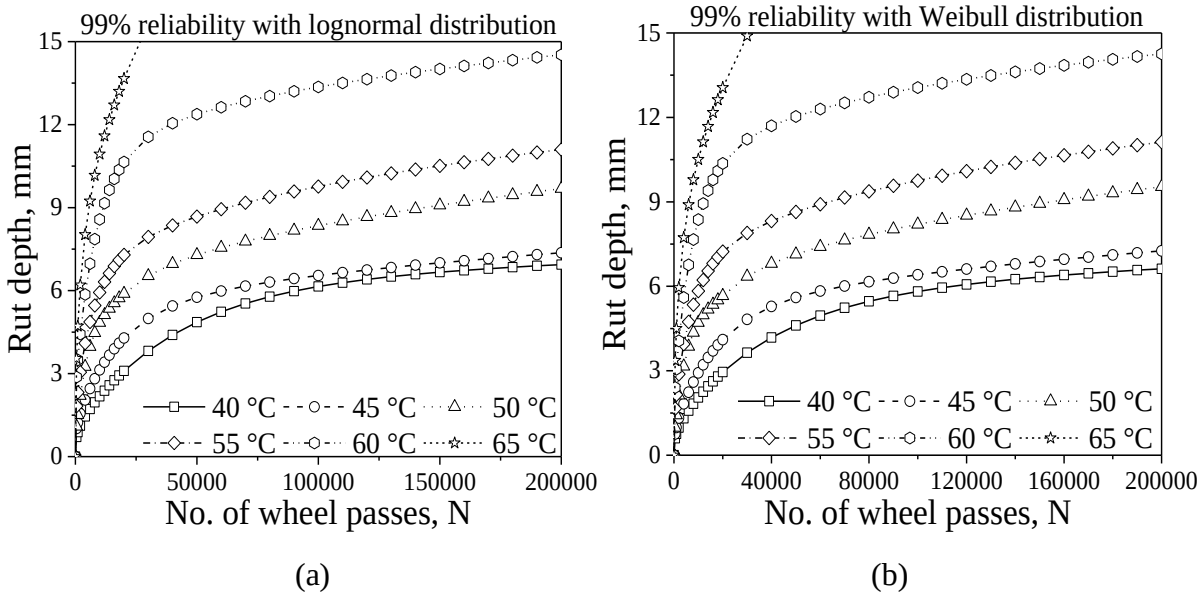

(a) (b)

Fig. 5.6 Reliability curves at 99% for the STA BC-2 prepared with VG40 binder

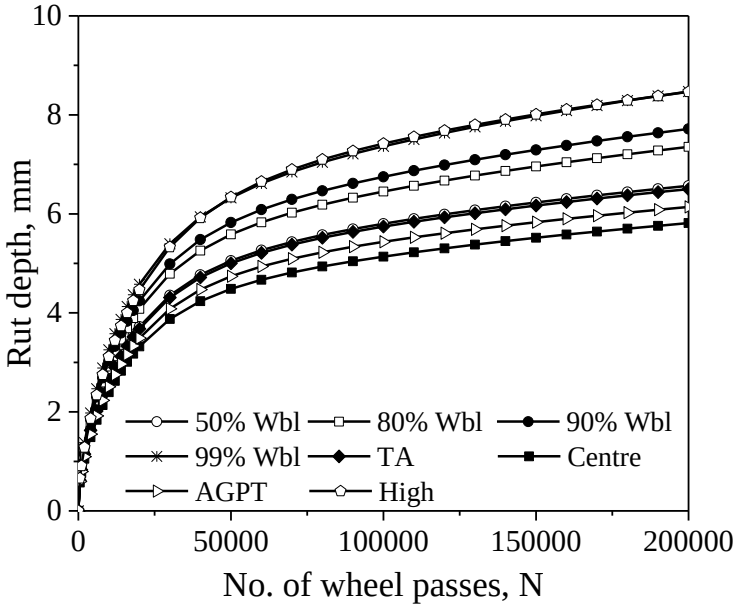

Fig. 5.7 Comparison of the Weibull probability curves with the rut curves from four methodologies for the STA BC-2 prepared with VG20 bitumen at 40 °C

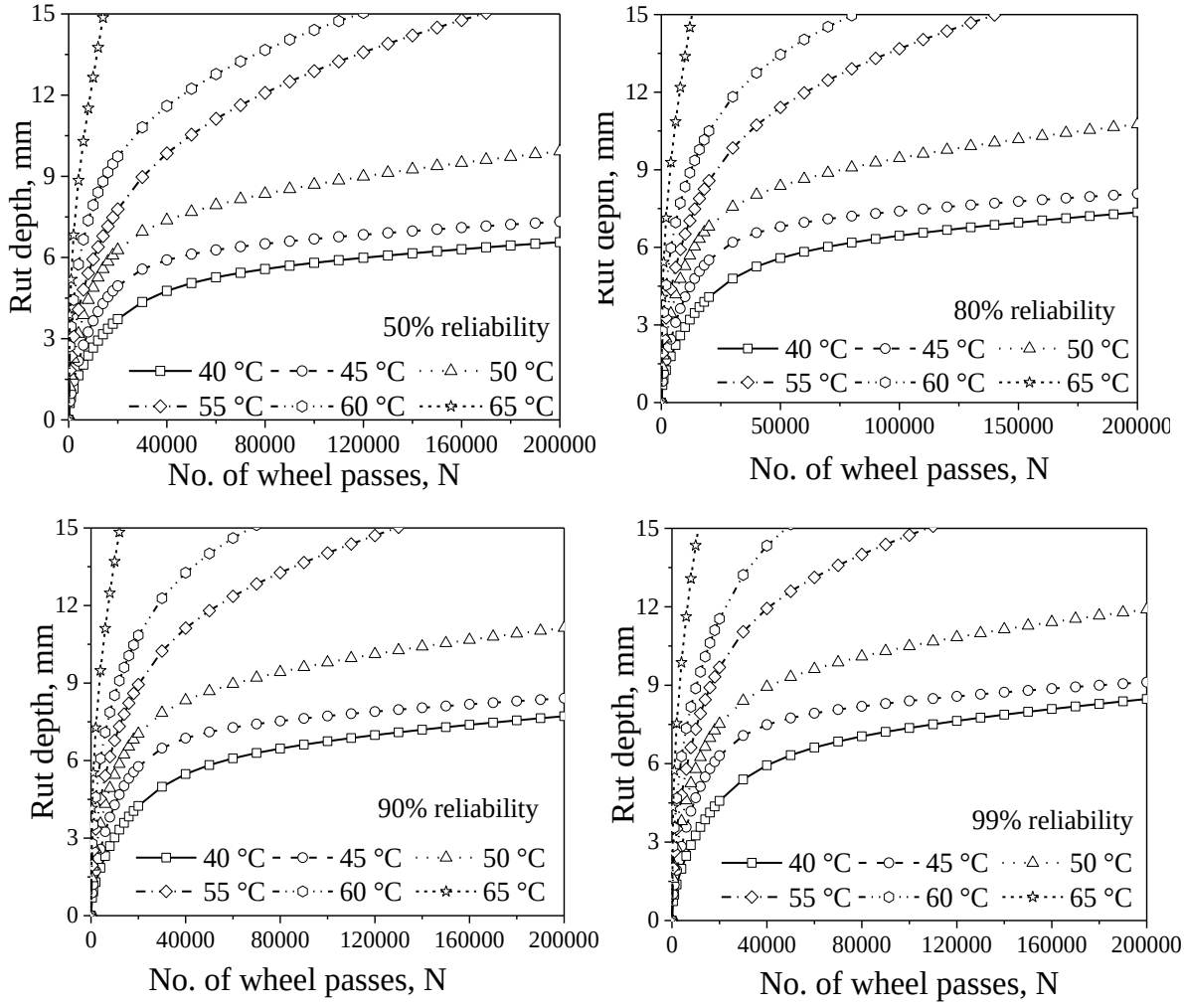

Fig. 5.8 Probabilistic rut curves at all temperatures with Weibull distribution for the STA BC-2 prepared with VG20 binder

Table 5.5 Comparison of rut data at 50% reliability level

Mixture	Temp., °C / Passes	20000	40000	60000	80000	100000	120000	140000	160000	180000	200000
STA-BC-2-VG20	**40**	3.72	4.77	5.27	5.57	5.80	5.99	6.16	6.30	6.44	6.57
	45	4.95	5.91	6.28	6.51	6.69	6.84	6.98	7.10	7.22	7.32
	50	6.27	7.38	7.94	8.35	8.69	8.99	9.26	9.50	9.72	9.92
	55	7.78	9.85	11.12	12.09	12.89	13.58	14.20	14.77	15.29	15.78
	60	9.73	11.60	12.78	13.67	14.41	15.04	15.61	16.12	16.59	17.02
	65	*14200*									
STA-BC-2-VG40	**40**	2.28	3.07	3.59	3.97	4.27	4.51	4.71	4.89	5.05	5.19
	45	3.42	4.28	4.69	4.98	5.20	5.39	5.57	5.72	5.87	6.00
	50	5.23	5.98	6.41	6.73	7.01	7.25	7.47	7.67	7.86	8.03
	55	6.40	7.31	7.78	8.14	8.44	8.70	8.93	9.14	9.33	9.51
	60	8.58	9.81	10.39	10.82	11.18	11.48	11.75	12.00	12.22	12.43
	65	11.21	14.39	*43780*							
LTA-BC-2-VG20	**40**	2.57	3.20	3.53	3.77	3.97	4.15	4.30	4.45	4.58	4.70
	45	2.96	3.83	4.34	4.70	4.98	5.22	5.43	5.62	5.79	5.94
	50	5.25	5.99	6.32	6.56	6.75	6.92	7.07	7.20	7.33	7.44
	55	6.42	7.31	7.76	8.09	8.36	8.60	8.81	9.00	9.17	9.33
	60	7.82	9.25	10.04	10.62	11.09	11.51	11.88	12.21	12.52	12.80
	65	11.95	31860								
LTA-BC-2-VG40	**40**	1.38	1.85	2.19	2.48	2.72	2.95	3.15	3.34	3.51	3.68
	45	2.35	3.18	3.68	4.01	4.27	4.48	4.65	4.81	4.95	5.08
	50	3.88	4.86	5.29	5.55	5.75	5.91	6.04	6.17	6.28	6.39
	55	4.91	5.67	6.05	6.33	6.57	6.78	6.97	7.14	7.30	7.45
	60	5.99	7.12	7.84	8.40	8.88	9.29	9.67	10.01	10.32	10.61
	65	8.57	10.53	11.95	13.11	14.11	15.00				
STA-DBM-2-VG20	**40**	2.95	3.85	4.42	4.84	5.17	5.44	5.67	5.88	6.07	6.23
	45	4.08	5.24	5.86	6.26	6.54	6.75	6.93	7.08	7.22	7.34
	50	5.78	6.74	7.27	7.65	7.97	8.24	8.48	8.70	8.89	9.07
	55	8.23	9.95	10.98	11.76	12.39	12.94	13.43	13.87	14.28	14.65
	60	9.60	11.67	12.89	13.75	14.42	14.98	15.46	15.89	16.27	16.63
	65	13.17	*30800*								
STA-DBM-2-VG40	**40**	2.12	2.99	3.60	4.04	4.37	4.62	4.82	4.98	5.10	5.21
	45	2.84	3.79	4.40	4.80	5.10	5.32	5.49	5.63	5.75	5.86
	50	4.48	5.43	5.94	6.28	6.54	6.76	6.94	7.11	7.26	7.40
	55	6.71	7.71	8.24	8.64	8.97	9.25	9.50	9.73	9.93	10.12
	60	8.34	9.69	10.50	11.13	11.64	12.09	12.48	12.84	13.16	13.47
	65	10.55	12.88	14.53	*66820*						
LTA-DBM-2-VG20	**40**	1.91	2.33	2.62	2.84	3.03	3.18	3.32	3.44	3.56	3.66
	45	3.07	3.63	3.97	4.24	4.45	4.64	4.81	4.96	5.10	5.22
	50	3.52	4.36	4.84	5.16	5.40	5.59	5.75	5.89	6.01	6.13
	55	5.87	7.03	7.62	8.03	8.37	8.65	8.90	9.13	9.33	9.52
	60	7.09	8.60	9.55	10.29	10.90	11.44	11.92	12.36	12.76	13.13
	65	9.38	11.90	13.67	15.05						
LTA-DBM-2-VG40	**40**	1.18	1.58	1.85	2.05	2.21	2.35	2.47	2.59	2.69	2.79
	45	2.22	2.82	3.15	3.39	3.58	3.74	3.88	4.01	4.13	4.23
	50	2.60	3.46	3.97	4.30	4.52	4.69	4.82	4.92	5.01	5.09
	55	3.85	4.66	5.11	5.44	5.71	5.94	6.15	6.34	6.52	6.68
	60	5.81	6.41	6.77	7.05	7.29	7.49	7.66	7.82	7.97	8.10
	65	8.00	9.16	9.96	10.60	11.14	11.60	12.02	12.40	12.75	13.07

5.4 COMPARING THE RUTTING RESISTANCE OF BITUMINOUS MIXTURES

The rutting resistance of the BC-2 and DBM-2 mixtures is analysed by comparing the rut data from the four reliability levels determined using the Weibull distribution. Table 5.5 show the comparison between the STA and LTA BC-2 and DBM-2 mixtures prepared with VG20 and VG40 bitumen respectively at 50% reliability level while Tables with 80, 90 and 99% reliability levels are shown in Appendix B (Tables B22 to B24). The wheel tracking tests are conducted for a total of 200,000 passes or a terminal rut depth of 15 mm. It is well known that the resistance to deformation decreases with an increase in temperature for the bituminous mixtures. This generic trend is clearly observed from Table 5.5 across all mixture types and for both the binders.

5.4.1 Comparing the performances of VG20 and VG40 binders

From the overall observations across the entire set of data, it is observed that higher the binder viscosity higher will be the rutting resistance as seen by the trend, wherein, the mixtures with the VG40 binders exhibited a higher resistance against permanent deformation than the mixtures with VG20 binders. This trend is seen for both the STA and LTA BC-2 and DBM-2 mixtures. STA BC-2 mixtures prepared with VG40 binder had an increase in rutting resistance by 63% at 60 and 65 °C, and by 20% at 40, 45, 50 and 55 °C when compared with STA BC-2 mixtures prepared with VG20 binder whereas the LTA BC-2 mixtures prepared with VG40 binder had an increase in rutting resistance by 73% at 65 °C, however the increase is only 20% at 40, 45, 50, 55 and 60 °C when compared with LTA BC-2 mixtures with VG20 binder. Moreover, STA DBM-2 mixtures with VG40 binder had an increase in rutting resistance by 44% at 60 and 65 °C, by 30% at 55 °C and by 20% at 40, 45 and 50 °C when compared with STA DBM-2 mixtures with VG20 binder, whereas, the LTA DBM-2 mixtures with VG40 binder had an increase in rutting resistance by 64% at 65 °C. However, the increase is only 34% at 55 and 60 °C and 20% at 40, 45 and 50 °C when compared with LTA BC-2 mixtures prepared with VG20 binder. Moreover, from Table 5.5, it is observed that, at 65 °C, the BC-2 mixtures prepared with VG20 binder reached the terminal rut depth of 15 mm at 14200 and 31860 wheel passes respectively for the STA and LTA mixture condition whereas the BC-2 mixture with VG40 binder reached the terminal (failure) rut depth at 43780 and 120,000 respectively for the STA and LTA mixture condition. Here, at 65 °C, the presence of VG40 binder in the STA BC-2 mixture improved the mixture resistance by more

than three times while for the LTA mixtures the presence of VG40 binder increased the rutting resistance by more than four times over the mixtures with VG20 binder. Similarly, at 65 °C, for the STA DBM-2 mixture type, the mixtures with VG20 binder achieved the terminal rut depth at 30800 while the mixture with VG40 binder reached the terminal rut depth at 66820 wheel passes which clearly shows an improvement by more than two times by having VG40 binder instead of VG20 binder. Further, the LTA DBM-2 mixture with VG20 binder reached the terminal condition at 80,000 wheel passes while the LTA DBM-2 mixture had a rut depth of 13.07 mm after 200,000 wheel passes clearly indicating the superior performance of the mixtures with VG40 binder over the mixtures with VG20 binder. This superior performance of the mixtures with VG40 binder over mixtures with VG20 binder is also seen at all other temperatures at different intervals of wheel passes and at all reliability levels as observed from Table 5.5 and Tables B22 to B24. As VG40 is the highest graded unmodified bitumen as per IS: 73 (BIS, 2013), the above trend of mixtures with VG40 binder having a greater resistance towards permanent deformation than the mixtures with VG20 binder is on expected lines. The VG40 binder is stiffer than the VG20 binder and thus will have higher resistance against permanent deformation than the VG20 binder. This shows that the use of a higher grade of bitumen substantially increases rutting resistance even at higher pavement temperatures.

5.4.2 Effect of Mixture Aging

Table 5.5 also compares the rutting performance of the STA and LTA aged BC-2 and DBM-2 mixtures at different passes. From Table 5.5, it is observed that, at 65 °C, the STA BC-2 mixture with VG20 binder reached the terminal rut depth of 15 mm at 14200 passes whereas the LTA BC-2 mixture with the VG20 binder reached the terminal rut depth at 31860 passes showing an improvement by more than 2 times. Similarly, for the mixtures with VG40 binder at 65 °C, the LTA mixtures showed an improvement by more than 4 times over the STA mixtures. Further, for the DBM-2 mixtures at 65 °C, the LTA mixtures had higher resistance to rutting than the STA mixtures for both the VG20 and VG40 binders. For the BC-2 mixtures with VG20 and VG40 binder respectively, the LTA mixtures showed an improvement over STA mixtures by 49% and 64% at 65 °C and by 24% and 20% at remaining test temperatures. For DBM-2 mixtures with VG20 and VG40 binder respectively, LTA mixtures showed an improvement over STA mixtures by 46% and 70% at 65 °C and by 36% at remaining test temperatures. However, a reasoning can be made that the LTA mixtures are prepared at 4% air voids and the STA mixtures are prepared at 6% air voids and the higher resistance of the LTA mixtures could be due to the presence of lower air voids. In order to study the effect of

aging, the number of passes corresponding to the start of the secondary phase of the permanent deformation curve is determined. The three staged permanent deformation behaviour of bituminous mixtures has already been discussed in Section 1.4. The procedure to calculate the number of passes corresponding to the start of the secondary stage has been explained previously (Khateeb and Basheer, 2009) and is determined using the onset of slope tool with the Origin software. Table 5.6 shows the passes corresponding to the start of the secondary stage for all the four reliability levels and also are illustrated in Figure 5.9. From Table 5.6 and Figure 5.9, it is observed that the passes corresponding to the start of the secondary stage are higher for the LTA mixtures when compared to the STA mixtures at all test temperatures and for both the mixture types. Since the LTA mixtures are prepared with a reduced air void content of 4%, theoretically the start of the secondary stage should be quicker for the LTA mixtures. However, as per the above results, the number of passes corresponding to the start of the secondary stage are more for the LTA mixtures than the STA mixtures. This could only be due to the increase in the stiffness of the binders in the LTA mixtures when compared to the stiffness of the binders in the STA mixtures. This result shows that the aging improves the rutting resistance of bituminous mixtures.

Table 5.6 Passes corresponding to the start of secondary stage

Mixture / Temp. °C	**50% reliability**					
	40	**45**	**50**	**55**	**60**	**65**
STA-BC2-VG20	27220	25660	24880	20130	13740	1374
STA-DBM2-VG20	33080	28140	24060	22960	18480	5420
STA-BC2-VG40	37100	33460	28160	22520	19000	5660
STA-DBM2-VG40	55400	43900	32280	23380	19100	13360
LTA-BC2-VG20	33780	32440	28660	22950	19620	4320
LTA-DBM2-VG20	38080	30820	27280	24780	20010	16960
LTA-BC2-VG40	45500	41340	33240	28680	23520	17180
LTA-DBM2-VG40	59180	49000	46590	31140	28880	21560

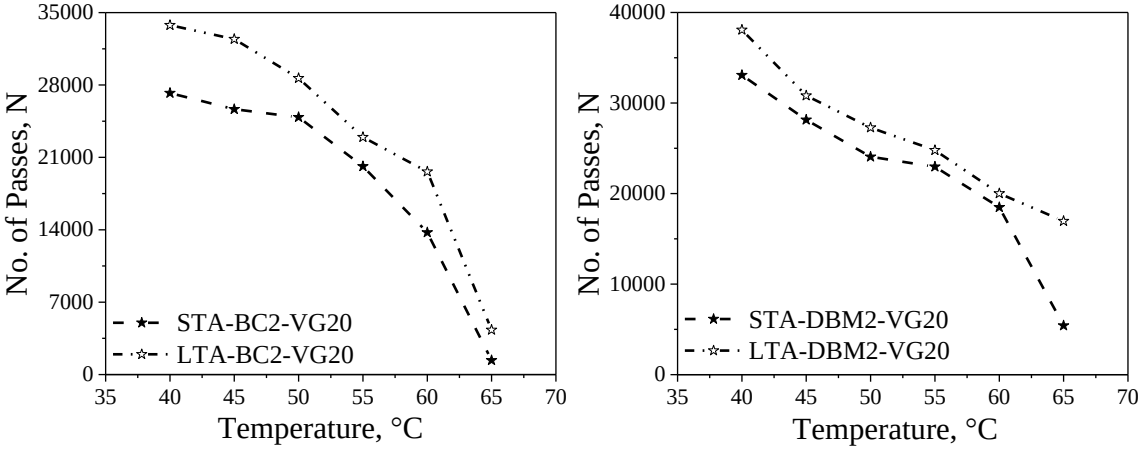

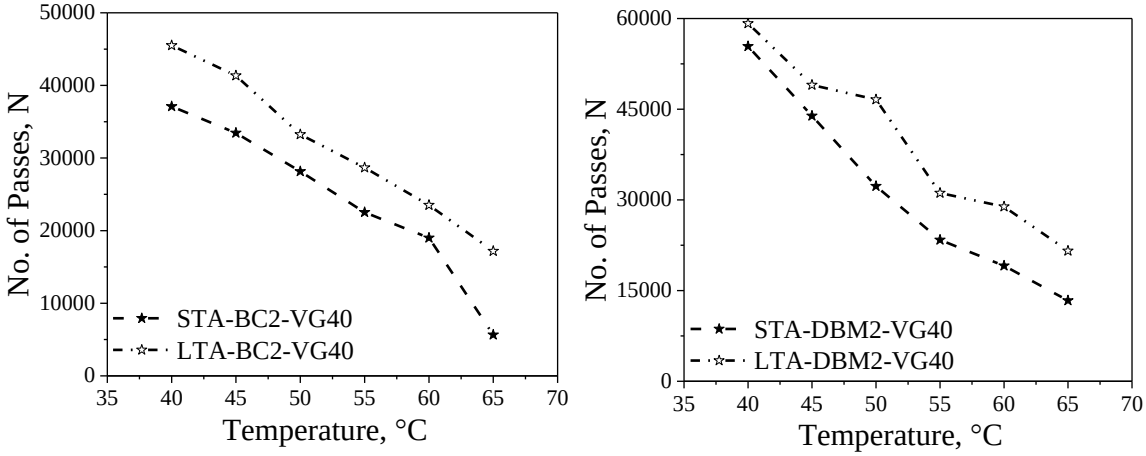

Fig. 5.9 Start of secondary stage at 50% reliability level

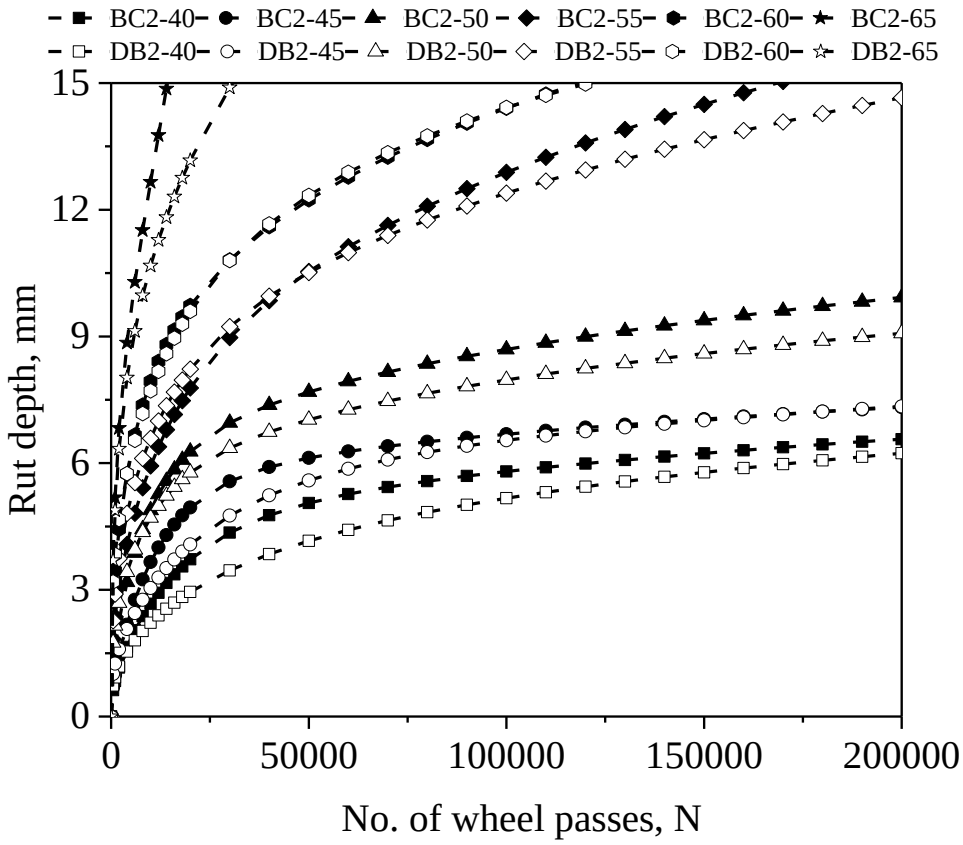

(a) STA BC-2 and DBM-2 prepared with VG20 binder

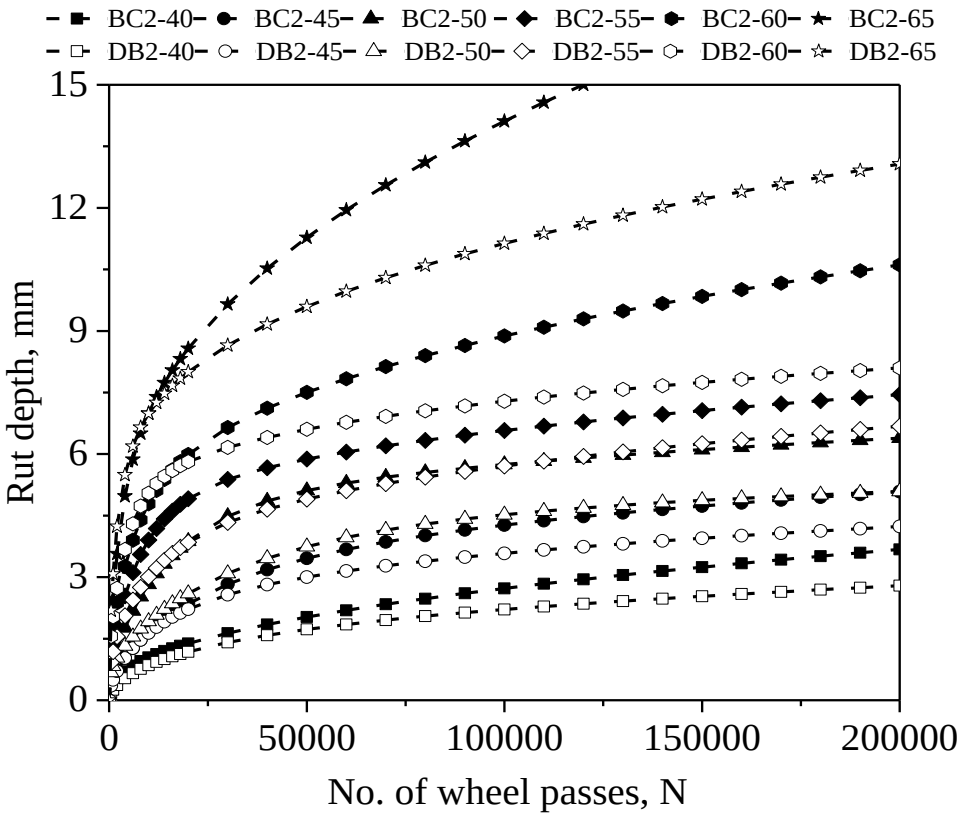

(b) LTA BC-2 and DBM-2 prepared with VG40 binder

Fig. 5.10 Comparison of two bituminous mixtures at 50% reliability

5.4.3 Comparing the Rutting Performance of Two Mixture Gradations

Both the BC-2 and DBM-2 mixtures are densely graded mixtures. Figure 5.10 (a) shows the comparison between the STA BC-2 and DBM-2 mixtures prepared with VG20 bitumen and Figure 5.10 (b) shows the comparison between the LTA BC-2 and DBM-2 mixtures prepared with VG40 bitumen at 50% reliability. From Tables 5.5, B22 to B24 and Figure 5.10 it is observed that both the BC-2 and DBM-2 mixtures had similar rut depths for an initial few thousand passes but gradually the DMB-2 mixtures showed a greater tendency to resist permanent deformation than the BC-2 mixtures. This is observed for almost all the cases of mixture aging condition, for both the binders and at various temperatures. At 65 °C, the DBM-2 mixtures showed an improvement in rutting resistance by 63% over the BC-2 mixtures, whereas, at temperatures other than 65 °C, the DBM-2 mixtures showed an improvement by 18% when compared with the BC-2 mixtures for most of the cases. This higher resistance offered by DBM-2 mixtures over the BC-2 mixtures is observed for both STA as well as LTA mixtures and with both VG20 and VG40 bitumen. DBM-2 mixtures showing an overall higher resistance towards permanent deformation than the BC-2 mixtures may be due to the presence of the higher nominal sized aggregate in the DBM-2 mixtures

resulting in a better interlocking between the aggregates than the interlocking in the BC-2 mixtures. This supposedly better interlocking in the DBM-2 mixtures might be due to the confined testing of the bituminous slabs in a WTD. From the overall comparison of the two mixture gradations for both the aging conditions, it can be said that the DBM-2 mixtures had a better resistance against permanent deformation than the BC-2 mixtures. These results are contrary to those reported earlier (Saboo and Kumar, 2006).

5.5 DETERMINING THE RUTTING RATES

From the wheel tracking tests, the rutting rate (*Rr*) is also considered as dry wheel test parameter along with accumulated rut depth. The rutting rate analysis is carried out only for the average of the data from 27 locations along the wheel traverse. The rutting rate (Rr_M) is determined as specified in Morea et al. (2013) as shown in Equation (5.4). Here, the test data is considered for a duration of 120 minutes only. Since, in this current research, the tests are conducted from 40 to 65 °C, it is possible that the mixtures at different temperatures could be in different zones (primary or secondary zone) for a duration of 120 minutes. From the wheel tracking tests it is observed that the secondary stage in the STA BC-2 mixtures prepared with VG20 bitumen at 65 °C starts at 35 minutes which is well below 120 minutes. Therefore, the Equation (5.4) is modified by using 30 minutes as the maximum duration and the modified form of the rutting rate (Rr_P) is shown as Equation (5.5). Using Equation (5.5) the rutting rate is calculated only in the primary zone for all mixture conditions. Additionally, one more rutting rate is determined at the terminal condition (Rr_T), and its form is shown in Equation (5.6). The terminal duration of the test is 4000 minutes. The three rutting rates are shown in Table 5.7.

5.6 SUMMARY

The wheel tracking tests are carried out on the STA and LTA BC-2 and DBM-2 mixtures prepared with the VG20 and VG40 binders using a small wheel tracking device. The raw permanent deformation data is analysed using a probabilistic approach. The rutting performance of the binders and mixtures types is compared. Also, the influence of mixture aging on the rutting resistance of bituminous mixtures is analysed. Moreover, different rutting rates are also determined.

Table 5.7 Rutting rates

Temp., °C	STA			LTA		
	VG20-BC					
	Rr_M	Rr_P	Rr_T	Rr_M	Rr_P	Rr_T
40	9.09	17.53	0.38	6.53	13.16	0.36
45	13.48	24.65	0.32	6.63	14.91	0.48
50	15.81	34.18	0.61	13.73	30.22	0.34
55	16.81	41.42	1.43	16.35	36.88	0.48
60	20.37	57.31	1.29	18.62	43.17	0.84
65	32.76	97.83		27.22	64.65	
VG20-DBM						
40	6.13	14.97	0.53	3.17	10.84	0.31
45	8.71	19.12	0.40	5.45	21.65	0.38
50	11.87	31.23	0.55	6.48	17.19	0.37
55	16.61	48.47	1.12	13.17	30.63	0.57
60	17.75	48.68	1.09	14.36	42.75	1.11
65	24.57	86.70		18.44	52.22	
VG40-BC						
40	4.91	11.44	0.46	3.01	9.01	0.47
45	8.61	16.97	0.40	5.47	11.09	0.40
50	14.67	32.51	0.51	9.52	18.28	0.32
55	16.48	37.15	0.53	12.81	28.17	0.43
60	21.87	47.99	0.63	14.41	35.45	0.86
65	22.86	76.09		19.32	61.73	
VG40-DBM						
40	4.34	8.97	0.42	2.82	6.09	0.29
45	5.63	12.99	0.38	5.37	11.15	0.33
50	8.57	21.95	0.42	5.28	11.52	0.29
55	15.49	37.05	0.57	8.65	20.44	0.48
60	18.90	50.93	0.91	13.39	39.34	0.41
65	19.16	72.17	-	14.38	68.61	0.96

$$Rr_M = \frac{(D_{120\,min} - D_{105\,min}) * 1000}{15\,min} \quad (5.4)$$

$$Rr_P = \frac{(D_{30\,min} - D_{15\,min}) * 1000}{15\,min} \quad (5.5)$$

$$Rr_T = \frac{(D_{4000\,min} - D_{2000\,min}) * 1000}{2000\,min} \quad (5.6)$$

where,

Rr = Rutting rate in µm/min,

D_{ti} = Rut depth after specified time, and

Dx = duration corresponding to the mid-point of secondary zone

CHAPTER-6

CORRELATIONS OF RUTTING PARAMETERS WITH MIXTURE RUT DATA

6.1 GENERAL

In the Chapter 4, the non-Newtonian behaviour of the VG20 and VG40 bitumen binders is analysed using the LSRS test and η_{TV} and $\eta_{0(L)}$ are determined. Here, η_{TV} is proposed as a non-Newtonian rutting parameter. From the SWSSRS tests using a RV and a DSR, $\eta_{0(S\text{-}RV)}$ and $\eta_{0(S\text{-}DSR)}$ are proposed as Newtonian rutting parameters. Since $\eta_{0(S\text{-}RV)}$ is determined at only four and three temperatures respectively for unaged and short-term aged VG20 binder, it is not considered for correlations with mixture rut data and rut rate. Since $\eta_{0(S\text{-}DSR)}$ is determined at all test conditions, it is used to correlate with the mixture rut data and mixture rutting rates. In addition three existing rutting parameters, the binder $|G^*|/\sin\delta$, $|G^*|/(1-(1/\tan\delta\sin\delta))$ and J_{nr} at 3.2 kPa are also determined. In order to validate the efficacy of $\eta_{0(S\text{-}DSR)}$ and η_{TV}, it is necessary to check the performance of the proposed parameters by correlating them with the mixture rutting parameters. As $\eta_{0(S\text{-}RV)}$ is not used in this section, $\eta_{0(S\text{-}DSR)}$ is henceforth denoted as $\eta_{0(S)}$.

6.2 RELATING THE BINDER PROPERTIES WITH THE RUT DEPTHS AT SPECIFIED NUMBER OF PASSES

Generally, in the Hamburg wheel tracking device (AASHTO, 2017) and in small wheel tracking devices (BS- EN, 2003) the specimens are tracked for 20,000 passes. The maximum number of passes specific to some other wheel tracking devices and their failure criteria have been summarized elsewhere (Singh and Swamy, 2018). In the past, researchers correlated the binder rutting parameters with the rut depths mostly at one specific number of passes that too, mostly at 20,000 passes. However, in this study, as mentioned previously, the slabs of bituminous mixture are tracked for a total of 200,000 passes or until a rut depth of 15 mm, whichever is the earliest. Moreover, as discussed in the Section 5.3, the probabilistic rut data at four reliability levels determined with the Weibull distribution is used for correlating with

the binder rutting parameters. Later, the rut depths at 20,000, 40,000, 60,000, 80,000, 100,000, 120,000, 140,000, 160,000, 180,000 and 200,000 wheel passes are then correlated with the six rutting parameters $\eta_{0(S)}$, η_{TV}, $\eta_{0(L)}$, $|G^*|/\sin\delta$, $|G^*|/(1-(1/\tan\delta\sin\delta))$ and J_{nr} at 3.2 kPa. The correlations are developed with the rut data determined at all the four reliability levels. All the six rutting parameters, $\eta_{0(S)}$, η_{TV}, $\eta_{0(L)}$, $|G^*|/\sin\delta$, $|G^*|/(1-(1/\tan\delta\sin\delta))$ and J_{nr} at 3.2 kPa are correlated with the rut data using a power law model whose form is shown in Equation (6.1).

$$y = a * x^b, \tag{6.1}$$

where,

y = dependent variable, here it is the rut depth in mm,

a,b = model coefficients,

x = independent variable, here it is $\eta_{0(S)}$, η_{TV}, $\eta_{0(L)}$, $|G^*|/\sin\delta$, $|G^*|/(1-(1/\tan\delta\sin\delta))$ and J_{nr} at 3.2 kPa.

Figures 6.1 to 6.4 show the relationship of the bitumen properties determined in this research with the rut depth of the STA BC-2 mixtures prepared with VG20 bitumen at 20,000 passes and at all the four reliability levels. The coefficient of correlation, R^2, is used a measure to determine the goodness of fit. Tables 6.1 to 6.4 show R^2 of the STA BC-2 mixtures prepared with VG20 bitumen at all the four reliability levels, whereas the R^2 of all the individual mixtures is shown in Appendix C (Tables C1 to C7). From Figures 6.1 to 6.4, it is observed that all the six rutting parameters exhibited a strong correlation with the mixture rut depth with an almost identical values of R^2. Moreover, relationships of the six rutting parameters with mixture rut depth of STA and LTA DBM-2 mixtures prepared with VG20 and VG40 binders at 20,000 passes are observed to exhibit a strong correlation. Similar correlations established at remaining set of wheel passes are consolidated wherein the R^2 values for the power law model are shown in Tables 6.1 to 6.4. From Tables 6.1 to 6.4, it is observed that there is not much difference between the R^2 values at four reliability levels for a particular mixture type i.e., the correlations are independent of the level of reliability. However, it is also observed that there is a slight decrease in R^2 at with an increase in the pre specified wheel passes at a particular reliability level. This trend is observed for all the mixture types when compared individually. From Figures 6.1 to 6.4 and Tables 6.1 to 6.4, it can be said that the proposed new rutting parameters, $\eta_{0(S)}$ and η_{TV}, show an equally strong correlation with the rut depth at 20,000 passes and also at an extended series of wheel passes in similar lines as that of

the well-established binder rutting parameters including $\eta_{0(L)}$, $|G^*|/\sin\delta$, $|G^*|/(1-(1/\tan\delta\sin\delta))$ and J_{nr} at 3.2 kPa.

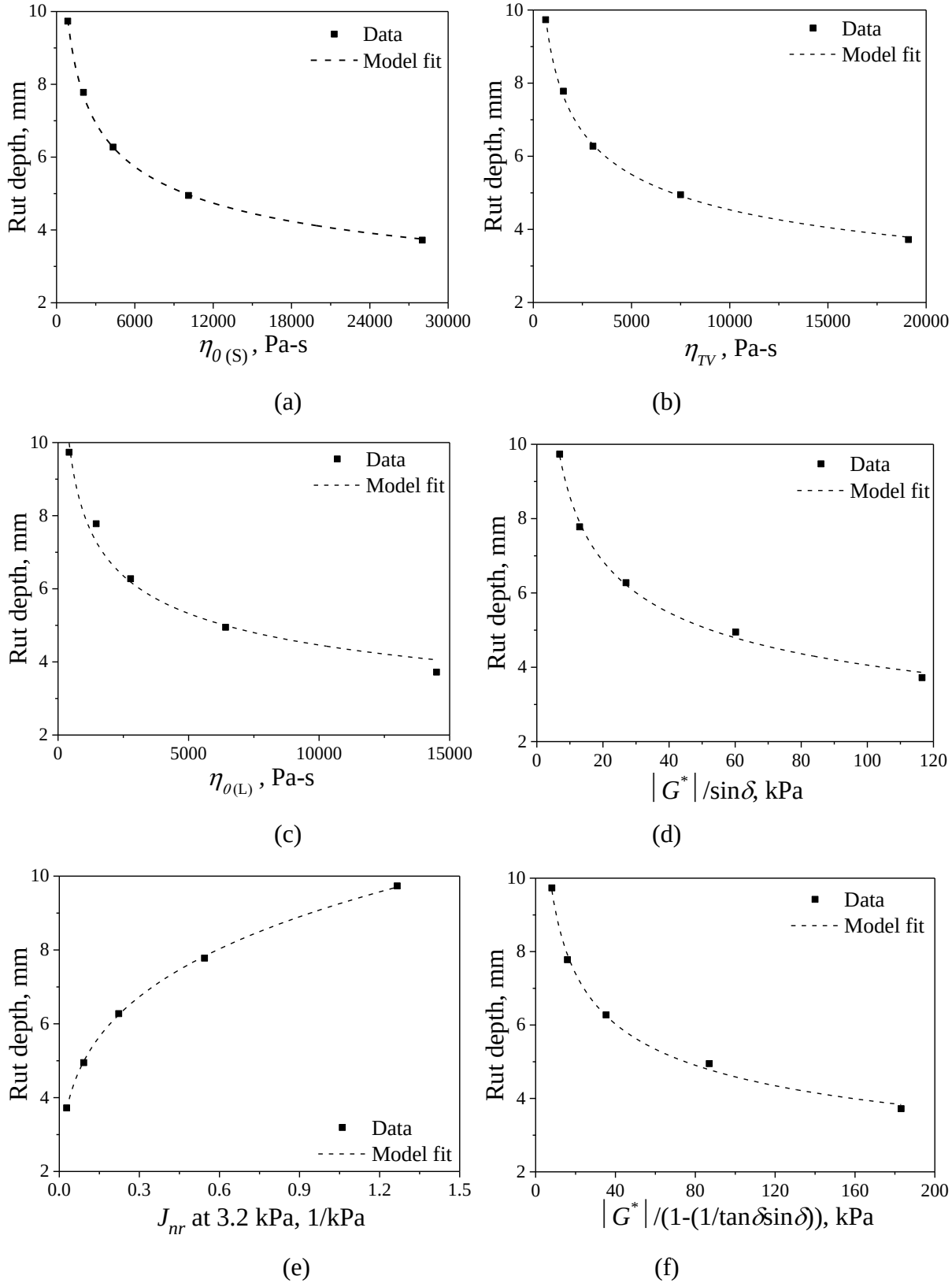

Fig. 6.1 Variation of rut depth of the STA BC-2 mixtures prepared with VG20 binder as a function of the six rutting parameters at 20,000 passes at 50% reliability

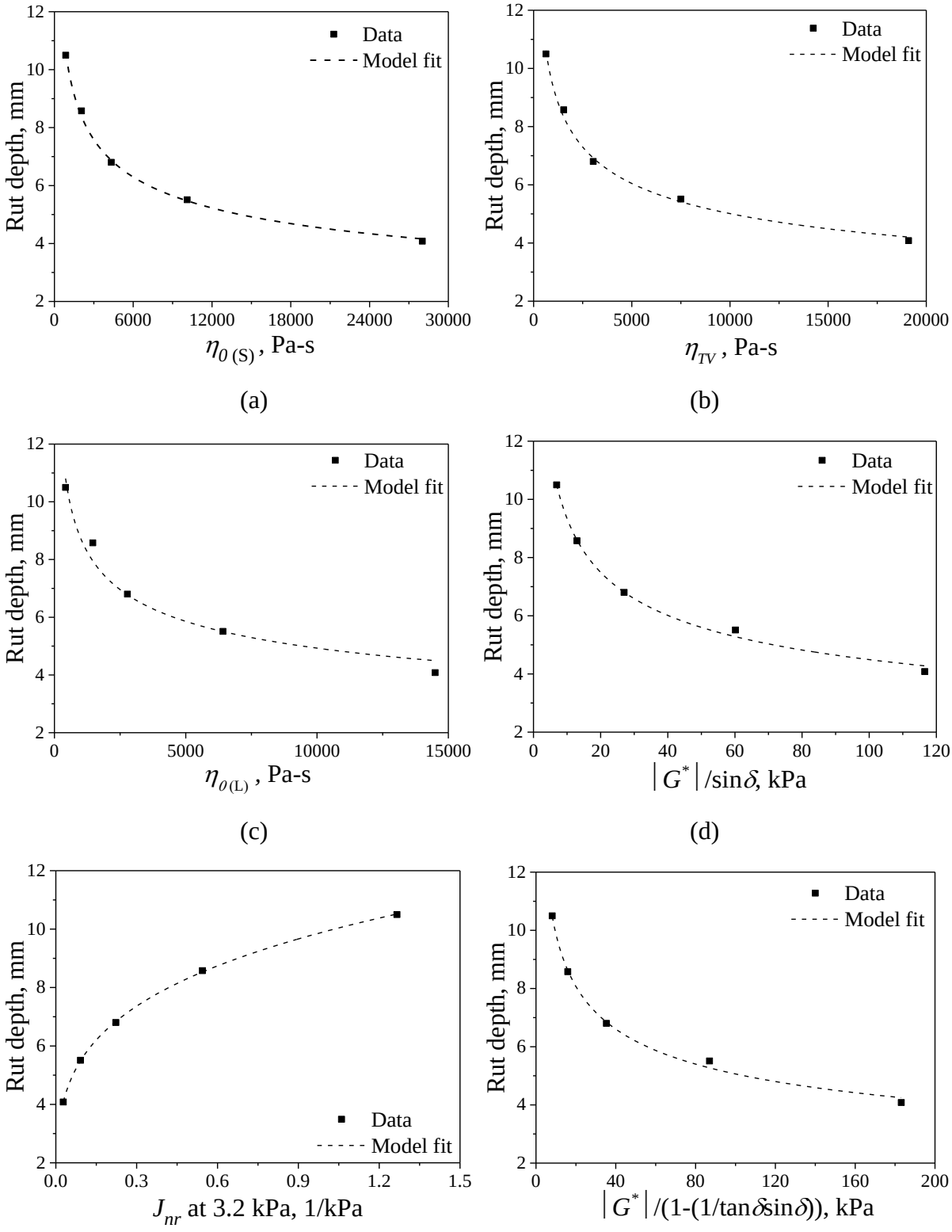

Fig. 6.2 Variation of rut depth of the STA BC-2 mixtures prepared with VG20 binder as a function of the six rutting parameters at 20,000 passes at 80% reliability

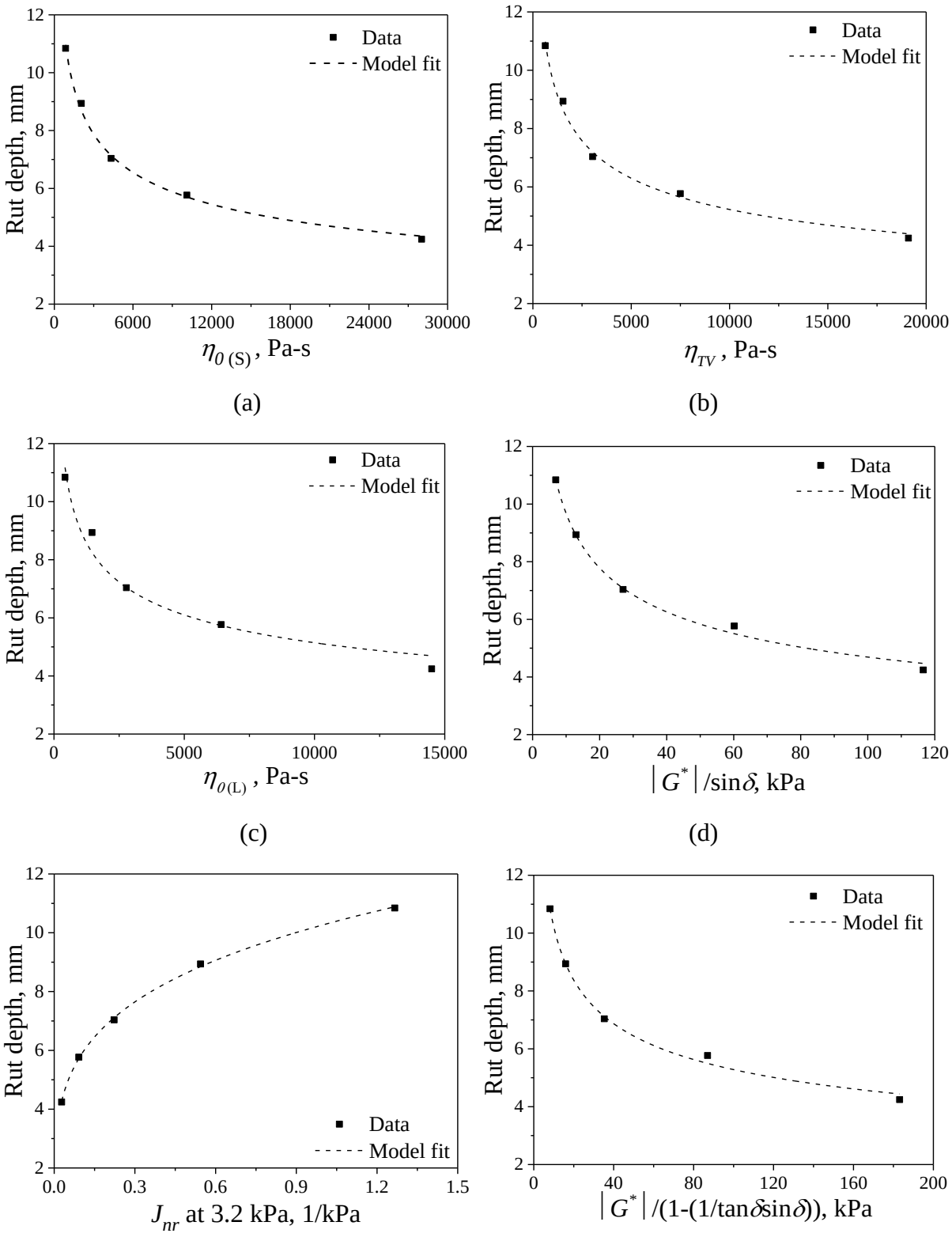

Fig. 6.3 Variation of rut depth of the STA BC-2 mixtures prepared with VG20 binder as a function of the six rutting parameters at 20,000 passes at 90% reliability

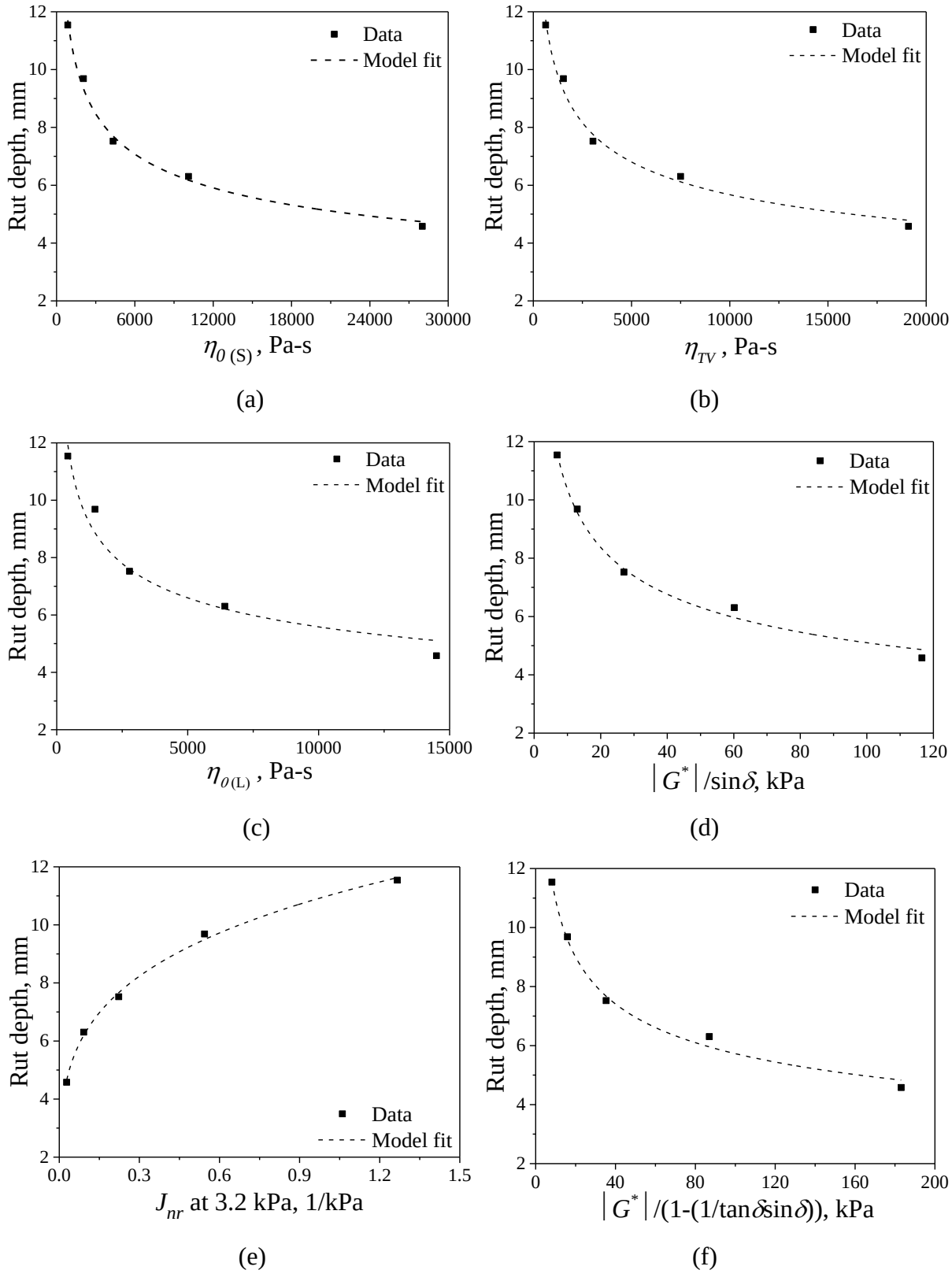

Fig. 6.4 Variation of rut depth of the STA BC-2 mixtures prepared with VG20 binder as a function of the six rutting parameters at 20,000 passes at 99% reliability

Table 6.1 Coefficient of correlation for the STA BC-2 prepared with VG20 bitumen at 50% reliability

Passes	$\eta_{0(S)}$	η_{TV}	$\eta_{0(L)}$	$\|G^*\|/\sin\delta$	J_{nr} *at 3.2 kPa*	$\|G^*\|/(1-(1/\tan\delta\sin\delta))$
20000	1.00	1.00	0.97	1.00	1.00	1.00
40000	0.98	0.98	0.94	0.99	0.99	0.99
60000	0.96	0.96	0.92	0.98	0.97	0.98
80000	0.95	0.94	0.90	0.97	0.96	0.97
100000	0.93	0.93	0.88	0.96	0.95	0.96
120000	0.92	0.92	0.87	0.96	0.94	0.96
140000	0.91	0.91	0.86	0.95	0.93	0.95
160000	0.91	0.90	0.85	0.94	0.92	0.94
180000	0.90	0.89	0.84	0.94	0.92	0.94
200000	0.89	0.89	0.83	0.93	0.91	0.93

Table 6.2 Coefficient of correlation for the STA BC-2 prepared with VG20 bitumen at 80% reliability

Passes	$\eta_{0(S)}$	η_{TV}	$\eta_{0(L)}$	$\|G^*\|/\sin\delta$	J_{nr} *at 3.2 kPa*	$\|G^*\|/(1-(1/\tan\delta\sin\delta))$
20000	1.00	0.99	0.97	1.00	1.00	1.00
40000	0.98	0.98	0.95	0.99	0.99	0.99
60000	0.97	0.97	0.93	0.99	0.98	0.99
80000	0.96	0.95	0.92	0.98	0.97	0.98
100000	0.95	0.94	0.91	0.97	0.96	0.97
120000	0.94	0.94	0.89	0.97	0.95	0.97
140000	0.93	0.93	0.88	0.96	0.94	0.96
160000	0.93	0.92	0.87	0.96	0.94	0.96
180000	0.92	0.91	0.87	0.95	0.93	0.95
200000	0.91	0.91	0.86	0.95	0.93	0.95

Table 6.3 Coefficient of correlation for the STA BC-2 prepared with VG20 bitumen at 90% reliability

Passes	$\eta_{0(S)}$	η_{TV}	$\eta_{0(L)}$	$\|G^*\|/\sin\delta$	J_{nr} *at 3.2 kPa*	$\|G^*\|/(1-(1/\tan\delta\sin\delta))$
20000	1.00	0.99	0.96	0.99	1.00	0.99
40000	0.99	0.98	0.95	0.99	0.99	0.99
60000	0.97	0.97	0.94	0.99	0.98	0.99
80000	0.96	0.96	0.93	0.98	0.97	0.98
100000	0.95	0.95	0.92	0.98	0.96	0.98
120000	0.95	0.94	0.91	0.97	0.96	0.97
140000	0.94	0.93	0.90	0.97	0.95	0.97
160000	0.93	0.93	0.89	0.96	0.94	0.96
180000	0.93	0.92	0.88	0.96	0.94	0.96
200000	0.92	0.91	0.87	0.95	0.93	0.95

Table 6.4 Coefficient of correlation for the STA BC-2 prepared with VG20 bitumen at 99% reliability

Passes	$\eta_{0(S)}$	η_{TV}	$\eta_{0(L)}$	$\lvert G^* \rvert / \sin\delta$	J_{nr} at 3.2 kPa	$\lvert G^* \rvert / (1-(1/\tan\delta \sin\delta))$
20000	0.99	0.99	0.95	0.99	1.00	0.99
40000	0.99	0.98	0.96	0.99	0.99	0.99
60000	0.98	0.97	0.95	0.99	0.98	0.99
80000	0.97	0.97	0.94	0.99	0.97	0.98
100000	0.96	0.96	0.93	0.98	0.97	0.98
120000	0.96	0.95	0.93	0.98	0.96	0.98
140000	0.95	0.95	0.92	0.97	0.96	0.97
160000	0.94	0.94	0.91	0.97	0.95	0.97
180000	0.94	0.93	0.90	0.97	0.94	0.96
200000	0.93	0.93	0.89	0.96	0.94	0.96

Moreover, relationships of the six rutting parameters with the rut data of a particular mixture independent of binder type are also developed. As discussed previously, with both VG20 and VG40 binders, STA BC-2 and DBM-2 mixtures are fabricated with an air void content of 6%, whereas, LTA BC-2 and DBM-2 mixtures are fabricated with an air void content of 4%. Therefore, for a particular mix type, air voids, aggregate type, aggregate gradation, speed of the wheel, wheel load are kept constant, thereby the only variable is the binder property. The correlations are made for four mixture types employed in this study namely STA BC-2, LTA BC-2, STA DBM-2 and LTA DBM-2. The correlations are established at the four reliability levels and also at all the pre specified number of wheel passes similar to the first set of correlations. Figures 6.5 and 6.6 show the correlations of the six rutting parameters with the rut data at 50% reliability level and at 20,000 passes for STA BC-2 and LTA BC-2 whereas similar figures for the STA DBM-2 and LTA BC-2 mixtures are shown in Appendix C (Figures C1 to C2). Correlations similar to those shown in Figures 6.5-6.6 but at all the remaining reliability levels and also at all the pre specified passes are shown in Appendix C (Tables C8 to C11). Tables 6.5 and 6.6 show the coefficient of correlation of the six rutting parameters with the rut data corresponding to the STA and LTA BC-2 mixtures at 50% reliability level and all the pre specified passes whereas similar tables at the remaining three reliability levels are shown in Appendix C (Tables C8 to C11). From Figures 6.5 and 6.6 it is observed that all the six rutting parameters had a strong correlation with mixture rut data. However, it is also observed that $\eta_{0(S)}$ shows the highest degree of correlation with mixture rut data for all the four mixture types with R^2 of 0.92, 0.971, 0.95

and 0.96 for the STA BC-2, LTA BC-2, STA DBM-2 and LTA DBM-2 mixtures respectively at 20,000 passes at 50% reliability. Moreover, from Tables C8 to C11 (in Appendix C) it is also observed that $\eta_{0(S)}$ has the highest correlation at 20,000 passes at all the three remaining reliability levels. It is also observed from Tables 6.5, 6.6 and C8 to C11 (in Appendix C) that $\eta_{0(S)}$ has the highest correlation at all the specified number of passes for almost all the cases. $\eta_{0(S)}$ is followed by J_{nr} which showed the second best correlation. η_{TV} has an overall third best correlation. $\eta_{0(L)}$, $|G^*|/\sin\delta$ and $|G^*|/(1-(1/\tan\delta\sin\delta))$ has similar coefficient of correlations for almost all the cases and equally stood fourth in the ranking of rutting parameters. These results clearly showed that there is a hierarchy in the six rutting parameters with an overall ranking wherein $\eta_{0(S)} > J_{nr} > \eta_{TV} > \eta_{0(L)} \approx |G^*|/\sin\delta \approx |G^*|/(1-(1/\tan\delta\sin\delta))$. This hierarchy is not observed when the first set of correlations are made.

However, the second set of correlations of the six rutting parameters independent of the bitumen type provides a realistic picture because of the more number of the data points. Here, twelve data points are used to determine the degree of correlations between the bitumen parameter and the mixture rut data whereas in the previous case only six data points are used to determine the relationships. It is also observed from Tables 6.5, 6.6 and Tables C8 to C11 (in Appendix C) that the coefficient of correlation at four reliability levels is more or less similar for a particular mixture type. Also there are no observable trends with the coefficient of correlations determined at different pre specified number of passes. These observations tend to show that the coefficient of correlation is independent of reliability level and the number of passes. The results as discussed above show that the newly identified Newtonian viscosity $\eta_{0(S)}$ is the best performing rutting parameter in this study. Its results are better than J_{nr} which is currently the most popular rutting parameter. It is worth mentioning here that both the rutting parameters exhibit a very strong correlation and are very close. Moreover, η_{TV}, proposed as a non-Newtonian rutting parameter, is closely behind the J_{nr} and is better than the other popular rutting parameters $\eta_{0(L)}$, $|G^*|/\sin\delta$ and $|G^*|/(1-(1/\tan\delta\sin\delta))$.

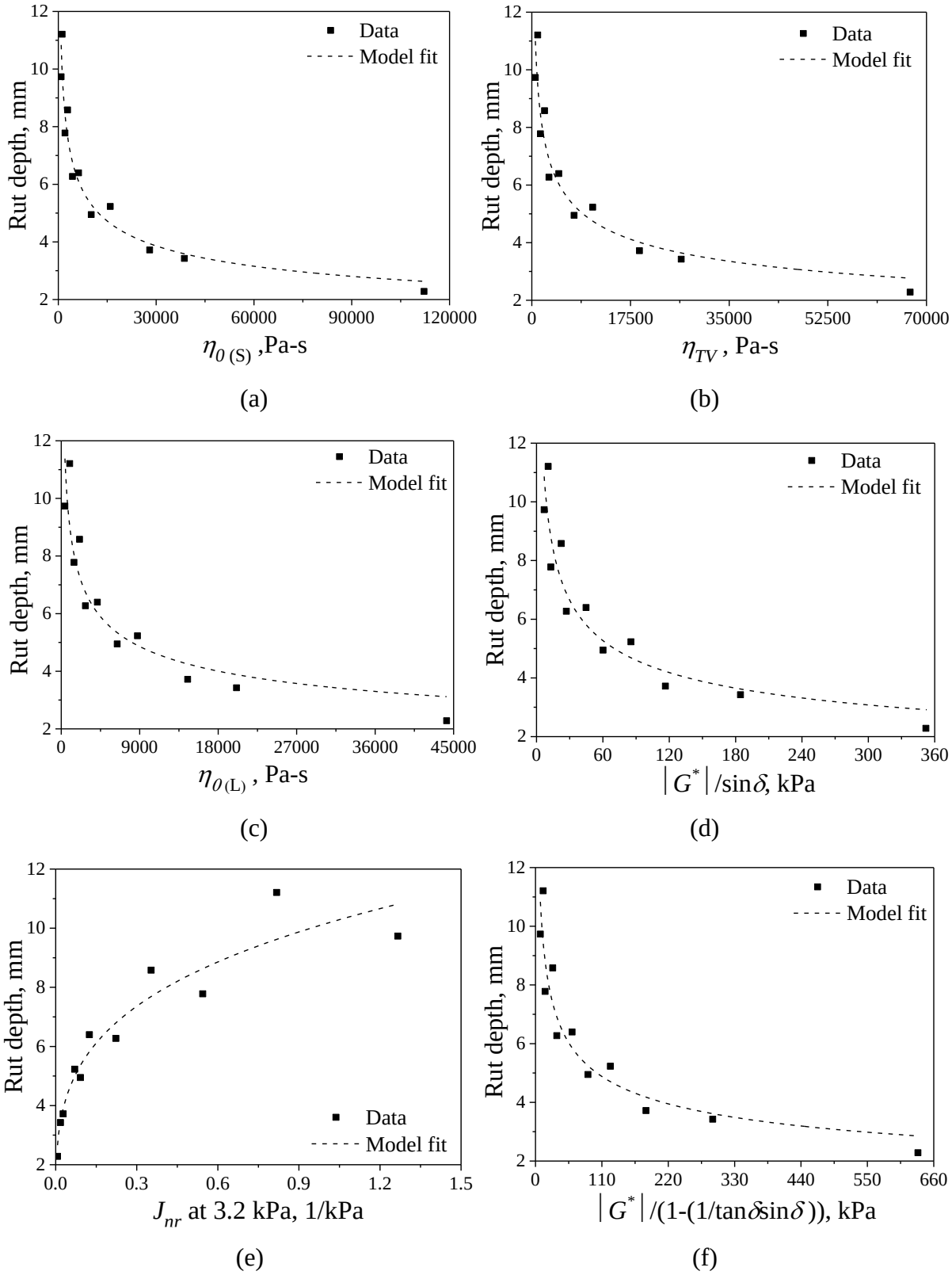

Fig. 6.5 Variation of rut depth of the STA BC-2 mixtures as function of the six rutting parameters at 20,000 passes at 50% reliability

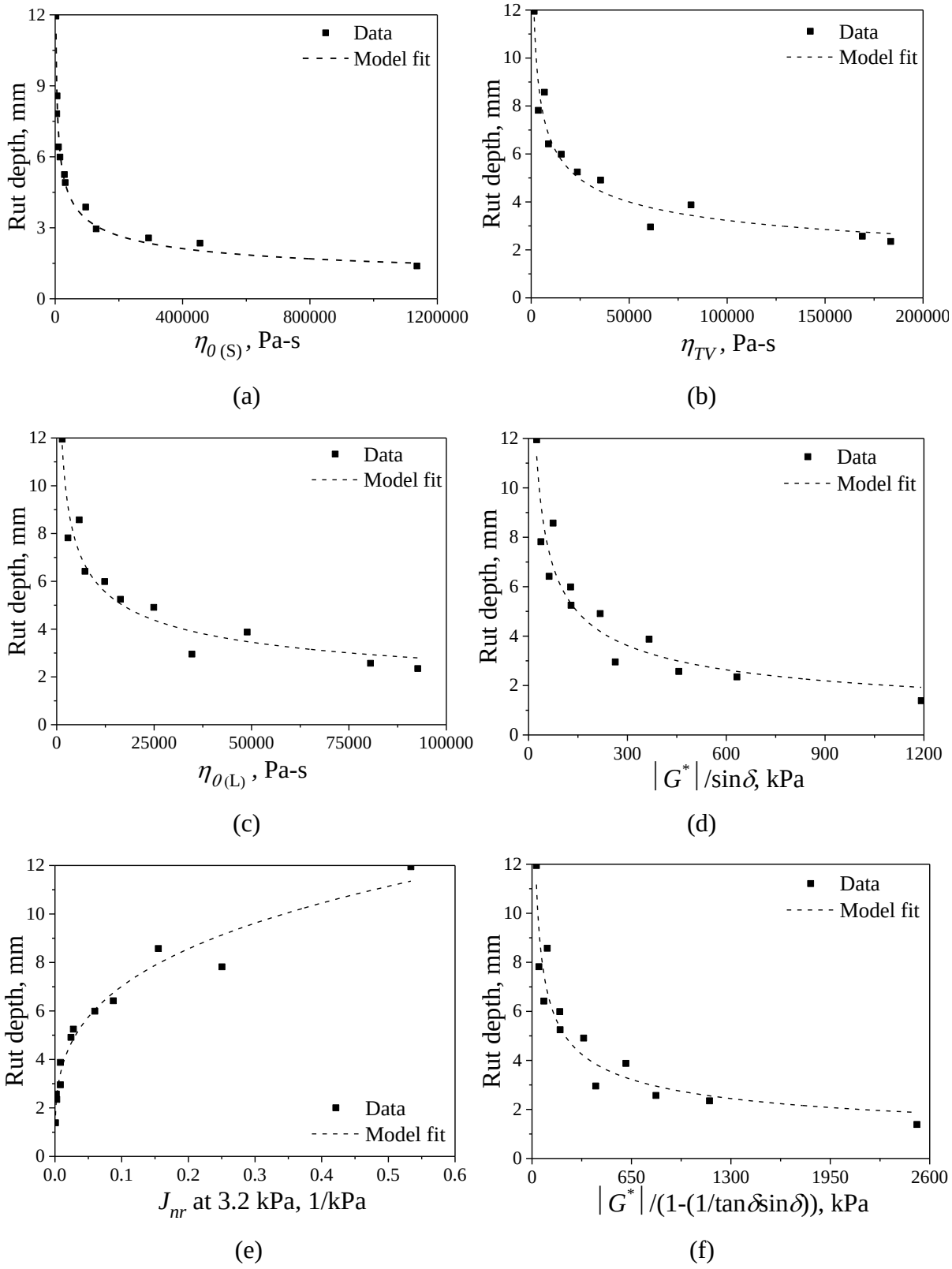

Fig. 6.6 Variation of rut depth of the LTA BC-2 mixtures as function of the six rutting parameters at 20,000 passes at 50% reliability

Table 6.5 Coefficient of correlation for STA BC-2 mixture at 50% reliability

Passes	$\eta_{0(S)}$	η_{TV}	$\eta_{0(L)}$	$\lvert G^*\rvert/\sin\delta$	J_{nr} at 3.2 kPa	$\lvert G^*\rvert/(1-(1/\tan\delta\sin\delta))$
20000	0.92	0.89	0.84	0.87	0.91	0.88
40000	0.91	0.87	0.82	0.86	0.89	0.87
60000	0.85	0.80	0.74	0.80	0.82	0.80
80000	0.97	0.96	0.93	0.96	0.97	0.97
100000	0.96	0.96	0.93	0.96	0.97	0.97
120000	0.95	0.95	0.92	0.96	0.96	0.96
140000	0.95	0.95	0.92	0.96	0.96	0.96
160000	0.94	0.94	0.91	0.96	0.95	0.96
180000	0.94	0.94	0.91	0.95	0.95	0.96
200000	0.93	0.93	0.91	0.95	0.94	0.95

Table 6.6 Coefficient of correlation for LTA BC-2 mixture at 50% reliability

Passes	$\eta_{0(S)}$	η_{TV}	$\eta_{0(L)}$	$\lvert G^*\rvert/\sin\delta$	J_{nr} at 3.2 kPa	$\lvert G^*\rvert/(1-(1/\tan\delta\sin\delta))$
20000	0.97	0.94	0.93	0.90	0.96	0.90
40000	0.92	0.92	0.91	0.87	0.92	0.86
60000	0.93	0.84	0.80	0.76	0.91	0.76
80000	0.90	0.80	0.77	0.73	0.89	0.73
100000	0.88	0.78	0.74	0.70	0.87	0.70
120000	0.86	0.75	0.72	0.68	0.85	0.67
140000	0.95	0.93	0.91	0.88	0.97	0.87
160000	0.95	0.92	0.90	0.87	0.97	0.87
180000	0.94	0.92	0.90	0.87	0.96	0.86
200000	0.93	0.91	0.89	0.86	0.96	0.86

6.3 RELATING THE BINDER PROPERTIES WITH RUTTING RATE

The six bitumen properties are also correlated with the rutting rate of bituminous mixtures. Figure 6.7 shows the relationship of $\eta_{0(S)}$ with the rutting rates of the STA BC-2 mixtures prepared with VG20 bitumen. Whereas, Figure 6.8 shows the relationship of $\eta_{0(S)}$ with the rutting rates of the STA BC-2 mixtures prepared with both the VG20 and VG40 bitumen binders. The coefficient of correlation of all the bitumen parameters with all the rut rates and all the test conditions are shown in Tables 6.7 and 6.8. From Figures 6.7 and 6.8, it is observed that the coefficient of correlation is relatively higher when the binder properties are related with Rr_P than with Rr_M. This may be because Rr_P is determined exclusively in the primary zone. Moreover, it is also observed that Rr_T shows a poor correlation with binder

properties. These results show that the use of *Rr* as a dry wheel tracking test parameter should only be considered during a short period of testing and in particular during the primary stage.

A comparison of the relationship of the six binder properties with Rr_P for the STA BC-2 mixture is shown in Figure 6.9. From Figure 6.9 and Table 6.8, it is observed that all the six binder properties exhibit a strong correlation with Rr_P. However, it is also observed that $\eta_{0\,(S)}$ has the highest correlation followed by J_{nr}. A strong correlation of all the six binder properties is also observed with Rr_M which is shown in Table 6.8. Again it is also observed that $\eta_{0\,(S)}$ has the highest correlation with Rr_M.

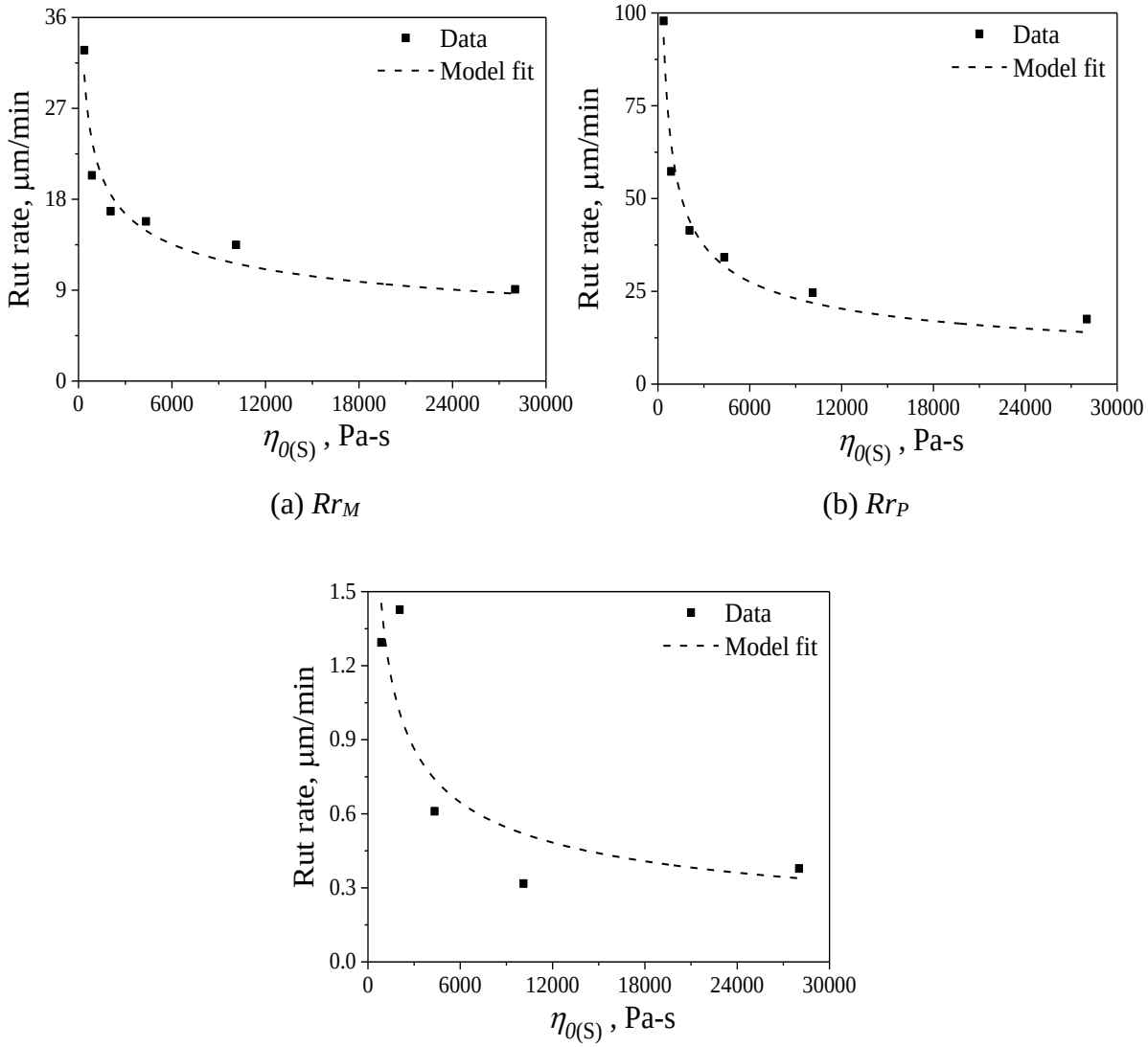

Fig. 6.7 Rutting rates as a function of $\eta_{0\,(S)}$ for the STA BC-2 mixtures prepared with VG20 bitumen

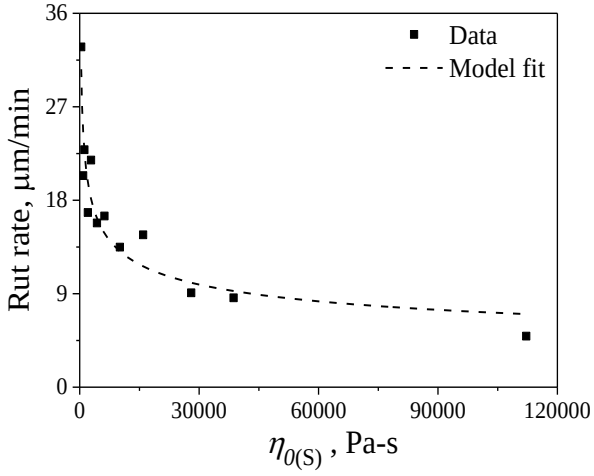

(a) Rr_M

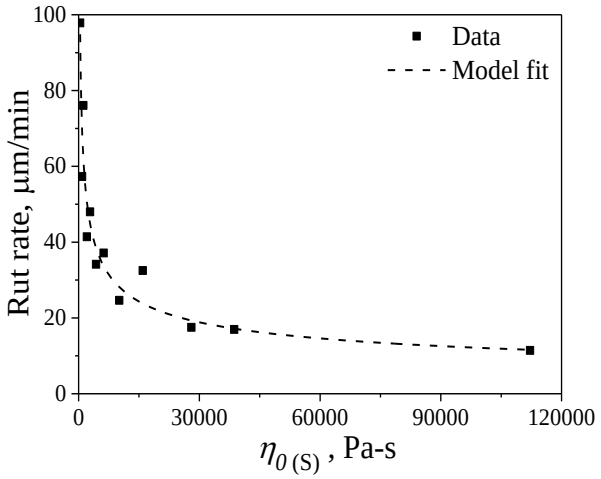

(b) Rr_P

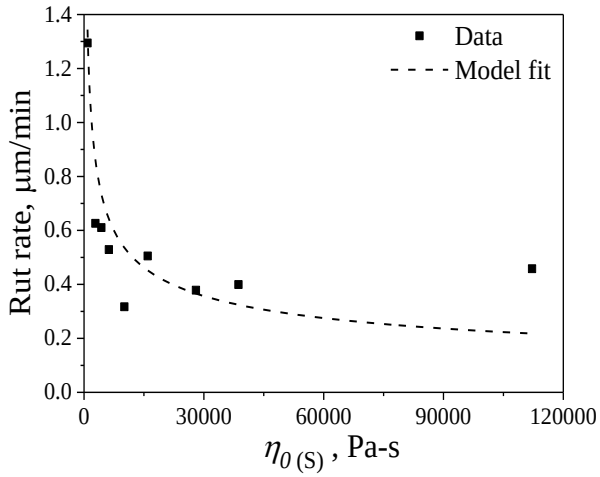

(c) Rr_T

Fig. 6.8 Rutting rates as function of $\eta_{0\,(S)}$ for the STA BC-2 mixture

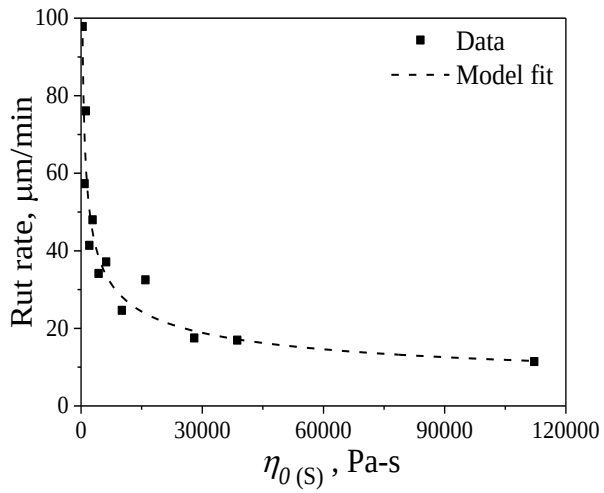

(a)

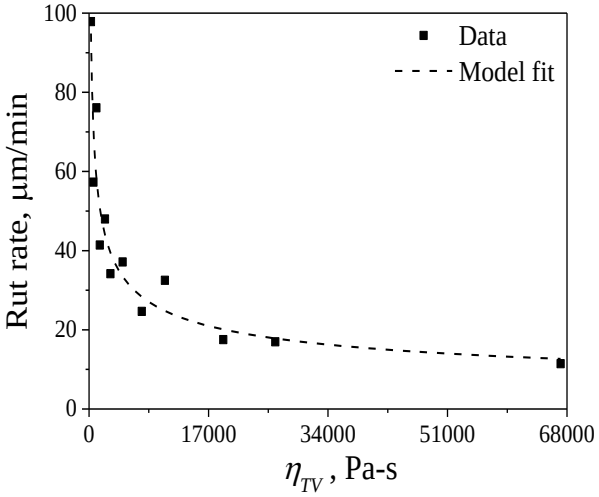

(b)

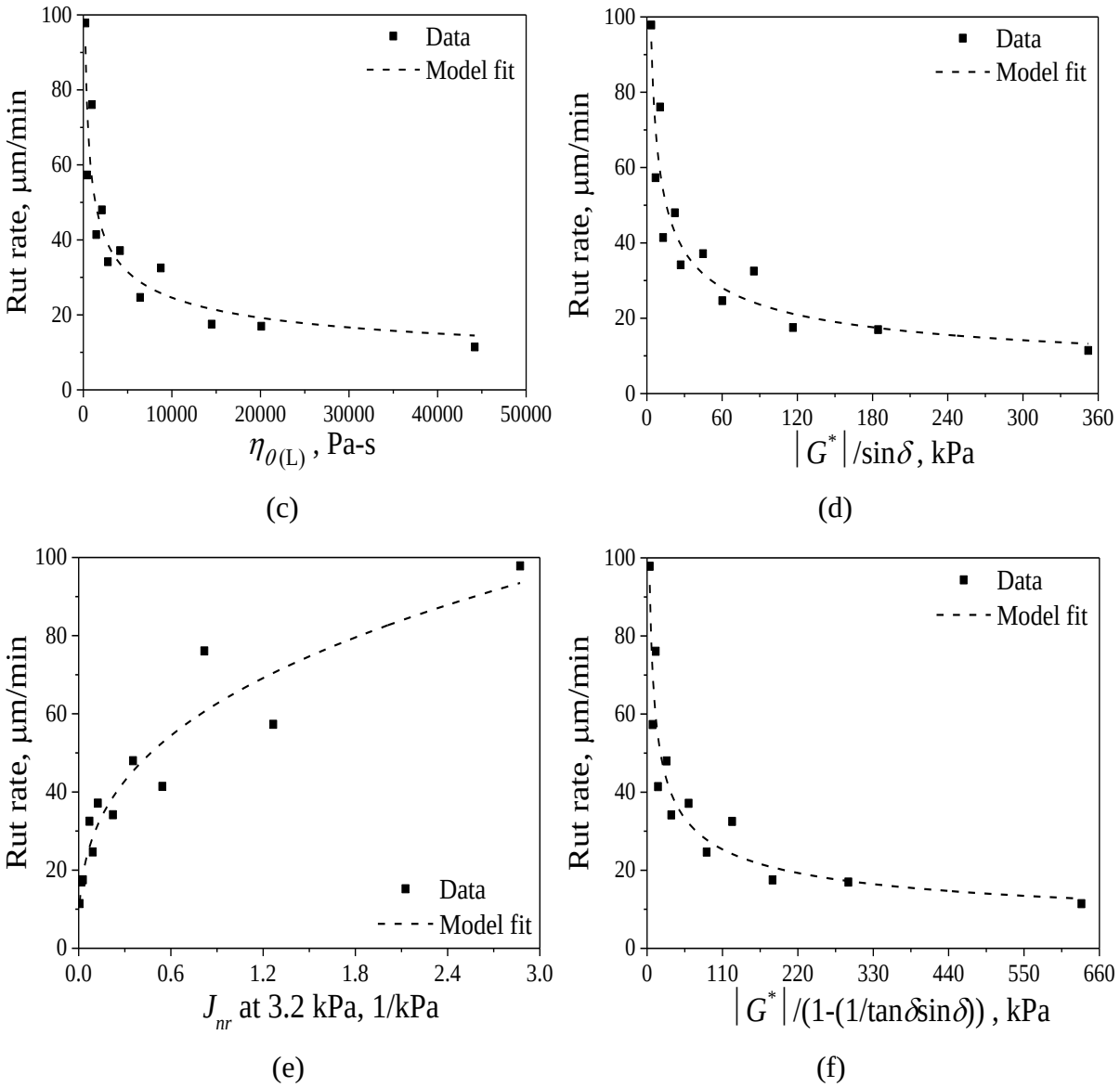

Fig. 6.9 Rr_P as a function of binder properties for the STA BC-2 mixtures

6.4 SUMMARY

In this chapter the four rutting parameters determined previously are correlated with the mixture rut depths at the pre-specified passes using a power law model. The correlations are made at all the four reliability levels for the STA and LTA BC-2 and DBM-2 mixtures with VG20 and VG40 bitumen binders. The results indicated a strong correlation of the six rutting parameters with the mixture rut depths and rutting rates. However, the new rutting parameter $\eta_{0(S)}$ is observed to be comparatively better performing rutting parameter among the six.

$\eta_{0(S)}$, J_{nr}, η_{TV}, $\eta_{0(L)}$, $|G^*|/\sin\delta$, $|G^*|/(1-(1/\tan\delta\sin\delta))$ are determined using a DSR. Among these, $|G^*|/\sin\delta$, $|G^*|/(1-(1/\tan\delta\sin\delta))$ take the least amount of time but require a preliminary test to determine LVE range. $|G^*|/\sin\delta$ is directly provided by the DSR whereas $|G^*|/(1-$

(1/tanδsinδ)) requires simple mathematics. The MSCR test to determine J_{nr} is easier to perform but time taking to analyse the data. The determination of the $\eta_{0(S)}$ η_{TV}, and $\eta_{0(L)}$ requires a predetermination of the lower and the higher shear rate. $\eta_{0(L)}$ and η_{TV} are directly measured from the shear rate versus viscosity plots. $\eta_{0(S)}$ is quite simple in its approach though time consuming test to conduct and analyse. The time consuming aspect of $\eta_{0(S)}$ should not be considered as a hindrance when pavement performance is concerned.

Table 6.7 Coefficient of correlation of binder properties with *Rr* for individual mixtures

Rr	$\eta_{0(S)}$	η_{TV}	$\eta_{0(L)}$	$\lvert G^*\rvert/\sin\delta$	J_{nr} ***at 3.2 kPa***	$\lvert G^*\rvert/(1-(1/\tan\delta\sin\delta))$
STA BC-2 VG20						
Rr_M	***0.91***	0.90	0.85	0.88	0.89	0.88
Rr_P	***0.97***	***0.97***	0.92	0.96	0.96	0.95
Rr_T	0.68	0.67	0.58	***0.75***	0.72	***0.75***
STA DBM-2 VG20						
Rr_M	0.97	0.96	0.92	***0.98***	0.97	***0.98***
Rr_P	***0.94***	0.93	0.86	***0.94***	0.93	***0.94***
Rr_T	0.65	0.64	0.59	***0.72***	0.67	***0.72***
STA BC-2 VG40						
Rr_M	0.89	0.90	0.89	0.87	***0.92***	0.88
Rr_P	0.97	0.97	0.97	***0.98***	***0.98***	***0.98***
Rr_T	0.67	0.69	0.71	***0.74***	0.73	0.72
STA DBM-2 VG40						
Rr_M	***0.87***	***0.87***	0.86	0.84	0.86	0.85
Rr_P	***0.99***	***0.99***	***0.99***	***0.99***	***0.99***	***0.99***
Rr_T	0.73	0.74	0.74	***0.78***	0.72	0.76
LTA BC-2 VG20						
Rr_M	***0.96***	0.95	0.93	0.94	0.94	0.93
Rr_P	***0.97***	0.96	0.95	0.95	0.95	0.94
Rr_T	0.40	0.54	***0.61***	0.49	0.51	0.47
LTA DBM-2 VG20						
Rr_M	0.96	0.94	0.92	0.96	0.95	***0.97***
Rr_P	0.91	0.94	***0.95***	0.93	0.94	0.93
Rr_T	0.73	0.84	***0.89***	0.81	0.82	0.79
LTA BC-2 VG40						
Rr_M	***0.98***	0.95	0.94	0.95	***0.97***	0.95
Rr_P	***0.98***	***0.98***	***0.98***	***0.98***	***0.98***	***0.98***
Rr_T	0.16	0.65	***0.67***	0.29	0.22	0.28
LTA DBM-2 VG40						
Rr_M	0.91	0.89	0.88	0.92	***0.93***	***0.93***
Rr_P	0.97	***0.99***	***0.99***	***0.99***	0.98	***0.99***
Rr_T	0.62	0.70	***0.73***	0.68	0.65	0.67

Table 6.8 Coefficient of correlation of binder properties with *Rr* for specific mixture

Rr	$\eta_{0(S)}$	η_{TV}	$\eta_{0(L)}$	$\lvert G^* \rvert/\sin\delta$	J_{nr} ***at 3.2 kPa***	$\lvert G^* \rvert/(1-(1/\tan\delta\sin\delta))$
STA BC-2						
Rr_M	***0.89***	0.87	0.83	0.85	0.88	0.85
Rr_P	***0.91***	0.89	0.85	0.87	0.90	0.87
Rr_T	0.66	0.67	0.65	***0.73***	0.68	***0.73***
STA DBM-2						
Rr_M	***0.88***	0.86	0.82	0.85	0.87	0.85
Rr_P	***0.89***	0.86	0.80	0.85	0.87	0.85
Rr_T	0.76	0.76	0.73	***0.79***	0.77	***0.79***
LTA BC-2						
Rr_M	***0.97***	0.94	0.92	0.90	0.95	0.90
Rr_P	***0.92***	0.82	0.79	0.78	0.89	0.78
Rr_T	0.31	***0.45***	***0.45***	0.28	0.37	0.27
LTA DBM-2						
Rr_M	***0.93***	0.87	0.84	0.84	0.93	0.84
Rr_P	***0.75***	0.61	0.59	0.59	0.72	0.59
Rr_T	0.72	0.81	***0.83***	0.73	0.78	0.71

CHAPTER-7

SUMMARY AND CONCLUSIONS

7.1 GENERAL

The main objective of this research work is to characterize the non-Newtonian response of the unmodified bitumen binders. Previous chapters dealt with the test protocols adopted to analyse the non-Newtonian and Newtonian responses of the bitumen binders and moreover the permanent deformation characteristics of the dense bituminous mixtures. This chapter contains the summary of the experimental investigations and the analysis carried out. The conclusions drawn from the research are also presented in this chapter.

7.2 SUMMARY

The experimental work consisted of mainly two phases. In the first phase, the rheological studies were conducted on unaged, short-term aged and long-term aged unmodified VG20 and VG40 bitumen binders using a RV and a DSR. It is observed that bitumen exhibits a non-Newtonian behavior. From the LSRS test protocol, it is observed that the response of the bitumen is Newtonian as well as non-Newtonian. An initial Newtonian plateau is followed by a non-Newtonian shear thickening region. This shear thickening region is followed by shear thinning regions. From the Newtonian region $\eta_{0(L)}$ is considered as the ZSV whereas, from the shear thickening (non-Newtonian) region a new viscosity, peak transient viscosity denoted as η_{TV}, is proposed as a non-Newtonian rutting parameter. $SWSSRS_{RV}$ and $SWSSRS_{DSR}$ tests are conducted at shear rates corresponding to the ZSV regime. It is observed that the stress overshoot appears in the first step of the first forward sweep and subsequently, a steady state appears. The response of the bitumen to the applied SWSSSRS test is observed to be independent of shear rate, time and shear history. A Newtonian viscosity is proposed from the first forward sweep and is denoted as $\eta_{0(S)}$. $\eta_{0(S)}$ is determined from the SWSSRS test conducted with RV and DSR. However, due to the limitations of test temperatures encountered with a RV, $\eta_{0(S)}$ determined by applying $SWSSRS_{DSR}$ test is used for correlations. In order to compare the proposed new rutting parameters, $\eta_{0(S)}$ and η_{TV}, existing rutting parameters, $|G^*|/\sin\delta$, $|G^*|/(1-(1/\tan\delta\sin\delta))$ and J_{nr} are also determined.

In the second phase of the experimental work, STA and LTA BC-2 and DBM-2 bituminous mixtures were tested using a small WTD to characterize their permanent deformation behavior. The distribution of the raw rut data is analyzed using a probabilistic approach and probabilistic rut curves at four reliability levels are determined. Moreover, three *Rr* are also determined from the wheel tracking tests.

In order to evaluate the efficacy of the proposed new rutting parameters, $\eta_{0(S)}$ and η_{TV}, correlations of all the six rutting parameters with mixture rut data are developed at the four reliability levels and mixture *Rr*. The analysis of results from this research lead to a set of conclusions which are shown in the following section.

7.3 CONCLUSIONS

Following conclusions are drawn from this study:

1) The response of unmodified bitumen from the linear shear rate sweep test is both Newtonian as well as multi-step non-Newtonian within a range of shear rate sweep at all aging conditions and most of the test temperatures except for the softest binder i.e., VG20 binder at 60 and 65 °C. At very low shear rates the response is Newtonian as seen by the appearance of a plateau region whereas with increased shear rates the response is non-Newtonian exhibiting shear thickening response initially followed by a two stage shear thinning responses. Even though such responses were reported in the past by some of the researchers for modified binders, such response is also characterized for unmodified unaged and aged binders in this study. The temperature, bitumen grade and bitumen aging has a significant effect on the shear thickening response whereas the critical shear rate at which the peak transient viscosity occurs is independent of these three parameters. The percentage difference between the peak transient viscosity and the primary Newtonian viscosity is observed to be temperature dependent. Thus, η_{TV} is proposed as a non-Newtonian rutting parameter.

2) In the SWSSRS test, the non-Newtonian response of bitumen is characterized by a stress overshoot whereas the Newtonian response is characterized by the appearance of a steady-state. Bitumen response in the first forward sweep of the SWSSRS test protocol is Newtonian. Also, the bitumen response is independent of time and the effect of shear history is negligible in the SWSSRS test. The SWSSRS test protocol can also be used to determine bitumen ZSV and $\eta_{0(S)}$ is proposed as a rutting parameter.

3) The $\eta_{0(S)}$, η_{TV} and $\eta_{0(L)}$ of the short-term aged VG20 bitumen are similar to that of the unaged VG40 binder at all test temperatures exhibiting a possible correspondence between the bitumen grade and the short-term aged binder.

4) $\eta_{0(S)}$ can be a possible candidate to grade bitumen binders as per viscosity grading system.

5) VG40 binder has superior indicators than the VG20 binder when the six rutting parameters are compared. This shows that VG40 binder is better at resisting permanent deformation than VG20 binder.

6) The two new rutting parameters obtained from this study are correlated with the existing four rutting parameters. It is observed that $\eta_{0(S)}$ and η_{TV} has the highest correlation with the binder J_{nr} at 3.2 kPa followed by $|G^*|/(1-(1/\tan\delta\sin\delta))$ and $|G^*|/\sin\delta$ indicating that the performance of bitumen when expressed in terms of $\eta_{0(S)}$ and η_{TV} will be closer to performance expressed in terms of J_{nr} at 3.2 kPa compared to $|G^*|/(1-(1/\tan\delta\sin\delta))$ and $|G^*|/\sin\delta$. This is because the $\eta_{0(S)}$, η_{TV} and J_{nr} at 3.2 kPa are determined in the non-linear regime whereas the $|G^*|/\sin\delta$ and $|G^*|/(1-(1/\tan\delta\sin\delta))$ are determined in the linear regime. The relationships developed between $\eta_{0(S)}$ and the corresponding binder $|G^*|/\sin\delta$, $|G^*|/(1-(1/\tan\delta\sin\delta))$ and J_{nr} at 3.2 kPa helps to estimate the binder $|G^*|/\sin\delta$, $|G^*|/(1-(1/\tan\delta\sin\delta))$ and J_{nr} at 3.2 kPa even in the absence of a DSR. The relationships developed between the $\eta_{0(S)}$ and η_{TV} with the corresponding binder $|G^*|/\sin\delta$, $|G^*|/(1-(1/\tan\delta\sin\delta))$ and J_{nr} at 3.2 kPa can lead to performance grade specifications for $\eta_{0(S)}$ and η_{TV} by stipulating minimum required $\eta_{0(S)}$ and η_{TV}.

7) A probabilistic approach is adopted to obtain a representative rut curve for each test specimen. Reliability-based rutting curves are developed to take into account the variability observed along the wheel traverse. Lognormal and Weibull distributions proved to be the best fits. However, based on various reliability levels, lognormal distribution overestimated the rut depths at different temperatures. Higher the reliability, lower is the resistance towards permanent deformation.

8) Rutting resistance decreases with an increase in temperature for all mixture types.

9) Higher the binder grade, higher is the resistance towards permanent deformation, wherein bituminous mixtures prepared with VG40 binder perform better than bituminous mixtures prepared with VG20 binder. This trend was seen in both the STA and LTA BC-2 and DBM-2 mixtures.

10) The influence binder aging on permanent deformation characteristics of bituminous mixtures is captured through the identification of the onset of second stage of permanent

deformation curve. Ideally, the number of wheel load passes required to reach the onset of second stage of permanent deformation curve should be higher for the bituminous mixtures with higher air voids (6%), i.e., for short-term aged bituminous mix. However, because of the long-term aging, the number wheel load passes to reach the second stage of permanent deformation curve increased significantly at all test temperatures even though the air voids are less (4%). Thus, the higher resistance offered by the LTA mixtures towards permanent deformation than the STA mixtures is due to an increase in the mixture aging and not the decrease in air voids.

11) The DBM-2 mixtures have a higher resistance towards permanent deformation than the BC-2 mixtures. The higher rutting resistance offered by the DBM-2 mixtures than the BC-2 mixtures is due to better aggregate interlocking and the confined testing conditions in the wheel tacking test.

12) The use of mixture *Rr* to develop relationships between binder properties and the mixture performance holds good when the mixture *Rr* is determined in the primary stage for all mixture types.

13) The overall ranking of rutting parameters in terms of correlation is:

$$\eta_{0(S)} > J_{nr} > \eta_{TV} > \eta_{0(L)} \approx |G^*|/\sin\delta \approx |G^*|/(1-(1/\tan\delta\sin\delta))$$

Coefficient of correlation is observed to be independent of a number of passes and the reliability level for most of the cases. The new parameter $\eta_{0(S)}$ showed stronger and better correlation with the rut depth than the established rutting parameters whereas η_{TV} has a performance very close to J_{nr}. Thus, this study identified a Newtonian viscosity ($\eta_{0(S)}$) and a non-Newtonian viscosity (η_{TV}) as new rutting parameters that are corroborated through rutting tests on two different bituminous mixtures using two different grades of unmodified bitumen under different aging conditions.

7.4 APPLICATONS

The main aim of PG specifications is the selection of an appropriate bitumen. This study provides a novel approach to determine ZSV of bitumen binders. Among all the rutting parameters measured in this study $\eta_{0(S)}$ is having the highest correlation with permanent deformation in bituminous mixtures. Therefore, it is proposed that the use of $\eta_{0(S)}$ will help in an improvement in selection of binder as per PG specifications.

7.4 WAY FORWARD

Following points can be considered to extend the current research study:

- The study focussed on only two unmodified bitumen binders i.e., VG20 and VG40. Even though, in theory it is expected that the other unmodified bitumen binders would exhibit a similar response, a similar study on other unmodified binders can be considered.

- Similarly, the response of the modified binders to SWSSRS test protocol can be evaluated.

- Relationship of $\eta_{0(S)}$ and η_{TV} with other mixture type such as SMA could also be evaluated.

APPENDIX A

A.1 RHEOLOGICAL STUDY USING ROTATIONAL VISCOMETER

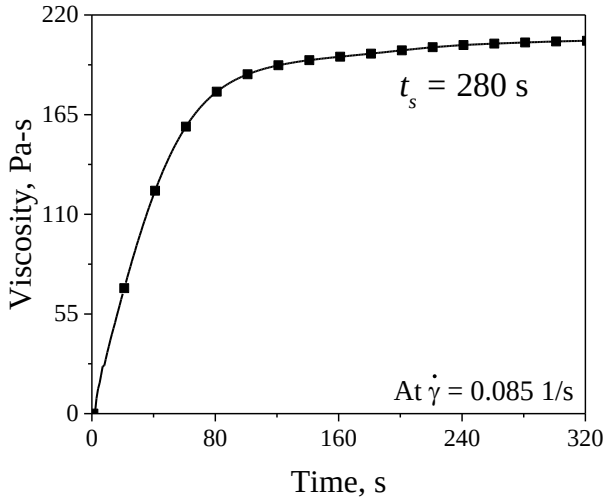

Fig. A1 Variation of viscosity as function of time for the unaged VG40 at 65 °C

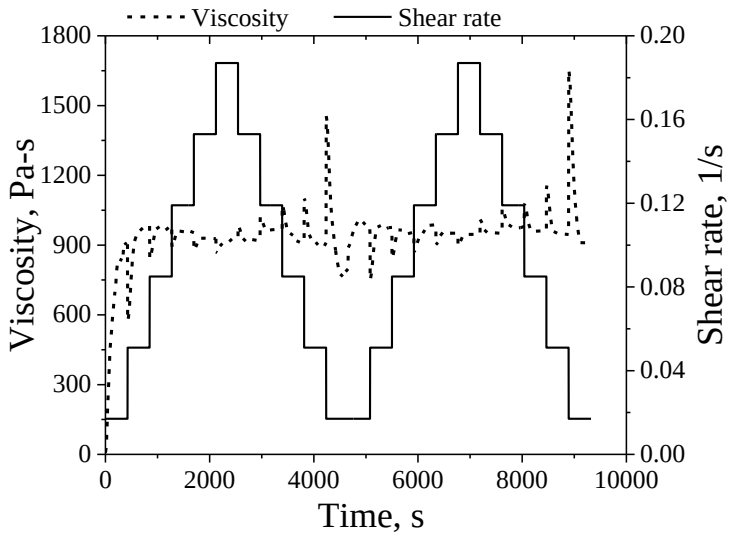

(a) Unaged VG20 at 50 °C

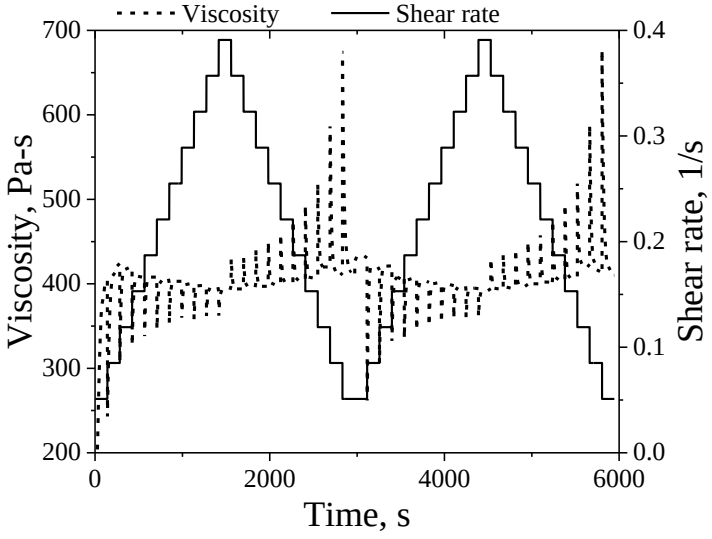

(b) Unaged VG20 at 55 °C

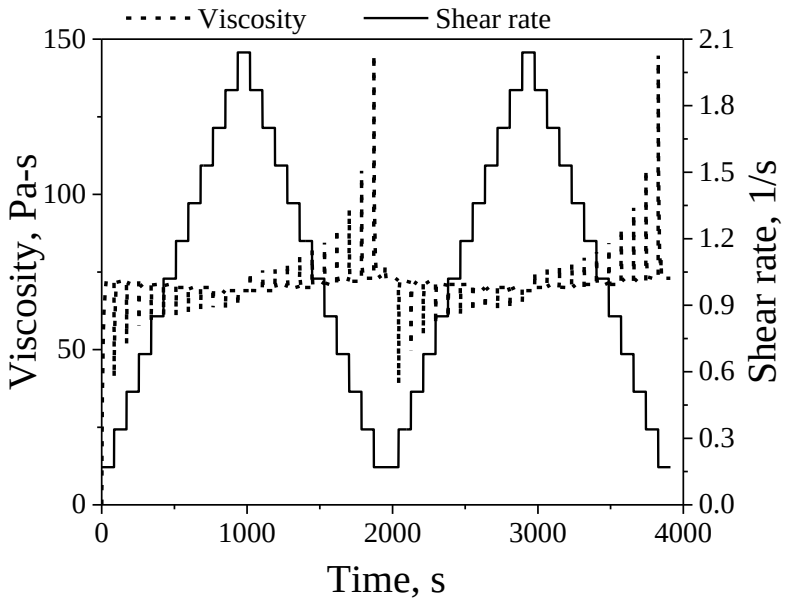

(c) Unaged VG20 at 65 °C

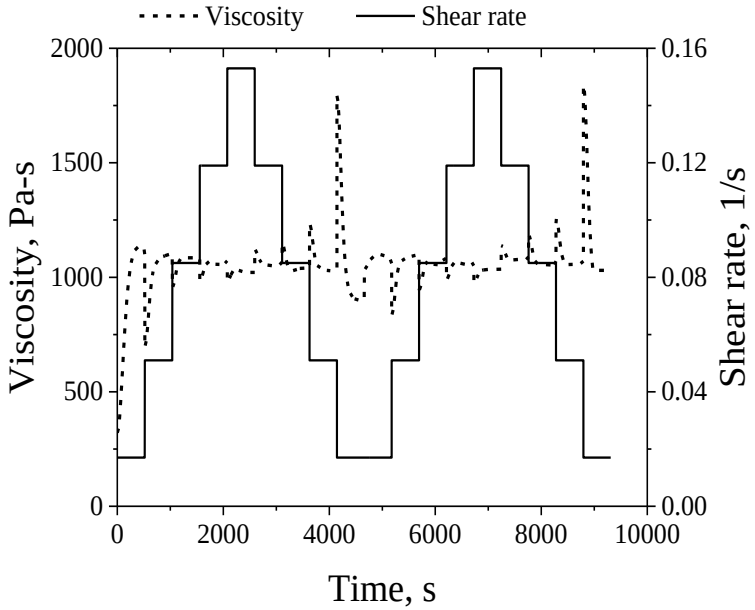

(d) Short-term aged VG20 at 55 °C

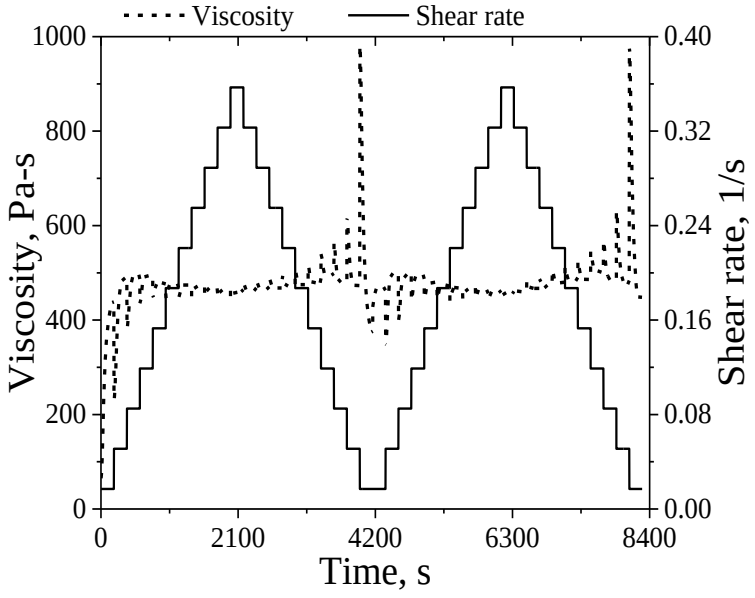

(d) Short-term aged VG20 at 60 °C

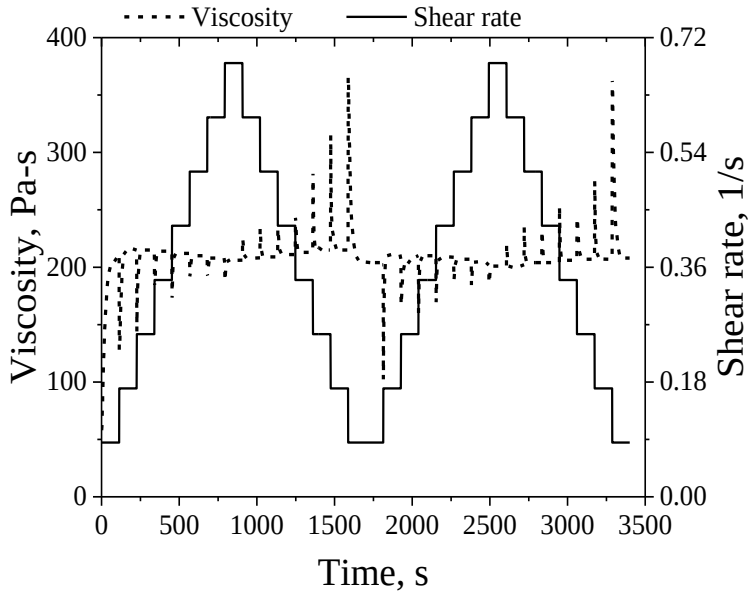

(e) Short-term aged VG20 at 65 °C

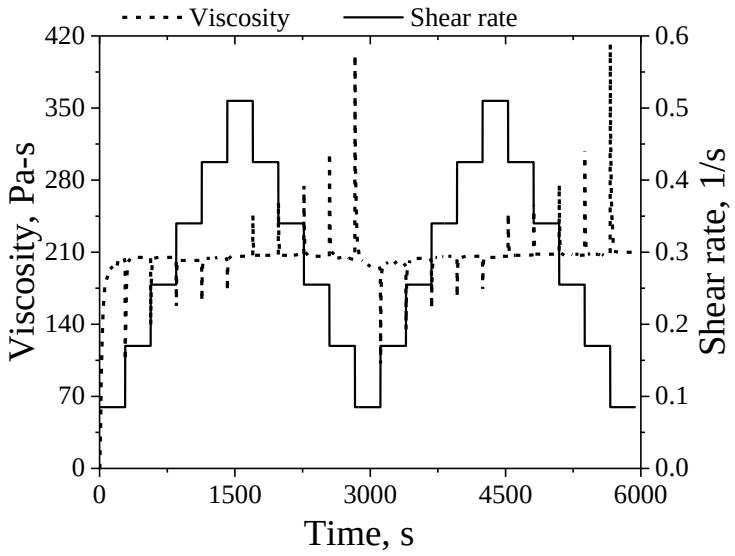

(f) Unaged VG40 at 65 °C

Fig. A2 Viscosity and shear rate as a function of time for the VG20 bitumen and VG40 bitumen

Table A1 Viscosity and shear stress at $ts_{(RV)}$ in the $SWSSRS_{RV}$ for the unaged VG20 bitumen at 50, 55, 65 °C

$\dot{\gamma}$, 1/s	Cycle 1				Cycle 2				Average.	
	Forward Sweep		Backward Sweep		Forward Sweep		Backward Sweep			
	σ, Pa	***η, Pa-s***	**σ, Pa**	**η, Pa-s**	**σ, Pa**	**η, Pa-s**	**σ, Pa**	**η, Pa-s**	**σ, Pa**	**η, Pa-s**
Unaged VG20, 50 °C										
0.017	***15.64***	***920***	16.46	968	16.46	968	15.47	910	16.01	942
0.051	***50.13***	***983***	45.75	897	49.95	979	48.14	944	48.49	951
0.085	***83.57***	***983***	78.1	919	81.17	955	81.71	961	81.14	955
0.119	***114***	***958***	115.22	968	117.51	987	116.11	976	115.71	972
0.153	***141.79***	***927***	141.41	924	145.56	951	145.53	951	143.57	938
0.187	***175.02***	***936***	175.02	936	176.96	946	176.96	946	175.99	941
Unaged VG20, 55 °C										
0.051	***20.6***	***404***	21	412	21	412	20.91	410	20.88	409
0.089	***37.73***	***424***	36.49	410	37.38	420	36.69	412	37.07	417
0.119	***49.73***	***418***	49.98	420	50.16	422	50.06	421	49.98	420
0.153	***62.47***	***408***	62.23	407	62.43	408	62.39	408	62.38	408
0.187	***76.42***	***409***	75.65	405	75.98	406	75.58	404	75.91	406
0.221	***89.74***	***406***	88.85	402	89.23	404	88.91	402	89.18	404
0.255	***102.85***	***403***	101.82	399	102.01	400	101.95	400	102.16	401
0.289	***115.61***	***400***	114.75	397	115.26	399	114.9	398	115.13	398
0.323	***128.52***	***398***	127.84	396	128.26	397	127.67	395	128.07	397
0.357	***141.19***	***395***	140.76	394	140.97	395	140.43	393	140.84	395
0.391	***153.63***	***393***	153.63	393	153.34	392	153.34	392	153.49	393
Unaged VG20, 65 °C										
0.17	***12.24***	***72***	12.41	73	12.41	73	12.41	73	12.37	73
0.34	***24.48***	***72***	24.82	73	24.31	72	24.82	73	24.61	72
0.51	***36.72***	***72***	36.72	72	36.55	72	36.72	72	36.68	72
0.68	***48.28***	***71***	48.96	72	48.62	72	48.96	72	48.71	72
0.85	***60.35***	***71***	60.35	71	60.52	71	60.35	71	60.39	71
1.02	***72.42***	***71***	72.42	71	72.42	71	72.42	71	72.42	71
1.19	***83.3***	***70***	83.3	70	84.15	71	84.49	71	83.81	70
1.36	***95.2***	***70***	95.2	70	95.71	70	95.2	70	95.33	70
1.53	***107.1***	***70***	107.1	70	107.44	70	107.1	70	107.19	70
1.7	***117.3***	***69***	117.3	69	118.66	70	119	70	118.07	69
1.87	***129.03***	***69***	129.03	69	130.05	70	130.9	70	129.75	69
2.04	***140.76***	***69***	140.76	69	140.76	69	140.76	69	140.76	69

Table A2 Viscosity and shear stress at $ts_{(RV)}$ in the $SWSSRS_{RV}$ for the short-term aged VG20 bitumen at 55, 60, 65 °C and unaged VG40 bitumen at 65 °C

$\dot{\gamma}$, 1/s	Cycle 1				Cycle 2				Average.	
	Forward Sweep		Backward Sweep		Forward Sweep		Backward Sweep			
	σ, Pa	***η, Pa-s***	**σ, Pa**	**η, Pa-s**	**σ, Pa**	**η, Pa-s**	**σ, Pa**	**η, Pa-s**	**σ, Pa**	**η, Pa-s**
Short-term aged VG20, 55 °C										
0.017	***19.86***	***1121***	20.43	1076	20.43	1076	18.87	1030	19.90	1076
0.051	***61.71***	***1102***	56.92	1042	60.54	1098	56.66	1061	58.96	1076
0.085	***100.05***	***1085***	96.65	1039	99.20	1083	94.78	1055	97.67	1065
0.119	***138.87***	***1073***	136.26	1055	136.49	1065	136.14	1078	136.94	1068
0.153	***167.69***	***1020***	167.69	1020	167.84	1035	167.84	1035	167.76	1028
Short-term aged VG20, 60 °C										
0.017	***7.50***	***441***	7.99	470	7.99	470	7.62	448	7.78	457
0.051	***24.99***	***490***	24.12	473	25.50	500	24.31	477	24.73	485
0.085	***42.16***	***496***	40.80	480	42.49	500	41.48	488	41.73	491
0.119	***58.80***	***494***	58.79	494	59.04	496	59.67	501	59.08	496
0.153	***73.27***	***479***	73.33	479	73.31	479	74.45	487	73.59	481
0.187	***89.13***	***477***	88.99	476	88.20	472	90.44	484	89.19	477
0.221	***104.75***	***474***	104.31	472	103.50	468	106.00	480	104.64	473
0.255	***120.26***	***472***	119.33	468	119.61	469	121.41	476	120.15	471
0.289	***134.97***	***467***	134.44	465	134.10	464	135.02	467	134.63	466
0.323	***149.29***	***462***	149.32	462	149.73	464	149.35	462	149.42	463
0.357	***164.01***	***459***	164.01	459	161.91	454	161.91	454	162.92	456
Short-term aged VG20, 65 °C										
0.085	***17.91***	***211***	17.51	206	17.51	206	17.68	208	17.65	208
0.170	***36.66***	***216***	36.55	215	35.87	211	35.36	208	36.11	212
0.255	***54.91***	***215***	54.74	215	53.88	211	53.03	208	54.14	212
0.340	***72.86***	***214***	72.58	213	71.74	211	70.04	206	71.80	211
0.425	***90.10***	***212***	89.59	211	88.91	209	86.91	204	88.88	209
0.510	***106.87***	***210***	106.67	209	105.37	207	104.04	204	105.74	207
0.595	***123.50***	***208***	123.92	208	121.65	204	119.31	201	122.10	205
0.680	***140.08***	***206***	140.08	206	136.68	201	136.44	201	138.32	203
0.085	***17.91***	***211***	17.51	206	17.51	206	17.68	208	17.65	208
Unaged VG40, 65 °C										
0.085	***17.31***	***204***	16.66	196	16.66	196	17.85	210	17.12	201
0.170	***34.85***	***205***	34.51	203	33.83	199	35.19	207	34.60	204
0.255	***52.19***	***205***	52.53	206	52.02	204	52.87	207	52.40	206
0.340	***68.51***	***202***	70.45	207	69.87	206	70.72	208	69.89	206
0.425	***87.21***	***205***	88.06	207	87.38	206	88.06	207	87.68	206
0.510	***104.89***	***206***	104.89	206	104.89	206	104.89	206	104.89	206

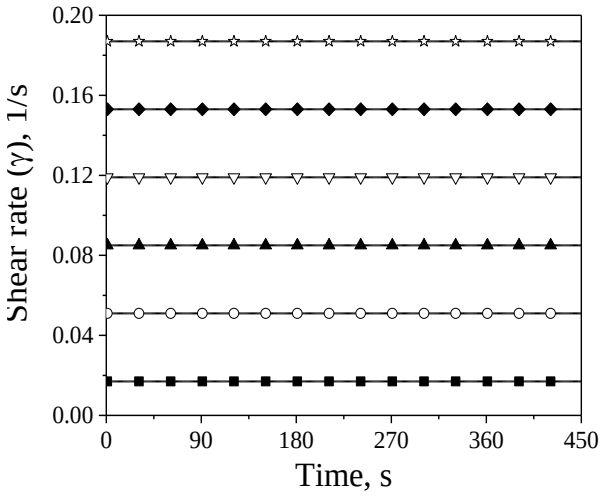

(a) Unaged VG20 at 50 °C

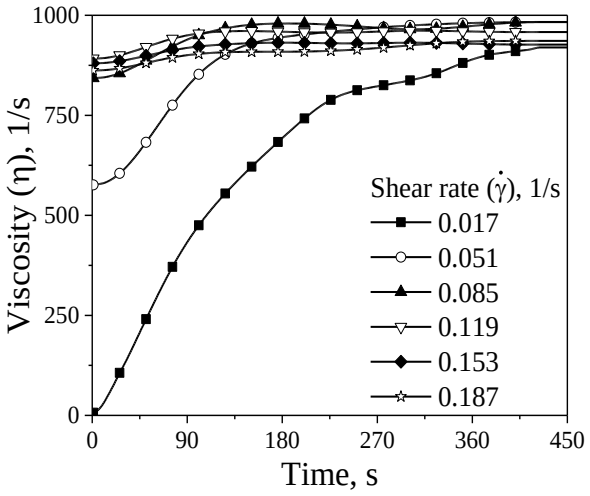

(b) Unaged VG20 at 50 °C

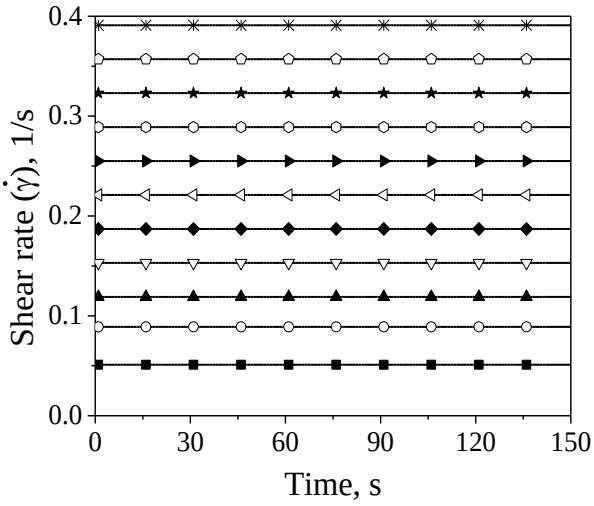

(c) Unaged VG20 at 55 °C

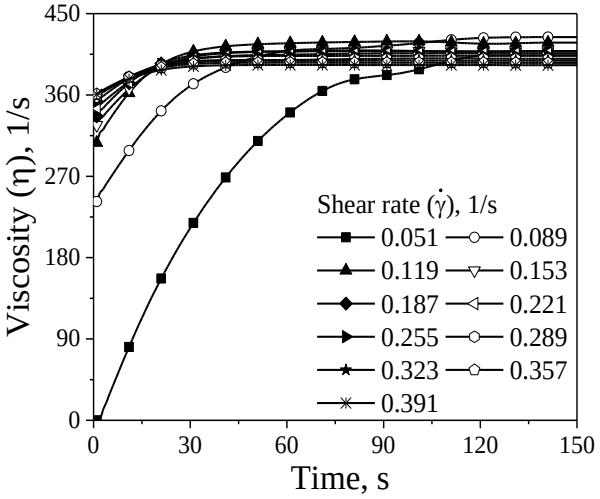

(d) Unaged VG20 at 55 °C

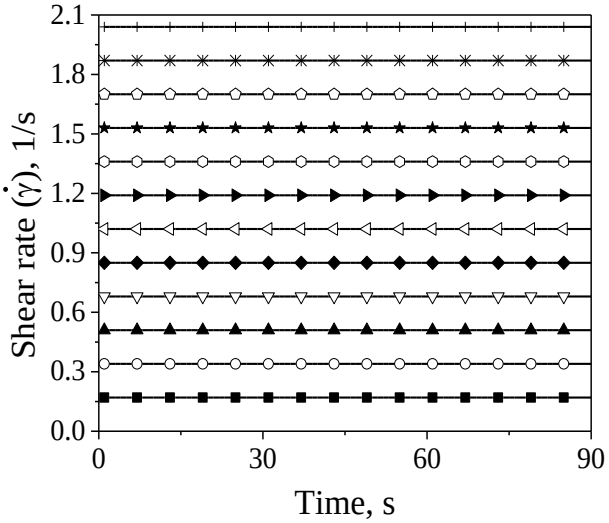

(c) Unaged VG20 at 65 °C

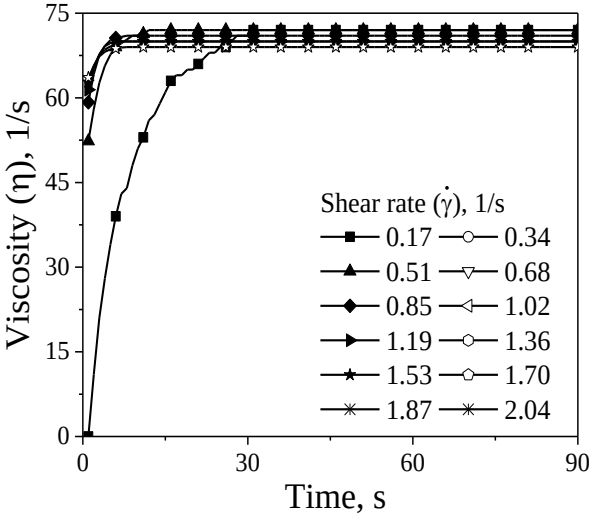

(d) Unaged VG20 at 65 °C

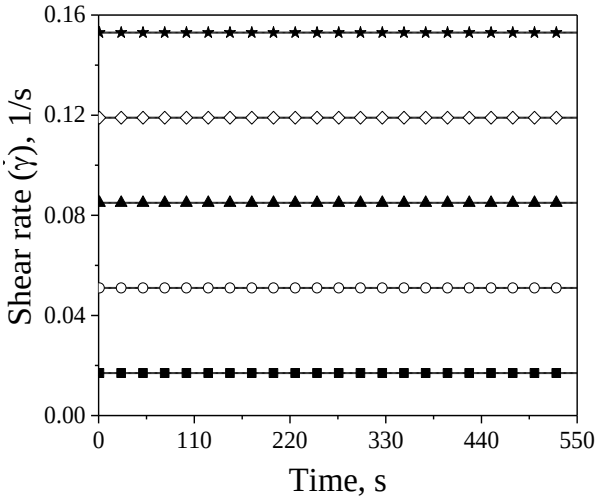

(g) Short-term aged VG20 at 55 °C

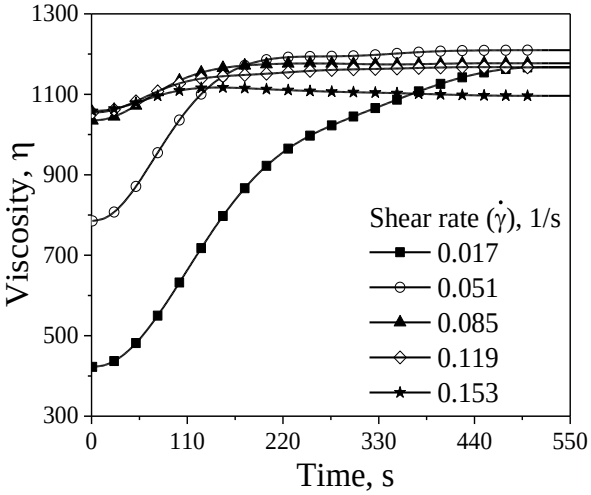

(h) Short-term aged VG20 at 55 °C

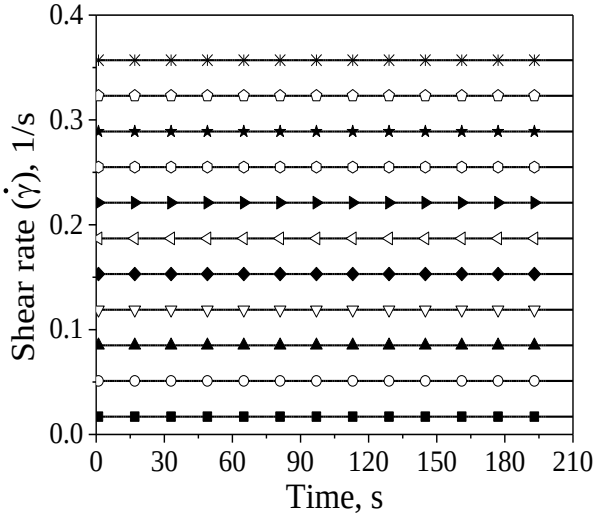

(g) Short-term aged VG20 at 60 °C

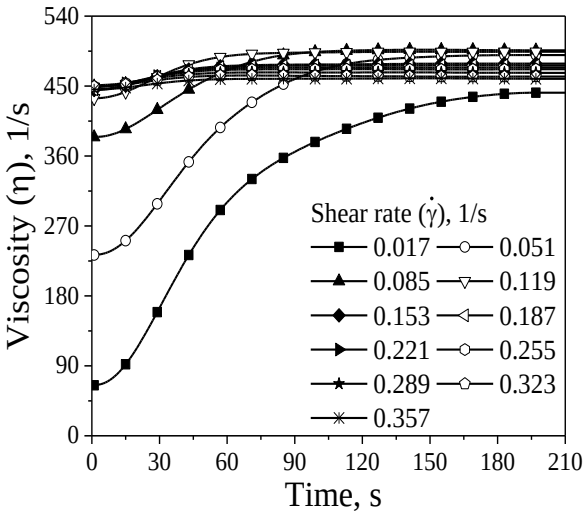

(h) Short-term aged VG20 at 60 °C

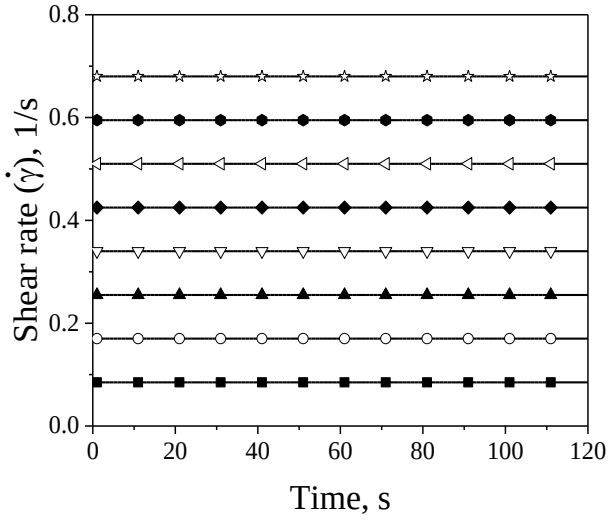

(i) Short-term aged VG20 at 65 °C

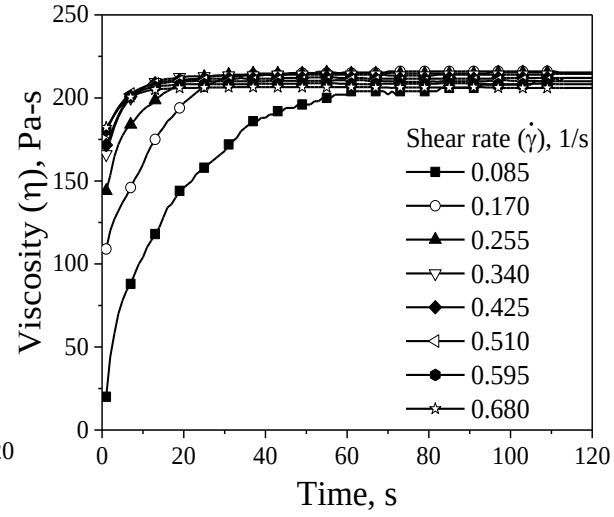

(j) Short-term aged VG20 at 65 °C

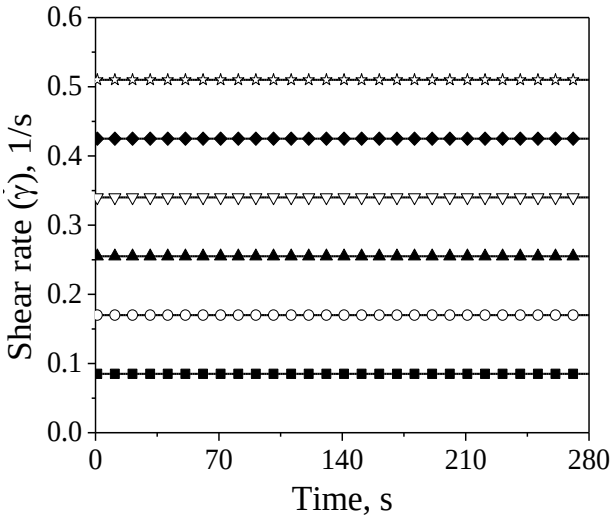

(k) Unaged VG40 at 65 °C

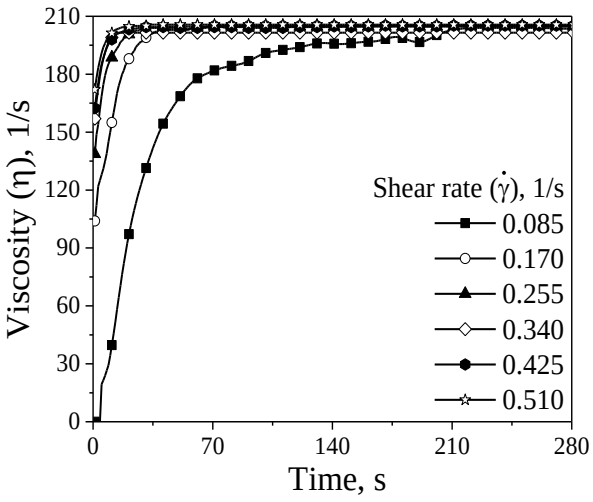

(l) Unaged VG40 at 65 °C

Fig. A3 Observed response in the first forward sweep of $SWSSRS_{RV}$ test for VG20 and VG40 bitumen (a) Shear rate as a function of time, (b) Viscosity as a function of time respectively

A.2 RHEOLOGICAL STUDIES USING DYNAMIC SHEAR REHOMETER

A.2.1 Time for Thermal Equilibrium

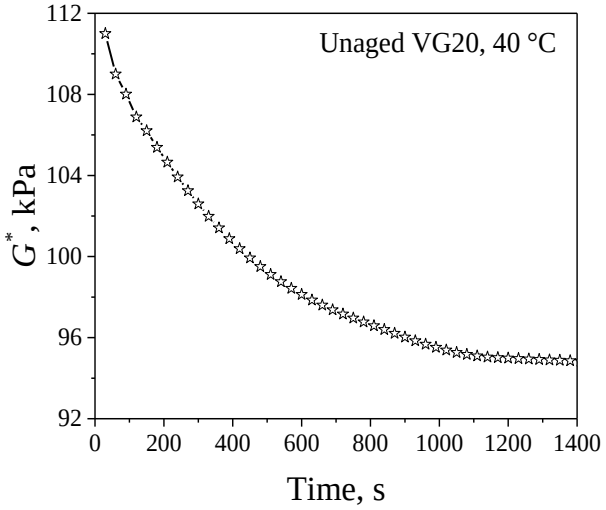

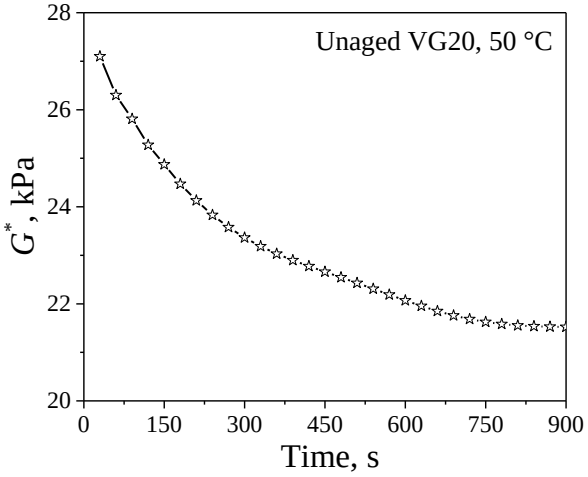

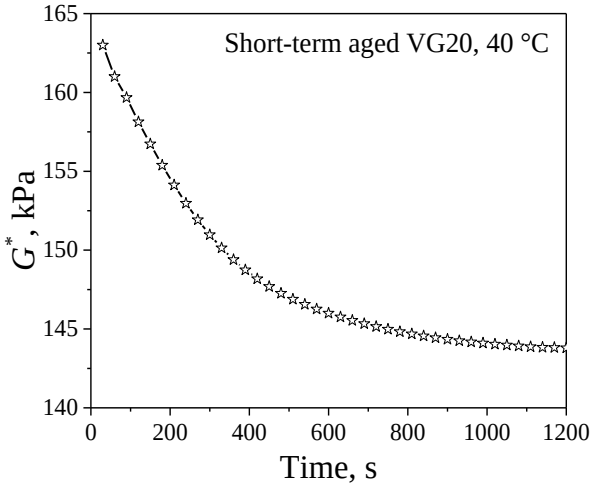

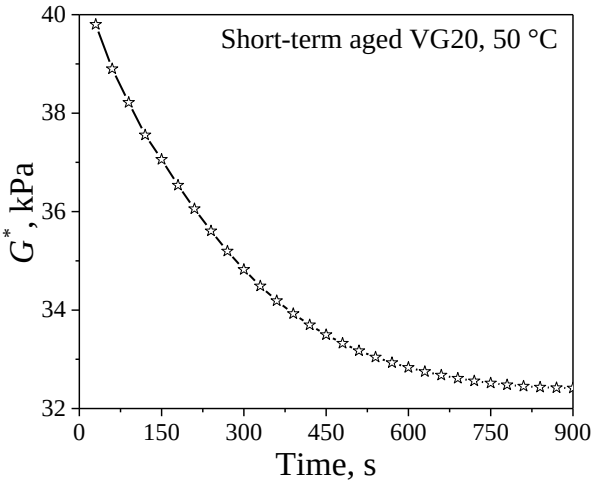

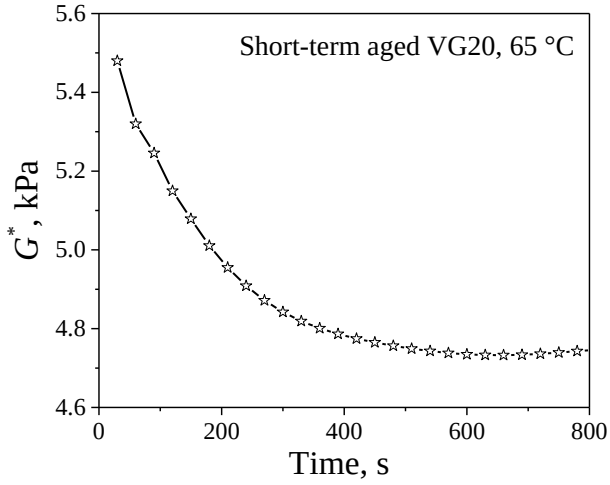

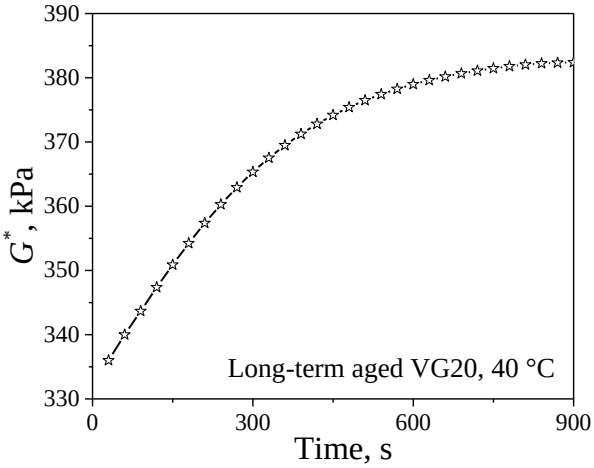

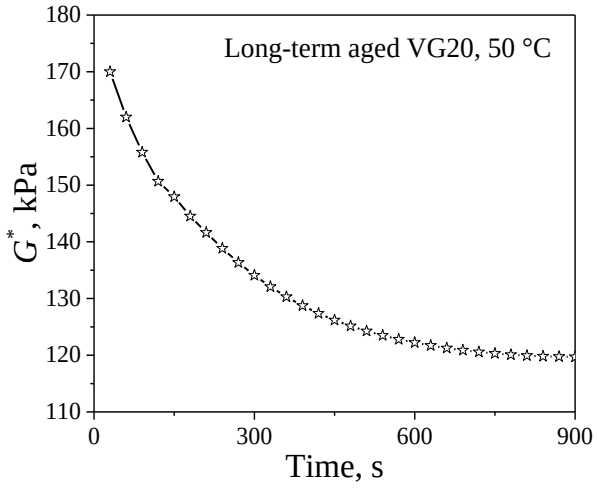
Long-term aged VG20, 50 °C
G*, kPa
Time, s
180
170
160
150
140
130
120
110
0
300
600
900

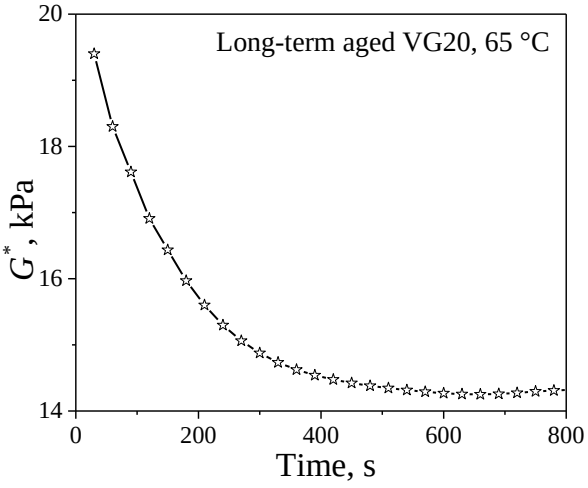
Long-term aged VG20, 65 °C
G*, kPa
Time, s
20
18
16
14
0
200
400
600
800

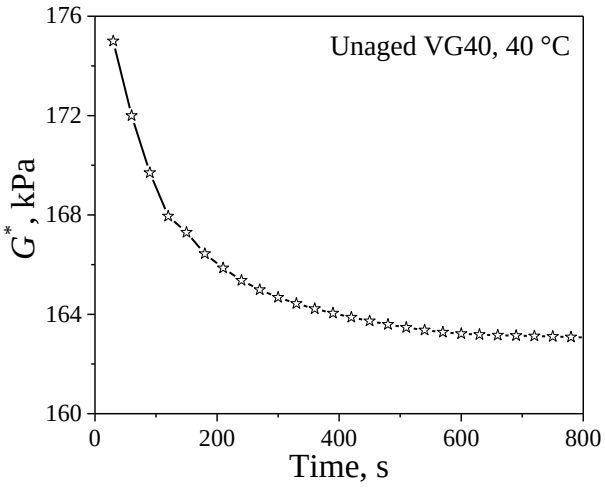
Unaged VG40, 40 °C
G*, kPa
Time, s
176
172
168
164
160
0
200
400
600
800

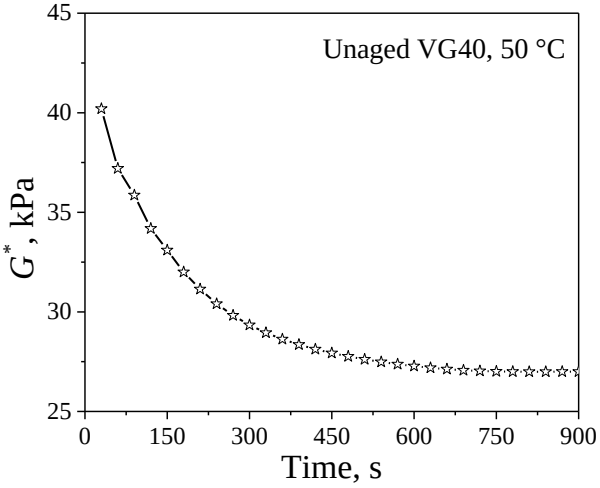
Unaged VG40, 50 °C
G*, kPa
Time, s
45
40
35
30
25
0
150
300
450
600
750
900

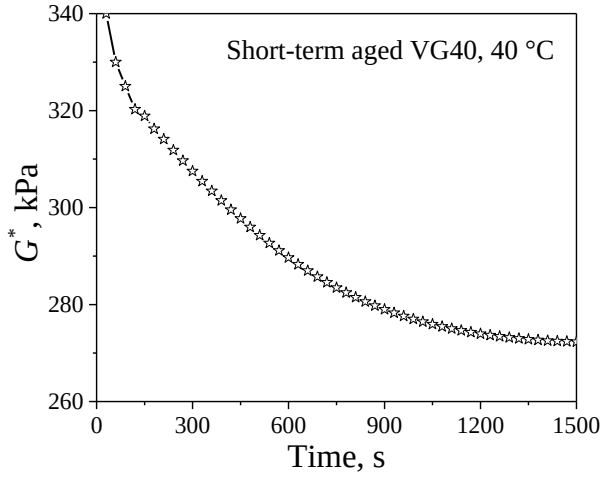
Short-term aged VG40, 40 °C
G*, kPa
Time, s
340
320
300
280
260
0
300
600
900
1200
1500

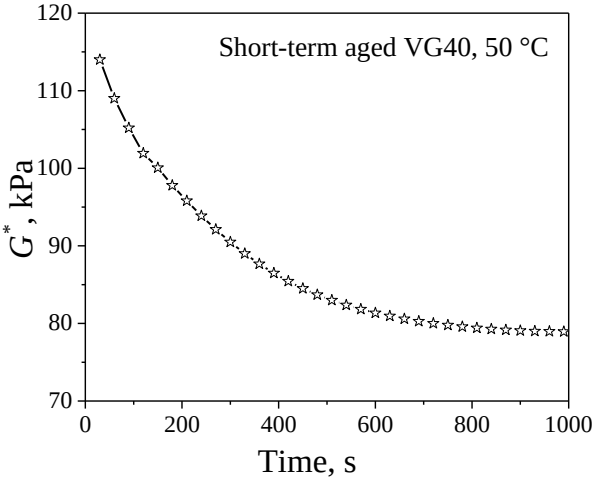
Short-term aged VG40, 50 °C
G*, kPa
Time, s
120
110
100
90
80
70
0
200
400
600
800
1000

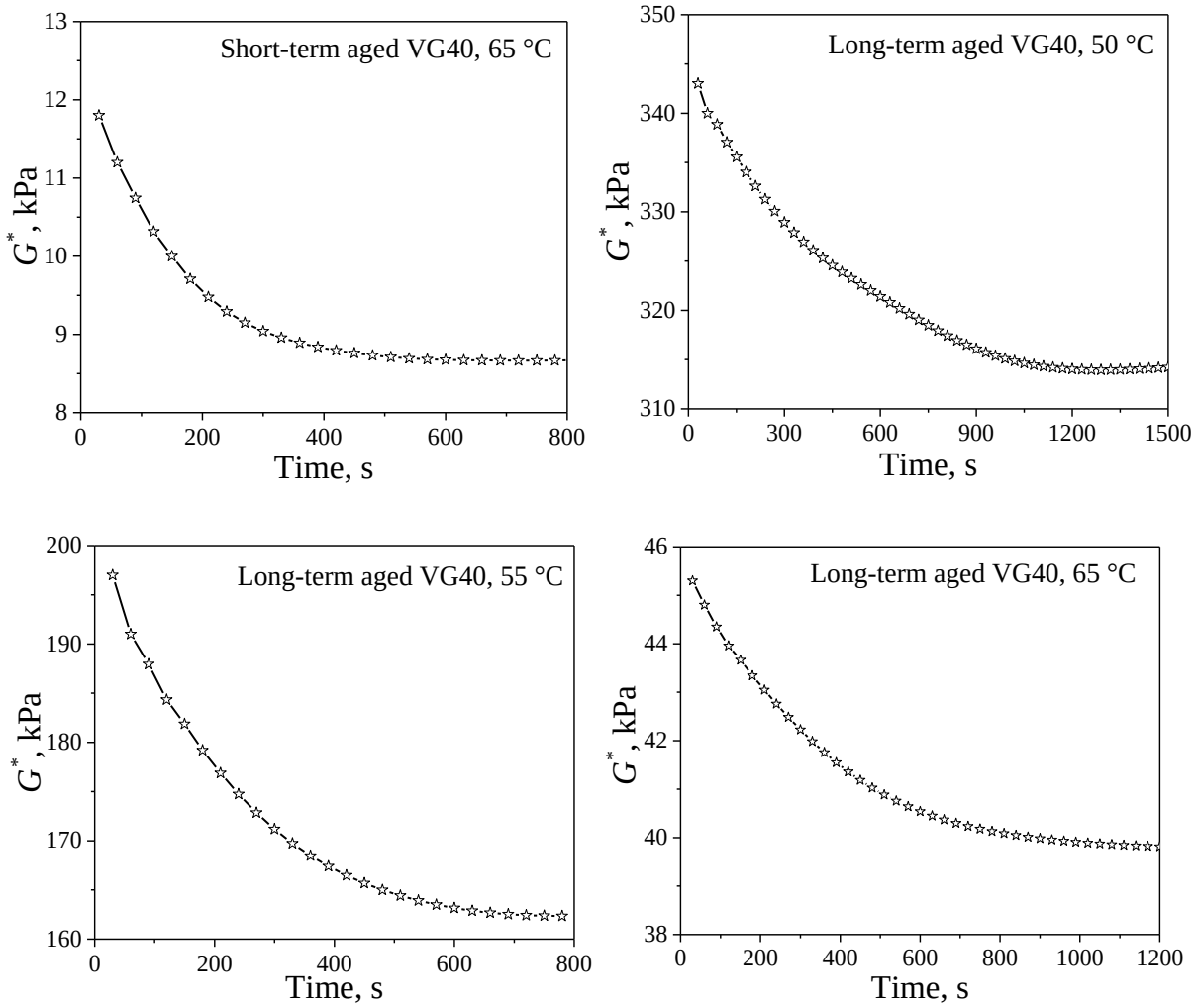

Fig. A4 G^*as a function of time VG20 bitumen and VG40 bitumen

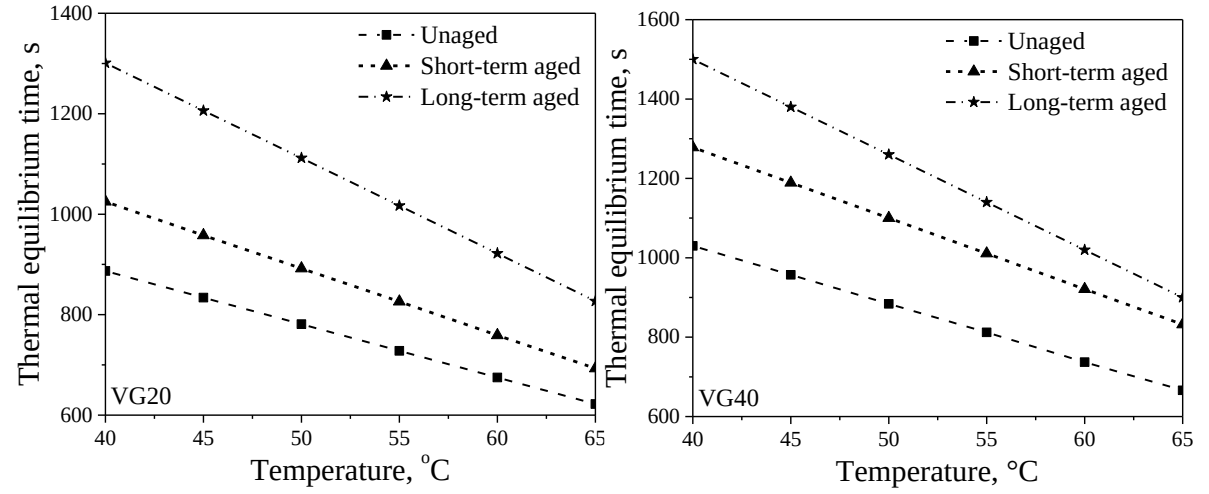

(a) VG20 (b) VG40

Fig. A5 Variation of thermal equilibrium time as a function of temperature at different aging condition

A.2.2 Step-wise Steady Shear Rate Sweep Test-DSR

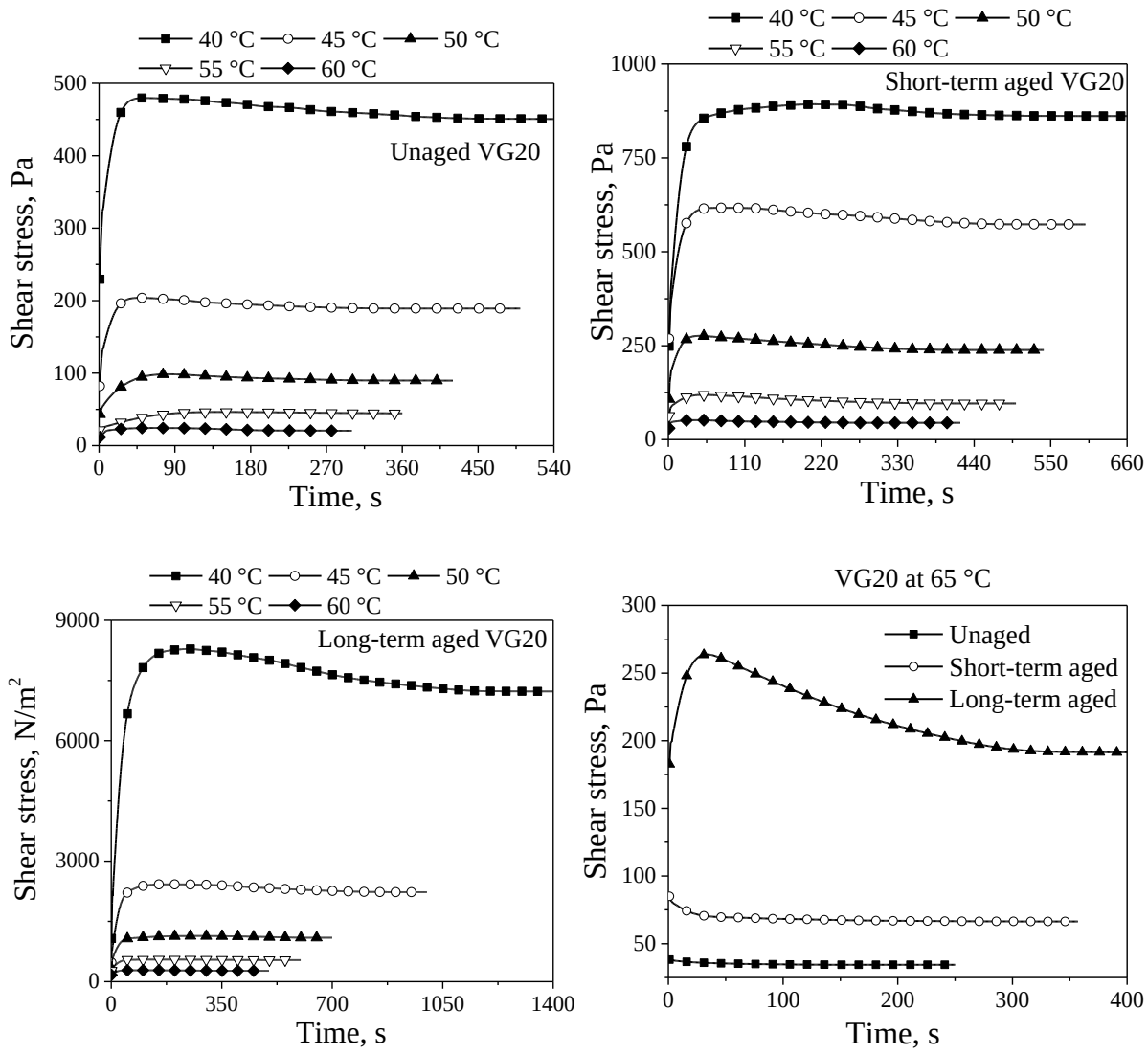

Fig. A6 Shear stress as a function of time in determining 't_s' for the VG20 bitumen

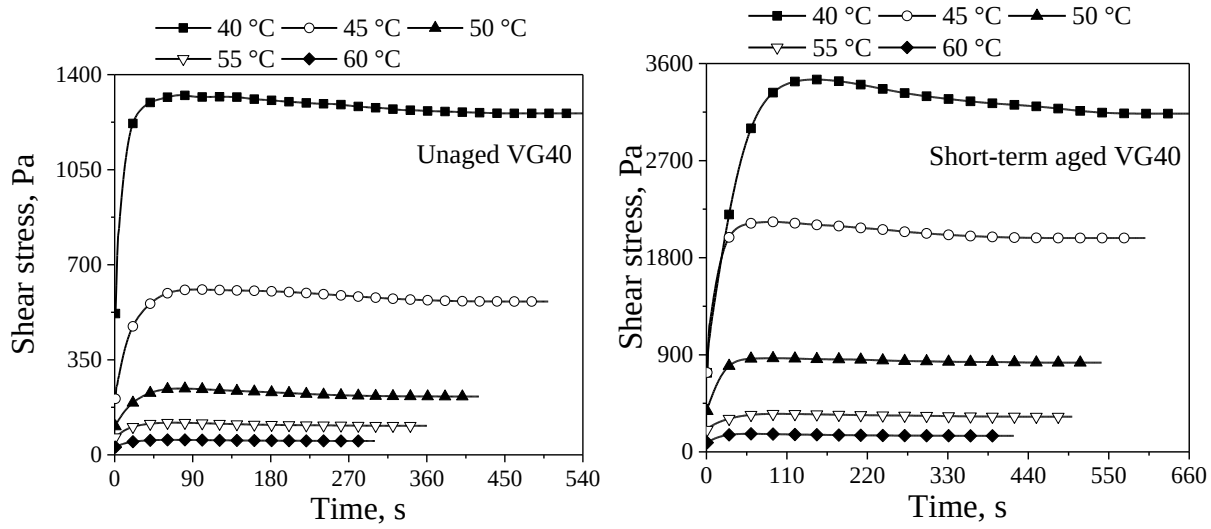

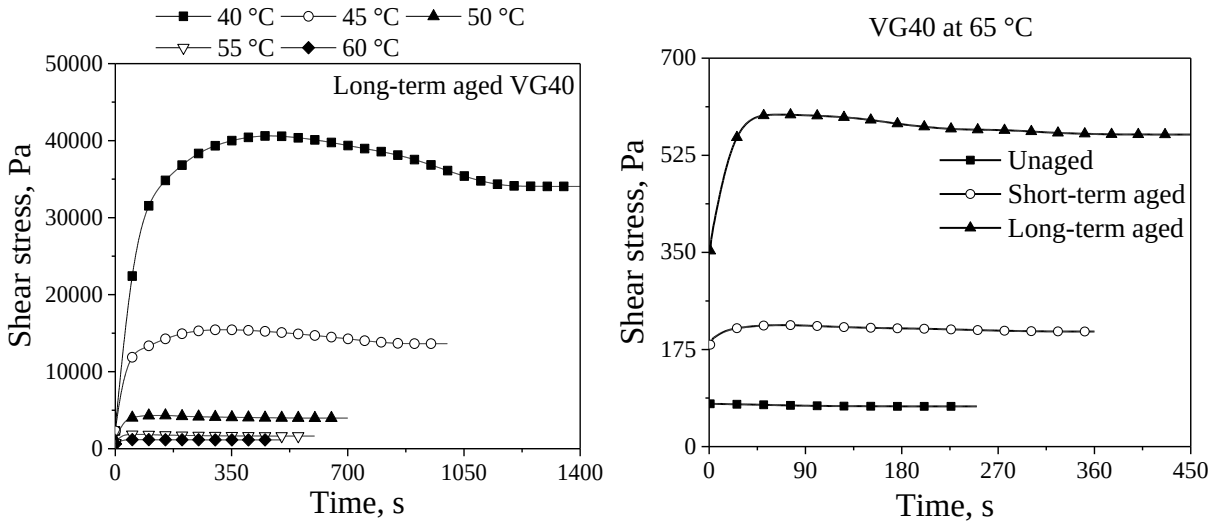

Fig. A7 Shear stress as a function of time in determining 't_s' for the VG20 bitumen

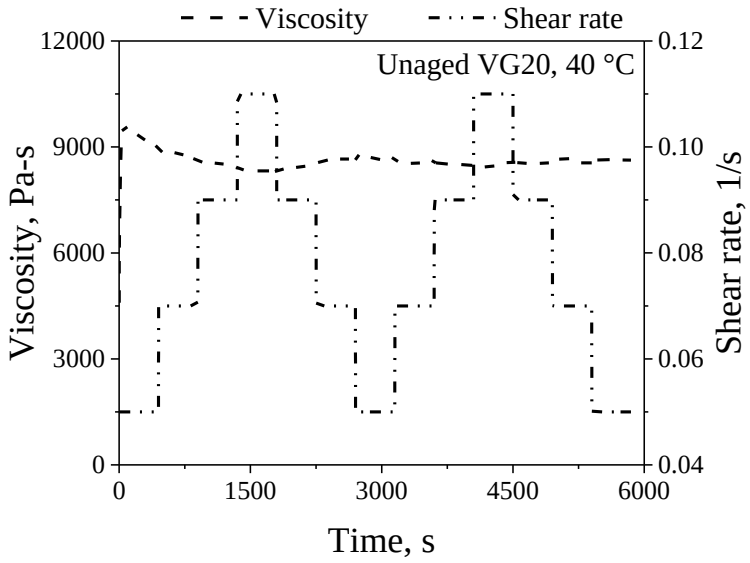
Viscosity
Shear rate
Unaged VG20, 40 °C
Viscosity, Pa-s
Shear rate, 1/s
Time, s
0
3000
6000
9000
12000
0.04
0.06
0.08
0.10
0.12
0
1500
3000
4500
6000

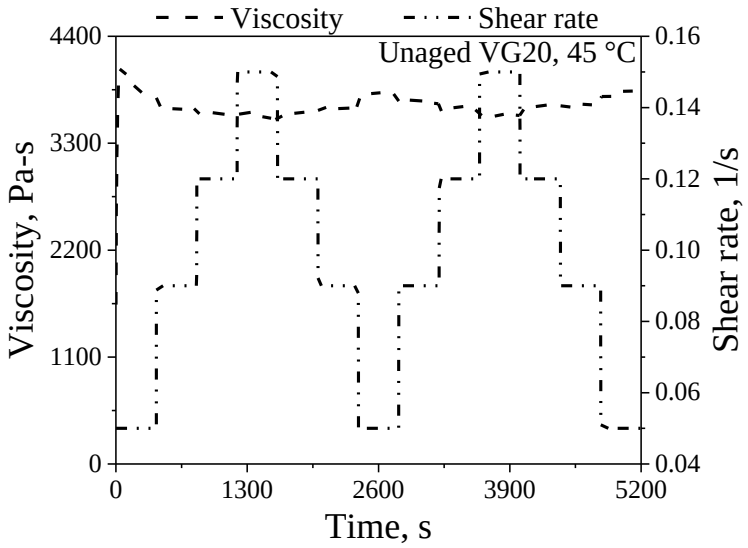
Viscosity
Shear rate
Unaged VG20, 45 °C
Viscosity, Pa-s
Shear rate, 1/s
Time, s
0
1100
2200
3300
4400
0.04
0.06
0.08
0.10
0.12
0.14
0.16
0
1300
2600
3900
5200

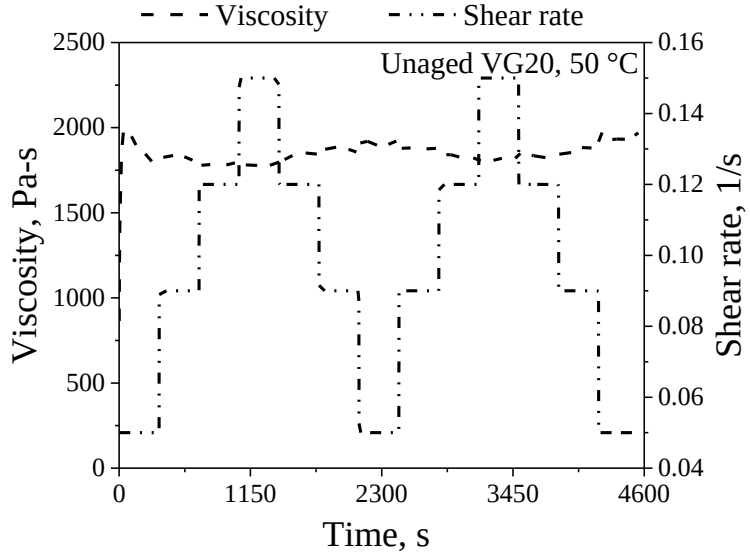
Viscosity
Shear rate
Unaged VG20, 50 °C
Viscosity, Pa-s
Shear rate, 1/s
Time, s
0
500
1000
1500
2000
2500
0.04
0.06
0.08
0.10
0.12
0.14
0.16
0
1150
2300
3450
4600

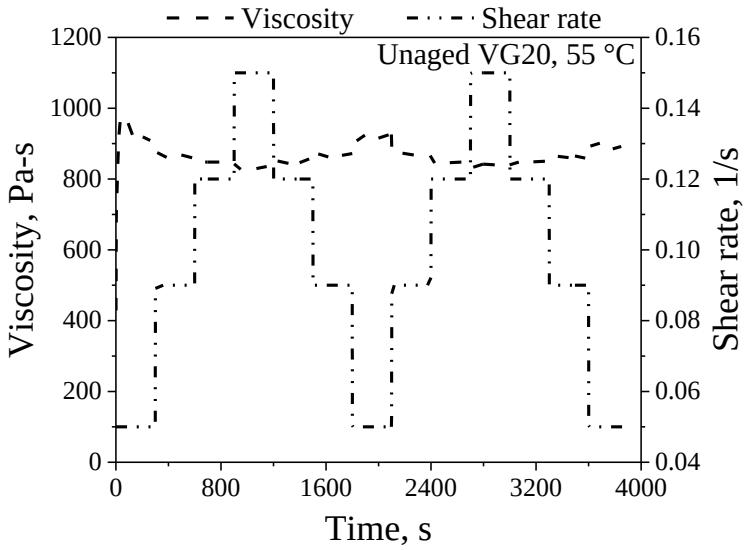
Viscosity
Shear rate
Unaged VG20, 55 °C
Viscosity, Pa-s
Shear rate, 1/s
Time, s
0
200
400
600
800
1000
1200
0.04
0.06
0.08
0.10
0.12
0.14
0.16
0
800
1600
2400
3200
4000

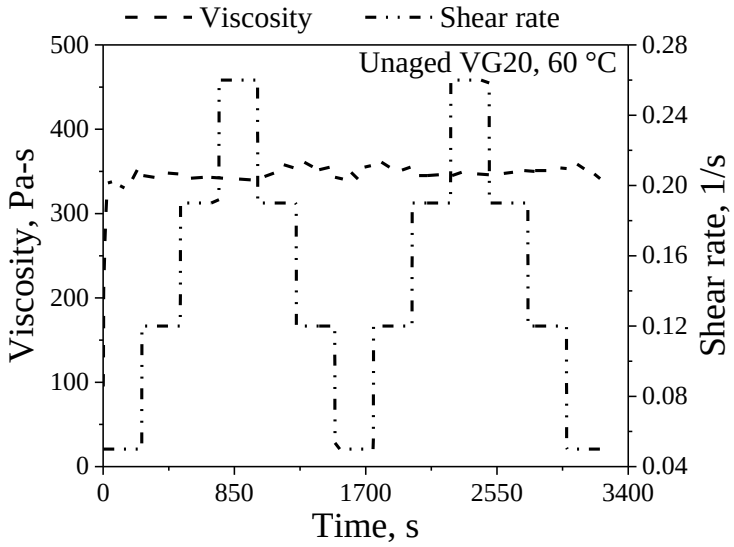
Viscosity
Shear rate
Unaged VG20, 60 °C
Viscosity, Pa-s
Shear rate, 1/s
Time, s
0
100
200
300
400
500
0.04
0.08
0.12
0.16
0.20
0.24
0.28
0
850
1700
2550
3400

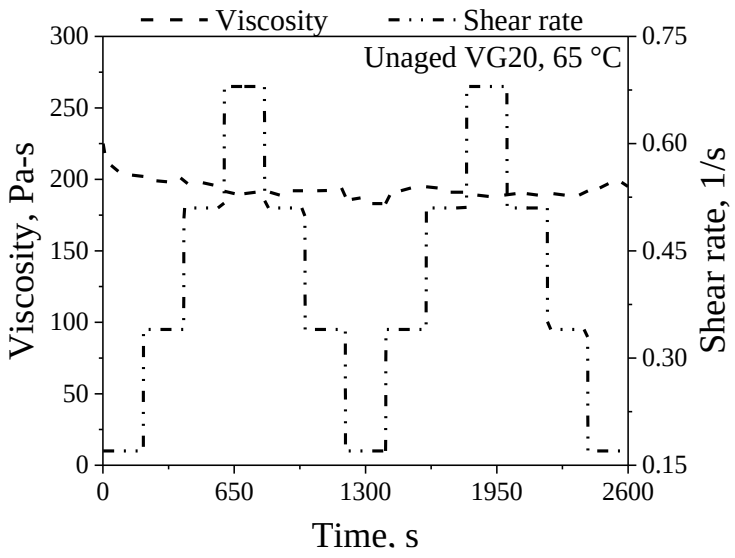
Viscosity
Shear rate
Unaged VG20, 65 °C
Viscosity, Pa-s
Shear rate, 1/s
Time. s
0
50
100
150
200
250
300
0.15
0.30
0.45
0.60
0.75
0
650
1300
1950
2600

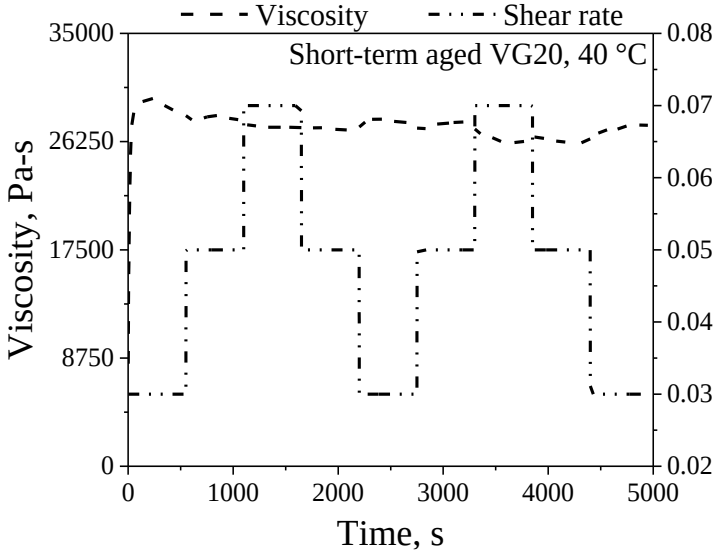
Viscosity
Shear rate
Short-term aged VG20, 40 °C
Viscosity, Pa-s
Shear rate, 1/s
Time, s
0
8750
17500
26250
35000
0.02
0.03
0.04
0.05
0.06
0.07
0.08
0
1000
2000
3000
4000
5000

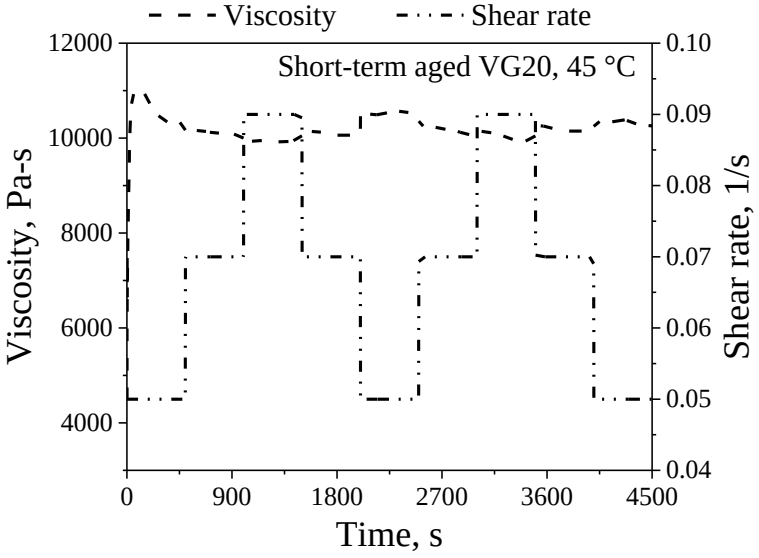
Viscosity
Shear rate
Short-term aged VG20, 45 °C
Viscosity, Pa-s
Shear rate, 1/s
Time, s
4000
6000
8000
10000
12000
0.04
0.05
0.06
0.07
0.08
0.09
0.10
0
900
1800
2700
3600
4500

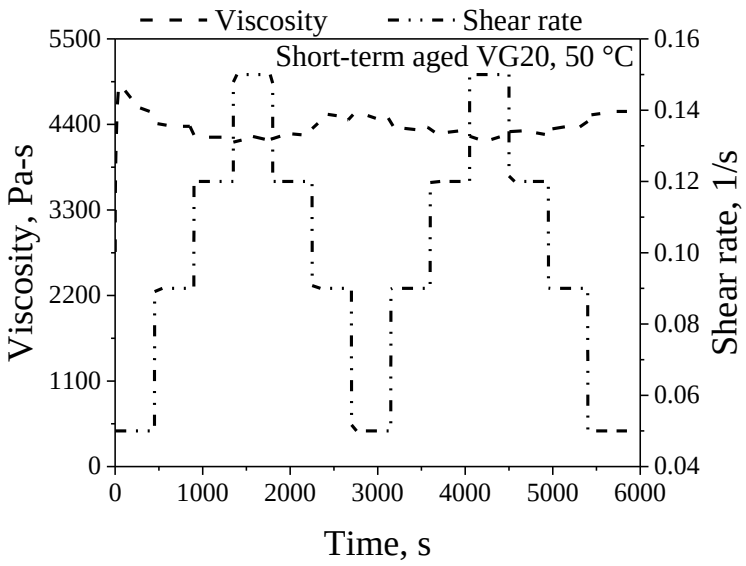
Viscosity
Shear rate
Short-term aged VG20, 50 °C
Viscosity, Pa-s
Shear rate, 1/s
Time, s
0
1100
2200
3300
4400
5500
0.04
0.06
0.08
0.10
0.12
0.14
0.16
0
1000
2000
3000
4000
5000
6000

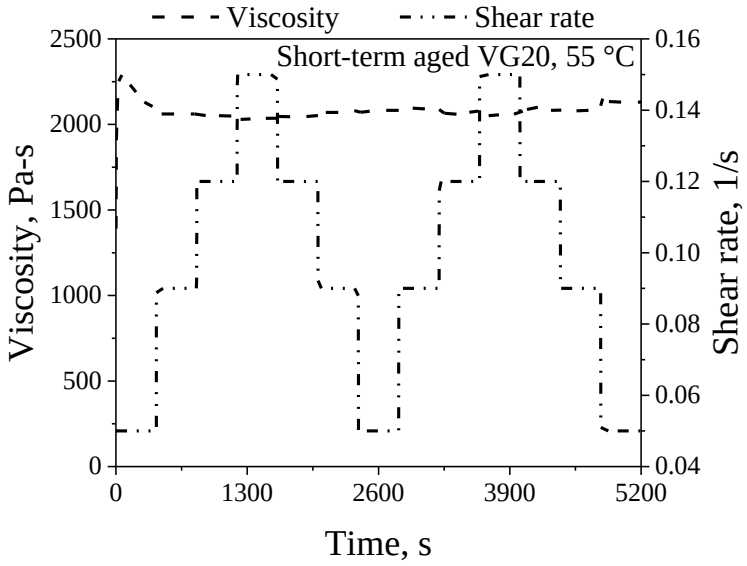
Viscosity
Shear rate
Short-term aged VG20, 55 °C
Viscosity, Pa-s
Shear rate, 1/s
Time, s
0
500
1000
1500
2000
2500
0.04
0.06
0.08
0.10
0.12
0.14
0.16
0
1300
2600
3900
5200

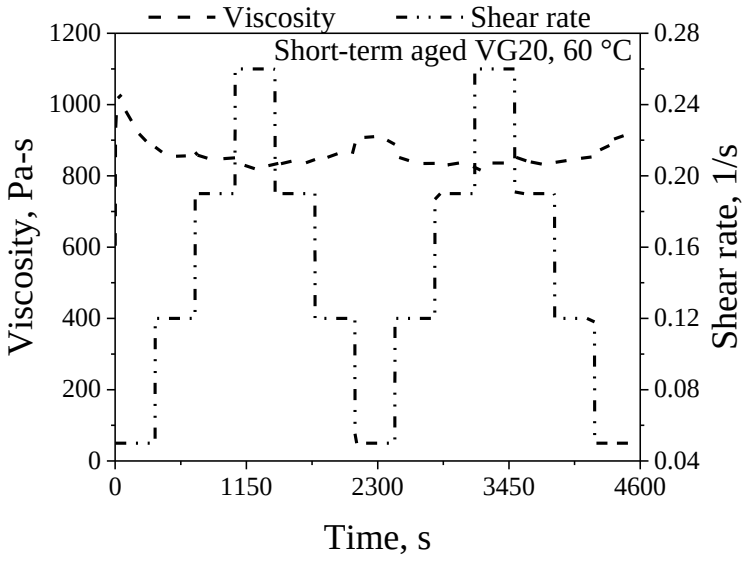
Viscosity
Shear rate
Short-term aged VG20, 60 °C
Viscosity, Pa-s
Shear rate, 1/s
Time, s
0
200
400
600
800
1000
1200
0.04
0.08
0.12
0.16
0.20
0.24
0.28
0
1150
2300
3450
4600

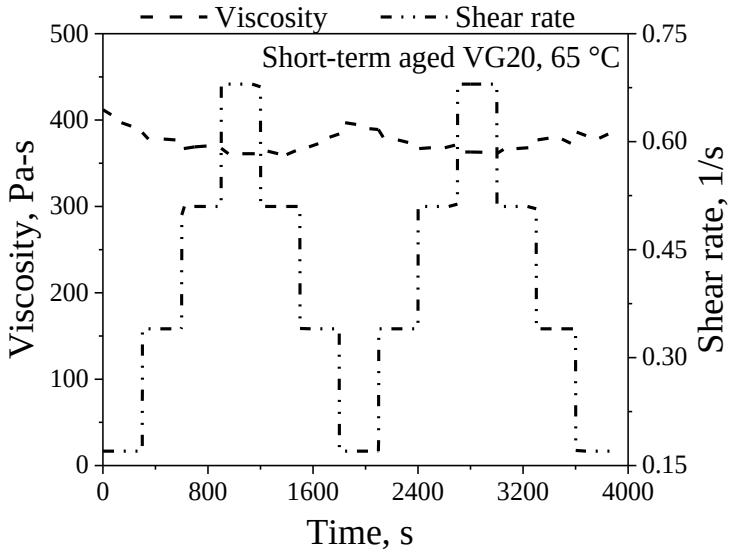
Viscosity
Shear rate
Short-term aged VG20, 65 °C
Viscosity, Pa-s
Shear rate, 1/s
Time, s
0
100
200
300
400
500
0.15
0.30
0.45
0.60
0.75
0
800
1600
2400
3200
4000

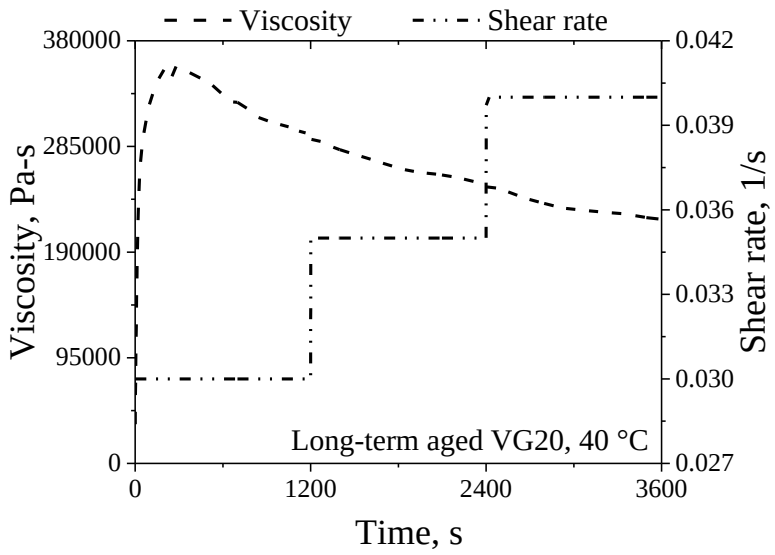
Viscosity
Shear rate
Viscosity, Pa-s
Shear rate, 1/s
Time, s
Long-term aged VG20, 40 °C
380000
285000
190000
95000
0
0.042
0.039
0.036
0.033
0.030
0.027
0
1200
2400
3600

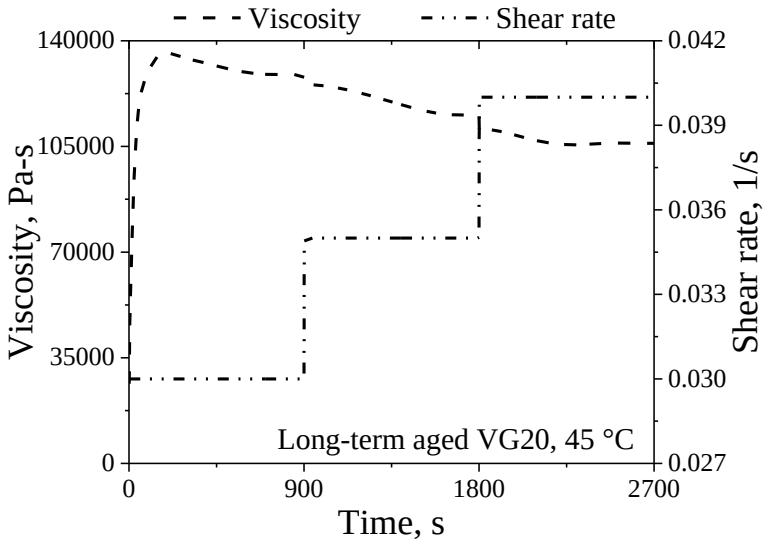
Viscosity
Shear rate
Viscosity, Pa-s
Shear rate, 1/s
Time, s
Long-term aged VG20, 45 °C
140000
105000
70000
35000
0
0.042
0.039
0.036
0.033
0.030
0.027
0
900
1800
2700

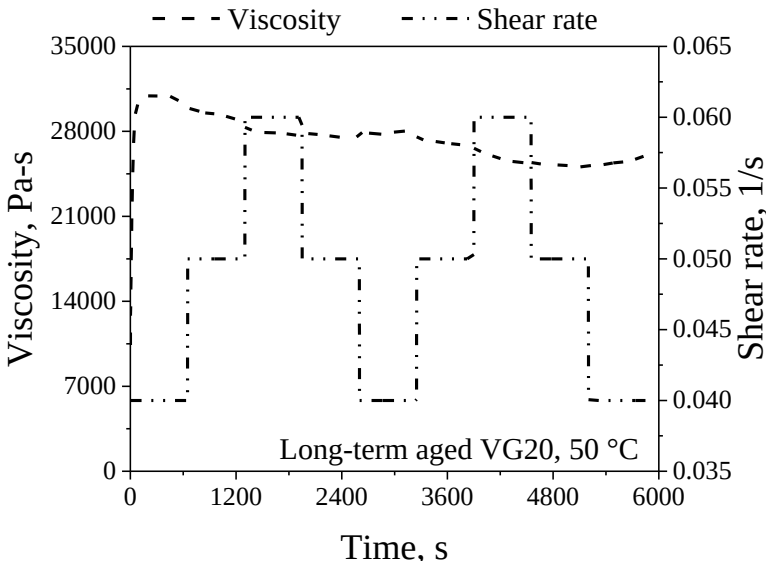
Viscosity
Shear rate
Viscosity, Pa-s
Shear rate, 1/s
Time, s
Long-term aged VG20, 50 °C
35000
28000
21000
14000
7000
0
0.065
0.060
0.055
0.050
0.045
0.040
0.035
0
1200
2400
3600
4800
6000

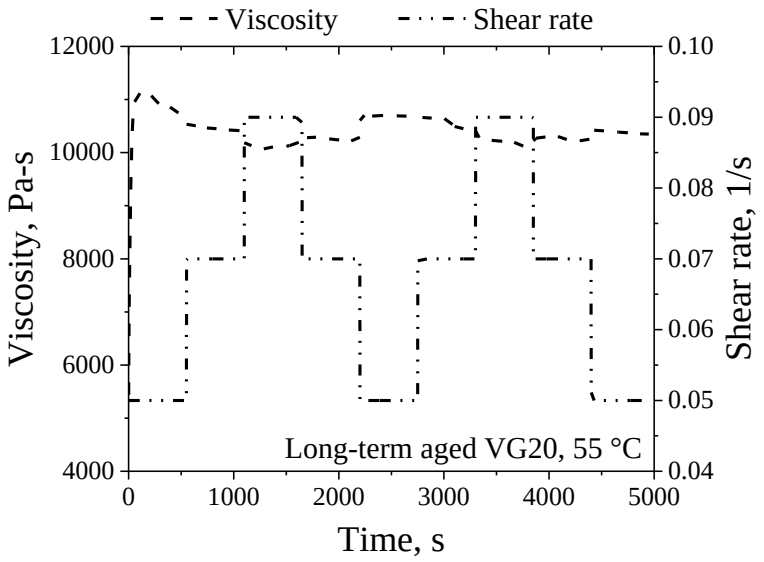
Viscosity
Shear rate
Viscosity, Pa-s
Shear rate, 1/s
Time, s
Long-term aged VG20, 55 °C
12000
10000
8000
6000
4000
0.10
0.09
0.08
0.07
0.06
0.05
0.04
0
1000
2000
3000
4000
5000

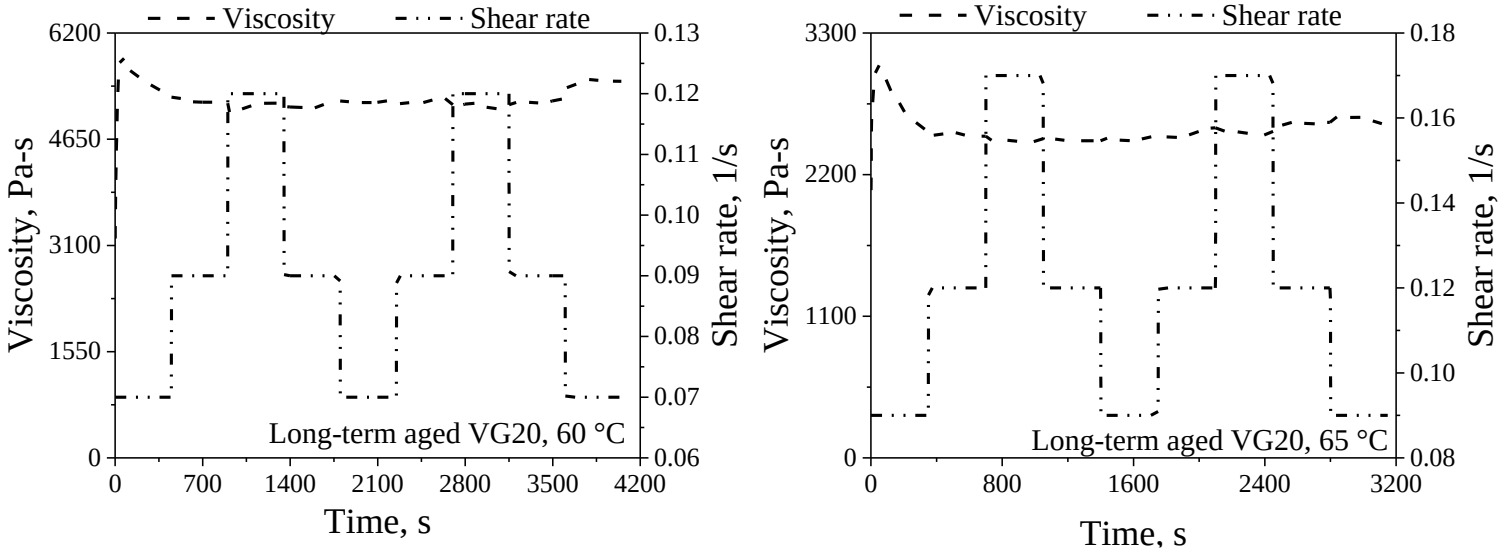

Fig. A8 Response of VG20 bitumen in the $SWSSRS_{DSR}$ test protocol

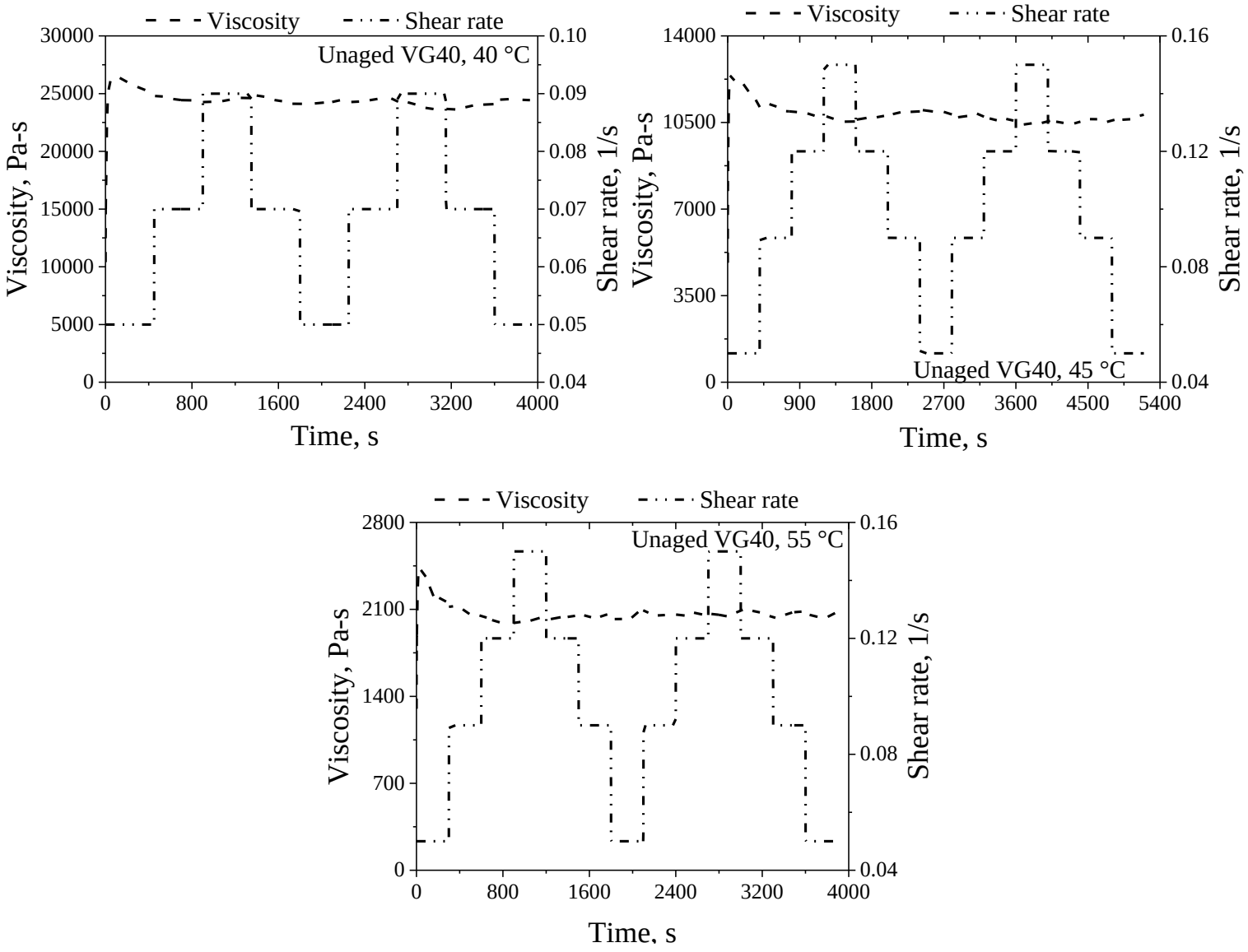
Viscosity
Shear rate
Unaged VG40, 40 °C
Viscosity, Pa-s
Shear rate, 1/s
Time, s
Unaged VG40, 45 °C
Unaged VG40, 55 °C

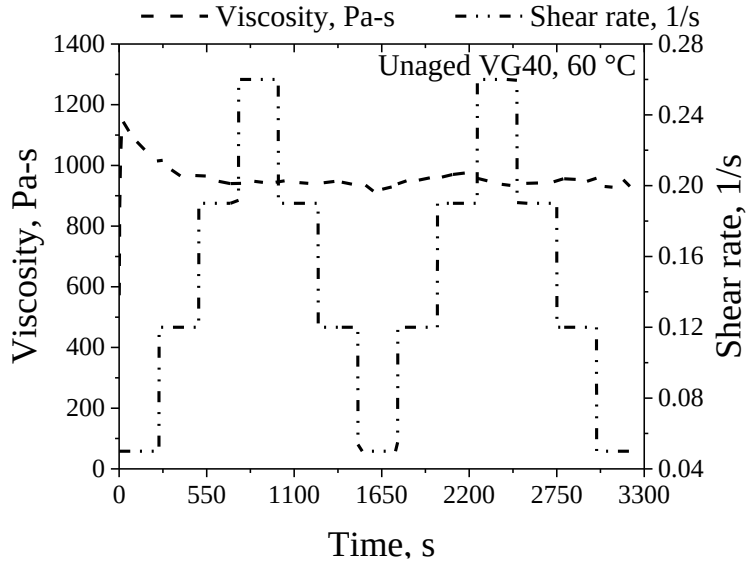
Viscosity, Pa-s
Shear rate, 1/s
Unaged VG40, 60 °C
Viscosity, Pa-s
Shear rate, 1/s
Time, s
0
200
400
600
800
1000
1200
1400
0.04
0.08
0.12
0.16
0.20
0.24
0.28
0
550
1100
1650
2200
2750
3300

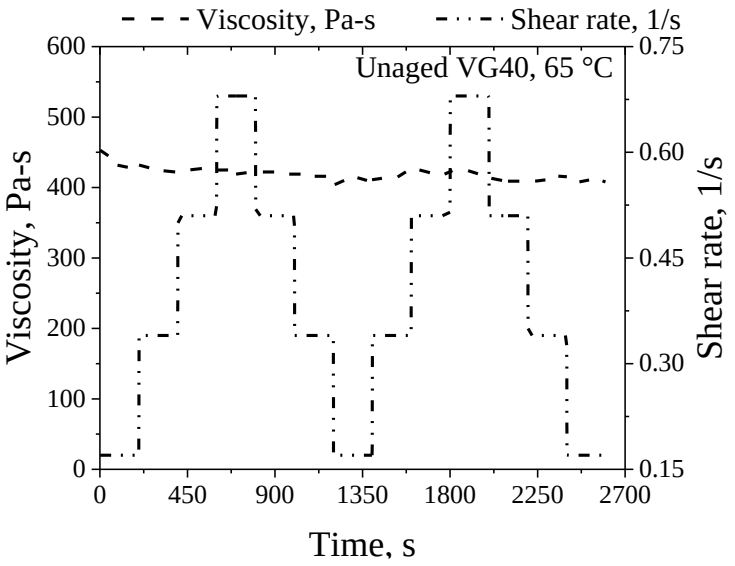
Viscosity, Pa-s
Shear rate, 1/s
Unaged VG40, 65 °C
Viscosity, Pa-s
Shear rate, 1/s
Time, s
0
100
200
300
400
500
600
0.15
0.30
0.45
0.60
0.75
0
450
900
1350
1800
2250
2700

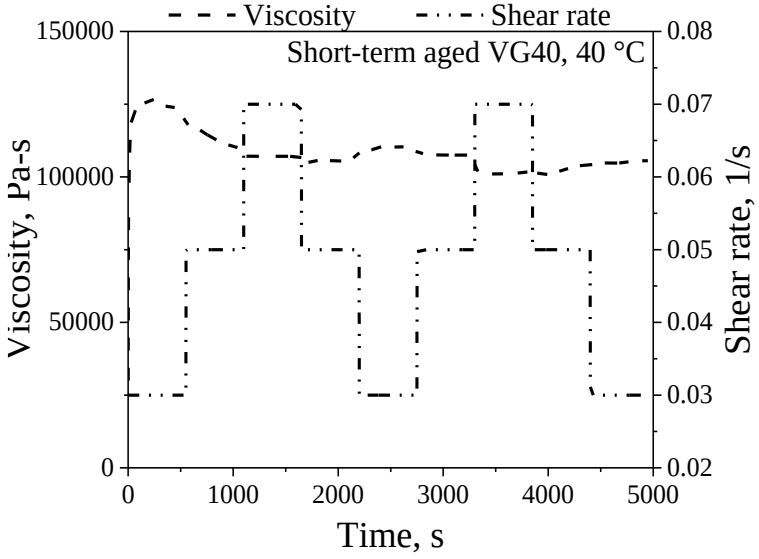
Viscosity
Shear rate
Short-term aged VG40, 40 °C
Viscosity, Pa-s
Shear rate, 1/s
Time, s
0
50000
100000
150000
0.02
0.03
0.04
0.05
0.06
0.07
0.08
0
1000
2000
3000
4000
5000

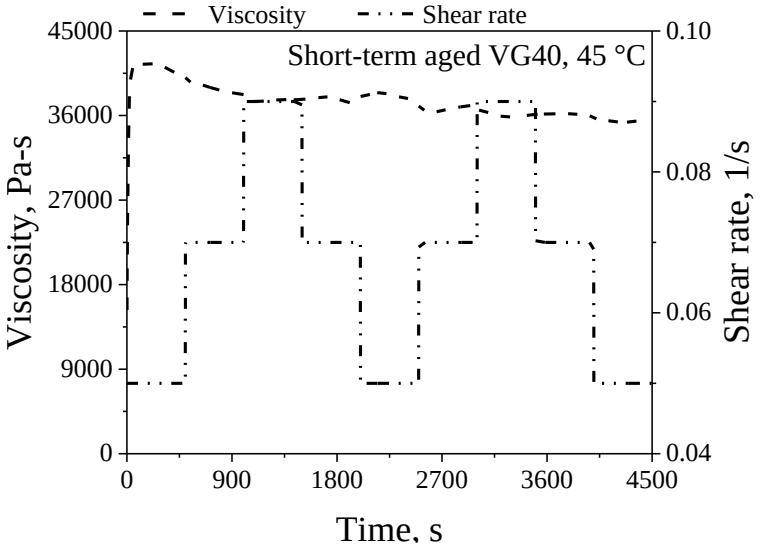
Viscosity
Shear rate
Short-term aged VG40, 45 °C
Viscosity, Pa-s
Shear rate, 1/s
Time, s
0
9000
18000
27000
36000
45000
0.04
0.06
0.08
0.10
0
900
1800
2700
3600
4500

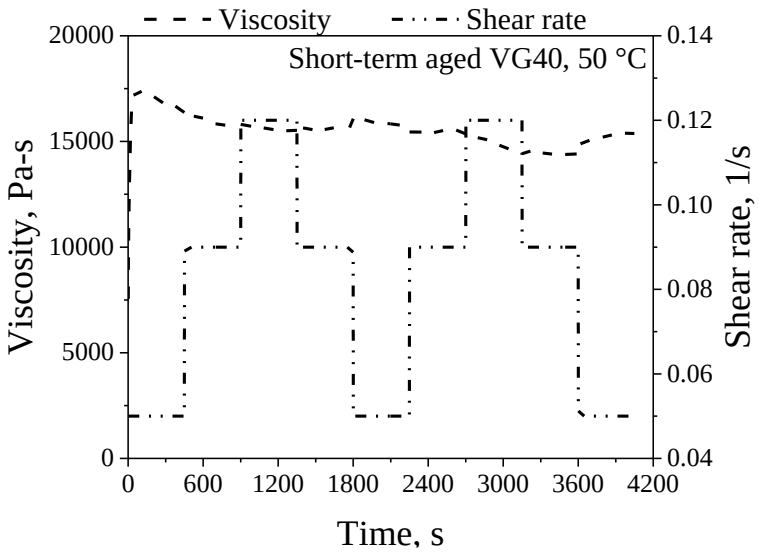
Viscosity
Shear rate
Short-term aged VG40, 50 °C
Viscosity, Pa-s
Shear rate, 1/s
Time, s
0
5000
10000
15000
20000
0.04
0.06
0.08
0.10
0.12
0.14
0
600
1200
1800
2400
3000
3600
4200

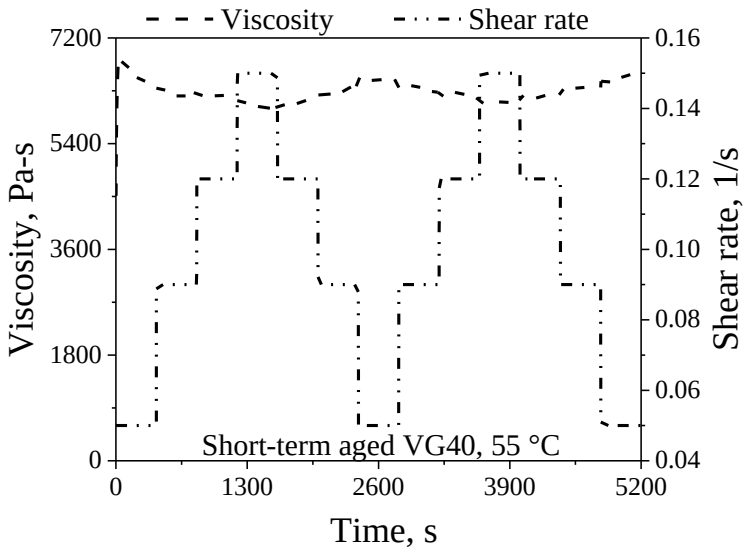
Viscosity
Shear rate
Short-term aged VG40, 55 °C
Viscosity, Pa-s
Shear rate, 1/s
Time, s
0
1800
3600
5400
7200
0.04
0.06
0.08
0.10
0.12
0.14
0.16
0
1300
2600
3900
5200

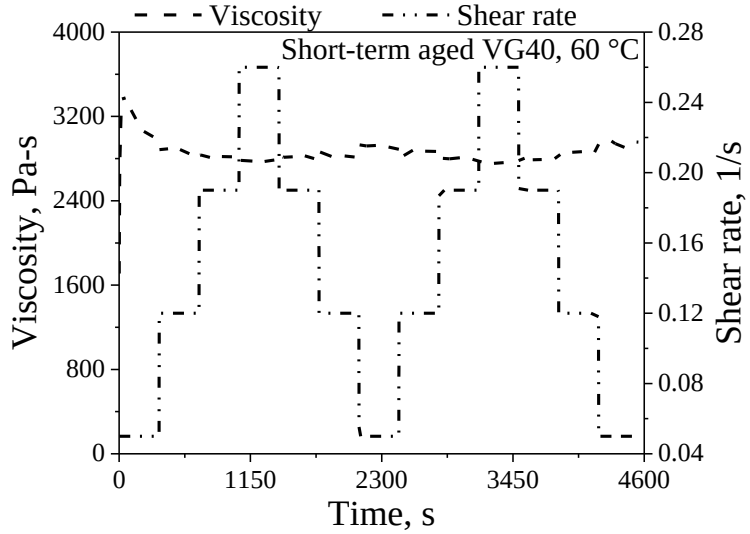
Viscosity
Shear rate
Short-term aged VG40, 60 °C
Viscosity, Pa-s
Shear rate, 1/s
Time, s
0
800
1600
2400
3200
4000
0.04
0.08
0.12
0.16
0.20
0.24
0.28
0
1150
2300
3450
4600

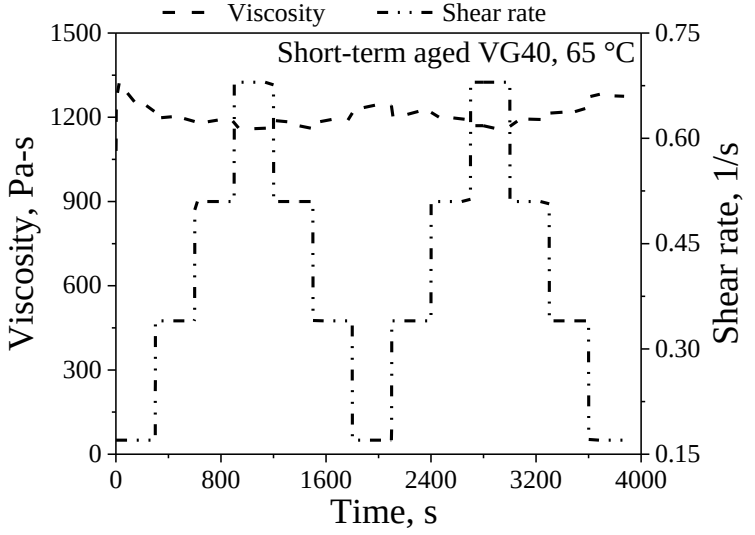
Viscosity
Shear rate
Short-term aged VG40, 65 °C
Viscosity, Pa-s
Shear rate, 1/s
Time, s
0
300
600
900
1200
1500
0.15
0.30
0.45
0.60
0.75
0
800
1600
2400
3200
4000

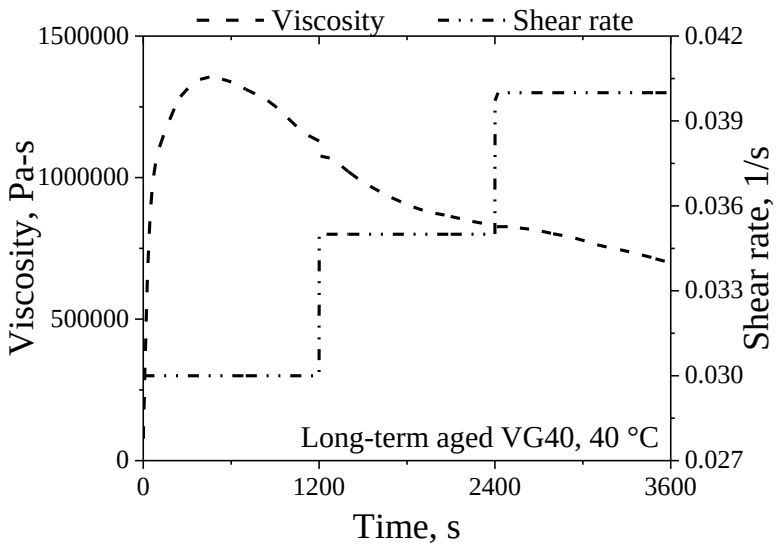
Viscosity
Shear rate
Long-term aged VG40, 40 °C
Viscosity, Pa-s
Shear rate, 1/s
Time, s
1500000
1000000
500000
0
0.042
0.039
0.036
0.033
0.030
0.027
0
1200
2400
3600

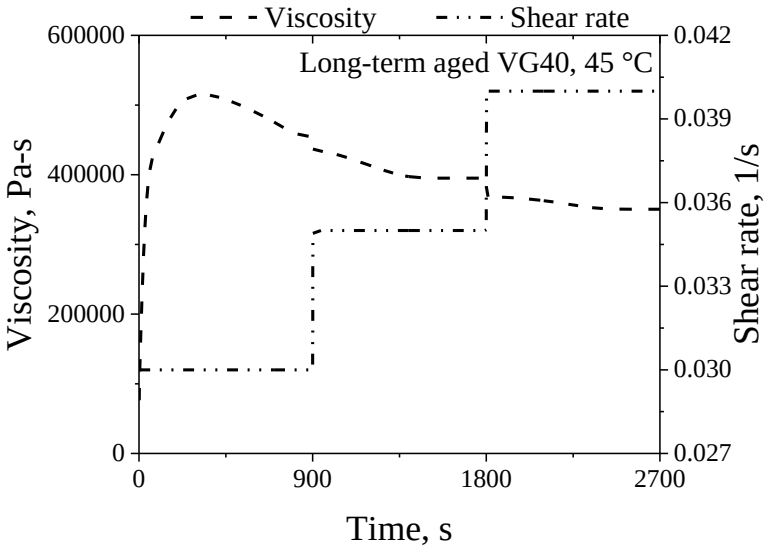
Viscosity
Shear rate
Long-term aged VG40, 45 °C
Viscosity, Pa-s
Shear rate, 1/s
Time, s
600000
400000
200000
0
0.042
0.039
0.036
0.033
0.030
0.027
0
900
1800
2700

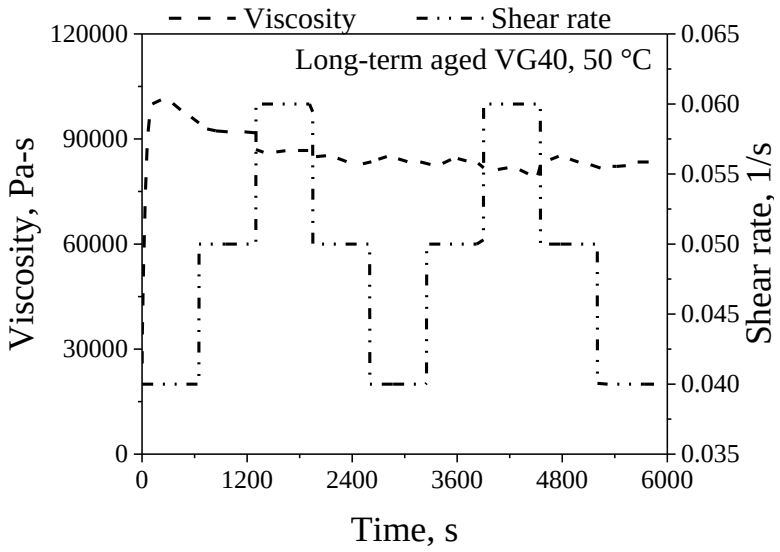
Viscosity
Shear rate
Long-term aged VG40, 50 °C
Viscosity, Pa-s
Shear rate, 1/s
Time, s
120000
90000
60000
30000
0
0.065
0.060
0.055
0.050
0.045
0.040
0.035
0
1200
2400
3600
4800
6000

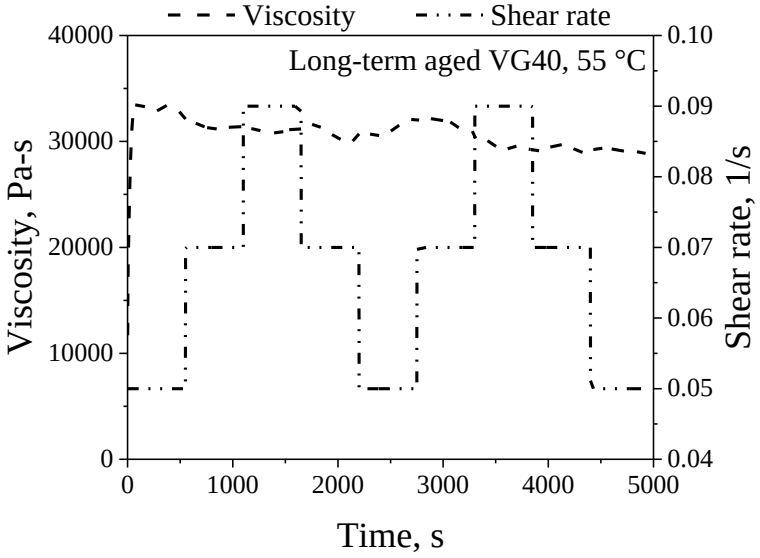
Viscosity
Shear rate
Long-term aged VG40, 55 °C
Viscosity, Pa-s
Shear rate, 1/s
Time, s
40000
30000
20000
10000
0
0.10
0.09
0.08
0.07
0.06
0.05
0.04
0
1000
2000
3000
4000
5000

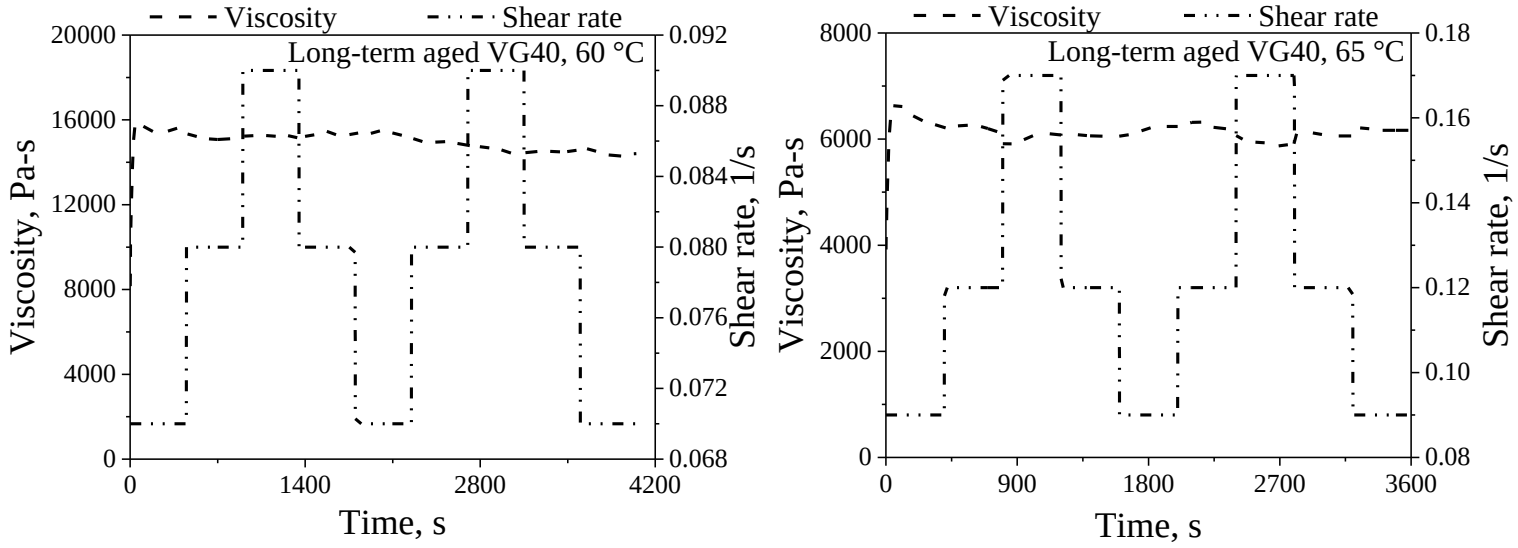

Fig. A9 Test Response of VG40 bitumen in the $SWSSRS_{DSR}$ test protocol

Table A3 Viscosity and shear stress at $t_{s(DSR)}$ in the $SWSSRS_{DSR}$ for the unaged VG20 bitumen

Bitumen	$\dot{\gamma}$, 1/s	Cycle 1				Cycle 2				Average.	
		Forward Sweep		Backward Sweep		Forward Sweep		Backward Sweep			
		σ, Pa	η, Pa-s	σ, Pa	η, Pa-s	σ, Pa	η, Pa-s	σ, Pa	η, Pa-s	σ, Pa	η, Pa-s
Unaged VG20 at 40 °C	*0.05*	***451.09***	***9022***	435.42	8708	435.42	8708	431.30	8626	438.31	8766
	0.07	***606.36***	***8662***	604.28	8633	603.23	8618	595.56	8508	602.36	8605
	0.09	***758.56***	***8428***	763.51	8483	762.80	8476	770.51	8561	763.85	8487
	0.11	***913.70***	***8306***	913.70	8306	941.40	8558	941.40	8558	927.55	8432
Unaged VG20 at 45 °C	*0.050*	***188.77***	***3783***	190.10	3810	190.10	3810	191.83	3844	190.20	3812
	0.090	***329.23***	***3658***	330.79	3675	333.51	3706	331.59	3684	331.28	3681
	0.120	***434.09***	***3617***	432.91	3608	436.54	3638	440.75	3673	436.07	3634
	0.150	***531.27***	***3542***	531.27	3542	537.81	3585	537.81	3585	534.54	3564
Unaged VG20 at 50 °C	*0.050*	***90.93***	***1819***	96.37	1927	96.37	1927	98.45	1969	95.53	1911
	0.090	***162.92***	***1810***	166.81	1853	168.96	1877	167.82	1865	166.63	1851
	0.120	***216.08***	***1801***	221.51	1846	219.47	1829	219.48	1829	219.13	1826
	0.150	***266.97***	***1780***	266.97	1780	272.86	1819	272.86	1819	269.91	1799
Unaged VG20 at 55 °C	*0.050*	***44.46***	***889***	46.31	926	46.31	926	44.04	881	45.28	906
	0.090	***77.24***	***858***	77.93	866	77.96	866	77.48	861	77.65	863
	0.120	***101.43***	***845***	103.06	859	101.27	844	102.16	851	101.98	850
	0.150	***125.84***	***839***	125.84	839	125.96	840	125.96	840	125.90	839
Unaged VG20 at 60 °C	*0.050*	***17.77***	***355***	17.76	355	17.76	355	16.42	328	17.43	349
	0.120	***41.63***	***347***	42.69	356	42.65	355	42.92	358	42.47	354
	0.190	***65.08***	***343***	67.29	354	65.85	347	66.44	350	66.17	348
	0.260	***88.37***	***340***	88.37	340	89.94	346	89.94	346	89.15	343
Unaged VG20 at 65 °C	*0.17*	***35.27***	***207***	33.03	194	33.03	194	33.56	197	33.72	198
	0.34	***65.57***	***193***	65.40	192	66.04	194	64.47	190	65.37	192
	0.51	***94.56***	***185***	95.52	187	97.32	191	95.46	187	95.71	188
	0.68	***124.39***	***183***	124.39	183	126.23	186	126.23	186	125.31	184

Table A4 Viscosity and shear stress at $t_{s(DSR)}$ in the $SWSSRS_{DSR}$ for the short-term aged VG20 bitumen

Bitumen	**$\dot{\gamma}$, 1/s**	**Cycle 1**				**Cycle 2**				**Average.**	
		Forward Sweep		**Backward Sweep**		**Forward Sweep**		**Backward Sweep**			
		***σ*, Pa**	***η*, Pa-s**	***σ*, Pa**	***η*, Pa-s**	***σ*, Pa**	***η*, Pa-s**	***σ*, Pa**	***η*, Pa-s**	***σ*, Pa**	***η*, Pa-s**
Short-term aged VG20 at 40 °C	***0.030***	***859.68***	***28656***	835.12	27837	835.12	27837	826.95	27565	839.22	27974
	0.050	***1399.92***	***27998***	1354.13	27083	1385.08	27702	1325.36	26507	1366.12	27322
	0.070	***1918.73***	***27410***	1918.73	27410	1843.53	26336	1843.53	26336	1881.13	26873
Short-term aged VG20 at 45 °C	***0.050***	***515.85***	***10317***	524.45	10489	524.45	10489	512.79	10256	519.38	10388
	0.070	***704.30***	***10061***	704.30	10061	705.09	10073	710.32	10147	706.00	10086
	0.090	***896.73***	***9964***	896.73	9964	899.11	9990	899.11	9990	897.92	9977
Short-term aged VG20 at 50 °C	***0.050***	***226.00***	***4520***	224.12	4482	224.12	4482	228.35	4567	225.65	4513
	0.090	***393.71***	***4375***	401.15	4457	392.91	4366	394.58	4384	395.59	4395
	0.120	***508.26***	***4236***	511.82	4265	517.87	4316	512.25	4269	512.55	4271
	0.150	***631.46***	***4210***	631.46	4210	639.19	4261	639.19	4261	635.32	4235
Short-term aged VG20 at 55 °C	***0.050***	***105.17***	***2103***	104.08	2082	104.08	2082	106.52	2130	104.97	2099
	0.090	***185.45***	***2061***	187.21	2080	188.95	2099	187.37	2082	187.25	2081
	0.120	***245.77***	***2048***	245.58	2046	249.43	2079	248.88	2074	247.41	2062
	0.150	***304.85***	***2032***	304.85	2032	309.04	2060	309.04	2060	306.95	2046
Short-term aged VG20 at 60 °C	***0.050***	***44.96***	***899***	45.04	901	45.04	901	45.13	903	45.04	901
	0.120	***105.03***	***875***	103.61	863	100.26	836	102.26	852	102.79	857
	0.190	***161.60***	***851***	159.01	837	156.88	826	157.81	831	158.83	836
	0.260	***215.83***	***830***	215.83	830	220.02	846	220.02	846	217.93	838
Short-term aged VG20 at 65 °C	***0.170***	***66.11***	***389***	66.06	389	66.06	389	66.18	389	66.10	389
	0.340	***128.02***	***377***	130.41	384	126.76	373	126.67	373	127.96	376
	0.510	***188.45***	***370***	186.18	365	189.28	371	187.92	368	187.96	369
	0.680	***245.18***	***361***	245.18	361	245.16	361	245.16	361	245.17	361

Table A5 Viscosity and shear stress at $t_{s(DSR)}$ in the $SWSSRS_{DSR}$ for the long-term aged VG20 bitumen

Bitumen	**$\dot{\gamma}$, 1/s**	**Cycle 1**				**Cycle 2**				**Average.**	
		Forward Sweep		**Backward Sweep**		**Forward Sweep**		**Backward Sweep**			
		σ, Pa	**η, Pa-s**	**σ, Pa**	**η, Pa-s**	**σ, Pa**	**η, Pa-s**	**σ, Pa**	**η, Pa-s**	**σ, Pa**	**η, Pa-s**
Long-term aged VG20 at 40 °C	***0.03***	***8805***	***293500***	-	-	-	-	-	-	-	-
	0.035	***8809***	251695	-	-	-	-	-	-	-	-
	0.04	***8788***	219706	-	-	-	-	-	-	-	-
Long-term aged VG20 at 45 °C	***0.030***	***3865***	***128824***	-	-	-	-	-	-	-	-
	0.035	***4038***	115374	-	-	-	-	-	-	-	-
	0.040	***4241***	106023	-	-	-	-	-	-	-	-
Long-term aged VG20 at 50 °C	***0.040***	***1211.73***	***30293***	1117.76	27944	1117.76	27944	1038.51	25963	1121.44	28036
	0.050	***1444.40***	***28888***	1376.82	27536	1342.53	26851	1251.34	25027	1353.78	27076
	0.060	***1659.39***	***27656***	1659.39	27656	1524.53	25409	1524.53	25409	1591.96	26533
Long-term aged VG20 at 55 °C	***0.050***	***534.69***	***10694***	533.92	10678	533.92	10678	517.38	10348	529.98	10600
	0.070	***728.83***	***10412***	715.11	10216	734.60	10494	717.75	10254	724.07	10344
	0.090	***917.93***	***10199***	917.93	10199	908.74	10097	908.74	10097	913.34	10148
Long-term aged VG20 at 60 °C	***0.070***	***373.89***	***5341***	365.78	5225	365.78	5225	384.63	5495	372.52	5322
	0.090	***467.37***	***5193***	468.17	5202	470.08	5223	471.43	5238	469.26	5214
	0.120	***621.08***	***5176***	621.08	5176	610.92	5091	610.92	5091	616.00	5133
Long-term aged VG20 at 65 °C	***0.090***	***229.00***	***2544***	225.00	2500	225.00	2500	233.24	2592	228.06	2534
	0.120	***299.85***	***2499***	295.57	2463	307.65	2564	312.77	2606	303.96	2533
	0.170	***417.62***	***2457***	417.62	2457	426.11	2507	426.11	2507	421.87	2482

Table A6 Viscosity and shear stress at $t_{s(DSR)}$ in the $SWSSRS_{DSR}$ for the unaged VG40 bitumen

Bitumen	$\dot{\gamma}$, 1/s	Cycle 1				Cycle 2				Average.	
		Forward Sweep		Backward Sweep		Forward Sweep		Backward Sweep			
		σ, Pa	η, Pa-s	σ, Pa	η, Pa-s	σ, Pa	η, Pa-s	σ, Pa	η, Pa-s	σ, Pa	η, Pa-s
Unaged VG40 at 40 °C	***0.050***	***1257.36***	***25147***	1225.06	24501	1225.06	24501	1220.21	24404	1231.92	24638
	0.070	***1715.83***	***24512***	1682.56	24037	1722.25	24604	1687.09	24101	1701.93	24313
	0.090	***2216.55***	***24628***	2216.55	24628	2113.74	23486	2113.74	23486	2165.14	24057
Unaged VG40 at 45 °C	***0.050***	***564.56***	***11291***	545.37	10907	545.37	10907	540.72	10814	549.00	10980
	0.090	***985.27***	***10947***	981.64	10907	977.71	10863	944.83	10498	972.36	10804
	0.120	***1287.95***	***10733***	1292.93	10774	1267.19	10560	1253.71	10448	1275.44	10629
	0.150	***1581.15***	***10541***	1581.15	10541	1573.54	10490	1573.54	10490	1577.35	10516
Unaged VG40 at 50 °C	***0.050***	***204.30***	***4094***	202.06	4049	202.06	4049	207.09	4150	203.88	4086
	0.090	***369.47***	***4105***	362.00	4022	367.60	4084	364.51	4050	365.89	4065
	0.120	***490.91***	***4091***	487.07	4059	481.85	4015	490.99	4092	487.71	4064
	0.150	***595.69***	***3971***	595.69	3971	597.67	3984	597.67	3984	596.68	3978
Unaged VG40 at 55 °C	***0.050***	***104.13***	***2087***	104.39	2092	104.39	2092	103.64	2077	104.14	2087
	0.090	***184.41***	***2049***	184.57	2051	183.60	2040	187.92	2088	185.12	2057
	0.120	***238.81***	***1990***	246.45	2054	246.48	2054	244.97	2041	244.18	2035
	0.150	***303.12***	***2021***	303.12	2021	313.72	2091	313.72	2091	308.42	2056
Unaged VG40 at 60 °C	***0.050***	***50.50***	***1010***	45.60	912	45.60	912	46.40	928	47.03	941
	0.120	***116.17***	***968***	113.28	944	115.32	961	115.32	961	115.02	959
	0.190	***177.88***	***936***	178.41	939	183.92	968	179.74	946	179.99	947
	0.260	***245.34***	***944***	245.34	944	244.66	941	244.66	941	245.00	942
Unaged VG40 at 65 °C	***0.170***	***72.47***	***426***	69.90	411	69.90	411	69.33	408	70.40	414
	0.340	***143.42***	***422***	141.18	415	145.14	427	142.46	419	143.05	421
	0.510	***216.87***	***425***	214.20	420	213.34	418	209.00	410	213.35	418
	0.680	***286.33***	***421***	286.33	421	281.54	414	281.54	414	283.94	418

Table A7 Viscosity and shear stress at $t_{s(DSR)}$ in the $SWSSRS_{DSR}$ for the short-term aged VG40 bitumen

Bitumen	**$\dot{\gamma}$, 1/s**	**Cycle 1**				**Cycle 2**				**Average.**	
		Forward Sweep		**Backward Sweep**		**Forward Sweep**		**Backward Sweep**			
		***σ*, Pa**	***η*, Pa-s**	***σ*, Pa**	***η*, Pa-s**	***σ*, Pa**	***η*, Pa-s**	***σ*, Pa**	***η*, Pa-s**	***σ*, Pa**	***η*, Pa-s**
Short-term aged VG40 at 40 °C	***0.030***	***3588.37***	***119612***	3263.08	108769	3263.08	108769	3166.10	105537	3320.16	110672
	0.050	***5493.03***	***109861***	5341.43	106829	5375.14	107503	5207.70	104154	5354.32	107086
	0.070	***7496.38***	***107091***	7496.38	107091	7125.33	101790	7125.33	101790	7310.86	104441
Short-term aged VG40 at 45 °C	***0.050***	***2000.00***	***40000***	1882.24	37645	1882.24	37645	1777.67	35553	1885.54	37711
	0.070	***2683.45***	***38335***	2617.06	37387	2597.47	37107	2517.18	35960	2603.79	37197
	0.090	***3389.37***	***37660***	3389.37	37660	3236.29	35959	3236.29	35959	3312.83	36809
Short-term aged VG40 at 50 °C	***0.050***	***826.63***	***16533***	789.04	15781	789.04	15781	768.58	15372	793.32	15866
	0.090	***1428.57***	***15873***	1409.38	15660	1394.17	15491	1296.99	14411	1382.28	15359
	0.120	***1852.94***	***15441***	1852.94	15441	1730.58	14421	1730.58	14421	1791.76	14931
Short-term aged VG40 at 55 °C	***0.050***	***321.57***	***6431***	324.68	6494	324.68	6494	328.24	6565	324.79	6496
	0.090	***564.61***	***6273***	573.92	6377	564.71	6275	572.14	6357	568.84	6320
	0.120	***742.41***	***6187***	738.70	6156	741.33	6178	747.87	6232	742.58	6188
	0.150	***902.62***	***6017***	902.62	6017	920.82	6139	920.82	6139	911.72	6078
Short-term aged VG40 at 60 °C	***0.050***	***148.55***	***2971***	145.44	2909	145.44	2909	147.79	2956	146.81	2936
	0.120	***341.94***	***2850***	338.20	2818	344.32	2869	342.76	2856	341.81	2848
	0.190	***536.81***	***2825***	531.63	2798	530.03	2790	531.74	2799	532.55	2803
	0.260	***724.31***	***2786***	724.31	2786	718.68	2764	718.68	2764	721.50	2775
Short-term aged VG40 at 65 °C	***0.170***	***208.55***	***1227***	211.21	1242	211.21	1242	216.22	1272	211.80	1246
	0.340	***404.00***	***1188***	403.99	1188	417.51	1228	419.42	1234	411.23	1210
	0.510	***604.96***	***1186***	592.15	1161	606.84	1190	607.66	1191	602.90	1182
	0.680	***793.90***	***1167***	793.90	1167	792.13	1165	792.13	1165	793.02	1166

Table A8 Viscosity and shear stress at $t_{s(DSR)}$ in the $SWSSRS_{DSR}$ for the long-term aged VG40 bitumen

Bitumen	**$\dot{\gamma}$, 1/s**	**Cycle 1**				**Cycle 2**				**Average.**	
		Forward Sweep		**Backward Sweep**		**Forward Sweep**		**Backward Sweep**			
		σ, Pa	**η, Pa-s**	**σ, Pa**	**η, Pa-s**	**σ, Pa**	**η, Pa-s**	**σ, Pa**	**η, Pa-s**	**σ, Pa**	**η, Pa-s**
Long-term aged VG40 at 40 °C	0.030	34078	***1135943***	-	-	-	-	-	-	-	-
	0.035	29198	834220	-	-	-	-	-	-	-	-
	0.040	28069	701731	-	-	-	-	-	-	-	-
Long-term aged VG40 at 45 °C	0.030	13645	***454819***	-	-	-	-	-	-	-	-
	0.035	13826	395017	-	-	-	-	-	-	-	-
	0.040	14015	350383	-	-	-	-	-	-	-	-
Long-term aged VG40 at 50 °C	0.040	3835.53	***95888***	3336.08	83402	3336.08	83402	3335.34	83384	3460.76	86519
	0.050	4601.93	92039	4143.34	82867	4149.26	82985	4114.15	82283	4252.17	85043
	0.060	5201.88	86698	5201.88	86698	4779.82	79664	4779.82	79664	4990.85	83181
Long-term aged VG40 at 55 °C	***0.050***	***1634.78***	***32696***	1607.60	32152	1607.60	32152	1442.47	28849	1573.11	31462
	0.070	***2197.76***	***31397***	2110.08	30144	2168.49	30978	2023.90	28913	2125.06	30358
	0.090	***2803.01***	***31145***	2803.01	31145	2631.21	29236	2631.21	29236	2717.11	30190
Long-term aged VG40 at 60 °C	***0.070***	***1090.27***	***15575***	1065.79	15226	1065.79	15226	1008.57	14408	1057.60	15109
	0.080	***1208.00***	***15100***	1225.26	15316	1181.99	14775	1165.81	14573	1195.26	14941
	0.090	***1363.81***	***15153***	1363.81	15153	1296.79	14409	1296.79	14409	1330.30	14781
Long-term aged VG40 at 65 °C	***0.090***	***562.45***	***6249***	561.29	6237	561.29	6237	554.96	6166	560.00	6222
	0.120	***735.31***	***6128***	726.53	6054	743.07	6192	727.24	6060	733.04	6109
	0.170	***1037.10***	***6101***	1037.10	6101	1005.05	5912	1005.05	5912	1021.08	6006

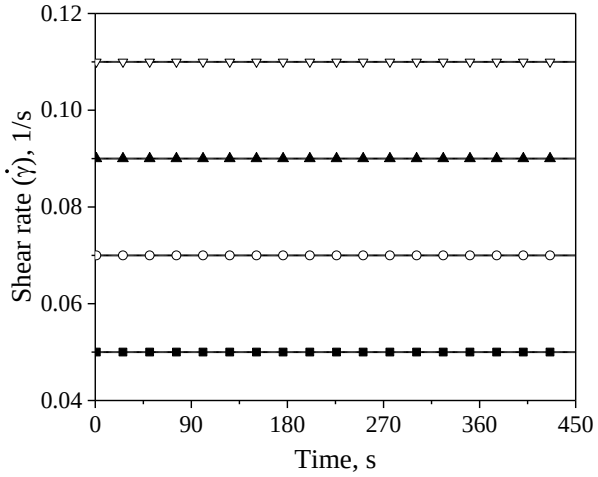

(a) Unaged VG20 at 40 °C

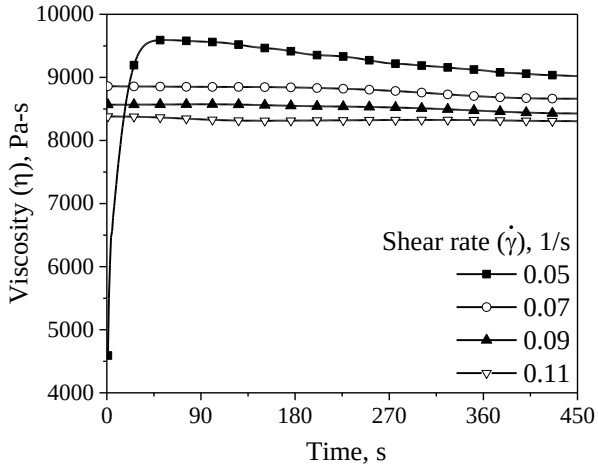

(b) Unaged VG20 at 40 °C

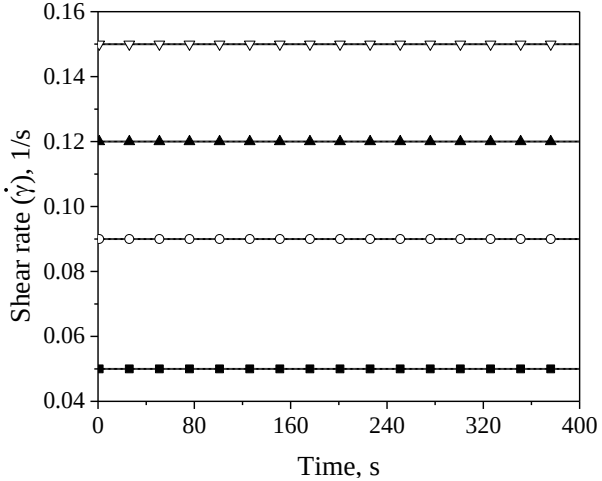

(c) Unaged VG20 at 45 °C

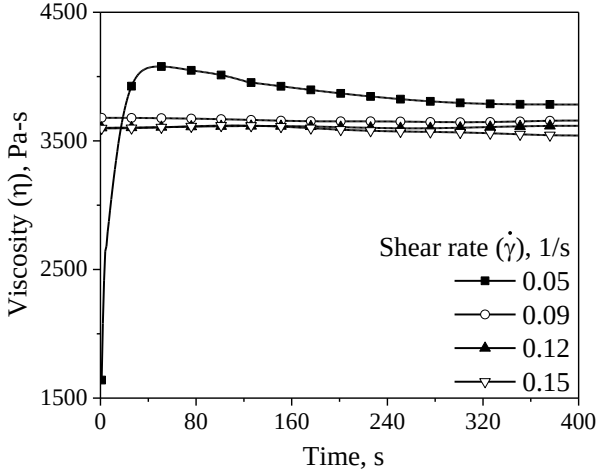

(d) Unaged VG20 at 45 °C

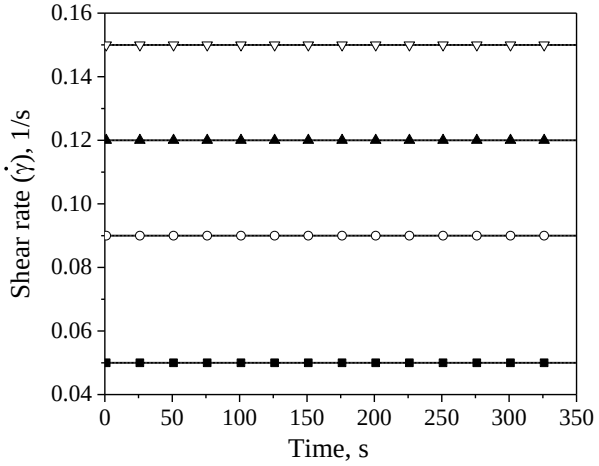

(e) Unaged VG20 at 50 °C

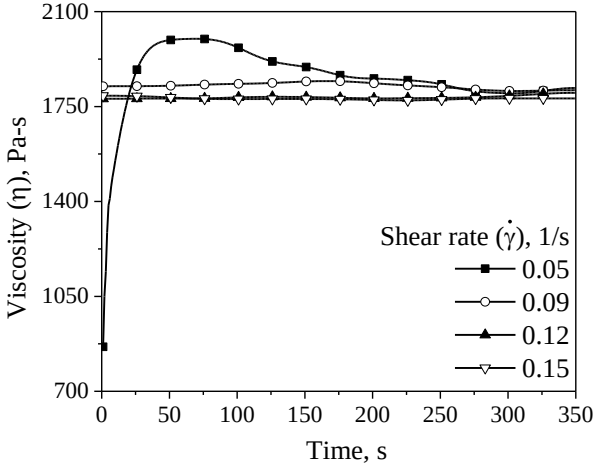

(f) Unaged VG20 at 50 °C

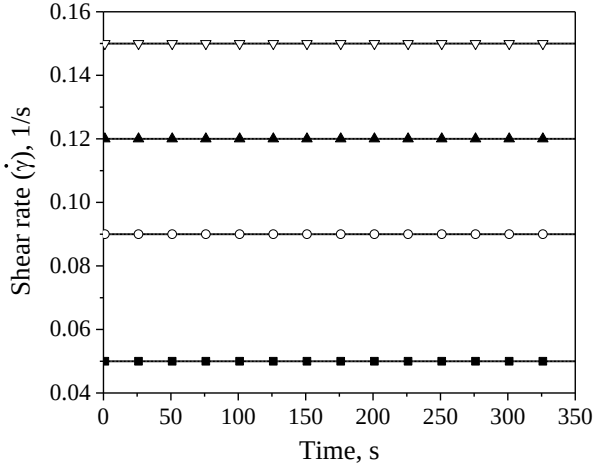

(g) Unaged VG20 at 55 °C

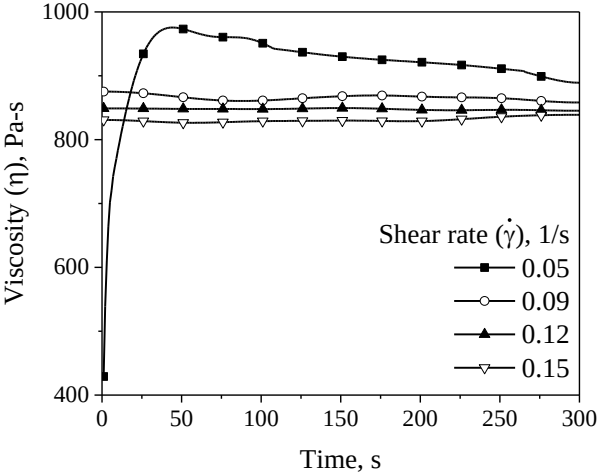

(h) Unaged VG20 at 55 °C

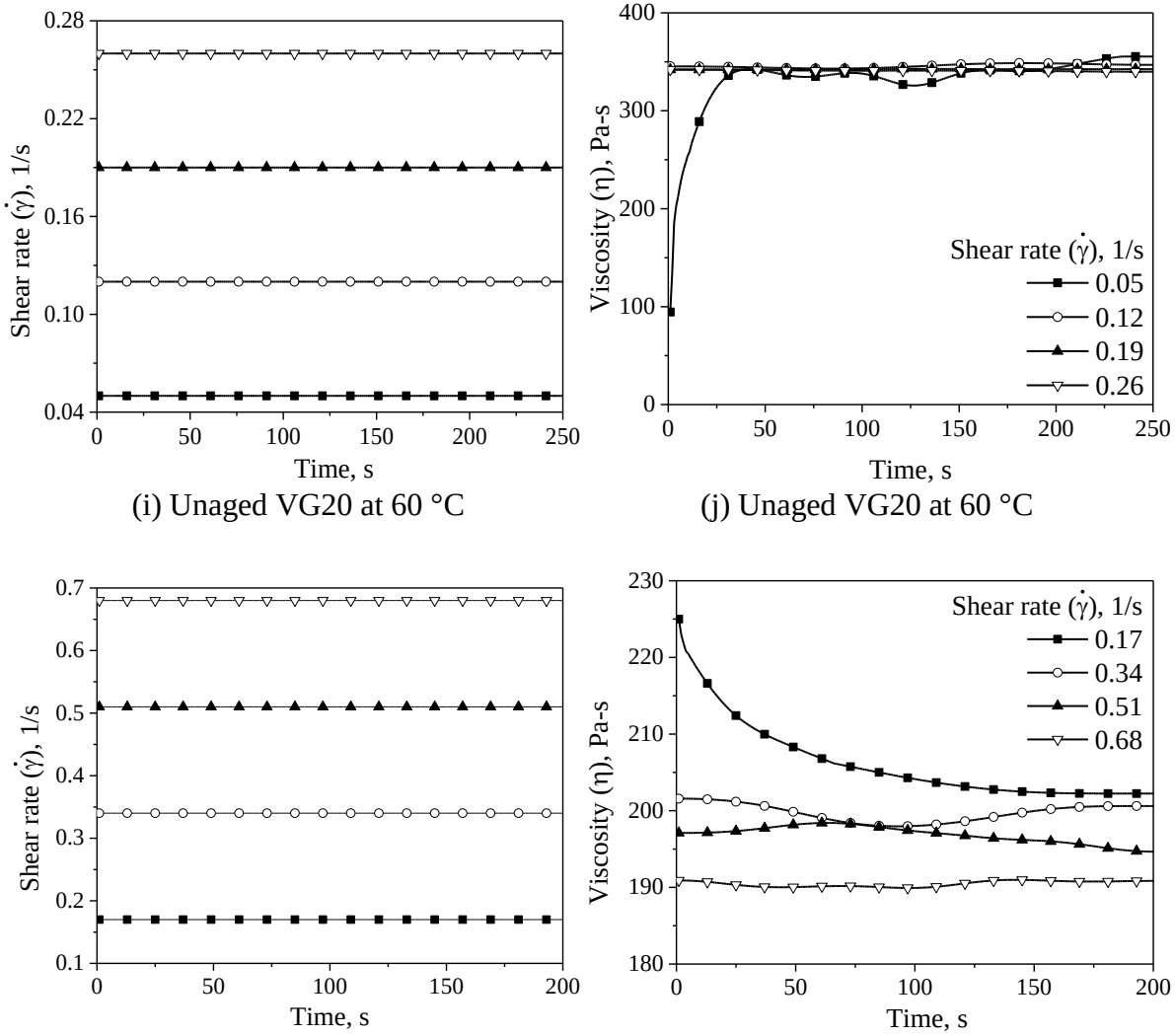

(i) Unaged VG20 at 60 °C (j) Unaged VG20 at 60 °C

(k) Unaged VG20 at 65 °C (l) Unaged VG20 at 65 °C

Fig. A10 Shear rate and viscosity as a function of time in the first forward sweep of the $SWSSRS_{DSR}$ test for the unaged VG20 bitumen

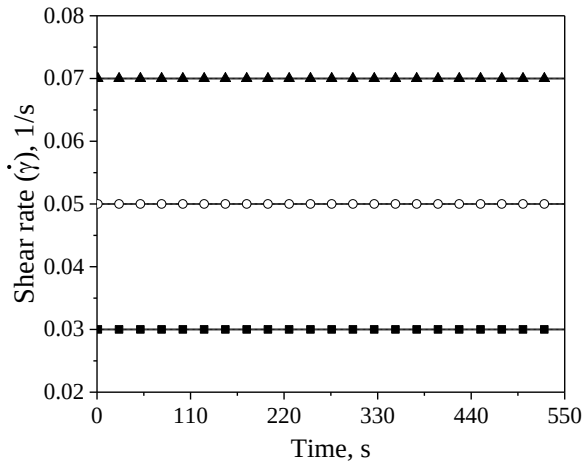

(a) Short-term aged VG20 at 40 °C

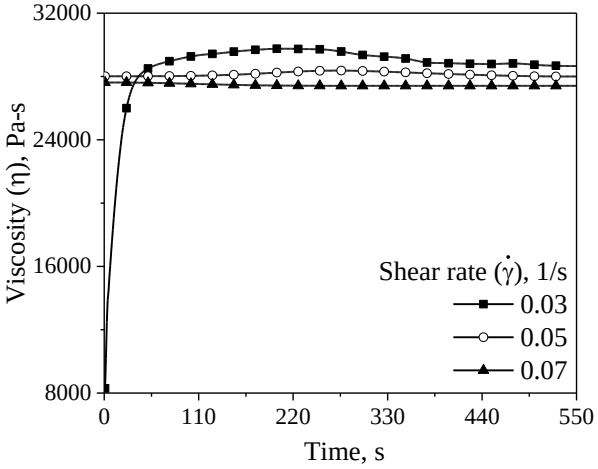

(b) Short-term aged VG20 at 40 °C

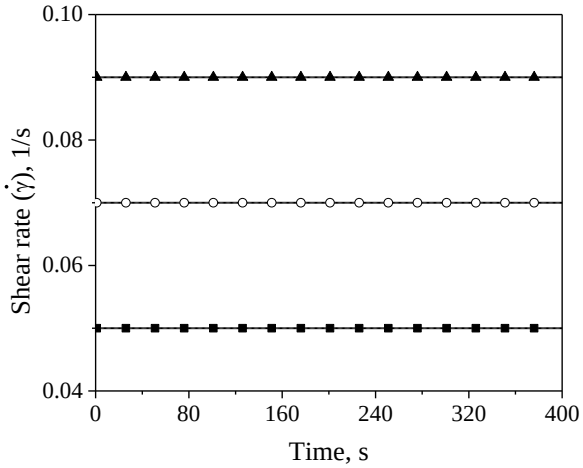

(c) Short-term aged VG20 at 45 °C

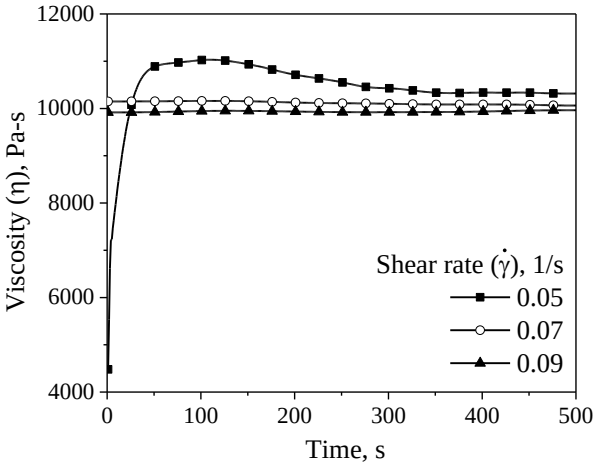

(d) Short-term aged VG20 at 45 °C

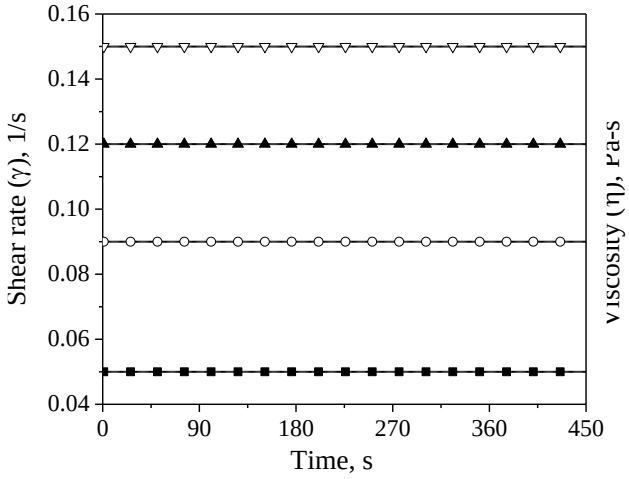

(e) Short-term aged VG20 at 50 °C

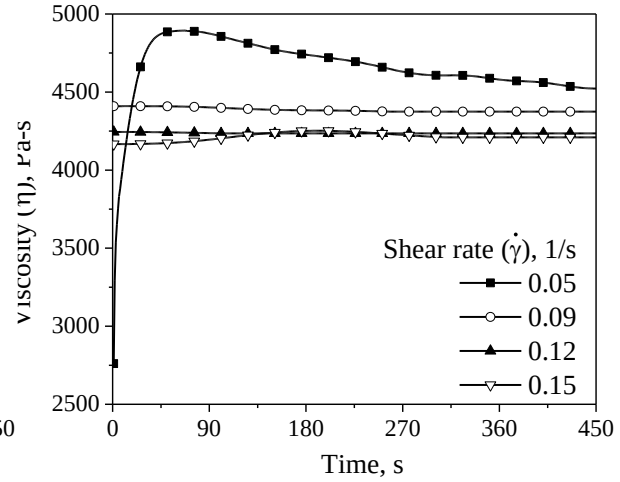

(f) Short-term aged VG20 at 50 °C

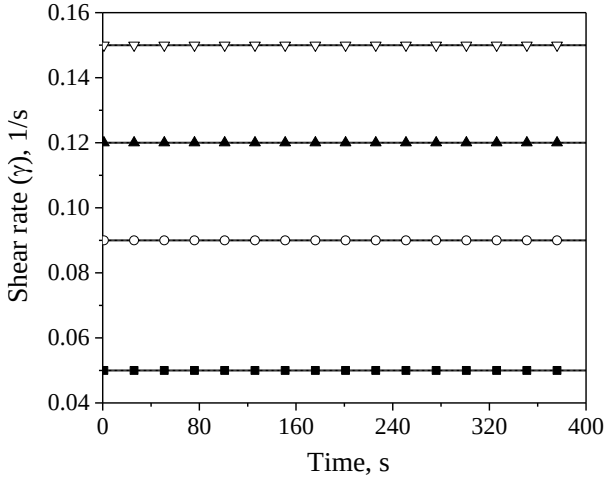

(g) Short-term aged VG20 at 55 °C

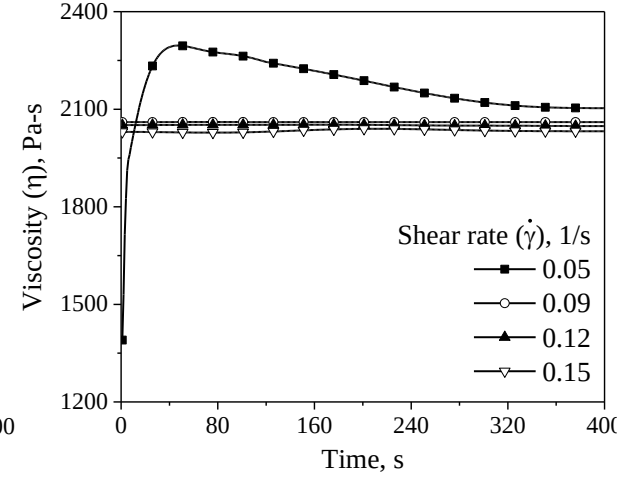

(h) Short-term aged VG20 at 55 °C

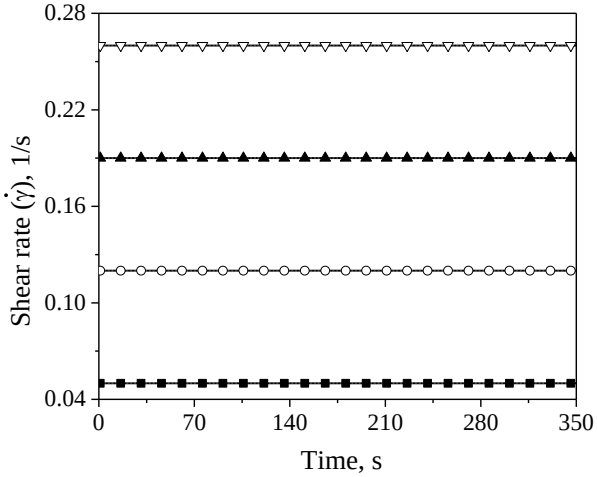

(i) Short-term aged VG20 at 60 °C

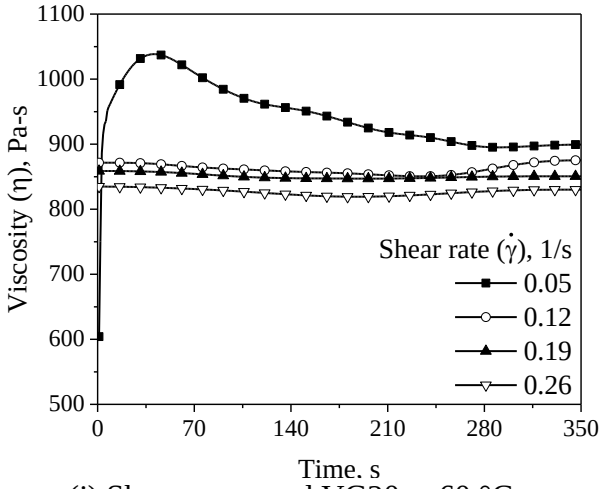

(j) Short-term aged VG20 at 60 °C

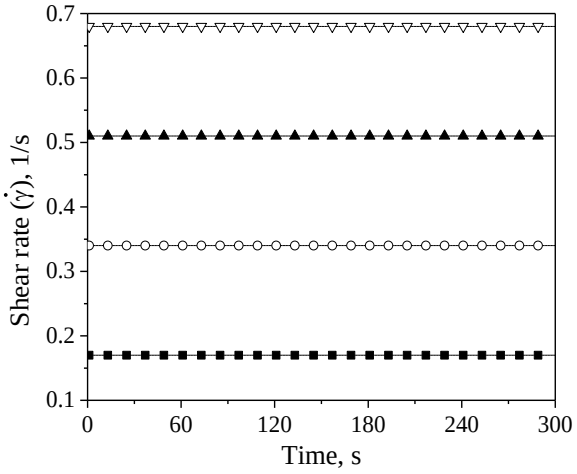

(k) Short-term aged VG20 at 65 °C

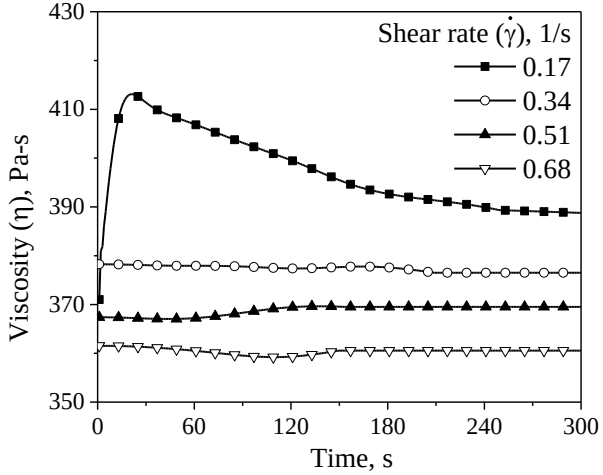

(l) Short-term aged VG20 at 65 °C

Fig. A11 Shear rate and viscosity as a function of time in the first forward sweep of the $SWSSRS_{DSR}$ test for the short-term aged VG20 bitumen

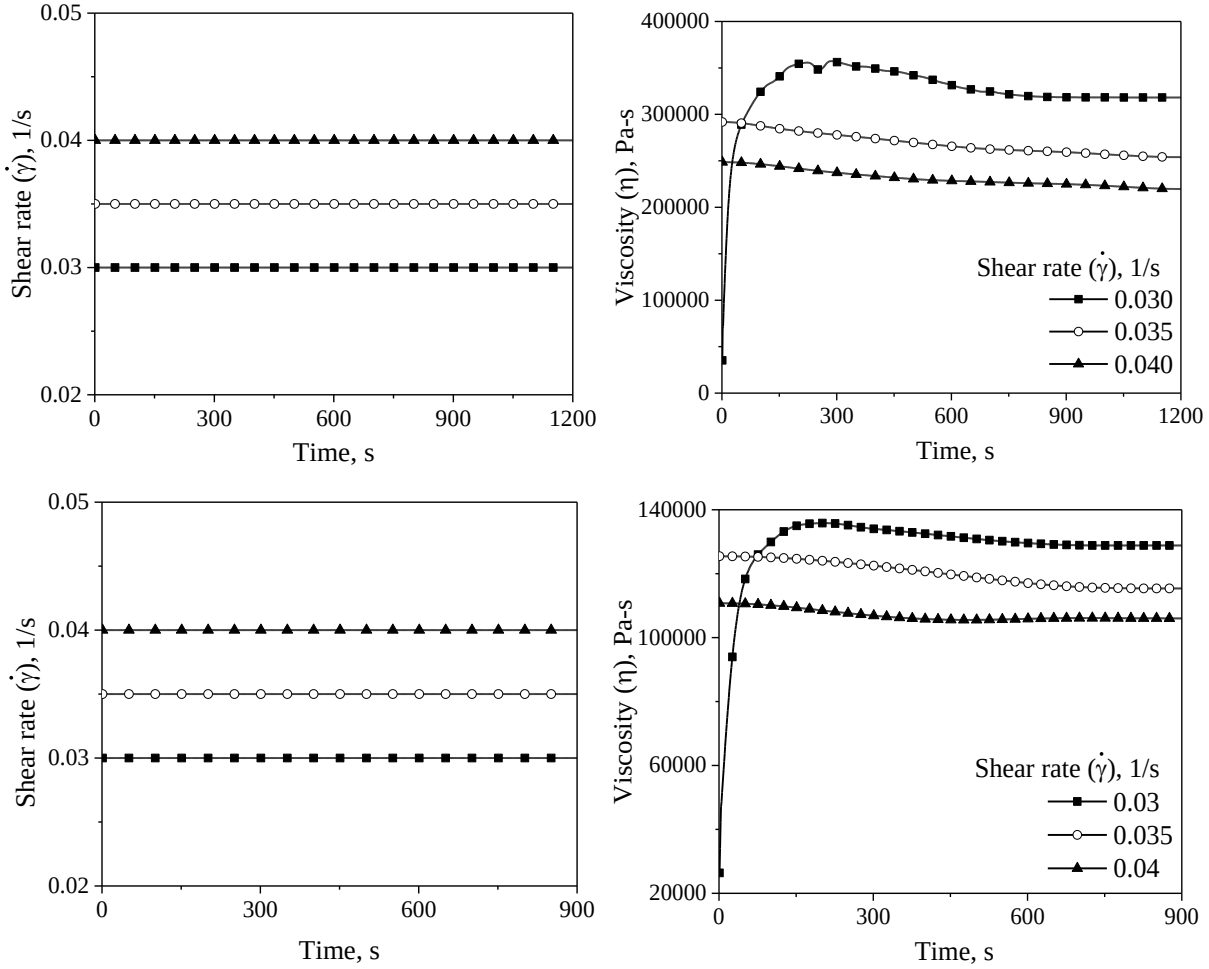
0.05
0.04
0.03
0.02
Shear rate ($\dot{\gamma}$), 1/s
0
300
600
900
1200
Time, s
400000
300000
200000
100000
0
Viscosity (η), Pa-s
Shear rate ($\dot{\gamma}$), 1/s
0.030
0.035
0.040
0.05
0.04
0.03
0.02
Shear rate ($\dot{\gamma}$), 1/s
0
300
600
900
Time, s
140000
100000
60000
20000
Viscosity (η), Pa-s
Shear rate ($\dot{\gamma}$), 1/s
0.03
0.035
0.04
0
300
600
900
Time, s

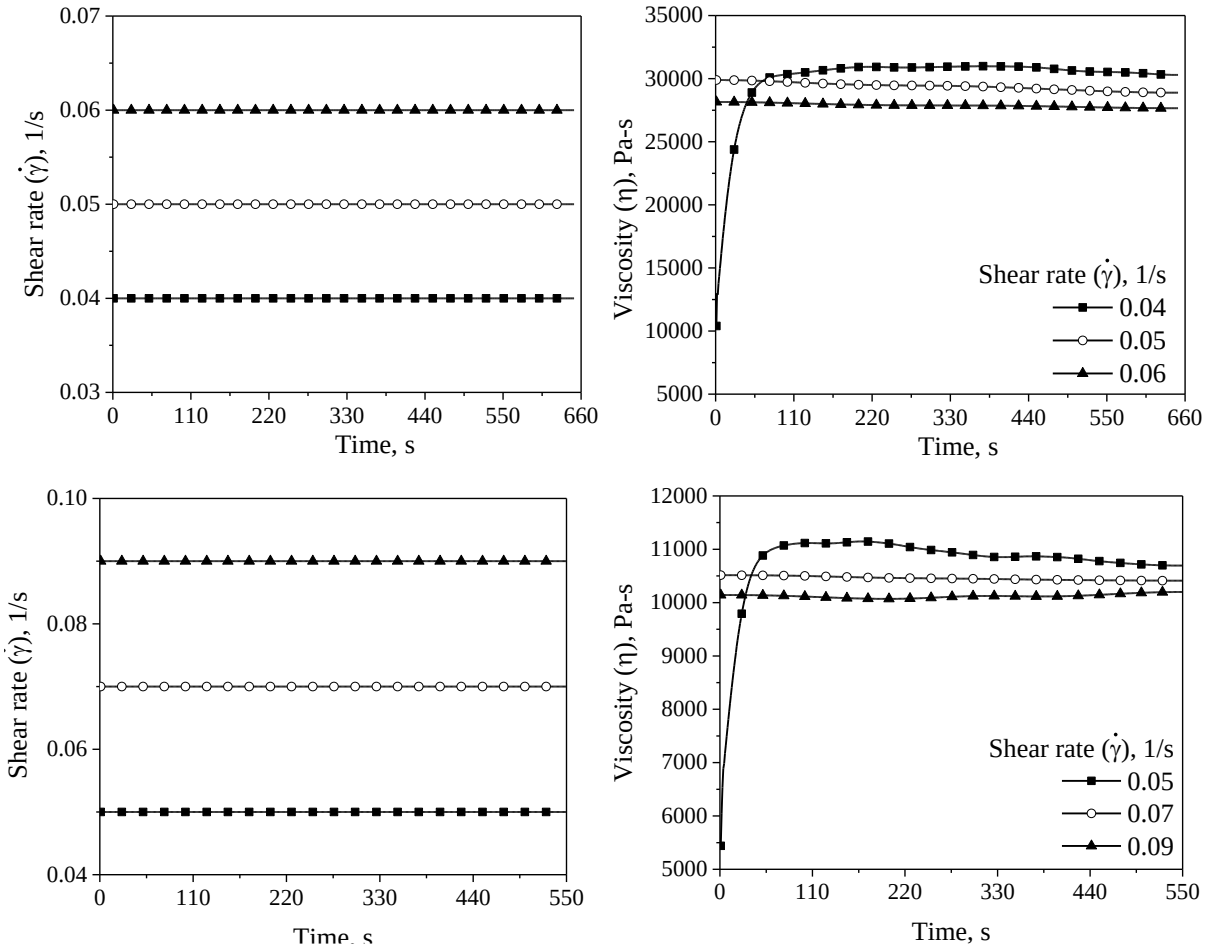
Shear rate ($\dot{\gamma}$), 1/s
Time, s
Viscosity (η), Pa-s
Shear rate ($\dot{\gamma}$), 1/s
0.04
0.05
0.06
Shear rate ($\dot{\gamma}$), 1/s
Time, s
Viscosity (η), Pa-s
Shear rate ($\dot{\gamma}$), 1/s
0.05
0.07
0.09

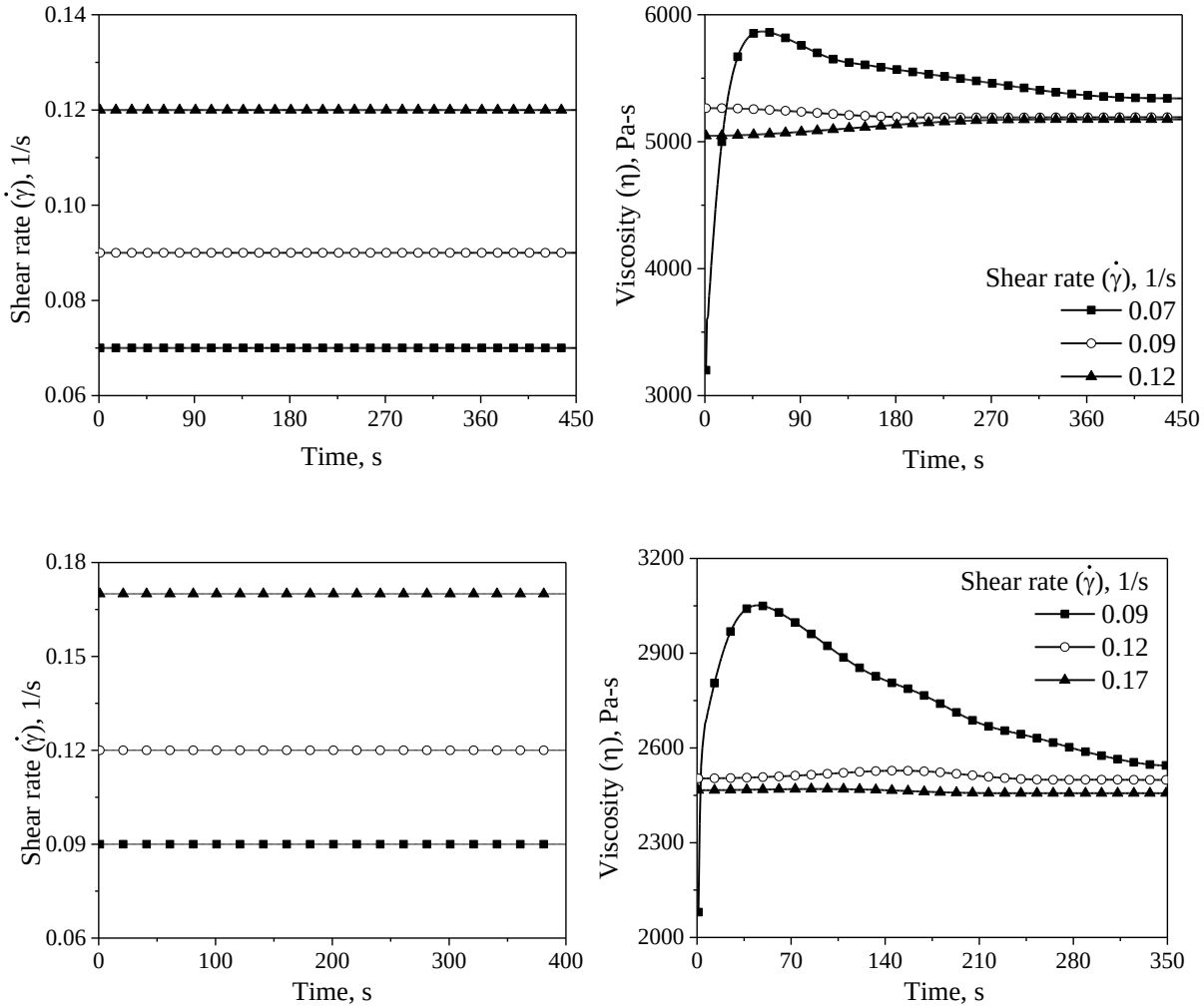

Fig. A12 Shear rate and viscosity as a function of time in the first forward sweep of the $SWSSRS_{DSR}$ test for the long-term aged VG20 bitumen

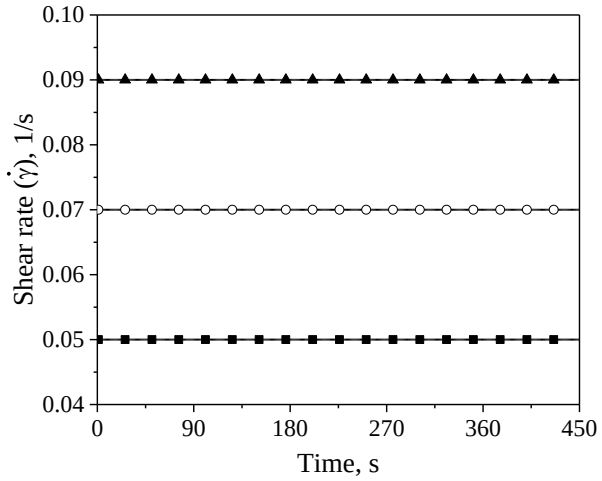

(a) Unaged VG40 at 40 °C

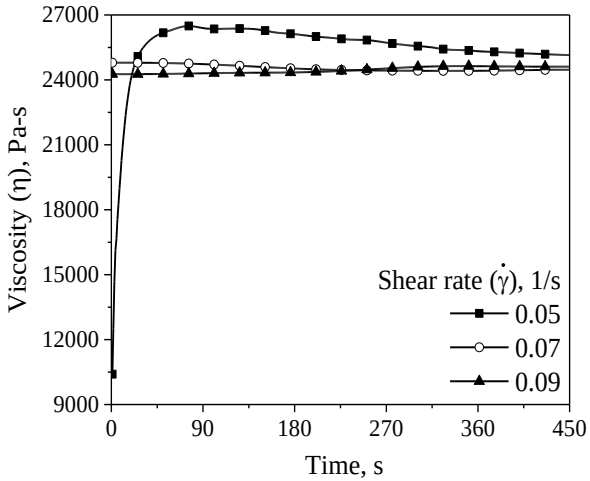

(b) Unaged VG40 at 40 °C

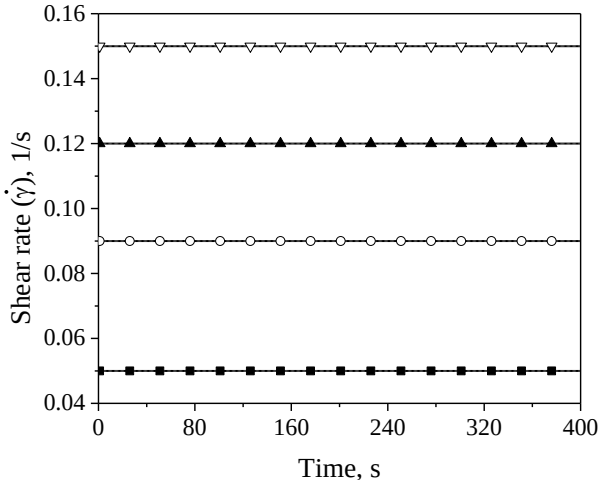

(c) Unaged VG40 at 45 °C

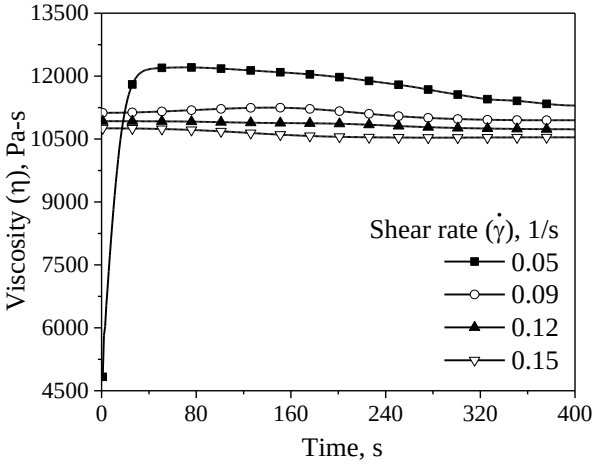

(d) Unaged VG40 at 45 °C

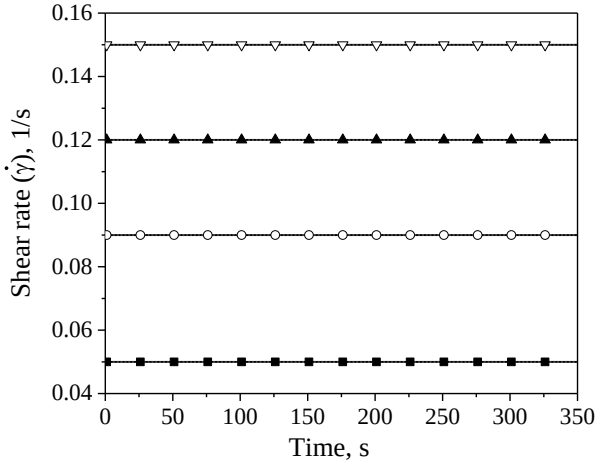

(e) Unaged VG40 at 50 °C

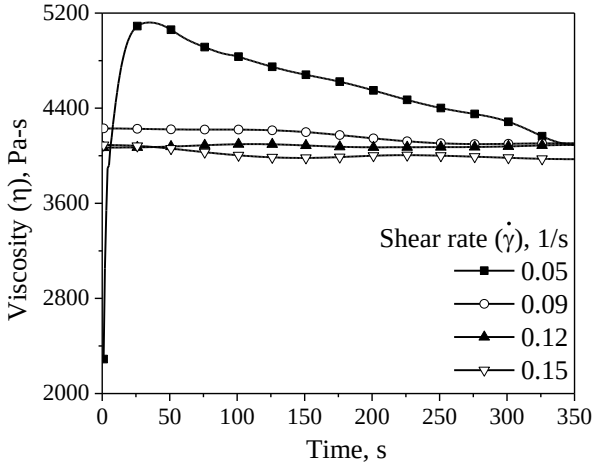

(f) Unaged VG40 at 50 °C

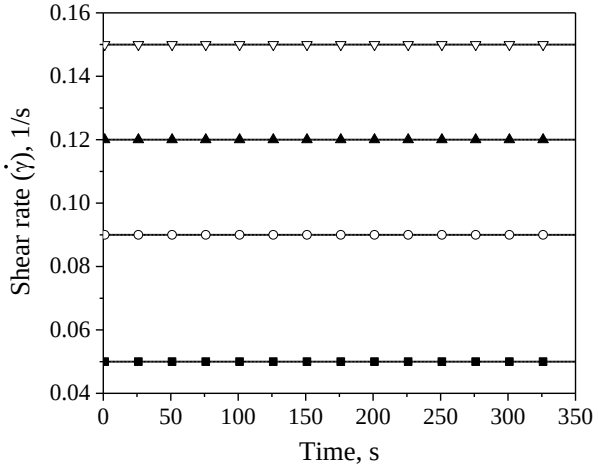

(g) Unaged VG40 at 55 °C

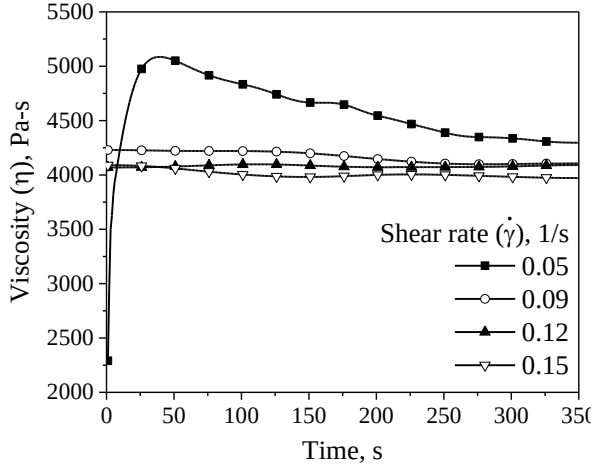

(h) Unaged VG40 at 55 °C

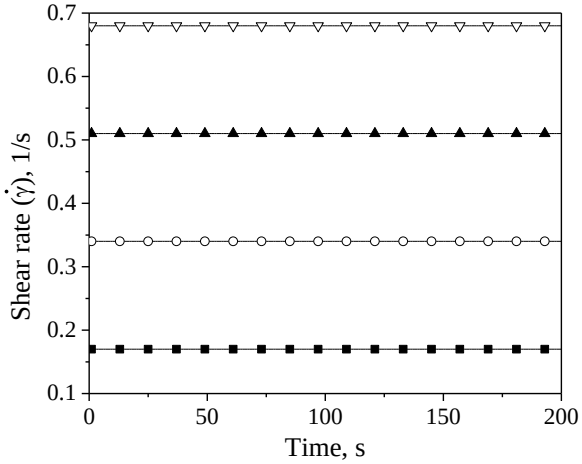

(i) Unaged VG40 at 65 °C

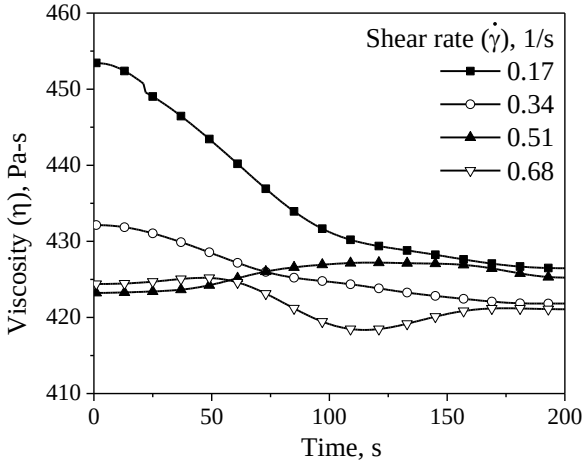

(j) Unaged VG40 at 65 °C

Fig. A13 Shear rate and viscosity as a function of time in the first forward sweep of the $SWSSRS_{DSR}$ test for the unaged VG40 bitumen

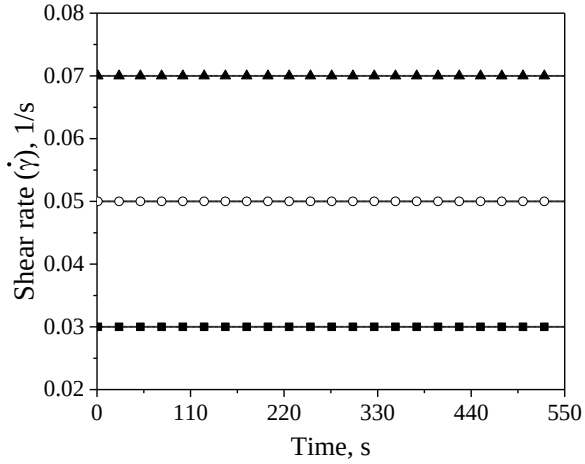

(a) Short-term aged VG40 at 40 °C

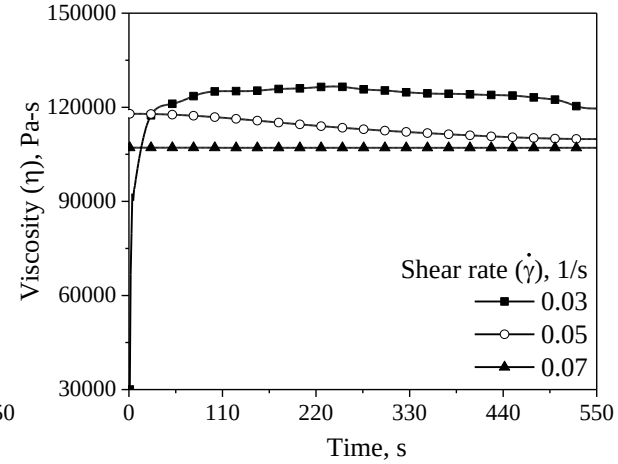

(b) Short-term aged VG40 at 40 °C

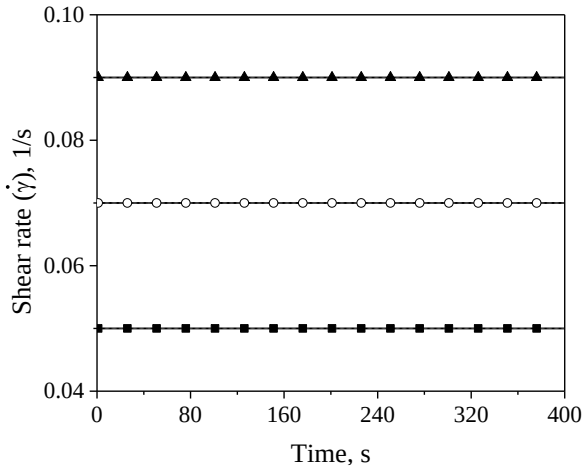

(c) Short-term aged VG40 at 45 °C

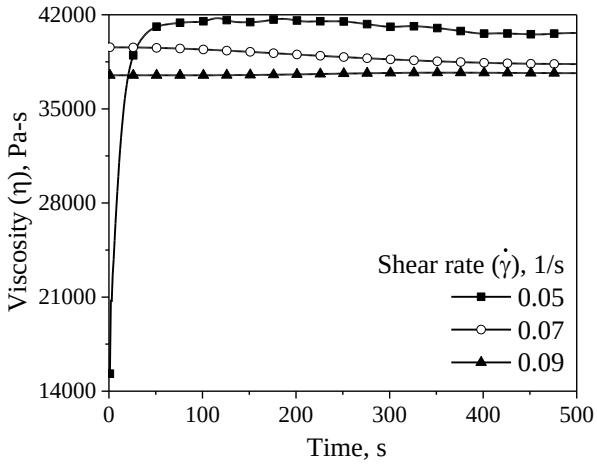

(d) Short-term aged VG40 at 45 °C

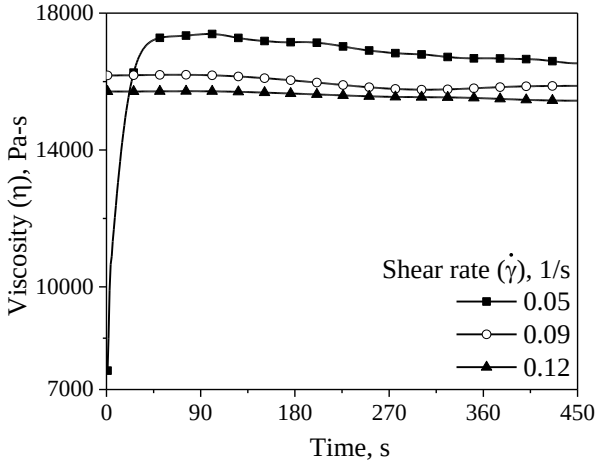

(e) Short-term aged VG40 at 50 °C

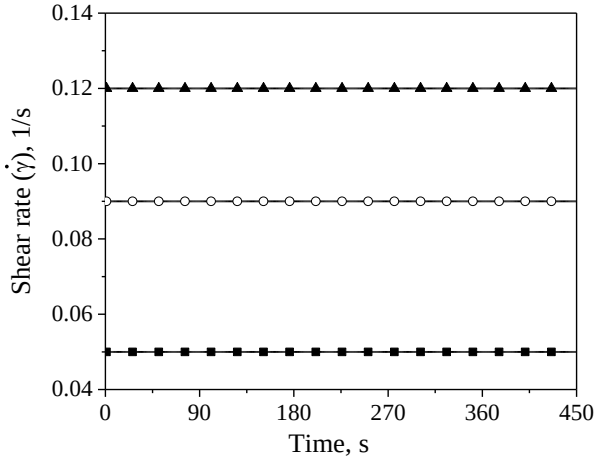

(f) Short-term aged VG40 at 50 °C

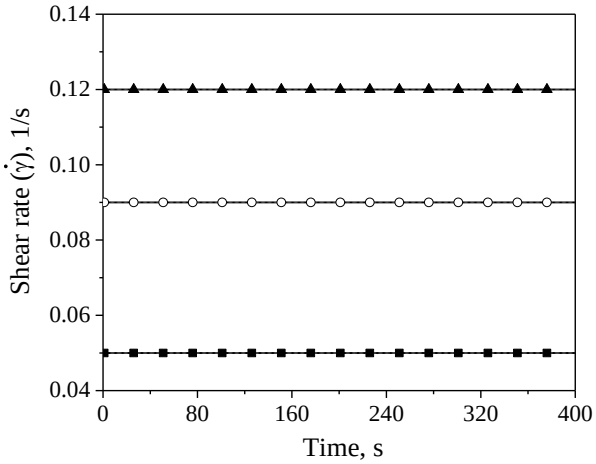

(g) Short-term aged VG40 at 55 °C

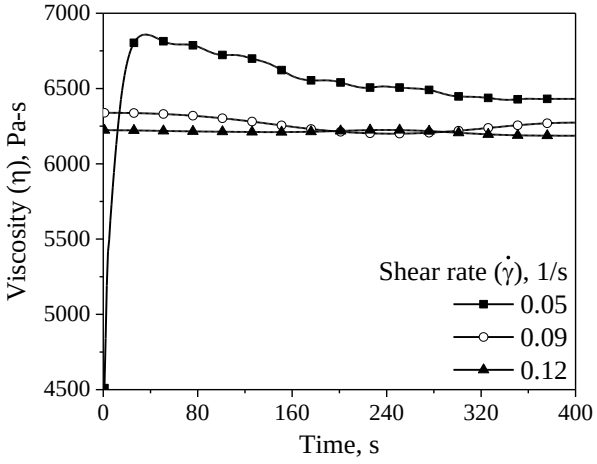

(h) Short-term aged VG40 at 55 °C

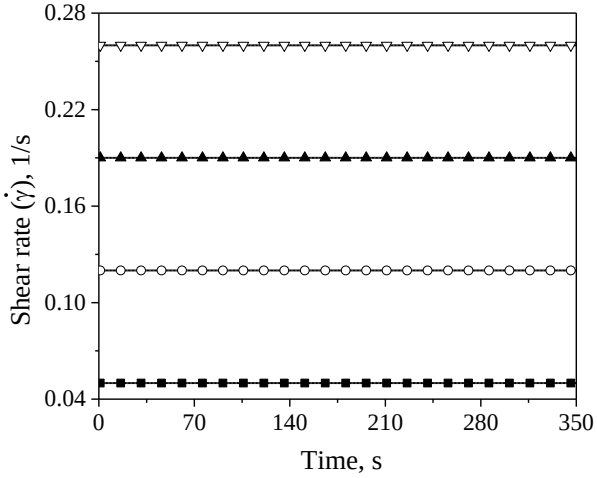

(i) Short-term aged VG40 at 60 °C

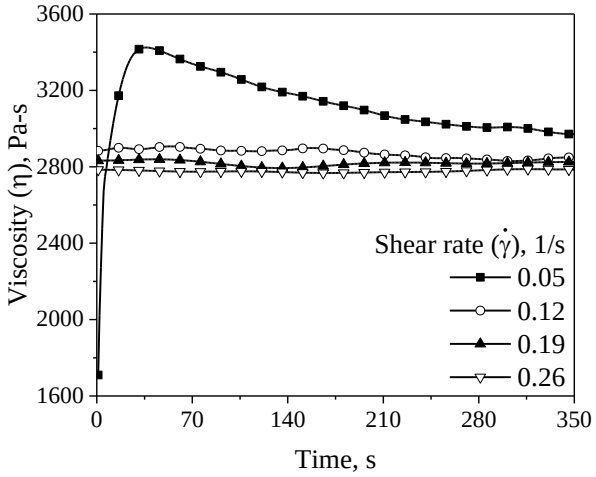

(j) Short-term aged VG40 at 60 °C

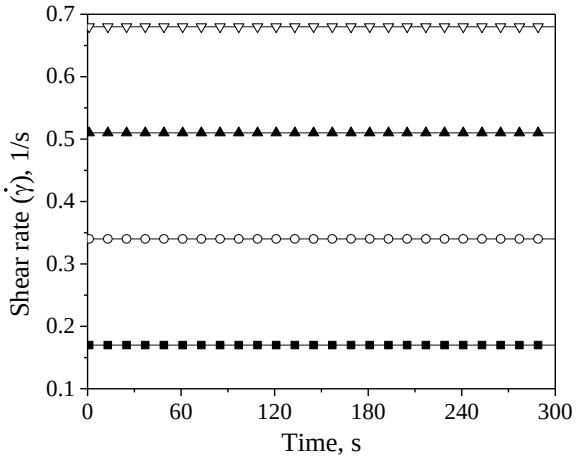

(k) Short-term aged VG40 at 65 °C

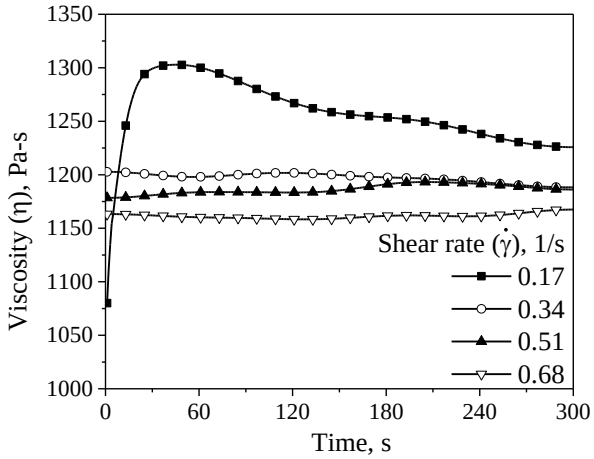

(l) Short-term aged VG40 at 65 °C

Fig. A14 Shear rate and viscosity as a function of time in the first forward sweep of the SWSSRS$_{DSR}$ test for the short-term aged VG40 bitumen

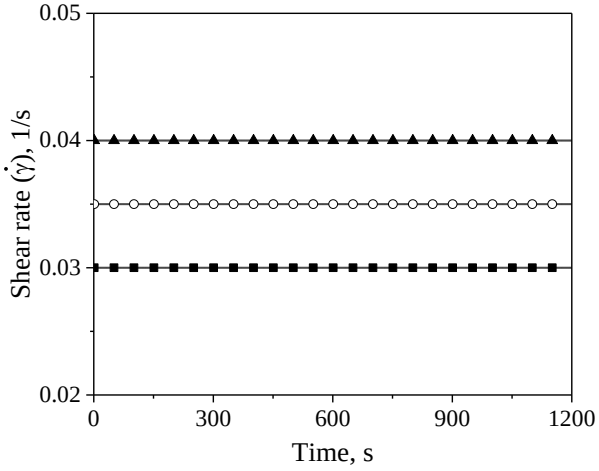

(a) Long-term aged VG40 at 40 °C

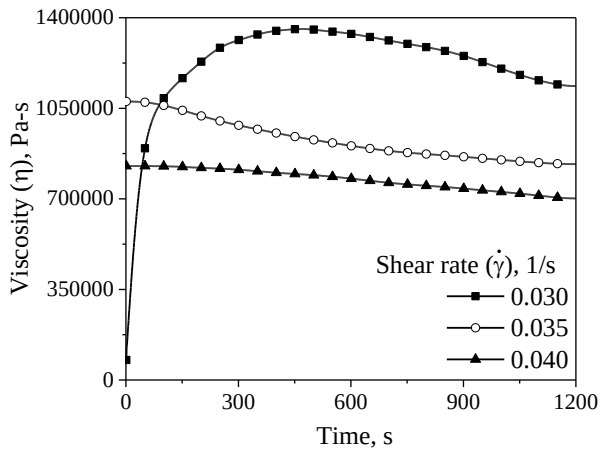

(b) Long-term aged VG40 at 40 °C

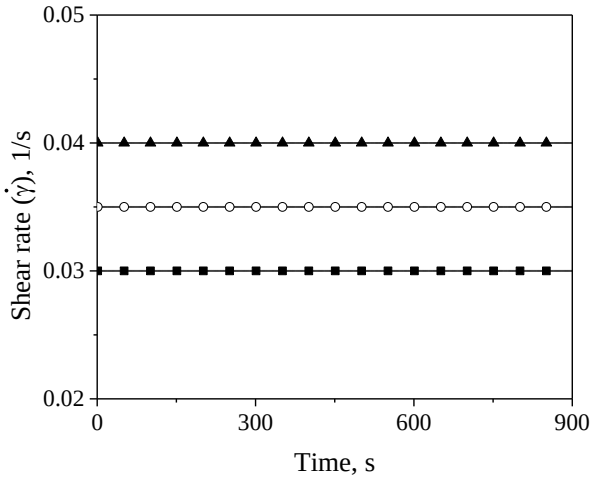

(c) Long-term aged VG40 at 45 °C

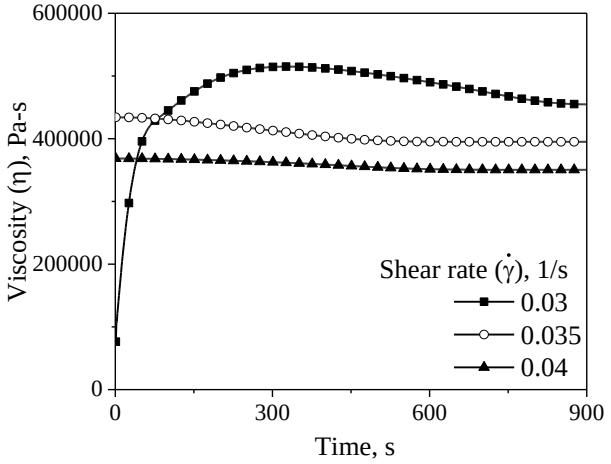

(d) Long-term aged VG40 at 45 °C

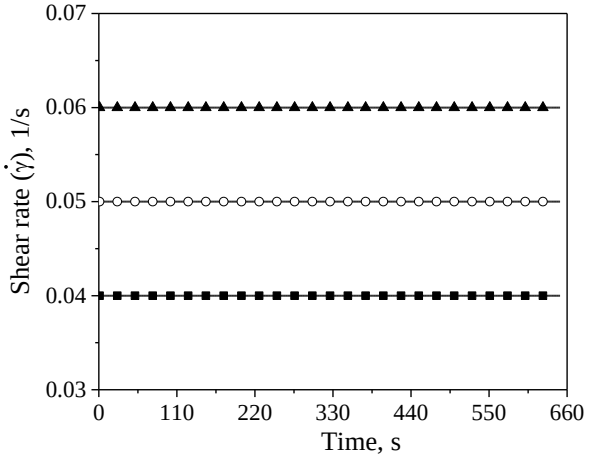

(e) Long-term aged VG40 at 50 °C

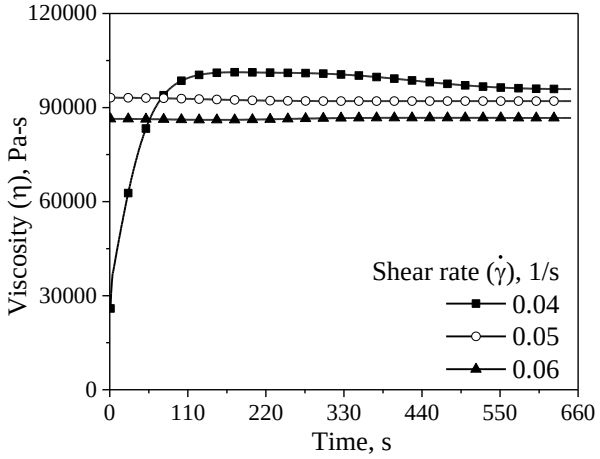

(f) Long-term aged VG40 at 50 °C

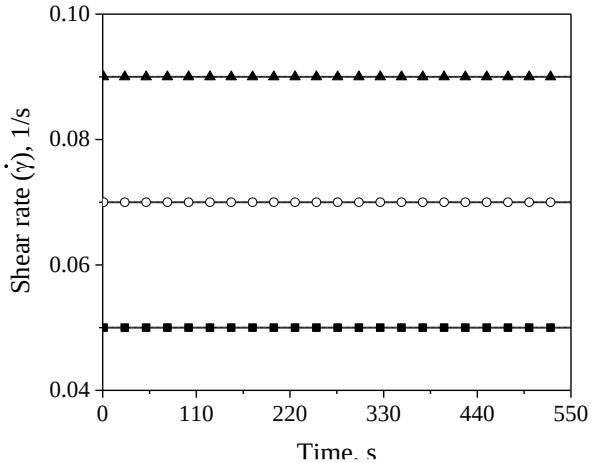

(g) Long-term aged VG40 at 55 °C

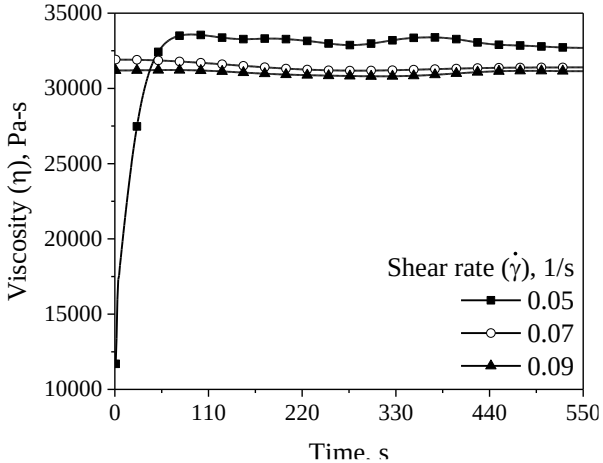

(h) Long-term aged VG40 at 55 °C

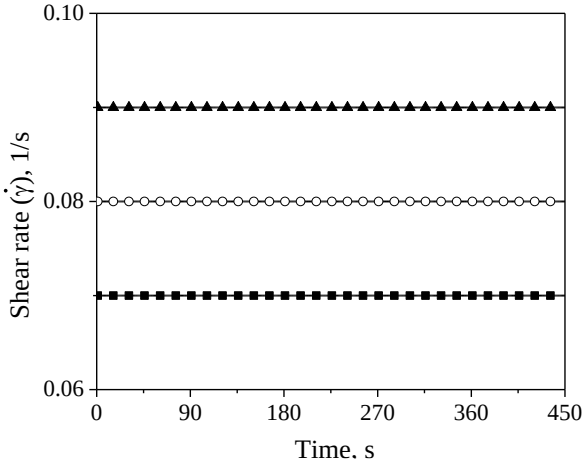

(i) Long-term aged VG40 at 60 °C

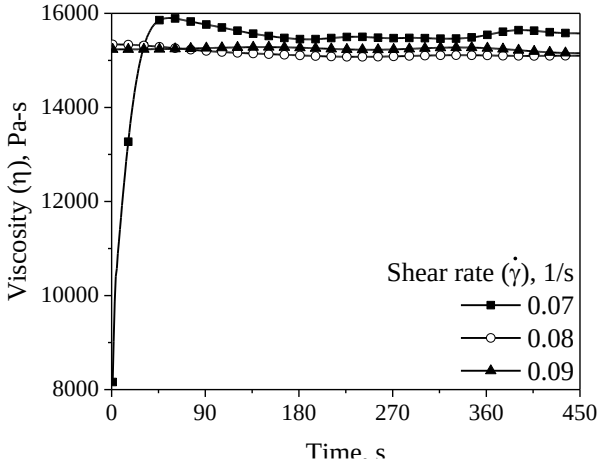

(j) Long-term aged VG40 at 60 °C

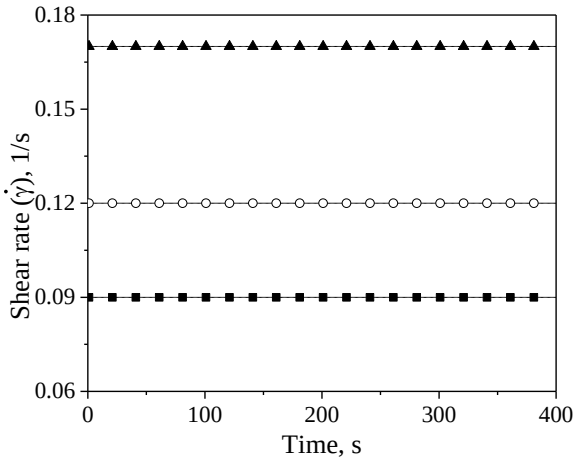

(k) Long-term aged VG40 at 65 °C

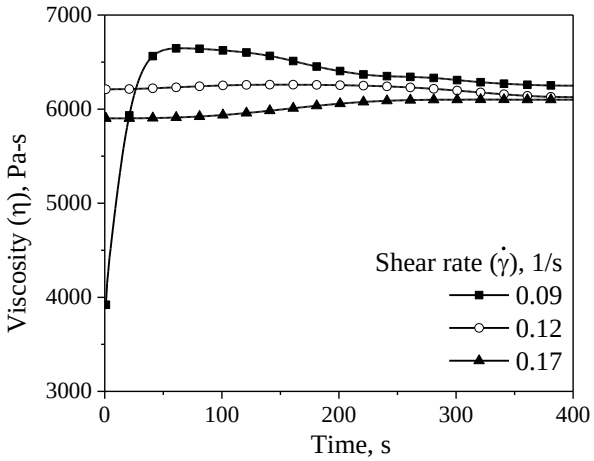

(l) Long-term aged VG40 at 65 °C

Fig. A15 Shear rate and viscosity as a function of time in the first forward sweep of the $SWSSRS_{DSR}$ test for the long-term aged VG40 bitumen

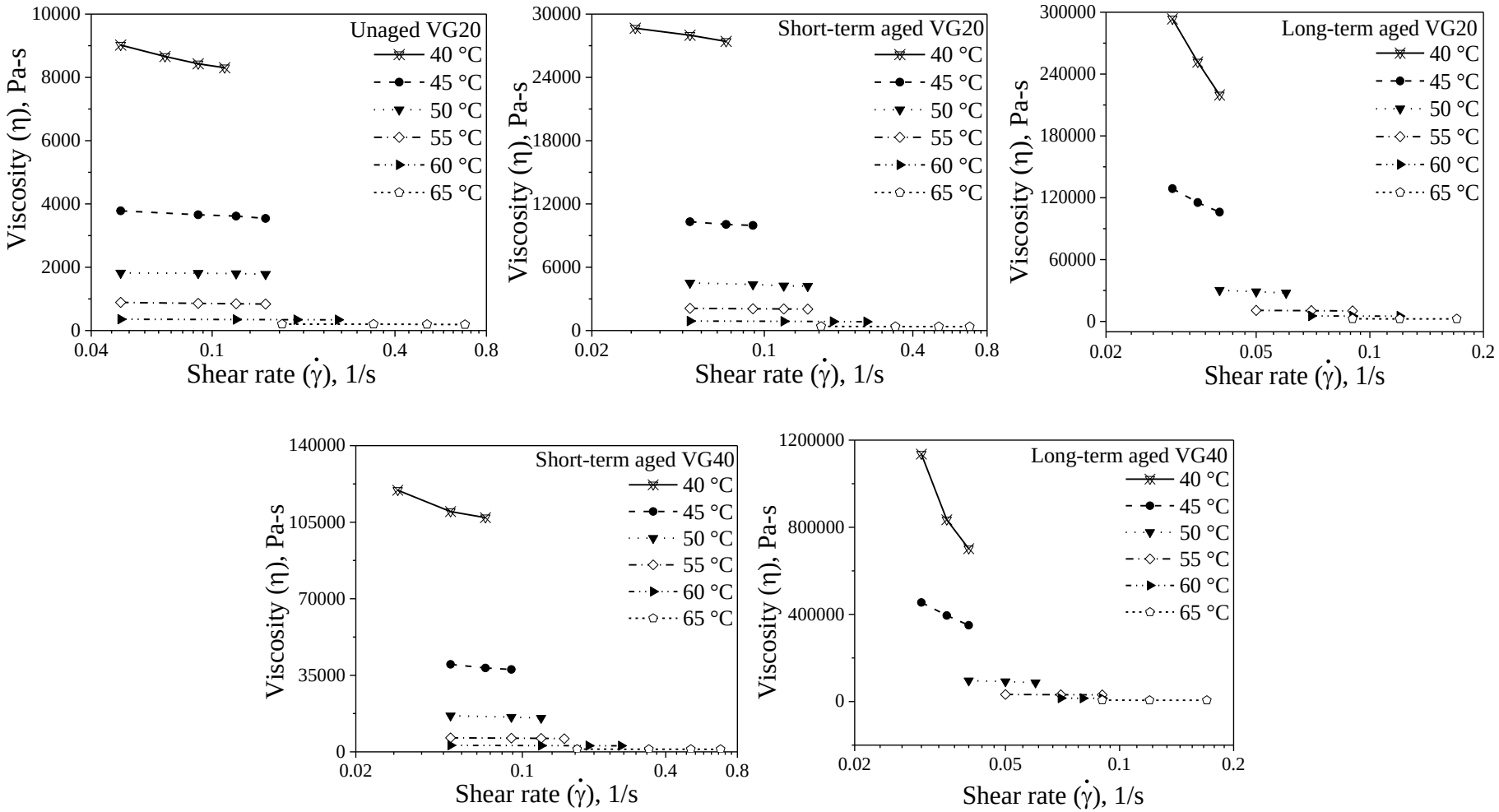

Fig. A 16 Viscosity at 't_s' as a function of shear rate in the first forward sweep of $SWSSRS_{DSR}$ test for the VG20 and VG40 bitumen

APPENDIX B

B.1 Performance Grade pass/fail Temperatures for the VG20 and VG40 Bitumen

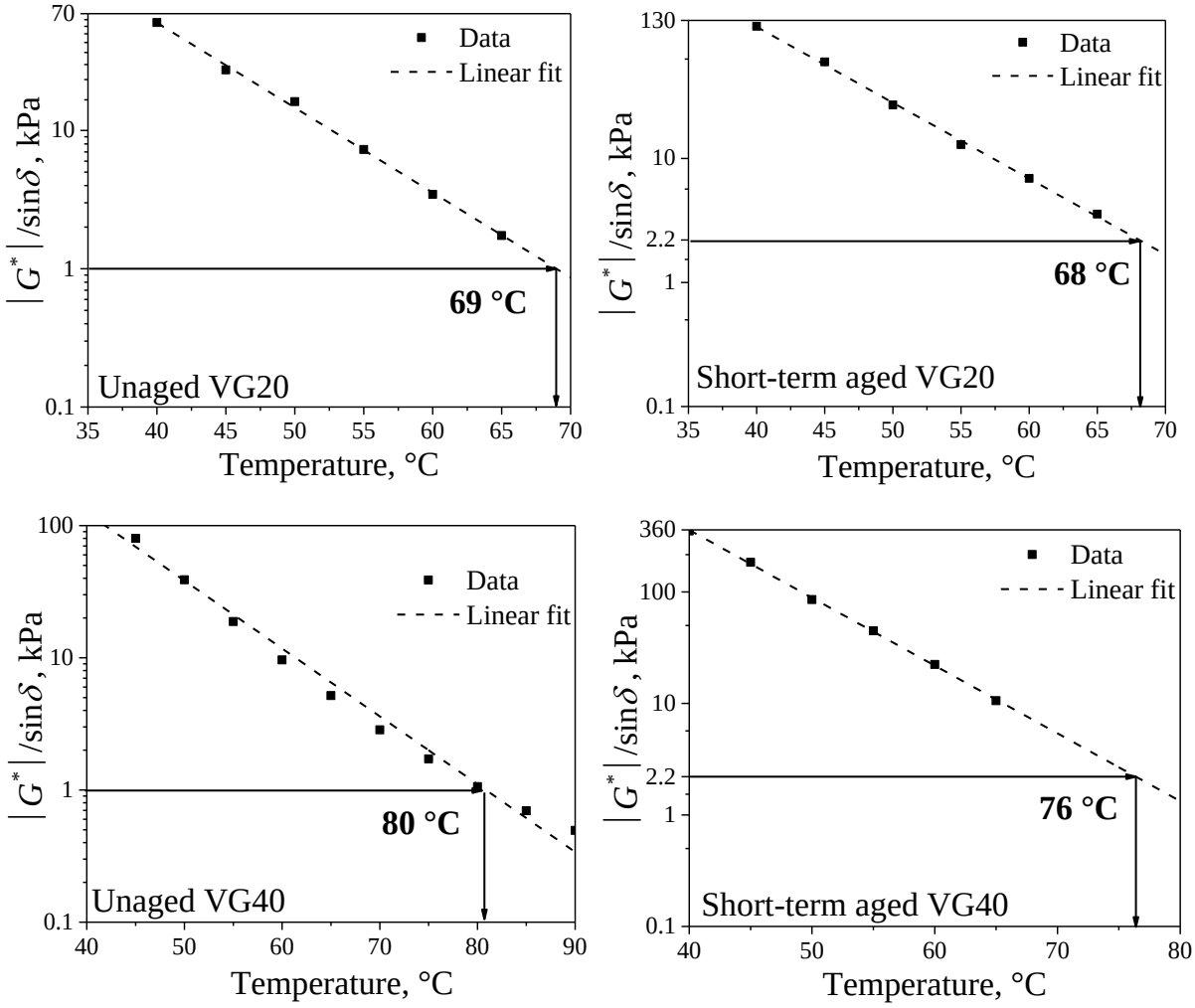

Fig. B1 Variation of $|G^*|/\sin\delta$ with temperature

Table B1(a) Statistical parameters for the LTA BC-2 prepared with VG20 bitumen

Passes	40 °C						45 °C						50 °C					
	Mean	**Median**	**Mode**	**Standard Deviation**	**Skewness**	**Kurtosis**	**Mean**	**Median**	**Mode**	**Standard Deviation**	**Skewness**	**Kurtosis**	**Mean**	**Median**	**Mode**	**Standard Deviation**	**Skewness**	**Kurtosis**
500	0.40	0.41	0.08	0.01	-0.08	**1.67**	0.61	0.62	0.10	0.01	-0.45	**2.63**	0.98	0.98	0.12	0.01	-0.34	**1.74**
1000	0.56	0.57	0.10	0.01	-0.06	**1.56**	0.80	0.82	0.12	0.01	-0.46	**2.56**	1.34	1.37	0.12	0.02	-0.68	**2.15**
2000	0.80	0.81	0.12	0.01	-0.09	**1.46**	1.06	1.08	0.15	0.02	-0.22	**2.65**	1.89	1.93	0.15	0.02	-0.38	**2.30**
4000	1.16	1.18	0.15	0.02	-0.07	**1.49**	1.43	1.44	0.21	0.05	0.25	**2.94**	2.71	2.71	0.21	0.04	0.46	**2.75**
6000	1.44	1.46	0.17	0.03	-0.08	**1.60**	1.72	1.72	0.27	0.07	0.54	*3.20*	3.32	3.30	0.24	0.06	0.62	**2.91**
8000	1.67	1.67	0.19	0.04	-0.09	**1.77**	1.96	1.95	0.31	0.10	0.75	*3.44*	3.79	3.79	0.25	0.06	0.54	**2.95**
10000	1.87	1.87	0.20	0.04	-0.11	**1.88**	2.17	2.14	0.34	0.12	0.86	*3.59*	4.16	4.17	0.25	0.06	0.29	**2.91**
12000	2.04	2.04	0.22	0.05	-0.11	**1.99**	2.35	2.32	0.37	0.14	0.92	*3.67*	4.45	4.50	0.25	0.06	-0.07	**2.78**
14000	2.19	2.19	0.23	0.05	-0.11	**2.09**	2.52	2.48	0.40	0.16	0.99	*3.76*	4.70	4.74	0.26	0.07	-0.35	**2.69**
16000	2.33	2.32	0.24	0.06	-0.10	**2.14**	2.67	2.62	0.41	0.17	1.02	*3.80*	4.90	4.97	0.27	0.07	-0.57	**2.62**
18000	2.44	2.43	0.25	0.06	-0.08	**2.16**	2.81	2.75	0.43	0.18	1.04	*3.85*	5.06	5.14	0.28	0.08	-0.69	**2.60**
20000	2.54	2.53	0.25	0.06	-0.07	**2.19**	2.93	2.87	0.44	0.19	1.05	*3.86*	5.21	5.29	0.30	0.09	-0.73	**2.53**
30000	2.92	2.89	0.28	0.08	0.03	**2.24**	3.44	3.36	0.45	0.21	1.07	*3.95*	5.67	5.77	0.37	0.14	-0.63	**2.40**
40000	3.17	3.16	0.30	0.09	0.14	**2.20**	3.80	3.71	0.44	0.19	1.01	*3.93*	5.93	6.05	0.43	0.18	-0.47	**2.38**
50000	3.35	3.33	0.32	0.10	0.22	**2.14**	4.09	3.99	0.41	0.17	0.95	*3.91*	6.12	6.21	0.46	0.21	-0.34	**2.40**
60000	3.50	3.46	0.33	0.11	0.27	**2.08**	4.31	4.23	0.39	0.15	0.83	*3.79*	6.26	6.34	0.48	0.23	-0.21	**2.43**
70000	3.62	3.58	0.35	0.12	0.30	**2.03**	4.51	4.45	0.36	0.13	0.73	*3.65*	6.39	6.49	0.50	0.25	-0.10	**2.46**
80000	3.73	3.68	0.36	0.13	0.32	**1.98**	4.67	4.63	0.34	0.11	0.59	*3.54*	6.50	6.58	0.52	0.27	0.01	**2.51**
90000	3.84	3.77	0.37	0.14	0.35	**1.95**	4.82	4.79	0.31	0.10	0.45	*3.38*	6.60	6.66	0.53	0.28	0.09	**2.54**
100000	3.93	3.86	0.38	0.15	0.35	**1.92**	4.96	4.94	0.30	0.09	0.30	*3.27*	6.69	6.73	0.55	0.30	0.16	**2.56**
110000	4.02	3.94	0.39	0.16	0.37	**1.90**	5.08	5.08	0.28	0.08	0.14	*3.17*	6.78	6.79	0.56	0.32	0.25	**2.59**
120000	4.10	4.02	0.41	0.16	0.37	**1.88**	5.19	5.21	0.26	0.07	-0.03	*3.04*	6.86	6.85	0.58	0.34	0.30	**2.60**
130000	4.18	4.09	0.41	0.17	0.39	**1.87**	5.30	5.33	0.25	0.06	-0.18	**2.98**	6.94	6.91	0.59	0.35	0.35	**2.61**
140000	4.26	4.16	0.42	0.18	0.39	**1.84**	5.40	5.43	0.24	0.06	-0.35	**2.97**	7.01	6.96	0.61	0.37	0.40	**2.64**
150000	4.33	4.23	0.43	0.19	0.39	**1.83**	5.49	5.53	0.23	0.05	-0.46	**2.99**	7.08	7.04	0.62	0.39	0.46	**2.65**
160000	4.40	4.29	0.44	0.19	0.39	**1.82**	5.59	5.63	0.22	0.05	-0.62	*3.01*	7.14	7.11	0.64	0.40	0.49	**2.66**
170000	4.47	4.35	0.45	0.20	0.40	**1.81**	5.67	5.72	0.22	0.05	-0.69	*3.03*	7.20	7.15	0.65	0.42	0.53	**2.67**
180000	4.53	4.41	0.46	0.21	0.41	**1.81**	5.76	5.81	0.21	0.04	-0.75	*3.06*	7.27	7.20	0.66	0.44	0.56	**2.68**
190000	4.59	4.47	0.46	0.21	0.41	**1.80**	5.84	5.88	0.21	0.04	-0.81	*3.07*	7.32	7.24	0.67	0.45	0.59	**2.69**
200000	4.65	4.52	0.47	0.22	0.42	**1.79**	5.91	5.96	0.20	0.04	-0.79	*3.06*	7.38	7.28	0.69	0.47	0.62	**2.70**

Table B1(b) Statistical parameters for the LTA BC-2 prepared with VG20 bitumen

Passes	55 °C						60 °C						65 °C					
	Mean	**Median**	**Mode**	**Standard Deviation**	**Skewness**	**Kurtosis**	**Mean**	**Median**	**Mode**	**Standard Deviation**	**Skewness**	**Kurtosis**	**Mean**	**Median**	**Mode**	**Standard Deviation**	**Skewness**	**Kurtosis**
500	1.29	1.39	0.24	0.06	-0.84	**2.39**	1.70	1.64	0.22	0.05	0.84	**2.48**	1.97	1.93	0.29	0.09	-0.05	**1.37**
1000	1.73	1.86	0.28	0.08	-0.81	**2.40**	2.24	2.16	0.26	0.07	0.87	**2.54**	2.78	2.83	0.33	0.11	-0.12	**1.73**
2000	2.40	2.44	0.34	0.12	-0.58	**2.23**	3.00	2.91	0.30	0.09	0.87	**2.56**	3.92	4.00	0.42	0.18	0.58	*3.18*
4000	3.38	3.34	0.44	0.19	-0.29	**1.92**	4.10	4.00	0.34	0.12	0.72	**2.40**	5.49	5.35	0.63	0.40	1.26	*3.97*
6000	4.10	4.07	0.49	0.24	-0.17	**1.74**	4.92	4.86	0.38	0.15	0.46	**2.07**	6.67	6.35	0.81	0.65	1.34	*3.76*
8000	4.66	4.60	0.52	0.27	-0.12	**1.66**	5.57	5.52	0.42	0.18	0.21	**1.76**	7.65	7.20	0.96	0.92	1.31	*3.47*
10000	5.11	5.01	0.53	0.28	-0.09	**1.62**	6.10	6.11	0.47	0.22	0.05	**1.56**	8.51	7.92	1.08	1.17	1.25	*3.21*
12000	5.46	5.34	0.53	0.28	-0.08	**1.59**	6.54	6.58	0.51	0.26	-0.02	**1.48**	9.28	8.67	1.18	1.40	1.19	*3.01*
14000	5.75	5.60	0.52	0.27	-0.08	**1.57**	6.91	6.91	0.56	0.31	-0.02	**1.50**	9.98	9.29	1.27	1.61	1.14	**2.83**
16000	5.99	5.89	0.51	0.26	-0.09	**1.57**	7.23	7.20	0.60	0.36	0.02	**1.56**	10.64	9.87	1.34	1.80	1.08	**2.68**
18000	6.18	6.14	0.50	0.25	-0.10	**1.57**	7.50	7.50	0.65	0.42	0.07	**1.64**	11.25	10.48	1.40	1.96	1.03	**2.55**
20000	6.35	6.36	0.49	0.24	-0.12	**1.57**	7.74	7.76	0.69	0.47	0.14	**1.74**	11.84	11.08	1.45	2.10	0.98	**2.43**
30000	6.91	6.94	0.44	0.19	-0.24	**1.66**	8.60	8.61	0.86	0.74	0.37	**2.08**	14.43	13.55	1.56	2.43	0.78	**2.00**
40000	7.25	7.28	0.42	0.18	-0.33	**1.77**	9.16	9.10	0.96	0.93	0.48	**2.25**	16.73	15.86	1.51	2.27	0.61	**1.70**
50000	7.50	7.52	0.41	0.17	-0.36	**1.80**	9.59	9.55	1.03	1.05	0.53	**2.33**						
60000	7.70	7.73	0.41	0.17	-0.37	**1.79**	9.94	9.91	1.07	1.14	0.55	**2.36**						
70000	7.87	7.90	0.41	0.17	-0.35	**1.75**	10.24	10.22	1.09	1.19	0.56	**2.38**						
80000	8.03	8.05	0.41	0.17	-0.34	**1.72**	10.51	10.50	1.11	1.23	0.55	**2.38**						
90000	8.17	8.19	0.41	0.17	-0.33	**1.69**	10.76	10.76	1.13	1.27	0.55	**2.37**						
100000	8.30	8.31	0.41	0.17	-0.32	**1.66**	10.99	10.99	1.14	1.30	0.55	**2.36**						
110000	8.42	8.43	0.41	0.17	-0.31	**1.65**	11.20	11.21	1.15	1.33	0.54	**2.36**						
120000	8.53	8.54	0.41	0.17	-0.32	**1.64**	11.40	11.42	1.17	1.36	0.54	**2.36**						
130000	8.64	8.65	0.41	0.17	-0.32	**1.64**	11.59	11.61	1.18	1.38	0.53	**2.35**						
140000	8.74	8.75	0.41	0.17	-0.32	**1.63**	11.77	11.79	1.19	1.41	0.53	**2.34**						
150000	8.84	8.86	0.41	0.17	-0.31	**1.63**	11.93	11.97	1.20	1.43	0.53	**2.33**						
160000	8.93	8.96	0.41	0.17	-0.31	**1.65**	12.10	12.12	1.21	1.46	0.52	**2.33**						
170000	9.02	9.06	0.41	0.17	-0.32	**1.65**	12.25	12.27	1.22	1.48	0.52	**2.32**						
180000	9.10	9.16	0.41	0.17	-0.33	**1.66**	12.40	12.42	1.23	1.50	0.52	**2.32**						
190000	9.18	9.24	0.41	0.17	-0.34	**1.70**	12.54	12.55	1.23	1.52	0.52	**2.32**						
200000	9.26	9.32	0.41	0.17	-0.34	**1.72**	12.68	12.69	1.24	1.54	0.51	**2.31**						

Table B2(a) Statistical parameters for the STA BC-2 prepared with VG40 bitumen

Passes	40 °C						45 °C						50 °C					
	Mean	**Median**	**Mode**	**Standard Deviation**	**Skewness**	**Kurtosis**	**Mean**	**Median**	**Mode**	**Standard Deviation**	**Skewness**	**Kurtosis**	**Mean**	**Median**	**Mode**	**Standard Deviation**	**Skewness**	**Kurtosis**
500	0.48	0.49	0.07	0.00	-1.39	*6.48*	0.55	0.57	0.12	0.01	-1.26	3.76	0.75	0.76	0.12	0.01	-0.21	**2.02**
1000	0.63	0.63	0.08	0.01	-1.48	*6.89*	0.76	0.79	0.14	0.02	-1.21	3.62	1.13	1.11	0.15	0.02	0.21	**1.88**
2000	0.83	0.83	0.10	0.01	-1.46	*6.51*	1.07	1.12	0.16	0.03	-1.11	3.29	1.73	1.67	0.19	0.04	0.61	**1.90**
4000	1.10	1.10	0.12	0.01	-1.06	*4.84*	1.53	1.61	0.18	0.03	-0.88	**2.51**	2.62	2.53	0.25	0.06	0.65	**1.90**
6000	1.32	1.30	0.15	0.02	-0.56	*3.56*	1.90	2.02	0.20	0.04	-0.68	**1.95**	3.28	3.16	0.28	0.08	0.56	**1.87**
8000	1.49	1.47	0.17	0.03	-0.22	**2.82**	2.22	2.35	0.23	0.05	-0.51	**1.71**	3.77	3.67	0.29	0.08	0.46	**1.90**
10000	1.65	1.61	0.20	0.04	0.03	**2.42**	2.48	2.60	0.25	0.06	-0.35	**1.69**	4.15	4.07	0.28	0.08	0.32	**1.96**
12000	1.79	1.73	0.22	0.05	0.23	**2.20**	2.71	2.82	0.27	0.07	-0.21	**1.77**	4.45	4.41	0.27	0.07	0.08	**2.01**
14000	1.92	1.83	0.25	0.06	0.36	**2.08**	2.91	3.01	0.29	0.09	-0.09	**1.89**	4.69	4.69	0.27	0.07	-0.18	**2.02**
16000	2.04	1.92	0.28	0.08	0.46	**2.02**	3.09	3.18	0.31	0.10	0.03	**2.02**	4.89	4.93	0.27	0.07	-0.40	**1.99**
18000	2.15	2.00	0.30	0.09	0.53	**1.98**	3.25	3.32	0.33	0.11	0.13	**2.16**	5.05	5.13	0.27	0.07	-0.50	**1.94**
20000	2.25	2.09	0.33	0.11	0.57	**1.96**	3.39	3.45	0.35	0.12	0.20	**2.26**	5.19	5.31	0.28	0.08	-0.50	**1.94**
30000	2.69	2.47	0.44	0.19	0.66	**1.93**	3.91	3.96	0.43	0.18	0.48	**2.67**	5.65	5.73	0.36	0.13	0.04	**2.22**
40000	3.03	2.78	0.52	0.27	0.68	**1.93**	4.24	4.28	0.48	0.23	0.61	**2.83**	5.94	6.01	0.42	0.17	0.37	**2.46**
50000	3.31	3.03	0.59	0.35	0.68	**1.92**	4.47	4.50	0.51	0.26	0.67	**2.92**	6.17	6.21	0.46	0.21	0.51	**2.54**
60000	3.55	3.25	0.64	0.41	0.66	**1.91**	4.65	4.67	0.53	0.28	0.71	**2.97**	6.36	6.38	0.49	0.24	0.60	**2.60**
70000	3.75	3.44	0.68	0.46	0.65	**1.90**	4.80	4.82	0.54	0.29	0.73	*3.01*	6.53	6.53	0.51	0.26	0.65	**2.63**
80000	3.92	3.62	0.70	0.50	0.64	**1.90**	4.93	4.95	0.55	0.30	0.75	*3.05*	6.68	6.66	0.53	0.29	0.70	**2.64**
90000	4.08	3.77	0.72	0.52	0.62	**1.89**	5.05	5.07	0.55	0.31	0.77	*3.09*	6.82	6.79	0.55	0.30	0.72	**2.65**
100000	4.22	3.91	0.73	0.54	0.61	**1.88**	5.16	5.17	0.56	0.31	0.79	*3.13*	6.95	6.90	0.57	0.32	0.75	**2.65**
110000	4.34	4.04	0.74	0.55	0.61	**1.88**	5.26	5.25	0.56	0.31	0.80	*3.17*	7.08	7.01	0.59	0.34	0.78	**2.67**
120000	4.45	4.16	0.74	0.55	0.60	**1.88**	5.35	5.35	0.56	0.32	0.80	*3.19*	7.19	7.11	0.60	0.36	0.80	**2.67**
130000	4.56	4.27	0.74	0.55	0.58	**1.87**	5.44	5.43	0.56	0.32	0.81	*3.22*	7.30	7.21	0.62	0.38	0.82	**2.68**
140000	4.65	4.37	0.74	0.55	0.57	**1.87**	5.52	5.52	0.56	0.32	0.81	*3.24*	7.41	7.30	0.63	0.40	0.83	**2.68**
150000	4.75	4.47	0.74	0.54	0.56	**1.87**	5.60	5.60	0.56	0.32	0.82	*3.27*	7.51	7.39	0.64	0.41	0.85	**2.69**
160000	4.83	4.57	0.73	0.54	0.56	**1.87**	5.68	5.67	0.57	0.32	0.83	*3.30*	7.61	7.48	0.66	0.43	0.86	**2.69**
170000	4.91	4.66	0.72	0.53	0.55	**1.87**	5.75	5.75	0.57	0.32	0.83	*3.33*	7.70	7.56	0.67	0.45	0.87	**2.70**
180000	4.99	4.74	0.72	0.51	0.54	**1.88**	5.82	5.82	0.57	0.32	0.84	*3.37*	7.79	7.63	0.68	0.47	0.88	**2.70**
190000	5.06	4.82	0.71	0.50	0.53	**1.88**	5.89	5.88	0.57	0.32	0.85	*3.40*	7.88	7.71	0.69	0.48	0.89	**2.70**
200000	5.13	4.90	0.70	0.49	0.52	**1.88**	5.96	5.95	0.57	0.33	0.84	*3.42*	7.96	7.79	0.71	0.50	0.90	**2.69**

Table B2(b) Statistical parameters for the STA BC-2 prepared with VG40 bitumen

Passes	55 °C						60 °C						65 °C					
	Mean	**Median**	**Mode**	**Standard Deviation**	**Skewness**	**Kurtosis**	**Mean**	**Median**	**Mode**	**Standard Deviation**	**Skewness**	**Kurtosis**	**Mean**	**Median**	**Mode**	**Standard Deviation**	**Skewness**	**Kurtosis**
500	1.27	1.32	0.20	0.04	-0.12	**1.50**	1.73	1.80	0.36	0.13	-0.51	**1.89**	2.70	2.71	0.33	0.11	0.23	**1.86**
1000	1.72	1.79	0.23	0.05	-0.10	**1.54**	2.30	2.33	0.41	0.16	-0.39	**1.84**	3.70	3.69	0.40	0.16	0.23	**1.90**
2000	2.39	2.44	0.25	0.06	-0.02	**1.70**	3.17	3.17	0.46	0.21	-0.10	**1.88**	4.98	4.96	0.48	0.23	0.23	**1.97**
4000	3.37	3.41	0.29	0.08	0.13	**2.03**	4.46	4.38	0.54	0.30	0.37	**2.24**	6.55	6.53	0.58	0.34	0.21	**2.00**
6000	4.10	4.17	0.31	0.10	0.26	**2.33**	5.42	5.25	0.61	0.38	0.62	**2.48**	7.58	7.55	0.66	0.43	0.18	**2.03**
8000	4.67	4.73	0.32	0.10	0.36	**2.60**	6.18	5.93	0.67	0.45	0.73	**2.57**	8.35	8.33	0.72	0.52	0.15	**2.05**
10000	5.11	5.18	0.34	0.11	0.44	**2.83**	6.78	6.47	0.72	0.52	0.76	**2.53**	8.97	8.97	0.77	0.60	0.12	**2.07**
12000	5.47	5.53	0.35	0.12	0.51	*3.05*	7.26	6.92	0.76	0.58	0.76	**2.45**	9.50	9.51	0.83	0.68	0.09	**2.10**
14000	5.76	5.82	0.36	0.13	0.59	*3.25*	7.66	7.25	0.80	0.63	0.74	**2.36**	9.95	9.98	0.88	0.77	0.07	**2.11**
16000	6.00	6.07	0.37	0.13	0.65	*3.41*	7.99	7.60	0.82	0.68	0.72	**2.29**	10.36	10.35	0.92	0.85	0.05	**2.12**
18000	6.20	6.28	0.37	0.14	0.69	*3.49*	8.27	7.90	0.85	0.71	0.70	**2.22**	10.74	10.69	0.97	0.94	0.03	**2.12**
20000	6.37	6.44	0.38	0.15	0.73	*3.58*	8.50	8.15	0.86	0.75	0.68	**2.17**	11.09	11.07	1.01	1.01	0.01	**2.11**
30000	6.93	6.99	0.42	0.18	0.88	*3.80*	9.27	8.95	0.92	0.85	0.61	**2.04**	12.69	12.90	1.16	1.35	-0.10	**2.01**
40000	7.27	7.35	0.45	0.20	0.96	*3.89*	9.71	9.42	0.94	0.88	0.59	**2.02**	14.23	14.52	1.23	1.50	-0.24	**1.90**
50000	7.53	7.59	0.48	0.23	1.04	*3.96*	10.03	9.75	0.94	0.89	0.59	**2.04**	15.83	16.17	1.22	1.49	-0.39	**1.88**
60000	7.75	7.80	0.50	0.25	1.09	*3.98*	10.30	10.02	0.94	0.89	0.61	**2.06**						
70000	7.93	7.99	0.52	0.27	1.14	*4.02*	10.52	10.25	0.94	0.88	0.62	**2.09**						
80000	8.10	8.16	0.54	0.29	1.18	*4.05*	10.73	10.47	0.93	0.87	0.63	**2.11**						
90000	8.26	8.30	0.56	0.31	1.22	*4.09*	10.91	10.66	0.93	0.87	0.64	**2.14**						
100000	8.40	8.43	0.57	0.33	1.25	*4.11*	11.08	10.84	0.93	0.86	0.65	**2.16**						
110000	8.53	8.55	0.59	0.34	1.28	*4.14*	11.24	11.01	0.92	0.85	0.65	**2.18**						
120000	8.66	8.66	0.60	0.36	1.30	*4.15*	11.39	11.16	0.92	0.85	0.66	**2.21**						
130000	8.78	8.77	0.61	0.38	1.32	*4.17*	11.53	11.29	0.92	0.84	0.67	**2.22**						
140000	8.89	8.87	0.63	0.39	1.34	*4.19*	11.66	11.42	0.91	0.83	0.67	**2.24**						
150000	8.99	8.96	0.64	0.41	1.37	*4.21*	11.78	11.52	0.91	0.83	0.68	**2.25**						
160000	9.09	9.05	0.65	0.42	1.37	*4.20*	11.90	11.60	0.91	0.82	0.68	**2.28**						
170000	9.19	9.14	0.66	0.44	1.39	*4.23*	12.02	11.72	0.90	0.82	0.68	**2.28**						
180000	9.28	9.22	0.67	0.45	1.41	*4.25*	12.13	11.85	0.90	0.81	0.68	**2.30**						
190000	9.37	9.30	0.68	0.47	1.42	*4.25*	12.23	11.97	0.90	0.81	0.67	**2.30**						
200000	9.46	9.37	0.69	0.48	1.44	*4.27*	12.33	12.08	0.90	0.81	0.67	**2.32**						

Table B3(a) Statistical parameters for the LTA BC-2 prepared with VG40 bitumen

Passes	40 °C						45 °C						50 °C					
	Mean	**Median**	**Mode**	**Standard Deviation**	**Skewness**	**Kurtosis**	**Mean**	**Median**	**Mode**	**Standard Deviation**	**Skewness**	**Kurtosis**	**Mean**	**Median**	**Mode**	**Standard Deviation**	**Skewness**	**Kurtosis**
500	0.25	0.26	0.12	0.01	-0.27	**1.71**	0.39	0.32	0.19	0.04	0.54	**2.21**	0.67	0.71	0.16	0.03	-0.94	**2.71**
1000	0.36	0.37	0.17	0.03	-0.17	**1.70**	0.53	0.44	0.23	0.05	0.48	**2.08**	0.89	0.94	0.19	0.03	-1.03	**2.89**
2000	0.52	0.54	0.24	0.06	-0.05	**1.70**	0.73	0.62	0.28	0.08	0.43	**1.95**	1.23	1.30	0.21	0.05	-1.11	**2.99**
4000	0.72	0.72	0.31	0.09	0.02	**1.67**	1.02	0.91	0.32	0.10	0.41	**1.80**	1.73	1.84	0.24	0.06	-1.06	**2.87**
6000	0.85	0.84	0.34	0.11	0.00	**1.67**	1.26	1.16	0.35	0.12	0.39	**1.71**	2.14	2.24	0.27	0.07	-0.92	**2.67**
8000	0.96	0.95	0.36	0.13	-0.02	**1.67**	1.46	1.38	0.36	0.13	0.38	**1.65**	2.49	2.57	0.28	0.08	-0.77	**2.52**
10000	1.04	1.03	0.37	0.13	-0.03	**1.67**	1.64	1.56	0.37	0.14	0.36	**1.62**	2.79	2.85	0.29	0.09	-0.65	**2.43**
12000	1.12	1.11	0.37	0.14	-0.04	**1.69**	1.80	1.71	0.38	0.15	0.34	**1.61**	3.05	3.13	0.31	0.09	-0.55	**2.37**
14000	1.19	1.18	0.38	0.14	-0.06	**1.68**	1.94	1.85	0.39	0.15	0.30	**1.61**	3.28	3.36	0.31	0.10	-0.48	**2.33**
16000	1.25	1.25	0.38	0.15	-0.07	**1.69**	2.08	1.97	0.39	0.15	0.27	**1.61**	3.49	3.56	0.32	0.10	-0.42	**2.29**
18000	1.31	1.31	0.39	0.15	-0.08	**1.69**	2.20	2.08	0.39	0.15	0.22	**1.63**	3.67	3.74	0.32	0.10	-0.37	**2.26**
20000	1.37	1.37	0.39	0.15	-0.09	**1.70**	2.32	2.19	0.39	0.15	0.18	**1.65**	3.84	3.90	0.32	0.10	-0.32	**2.23**
30000	1.61	1.63	0.40	0.16	-0.12	**1.68**	2.79	2.70	0.39	0.15	-0.07	**1.80**	4.44	4.49	0.32	0.10	-0.26	**2.17**
40000	1.82	1.85	0.41	0.17	-0.16	**1.67**	3.14	3.13	0.38	0.15	-0.29	**1.92**	4.81	4.84	0.32	0.10	-0.24	**2.12**
50000	1.99	2.04	0.42	0.18	-0.20	**1.66**	3.41	3.44	0.38	0.15	-0.45	**2.01**	5.07	5.09	0.31	0.10	-0.26	**2.07**
60000	2.15	2.22	0.43	0.19	-0.25	**1.66**	3.63	3.69	0.38	0.14	-0.54	**2.06**	5.25	5.27	0.32	0.10	-0.28	**2.04**
70000	2.30	2.38	0.44	0.20	-0.29	**1.67**	3.81	3.88	0.38	0.14	-0.59	**2.10**	5.39	5.41	0.32	0.10	-0.27	**1.99**
80000	2.43	2.54	0.45	0.21	-0.33	**1.67**	3.96	4.04	0.38	0.14	-0.61	**2.13**	5.51	5.52	0.32	0.10	-0.28	**1.96**
90000	2.56	2.68	0.46	0.21	-0.36	**1.69**	4.10	4.16	0.37	0.14	-0.60	**2.15**	5.61	5.62	0.33	0.11	-0.28	**1.92**
100000	2.67	2.81	0.47	0.22	-0.40	**1.71**	4.22	4.26	0.37	0.14	-0.58	**2.14**	5.70	5.71	0.33	0.11	-0.27	**1.91**
110000	2.79	2.94	0.48	0.23	-0.44	**1.72**	4.32	4.37	0.37	0.14	-0.55	**2.12**	5.78	5.79	0.33	0.11	-0.25	**1.88**
120000	2.89	3.06	0.49	0.24	-0.46	**1.74**	4.42	4.49	0.38	0.14	-0.50	**2.08**	5.86	5.86	0.34	0.11	-0.23	**1.87**
130000	2.99	3.18	0.50	0.25	-0.49	**1.76**	4.51	4.59	0.38	0.14	-0.44	**2.02**	5.93	5.93	0.34	0.12	-0.21	**1.86**
140000	3.09	3.29	0.51	0.26	-0.52	**1.78**	4.60	4.66	0.38	0.15	-0.37	**1.94**	5.99	5.99	0.35	0.12	-0.19	**1.87**
150000	3.18	3.40	0.51	0.26	-0.55	**1.80**	4.68	4.71	0.39	0.15	-0.30	**1.86**	6.06	6.05	0.35	0.13	-0.17	**1.88**
160000	3.27	3.50	0.52	0.27	-0.57	**1.82**	4.75	4.77	0.39	0.15	-0.24	**1.78**	6.12	6.11	0.36	0.13	-0.14	**1.88**
170000	3.36	3.60	0.53	0.28	-0.59	**1.84**	4.83	4.81	0.40	0.16	-0.17	**1.70**	6.18	6.17	0.36	0.13	-0.12	**1.89**
180000	3.44	3.69	0.54	0.29	-0.61	**1.87**	4.90	4.86	0.41	0.16	-0.12	**1.63**	6.23	6.22	0.37	0.13	-0.09	**1.89**
190000	3.53	3.78	0.54	0.29	-0.63	**1.89**	4.96	4.90	0.41	0.17	-0.07	**1.56**	6.29	6.27	0.37	0.14	-0.07	**1.92**
200000	3.61	3.87	0.55	0.30	-0.65	**1.92**	5.03	4.94	0.42	0.18	-0.03	**1.51**	6.34	6.32	0.37	0.14	-0.05	**1.93**

Table B3(b) Statistical parameters for the LTA BC-2 prepared with VG40 bitumen

Passes	55 °C						60 °C						65 °C					
	Mean	**Median**	**Mode**	**Standard Deviation**	**Skewness**	**Kurtosis**	**Mean**	**Median**	**Mode**	**Standard Deviation**	**Skewness**	**Kurtosis**	**Mean**	**Median**	**Mode**	**Standard Deviation**	**Skewness**	**Kurtosis**
500	0.90	0.98	0.23	0.06	-0.60	**2.02**	1.29	1.31	0.13	0.02	-0.18	**1.47**	1.69	1.60	0.25	0.06	0.93	**2.48**
1000	1.23	1.33	0.25	0.06	-0.73	**2.27**	1.72	1.76	0.16	0.02	-0.22	**1.61**	2.45	2.33	0.33	0.11	0.88	**2.42**
2000	1.75	1.86	0.26	0.07	-0.83	**2.68**	2.35	2.40	0.18	0.03	-0.24	**1.82**	3.53	3.40	0.43	0.19	0.81	**2.35**
4000	2.51	2.57	0.28	0.08	-0.79	**3.00**	3.23	3.30	0.21	0.04	-0.23	**2.14**	4.93	4.74	0.52	0.27	0.72	**2.27**
6000	3.07	3.12	0.29	0.09	-0.67	**2.89**	3.87	3.92	0.22	0.05	-0.17	**2.39**	5.82	5.58	0.56	0.32	0.69	**2.20**
8000	3.51	3.53	0.31	0.10	-0.49	**2.68**	4.37	4.40	0.23	0.05	-0.11	**2.58**	6.45	6.17	0.60	0.36	0.68	**2.16**
10000	3.86	3.85	0.33	0.11	-0.29	**2.53**	4.76	4.78	0.24	0.06	-0.01	**2.78**	6.93	6.63	0.63	0.40	0.68	**2.13**
12000	4.15	4.14	0.35	0.12	-0.12	**2.52**	5.09	5.10	0.25	0.06	0.09	*3.01*	7.33	7.01	0.66	0.44	0.69	**2.15**
14000	4.38	4.38	0.37	0.14	0.05	**2.53**	5.36	5.37	0.25	0.06	0.18	*3.14*	7.67	7.35	0.69	0.48	0.69	**2.17**
16000	4.57	4.58	0.39	0.16	0.15	**2.57**	5.59	5.60	0.26	0.07	0.26	*3.29*	7.97	7.65	0.72	0.53	0.70	**2.20**
18000	4.73	4.75	0.41	0.17	0.26	**2.62**	5.79	5.80	0.26	0.07	0.31	*3.37*	8.24	7.93	0.76	0.57	0.71	**2.23**
20000	4.87	4.89	0.43	0.19	0.32	**2.67**	5.96	5.97	0.27	0.07	0.35	*3.43*	8.50	8.19	0.78	0.61	0.73	**2.28**
30000	5.34	5.29	0.49	0.24	0.47	**2.82**	6.62	6.63	0.28	0.08	0.47	*3.60*	9.56	9.29	0.92	0.84	0.77	**2.40**
40000	5.62	5.59	0.50	0.25	0.53	**2.96**	7.09	7.10	0.29	0.08	0.48	*3.58*	10.43	10.07	1.03	1.06	0.80	**2.46**
50000	5.83	5.78	0.50	0.25	0.58	*3.08*	7.47	7.51	0.30	0.09	0.49	*3.52*	11.18	10.80	1.13	1.27	0.82	**2.48**
60000	6.00	5.98	0.49	0.24	0.61	*3.18*	7.81	7.84	0.31	0.09	0.50	*3.49*	11.84	11.49	1.21	1.47	0.83	**2.48**
70000	6.16	6.14	0.49	0.24	0.64	*3.26*	8.10	8.13	0.31	0.10	0.49	*3.38*	12.44	12.12	1.30	1.68	0.83	**2.48**
80000	6.29	6.27	0.48	0.23	0.69	*3.33*	8.37	8.40	0.32	0.10	0.50	*3.37*	12.99	12.69	1.37	1.88	0.83	**2.48**
90000	6.42	6.37	0.47	0.22	0.73	*3.39*	8.62	8.64	0.32	0.10	0.50	*3.27*	13.50	13.23	1.44	2.07	0.83	**2.46**
100000	6.53	6.48	0.46	0.21	0.77	*3.43*	8.85	8.87	0.33	0.11	0.52	*3.26*	13.98	13.69	1.51	2.27	0.83	**2.45**
110000	6.64	6.56	0.46	0.21	0.80	*3.42*	9.06	9.08	0.33	0.11	0.50	*3.14*	14.44	14.10	1.57	2.46	0.83	**2.44**
120000	6.74	6.67	0.45	0.21	0.83	*3.41*	9.26	9.27	0.33	0.11	0.54	*3.15*	14.86	14.48	1.63	2.65	0.83	**2.43**
130000	6.84	6.77	0.45	0.20	0.85	*3.39*	9.45	9.46	0.34	0.12	0.55	*3.13*						
140000	6.93	6.87	0.45	0.20	0.86	*3.34*	9.63	9.64	0.34	0.12	0.55	*3.06*						
150000	7.02	6.98	0.45	0.20	0.87	*3.28*	9.80	9.81	0.35	0.12	0.57	*3.05*						
160000	7.10	7.07	0.45	0.20	0.87	*3.25*	9.97	9.97	0.35	0.12	0.58	**2.96**						
170000	7.18	7.15	0.45	0.20	0.86	*3.18*	10.13	10.12	0.35	0.13	0.61	**2.98**						
180000	7.26	7.22	0.45	0.20	0.84	*3.12*	10.28	10.27	0.36	0.13	0.62	**2.95**						
190000	7.33	7.29	0.45	0.21	0.82	*3.07*	10.43	10.42	0.36	0.13	0.62	**2.92**						
200000	7.40	7.37	0.46	0.21	0.77	*2.98*	10.57	10.55	0.36	0.13	0.64	**2.90**						

Table B4(a) Statistical parameters for the STA DBM-2 prepared with VG20 bitumen

Passes	40 °C						45 °C						50 °C					
	Mean	**Median**	**Mode**	**Standard Deviation**	**Skewness**	**Kurtosis**	**Mean**	**Median**	**Mode**	**Standard Deviation**	**Skewness**	**Kurtosis**	**Mean**	**Median**	**Mode**	**Standard Deviation**	**Skewness**	**Kurtosis**
500	0.72	0.75	0.11	0.01	-0.15	**1.35**	0.99	1.04	0.20	0.04	-1.31	*3.79*	1.73	1.75	0.22	0.05	-0.32	**2.37**
1000	0.91	0.94	0.11	0.01	-0.23	**1.45**	1.23	1.29	0.22	0.05	-1.28	*3.82*	2.13	2.15	0.27	0.07	-0.08	**2.33**
2000	1.17	1.21	0.09	0.01	-0.38	**1.86**	1.57	1.64	0.24	0.06	-1.20	*3.79*	2.67	2.68	0.35	0.12	0.42	**2.89**
4000	1.52	1.54	0.08	0.01	-0.79	**3.05**	2.04	2.13	0.26	0.07	-0.92	*3.63*	3.40	3.41	0.47	0.22	0.87	*3.71*
6000	1.79	1.82	0.09	0.01	-0.76	**3.36**	2.42	2.49	0.28	0.08	-0.58	*3.52*	3.92	3.95	0.54	0.29	0.96	*3.83*
8000	2.01	2.03	0.11	0.01	-0.31	**2.71**	2.74	2.78	0.29	0.09	-0.24	*3.51*	4.33	4.36	0.58	0.34	0.90	*3.62*
10000	2.21	2.22	0.13	0.02	-0.08	**2.48**	3.02	3.04	0.31	0.09	0.06	*3.61*	4.67	4.69	0.61	0.37	0.83	*3.35*
12000	2.38	2.39	0.15	0.02	0.07	**2.31**	3.27	3.27	0.32	0.10	0.33	*3.76*	4.95	4.97	0.63	0.39	0.73	*3.06*
14000	2.53	2.55	0.17	0.03	0.15	**2.22**	3.49	3.48	0.33	0.11	0.56	*3.97*	5.18	5.21	0.64	0.41	0.65	**2.83**
16000	2.68	2.68	0.18	0.03	0.19	**2.21**	3.70	3.67	0.34	0.11	0.76	*4.19*	5.38	5.41	0.65	0.42	0.57	**2.61**
18000	2.81	2.81	0.20	0.04	0.22	**2.22**	3.88	3.85	0.34	0.12	0.93	*4.43*	5.56	5.59	0.65	0.43	0.52	**2.45**
20000	2.93	2.93	0.22	0.05	0.21	**2.18**	4.05	4.02	0.35	0.12	1.09	*4.68*	5.72	5.75	0.66	0.43	0.47	**2.32**
30000	3.43	3.46	0.26	0.07	0.27	**2.50**	4.74	4.69	0.36	0.13	1.65	*5.88*	6.29	6.31	0.68	0.46	0.35	**2.03**
40000	3.82	3.87	0.30	0.09	0.31	**2.79**	5.22	5.15	0.36	0.13	1.94	*6.71*	6.67	6.68	0.69	0.48	0.33	**1.96**
50000	4.13	4.22	0.32	0.10	0.39	*3.06*	5.57	5.53	0.35	0.13	2.01	*6.99*	6.95	6.95	0.71	0.50	0.35	**1.98**
60000	4.39	4.47	0.34	0.12	0.47	*3.25*	5.85	5.82	0.36	0.13	1.96	*6.85*	7.19	7.17	0.72	0.51	0.37	**2.00**
70000	4.61	4.71	0.36	0.13	0.54	*3.35*	6.06	6.00	0.36	0.13	1.85	*6.54*	7.40	7.36	0.73	0.53	0.40	**2.04**
80000	4.81	4.89	0.38	0.14	0.61	*3.44*	6.24	6.18	0.37	0.13	1.74	*6.22*	7.58	7.56	0.73	0.54	0.42	**2.07**
90000	4.98	5.05	0.39	0.16	0.67	*3.50*	6.39	6.34	0.37	0.14	1.66	*5.98*	7.74	7.74	0.74	0.55	0.44	**2.11**
100000	5.14	5.20	0.41	0.17	0.71	*3.50*	6.52	6.48	0.37	0.14	1.62	*5.84*	7.89	7.90	0.75	0.56	0.46	**2.15**
110000	5.28	5.32	0.42	0.18	0.76	*3.51*	6.63	6.60	0.38	0.14	1.59	*5.79*	8.03	8.06	0.76	0.58	0.48	**2.19**
120000	5.41	5.42	0.44	0.19	0.80	*3.54*	6.73	6.71	0.38	0.14	1.59	*5.81*	8.17	8.20	0.77	0.59	0.50	**2.22**
130000	5.53	5.54	0.45	0.20	0.84	*3.55*	6.83	6.81	0.38	0.15	1.61	*5.88*	8.29	8.33	0.77	0.60	0.52	**2.25**
140000	5.64	5.65	0.46	0.21	0.88	*3.56*	6.91	6.90	0.38	0.15	1.64	*5.99*	8.41	8.44	0.78	0.61	0.54	**2.28**
150000	5.75	5.74	0.47	0.22	0.90	*3.54*	6.99	6.98	0.38	0.15	1.67	*6.13*	8.52	8.54	0.79	0.62	0.56	**2.30**
160000	5.84	5.80	0.49	0.24	0.93	*3.55*	7.06	7.04	0.39	0.15	1.71	*6.29*	8.62	8.64	0.79	0.63	0.58	**2.34**
170000	5.94	5.88	0.50	0.25	0.96	*3.56*	7.13	7.10	0.39	0.15	1.75	*6.46*	8.72	8.73	0.80	0.64	0.59	**2.37**
180000	6.03	5.97	0.51	0.26	0.99	*3.57*	7.20	7.16	0.39	0.15	1.80	*6.63*	8.82	8.82	0.80	0.64	0.61	**2.39**
190000	6.11	6.06	0.52	0.28	1.01	*3.56*	7.26	7.22	0.39	0.15	1.84	*6.80*	8.91	8.91	0.81	0.65	0.61	**2.41**
200000	6.20	6.15	0.54	0.29	1.02	*3.55*	7.33	7.27	0.39	0.15	1.88	*6.96*	9.00	8.99	0.81	0.66	0.64	**2.45**

Table B4(b) Statistical parameters for the STA DBM-2 prepared with VG20 bitumen

Passes	55 °C						60 °C						65 °C					
	Mean	**Median**	**Mode**	**Standard Deviation**	**Skewness**	**Kurtosis**	**Mean**	**Median**	**Mode**	**Standard Deviation**	**Skewness**	**Kurtosis**	**Mean**	**Median**	**Mode**	**Standard Deviation**	**Skewness**	**Kurtosis**
500	2.26	2.24	0.28	0.08	1.22	*5.92*	3.15	3.19	0.26	0.07	-0.37	**2.43**	3.66	3.67	0.44	0.19	0.35	**1.95**
1000	2.88	2.85	0.31	0.10	0.77	*4.76*	3.80	3.84	0.29	0.09	-0.35	**2.49**	4.82	4.90	0.51	0.26	-0.29	**1.64**
2000	3.71	3.70	0.36	0.13	0.49	*3.33*	4.62	4.62	0.35	0.12	-0.31	**2.64**	6.25	6.54	0.65	0.42	-0.41	**1.57**
4000	4.78	4.85	0.39	0.15	0.56	*3.17*	5.70	5.70	0.44	0.19	-0.23	**2.59**	7.91	8.29	0.75	0.57	-0.37	**1.51**
6000	5.51	5.48	0.38	0.14	0.80	*4.00*	6.48	6.49	0.50	0.25	-0.16	**2.47**	9.01	9.30	0.78	0.60	-0.31	**1.56**
8000	6.09	6.11	0.38	0.15	1.12	*5.10*	7.11	7.12	0.55	0.30	-0.11	**2.38**	9.86	9.95	0.78	0.60	-0.23	**1.62**
10000	6.57	6.54	0.40	0.16	1.29	*5.50*	7.64	7.65	0.58	0.33	-0.07	**2.32**	10.57	10.67	0.77	0.60	-0.16	**1.64**
12000	6.98	6.88	0.43	0.19	1.32	*5.27*	8.10	8.12	0.59	0.35	-0.05	**2.28**	11.18	11.23	0.77	0.59	-0.09	**1.62**
14000	7.33	7.15	0.47	0.22	1.27	*4.87*	8.51	8.52	0.60	0.36	-0.02	**2.24**	11.71	11.84	0.78	0.60	-0.02	**1.61**
16000	7.65	7.46	0.51	0.26	1.20	*4.45*	8.88	8.87	0.60	0.36	-0.01	**2.22**	12.20	12.22	0.78	0.61	0.03	**1.61**
18000	7.93	7.69	0.54	0.30	1.13	*4.09*	9.21	9.18	0.60	0.36	0.01	**2.21**	12.65	12.59	0.79	0.63	0.06	**1.63**
20000	8.18	7.91	0.58	0.33	1.07	*3.80*	9.52	9.49	0.59	0.35	0.02	**2.20**	13.06	13.03	0.81	0.65	0.08	**1.69**
30000	9.17	8.78	0.71	0.51	0.94	*3.09*	10.73	10.76	0.52	0.27	0.11	**2.23**	14.78	14.77	0.91	0.83	-0.07	**2.20**
40000	9.88	9.42	0.79	0.62	0.91	**2.81**	11.61	11.64	0.45	0.20	0.23	**2.31**	16.13	16.17	1.04	1.08	-0.36	**2.70**
50000	10.44	9.93	0.83	0.69	0.92	**2.70**	12.29	12.30	0.38	0.15	0.35	**2.41**						
60000	10.90	10.41	0.85	0.73	0.91	**2.58**	12.85	12.86	0.34	0.12	0.49	**2.57**						
70000	11.31	10.81	0.87	0.75	0.90	**2.50**	13.31	13.33	0.32	0.10	0.61	**2.78**						
80000	11.67	11.14	0.88	0.77	0.88	**2.41**	13.71	13.69	0.30	0.09	0.71	**2.99**						
90000	12.00	11.44	0.88	0.78	0.85	**2.33**	14.07	14.03	0.30	0.09	0.79	*3.12*						
100000	12.30	11.77	0.89	0.79	0.83	**2.26**	14.39	14.36	0.30	0.09	0.82	*3.23*						
110000	12.58	12.07	0.89	0.79	0.80	**2.19**	14.68	14.64	0.31	0.09	0.82	*3.34*						
120000	12.85	12.35	0.89	0.80	0.77	**2.13**	14.94	14.87	0.32	0.10	0.74	*3.37*						
130000	13.10	12.61	0.90	0.81	0.74	**2.08**												
140000	13.33	12.85	0.91	0.82	0.71	**2.04**												
150000	13.56	13.08	0.91	0.83	0.67	**1.99**												
160000	13.77	13.32	0.91	0.83	0.64	**1.96**												
170000	13.97	13.56	0.92	0.84	0.61	**1.92**												
180000	14.17	13.80	0.93	0.86	0.58	**1.89**												
190000	14.36	14.03	0.93	0.86	0.55	**1.87**												
200000	14.54	14.25	0.93	0.87	0.53	**1.85**												

Table B5 Statistical parameters for the LTA DBM-2 prepared with VG20 bitumen

Passes	40 °C						45 °C						50 °C					
	Mean	**Median**	**Mode**	**Standard Deviation**	**Skewness**	**Kurtosis**	**Mean**	**Median**	**Mode**	**Standard Deviation**	**Skewness**	**Kurtosis**	**Mean**	**Median**	**Mode**	**Standard Deviation**	**Skewness**	**Kurtosis**
500	0.66	0.73	0.19	0.04	-1.18	*3.17*	0.89	0.83	0.35	0.12	-0.09	**1.60**	1.15	1.13	0.17	0.03	0.57	**2.82**
1000	0.82	0.89	0.22	0.05	-1.23	*3.28*	1.17	1.04	0.46	0.22	-0.06	**1.44**	1.38	1.35	0.19	0.04	0.69	*3.22*
2000	0.99	1.08	0.25	0.06	-1.20	*3.25*	1.53	1.32	0.58	0.34	-0.03	**1.44**	1.67	1.63	0.22	0.05	0.82	*3.59*
4000	1.20	1.27	0.29	0.08	-1.06	*3.06*	1.92	1.74	0.62	0.38	-0.12	**1.47**	2.05	2.00	0.26	0.07	1.00	*4.07*
6000	1.34	1.41	0.31	0.10	-0.94	**2.88**	2.16	2.04	0.60	0.36	-0.22	**1.52**	2.33	2.28	0.29	0.08	1.12	*4.35*
8000	1.45	1.53	0.33	0.11	-0.82	**2.77**	2.35	2.25	0.58	0.34	-0.29	**1.57**	2.57	2.51	0.31	0.10	1.22	*4.61*
10000	1.54	1.62	0.34	0.12	-0.73	**2.67**	2.50	2.46	0.56	0.32	-0.34	**1.61**	2.76	2.71	0.33	0.11	1.29	*4.76*
12000	1.62	1.69	0.36	0.13	-0.62	**2.59**	2.63	2.64	0.55	0.30	-0.38	**1.63**	2.94	2.90	0.35	0.12	1.35	*4.91*
14000	1.70	1.76	0.37	0.14	-0.53	**2.53**	2.75	2.80	0.53	0.29	-0.40	**1.65**	3.10	3.07	0.36	0.13	1.39	*5.00*
16000	1.76	1.82	0.38	0.14	-0.45	**2.48**	2.85	2.94	0.52	0.27	-0.41	**1.66**	3.25	3.23	0.37	0.14	1.43	*5.09*
18000	1.82	1.87	0.39	0.15	-0.36	**2.44**	2.94	3.06	0.52	0.27	-0.42	**1.66**	3.38	3.37	0.38	0.15	1.45	*5.15*
20000	1.88	1.92	0.40	0.16	-0.29	**2.42**	3.02	3.17	0.51	0.26	-0.42	**1.66**	3.50	3.49	0.39	0.15	1.46	*5.18*
30000	2.12	2.12	0.43	0.19	0.01	**2.37**	3.34	3.48	0.50	0.25	-0.39	**1.63**	3.98	4.00	0.42	0.18	1.53	*5.36*
40000	2.30	2.28	0.46	0.21	0.22	**2.40**	3.57	3.70	0.51	0.26	-0.36	**1.61**	4.34	4.34	0.44	0.19	1.55	*5.39*
50000	2.46	2.41	0.48	0.23	0.37	**2.42**	3.75	3.88	0.52	0.27	-0.34	**1.59**	4.61	4.59	0.45	0.20	1.57	*5.46*
60000	2.59	2.53	0.50	0.25	0.46	**2.46**	3.91	4.04	0.54	0.29	-0.33	**1.57**	4.82	4.79	0.45	0.21	1.58	*5.54*
70000	2.71	2.63	0.52	0.27	0.53	**2.47**	4.04	4.18	0.55	0.30	-0.33	**1.56**	4.99	4.96	0.46	0.21	1.59	*5.58*
80000	2.81	2.72	0.53	0.28	0.58	**2.48**	4.17	4.31	0.56	0.32	-0.32	**1.54**	5.14	5.10	0.47	0.22	1.58	*5.61*
90000	2.91	2.80	0.54	0.29	0.62	**2.47**	4.28	4.42	0.57	0.33	-0.32	**1.53**	5.26	5.23	0.48	0.23	1.59	*5.65*
100000	3.00	2.87	0.54	0.30	0.65	**2.48**	4.38	4.53	0.58	0.34	-0.32	**1.52**	5.38	5.34	0.48	0.23	1.60	*5.73*
110000	3.08	2.94	0.55	0.31	0.67	**2.47**	4.48	4.63	0.59	0.35	-0.32	**1.51**	5.48	5.45	0.49	0.24	1.60	*5.76*
120000	3.15	3.01	0.56	0.31	0.68	**2.47**	4.57	4.73	0.60	0.37	-0.32	**1.50**	5.57	5.55	0.50	0.25	1.61	*5.81*
130000	3.22	3.07	0.56	0.32	0.69	**2.47**	4.65	4.81	0.61	0.37	-0.32	**1.50**	5.65	5.63	0.51	0.26	1.62	*5.90*
140000	3.29	3.13	0.57	0.33	0.71	**2.46**	4.73	4.90	0.62	0.39	-0.32	**1.49**	5.73	5.71	0.51	0.26	1.62	*5.89*
150000	3.35	3.18	0.57	0.33	0.71	**2.45**	4.81	4.98	0.63	0.40	-0.31	**1.48**	5.80	5.78	0.52	0.27	1.64	*5.96*
160000	3.41	3.23	0.58	0.33	0.72	**2.44**	4.88	5.05	0.64	0.40	-0.31	**1.48**	5.87	5.85	0.53	0.28	1.64	*6.00*
170000	3.47	3.28	0.58	0.34	0.72	**2.44**	4.95	5.12	0.64	0.41	-0.30	**1.48**	5.93	5.92	0.53	0.28	1.63	*6.02*
180000	3.52	3.33	0.59	0.34	0.72	**2.43**	5.01	5.19	0.65	0.42	-0.30	**1.47**	5.99	5.98	0.54	0.29	1.65	*6.07*
190000	3.57	3.38	0.59	0.35	0.72	**2.43**	5.08	5.24	0.66	0.43	-0.30	**1.47**	6.05	6.03	0.55	0.30	1.65	*6.09*
200000	3.62	3.43	0.59	0.35	0.72	**2.42**	5.14	5.29	0.66	0.44	-0.29	**1.47**	6.11	6.08	0.55	0.30	1.65	*6.11*

Table B5(b) Statistical parameters for the LTA DBM-2 prepared with VG20 bitumen

Passes	55 °C						60 °C						65 °C					
	Mean	**Median**	**Mode**	**Standard Deviation**	**Skewness**	**Kurtosis**	**Mean**	**Median**	**Mode**	**Standard Deviation**	**Skewness**	**Kurtosis**	**Mean**	**Median**	**Mode**	**Standard Deviation**	**Skewness**	**Kurtosis**
500	1.41	1.55	0.38	0.15	-0.64	**2.46**	1.89	1.94	0.27	0.07	-0.27	**1.76**	2.61	2.48	0.30	0.09	0.46	**1.91**
1000	1.79	1.92	0.39	0.15	-0.70	**2.61**	2.45	2.45	0.33	0.11	-0.39	**1.92**	3.30	3.20	0.32	0.10	0.36	**1.85**
2000	2.33	2.46	0.38	0.14	-0.64	**2.57**	3.17	3.16	0.40	0.16	-0.35	**1.93**	4.19	4.11	0.34	0.12	0.21	**1.77**
4000	3.09	3.09	0.35	0.12	-0.31	**2.24**	4.10	4.07	0.47	0.22	0.00	**1.70**	5.32	5.30	0.34	0.12	0.01	**1.71**
6000	3.67	3.70	0.37	0.14	-0.19	**2.59**	4.74	4.59	0.52	0.27	0.26	**1.57**	6.14	6.15	0.34	0.11	-0.11	**1.75**
8000	4.13	4.14	0.42	0.17	-0.34	*3.23*	5.23	5.12	0.56	0.31	0.38	**1.56**	6.79	6.83	0.33	0.11	-0.19	**1.86**
10000	4.52	4.54	0.47	0.22	-0.49	*3.62*	5.64	5.54	0.59	0.34	0.43	**1.62**	7.34	7.41	0.31	0.10	-0.23	**2.04**
12000	4.86	4.86	0.52	0.27	-0.60	*3.83*	5.99	5.83	0.61	0.37	0.43	**1.68**	7.83	7.92	0.29	0.09	-0.22	**2.30**
14000	5.14	5.19	0.57	0.32	-0.65	*3.91*	6.29	6.09	0.62	0.39	0.41	**1.74**	8.26	8.38	0.28	0.08	-0.16	**2.65**
16000	5.39	5.47	0.60	0.36	-0.68	*3.94*	6.56	6.41	0.63	0.40	0.36	**1.77**	8.66	8.74	0.26	0.07	-0.04	*3.13*
18000	5.61	5.71	0.63	0.40	-0.69	*3.97*	6.80	6.66	0.64	0.41	0.32	**1.80**	9.02	9.06	0.25	0.06	0.16	*3.72*
20000	5.80	5.92	0.66	0.43	-0.68	*4.00*	7.02	6.92	0.64	0.41	0.29	**1.81**	9.36	9.40	0.24	0.06	0.43	*4.40*
30000	6.51	6.58	0.73	0.53	-0.59	*4.09*	7.88	7.74	0.64	0.41	0.16	**1.83**	10.77	10.69	0.24	0.06	1.69	*6.26*
40000	6.96	7.02	0.75	0.56	-0.49	*4.17*	8.52	8.38	0.63	0.39	0.14	**1.81**	11.88	11.82	0.30	0.09	1.16	*4.21*
50000	7.29	7.31	0.75	0.56	-0.39	*4.18*	9.03	8.92	0.61	0.37	0.19	**1.80**	12.80	12.83	0.39	0.15	0.56	**2.88**
60000	7.55	7.58	0.74	0.55	-0.31	*4.18*	9.47	9.38	0.60	0.35	0.27	**1.78**	13.61	13.68	0.47	0.22	0.24	**2.31**
70000	7.77	7.77	0.74	0.55	-0.24	*4.14*	9.86	9.73	0.59	0.34	0.35	**1.75**	14.32	14.47	0.56	0.31	0.09	**2.06**
80000	7.97	7.96	0.74	0.54	-0.20	*4.10*	10.21	10.06	0.58	0.33	0.41	**1.72**	14.96	15.17	0.63	0.40	0.00	**1.93**
90000	8.14	8.16	0.74	0.54	-0.15	*4.05*	10.53	10.37	0.58	0.33	0.46	**1.70**	15.55	15.80	0.70	0.49	-0.04	**1.87**
100000	8.30	8.30	0.73	0.54	-0.12	*3.97*	10.83	10.69	0.57	0.33	0.47	**1.69**	16.09	16.36	0.77	0.59	-0.07	**1.83**
110000	8.45	8.43	0.73	0.54	-0.09	*3.91*	11.10	10.99	0.58	0.33	0.47	**1.69**	16.60	16.89	0.83	0.69	-0.08	**1.82**
120000	8.58	8.55	0.73	0.54	-0.08	*3.85*	11.37	11.27	0.58	0.34	0.45	**1.69**	17.07	17.37	0.89	0.79	-0.09	**1.81**
130000	8.71	8.67	0.74	0.54	-0.05	*3.77*	11.61	11.49	0.58	0.34	0.42	**1.72**						
140000	8.83	8.78	0.74	0.54	-0.04	*3.71*	11.84	11.69	0.59	0.35	0.38	**1.74**						
150000	8.95	8.88	0.74	0.55	-0.03	*3.65*	12.06	11.88	0.60	0.36	0.32	**1.77**						
160000	9.05	8.98	0.74	0.55	-0.02	*3.60*	12.28	12.07	0.60	0.36	0.26	**1.80**						
170000	9.16	9.08	0.75	0.56	-0.03	*3.55*	12.48	12.29	0.61	0.37	0.20	**1.84**						
180000	9.26	9.18	0.75	0.57	-0.03	*3.52*	12.67	12.50	0.62	0.38	0.14	**1.87**						
190000	9.35	9.28	0.75	0.57	-0.03	*3.48*	12.86	12.70	0.63	0.40	0.07	**1.91**						
200000	9.44	9.37	0.76	0.58	-0.04	*3.45*	13.04	12.89	0.64	0.41	0.01	**1.94**						

Table B6(a) Statistical parameters for the STA DBM-2 prepared with VG40 bitumen

Passes	40 °C						45 °C						50 °C					
	Mean	**Median**	**Mode**	**Standard Deviation**	**Skewness**	**Kurtosis**	**Mean**	**Median**	**Mode**	**Standard Deviation**	**Skewness**	**Kurtosis**	**Mean**	**Median**	**Mode**	**Standard Deviation**	**Skewness**	**Kurtosis**
500	0.48	0.49	0.17	0.03	0.10	**2.13**	0.74	0.77	0.14	0.02	-0.76	**2.87**	1.43	1.41	0.23	0.05	0.10	**2.69**
1000	0.60	0.62	0.19	0.03	-0.10	**1.89**	0.91	0.95	0.15	0.02	-0.70	**2.71**	1.72	1.70	0.24	0.06	0.19	**2.65**
2000	0.75	0.79	0.21	0.04	-0.25	**1.79**	1.14	1.15	0.17	0.03	-0.61	**2.48**	2.09	2.08	0.25	0.06	0.31	**2.59**
4000	0.98	1.02	0.24	0.06	-0.30	**1.82**	1.45	1.46	0.20	0.04	-0.45	**2.13**	2.60	2.55	0.27	0.07	0.48	**2.53**
6000	1.17	1.20	0.25	0.06	-0.27	**1.87**	1.69	1.71	0.21	0.04	-0.35	**1.91**	2.97	2.94	0.28	0.08	0.58	**2.51**
8000	1.33	1.34	0.26	0.07	-0.24	**1.93**	1.90	1.93	0.22	0.05	-0.30	**1.79**	3.28	3.25	0.29	0.09	0.67	**2.55**
10000	1.48	1.50	0.26	0.07	-0.22	**1.97**	2.08	2.14	0.23	0.05	-0.24	**1.69**	3.54	3.50	0.30	0.09	0.75	**2.61**
12000	1.61	1.64	0.26	0.07	-0.19	**2.02**	2.25	2.32	0.24	0.06	-0.20	**1.62**	3.76	3.73	0.31	0.09	0.77	**2.64**
14000	1.74	1.77	0.27	0.07	-0.20	**2.07**	2.40	2.48	0.25	0.06	-0.17	**1.58**	3.96	3.94	0.31	0.10	0.83	**2.72**
16000	1.86	1.89	0.27	0.07	-0.18	**2.09**	2.55	2.62	0.25	0.06	-0.14	**1.55**	4.14	4.12	0.31	0.10	0.84	**2.75**
18000	1.98	2.00	0.27	0.07	-0.16	**2.11**	2.68	2.75	0.26	0.07	-0.13	**1.53**	4.31	4.28	0.31	0.10	0.86	**2.79**
20000	2.09	2.11	0.26	0.07	-0.16	**2.12**	2.81	2.87	0.26	0.07	-0.12	**1.51**	4.45	4.42	0.31	0.10	0.88	**2.84**
30000	2.57	2.58	0.25	0.06	-0.16	**2.07**	3.34	3.37	0.28	0.08	-0.05	**1.47**	5.02	4.95	0.31	0.09	0.96	*3.08*
40000	2.96	2.96	0.24	0.06	-0.17	**1.95**	3.76	3.77	0.28	0.08	-0.02	**1.46**	5.41	5.30	0.30	0.09	1.02	*3.35*
50000	3.29	3.27	0.23	0.05	-0.14	**1.81**	4.09	4.09	0.28	0.08	0.00	**1.46**	5.69	5.56	0.31	0.09	1.07	*3.53*
60000	3.57	3.59	0.23	0.05	-0.08	**1.75**	4.35	4.34	0.28	0.08	0.02	**1.47**	5.91	5.82	0.31	0.10	1.04	*3.63*
70000	3.80	3.80	0.23	0.05	0.00	**1.74**	4.58	4.55	0.28	0.08	0.03	**1.47**	6.10	6.03	0.32	0.10	0.99	*3.63*
80000	4.01	4.00	0.24	0.06	0.07	**1.76**	4.76	4.73	0.28	0.08	0.03	**1.47**	6.25	6.21	0.33	0.11	0.91	*3.50*
90000	4.19	4.19	0.24	0.06	0.14	**1.80**	4.92	4.88	0.28	0.08	0.03	**1.48**	6.39	6.38	0.34	0.11	0.81	*3.38*
100000	4.34	4.36	0.25	0.06	0.15	**1.85**	5.06	5.01	0.28	0.08	0.04	**1.48**	6.51	6.53	0.35	0.12	0.75	*3.27*
110000	4.47	4.50	0.25	0.06	0.18	**1.88**	5.17	5.12	0.29	0.08	0.04	**1.47**	6.62	6.67	0.35	0.13	0.66	*3.13*
120000	4.59	4.62	0.26	0.07	0.20	**1.89**	5.27	5.22	0.29	0.08	0.03	**1.48**	6.72	6.77	0.36	0.13	0.58	**3.01**
130000	4.70	4.73	0.26	0.07	0.20	**1.92**	5.36	5.31	0.29	0.09	0.03	**1.47**	6.81	6.88	0.37	0.14	0.54	**2.91**
140000	4.79	4.82	0.26	0.07	0.21	**1.92**	5.44	5.38	0.30	0.09	0.04	**1.46**	6.90	6.97	0.38	0.15	0.47	**2.77**
150000	4.87	4.90	0.27	0.07	0.20	**1.94**	5.52	5.46	0.30	0.09	0.03	**1.45**	6.99	7.04	0.39	0.15	0.41	**2.64**
160000	4.94	4.97	0.27	0.07	0.20	**1.95**	5.58	5.52	0.31	0.10	0.03	**1.45**	7.06	7.10	0.40	0.16	0.38	**2.58**
170000	5.01	5.03	0.27	0.07	0.19	**1.92**	5.64	5.58	0.32	0.10	0.02	**1.44**	7.14	7.19	0.41	0.17	0.33	**2.46**
180000	5.07	5.09	0.27	0.07	0.18	**1.91**	5.70	5.64	0.32	0.10	0.02	**1.43**	7.21	7.28	0.42	0.18	0.30	**2.39**
190000	5.12	5.14	0.27	0.07	0.16	**1.87**	5.76	5.69	0.33	0.11	0.02	**1.42**	7.28	7.37	0.43	0.18	0.27	**2.32**
200000	5.17	5.18	0.27	0.07	0.17	**1.86**	5.81	5.74	0.34	0.11	0.01	**1.42**	7.35	7.44	0.44	0.19	0.24	**2.24**

Table B6(b) Statistical parameters for the STA DBM-2 prepared with VG40 bitumen

Passes	55 °C						60 °C						65 °C					
	Mean	**Median**	**Mode**	**Standard Deviation**	**Skewness**	**Kurtosis**	**Mean**	**Median**	**Mode**	**Standard Deviation**	**Skewness**	**Kurtosis**	**Mean**	**Median**	**Mode**	**Standard Deviation**	**Skewness**	**Kurtosis**
500	1.67	1.75	0.38	0.14	-0.17	**1.82**	2.08	2.11	0.14	0.02	0.16	**2.63**	3.01	3.01	0.12	0.02	0.08	**2.40**
1000	2.12	2.26	0.43	0.18	-0.26	**1.71**	2.71	2.72	0.15	0.02	0.03	**2.86**	3.97	3.99	0.16	0.02	-0.22	**2.18**
2000	2.78	2.98	0.48	0.23	-0.34	**1.60**	3.61	3.62	0.18	0.03	-0.15	**3.10**	5.17	5.29	0.27	0.07	-0.70	**2.39**
4000	3.71	3.99	0.55	0.30	-0.40	**1.52**	4.83	4.86	0.25	0.06	-0.04	**2.76**	6.55	6.67	0.42	0.18	-0.71	**2.14**
6000	4.40	4.72	0.59	0.35	-0.42	**1.52**	5.68	5.67	0.33	0.11	0.19	**2.49**	7.42	7.53	0.50	0.25	-0.56	**1.96**
8000	4.93	5.24	0.62	0.38	-0.42	**1.54**	6.31	6.33	0.42	0.18	0.32	**2.32**	8.07	8.19	0.54	0.29	-0.46	**1.89**
10000	5.36	5.66	0.64	0.40	-0.40	**1.56**	6.81	6.79	0.51	0.26	0.36	**2.25**	8.60	8.75	0.56	0.31	-0.41	**1.86**
12000	5.71	6.00	0.65	0.42	-0.38	**1.57**	7.20	7.20	0.59	0.34	0.37	**2.19**	9.05	9.23	0.57	0.32	-0.37	**1.83**
14000	6.00	6.28	0.66	0.44	-0.36	**1.58**	7.53	7.49	0.66	0.43	0.37	**2.13**	9.45	9.58	0.58	0.33	-0.34	**1.79**
16000	6.24	6.51	0.67	0.45	-0.34	**1.60**	7.81	7.71	0.72	0.52	0.35	**2.07**	9.82	9.97	0.59	0.34	-0.32	**1.75**
18000	6.44	6.71	0.68	0.46	-0.31	**1.61**	8.05	7.94	0.77	0.60	0.34	**2.00**	10.15	10.33	0.59	0.35	-0.31	**1.71**
20000	6.62	6.88	0.68	0.47	-0.28	**1.62**	8.25	8.19	0.82	0.67	0.32	**1.93**	10.46	10.67	0.60	0.36	-0.29	**1.67**
30000	7.23	7.47	0.71	0.51	-0.15	**1.69**	9.02	9.14	0.97	0.94	0.21	**1.61**	11.75	12.07	0.65	0.43	-0.28	**1.58**
40000	7.62	7.82	0.75	0.56	-0.05	**1.76**	9.56	9.65	1.05	1.11	0.11	**1.37**	12.78	13.11	0.71	0.50	-0.32	**1.63**
50000	7.91	8.09	0.79	0.62	0.02	**1.83**	9.99	10.04	1.11	1.24	0.05	**1.21**	13.64	13.98	0.76	0.58	-0.38	**1.77**
60000	8.15	8.31	0.82	0.67	0.08	**1.89**	10.35	10.37	1.16	1.36	0.02	**1.14**	14.40	14.74	0.82	0.67	-0.45	**1.94**
70000	8.36	8.50	0.86	0.73	0.13	**1.95**	10.68	10.66	1.22	1.48	0.01	**1.12**	15.08	15.41	0.87	0.76	-0.51	**2.13**
80000	8.55	8.68	0.89	0.79	0.16	**2.00**	10.97	10.92	1.27	1.61	0.02	**1.14**	15.70	16.01	0.92	0.85	-0.57	**2.31**
90000	8.72	8.83	0.92	0.84	0.20	**2.04**	11.23	11.15	1.32	1.74	0.04	**1.17**						
100000	8.87	8.98	0.94	0.89	0.23	**2.08**	11.48	11.37	1.37	1.87	0.07	**1.21**						
110000	9.02	9.11	0.97	0.94	0.26	**2.12**	11.70	11.58	1.42	2.00	0.09	**1.26**						
120000	9.15	9.23	0.99	0.98	0.29	**2.15**	11.92	11.77	1.46	2.14	0.12	**1.30**						
130000	9.28	9.35	1.01	1.03	0.31	**2.18**	12.12	11.95	1.51	2.28	0.15	**1.35**						
140000	9.40	9.46	1.04	1.07	0.33	**2.21**	12.31	12.12	1.56	2.42	0.17	**1.39**						
150000	9.52	9.56	1.06	1.12	0.35	**2.23**	12.49	12.28	1.60	2.56	0.20	**1.43**						
160000	9.63	9.66	1.08	1.16	0.37	**2.26**	12.66	12.43	1.65	2.71	0.22	**1.47**						
170000	9.73	9.76	1.10	1.20	0.39	**2.27**	12.83	12.58	1.69	2.85	0.24	**1.50**						
180000	9.83	9.85	1.11	1.24	0.41	**2.29**	12.99	12.72	1.73	3.00	0.26	**1.54**						
190000	9.93	9.94	1.13	1.28	0.42	**2.31**	13.14	12.86	1.77	3.14	0.28	**1.57**						
200000	10.02	10.02	1.15	1.32	0.44	**2.34**	13.29	12.99	1.81	3.28	0.30	**1.60**						

Table B7(a) Statistical parameters for the LTA DBM-2 prepared with VG40 bitumen

Passes	40 °C						45 °C						50 °C					
	Mean	**Median**	**Mode**	**Standard Deviation**	**Skewness**	**Kurtosis**	**Mean**	**Median**	**Mode**	**Standard Deviation**	**Skewness**	**Kurtosis**	**Mean**	**Median**	**Mode**	**Standard Deviation**	**Skewness**	**Kurtosis**
500	0.19	0.15	0.11	0.01	0.94	**2.49**	0.40	0.28	0.31	0.10	1.23	**2.77**	0.67	0.72	0.19	0.04	-0.67	**2.66**
1000	0.27	0.22	0.13	0.02	0.87	**2.37**	0.54	0.43	0.34	0.12	1.19	**2.70**	0.82	0.88	0.21	0.04	-0.62	**2.61**
2000	0.38	0.32	0.16	0.02	0.72	**2.17**	0.74	0.62	0.37	0.14	1.09	**2.56**	1.02	1.10	0.22	0.05	-0.51	**2.46**
4000	0.53	0.47	0.18	0.03	0.48	**1.93**	1.04	0.86	0.40	0.16	0.92	**2.31**	1.30	1.41	0.23	0.05	-0.30	**2.30**
6000	0.66	0.59	0.20	0.04	0.40	**1.94**	1.27	1.14	0.41	0.17	0.82	**2.18**	1.53	1.64	0.23	0.05	-0.14	**2.28**
8000	0.76	0.69	0.21	0.04	0.36	**2.00**	1.46	1.31	0.42	0.18	0.77	**2.13**	1.73	1.84	0.24	0.06	-0.04	**2.37**
10000	0.85	0.78	0.22	0.05	0.34	**2.06**	1.63	1.49	0.42	0.18	0.75	**2.13**	1.90	2.01	0.25	0.06	0.00	**2.52**
12000	0.92	0.87	0.22	0.05	0.36	**2.11**	1.77	1.64	0.42	0.18	0.76	**2.15**	2.06	2.16	0.25	0.06	0.03	**2.77**
14000	0.99	0.95	0.23	0.05	0.36	**2.15**	1.90	1.76	0.42	0.18	0.78	**2.17**	2.20	2.30	0.26	0.07	-0.02	**2.95**
16000	1.06	1.03	0.24	0.06	0.41	**2.19**	2.01	1.87	0.42	0.18	0.81	**2.22**	2.34	2.43	0.27	0.07	-0.04	*3.20*
18000	1.12	1.09	0.25	0.06	0.41	**2.18**	2.11	1.97	0.42	0.18	0.85	**2.25**	2.46	2.56	0.28	0.08	-0.06	*3.41*
20000	1.17	1.12	0.25	0.06	0.42	**2.17**	2.20	2.06	0.42	0.18	0.89	**2.28**	2.58	2.67	0.28	0.08	-0.12	*3.59*
30000	1.39	1.30	0.28	0.08	0.44	**1.96**	2.55	2.39	0.43	0.18	1.03	**2.38**	3.06	3.15	0.32	0.10	-0.31	*4.58*
40000	1.56	1.46	0.31	0.09	0.40	**1.73**	2.79	2.59	0.44	0.19	1.05	**2.41**	3.43	3.52	0.34	0.12	-0.43	*5.14*
50000	1.70	1.58	0.32	0.11	0.34	**1.58**	2.97	2.75	0.45	0.21	1.01	**2.38**	3.71	3.80	0.36	0.13	-0.49	*5.61*
60000	1.82	1.70	0.34	0.12	0.32	**1.53**	3.12	2.89	0.47	0.22	0.93	**2.33**	3.94	4.02	0.38	0.14	-0.52	*5.89*
70000	1.93	1.81	0.36	0.13	0.32	**1.56**	3.24	3.02	0.48	0.23	0.85	**2.28**	4.12	4.20	0.39	0.15	-0.50	*6.05*
80000	2.02	1.92	0.37	0.14	0.33	**1.62**	3.35	3.13	0.49	0.24	0.78	**2.21**	4.27	4.34	0.40	0.16	-0.49	*6.14*
90000	2.11	2.03	0.38	0.15	0.36	**1.73**	3.45	3.22	0.50	0.25	0.72	**2.17**	4.39	4.46	0.40	0.16	-0.46	*6.21*
100000	2.18	2.13	0.39	0.15	0.39	**1.85**	3.54	3.30	0.51	0.26	0.68	**2.14**	4.49	4.56	0.41	0.17	-0.43	*6.29*
110000	2.25	2.22	0.40	0.16	0.41	**1.96**	3.62	3.37	0.52	0.27	0.64	**2.14**	4.58	4.65	0.41	0.17	-0.41	*6.38*
120000	2.32	2.29	0.41	0.17	0.45	**2.09**	3.70	3.44	0.53	0.28	0.62	**2.19**	4.66	4.72	0.41	0.17	-0.38	*6.40*
130000	2.39	2.35	0.42	0.18	0.48	**2.20**	3.77	3.52	0.54	0.30	0.62	**2.27**	4.73	4.79	0.41	0.17	-0.37	*6.49*
140000	2.45	2.41	0.43	0.19	0.51	**2.30**	3.84	3.59	0.56	0.31	0.63	**2.38**	4.79	4.85	0.41	0.17	-0.33	*6.57*
150000	2.51	2.47	0.45	0.20	0.53	**2.36**	3.91	3.66	0.57	0.32	0.66	**2.53**	4.85	4.91	0.41	0.17	-0.31	*6.61*
160000	2.56	2.53	0.46	0.21	0.55	**2.44**	3.97	3.72	0.58	0.34	0.69	**2.74**	4.89	4.96	0.41	0.17	-0.29	*6.71*
170000	2.62	2.58	0.46	0.22	0.57	**2.52**	4.03	3.78	0.59	0.35	0.73	**2.97**	4.94	5.01	0.41	0.17	-0.28	*6.82*
180000	2.67	2.63	0.47	0.22	0.58	**2.57**	4.09	3.85	0.60	0.37	0.78	*3.25*	4.99	5.06	0.41	0.17	-0.26	*6.86*
190000	2.72	2.68	0.48	0.23	0.60	**2.63**	4.15	3.90	0.62	0.38	0.84	*3.54*	5.03	5.10	0.41	0.17	-0.26	*6.88*
200000	2.76	2.73	0.49	0.24	0.61	**2.68**	4.20	3.96	0.63	0.40	0.92	*3.89*	5.06	5.14	0.42	0.17	-0.24	*6.96*

Table B7(b) Statistical parameters for the LTA DBM-2 prepared with VG40 bitumen

Passes	55 °C						60 °C						65 °C					
	Mean	**Median**	**Mode**	**Standard Deviation**	**Skewness**	**Kurtosis**	**Mean**	**Median**	**Mode**	**Standard Deviation**	**Skewness**	**Kurtosis**	**Mean**	**Median**	**Mode**	**Standard Deviation**	**Skewness**	**Kurtosis**
500	0.91	0.92	0.20	0.04	-0.02	**2.24**	1.53	1.56	0.18	0.03	-0.38	2.41	2.17	2.14	0.25	0.06	1.20	*3.85*
1000	1.17	1.18	0.22	0.05	-0.16	**2.19**	2.01	2.05	0.17	0.03	-0.29	2.84	3.05	2.99	0.33	0.11	1.07	*4.10*
2000	1.52	1.57	0.22	0.05	-0.30	**2.08**	2.71	2.75	0.17	0.03	0.04	2.99	4.20	4.20	0.42	0.17	0.68	*3.29*
4000	2.03	2.08	0.23	0.05	-0.42	**1.85**	3.65	3.62	0.20	0.04	0.10	2.63	5.45	5.21	0.52	0.27	0.75	**2.79**
6000	2.41	2.48	0.23	0.05	-0.41	**1.67**	4.27	4.18	0.25	0.06	0.02	2.49	6.13	5.84	0.63	0.39	0.72	**2.24**
8000	2.71	2.78	0.25	0.06	-0.34	**1.58**	4.70	4.61	0.30	0.09	0.03	2.31	6.58	6.31	0.71	0.50	0.65	**2.00**
10000	2.97	3.03	0.26	0.07	-0.22	**1.57**	5.00	4.93	0.34	0.11	0.06	2.17	6.91	6.66	0.75	0.57	0.60	**1.92**
12000	3.19	3.25	0.28	0.08	-0.10	**1.60**	5.23	5.17	0.37	0.13	0.09	2.07	7.17	6.94	0.78	0.61	0.58	**1.88**
14000	3.37	3.42	0.30	0.09	0.01	**1.64**	5.41	5.35	0.39	0.15	0.10	2.02	7.40	7.16	0.79	0.63	0.56	**1.86**
16000	3.54	3.57	0.31	0.10	0.10	**1.67**	5.55	5.49	0.40	0.16	0.12	2.01	7.59	7.36	0.80	0.64	0.54	**1.83**
18000	3.68	3.70	0.33	0.11	0.18	**1.71**	5.66	5.59	0.42	0.17	0.13	2.01	7.76	7.54	0.81	0.65	0.53	**1.80**
20000	3.81	3.82	0.35	0.12	0.24	**1.74**	5.76	5.67	0.43	0.18	0.14	2.03	7.92	7.69	0.81	0.65	0.51	**1.78**
30000	4.29	4.24	0.43	0.19	0.42	**1.81**	6.11	6.01	0.46	0.21	0.20	2.20	8.56	8.31	0.81	0.65	0.46	**1.66**
40000	4.61	4.53	0.49	0.24	0.49	**1.83**	6.35	6.26	0.48	0.23	0.26	2.43	9.07	8.84	0.80	0.65	0.42	**1.60**
50000	4.85	4.79	0.54	0.29	0.51	**1.83**	6.55	6.47	0.50	0.25	0.31	2.65	9.49	9.32	0.80	0.65	0.40	**1.58**
60000	5.05	4.99	0.58	0.33	0.51	**1.81**	6.72	6.65	0.51	0.26	0.36	2.85	9.87	9.73	0.81	0.65	0.38	**1.59**
70000	5.22	5.14	0.61	0.37	0.52	**1.79**	6.87	6.81	0.52	0.27	0.40	*3.04*	10.20	10.08	0.81	0.66	0.36	**1.62**
80000	5.37	5.27	0.64	0.41	0.52	**1.77**	7.01	6.95	0.54	0.29	0.45	*3.21*	10.50	10.40	0.82	0.67	0.34	**1.66**
90000	5.51	5.39	0.67	0.44	0.51	**1.76**	7.13	7.08	0.55	0.30	0.48	*3.37*	10.78	10.69	0.82	0.68	0.33	**1.72**
100000	5.64	5.50	0.69	0.48	0.51	**1.74**	7.24	7.21	0.56	0.31	0.52	*3.51*	11.03	10.96	0.83	0.69	0.31	**1.77**
110000	5.76	5.60	0.72	0.51	0.52	**1.72**	7.35	7.32	0.57	0.32	0.55	*3.64*	11.27	11.21	0.84	0.70	0.29	**1.83**
120000	5.87	5.70	0.74	0.54	0.52	**1.71**	7.44	7.43	0.58	0.34	0.58	*3.76*	11.50	11.45	0.85	0.72	0.27	**1.89**
130000	5.98	5.78	0.76	0.58	0.52	**1.69**	7.53	7.54	0.59	0.35	0.61	*3.87*	11.71	11.67	0.86	0.74	0.24	**1.95**
140000	6.08	5.86	0.78	0.61	0.52	**1.68**	7.62	7.63	0.60	0.36	0.63	*3.97*	11.91	11.88	0.87	0.75	0.22	**2.01**
150000	6.17	5.94	0.80	0.64	0.52	**1.67**	7.70	7.73	0.61	0.37	0.65	*4.06*	12.11	12.08	0.88	0.77	0.20	**2.07**
160000	6.26	6.02	0.82	0.67	0.52	**1.66**	7.78	7.82	0.62	0.38	0.67	*4.15*	12.29	12.28	0.89	0.79	0.17	**2.13**
170000	6.35	6.09	0.84	0.70	0.52	**1.65**	7.85	7.90	0.62	0.39	0.69	*4.23*	12.47	12.46	0.90	0.81	0.15	**2.18**
180000	6.44	6.15	0.86	0.73	0.52	**1.64**	7.92	7.98	0.63	0.40	0.71	*4.30*	12.64	12.56	0.91	0.83	0.13	**2.23**
190000	6.52	6.22	0.87	0.76	0.53	**1.63**	7.99	8.06	0.64	0.41	0.73	*4.37*	12.80	12.71	0.92	0.85	0.10	**2.27**
200000	6.59	6.28	0.89	0.79	0.53	**1.62**	8.06	8.14	0.65	0.42	0.75	*4.44*	12.96	12.90	0.93	0.87	0.08	**2.32**

Table B8 Goodness of fit using K-S statistic for the LTA BC-2 preparedwith VG20 bitumen

Passes	40 °C			45 °C			50 °C			55 °C			60 °C			65 °C		
	Normal	Lognormal	Weibull	Normal	Lognormal	Weibull	Normal	Lognormal	Weibull	Normal	Lognormal	Weibull	Normal	Lognormal	Weibull	Normal	Lognormal	Weibull
500	***0.130***	0.145	0.140	0.152	0.186	***0.085***	0.170	0.164	***0.146***	0.235	0.257	0.166	0.223	***0.198***	0.252	0.203	0.202	***0.177***
1000	***0.147***	0.158	0.159	0.153	0.185	***0.084***	0.146	0.148	***0.115***	0.193	0.217	0.153	0.270	***0.250***	0.294	0.191	0.198	***0.132***
2000	0.166	***0.152***	0.186	0.148	0.178	***0.103***	0.120	0.130	***0.094***	0.140	0.171	0.146	0.275	***0.257***	0.299	0.152	***0.134***	0.195
4000	0.164	***0.156***	0.177	0.126	***0.133***	0.158	0.135	***0.121***	0.183	0.135	0.133	0.105	0.156	***0.149***	0.192	0.214	***0.193***	0.230
6000	0.140	***0.136***	0.156	0.150	***0.122***	0.180	0.154	***0.140***	0.201	0.137	0.138	0.131	0.173	0.171	***0.161***	0.257	***0.239***	0.264
8000	***0.121***	0.128	0.140	0.160	***0.130***	0.188	0.184	***0.171***	0.227	0.138	0.145	0.134	0.166	***0.162***	0.169	0.267	***0.255***	0.265
10000	0.107	***0.107***	0.127	0.155	***0.125***	0.183	0.153	***0.142***	0.200	0.141	0.151	0.159	0.158	***0.154***	0.165	0.293	***0.281***	0.287
12000	0.097	***0.096***	0.117	0.169	***0.139***	0.191	0.143	***0.135***	0.192	0.146	0.156	0.163	0.161	***0.156***	0.172	0.270	***0.260***	0.270
14000	0.090	***0.088***	0.110	0.181	***0.151***	0.200	0.130	***0.141***	0.145	0.149	0.154	0.172	0.145	***0.143***	0.160	0.279	***0.269***	0.271
16000	0.085	***0.080***	0.105	0.191	***0.161***	0.208	0.141	0.153	***0.118***	0.152	0.152	***0.152***	***0.137***	0.143	0.143	0.283	***0.273***	0.276
18000	0.081	***0.072***	0.103	0.199	***0.170***	0.215	0.152	0.162	***0.104***	0.147	0.148	***0.143***	0.140	***0.137***	0.139	0.264	***0.251***	0.263
20000	0.079	***0.072***	0.102	0.205	***0.177***	0.221	0.167	0.178	***0.098***	0.142	0.144	***0.133***	0.142	0.140	***0.136***	0.252	***0.248***	0.251
30000	0.084	***0.076***	0.104	0.221	***0.197***	0.235	0.156	0.168	***0.109***	0.149	0.151	***0.126***	0.147	0.148	***0.127***	0.238	***0.227***	0.245
40000	0.098	***0.085***	0.112	0.199	***0.177***	0.219	0.141	0.154	***0.123***	0.176	0.179	***0.126***	0.135	0.136	***0.113***	0.246	***0.239***	0.251
50000	0.110	***0.100***	0.120	0.186	***0.168***	0.203	0.133	0.147	***0.123***	0.176	0.179	***0.138***	0.127	0.128	***0.104***			
60000	0.121	***0.112***	0.127	0.166	***0.149***	0.189	0.112	0.126	***0.120***	0.176	0.179	***0.132***	0.121	0.121	***0.105***			
70000	0.130	***0.122***	0.134	***0.162***	0.147	0.181	***0.099***	0.112	0.123	0.178	0.180	***0.128***	0.117	0.121	***0.106***			
80000	0.137	***0.130***	0.140	***0.154***	0.140	0.177	***0.089***	0.103	0.119	0.179	0.182	***0.125***	0.118	0.122	***0.106***			
90000	0.144	***0.137***	0.144	***0.138***	0.125	0.167	***0.080***	0.095	0.121	0.177	0.180	***0.123***	0.119	0.123	***0.106***			
100000	0.149	***0.143***	0.149	***0.117***	0.126	0.151	***0.073***	0.081	0.119	0.175	0.178	***0.122***	0.120	0.124	***0.105***			
110000	0.154	***0.148***	0.152	***0.128***	0.137	0.131	***0.077***	***0.070***	0.123	0.172	0.175	***0.124***	0.121	0.125	***0.105***			
120000	0.158	***0.153***	0.155	***0.142***	0.151	0.163	0.082	***0.069***	0.128	0.170	0.173	***0.126***	0.122	0.126	***0.106***			
130000	0.161	***0.157***	0.158	***0.159***	0.168	0.165	0.093	***0.076***	0.135	0.167	0.171	***0.124***	0.122	0.127	***0.107***			
140000	0.165	***0.161***	0.161	0.179	0.188	***0.153***	0.103	***0.087***	0.145	0.165	0.168	***0.121***	0.123	0.127	***0.108***			
150000	0.159	***0.155***	0.162	0.201	0.210	***0.154***	0.114	***0.097***	0.154	0.163	0.166	***0.117***	0.123	0.128	***0.109***			
160000	0.161	***0.153***	0.165	0.226	0.234	***0.181***	0.123	***0.106***	0.162	0.160	0.164	***0.114***	0.124	0.128	***0.109***			
170000	0.165	***0.157***	0.168	0.230	0.237	***0.138***	0.132	***0.114***	0.169	0.158	0.162	***0.114***	0.125	0.129	***0.110***			
180000	0.168	***0.161***	0.171	0.241	0.247	***0.145***	0.140	***0.122***	0.176	0.156	0.159	***0.113***	0.125	0.129	***0.111***			
190000	0.164	***0.156***	0.168	0.267	0.273	***0.173***	0.147	***0.130***	0.182	0.154	0.157	***0.117***	0.125	0.129	***0.110***			
200000	0.158	***0.149***	0.170	0.242	0.247	***0.149***	0.154	***0.136***	0.187	0.151	0.155	***0.121***	0.125	0.130	***0.109***			

Table B9 Goodness of fit using K-S statistic for the STA BC-2 prepared with VG40 bitumen

Passes	40 °C			45 °C			50 °C			55 °C			60 °C			65 °C		
	Normal	**Lognormal**	**Weibull**	**Normal**	**Lognormal**	**Weibull**	**Normal**	**Lognormal**	**Weibull**	**Normal**	**Lognormal**	**Weibull**	**Normal**	**Lognormal**	**Weibull**	**Normal**	**Lognormal**	**Weibull**
500	0.121	0.154	***0.074***	0.183	0.224	***0.140***	0.130	0.140	0.107	0.176	***0.173***	0.189	0.138	0.163	***0.127***	0.131	***0.128***	0.131
1000	0.124	0.151	***0.086***	0.177	0.206	***0.136***	0.130	0.124	0.144	***0.162***	0.163	0.168	0.122	0.143	***0.121***	0.116	***0.104***	0.125
2000	0.132	0.170	***0.124***	0.199	0.215	***0.140***	0.201	0.180	0.236	0.166	0.165	***0.165***	0.118	0.126	***0.106***	0.141	***0.133***	0.145
4000	***0.130***	0.133	0.143	0.210	0.231	***0.161***	0.246	0.231	0.271	0.143	0.141	***0.131***	0.114	0.121	***0.121***	0.134	***0.126***	0.139
6000	0.132	***0.111***	0.180	0.235	0.235	***0.203***	0.251	0.237	0.278	0.133	0.135	***0.111***	0.127	***0.112***	0.149	0.119	***0.110***	0.128
8000	0.138	***0.115***	0.180	0.240	0.245	***0.209***	0.271	0.260	0.298	***0.132***	0.134	0.146	0.164	***0.150***	0.173	0.090	***0.079***	0.106
10000	0.138	***0.114***	0.176	0.207	0.216	***0.178***	0.237	0.225	0.273	***0.130***	0.133	0.166	0.198	***0.186***	0.200	0.086	***0.073***	0.111
12000	0.169	***0.148***	0.193	0.177	0.189	***0.158***	0.143	0.140	0.183	***0.129***	0.132	0.156	0.219	***0.209***	0.217	0.078	***0.074***	0.098
14000	0.179	***0.159***	0.198	0.156	0.165	***0.147***	0.120	0.117	0.129	***0.128***	0.133	0.171	0.217	***0.210***	0.216	0.076	***0.072***	0.104
16000	0.190	***0.174***	0.200	0.149	0.156	***0.135***	0.127	0.129	0.144	***0.131***	0.136	0.184	0.210	***0.199***	0.213	0.066	***0.062***	0.085
18000	0.208	***0.195***	0.212	0.142	0.149	***0.129***	0.169	0.177	0.175	***0.130***	0.134	0.183	0.203	***0.192***	0.209	***0.067***	0.075	0.086
20000	0.211	***0.198***	0.212	***0.136***	0.156	0.147	0.208	0.214	0.187	0.138	***0.133***	0.194	0.197	***0.185***	0.205	***0.071***	0.078	0.095
30000	0.212	***0.200***	0.211	***0.163***	0.163	0.204	0.138	0.136	0.128	***0.181***	0.169	0.231	0.170	***0.156***	0.186	0.091	0.107	***0.097***
40000	0.207	***0.193***	0.206	0.193	***0.171***	0.231	0.120	***0.119***	0.147	0.202	***0.189***	0.249	0.156	***0.142***	0.176	0.113	0.127	***0.103***
50000	0.202	***0.187***	0.201	0.203	***0.182***	0.243	0.137	***0.123***	0.184	0.219	***0.205***	*0.263*	0.151	***0.136***	0.171	0.149	0.163	***0.104***
60000	0.197	***0.181***	0.197	0.186	***0.165***	0.228	0.162	***0.147***	0.207	0.231	***0.217***	0.273	0.149	***0.135***	0.169	0.210	0.219	***0.123***
70000	0.192	***0.175***	0.194	0.171	***0.150***	0.214	0.164	***0.148***	0.208	0.231	***0.217***	0.272	0.149	***0.135***	0.169			
80000	0.188	***0.170***	0.191	0.159	***0.139***	0.203	0.163	***0.147***	0.206	0.230	***0.216***	0.272	0.149	***0.136***	0.169			
90000	0.184	***0.169***	0.188	0.149	***0.129***	0.193	0.176	***0.160***	0.213	0.230	***0.215***	0.272	0.150	***0.138***	0.170			
100000	0.181	***0.173***	0.185	0.143	***0.124***	0.185	0.189	***0.173***	0.224	0.236	***0.222***	0.272	0.152	***0.139***	0.171			
110000	0.177	***0.173***	0.182	0.142	***0.138***	0.178	0.201	***0.185***	0.233	0.239	***0.224***	0.271	0.156	***0.141***	0.187			
120000	0.173	***0.169***	0.180	0.142	***0.138***	0.173	0.212	***0.196***	0.242	0.241	***0.227***	0.272	0.167	***0.153***	0.197			
130000	0.170	***0.164***	0.178	0.141	***0.135***	0.172	0.222	***0.207***	0.250	0.243	***0.229***	0.274	0.169	***0.155***	0.199			
140000	0.167	***0.160***	0.175	0.141	***0.132***	0.171	0.232	***0.216***	0.257	0.245	***0.230***	0.275	0.173	***0.160***	0.200			
150000	0.163	**0.156**	0.173	0.141	***0.128***	0.177	0.240	***0.225***	0.264	0.246	***0.232***	0.276	0.174	***0.160***	0.202			
160000	0.160	**0.152**	0.171	0.141	***0.124***	0.188	0.249	***0.234***	0.271	0.247	***0.233***	0.277	0.176	***0.163***	0.204			
170000	0.157	**0.149**	0.168	0.141	***0.121***	0.182	0.256	***0.241***	0.276	0.249	***0.234***	0.278	0.178	***0.165***	0.206			
180000	0.154	**0.150**	0.166	0.141	0.121	0.177	0.252	***0.238***	0.273	0.250	***0.235***	0.278	0.181	***0.168***	0.208			
190000	0.150	**0.150**	0.164	0.141	0.122	0.172	0.249	***0.234***	0.270	0.250	***0.236***	0.279	0.182	***0.170***	0.209			
200000	0.147	**0.147**	0.162	0.141	0.122	0.170	0.246	***0.231***	0.268	0.251	***0.236***	0.279	0.177	***0.164***	0.205			

Table B10 Goodness of fit using K-S statistic for the LTA BC-2 prepared with VG40 bitumen

Passes	40 °C			45 °C			50 °C			55 °C			60 °C			65 °C		
	Normal	**Lognormal**	**Weibull**	**Normal**	**Lognormal**	**Weibull**	**Normal**	**Lognormal**	**Weibull**	**Normal**	**Lognormal**	**Weibull**	**Normal**	**Lognormal**	**Weibull**	**Normal**	**Lognormal**	**Weibull**
500	0.153	0.179	***0.121***	0.170	***0.092***	0.143	0.199	0.198	***0.170***	0.190	0.225	***0.135***	0.207	0.211	***0.206***	0.197	***0.173***	0.209
1000	0.116	0.158	***0.114***	0.178	***0.107***	0.160	0.191	0.210	***0.160***	0.235	0.254	***0.178***	0.205	0.209	***0.188***	0.193	0.193	***0.179***
2000	0.134	0.138	***0.098***	0.176	***0.117***	0.166	0.211	0.234	***0.136***	0.223	0.238	***0.157***	0.185	0.192	***0.154***	0.178	0.181	***0.175***
4000	0.151	0.130	***0.115***	0.184	***0.149***	0.182	0.206	0.221	***0.136***	0.136	0.145	***0.071***	0.150	0.159	***0.098***	0.169	0.169	***0.164***
6000	0.165	0.141	***0.130***	0.192	***0.165***	0.192	0.184	0.204	***0.111***	0.114	0.129	***0.064***	0.134	0.141	***0.101***	0.187	***0.181***	0.184
8000	0.171	0.147	***0.136***	0.202	***0.183***	0.203	0.177	0.199	***0.093***	***0.080***	0.092	0.089	0.119	***0.117***	0.151	0.212	***0.209***	0.201
10000	0.172	0.149	***0.139***	0.213	***0.195***	0.215	0.163	0.182	***0.085***	***0.064***	0.073	0.084	0.129	***0.128***	0.167	0.219	***0.217***	0.206
12000	0.172	0.150	***0.139***	0.216	***0.199***	0.219	0.146	0.165	***0.078***	0.078	***0.076***	0.110	***0.132***	0.142	0.170	0.218	***0.215***	0.205
14000	0.170	0.150	***0.138***	0.201	***0.183***	0.207	0.119	0.137	***0.072***	0.088	***0.083***	0.127	***0.135***	0.144	0.172	0.213	***0.210***	0.201
16000	0.169	0.149	***0.137***	0.186	***0.165***	0.196	0.112	0.126	***0.068***	0.103	***0.093***	0.144	***0.126***	0.129	0.173	0.207	***0.204***	0.196
18000	0.167	0.149	***0.136***	0.170	***0.148***	0.184	0.106	0.120	***0.066***	0.117	***0.106***	0.160	0.140	***0.137***	0.187	0.201	***0.197***	0.190
20000	0.166	0.148	***0.135***	0.154	***0.130***	0.171	0.101	0.115	***0.067***	0.126	***0.113***	0.170	0.151	***0.147***	0.201	0.194	***0.189***	0.184
30000	0.159	0.145	***0.129***	0.126	***0.141***	0.146	0.082	0.092	***0.104***	0.134	***0.133***	0.179	***0.130***	0.135	0.182	0.164	***0.154***	*0.175*
40000	0.152	0.141	***0.124***	0.119	0.132	***0.110***	0.080	0.088	***0.098***	0.150	***0.133***	0.188	***0.120***	0.121	0.171	0.157	***0.146***	*0.160*
50000	0.147	0.136	***0.122***	0.120	0.143	***0.113***	0.101	0.103	***0.096***	0.160	***0.143***	*0.197*	0.113	***0.108***	0.169	0.155	***0.145***	0.160
60000	0.142	0.136	***0.127***	0.161	0.181	***0.111***	0.109	0.110	***0.093***	0.151	***0.135***	0.189	0.127	***0.121***	0.183	0.154	***0.144***	0.177
70000	0.137	0.156	***0.131***	0.181	0.199	***0.111***	0.113	0.114	***0.086***	0.134	***0.119***	0.174	0.104	***0.099***	0.160	0.153	***0.143***	0.165
80000	0.155	0.173	***0.133***	0.183	0.201	***0.119***	0.116	0.116	***0.096***	0.142	***0.127***	0.186	0.118	***0.112***	0.174	0.153	***0.142***	0.181
90000	0.169	0.184	***0.136***	0.171	0.189	***0.121***	0.116	0.117	***0.100***	0.122	***0.107***	0.164	0.131	***0.124***	0.187	0.162	***0.141***	0.197
100000	0.180	0.192	***0.138***	0.149	0.167	***0.120***	0.116	0.117	***0.095***	0.125	***0.112***	0.156	0.137	***0.131***	0.193	0.178	***0.157***	0.211
110000	0.189	0.200	***0.139***	0.122	0.140	***0.111***	0.116	0.117	***0.091***	0.124	***0.110***	0.153	0.121	***0.115***	0.178	0.168	***0.147***	0.203
120000	0.197	0.206	***0.148***	0.110	0.116	***0.102***	0.109	0.111	***0.089***	0.123	***0.110***	0.152	0.129	***0.122***	0.184	0.168	***0.147***	0.197
130000	0.203	0.210	***0.155***	0.126	0.130	***0.104***	0.109	0.112	***0.090***	0.122	***0.109***	0.154	0.140	***0.133***	0.194			
140000	0.207	0.213	***0.161***	0.141	0.145	***0.131***	0.109	0.113	***0.092***	0.121	***0.109***	0.151	0.150	***0.144***	0.204			
150000	0.205	0.212	***0.160***	0.155	0.159	***0.155***	0.109	*0.113*	***0.094***	0.121	***0.108***	0.151	0.161	***0.154***	0.214			
160000	0.203	0.210	***0.158***	***0.148***	0.153	0.175	0.109	*0.113*	***0.096***	0.121	***0.109***	0.151	0.170	***0.163***	0.222			
170000	0.202	0.208	***0.156***	***0.160***	0.149	0.192	0.109	0.113	***0.097***	0.119	***0.114***	0.148	0.166	***0.160***	0.219			
180000	0.200	0.208	***0.155***	***0.172***	0.163	0.207	0.109	0.113	***0.100***	0.122	***0.118***	0.151	0.163	***0.156***	0.216			
190000	0.201	0.211	***0.153***	***0.182***	0.171	0.214	0.106	0.112	***0.102***	0.115	***0.120***	0.152	0.159	***0.153***	0.213			
200000	0.205	0.215	***0.154***	***0.169***	0.157	0.202	0.106	0.112	***0.105***	0.123	***0.111***	0.155	0.156	***0.149***	0.211			

Table B11 Goodness of fit using K-S statistic for the STA DBM-2 prepared with VG20 bitumen

Passes	40 °C			45 °C			50 °C			55 °C			60 °C			65 °C		
	Normal	**Lognormal**	**Weibull**	**Normal**	**Lognormal**	**Weibull**	**Normal**	**Lognormal**	**Weibull**	**Normal**	**Lognormal**	**Weibull**	**Normal**	**Lognormal**	**Weibull**	**Normal**	**Lognormal**	**Weibull**
500	***0.199***	0.200	0.213	0.224	0.260	***0.142***	0.146	0.169	***0.132***	0.124	***0.098***	0.157	0.130	0.146	***0.084***	0.135	0.119	0.149
1000	***0.201***	0.207	0.220	0.218	0.257	***0.123***	0.136	0.161	***0.123***	0.143	***0.135***	0.188	0.134	0.149	***0.087***	0.187	0.192	***0.147***
2000	0.206	0.211	***0.177***	0.162	0.200	***0.098***	0.144	***0.123***	0.181	***0.126***	0.143	0.151	0.095	0.110	***0.086***	0.194	0.204	***0.177***
4000	0.122	0.133	***0.070***	0.169	0.201	***0.113***	0.167	***0.140***	0.201	***0.129***	0.132	0.157	***0.072***	0.087	0.091	0.211	0.220	***0.176***
6000	0.164	0.174	***0.101***	0.144	0.161	***0.134***	0.135	***0.109***	0.173	0.135	***0.133***	0.139	***0.072***	0.076	0.091	0.186	0.193	***0.150***
8000	0.098	0.107	***0.091***	***0.146***	0.148	0.174	0.125	***0.099***	0.161	0.140	***0.140***	0.201	***0.093***	0.099	0.120	0.134	0.142	***0.140***
10000	***0.087***	0.097	0.108	***0.159***	0.174	0.196	0.117	***0.092***	0.155	0.171	0.172	***0.159***	***0.087***	0.091	0.129	***0.115***	0.117	0.117
12000	0.096	***0.085***	0.145	0.165	***0.155***	0.208	0.109	***0.091***	0.148	0.153	0.152	***0.147***	***0.080***	0.083	0.130	0.138	0.146	***0.128***
14000	0.096	***0.094***	0.143	0.174	***0.162***	0.221	0.101	***0.092***	0.141	0.170	0.166	***0.163***	0.080	***0.077***	0.129	0.142	0.143	***0.137***
16000	0.100	***0.098***	0.145	0.186	***0.172***	0.236	0.106	***0.097***	0.134	0.228	0.222	***0.213***	0.088	***0.076***	0.139	***0.134***	0.138	0.138
18000	***0.100***	0.102	0.137	0.191	***0.175***	0.242	0.112	***0.102***	0.127	0.253	0.246	***0.242***	0.095	***0.084***	0.147	0.137	0.139	***0.137***
20000	***0.106***	0.108	0.139	0.189	***0.173***	0.243	0.114	***0.105***	0.122	0.242	***0.236***	0.237	0.095	***0.083***	0.146	0.149	0.153	***0.142***
30000	***0.097***	0.102	0.141	0.232	***0.217***	0.273	0.117	***0.114***	0.120	0.243	***0.233***	0.244	0.083	***0.078***	0.135	**0.**140	***0.133***	0.161
40000	0.124	0.139	***0.110***	0.304	***0.291***	0.320	***0.112***	0.116	0.119	0.268	***0.260***	0.266	0.113	***0.106***	0.167	0.128	0.136	***0.113***
50000	***0.133***	0.148	0.147	0.308	***0.292***	0.345	0.116	***0.111***	0.128	0.294	0.288	***0.287***	0.118	***0.112***	0.168			
60000	***0.143***	0.158	0.166	0.267	***0.251***	0.315	0.127	***0.116***	0.136	0.317	0.313	***0.305***	0.106	***0.106***	0.138			
70000	***0.125***	0.140	0.159	0.232	***0.216***	0.288	0.129	***0.121***	0.137	0.332	0.329	***0.318***	0.131	***0.126***	0.181			
80000	***0.106***	0.118	0.152	0.210	***0.195***	0.270	0.129	***0.125***	0.131	0.318	0.314	***0.308***	0.136	***0.131***	0.185			
90000	0.111	***0.109***	0.160	0.197	***0.182***	0.259	0.133	0.130	***0.126***	0.304	0.299	***0.299***	0.125	***0.125***	0.180			
100000	0.114	***0.110***	0.164	0.192	***0.178***	0.255	0.136	0.134	***0.123***	0.290	***0.284***	0.290	0.140	***0.136***	0.194			
110000	***0.114***	0.117	0.163	0.192	***0.178***	0.255	0.139	0.138	***0.124***	0.277	***0.270***	0.282	0.122	***0.118***	0.179			
120000	***0.119***	0.123	0.163	0.195	***0.181***	0.257	0.142	0.141	***0.126***	0.264	***0.257***	0.273	0.118	***0.114***	0.161			
130000	***0.124***	0.127	0.159	0.192	***0.178***	0.255	0.145	0.144	***0.128***	0.251	***0.242***	0.264						
140000	0.127	***0.122***	0.155	0.190	***0.177***	0.254	0.147	0.147	***0.130***	0.236	***0.227***	0.254						
150000	0.129	***0.118***	0.155	0.184	***0.170***	0.249	0.150	*0.150*	***0.133***	0.222	***0.212***	0.244						
160000	0.129	***0.118***	0.155	0.177	***0.172***	0.244	0.152	*0.152*	***0.135***	0.208	***0.203***	0.234						
170000	0.126	***0.114***	0.157	0.173	***0.168***	0.239	0.153	0.154	***0.137***	0.195	***0.185***	0.224						
180000	0.124	***0.112***	0.166	0.171	***0.159***	0.235	0.156	0.155	***0.139***	0.182	***0.171***	0.214						
190000	0.122	***0.117***	0.175	0.170	***0.156***	0.235	0.159	0.157	***0.141***	0.170	***0.158***	0.205						
200000	0.122	***0.120***	0.171	0.169	***0.155***	0.238	0.162	0.160	***0.143***	0.158	***0.152***	0.196						

Table B12 Goodness of fit using K-S statistic for the LTA DBMC-2 with VG20 bitumen

Passes	40 °C			45 °C			50 °C			55 °C			60 °C			65 °C		
	Normal	**Lognormal**	**Weibull**	**Normal**	**Lognormal**	**Weibull**	**Normal**	**Lognormal**	**Weibull**	**Normal**	**Lognormal**	**Weibull**	**Normal**	**Lognormal**	**Weibull**	**Normal**	**Lognormal**	**Weibull**
500	0.283	0.320	***0.235***	0.158	0.161	***0.133***	0.108	***0.080***	0.129	0.191	0.226	***0.140***	0.127	0.141	***0.120***	0.187	***0.174***	0.197
1000	0.245	0.291	***0.197***	0.175	0.173	***0.141***	0.129	***0.104***	0.145	0.200	0.226	***0.140***	0.139	0.145	***0.111***	0.170	***0.155***	0.194
2000	0.233	0.262	***0.183***	0.164	0.192	***0.159***	0.142	***0.119***	0.157	0.165	0.189	***0.095***	0.146	0.147	***0.110***	0.172	0.176	***0.165***
4000	0.219	0.249	***0.162***	0.170	0.191	***0.139***	0.182	***0.158***	0.196	0.112	0.113	***0.083***	0.135	0.116	***0.166***	0.171	0.173	***0.148***
6000	0.188	0.225	***0.123***	0.161	0.180	***0.127***	0.156	***0.134***	0.177	0.087	0.073	***0.114***	0.175	0.169	***0.185***	0.161	0.163	***0.136***
8000	0.175	0.220	***0.104***	0.159	0.182	***0.135***	0.155	***0.134***	0.205	0.075	0.086	***0.116***	0.213	0.210	***0.210***	0.149	0.151	***0.128***
10000	0.172	0.216	***0.101***	0.170	0.187	***0.140***	0.176	***0.153***	0.226	0.110	0.132	***0.105***	0.188	***0.180***	0.196	0.156	0.158	***0.118***
12000	0.161	0.205	***0.096***	0.180	0.174	***0.153***	0.193	***0.168***	0.241	0.147	0.169	***0.103***	0.163	***0.152***	0.175	0.147	0.152	***0.111***
14000	0.145	0.190	***0.099***	0.176	0.171	***0.148***	0.205	***0.181***	0.253	0.153	0.178	***0.115***	0.149	***0.136***	0.171	0.175	0.180	***0.108***
16000	0.131	0.176	***0.101***	0.172	0.168	***0.149***	0.215	***0.190***	0.262	0.174	0.199	***0.117***	0.141	***0.125***	0.171	0.161	0.165	***0.142***
18000	0.118	0.163	***0.105***	0.168	0.165	***0.150***	0.222	***0.197***	0.268	0.194	0.220	***0.140***	0.140	***0.122***	0.176	***0.120***	0.119	0.165
20000	***0.106***	0.151	0.112	0.166	0.163	***0.151***	0.229	***0.204***	0.273	0.184	0.209	***0.156***	0.129	***0.112***	0.168	***0.116***	0.115	0.172
30000	0.113	***0.112***	0.139	0.163	0.176	***0.155***	0.250	***0.227***	0.279	***0.156***	0.181	0.172	0.108	***0.104***	0.143	0.201	0.198	***0.195***
40000	0.134	***0.095***	0.156	0.170	0.183	***0.158***	0.239	***0.216***	0.271	0.179	0.202	***0.175***	0.106	***0.102***	0.144	0.140	***0.136***	0.184
50000	0.149	***0.111***	0.169	0.182	0.193	***0.161***	0.222	***0.200***	0.258	***0.168***	0.190	0.173	0.100	***0.096***	0.136	0.132	0.133	***0.132***
60000	0.151	***0.114***	0.169	0.195	0.205	***0.164***	0.205	***0.184***	0.245	***0.159***	0.178	0.167	0.127	***0.115***	0.170	0.145	0.145	***0.119***
70000	0.150	***0.114***	0.168	0.191	0.201	***0.166***	0.188	***0.167***	0.235	***0.150***	0.168	0.160	0.136	***0.127***	0.177	0.140	0.139	***0.130***
80000	0.148	***0.113***	0.166	0.191	0.192	***0.169***	0.175	***0.153***	0.226	***0.142***	0.158	0.163	0.127	***0.127***	0.162	0.148	0.155	***0.145***
90000	0.146	***0.114***	0.164	0.194	0.199	***0.167***	0.165	***0.144***	0.220	***0.134***	0.150	0.165	***0.149***	0.150	0.159	0.154	0.161	***0.154***
100000	0.151	***0.120***	0.165	0.204	0.208	***0.166***	0.162	***0.143***	0.216	***0.129***	0.147	0.167	0.162	***0.159***	0.171	***0.157***	0.164	0.159
110000	0.156	***0.125***	0.168	0.213	0.216	***0.170***	0.165	***0.146***	0.213	***0.128***	0.145	0.168	0.176	***0.174***	0.186	***0.157***	0.165	0.162
120000	0.159	***0.129***	0.171	0.221	0.223	***0.181***	0.167	***0.148***	0.212	***0.129***	0.145	0.169	0.177	***0.177***	0.182	***0.150***	0.158	0.159
130000	0.162	***0.133***	0.174	0.221	0.223	***0.181***	0.163	***0.144***	0.212	***0.130***	0.146	0.170	0.185	***0.183***	0.185			
140000	0.165	***0.137***	0.176	0.219	0.222	***0.179***	0.156	***0.137***	0.212	***0.132***	0.148	0.171	0.183	***0.180***	0.185			
150000	0.167	***0.141***	0.178	0.218	0.220	***0.176***	0.155	***0.134***	0.213	***0.135***	0.150	0.172	0.159	***0.155***	0.170			
160000	0.169	***0.145***	0.180	0.216	0.219	***0.181***	0.157	***0.136***	0.215	***0.138***	0.154	0.172	0.154	***0.147***	0.183			
170000	0.172	***0.149***	0.182	0.215	0.218	***0.184***	0.159	***0.138***	0.217	***0.142***	0.157	0.172	0.142	***0.135***	0.175			
180000	0.175	***0.152***	0.183	0.217	0.217	***0.186***	0.161	***0.140***	0.218	***0.145***	0.160	0.172	0.131	***0.123***	0.168			
190000	0.177	***0.155***	0.184	0.219	0.217	***0.188***	0.163	***0.141***	0.220	***0.144***	0.159	0.172	0.121	***0.112***	0.160			
200000	0.178	***0.156***	0.186	0.221	0.219	***0.190***	0.163	***0.142***	0.222	***0.140***	0.155	0.172	0.111	***0.109***	0.154			

Table B13 Goodness of fit using K-S statistic for the STA DBM-2 prepared with VG40 bitumen

Passes	40 °C			45 °C			50 °C			55 °C			60 °C			65 °C		
	Normal	**Lognormal**	**Weibull**	**Normal**	**Lognormal**	**Weibull**	**Normal**	**Lognormal**	**Weibull**	**Normal**	**Lognormal**	**Weibull**	**Normal**	**Lognormal**	**Weibull**	**Normal**	**Lognormal**	**Weibull**
500	0.106	***0.105***	0.107	0.154	0.182	***0.092***	0.116	0.145	***0.112***	***0.130***	0.174	0.138	***0.105***	0.112	0.134	***0.066***	0.067	0.091
1000	***0.109***	0.123	0.115	0.124	0.146	***0.074***	***0.112***	0.130	0.146	***0.142***	0.169	0.158	***0.082***	0.091	0.103	***0.106***	0.107	0.110
2000	***0.114***	0.139	0.118	0.142	0.164	***0.092***	0.164	***0.141***	0.196	0.181	0.199	***0.172***	***0.091***	0.093	0.108	0.191	0.195	***0.119***
4000	0.127	0.132	***0.111***	***0.099***	0.125	0.106	0.150	***0.130***	0.180	0.226	0.241	***0.171***	***0.097***	0.103	0.125	0.225	0.234	***0.137***
6000	0.113	0.134	***0.102***	0.113	0.136	***0.107***	0.137	***0.119***	0.174	0.228	0.237	***0.173***	0.114	***0.110***	0.119	0.166	0.179	***0.130***
8000	0.102	0.136	***0.092***	0.127	0.131	***0.105***	0.151	***0.134***	0.180	0.212	0.222	***0.163***	0.135	0.134	***0.114***	0.154	0.158	***0.125***
10000	0.105	0.141	***0.083***	0.132	0.136	***0.116***	0.136	***0.120***	0.167	0.202	0.217	***0.158***	0.129	0.131	***0.101***	0.158	0.170	***0.121***
12000	0.080	0.103	***0.074***	0.134	0.150	***0.127***	0.127	***0.112***	0.167	0.197	0.214	***0.160***	0.140	0.143	***0.111***	0.174	0.185	***0.122***
14000	***0.072***	0.101	0.076	0.138	0.154	***0.126***	0.123	***0.117***	0.164	0.192	0.209	***0.167***	0.135	0.138	***0.110***	0.186	0.197	***0.152***
16000	***0.077***	0.104	0.082	0.129	0.143	***0.126***	0.129	***0.127***	0.172	0.186	0.203	***0.162***	0.132	0.135	***0.131***	0.162	0.172	***0.158***
18000	***0.070***	0.086	0.080	0.137	0.150	***0.133***	0.141	***0.136***	0.182	0.180	0.197	***0.158***	0.131	0.139	***0.131***	0.174	0.183	***0.159***
20000	0.075	0.079	0***.072***	0.143	0.156	***0.138***	0.157	***0.144***	0.190	0.173	0.190	***0.154***	0.138	0.149	***0.112***	0.189	0.197	***0.160***
30000	***0.08***7	0.088	0.101	0.151	0.162	***0.151***	0.167	***0.155***	0.205	0.149	0.164	***0.143***	***0.165***	0.174	0.184	0.237	0.243	***0.176***
40000	0.108	***0.105***	0.111	0.137	***0.144***	0.161	0.221	***0.214***	0.228	0.134	0.151	***0.131***	0.213	***0.203***	0.231	0.244	0.250	***0.195***
50000	0.137	0.133	***0.114***	0.139	***0.140***	0.163	0.183	***0.179***	0.192	0.124	0.142	***0.124***	0.245	***0.237***	0.263	0.227	0.234	***0.193***
60000	0.147	0.148	***0.120***	0.136	***0.137***	0.160	0.153	***0.147***	0.182	0.119	0.134	***0.118***	0.267	***0.261***	0.284	0.196	0.202	***0.175***
70000	0.122	0.123	***0.119***	0.132	***0.133***	0.154	0.133	***0.123***	0.168	0.116	0.126	***0.113***	0.257	***0.256***	0.277	0.169	0.177	***0.158***
80000	0.128	0.126	***0.128***	0.129	0.136	0.150	***0.111***	***0.101***	0.158	0.110	0.120	0.113	***0.244***	0.252	0.264	0.152	0.159	***0.147***
90000	0.129	0.129	***0.116***	0.132	0.141	0.149	***0.122***	***0.114***	0.180	***0.103***	0.114	0.126	***0.237***	0.245	0.251			
100000	0.137	0.138	***0.120***	0.137	0.146	0.147	***0.122***	***0.114***	0.179	***0.098***	0.109	0.136	***0.230***	0.239	0.238			
110000	0.130	0.130	***0.115***	0.143	0.150	0.147	***0.120***	***0.110***	0.174	***0.103***	0.104	0.146	***0.216***	0.227	0.226			
120000	0.116	0.116	***0.109***	0.147	0.155	0.154	***0.114***	***0.104***	0.165	0.112	***0.100***	0.155	***0.199***	0.208	0.215			
130000	0.106	***0.106***	0.111	0.151	0.159	0.162	***0.093***	***0.096***	0.145	0.120	***0.101***	0.162	0.193	***0.188***	0.205			
140000	0.100	***0.100***	0.112	0.154	0.162	0.166	***0.089***	0.100	0.136	0.127	***0.108***	0.170	0.186	***0.181***	0.195			
150000	0.098	***0.097***	0.112	0.157	0.164	0.161	***0.084***	*0.086*	0.134	0.134	***0.115***	0.176	0.180	***0.174***	0.187			
160000	0.102	***0.098***	0.119	0.159	0.166	0.160	***0.086***	*0.097*	0.124	0.141	***0.121***	0.183	0.175	***0.169***	0.180			
170000	0.111	***0.107***	0.127	0.161	0.168	0.164	***0.088***	0.088	0.109	0.147	***0.127***	0.188	0.169	***0.166***	0.174			
180000	0.122	***0.119***	0.124	0.162	0.169	0.169	***0.090***	0.096	0.096	0.153	***0.132***	0.194	0.164	***0.163***	0.169			
190000	0.135	***0.132***	0.134	0.163	0.170	0.174	0.099	0.110	***0.085***	0.159	***0.137***	0.199	0.160	***0.160***	0.164			
200000	0.145	***0.142***	0.142	0.163	0.170	0.176	0.100	0.111	***0.088***	0.164	***0.142***	0.203	***0.155***	0.157	0.159			

Table B14 Goodness of fit using K-S statistic for the LTA DBMC-2 prepared with VG40 bitumen

Passes	40 °C			45 °C			50 °C			55 °C			60 °C			65 °C		
	Normal	**Lognormal**	**Weibull**	**Normal**	**Lognormal**	**Weibull**	**Normal**	**Lognormal**	**Weibull**	**Normal**	**Lognormal**	**Weibull**	**Normal**	**Lognormal**	**Weibull**	**Normal**	**Lognormal**	**Weibull**
500	0.264	***0.184***	0.227	0.304	***0.177***	0.234	0.172	0.212	0.123	0.099	0.130	0.118	0.082	0.106	***0.059***	0.152	***0.128***	0.197
1000	0.221	***0.151***	0.194	0.308	***0.198***	0.258	0.196	0.228	0.143	0.112	0.149	0.088	0.140	0.156	***0.123***	0.153	***0.131***	0.194
2000	0.190	***0.140***	0.173	0.254	***0.171***	0.224	0.224	0.248	0.167	0.093	0.118	0.093	***0.141***	0.150	0.165	0.170	***0.154***	0.217
4000	0.151	***0.128***	0.146	0.253	***0.187***	0.239	0.244	0.264	0.181	0.150	0.158	0.097	***0.112***	0.115	0.139	0.208	***0.196***	0.213
6000	0.160	***0.113***	0.160	0.244	***0.187***	0.241	0.218	0.236	0.151	0.181	0.185	0.185	0.159	***0.149***	0.185	0.212	***0.202***	0.214
8000	0.153	***0.108***	0.157	0.228	***0.179***	0.229	0.200	0.216	0.158	0.223	0.225	0.182	0.131	***0.122***	0.165	0.213	***0.196***	0.233
10000	0.133	***0.094***	0.139	0.205	***0.159***	0.212	0.187	0.202	0.140	0.188	0.193	0.163	0.125	***0.125***	0.140	0.221	***0.204***	0.242
12000	0.115	***0.080***	0.122	0.191	***0.153***	0.205	0.186	0.198	0.143	0.154	0.162	0.150	0.126	***0.126***	0.141	0.207	***0.189***	0.231
14000	0.116	***0.083***	0.137	0.193	***0.155***	0.212	0.177	0.197	0.162	0.132	0.134	0.150	***0.125***	0.126	0.150	0.202	***0.185***	0.228
16000	0.135	***0.097***	0.157	0.196	***0.157***	0.217	0.164	0.184	0.176	0.140	0.137	0.152	***0.123***	0.125	0.148	0.204	***0.187***	0.230
18000	0.133	***0.095***	0.156	0.215	***0.181***	0.227	0.154	0.173	0.178	0.146	0.143	0.153	***0.122***	0.123	0.145	0.196	***0.179***	0.225
20000	0.130	***0.095***	0.154	0.241	***0.211***	0.249	0.156	0.172	0.180	0.150	0.147	0.157	***0.120***	0.122	0.144	0.187	***0.170***	0.218
30000	0.150	***0.122***	0.159	0.267	***0.249***	0.271	0.156	0.168	0.187	0.163	0.161	0.175	***0.111***	0.114	0.139	0.186	***0.171***	0.214
40000	0.146	***0.143***	0.164	0.296	***0.280***	0.296	0.163	0.161	0.193	0.169	0.167	0.210	***0.104***	0.106	0.136	0.186	***0.185***	0.204
50000	0.171	***0.152***	0.185	0.314	***0.296***	0.318	0.168	0.166	0.199	0.195	0.174	0.233	0.105	***0.100***	0.133	0.171	***0.169***	0.181
60000	***0.171***	0.176	0.176	0.306	***0.286***	0.313	0.173	0.171	0.206	0.199	0.177	0.236	0.105	***0.095***	0.130	0.191	***0.187***	0.192
70000	0.163	***0.161***	0.172	0.286	***0.268***	0.295	0.176	0.174	0.209	0.195	0.174	0.228	0.099	***0.094***	0.123	0.173	***0.167***	0.179
80000	0.165	***0.146***	0.176	0.279	***0.263***	0.283	0.160	0.170	0.193	0.209	0.188	0.240	***0.095***	0.097	0.132	0.155	***0.148***	0.169
90000	0.169	***0.148***	0.177	0.267	***0.249***	0.275	0.149	0.162	0.183	0.221	0.200	0.250	0.102	***0.101***	0.142	0.157	***0.148***	0.174
100000	0.160	***0.155***	0.162	0.259	***0.245***	0.270	0.149	0.163	0.185	0.232	0.211	0.260	0.108	***0.104***	0.154	0.157	***0.148***	0.174
110000	0.167	***0.160***	0.161	0.257	***0.242***	0.267	0.150	0.164	0.186	0.242	0.221	0.268	0.118	***0.110***	0.166	0.140	***0.130***	0.160
120000	0.171	0.165	0.162	0.255	***0.239***	0.266	0.151	0.166	0.187	0.244	0.224	0.270	0.122	***0.114***	0.171	0.138	***0.130***	0.151
130000	0.161	0.152	***0.151***	0.252	***0.236***	0.265	0.155	0.169	0.187	0.237	0.216	0.264	0.126	***0.119***	0.175	0.131	***0.122***	0.145
140000	0.150	***0.140***	0.140	0.249	***0.232***	0.264	0.162	0.174	0.187	0.231	0.209	0.258	0.130	***0.123***	0.179	0.121	***0.112***	0.138
150000	***0***.145	0.148	***0.132***	0.246	***0.229***	0.263	0.172	0.184	0.187	0.235	0.215	0.256	0.134	***0.127***	0.184	0.114	***0.107***	0.130
160000	0.147	0.149	***0.130***	0.245	***0.226***	0.263	0.183	0.195	0.186	0.241	0.221	0.261	0.139	***0.131***	0.189	0.118	***0.111***	0.128
170000	0.148	0.149	***0.130***	0.245	***0.221***	0.261	0.187	0.200	0.187	0.246	0.227	0.266	0.143	***0.135***	0.194	0.115	***0.108***	0.126
180000	0.149	0.147	***0.129***	0.243	***0.217***	0.257	0.184	0.196	0.189	0.251	0.233	0.270	0.147	***0.138***	0.198	0.108	***0.100***	0.120
190000	0.149	0.148	***0.129***	0.242	***0.216***	0.254	0.180	0.192	0.191	0.256	0.238	0.274	0.150	***0.141***	0.202	0.101	***0.093***	0.115
200000	0.149	0.148	***0.128***	0.241	***0.214***	0.250	0.176	0.187	0.197	0.261	0.243	0.278	0.154	***0.144***	0.206	0.091	***0.099***	0.124

Table B15 Distribution parameters for the LTA BC-2 prepared with VG20 bitumen

	40 °C				45 °C				50 °C				55 °C				60 °C				65 °C			
	Normal		Lognormal		Weibull		Normal		Lognormal		Weibull		Normal		Lognormal		Weibull		Normal		Lognormal		Weibull	
Passes	μ	σ	A	B	μ	σ	A	B	μ	σ	A	B	μ	σ	A	B	μ	σ	A	B	μ	σ	A	B
0	0	0	0	0	0	0	0	0	0	0	0	0	0	0	0	0	0	0	0	0	0	0	0	0
500	-0.93	0.20	0.43	6.03	-0.50	0.17	0.65	7.57	-0.03	0.13	1.03	10.26	0.24	0.21	1.38	7.53	0.52	0.13	1.80	7.71	0.67	0.15	2.10	8.08
1000	-0.59	0.18	0.60	6.88	-0.23	0.16	0.85	8.12	0.29	0.10	1.39	14.76	0.54	0.17	1.84	8.61	0.80	0.11	2.35	8.68	1.02	0.12	2.93	10.03
2000	-0.24	0.15	0.85	8.00	0.05	0.15	1.13	7.93	0.63	0.08	1.95	15.14	0.86	0.15	2.54	9.13	1.09	0.10	3.14	10.01	1.36	0.11	4.11	9.21
4000	0.14	0.13	1.22	9.25	0.35	0.15	1.53	7.11	0.99	0.08	2.81	13.01	1.21	0.13	3.57	9.52	1.41	0.08	4.27	11.90	1.70	0.11	5.78	8.07
6000	0.36	0.12	1.52	9.96	0.53	0.15	1.84	6.63	1.20	0.07	3.43	13.57	1.40	0.12	4.32	10.04	1.59	0.08	5.10	13.39	1.89	0.11	7.05	7.66
8000	0.51	0.11	1.76	10.43	0.66	0.15	2.09	6.37	1.33	0.07	3.90	15.06	1.53	0.11	4.89	10.70	1.71	0.08	5.76	14.53	2.03	0.12	8.10	7.51
10000	0.62	0.11	1.96	10.77	0.76	0.15	2.32	6.24	1.42	0.06	4.27	17.02	1.62	0.11	5.34	11.46	1.81	0.08	6.31	15.14	2.13	0.12	9.01	7.48
12000	0.71	0.11	2.14	11.03	0.84	0.15	2.52	6.20	1.49	0.06	4.57	19.20	1.69	0.10	5.70	12.28	1.87	0.08	6.77	15.14	2.22	0.12	9.82	7.52
14000	0.78	0.11	2.29	11.22	0.91	0.15	2.69	6.21	1.55	0.06	4.81	21.24	1.74	0.09	5.98	13.15	1.93	0.08	7.16	14.64	2.29	0.12	10.57	7.61
16000	0.84	0.10	2.43	11.37	0.97	0.15	2.85	6.26	1.59	0.06	5.02	22.75	1.79	0.09	6.22	14.03	1.97	0.08	7.50	13.94	2.36	0.12	11.25	7.74
18000	0.89	0.10	2.55	11.48	1.02	0.14	3.00	6.34	1.62	0.06	5.19	23.39	1.82	0.08	6.41	14.91	2.01	0.09	7.79	13.22	2.41	0.12	11.90	7.91
20000	0.93	0.10	2.65	11.55	1.07	0.14	3.13	6.45	1.65	0.06	5.33	23.22	1.85	0.08	6.57	15.78	2.04	0.09	8.05	12.58	2.46	0.12	12.50	8.10
30000	1.07	0.10	3.05	11.66	1.23	0.13	3.64	7.17	1.73	0.07	5.83	19.42	1.93	0.06	7.11	19.44	2.15	0.10	8.99	10.62	2.66	0.10	15.15	9.44
40000	1.15	0.10	3.30	11.57	1.33	0.11	4.01	8.14	1.78	0.07	6.12	17.13	1.98	0.06	7.44	21.72	2.21	0.10	9.60	9.89	2.81	0.09	17.44	11.64
50000	1.20	0.09	3.50	11.45	1.40	0.10	4.28	9.25	1.81	0.08	6.32	15.83	2.01	0.06	7.68	23.02	2.26	0.11	10.06	9.65				
60000	1.25	0.10	3.65	11.34	1.46	0.09	4.50	10.50	1.83	0.08	6.48	14.97	2.04	0.05	7.88	23.82	2.29	0.11	10.43	9.60				
70000	1.28	0.10	3.78	11.24	1.50	0.08	4.68	11.87	1.85	0.08	6.62	14.31	2.06	0.05	8.06	24.39	2.32	0.10	10.74	9.65				
80000	1.31	0.10	3.90	11.16	1.54	0.07	4.83	13.37	1.87	0.08	6.74	13.78	2.08	0.05	8.21	24.85	2.35	0.10	11.02	9.72				
90000	1.34	0.10	4.01	11.09	1.57	0.06	4.97	15.00	1.88	0.08	6.85	13.34	2.10	0.05	8.35	25.26	2.37	0.10	11.28	9.81				
100000	1.36	0.10	4.11	11.03	1.60	0.06	5.09	16.77	1.90	0.08	6.95	12.96	2.11	0.05	8.48	25.63	2.39	0.10	11.51	9.90				
110000	1.39	0.10	4.20	10.97	1.62	0.05	5.21	18.70	1.91	0.08	7.04	12.63	2.13	0.05	8.61	25.98	2.41	0.10	11.73	9.99				
120000	1.41	0.10	4.29	10.92	1.65	0.05	5.31	20.80	1.92	0.08	7.13	12.33	2.14	0.05	8.72	26.31	2.43	0.10	11.94	10.06				
130000	1.43	0.10	4.37	10.88	1.67	0.05	5.41	23.06	1.93	0.09	7.21	12.07	2.16	0.05	8.83	26.62	2.45	0.10	12.13	10.14				
140000	1.44	0.10	4.45	10.84	1.69	0.04	5.51	25.45	1.94	0.09	7.29	11.84	2.17	0.05	8.93	26.92	2.46	0.10	12.31	10.21				
150000	1.46	0.10	4.53	10.80	1.70	0.04	5.60	27.92	1.95	0.09	7.37	11.63	2.18	0.05	9.02	27.21	2.47	0.10	12.49	10.27				
160000	1.48	0.10	4.60	10.76	1.72	0.04	5.68	30.33	1.96	0.09	7.44	11.43	2.19	0.05	9.12	27.48	2.49	0.10	12.65	10.33				
170000	1.49	0.10	4.67	10.73	1.73	0.04	5.77	32.54	1.97	0.09	7.51	11.26	2.20	0.05	9.20	27.74	2.50	0.10	12.81	10.39				
180000	1.51	0.10	4.74	10.70	1.75	0.04	5.85	34.41	1.98	0.09	7.57	11.09	2.21	0.05	9.29	27.99	2.51	0.10	12.96	10.44				
190000	1.52	0.10	4.81	10.67	1.76	0.04	5.93	35.86	1.99	0.09	7.64	10.94	2.22	0.05	9.37	28.22	2.52	0.10	13.11	10.49				
200000	1.53	0.10	4.87	10.64	1.78	0.04	6.00	36.89	1.99	0.09	7.70	10.80	2.22	0.04	9.45	28.45	2.54	0.10	13.25	10.53				

Table B16 Distribution parameters for the STA BC-2 prepared with VG40 bitumen

	40 °C				45 °C				50 °C				55 °C				60 °C				65 °C			
	Normal		**Lognormal**		**Weibull**		**Normal**		**Lognormal**		**Weibull**		**Normal**		**Lognormal**		**Weibull**		**Normal**		**Lognormal**		**Weibull**	
Passes	μ	σ	A	B	μ	σ	A	B	μ	σ	A	B	μ	σ	A	B	μ	σ	A	B	μ	σ	A	B
0	0	0	0	0	0	0	0	0	0	0	0	0	0	0	0	0	0	0	0	0	0	0	0	0
500	-0.75	0.17	0.51	9.00	-0.62	0.27	0.60	6.47	-0.30	0.17	0.80	7.54	0.23	0.16	1.35	7.62	0.52	0.23	1.87	6.09	0.99	0.12	2.85	9.12
1000	-0.48	0.15	0.66	10.46	-0.30	0.22	0.81	7.80	0.11	0.13	1.19	8.60	0.53	0.13	1.81	9.06	0.82	0.19	2.47	7.14	1.30	0.11	3.88	10.26
2000	-0.20	0.13	0.86	11.77	0.05	0.17	1.13	9.66	0.54	0.11	1.81	9.49	0.86	0.11	2.50	10.87	1.14	0.15	3.37	8.11	1.60	0.10	5.20	11.31
4000	0.09	0.12	1.15	11.79	0.42	0.13	1.61	11.97	0.96	0.09	2.74	10.76	1.21	0.09	3.50	12.85	1.49	0.12	4.70	8.71	1.88	0.09	6.82	12.22
6000	0.27	0.12	1.38	10.91	0.64	0.11	1.99	12.96	1.18	0.08	3.41	12.21	1.41	0.07	4.25	13.97	1.68	0.11	5.70	8.97	2.02	0.09	7.88	12.63
8000	0.40	0.12	1.57	10.04	0.79	0.11	2.31	13.00	1.32	0.07	3.91	13.96	1.54	0.07	4.82	14.67	1.82	0.11	6.49	9.18	2.12	0.09	8.68	12.79
10000	0.49	0.12	1.74	9.32	0.90	0.10	2.59	12.60	1.42	0.07	4.28	16.00	1.63	0.07	5.27	15.11	1.91	0.10	7.11	9.37	2.19	0.09	9.33	12.82
12000	0.58	0.13	1.89	8.74	0.99	0.10	2.83	12.09	1.49	0.06	4.58	18.32	1.70	0.06	5.63	15.36	1.98	0.10	7.62	9.54	2.25	0.09	9.87	12.76
14000	0.64	0.13	2.03	8.28	1.06	0.10	3.04	11.59	1.54	0.06	4.81	20.78	1.75	0.06	5.93	15.49	2.03	0.10	8.03	9.68	2.29	0.09	10.35	12.67
16000	0.70	0.13	2.16	7.90	1.12	0.10	3.23	11.15	1.59	0.06	5.01	23.01	1.79	0.06	6.17	15.54	2.07	0.10	8.37	9.81	2.33	0.09	10.78	12.58
18000	0.76	0.14	2.28	7.58	1.17	0.10	3.40	10.77	1.62	0.05	5.17	24.24	1.82	0.06	6.38	15.54	2.11	0.10	8.66	9.92	2.37	0.09	11.17	12.49
20000	0.80	0.14	2.40	7.32	1.22	0.10	3.55	10.44	1.64	0.06	5.31	23.89	1.85	0.06	6.55	15.50	2.14	0.10	8.90	10.02	2.40	0.09	11.54	12.43
30000	0.98	0.16	2.88	6.50	1.36	0.11	4.10	9.40	1.73	0.06	5.81	17.34	1.93	0.06	7.13	15.09	2.22	0.10	9.69	10.40	2.54	0.09	13.21	12.69
40000	1.10	0.17	3.26	6.12	1.44	0.11	4.46	8.94	1.78	0.07	6.14	14.70	1.98	0.06	7.49	14.65	2.27	0.09	10.15	10.71	2.65	0.09	14.77	13.98
50000	1.18	0.17	3.57	5.94	1.49	0.11	4.71	8.76	1.82	0.07	6.38	13.60	2.02	0.06	7.76	14.28	2.30	0.09	10.47	11.00	2.76	0.08	16.37	16.29
60000	1.25	0.17	3.82	5.87	1.53	0.11	4.90	8.73	1.85	0.08	6.59	13.03	2.05	0.06	7.99	13.96	2.33	0.09	10.74	11.27	2.86	0.07	18.02	19.22
70000	1.31	0.17	4.04	5.88	1.56	0.11	5.05	8.78	1.87	0.08	6.77	12.67	2.07	0.06	8.19	13.70	2.35	0.09	10.96	11.51				
80000	1.35	0.17	4.22	5.92	1.59	0.11	5.19	8.86	1.90	0.08	6.93	12.41	2.09	0.06	8.37	13.48	2.37	0.09	11.17	11.74				
90000	1.39	0.17	4.39	6.01	1.61	0.11	5.31	8.97	1.92	0.08	7.08	12.20	2.11	0.06	8.53	13.28	2.39	0.08	11.35	11.96				
100000	1.43	0.17	4.53	6.11	1.64	0.10	5.42	9.08	1.94	0.08	7.22	12.03	2.13	0.07	8.68	13.11	2.40	0.08	11.52	12.16				
110000	1.45	0.17	4.66	6.24	1.65	0.10	5.52	9.19	1.95	0.08	7.36	11.87	2.14	0.07	8.82	12.95	2.42	0.08	11.68	12.35				
120000	1.48	0.16	4.77	6.38	1.67	0.10	5.61	9.29	1.97	0.08	7.48	11.74	2.16	0.07	8.96	12.82	2.43	0.08	11.82	12.54				
130000	1.50	0.16	4.88	6.54	1.69	0.10	5.70	9.39	1.99	0.08	7.60	11.61	2.17	0.07	9.08	12.69	2.44	0.08	11.96	12.71				
140000	1.53	0.15	4.98	6.70	1.70	0.10	5.78	9.49	2.00	0.08	7.71	11.50	2.18	0.07	9.20	12.58	2.45	0.08	12.09	12.88				
150000	1.55	0.15	5.07	6.87	1.72	0.10	5.87	9.58	2.01	0.08	7.82	11.40	2.19	0.07	9.31	12.47	2.46	0.08	12.22	13.05				
160000	1.56	0.15	5.15	7.04	1.73	0.10	5.94	9.66	2.03	0.08	7.92	11.31	2.21	0.07	9.42	12.37	2.47	0.07	12.34	13.20				
170000	1.58	0.14	5.23	7.23	1.75	0.10	6.02	9.74	2.04	0.08	8.02	11.22	2.22	0.07	9.52	12.28	2.48	0.07	12.45	13.36				
180000	1.60	0.14	5.31	7.41	1.76	0.09	6.09	9.82	2.05	0.08	8.12	11.14	2.23	0.07	9.62	12.19	2.49	0.07	12.56	13.50				
190000	1.61	0.14	5.38	7.60	1.77	0.09	6.16	9.89	2.06	0.09	8.21	11.07	2.24	0.07	9.71	12.11	2.50	0.07	12.66	13.65				
200000	1.63	0.13	5.44	7.80	1.78	0.09	6.23	9.96	2.07	0.09	8.30	11.00	2.24	0.07	9.80	12.04	2.51	0.07	12.76	13.79				

Table B17 Distribution parameters for the LTA BC-2 prepared with VG40 bitumen

	40 °C				45 °C				50 °C				55 °C				60 °C				65 °C			
	Normal		Lognormal		Weibull		Normal		Lognormal		Weibull		Normal		Lognormal		Weibull		Normal		Lognormal		Weibull	
Passes	μ	σ	A	B	μ	σ	A	B	μ	σ	A	B	μ	σ	A	B	μ	σ	A	B	μ	σ	A	B
0	0	0	0	0	0	0	0	0	0	0	0	0	0	0	0	0	0	0	0	0	0	0	0	0
500	-1.54	0.62	0.28	2.33	-1.05	0.52	0.45	2.24	-0.43	0.29	0.73	5.53	-0.15	0.30	0.99	4.89	0.25	0.11	1.35	11.87	0.52	0.14	1.81	6.80
1000	-1.16	0.59	0.41	2.38	-0.73	0.46	0.60	2.53	-0.14	0.24	0.96	6.71	0.19	0.23	1.33	6.55	0.54	0.09	1.79	13.61	0.89	0.13	2.60	7.38
2000	-0.79	0.55	0.59	2.44	-0.39	0.39	0.82	2.94	0.19	0.20	1.31	8.42	0.54	0.17	1.85	8.96	0.85	0.08	2.43	15.80	1.26	0.12	3.73	8.28
4000	-0.44	0.50	0.81	2.64	-0.03	0.31	1.14	3.54	0.54	0.15	1.83	10.44	0.91	0.12	2.62	11.75	1.17	0.06	3.33	18.27	1.59	0.10	5.17	9.63
6000	-0.25	0.45	0.96	2.86	0.19	0.27	1.39	4.03	0.75	0.13	2.25	11.38	1.12	0.10	3.20	13.38	1.35	0.06	3.97	19.60	1.76	0.09	6.08	10.48
8000	-0.12	0.42	1.07	3.09	0.35	0.25	1.60	4.46	0.91	0.12	2.61	11.91	1.25	0.09	3.65	14.02	1.47	0.05	4.47	20.34	1.86	0.09	6.73	10.95
10000	-0.02	0.39	1.17	3.30	0.47	0.23	1.78	4.87	1.02	0.11	2.91	12.32	1.35	0.09	4.01	13.87	1.56	0.05	4.87	20.76	1.93	0.09	7.23	11.16
12000	0.05	0.37	1.25	3.49	0.56	0.21	1.95	5.26	1.11	0.10	3.18	12.72	1.42	0.09	4.30	13.38	1.63	0.05	5.20	21.01	1.99	0.09	7.64	11.22
14000	0.12	0.35	1.32	3.67	0.65	0.20	2.10	5.64	1.18	0.10	3.42	13.13	1.47	0.09	4.55	12.85	1.68	0.05	5.48	21.18	2.03	0.09	7.99	11.18
16000	0.18	0.33	1.39	3.84	0.71	0.19	2.24	6.01	1.25	0.09	3.63	13.55	1.52	0.09	4.75	12.39	1.72	0.05	5.71	21.32	2.07	0.09	8.31	11.11
18000	0.23	0.32	1.45	3.99	0.77	0.18	2.37	6.37	1.30	0.09	3.81	13.98	1.55	0.09	4.92	12.01	1.75	0.05	5.91	21.45	2.11	0.09	8.60	11.01
20000	0.27	0.31	1.51	4.14	0.83	0.17	2.48	6.72	1.34	0.09	3.98	14.42	1.58	0.09	5.07	11.71	1.78	0.04	6.09	21.58	2.14	0.09	8.87	10.90
30000	0.45	0.27	1.77	4.76	1.02	0.14	2.95	8.44	1.49	0.07	4.58	16.45	1.67	0.09	5.56	11.08	1.89	0.04	6.76	22.25	2.25	0.09	9.99	10.43
40000	0.57	0.24	1.98	5.27	1.14	0.13	3.30	10.00	1.57	0.07	4.96	18.06	1.72	0.09	5.86	11.17	1.96	0.04	7.23	22.95	2.34	0.10	10.91	10.10
50000	0.67	0.22	2.16	5.71	1.22	0.12	3.57	11.33	1.62	0.06	5.21	19.24	1.76	0.08	6.07	11.50	2.01	0.04	7.62	23.59	2.41	0.10	11.71	9.87
60000	0.75	0.21	2.33	6.08	1.28	0.11	3.79	12.41	1.66	0.06	5.39	20.05	1.79	0.08	6.24	11.91	2.05	0.04	7.95	24.14	2.47	0.10	12.41	9.69
70000	0.81	0.20	2.48	6.41	1.33	0.10	3.97	13.26	1.68	0.06	5.53	20.58	1.81	0.08	6.39	12.31	2.09	0.04	8.25	24.63	2.52	0.10	13.05	9.55
80000	0.87	0.20	2.62	6.70	1.37	0.10	4.12	13.92	1.70	0.06	5.65	20.89	1.84	0.07	6.52	12.69	2.12	0.04	8.52	25.05	2.56	0.10	13.63	9.43
90000	0.92	0.19	2.74	6.97	1.41	0.09	4.26	14.41	1.72	0.06	5.75	21.03	1.86	0.07	6.64	13.05	2.15	0.04	8.77	25.43	2.60	0.10	14.17	9.34
100000	0.97	0.19	2.87	7.21	1.43	0.09	4.38	14.77	1.74	0.06	5.85	21.05	1.87	0.07	6.76	13.37	2.18	0.04	9.00	25.76	2.63	0.10	14.68	9.26
110000	1.01	0.18	2.98	7.43	1.46	0.09	4.49	15.00	1.75	0.06	5.93	20.99	1.89	0.07	6.86	13.66	2.20	0.04	9.22	26.07	2.66	0.10	15.16	9.19
120000	1.05	0.18	3.09	7.63	1.48	0.09	4.59	15.11	1.77	0.06	6.01	20.87	1.91	0.07	6.96	13.93	2.23	0.04	9.43	26.34	2.69	0.11	15.62	9.12
130000	1.08	0.18	3.20	7.83	1.50	0.09	4.68	15.13	1.78	0.06	6.08	20.72	1.92	0.06	7.06	14.18	2.25	0.04	9.62	26.58				
140000	1.11	0.17	3.30	8.00	1.52	0.08	4.77	15.08	1.79	0.06	6.15	20.55	1.93	0.06	7.15	14.41	2.26	0.04	9.80	26.81				
150000	1.14	0.17	3.39	8.17	1.54	0.08	4.85	14.97	1.80	0.06	6.22	20.36	1.95	0.06	7.24	14.62	2.28	0.04	9.98	27.01				
160000	1.17	0.17	3.49	8.33	1.56	0.08	4.93	14.82	1.81	0.06	6.28	20.17	1.96	0.06	7.32	14.81	2.30	0.03	10.14	27.20				
170000	1.20	0.17	3.58	8.48	1.57	0.08	5.01	14.65	1.82	0.06	6.34	19.97	1.97	0.06	7.40	14.99	2.31	0.03	10.30	27.37				
180000	1.22	0.17	3.66	8.63	1.59	0.08	5.08	14.47	1.83	0.06	6.40	19.78	1.98	0.06	7.48	15.16	2.33	0.03	10.46	27.52				
190000	1.25	0.16	3.75	8.77	1.60	0.08	5.15	14.29	1.84	0.06	6.46	19.58	1.99	0.06	7.55	15.31	2.34	0.03	10.61	27.67				
200000	1.27	0.16	3.83	8.90	1.61	0.08	5.22	14.10	1.84	0.06	6.51	19.39	2.00	0.06	7.63	15.46	2.36	0.03	10.75	27.80				

Table B18 Distribution parameters for the STA DBM-2 prepared with VG20 bitumen

	40 °C				45 °C				50 °C				55 °C				60 °C				65 °C			
	Normal		Lognormal		Weibull		Normal		Lognormal		Weibull		Normal		Lognormal		Weibull		Normal		Lognormal		Weibull	
Passes	μ	σ	A	B	μ	σ	A	B	μ	σ	A	B	μ	σ	A	B	μ	σ	A	B	μ	σ	A	B
0	0	0	0	0	0	0	0	0	0	0	0	0	0	0	0	0	0	0	0	0	0	0	0	0
500	-0.34	0.16	0.77	7.97	-0.04	0.24	1.06	7.37	0.54	0.13	1.82	9.46	0.81	0.12	2.38	7.23	1.14	0.08	3.27	14.61	1.29	0.12	3.85	8.99
1000	-0.10	0.12	0.96	10.65	0.19	0.21	1.31	8.27	0.75	0.13	2.24	9.07	1.05	0.11	3.02	8.63	1.33	0.08	3.93	15.35	1.57	0.11	5.04	11.76
2000	0.16	0.08	1.21	15.68	0.43	0.17	1.66	9.30	0.97	0.13	2.82	7.88	1.31	0.10	3.88	10.13	1.53	0.08	4.78	15.35	1.83	0.11	6.53	12.47
4000	0.42	0.05	1.56	24.65	0.71	0.14	2.15	10.06	1.21	0.13	3.61	7.05	1.56	0.08	4.96	12.00	1.74	0.08	5.90	14.91	2.06	0.10	8.24	13.57
6000	0.58	0.05	1.83	24.92	0.88	0.12	2.54	10.20	1.36	0.13	4.16	6.99	1.70	0.07	5.69	13.25	1.87	0.08	6.70	14.70	2.20	0.09	9.35	14.68
8000	0.70	0.05	2.06	21.65	1.00	0.11	2.87	10.21	1.46	0.13	4.59	7.19	1.80	0.06	6.28	13.76	1.96	0.08	7.35	14.75	2.29	0.08	10.21	15.63
10000	0.79	0.06	2.26	19.13	1.10	0.10	3.15	10.21	1.53	0.13	4.94	7.49	1.88	0.06	6.77	13.82	2.03	0.08	7.90	15.00	2.36	0.07	10.92	16.44
12000	0.86	0.06	2.45	17.46	1.18	0.10	3.41	10.23	1.59	0.12	5.23	7.83	1.94	0.06	7.19	13.68	2.09	0.07	8.37	15.40	2.41	0.07	11.53	17.09
14000	0.93	0.07	2.61	16.34	1.25	0.09	3.64	10.27	1.64	0.12	5.47	8.17	1.99	0.06	7.56	13.45	2.14	0.07	8.79	15.92	2.46	0.07	12.07	17.57
16000	0.98	0.07	2.76	15.57	1.30	0.09	3.85	10.34	1.68	0.12	5.68	8.50	2.03	0.06	7.90	13.21	2.18	0.07	9.16	16.54	2.50	0.06	12.56	17.91
18000	1.03	0.07	2.90	15.01	1.35	0.09	4.04	10.42	1.71	0.12	5.86	8.79	2.07	0.07	8.20	12.99	2.22	0.07	9.49	17.23	2.54	0.06	13.01	18.13
20000	1.07	0.07	3.03	14.60	1.40	0.08	4.22	10.53	1.74	0.11	6.02	9.05	2.10	0.07	8.47	12.79	2.25	0.06	9.79	17.98	2.57	0.06	13.43	18.27
30000	1.23	0.08	3.55	13.56	1.55	0.07	4.92	11.16	1.83	0.11	6.60	9.92	2.21	0.08	9.52	12.16	2.37	0.05	10.98	22.42	2.69	0.06	15.19	18.42
40000	1.34	0.08	3.96	13.07	1.65	0.06	5.40	11.87	1.89	0.10	6.98	10.35	2.29	0.08	10.26	12.00	2.45	0.04	11.82	27.46	2.78	0.07	16.60	18.29
50000	1.42	0.08	4.28	12.75	1.72	0.06	5.76	12.52	1.93	0.10	7.28	10.57	2.34	0.08	10.84	12.10	2.51	0.03	12.48	32.48				
60000	1.48	0.08	4.55	12.51	1.76	0.06	6.03	13.08	1.97	0.10	7.52	10.71	2.39	0.08	11.31	12.34	2.55	0.03	13.02	36.86				
70000	1.53	0.08	4.78	12.32	1.80	0.06	6.25	13.52	2.00	0.10	7.73	10.80	2.42	0.07	11.73	12.64	2.59	0.02	13.47	40.18				
80000	1.57	0.08	4.99	12.17	1.83	0.06	6.43	13.87	2.02	0.10	7.92	10.87	2.45	0.07	12.09	12.96	2.62	0.02	13.87	42.39				
90000	1.60	0.08	5.17	12.04	1.85	0.06	6.58	14.14	2.04	0.09	8.09	10.92	2.48	0.07	12.42	13.30	2.64	0.02	14.22	43.64				
100000	1.63	0.08	5.33	11.93	1.87	0.06	6.71	14.34	2.06	0.09	8.24	10.97	2.51	0.07	12.73	13.63	2.67	0.02	14.54	44.14				
110000	1.66	0.08	5.48	11.82	1.89	0.05	6.82	14.49	2.08	0.09	8.39	11.00	2.53	0.07	13.01	13.95	2.69	0.02	14.83	44.09				
120000	1.68	0.08	5.61	11.71	1.91	0.05	6.93	14.60	2.10	0.09	8.52	11.03	2.55	0.07	13.28	14.26	2.70	0.02	15.10	43.67				
130000	1.71	0.08	5.74	11.60	1.92	0.05	7.02	14.68	2.11	0.09	8.65	11.06	2.57	0.07	13.53	14.55								
140000	1.73	0.08	5.86	11.48	1.93	0.05	7.11	14.74	2.12	0.09	8.77	11.08	2.59	0.07	13.77	14.83								
150000	1.75	0.08	5.97	11.36	1.94	0.05	7.19	14.78	2.14	0.09	8.88	11.10	2.60	0.07	13.99	15.09								
160000	1.76	0.08	6.08	11.24	1.95	0.05	7.26	14.80	2.15	0.09	8.99	11.11	2.62	0.07	14.21	15.33								
170000	1.78	0.08	6.18	11.12	1.96	0.05	7.33	14.82	2.16	0.09	9.09	11.12	2.64	0.06	14.42	15.56								
180000	1.79	0.08	6.27	10.99	1.97	0.05	7.40	14.82	2.17	0.09	9.19	11.13	2.65	0.06	14.61	15.77								
190000	1.81	0.08	6.36	10.86	1.98	0.05	7.47	14.83	2.18	0.09	9.29	11.14	2.66	0.06	14.80	15.97								
200000	1.82	0.08	6.45	10.73	1.99	0.05	7.53	14.82	2.19	0.09	9.38	11.15	2.67	0.06	14.99	16.16								

Table B19 Distribution parameters for the LTA DBM-2 prepared with VG20 bitumen

	40 °C				45 °C				50 °C				55 °C				60 °C				65 °C			
	Normal		**Lognormal**		**Weibull**		**Normal**		**Lognormal**		**Weibull**		**Normal**		**Lognormal**		**Weibull**		**Normal**		**Lognormal**		**Weibull**	
Passes	μ	σ	A	B	μ	σ	A	B	μ	σ	A	B	μ	σ	A	B	μ	σ	A	B	μ	σ	A	B
0	0	0	0	0	0	0	0	0	0	0	0	0	0	0	0	0	0	0	0	0	0	0	0	0
500	-0.47	0.38	0.73	4.73	-0.21	0.44	1.00	2.94	0.13	0.15	1.22	6.90	0.30	0.32	1.55	4.65	0.63	0.15	2.01	8.60	0.95	0.11	2.75	9.30
1000	-0.25	0.36	0.89	5.14	0.07	0.44	1.32	2.91	0.31	0.14	1.46	7.10	0.56	0.25	1.94	5.91	0.89	0.14	2.58	9.34	1.19	0.10	3.45	11.06
2000	-0.05	0.33	1.08	5.44	0.35	0.42	1.72	3.05	0.50	0.13	1.77	7.28	0.83	0.17	2.48	7.97	1.15	0.13	3.34	9.84	1.43	0.08	4.34	13.65
4000	0.14	0.30	1.30	5.66	0.59	0.35	2.13	3.66	0.71	0.12	2.17	7.45	1.12	0.12	3.24	10.61	1.40	0.12	4.31	10.04	1.67	0.06	5.48	17.77
6000	0.26	0.28	1.45	5.74	0.73	0.30	2.39	4.34	0.84	0.12	2.46	7.52	1.29	0.10	3.83	11.42	1.55	0.11	4.97	10.12	1.81	0.06	6.29	21.42
8000	0.34	0.27	1.57	5.76	0.82	0.27	2.57	4.97	0.94	0.11	2.71	7.58	1.41	0.10	4.32	11.44	1.65	0.11	5.49	10.24	1.91	0.05	6.94	24.78
10000	0.40	0.26	1.67	5.76	0.89	0.24	2.72	5.56	1.01	0.11	2.92	7.63	1.50	0.11	4.73	11.26	1.73	0.10	5.91	10.42	1.99	0.04	7.49	27.77
12000	0.46	0.25	1.76	5.74	0.95	0.22	2.85	6.08	1.07	0.11	3.10	7.68	1.57	0.11	5.08	11.05	1.79	0.10	6.27	10.66	2.06	0.04	7.96	30.26
14000	0.50	0.24	1.84	5.71	0.99	0.21	2.96	6.54	1.13	0.11	3.27	7.74	1.63	0.12	5.38	10.86	1.83	0.10	6.58	10.94	2.11	0.03	8.39	32.19
16000	0.54	0.24	1.91	5.69	1.03	0.20	3.06	6.94	1.17	0.11	3.42	7.81	1.68	0.12	5.64	10.71	1.88	0.10	6.85	11.25	2.16	0.03	8.78	33.58
18000	0.58	0.23	1.98	5.66	1.06	0.19	3.15	7.28	1.21	0.11	3.56	7.87	1.72	0.12	5.87	10.59	1.91	0.09	7.09	11.58	2.20	0.03	9.14	34.54
20000	0.61	0.23	2.04	5.64	1.09	0.18	3.23	7.58	1.25	0.10	3.68	7.95	1.75	0.12	6.08	10.51	1.94	0.09	7.31	11.92	2.24	0.03	9.48	35.15
30000	0.73	0.21	2.29	5.55	1.19	0.16	3.55	8.48	1.38	0.10	4.18	8.32	1.87	0.12	6.81	10.39	2.06	0.08	8.17	13.65	2.38	0.02	10.89	35.44
40000	0.81	0.20	2.49	5.51	1.26	0.15	3.78	8.88	1.46	0.09	4.55	8.67	1.93	0.11	7.28	10.54	2.14	0.07	8.81	15.15	2.47	0.02	12.03	33.82
50000	0.88	0.20	2.66	5.51	1.31	0.14	3.97	9.08	1.52	0.09	4.82	8.95	1.98	0.11	7.61	10.79	2.20	0.07	9.32	16.36	2.55	0.03	13.00	31.74
60000	0.93	0.19	2.80	5.54	1.35	0.14	4.14	9.21	1.57	0.09	5.04	9.16	2.02	0.10	7.88	11.05	2.25	0.06	9.75	17.33	2.61	0.03	13.84	29.70
70000	0.98	0.19	2.92	5.58	1.39	0.14	4.28	9.30	1.60	0.09	5.21	9.30	2.05	0.10	8.10	11.32	2.29	0.06	10.14	18.12	2.66	0.04	14.59	27.90
80000	1.02	0.18	3.03	5.63	1.42	0.14	4.40	9.38	1.63	0.09	5.37	9.40	2.07	0.09	8.29	11.56	2.32	0.06	10.49	18.79	2.70	0.04	15.26	26.37
90000	1.05	0.18	3.13	5.68	1.44	0.14	4.52	9.44	1.66	0.09	5.50	9.45	2.09	0.09	8.47	11.78	2.35	0.05	10.81	19.37	2.74	0.05	15.88	25.08
100000	1.08	0.18	3.23	5.74	1.47	0.14	4.63	9.50	1.68	0.08	5.61	9.48	2.11	0.09	8.63	11.97	2.38	0.05	11.11	19.88	2.78	0.05	16.45	23.99
110000	1.11	0.17	3.31	5.80	1.49	0.14	4.73	9.55	1.70	0.08	5.71	9.50	2.13	0.09	8.77	12.15	2.41	0.05	11.38	20.34	2.81	0.05	16.98	23.05
120000	1.13	0.17	3.39	5.86	1.51	0.14	4.82	9.59	1.71	0.08	5.81	9.50	2.15	0.09	8.91	12.30	2.43	0.05	11.64	20.76	2.84	0.05	17.48	22.23
130000	1.16	0.17	3.46	5.92	1.53	0.14	4.91	9.63	1.73	0.08	5.89	9.49	2.16	0.09	9.04	12.44	2.45	0.05	11.89	21.14				
140000	1.18	0.17	3.53	5.98	1.55	0.14	4.99	9.67	1.74	0.08	5.97	9.47	2.17	0.08	9.16	12.57	2.47	0.05	12.13	21.49				
150000	1.20	0.17	3.60	6.04	1.56	0.13	5.07	9.70	1.75	0.08	6.05	9.45	2.19	0.08	9.28	12.69	2.49	0.05	12.35	21.81				
160000	1.21	0.16	3.66	6.09	1.58	0.13	5.15	9.72	1.77	0.08	6.12	9.43	2.20	0.08	9.39	12.79	2.51	0.05	12.56	22.11				
170000	1.23	0.16	3.72	6.15	1.59	0.13	5.22	9.75	1.78	0.08	6.19	9.41	2.21	0.08	9.50	12.89	2.52	0.05	12.77	22.39				
180000	1.25	0.16	3.77	6.20	1.60	0.13	5.29	9.77	1.79	0.08	6.25	9.38	2.22	0.08	9.60	12.98	2.54	0.05	12.97	22.65				
190000	1.26	0.16	3.83	6.25	1.62	0.13	5.36	9.79	1.80	0.09	6.32	9.36	2.23	0.08	9.70	13.06	2.55	0.05	13.16	22.89				
200000	1.27	0.16	3.88	6.30	1.63	0.13	5.42	9.80	1.81	0.09	6.37	9.34	2.24	0.08	9.79	13.14	2.57	0.05	13.34	23.11				

Table B20 Distribution parameters for the STA DBM-2 with VG40 prepared bitumen

	40 °C				45 °C				50 °C				55 °C				60 °C				65 °C			
	Normal		Lognormal		Weibull		Normal		Lognormal		Weibull		Normal		Lognormal		Weibull		Normal		Lognormal		Weibull	
Passes	μ	σ	A	B	μ	σ	A	B	μ	σ	A	B	μ	σ	A	B	μ	σ	A	B	μ	σ	A	B
0	0	0	0	0	0	0	0	0	0	0	0	0	0	0	0	0	0	0	0	0	0	0	0	0
500	-0.79	0.37	0.54	3.33	-0.31	0.20	0.80	7.18	0.34	0.16	1.52	6.97	0.48	0.24	1.81	5.27	0.73	0.07	2.14	15.28	1.10	0.04	3.07	25.82
1000	-0.57	0.34	0.66	3.78	-0.11	0.18	0.97	7.80	0.53	0.14	1.82	7.76	0.73	0.21	2.29	6.12	1.00	0.06	2.78	19.12	1.38	0.04	4.04	29.75
2000	-0.32	0.30	0.83	4.36	0.12	0.16	1.21	8.49	0.73	0.12	2.20	8.77	1.01	0.18	2.98	7.28	1.28	0.05	3.69	21.92	1.64	0.05	5.28	26.04
4000	-0.05	0.26	1.07	5.12	0.36	0.14	1.53	9.35	0.95	0.10	2.72	9.95	1.30	0.15	3.94	8.77	1.57	0.05	4.95	20.63	1.88	0.07	6.73	21.48
6000	0.13	0.23	1.27	5.72	0.52	0.13	1.78	9.99	1.08	0.09	3.10	10.66	1.47	0.14	4.64	9.73	1.73	0.06	5.83	17.95	2.00	0.07	7.64	19.62
8000	0.27	0.20	1.43	6.26	0.63	0.12	1.99	10.51	1.18	0.09	3.41	11.19	1.59	0.13	5.19	10.41	1.84	0.07	6.51	15.70	2.09	0.07	8.31	19.24
10000	0.37	0.19	1.59	6.77	0.73	0.11	2.18	10.98	1.26	0.08	3.68	11.63	1.67	0.12	5.63	10.91	1.92	0.07	7.04	14.06	2.15	0.07	8.85	19.44
12000	0.47	0.17	1.72	7.27	0.81	0.11	2.35	11.40	1.32	0.08	3.91	12.04	1.74	0.12	5.99	11.29	1.97	0.08	7.48	12.91	2.20	0.06	9.31	19.84
14000	0.54	0.16	1.85	7.77	0.87	0.10	2.51	11.78	1.37	0.08	4.11	12.45	1.79	0.11	6.28	11.58	2.02	0.09	7.84	12.10	2.24	0.06	9.71	20.28
16000	0.61	0.15	1.98	8.27	0.93	0.10	2.66	12.15	1.42	0.07	4.29	12.85	1.83	0.11	6.53	11.79	2.05	0.09	8.14	11.53	2.28	0.06	10.08	20.69
18000	0.67	0.14	2.09	8.77	0.98	0.10	2.80	12.49	1.46	0.07	4.46	13.25	1.86	0.11	6.74	11.94	2.08	0.10	8.40	11.13	2.32	0.06	10.42	21.06
20000	0.73	0.13	2.20	9.28	1.03	0.09	2.92	12.82	1.49	0.07	4.60	13.64	1.88	0.11	6.92	12.04	2.11	0.10	8.63	10.85	2.35	0.06	10.73	21.37
30000	0.94	0.10	2.68	11.92	1.20	0.08	3.47	14.31	1.61	0.06	5.17	15.34	1.97	0.10	7.55	12.09	2.19	0.11	9.46	10.41	2.46	0.06	12.04	22.35
40000	1.08	0.08	3.07	14.56	1.32	0.08	3.88	15.64	1.69	0.05	5.56	16.42	2.03	0.10	7.95	11.80	2.25	0.11	10.03	10.52	2.55	0.06	13.09	22.69
50000	1.19	0.07	3.39	16.73	1.41	0.07	4.22	16.85	1.74	0.05	5.84	16.99	2.06	0.10	8.26	11.46	2.30	0.11	10.48	10.66	2.61	0.06	13.99	22.73
60000	1.27	0.07	3.67	18.11	1.47	0.07	4.49	17.92	1.78	0.05	6.07	17.29	2.09	0.10	8.52	11.14	2.33	0.11	10.87	10.67	2.67	0.06	14.77	22.61
70000	1.33	0.06	3.91	18.81	1.52	0.06	4.71	18.84	1.81	0.05	6.25	17.46	2.12	0.10	8.74	10.86	2.36	0.11	11.21	10.56	2.71	0.06	15.47	22.41
80000	1.39	0.06	4.12	19.11	1.56	0.06	4.90	19.61	1.83	0.05	6.41	17.58	2.14	0.10	8.94	10.62	2.39	0.12	11.53	10.37	2.75	0.06	16.11	22.16
90000	1.43	0.06	4.30	19.24	1.59	0.06	5.05	20.21	1.85	0.05	6.55	17.67	2.16	0.10	9.13	10.42	2.41	0.12	11.81	10.15	2.79	0.06	16.69	21.90
100000	1.47	0.06	4.46	19.32	1.62	0.06	5.19	20.67	1.87	0.05	6.68	17.74	2.18	0.11	9.30	10.24	2.43	0.12	12.08	9.91	2.82	0.06	17.24	21.64
110000	1.50	0.06	4.59	19.39	1.64	0.06	5.31	20.98	1.89	0.05	6.79	17.79	2.19	0.11	9.45	10.08	2.45	0.12	12.33	9.68	2.85	0.06	17.75	21.37
120000	1.52	0.06	4.71	19.48	1.66	0.05	5.41	21.18	1.90	0.05	6.90	17.84	2.21	0.11	9.60	9.93	2.47	0.12	12.56	9.46	2.87	0.06	18.24	21.12
130000	1.55	0.06	4.82	19.59	1.68	0.05	5.50	21.26	1.92	0.05	6.99	17.87	2.22	0.11	9.74	9.80	2.49	0.12	12.79	9.25	2.90	0.07	18.69	20.87
140000	1.56	0.05	4.91	19.73	1.69	0.05	5.58	21.27	1.93	0.05	7.09	17.88	2.24	0.11	9.87	9.69	2.50	0.13	13.00	9.05	2.92	0.07	19.13	20.64
150000	1.58	0.05	5.00	19.90	1.71	0.06	5.66	21.20	1.94	0.06	7.17	17.89	2.25	0.11	9.99	9.58	2.52	0.13	13.20	8.88	2.94	0.07	19.54	20.41
160000	1.60	0.05	5.07	20.08	1.72	0.06	5.73	21.07	1.95	0.06	7.26	17.88	2.26	0.11	10.11	9.48	2.53	0.13	13.39	8.71	2.96	0.07	19.94	20.20
170000	1.61	0.05	5.14	20.28	1.73	0.06	5.79	20.90	1.96	0.06	7.33	17.86	2.27	0.11	10.22	9.39	2.54	0.13	13.57	8.55	2.98	0.07	20.32	19.99
180000	1.62	0.05	5.20	20.49	1.74	0.06	5.85	20.70	1.97	0.06	7.41	17.83	2.28	0.11	10.33	9.31	2.56	0.13	13.75	8.41	3.00	0.07	20.69	19.80
190000	1.63	0.05	5.25	20.70	1.75	0.06	5.91	20.48	1.98	0.06	7.48	17.80	2.29	0.11	10.44	9.23	2.57	0.13	13.92	8.28	3.02	0.07	21.04	19.61
200000	1.64	0.05	5.30	20.90	1.76	0.06	5.96	20.25	1.99	0.06	7.55	17.75	2.30	0.11	10.54	9.15	2.58	0.14	14.09	8.15	3.03	0.07	21.38	19.43

Table B21 Distribution parameters for the LTA DBM-2 prepared with VG40 bitumen

	40 °C				45 °C				50 °C				55 °C				60 °C				65 °C			
	Normal		**Lognormal**		**Weibull**		**Normal**		**Lognormal**		**Weibull**		**Normal**		**Lognormal**		**Weibull**		**Normal**		**Lognormal**		**Weibull**	
Passes	μ	σ	A	B	μ	σ	A	B	μ	σ	A	B	μ	σ	A	B	μ	σ	A	B	μ	σ	A	B
0	0	0	0	0	0	0	0	0	0	0	0	0	0	0	0	0	0	0	0	0	0	0	0	0
500	-1.80	0.55	0.22	1.86	-1.13	0.64	0.45	1.48	-0.45	0.35	0.74	4.33	-0.12	0.23	0.99	5.22	0.42	0.12	1.61	10.12	0.77	0.11	2.29	8.00
1000	-1.43	0.47	0.30	2.19	-0.78	0.54	0.61	1.76	-0.24	0.30	0.89	4.94	0.14	0.19	1.25	6.38	0.70	0.09	2.09	13.23	1.11	0.10	3.21	8.53
2000	-1.06	0.40	0.42	2.64	-0.41	0.44	0.84	2.18	-0.01	0.24	1.10	5.75	0.41	0.15	1.62	8.27	1.00	0.06	2.79	16.93	1.43	0.10	4.39	9.88
4000	-0.68	0.34	0.60	3.26	-0.03	0.35	1.17	2.81	0.25	0.18	1.40	6.82	0.70	0.12	2.13	11.32	1.29	0.06	3.75	19.00	1.69	0.09	5.69	10.28
6000	-0.46	0.30	0.73	3.71	0.19	0.30	1.42	3.31	0.41	0.16	1.63	7.55	0.87	0.10	2.51	13.33	1.45	0.06	4.39	18.39	1.81	0.10	6.42	9.87
8000	-0.31	0.28	0.84	4.06	0.34	0.27	1.62	3.74	0.54	0.14	1.83	8.10	0.99	0.09	2.82	14.12	1.54	0.06	4.84	17.36	1.88	0.10	6.91	9.64
10000	-0.20	0.26	0.93	4.33	0.46	0.25	1.79	4.12	0.63	0.13	2.00	8.54	1.08	0.09	3.08	14.09	1.61	0.07	5.16	16.53	1.93	0.11	7.26	9.59
12000	-0.11	0.24	1.01	4.54	0.55	0.23	1.94	4.45	0.71	0.12	2.17	8.89	1.15	0.09	3.31	13.72	1.65	0.07	5.40	15.93	1.97	0.11	7.53	9.65
14000	-0.03	0.23	1.08	4.71	0.62	0.21	2.07	4.73	0.78	0.12	2.32	9.17	1.21	0.09	3.51	13.25	1.69	0.07	5.59	15.51	2.00	0.11	7.76	9.79
16000	0.03	0.23	1.15	4.84	0.68	0.20	2.18	4.98	0.84	0.12	2.45	9.41	1.26	0.09	3.68	12.79	1.71	0.07	5.74	15.20	2.02	0.10	7.96	9.98
18000	0.09	0.22	1.21	4.95	0.73	0.19	2.28	5.19	0.89	0.11	2.58	9.62	1.30	0.09	3.83	12.37	1.73	0.07	5.86	14.98	2.04	0.10	8.13	10.18
20000	0.13	0.21	1.27	5.04	0.77	0.18	2.38	5.37	0.94	0.11	2.70	9.79	1.33	0.09	3.97	11.99	1.75	0.07	5.96	14.80	2.06	0.10	8.29	10.39
30000	0.31	0.20	1.51	5.39	0.92	0.16	2.73	6.00	1.11	0.11	3.20	10.37	1.45	0.10	4.48	10.69	1.81	0.08	6.32	14.27	2.14	0.09	8.93	11.39
40000	0.43	0.19	1.69	5.65	1.01	0.15	2.98	6.34	1.23	0.10	3.58	10.69	1.52	0.10	4.83	10.00	1.85	0.08	6.58	13.92	2.20	0.09	9.44	12.18
50000	0.52	0.19	1.84	5.85	1.08	0.14	3.17	6.57	1.31	0.10	3.87	10.89	1.57	0.11	5.09	9.59	1.88	0.08	6.78	13.61	2.25	0.08	9.87	12.79
60000	0.58	0.19	1.96	5.98	1.13	0.14	3.33	6.74	1.37	0.10	4.10	11.02	1.61	0.11	5.31	9.33	1.90	0.08	6.96	13.33	2.29	0.08	10.24	13.27
70000	0.64	0.18	2.08	6.06	1.17	0.14	3.46	6.88	1.41	0.10	4.29	11.12	1.65	0.11	5.50	9.13	1.92	0.08	7.12	13.09	2.32	0.08	10.58	13.65
80000	0.69	0.18	2.17	6.10	1.20	0.14	3.57	7.01	1.45	0.10	4.44	11.20	1.67	0.12	5.66	8.98	1.94	0.08	7.26	12.88	2.35	0.08	10.88	13.96
90000	0.73	0.18	2.26	6.10	1.23	0.14	3.67	7.11	1.47	0.10	4.56	11.27	1.70	0.12	5.81	8.85	1.96	0.08	7.39	12.69	2.37	0.08	11.16	14.21
100000	0.77	0.18	2.35	6.09	1.25	0.14	3.76	7.18	1.50	0.09	4.67	11.33	1.72	0.12	5.95	8.74	1.98	0.08	7.50	12.52	2.40	0.07	11.42	14.41
110000	0.80	0.18	2.42	6.07	1.28	0.14	3.85	7.23	1.52	0.09	4.76	11.39	1.74	0.12	6.08	8.63	1.99	0.08	7.61	12.36	2.42	0.07	11.67	14.58
120000	0.83	0.18	2.50	6.04	1.30	0.14	3.93	7.25	1.53	0.09	4.84	11.45	1.76	0.12	6.20	8.54	2.00	0.08	7.71	12.22	2.44	0.07	11.89	14.72
130000	0.86	0.17	2.57	6.02	1.32	0.14	4.01	7.23	1.55	0.09	4.91	11.51	1.78	0.12	6.32	8.45	2.02	0.08	7.81	12.10	2.46	0.07	12.11	14.83
140000	0.88	0.17	2.63	5.99	1.34	0.14	4.09	7.18	1.56	0.09	4.97	11.57	1.80	0.13	6.43	8.37	2.03	0.08	7.90	11.98	2.48	0.07	12.32	14.92
150000	0.90	0.17	2.69	5.96	1.35	0.14	4.16	7.10	1.57	0.09	5.03	11.62	1.81	0.13	6.53	8.29	2.04	0.08	7.99	11.87	2.49	0.07	12.52	15.00
160000	0.93	0.17	2.75	5.94	1.37	0.14	4.23	7.00	1.58	0.09	5.08	11.67	1.83	0.13	6.63	8.22	2.05	0.08	8.07	11.77	2.51	0.07	12.70	15.06
170000	0.95	0.17	2.81	5.91	1.38	0.14	4.29	6.88	1.59	0.09	5.13	11.72	1.84	0.13	6.73	8.15	2.06	0.08	8.15	11.67	2.52	0.07	12.89	15.11
180000	0.97	0.17	2.87	5.89	1.40	0.14	4.36	6.75	1.60	0.09	5.17	11.77	1.85	0.13	6.82	8.09	2.07	0.08	8.22	11.59	2.53	0.07	13.06	15.15
190000	0.98	0.17	2.92	5.86	1.41	0.14	4.42	6.62	1.61	0.08	5.21	11.82	1.87	0.13	6.91	8.03	2.08	0.08	8.29	11.50	2.55	0.07	13.23	15.18
200000	1.00	0.17	2.97	5.83	1.43	0.14	4.48	6.48	1.62	0.08	5.25	11.87	1.88	0.13	6.99	7.97	2.08	0.08	8.36	11.43	2.56	0.07	13.39	15.21

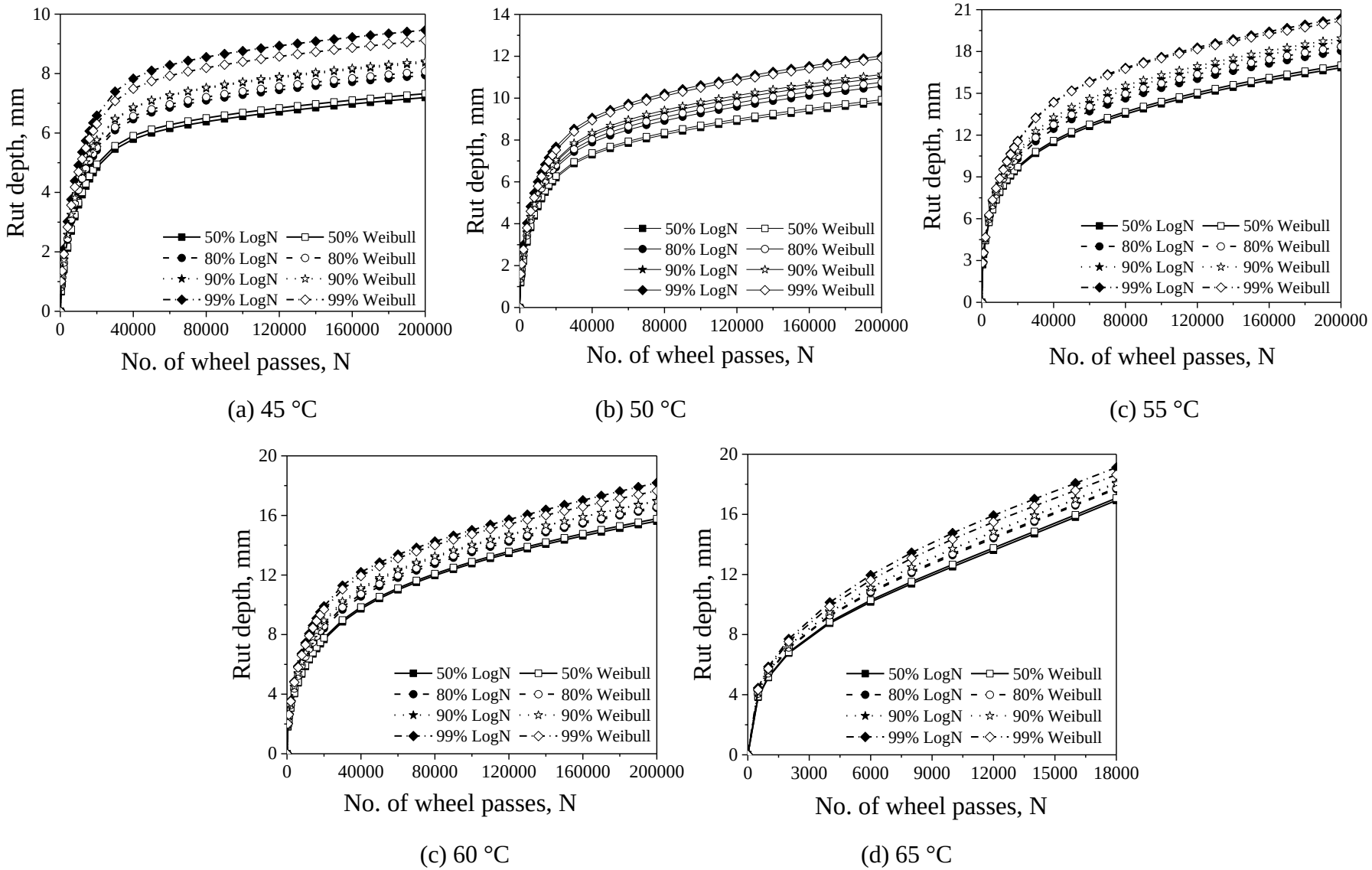

Fig. B2 Reliability rut curves for the STA BC-2 with VG20 bitumen

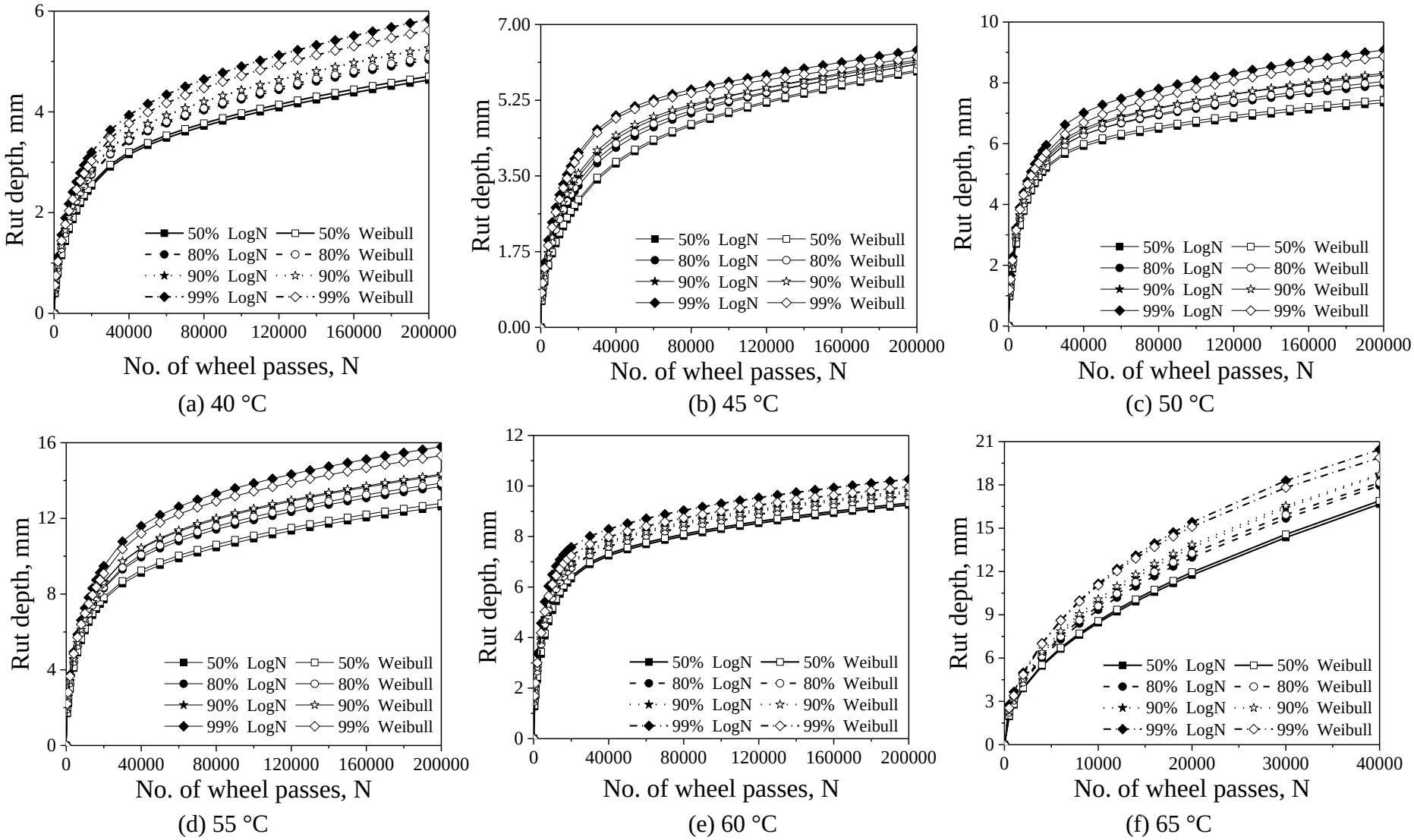

Fig. B3 Reliability rut curves for the LTA BC-2 with VG20 bitumen

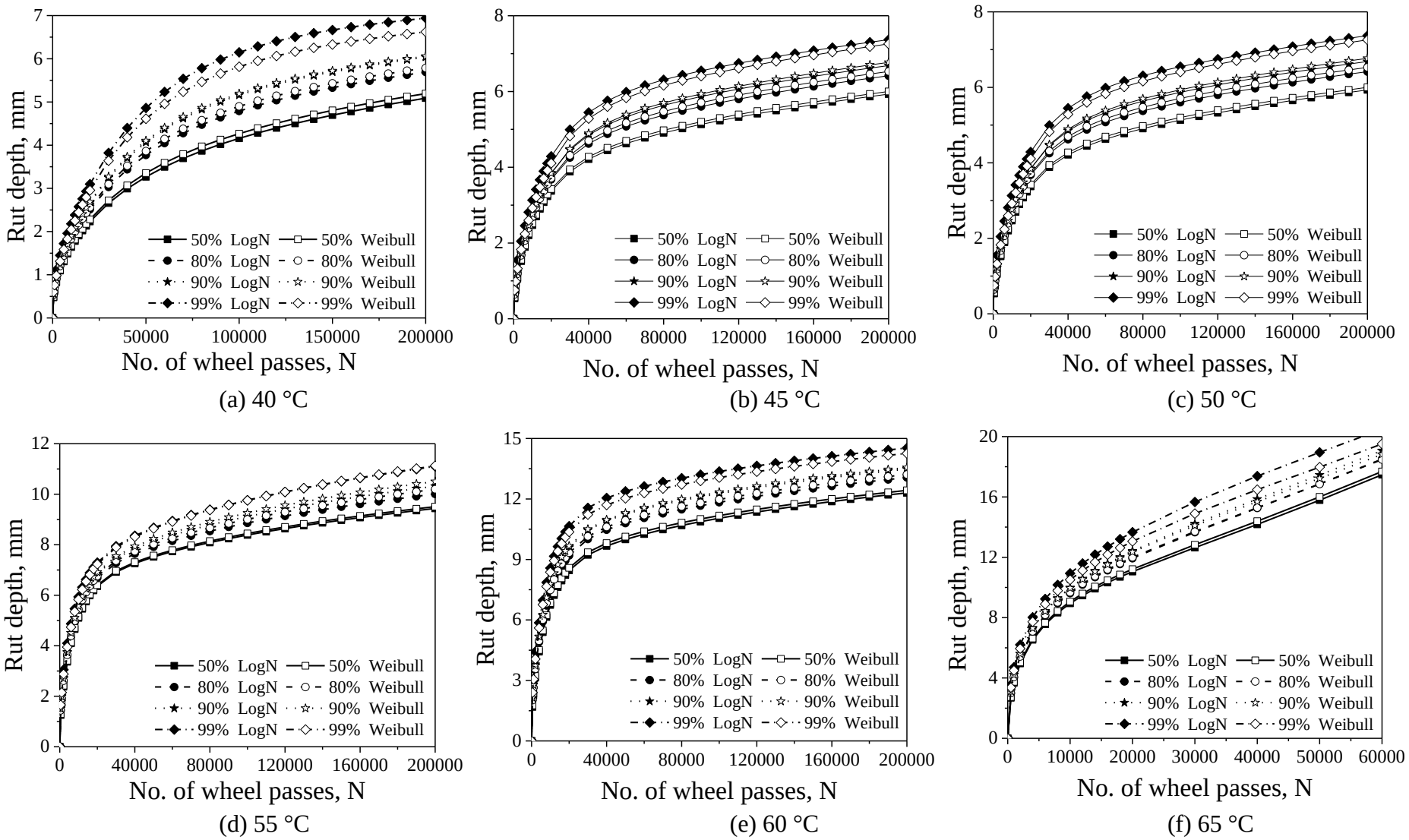

Fig. B4 Reliability rut curves for the STA BC-2 with VG40 bitumen

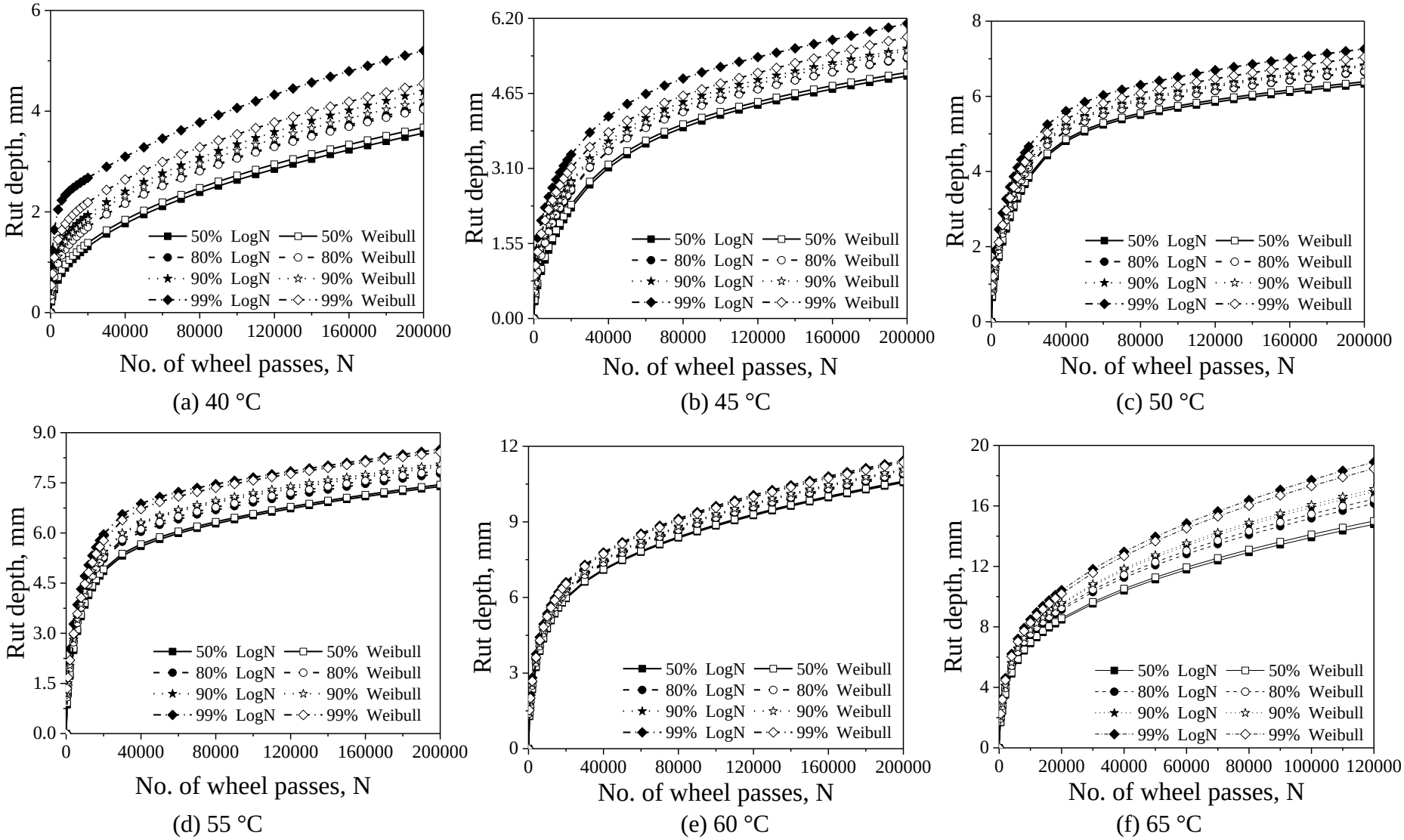

Fig. B5 Reliability rut curves for the LTA BC-2 with VG40 bitumen

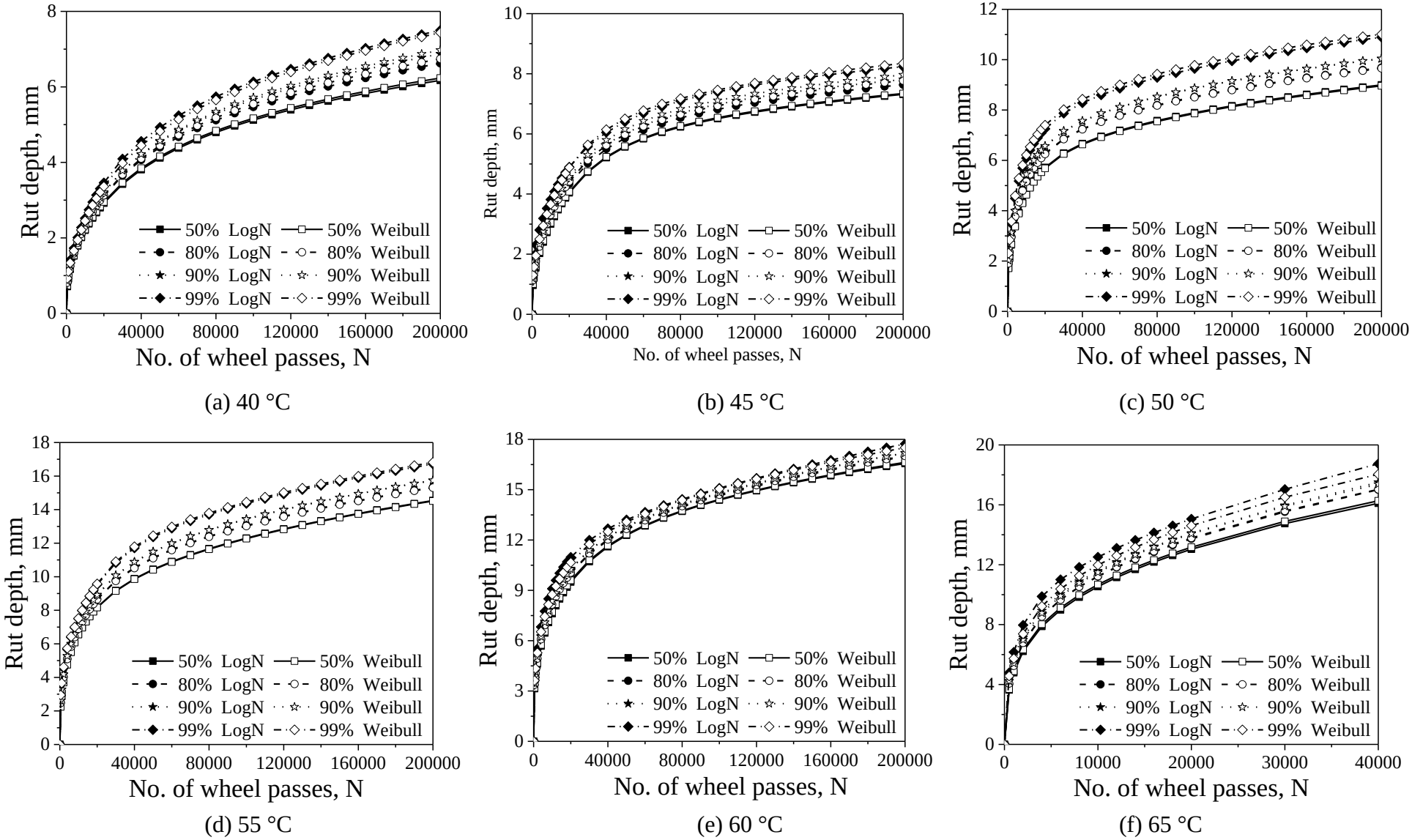

(a) 40 °C (b) 45 °C (c) 50 °C

(d) 55 °C (e) 60 °C (f) 65 °C

Fig. B6 Reliability rut curves for the STA DBM-2 with VG20 bitumen

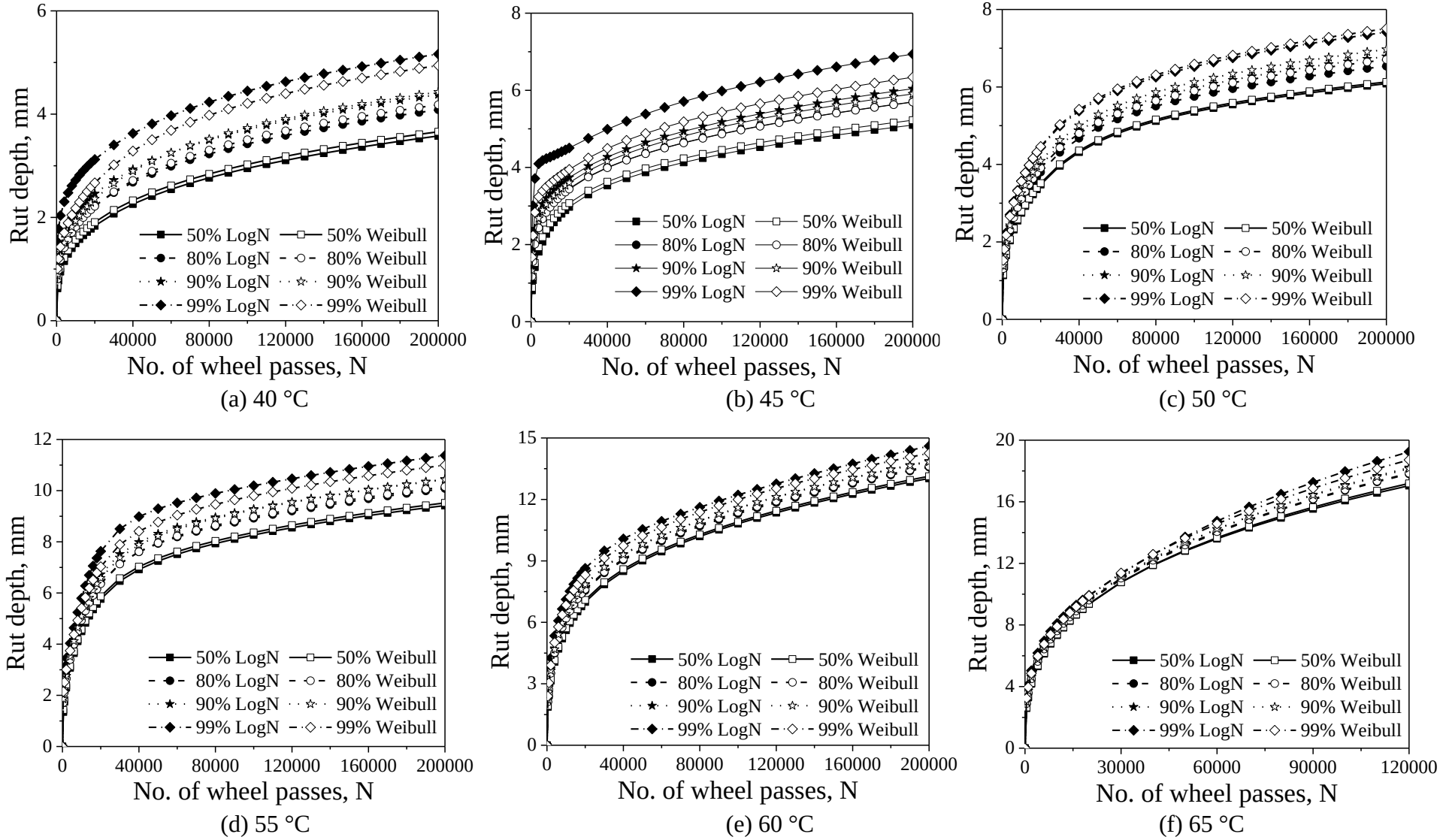

Fig. B7 Reliability rut curves for the LTA DBM-2 with VG20 bitumen

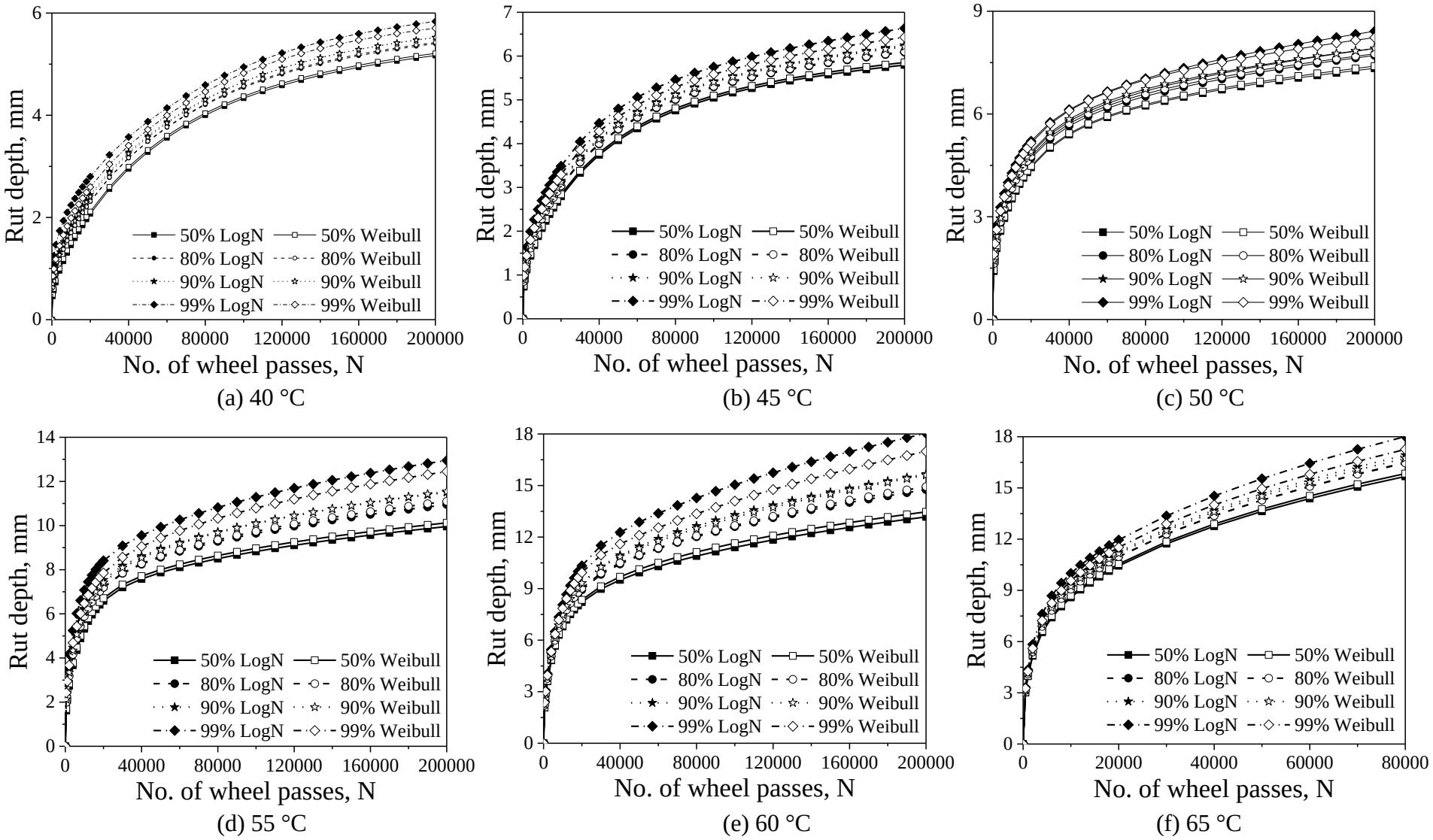

Fig. B8 Reliability rut curves for the STA DBM-2 with VG40 bitumen

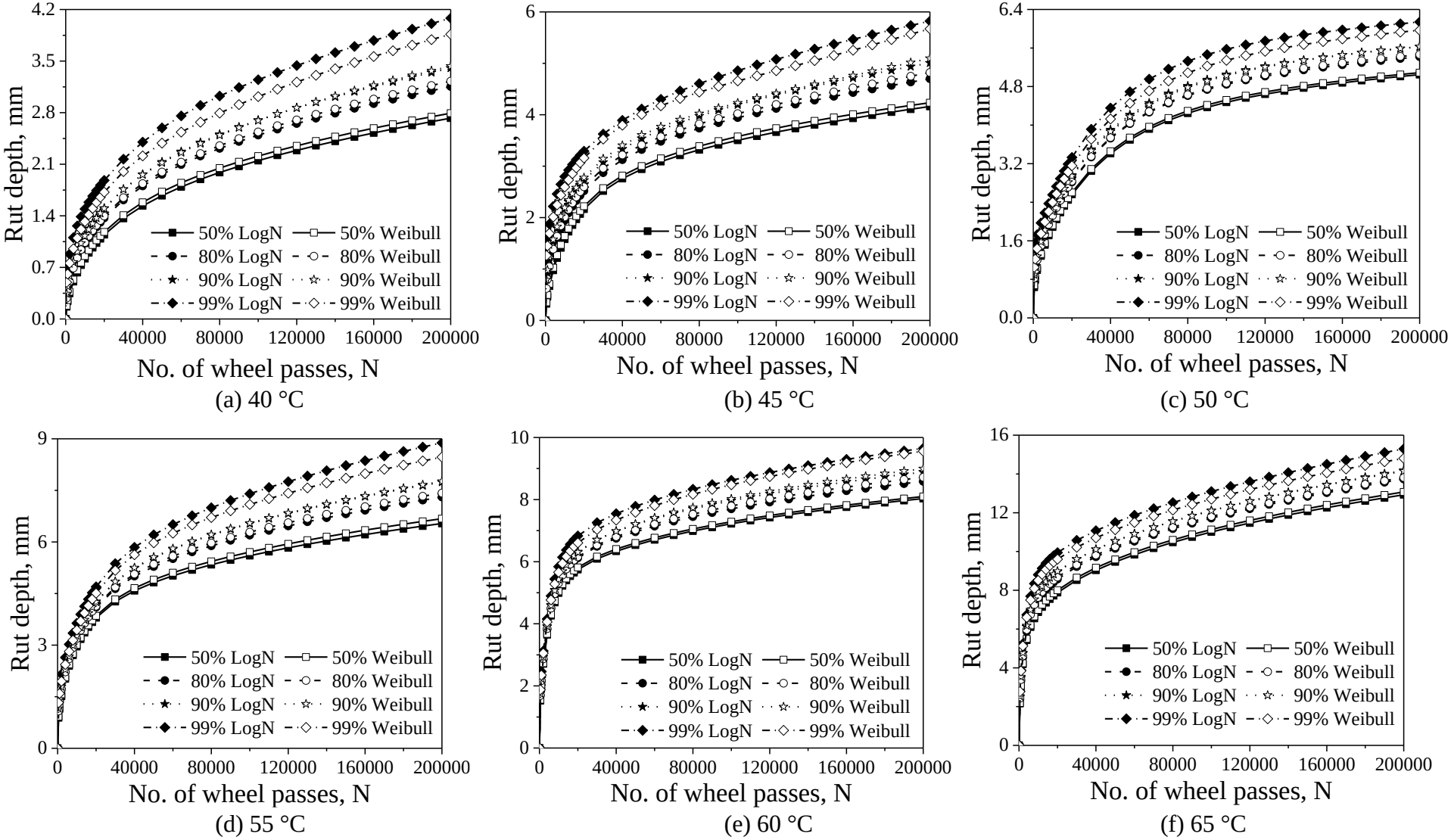

Fig. B9 Reliability rut curves for the LTA DBM-2 with VG40 bitumen

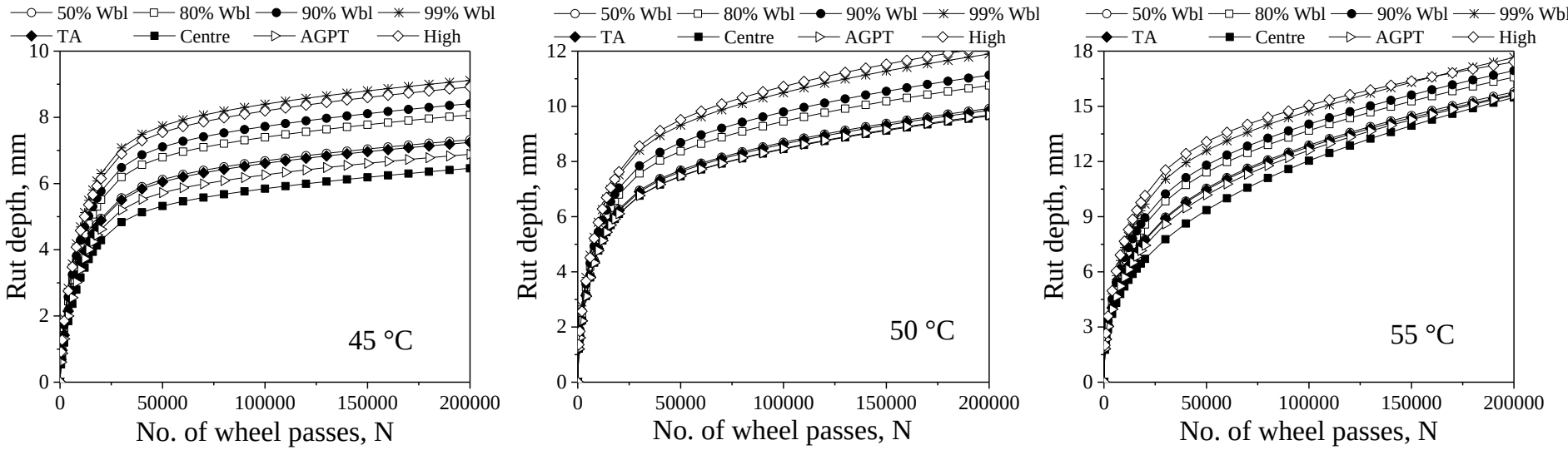

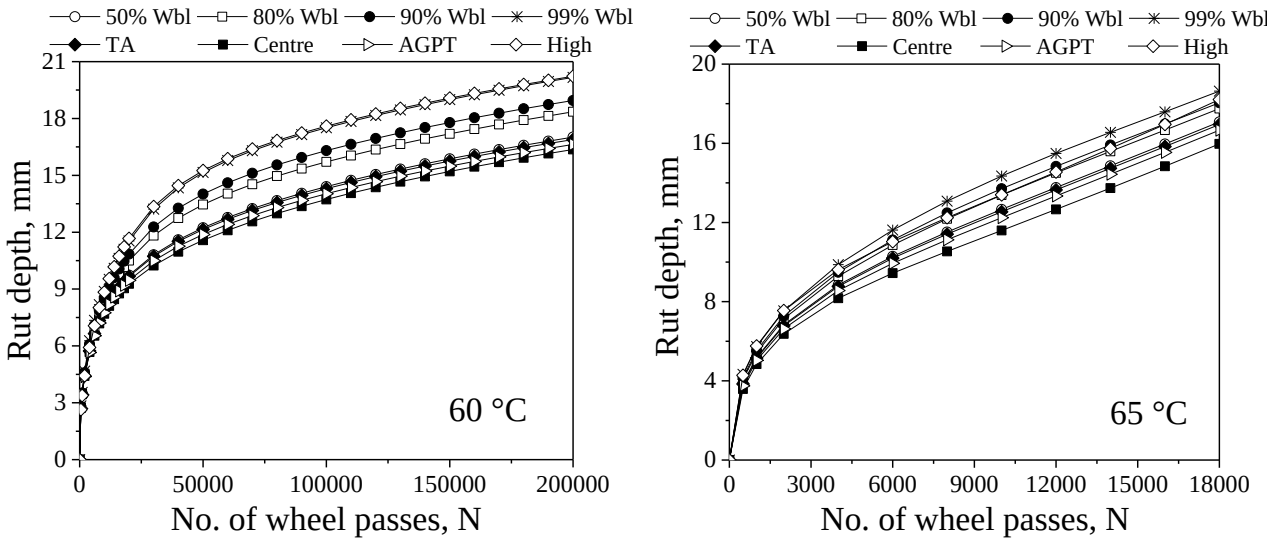

(a) STA BC-2 with VG20 bitumen

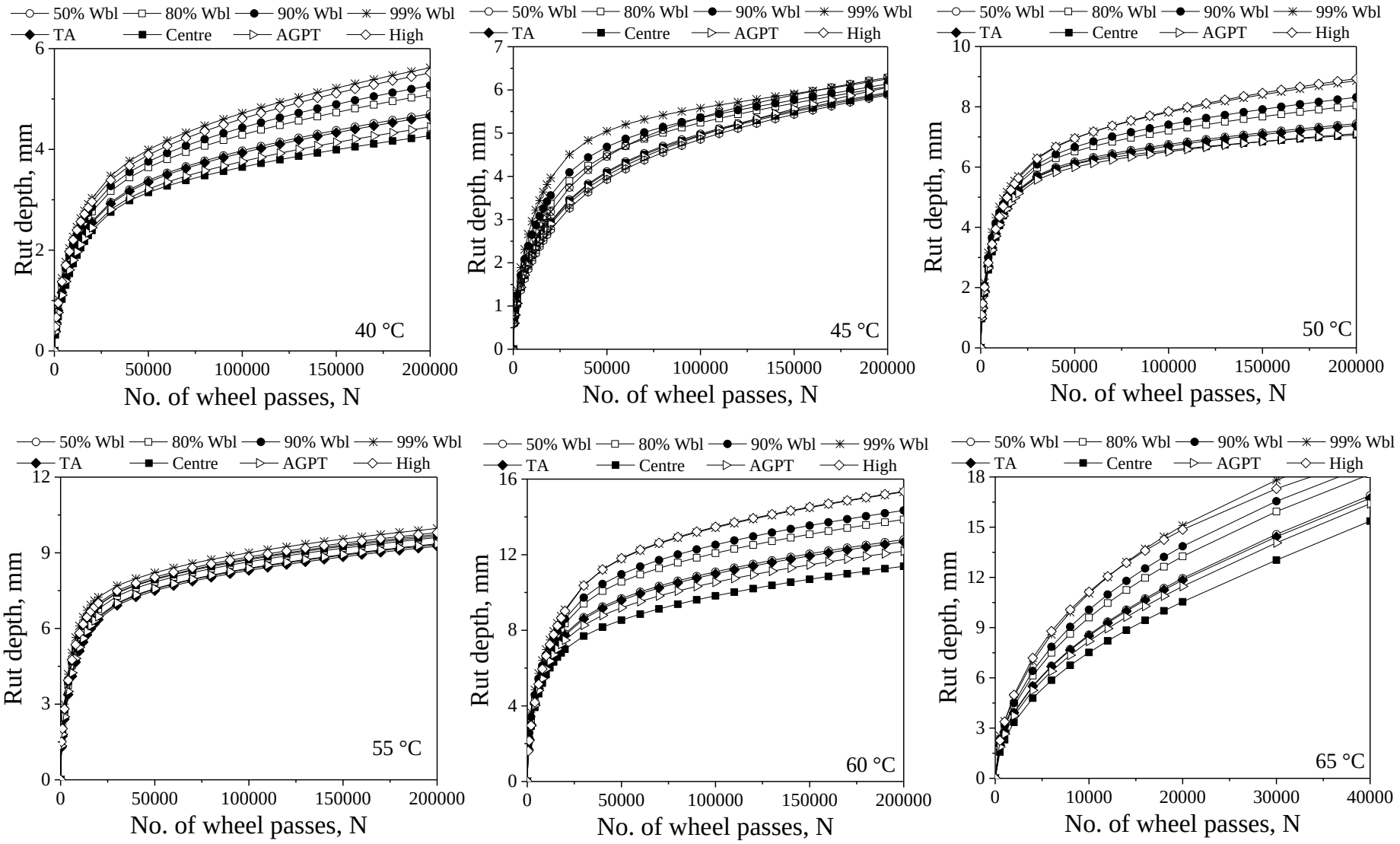

(b) LTA BC-2 with VG20 bitumen

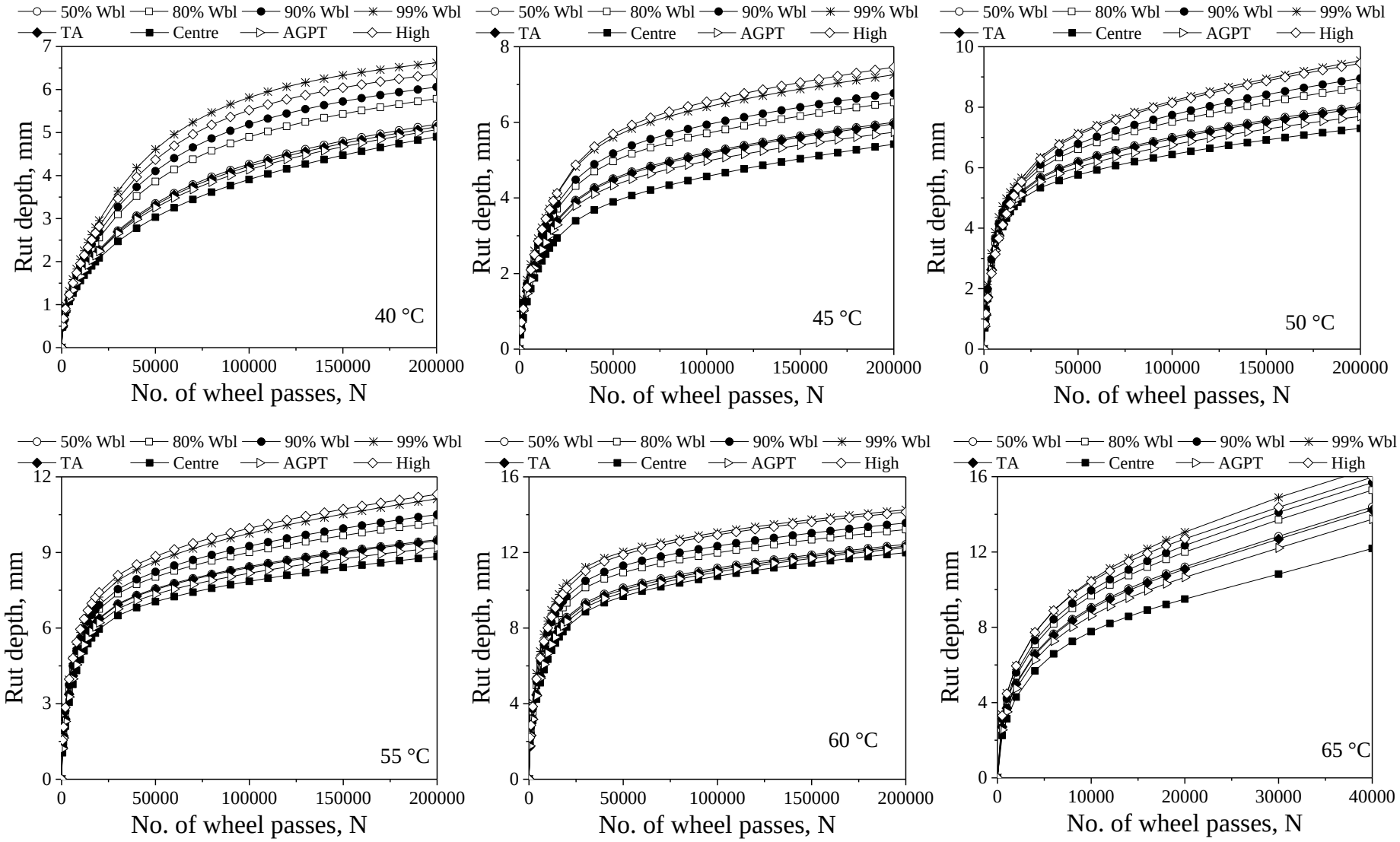

(c) STA BC-2 with VG40 bitumen

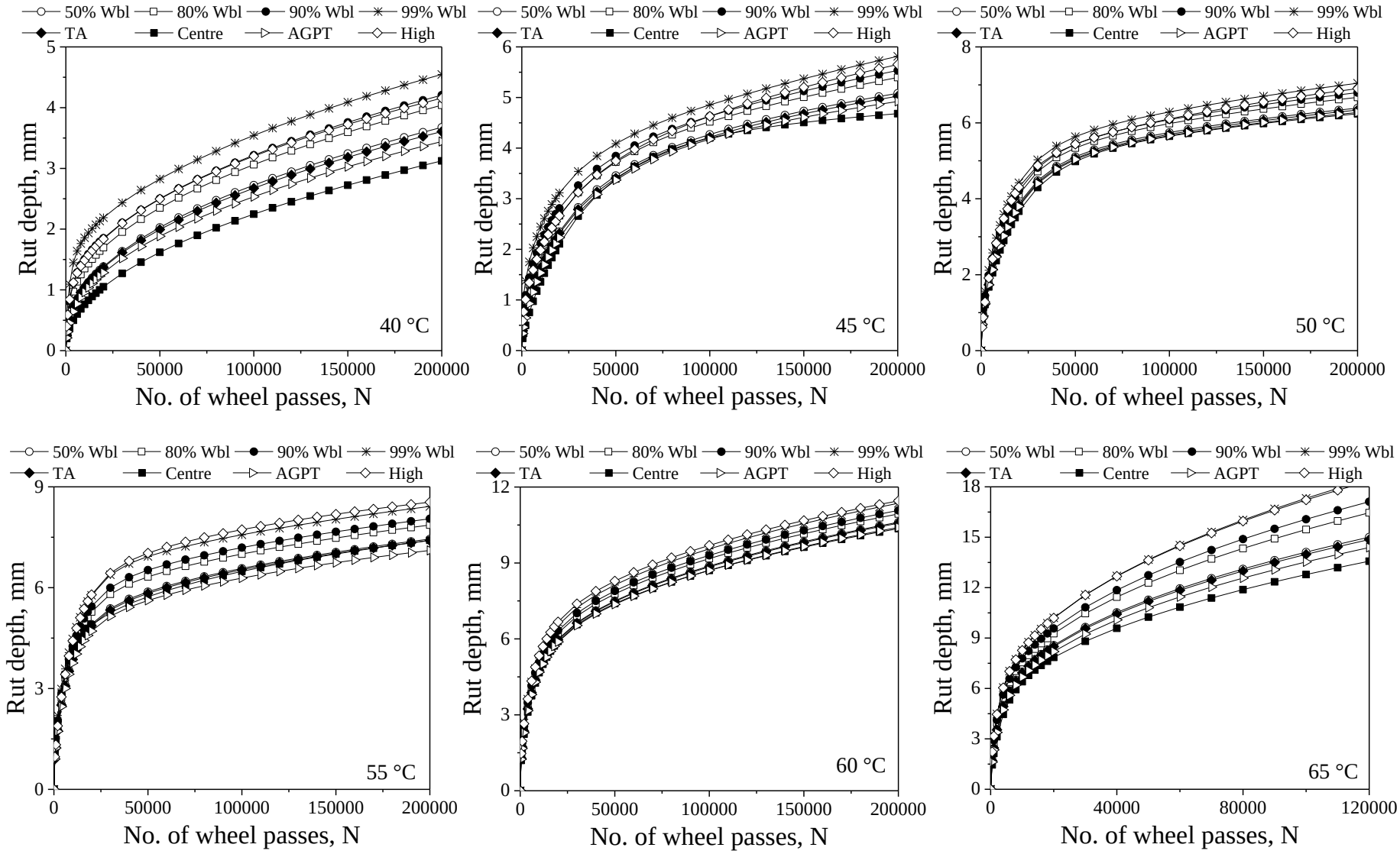

(d) LTA BC-2 with VG40 bitumen

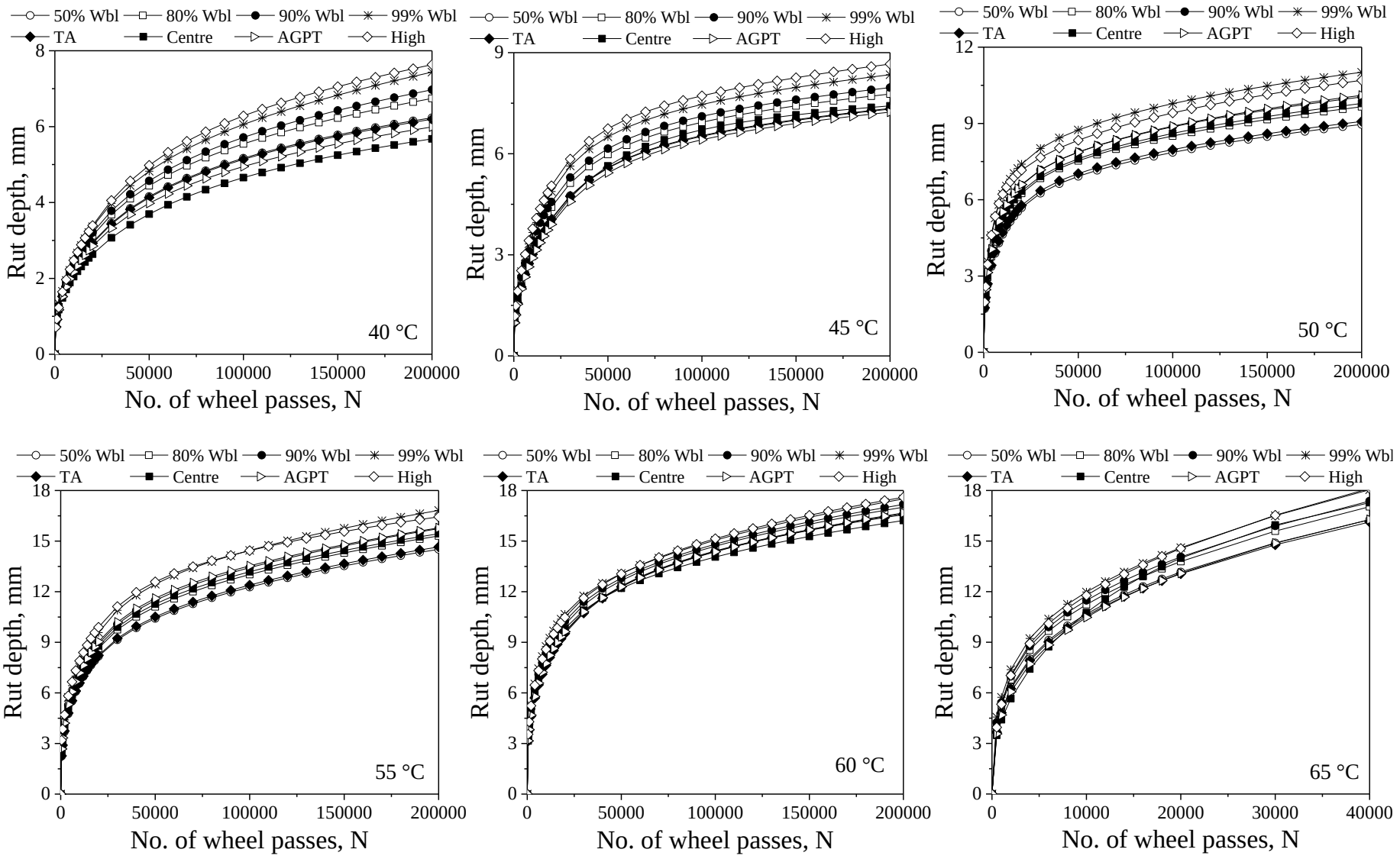

(e) STA DBM-2 with VG20 bitumen

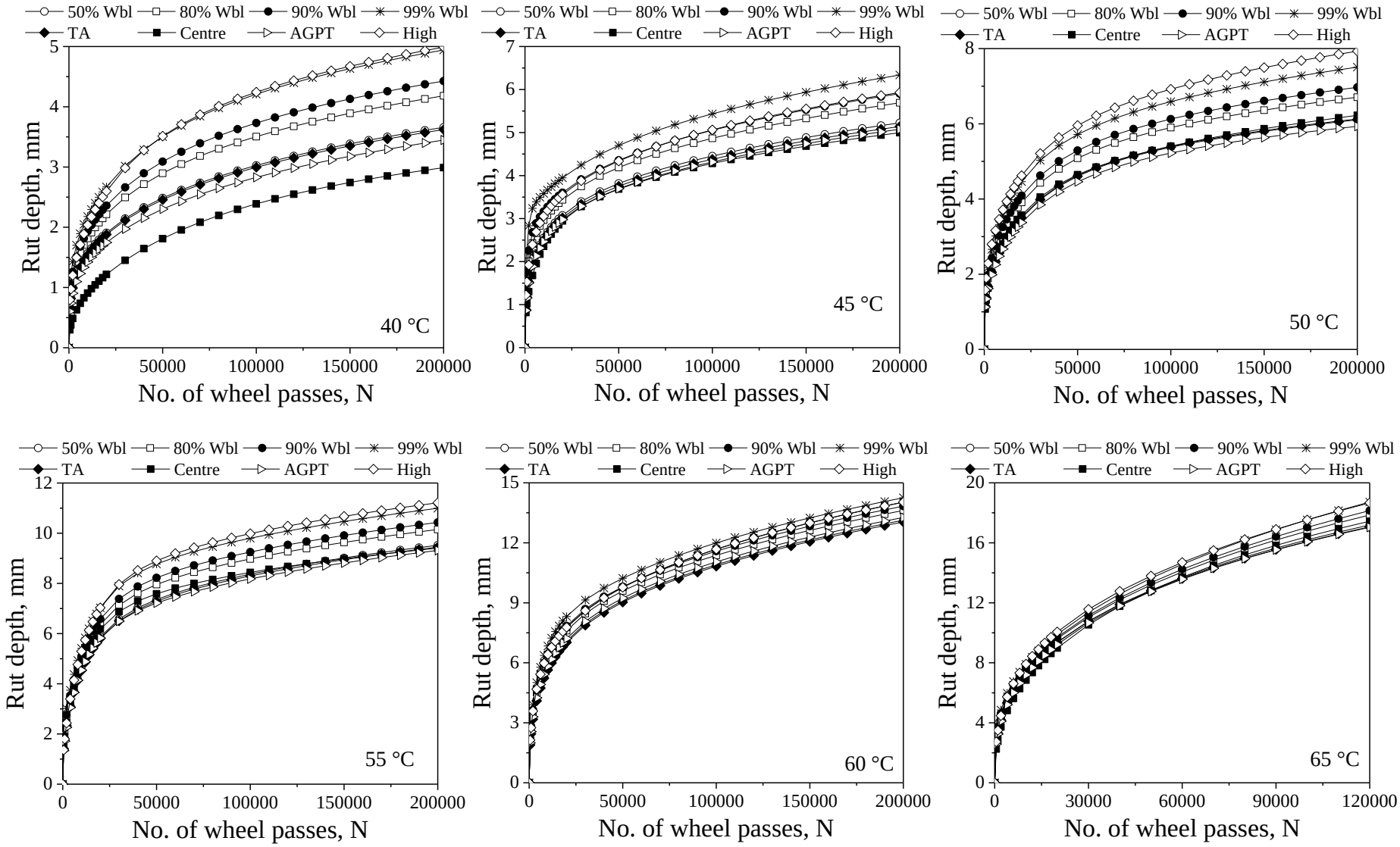

(f) LTA DBM -2 with VG20 bitumen

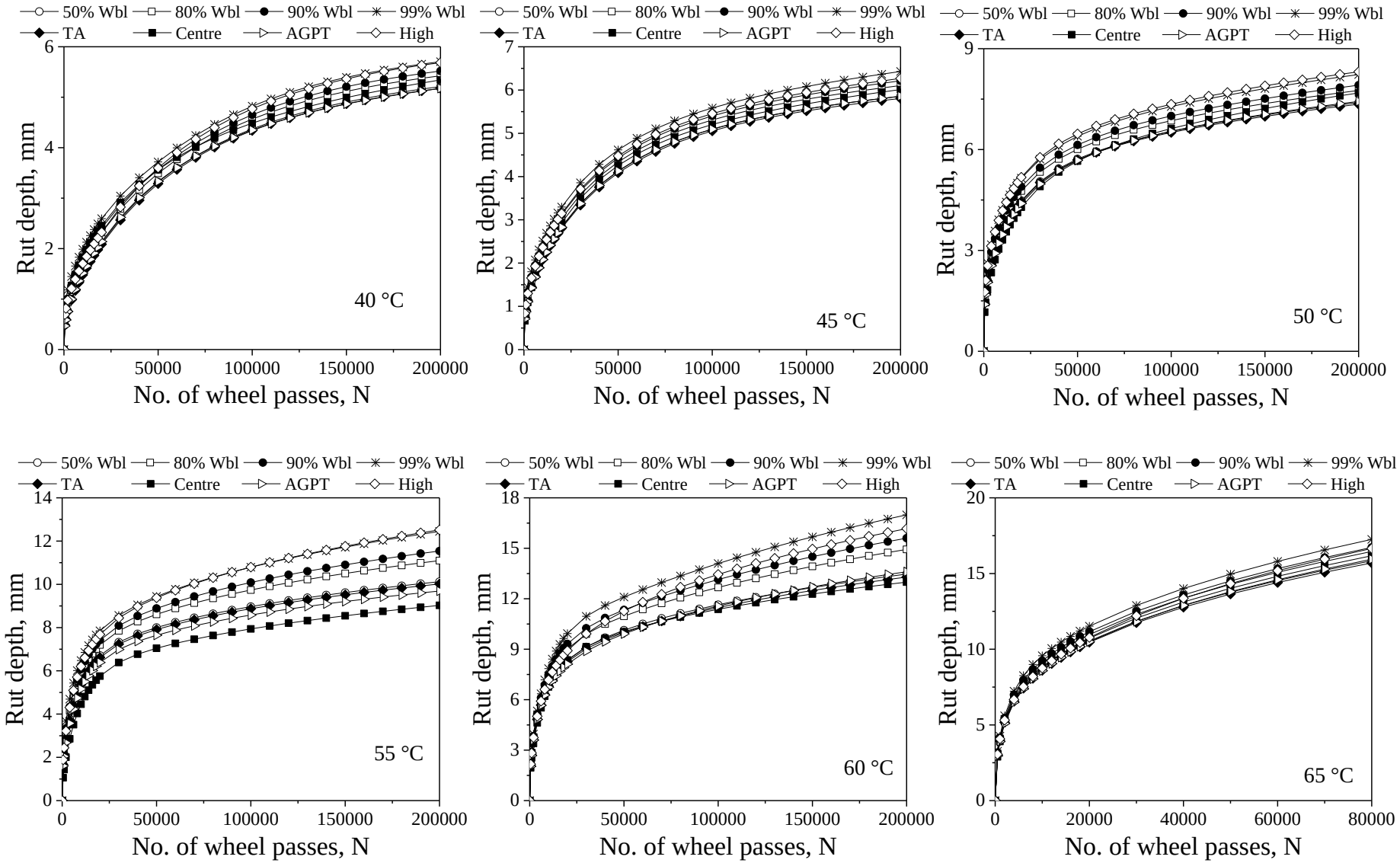

(g) STA DBM -2 with VG40 bitumen

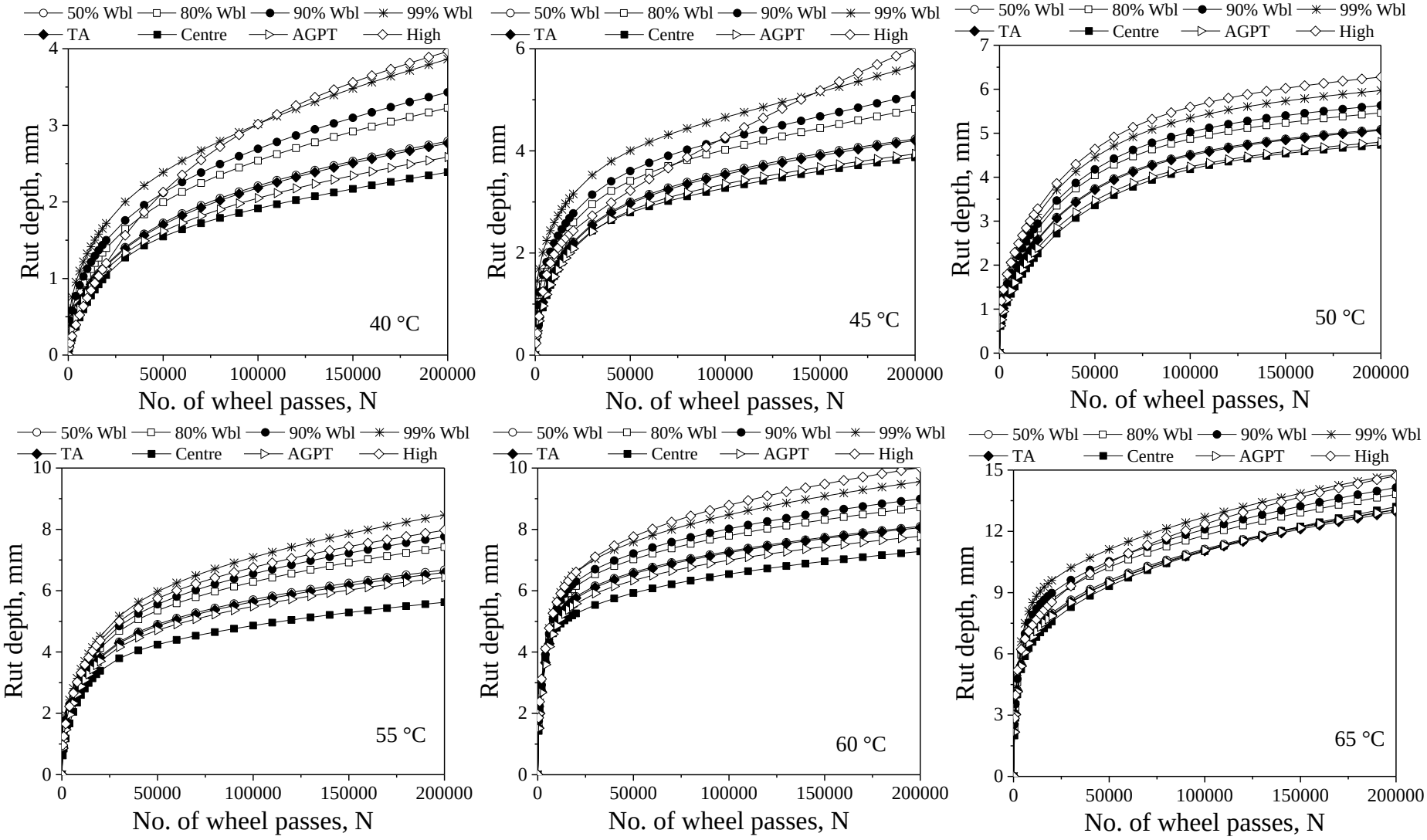

(h) LTA DBM -2 with VG40 bitumen

Fig. B10 Comparison of the Weibull probability curves with the rut curves from four methodologies

Table B22 Comparison of rut data at 80% reliability level

Mixture	Temp., °C / Passes	20000	40000	60000	80000	100000	120000	140000	160000	180000	200000
STA - BC-2 - VG20	40	4.08	5.26	5.83	6.19	6.45	6.67	6.87	7.04	7.21	7.35
	45	5.51	6.57	6.96	7.21	7.40	7.56	7.71	7.84	7.96	8.07
	50	6.80	8.04	8.65	9.09	9.45	9.77	10.05	10.31	10.54	10.76
	55	8.58	10.73	11.97	12.90	13.68	14.36	14.98	15.55	16.09	16.59
	60	10.50	12.75	14.04	14.96	15.71	16.36	16.93	17.44	17.92	18.35
	65										
STA - BC-2 - VG40	40	2.56	3.52	4.14	4.58	4.90	5.14	5.34	5.51	5.66	5.79
	45	3.71	4.70	5.17	5.47	5.71	5.91	6.08	6.24	6.39	6.53
	50	5.42	6.34	6.83	7.20	7.52	7.79	8.04	8.26	8.47	8.67
	55	6.76	7.74	8.27	8.67	9.00	9.29	9.55	9.79	10.00	10.20
	60	9.33	10.61	11.20	11.63	11.98	12.28	12.55	12.79	13.01	13.21
	65	12.00	15.28	18.48							
LTA - BC-2 - VG20	40	2.77	3.44	3.81	4.07	4.29	4.48	4.65	4.81	4.96	5.09
	45	3.37	4.25	4.71	5.01	5.24	5.44	5.61	5.77	5.93	6.08
	50	5.44	6.29	6.69	6.97	7.21	7.41	7.59	7.75	7.90	8.04
	55	6.77	7.60	8.04	8.37	8.64	8.88	9.09	9.28	9.45	9.61
	60	8.36	10.08	10.96	11.58	12.08	12.51	12.90	13.25	13.57	13.86
	65	13.26	18.16								
LTA - BC-2 - VG40	40	1.70	2.16	2.52	2.81	3.06	3.29	3.50	3.69	3.87	4.04
	45	2.66	3.46	3.94	4.27	4.52	4.73	4.92	5.09	5.25	5.40
	50	4.11	5.09	5.52	5.78	5.98	6.15	6.30	6.43	6.56	6.67
	55	5.28	6.11	6.49	6.77	7.00	7.21	7.39	7.56	7.72	7.86
	60	6.23	7.38	8.11	8.69	9.17	9.60	9.98	10.32	10.64	10.94
	65	9.26	11.44	13.03	14.34	15.46	16.45				
STA - DBM-2 - VG20	40	3.13	4.10	4.73	5.18	5.55	5.85	6.11	6.34	6.55	6.74
	45	4.42	5.62	6.25	6.65	6.93	7.16	7.34	7.50	7.64	7.77
	50	6.34	7.31	7.86	8.27	8.61	8.90	9.15	9.38	9.59	9.79
	55	8.79	10.67	11.76	12.55	13.18	13.73	14.22	14.66	15.06	15.44
	60	10.06	12.03	13.18	14.02	14.70	15.27	15.77	16.22	16.63	17.01
	65	13.79	17.04								
STA - DBM-2 - VG40	40	2.32	3.17	3.77	4.22	4.57	4.83	5.03	5.19	5.32	5.43
	45	3.04	4.00	4.61	5.02	5.31	5.53	5.71	5.86	5.99	6.10
	50	4.77	5.72	6.24	6.59	6.86	7.08	7.28	7.45	7.61	7.76
	55	7.20	8.28	8.89	9.35	9.74	10.07	10.37	10.63	10.87	11.10
	60	9.01	10.50	11.37	12.07	12.67	13.21	13.70	14.14	14.55	14.93
	65	10.97	13.37	15.08	16.46						
LTA - DBM-2 - VG20	40	2.22	2.71	3.05	3.30	3.50	3.68	3.82	3.96	4.07	4.18
	45	3.44	3.99	4.35	4.63	4.87	5.07	5.25	5.41	5.56	5.69
	50	3.91	4.80	5.31	5.64	5.90	6.11	6.28	6.44	6.58	6.71
	55	6.36	7.61	8.22	8.64	8.98	9.26	9.52	9.75	9.96	10.15
	60	7.61	9.09	10.02	10.76	11.38	11.92	12.40	12.84	13.24	13.62
	65	9.61	12.20	14.06	15.54	16.78					
LTA - DBM-2 - VG40	40	1.40	1.84	2.13	2.35	2.54	2.70	2.85	2.98	3.11	3.23
	45	2.60	3.22	3.57	3.82	4.02	4.20	4.36	4.52	4.68	4.82
	50	2.84	3.74	4.28	4.63	4.87	5.05	5.18	5.29	5.38	5.46
	55	4.13	5.07	5.59	5.97	6.29	6.56	6.81	7.03	7.23	7.42
	60	6.15	6.81	7.21	7.53	7.79	8.02	8.22	8.40	8.57	8.72
	65	8.68	9.82	10.62	11.26	11.81	12.29	12.72	13.11	13.48	13.81

Table B23 Comparison of rut data at 90% reliability level

Mixture	Temp., °C / Passes	20000	40000	60000	80000	100000	120000	140000	160000	180000	200000
STA-BC-2-VG20	40	4.24	5.48	6.09	6.47	6.75	6.99	7.19	7.38	7.56	7.72
	45	5.77	6.87	7.28	7.53	7.73	7.89	8.04	8.18	8.30	8.41
	50	7.04	8.33	8.97	9.42	9.80	10.12	10.41	10.67	10.91	11.13
	55	8.94	11.12	12.35	13.27	14.03	14.71	15.33	15.90	16.44	16.94
	60	10.84	13.27	14.61	15.55	16.30	16.95	17.52	18.04	18.51	18.95
	65										
STA-BC-2-VG40	40	2.69	3.73	4.41	4.86	5.19	5.44	5.64	5.80	5.94	6.06
	45	3.84	4.89	5.39	5.70	5.94	6.14	6.32	6.48	6.63	6.77
	50	5.50	6.49	7.02	7.42	7.74	8.03	8.29	8.53	8.75	8.95
	55	6.91	7.93	8.48	8.90	9.25	9.56	9.83	10.07	10.30	10.50
	60	9.67	10.97	11.56	11.99	12.34	12.64	12.90	13.14	13.36	13.56
	65	12.35	15.68	18.82							
LTA-BC-2-VG20	40	2.85	3.55	3.93	4.20	4.43	4.63	4.81	4.97	5.13	5.27
	45	3.56	4.44	4.87	5.14	5.35	5.53	5.69	5.84	5.99	6.14
	50	5.53	6.43	6.85	7.16	7.41	7.63	7.82	8.00	8.16	8.31
	55	6.93	7.73	8.16	8.49	8.76	9.00	9.21	9.40	9.57	9.73
	60	8.60	10.45	11.37	12.01	12.52	12.97	13.36	13.72	14.04	14.34
	65	13.86	18.73								
LTA-BC-2-VG40	40	1.85	2.32	2.67	2.96	3.22	3.45	3.66	3.85	4.03	4.21
	45	2.81	3.59	4.05	4.38	4.63	4.85	5.04	5.21	5.38	5.53
	50	4.21	5.19	5.62	5.88	6.08	6.25	6.41	6.55	6.68	6.80
	55	5.44	6.31	6.69	6.96	7.19	7.39	7.58	7.75	7.90	8.05
	60	6.33	7.50	8.23	8.81	9.30	9.73	10.11	10.46	10.78	11.08
	65	9.57	11.85	13.52	14.89	16.07	17.11				
STA-DBM-2-VG20	40	3.20	4.22	4.86	5.34	5.71	6.03	6.30	6.54	6.77	6.97
	45	4.57	5.79	6.43	6.83	7.11	7.33	7.52	7.68	7.83	7.96
	50	6.60	7.57	8.13	8.55	8.89	9.19	9.45	9.69	9.91	10.11
	55	9.04	11.00	12.11	12.90	13.53	14.08	14.56	15.00	15.41	15.78
	60	10.26	12.19	13.31	14.14	14.82	15.39	15.90	16.36	16.78	17.18
	65	14.06	17.37								
STA-DBM-2-VG40	40	2.41	3.25	3.85	4.30	4.65	4.92	5.12	5.28	5.41	5.52
	45	3.12	4.10	4.70	5.11	5.40	5.63	5.81	5.96	6.09	6.21
	50	4.89	5.85	6.37	6.72	7.00	7.23	7.42	7.60	7.76	7.92
	55	7.41	8.54	9.18	9.67	10.09	10.44	10.76	11.04	11.30	11.54
	60	9.32	10.86	11.75	12.49	13.14	13.72	14.25	14.74	15.18	15.60
	65	11.15	13.58	15.32	16.72						
LTA-DBM-2-VG20	40	2.36	2.90	3.25	3.52	3.73	3.91	4.06	4.19	4.32	4.43
	45	3.60	4.16	4.53	4.81	5.05	5.26	5.44	5.61	5.76	5.91
	50	4.09	5.00	5.52	5.86	6.13	6.34	6.53	6.69	6.84	6.97
	55	6.58	7.88	8.49	8.91	9.25	9.54	9.79	10.02	10.23	10.43
	60	7.84	9.30	10.23	10.97	11.58	12.12	12.61	13.05	13.45	13.83
	65	9.71	12.33	14.23	15.75	17.03					
LTA-DBM-2-VG40	40	1.50	1.96	2.26	2.49	2.69	2.87	3.02	3.17	3.30	3.43
	45	2.78	3.40	3.77	4.02	4.23	4.41	4.59	4.76	4.93	5.10
	50	2.94	3.87	4.42	4.78	5.03	5.21	5.34	5.45	5.55	5.63
	55	4.26	5.25	5.81	6.21	6.55	6.84	7.10	7.34	7.56	7.76
	60	6.31	6.98	7.41	7.74	8.02	8.26	8.47	8.66	8.84	9.00
	65	8.98	10.11	10.91	11.55	12.10	12.59	13.03	13.43	13.80	14.14

Table B24 Comparison of rut data at 99% reliability level

Mixture	Temp., °C / Passes	20000	40000	60000	80000	100000	120000	140000	160000	180000	200000
STA - BC-2 - VG20	40	4.58	5.94	6.62	7.04	7.37	7.64	7.87	8.09	8.29	8.47
	45	6.30	7.49	7.93	8.19	8.40	8.57	8.73	8.87	9.00	9.12
	50	7.52	8.94	9.62	10.10	10.49	10.83	11.14	11.41	11.66	11.90
	55	9.69	11.93	13.13	14.00	14.74	15.40	16.01	16.59	17.13	17.65
	60	11.54	14.34	15.78	16.75	17.51	18.16	18.73	19.25	19.73	20.17
	65										
STA - BC-2 - VG40	40	2.95	4.18	4.96	5.47	5.82	6.07	6.25	6.40	6.52	6.62
	45	4.11	5.29	5.83	6.16	6.41	6.61	6.80	6.96	7.11	7.26
	50	5.66	6.81	7.41	7.84	8.20	8.52	8.81	9.07	9.31	9.54
	55	7.23	8.32	8.91	9.37	9.76	10.09	10.38	10.65	10.90	11.13
	60	10.37	11.70	12.30	12.72	13.06	13.35	13.61	13.85	14.06	14.26
	65	13.05	16.48	19.51							
LTA - BC-2 - VG20	40	3.03	3.77	4.18	4.47	4.72	4.93	5.13	5.30	5.47	5.62
	45	3.96	4.83	5.20	5.42	5.58	5.72	5.85	5.98	6.11	6.26
	50	5.70	6.69	7.18	7.53	7.82	8.07	8.30	8.50	8.69	8.87
	55	7.24	7.98	8.40	8.73	9.00	9.24	9.45	9.64	9.81	9.97
	60	9.09	11.21	12.22	12.90	13.43	13.89	14.30	14.67	15.01	15.32
	65	15.10	19.88								
LTA - BC-2 - VG40	40	2.19	2.64	2.99	3.28	3.54	3.78	3.99	4.19	4.37	4.55
	45	3.11	3.85	4.28	4.60	4.85	5.07	5.28	5.46	5.64	5.81
	50	4.42	5.39	5.82	6.08	6.29	6.47	6.63	6.78	6.91	7.04
	55	5.77	6.71	7.09	7.35	7.57	7.77	7.95	8.12	8.27	8.42
	60	6.54	7.73	8.47	9.06	9.55	9.99	10.38	10.73	11.05	11.36
	65	10.20	12.70	14.53	16.03	17.32	18.46				
STA - DBM-2 - VG20	40	3.36	4.45	5.14	5.65	6.06	6.40	6.69	6.96	7.21	7.44
	45	4.88	6.14	6.78	7.17	7.46	7.69	7.88	8.05	8.20	8.34
	50	7.12	8.09	8.67	9.11	9.47	9.79	10.06	10.31	10.54	10.75
	55	9.54	11.65	12.80	13.60	14.24	14.78	15.26	15.70	16.10	16.47
	60	10.66	12.50	13.57	14.38	15.05	15.64	16.17	16.65	17.09	17.50
	65	14.61	18.04								
STA - DBM-2 - VG40	40	2.59	3.41	4.00	4.46	4.82	5.10	5.31	5.47	5.60	5.70
	45	3.30	4.28	4.89	5.29	5.59	5.81	6.00	6.16	6.30	6.43
	50	5.15	6.10	6.63	7.00	7.28	7.51	7.72	7.90	8.07	8.23
	55	7.85	9.05	9.77	10.33	10.79	11.20	11.55	11.88	12.17	12.45
	60	9.93	11.60	12.54	13.36	14.09	14.77	15.38	15.96	16.49	16.99
	65	11.52	14.01	15.80	17.26						
LTA - DBM-2 - VG20	40	2.67	3.28	3.69	3.98	4.21	4.40	4.56	4.70	4.83	4.94
	45	3.95	4.49	4.88	5.18	5.44	5.65	5.85	6.02	6.19	6.34
	50	4.46	5.42	5.95	6.31	6.59	6.82	7.02	7.20	7.36	7.51
	55	7.03	8.41	9.04	9.46	9.80	10.09	10.35	10.58	10.80	11.00
	60	8.31	9.74	10.65	11.38	11.99	12.53	13.02	13.46	13.87	14.25
	65	9.90	12.59	14.57	16.17	17.53					
LTA - DBM-2 - VG40	40	1.72	2.21	2.54	2.79	3.02	3.21	3.40	3.56	3.72	3.86
	45	3.16	3.80	4.17	4.44	4.66	4.86	5.05	5.26	5.46	5.67
	50	3.16	4.13	4.71	5.09	5.34	5.53	5.67	5.79	5.88	5.97
	55	4.51	5.63	6.25	6.71	7.09	7.42	7.72	7.99	8.24	8.47
	60	6.61	7.34	7.81	8.17	8.48	8.74	8.98	9.19	9.38	9.56
	65	9.60	10.70	11.49	12.14	12.70	13.20	13.65	14.06	14.44	14.80

APPENDIX C - Correlations

Table C1 Coefficient of correlations for the LTA BC-2 with VG20 bitumen

Passes	$\eta_{0(S)}$	η_{0TV}	$\eta_{0(L)}$	$\|G^*\|/\sin\delta$	J_{nr} *at 3.2 kPa*	$\|G^*\|/(1-(1/\tan\delta\sin\delta))$
50%						
20000	0.96	0.97	0.96	0.95	0.95	0.94
40000	0.90	0.94	0.93	0.89	0.89	0.88
60000	0.99	0.99	0.98	0.99	0.99	0.99
80000	0.98	0.99	0.99	0.99	0.99	0.98
100000	0.97	0.99	1.00	0.99	0.99	0.98
120000	0.97	0.99	1.00	0.98	0.99	0.98
140000	0.96	0.99	1.00	0.98	0.99	0.97
160000	0.95	0.99	1.00	0.98	0.99	0.97
180000	0.95	0.99	1.00	0.97	0.98	0.97
200000	0.94	0.99	1.00	0.97	0.98	0.96
80%						
20000	0.95	0.97	0.96	0.94	0.94	0.93
40000	0.90	0.94	0.94	0.89	0.90	0.88
60000	0.97	0.99	0.99	0.98	0.99	0.97
80000	0.96	0.98	0.99	0.97	0.98	0.97
100000	0.95	0.98	0.99	0.97	0.98	0.96
120000	0.94	0.98	0.99	0.96	0.97	0.96
140000	0.94	0.98	0.99	0.96	0.97	0.95
160000	0.93	0.97	0.99	0.96	0.97	0.95
180000	0.93	0.97	0.99	0.95	0.96	0.94
200000	0.92	0.97	0.98	0.95	0.96	0.94
90%						
20000	0.94	0.97	0.96	0.93	0.94	0.92
40000	0.90	0.94	0.94	0.89	0.90	0.88
60000	0.96	0.98	0.99	0.97	0.98	0.96
80000	0.95	0.98	0.99	0.96	0.98	0.96
100000	0.94	0.97	0.99	0.96	0.97	0.95
120000	0.93	0.97	0.98	0.95	0.97	0.94
140000	0.93	0.97	0.98	0.95	0.96	0.94
160000	0.92	0.96	0.98	0.95	0.96	0.93
180000	0.91	0.96	0.98	0.94	0.95	0.93
200000	0.91	0.96	0.98	0.94	0.95	0.93
99%						
20000	0.93	0.96	0.96	0.92	0.93	0.91
40000	0.89	0.94	0.94	0.89	0.90	0.87
60000	0.93	0.97	0.98	0.95	0.97	0.94
80000	0.92	0.96	0.98	0.94	0.96	0.93
100000	0.91	0.96	0.97	0.94	0.95	0.93
120000	0.91	0.95	0.97	0.93	0.94	0.92
140000	0.90	0.95	0.97	0.93	0.94	0.91
160000	0.89	0.94	0.96	0.92	0.93	0.91
180000	0.89	0.94	0.96	0.92	0.93	0.90
200000	0.88	0.93	0.96	0.91	0.92	0.90

Table C2 Coefficient of correlations for the STA BC-2 with VG40 bitumen

Passes	$\eta_{0(S)}$	η_{TV}	$\eta_{0(L)}$	$\|G^*\|/\sin\delta$	J_{nr} *at 3.2 kPa*	$\|G^*\|/(1-(1/\tan\delta\sin\delta))$
50%						
20000	0.99	0.99	0.99	0.99	1.00	0.99
40000	0.99	0.99	0.99	0.99	0.99	0.99
60000	0.95	0.95	0.96	0.97	0.95	0.96
80000	0.99	0.99	0.99	1.00	0.99	1.00
100000	0.99	0.99	0.99	1.00	0.99	1.00
120000	0.98	0.99	0.99	1.00	0.99	0.99
140000	0.98	0.99	0.99	0.99	0.99	0.99
160000	0.98	0.98	0.99	0.99	0.99	0.99
180000	0.98	0.98	0.99	0.99	0.99	0.99
200000	0.98	0.98	0.98	0.99	0.99	0.99
80%						
20000	0.99	1.00	1.00	0.99	1.00	0.99
40000	0.99	0.98	0.99	0.99	0.98	0.99
60000	0.95	0.95	0.96	0.97	0.94	0.96
80000	0.98	0.98	0.98	0.99	0.98	0.99
100000	0.98	0.98	0.98	0.99	0.98	0.99
120000	0.97	0.98	0.98	0.99	0.98	0.99
140000	0.97	0.98	0.98	0.99	0.98	0.99
160000	0.97	0.98	0.98	0.99	0.98	0.99
180000	0.97	0.98	0.98	0.99	0.98	0.99
200000	0.97	0.98	0.98	0.99	0.98	0.99
90%						
20000	0.99	1.00	0.99	0.99	1.00	0.99
40000	0.98	0.98	0.99	0.99	0.98	0.99
60000	0.95	0.95	0.96	0.97	0.94	0.96
80000	0.97	0.98	0.98	0.99	0.98	0.99
100000	0.97	0.97	0.98	0.99	0.98	0.98
120000	0.97	0.97	0.98	0.99	0.98	0.98
140000	0.97	0.97	0.98	0.99	0.98	0.98
160000	0.97	0.97	0.98	0.99	0.98	0.98
180000	0.97	0.98	0.98	0.99	0.98	0.99
200000	0.97	0.98	0.98	0.99	0.98	0.99
99%						
20000	0.99	0.99	0.99	0.99	1.00	0.99
40000	0.98	0.98	0.98	0.99	0.98	0.99
60000	0.95	0.94	0.95	0.96	0.94	0.96
80000	0.96	0.96	0.96	0.98	0.96	0.97
100000	0.95	0.96	0.96	0.98	0.96	0.97
120000	0.96	0.96	0.96	0.98	0.96	0.97
140000	0.96	0.96	0.97	0.98	0.97	0.98
160000	0.96	0.97	0.97	0.98	0.97	0.98
180000	0.96	0.97	0.97	0.98	0.97	0.98
200000	0.97	0.97	0.98	0.99	0.98	0.98

Table C3 Coefficient of correlations for the LTA BC-2 with VG40 bitumen

Passes	$\eta_{0(S)}$	η_{TV}	$\eta_{0(L)}$	$\|G^*\|/\sin\delta$	J_{nr} *at 3.2 kPa*	$\|G^*\|/(1-(1/\tan\delta\sin\delta))$
50%						
20000	0.99	0.98	0.98	0.98	0.99	0.98
40000	0.97	0.97	0.98	0.98	0.98	0.98
60000	0.95	0.96	0.97	0.98	0.97	0.97
80000	0.94	0.95	0.97	0.97	0.96	0.97
100000	0.93	0.95	0.96	0.97	0.96	0.97
120000	0.93	0.95	0.96	0.96	0.95	0.96
140000	0.94	0.97	0.97	0.98	0.97	0.98
160000	0.93	0.96	0.97	0.98	0.97	0.98
180000	0.93	0.96	0.97	0.98	0.97	0.98
200000	0.92	0.96	0.96	0.98	0.96	0.98
80%						
20000	0.98	0.97	0.97	0.98	0.98	0.98
40000	0.96	0.96	0.97	0.97	0.97	0.97
60000	0.94	0.95	0.96	0.97	0.96	0.96
80000	0.93	0.94	0.96	0.96	0.95	0.96
100000	0.92	0.94	0.95	0.95	0.94	0.95
120000	0.91	0.93	0.95	0.95	0.93	0.94
140000	0.95	0.98	0.98	0.99	0.98	0.99
160000	0.94	0.98	0.98	0.99	0.98	0.99
180000	0.93	0.97	0.98	0.98	0.97	0.98
200000	0.93	0.97	0.97	0.98	0.96	0.98
90%						
20000	0.98	0.97	0.97	0.98	0.98	0.98
40000	0.95	0.95	0.96	0.97	0.96	0.97
60000	0.93	0.94	0.95	0.96	0.95	0.96
80000	0.92	0.93	0.95	0.95	0.94	0.95
100000	0.91	0.93	0.95	0.95	0.93	0.94
120000	0.90	0.93	0.94	0.94	0.92	0.94
140000	0.95	0.98	0.99	0.99	0.98	0.99
160000	0.95	0.98	0.98	0.99	0.98	0.99
180000	0.94	0.97	0.98	0.99	0.97	0.99
200000	0.93	0.97	0.98	0.98	0.97	0.98
99%						
20000	0.96	0.95	0.96	0.97	0.97	0.97
40000	0.94	0.94	0.95	0.96	0.95	0.96
60000	0.92	0.93	0.94	0.95	0.94	0.94
80000	0.90	0.92	0.94	0.94	0.92	0.93
100000	0.89	0.92	0.93	0.93	0.91	0.93
120000	0.88	0.91	0.93	0.93	0.91	0.92
140000	0.96	0.99	0.99	1.00	0.99	1.00
160000	0.95	0.99	0.99	0.99	0.98	0.99
180000	0.94	0.98	0.99	0.99	0.98	0.99
200000	0.93	0.98	0.98	0.98	0.97	0.98

Table C4 Coefficient of correlations for the STA DBM-2 with VG20 bitumen

Passes	$\eta_{0(S)}$	η_{TV}	$\eta_{0(L)}$	$\|G^*\|/\sin\delta$	J_{nr} *at 3.2 kPa*	$\|G^*\|/(1-(1/\tan\delta\sin\delta))$
50%						
20000	0.99	0.98	0.95	0.99	0.99	0.99
40000	0.99	0.98	0.95	0.99	0.99	0.99
60000	0.96	0.95	0.91	0.98	0.97	0.98
80000	0.95	0.95	0.91	0.97	0.97	0.97
100000	0.95	0.94	0.90	0.97	0.96	0.97
120000	0.94	0.93	0.89	0.97	0.95	0.97
140000	0.94	0.93	0.89	0.96	0.95	0.96
160000	0.93	0.92	0.88	0.96	0.94	0.96
180000	0.93	0.92	0.88	0.96	0.94	0.95
200000	0.92	0.91	0.87	0.95	0.94	0.95
80%						
20000	0.98	0.98	0.94	0.99	0.99	0.99
40000	0.98	0.98	0.94	0.99	0.98	0.99
60000	0.95	0.94	0.88	0.97	0.96	0.97
80000	0.94	0.93	0.88	0.96	0.95	0.96
100000	0.93	0.93	0.87	0.96	0.95	0.96
120000	0.93	0.92	0.87	0.96	0.94	0.96
140000	0.92	0.92	0.87	0.95	0.94	0.95
160000	0.92	0.91	0.86	0.95	0.93	0.95
180000	0.91	0.91	0.86	0.95	0.93	0.95
200000	0.91	0.90	0.85	0.95	0.93	0.94
90%						
20000	0.98	0.98	0.94	0.99	0.98	0.99
40000	0.98	0.97	0.93	0.98	0.98	0.98
60000	0.94	0.93	0.87	0.96	0.95	0.96
80000	0.93	0.92	0.86	0.96	0.95	0.96
100000	0.93	0.92	0.86	0.95	0.94	0.96
120000	0.92	0.91	0.86	0.95	0.94	0.95
140000	0.92	0.91	0.86	0.95	0.93	0.95
160000	0.91	0.91	0.85	0.95	0.93	0.95
180000	0.91	0.90	0.85	0.94	0.92	0.94
200000	0.91	0.90	0.85	0.94	0.92	0.94
99%						
20000	0.98	0.97	0.93	0.98	0.98	0.98
40000	0.97	0.97	0.92	0.98	0.97	0.97
60000	0.91	0.91	0.84	0.94	0.93	0.95
80000	0.91	0.90	0.83	0.94	0.93	0.94
100000	0.91	0.90	0.83	0.94	0.93	0.94
120000	0.90	0.90	0.83	0.94	0.92	0.94
140000	0.90	0.89	0.83	0.94	0.92	0.94
160000	0.90	0.89	0.83	0.93	0.92	0.94
180000	0.89	0.89	0.83	0.93	0.91	0.93
200000	0.89	0.89	0.83	0.93	0.91	0.93

Table C5 Coefficient of correlations for the LTA DBM-2 with VG20 bitumen

Passes	$\eta_{0(S)}$	η_{TV}	$\eta_{0(L)}$	$\|G^*\|/\sin\delta$	J_{nr} *at 3.2 kPa*	$\|G^*\|/(1-(1/\tan\delta\sin\delta))$
50%						
20000	0.98	0.98	0.98	0.99	0.98	0.98
40000	0.98	0.99	0.98	0.98	0.98	0.98
60000	0.98	0.99	0.99	0.98	0.98	0.98
80000	0.97	0.99	0.99	0.98	0.98	0.97
100000	0.97	0.99	0.99	0.97	0.97	0.96
120000	0.96	0.99	0.99	0.99	0.99	0.99
140000	0.96	0.99	0.99	0.99	0.98	0.98
160000	0.95	0.99	0.99	0.98	0.98	0.98
180000	0.95	0.99	0.99	0.98	0.98	0.98
200000	0.94	0.99	0.99	0.98	0.98	0.97
80%						
20000	0.98	0.98	0.97	0.99	0.98	0.99
40000	0.98	0.99	0.98	0.99	0.98	0.98
60000	0.98	0.99	0.99	0.98	0.98	0.98
80000	0.97	0.99	0.99	0.97	0.97	0.97
100000	0.96	0.99	0.99	0.97	0.97	0.96
120000	0.96	0.99	0.98	0.99	0.98	0.99
140000	0.96	0.99	0.99	0.99	0.98	0.99
160000	0.95	0.99	0.99	0.98	0.98	0.98
180000	0.95	0.99	0.99	0.98	0.98	0.98
200000	0.95	0.99	0.99	0.98	0.98	0.98
90%						
20000	0.98	0.98	0.97	0.99	0.98	0.99
40000	0.98	0.99	0.98	0.99	0.98	0.99
60000	0.98	0.99	0.99	0.98	0.98	0.98
80000	0.97	0.99	0.99	0.97	0.97	0.97
100000	0.96	0.99	0.98	0.97	0.97	0.96
120000	0.96	0.99	0.98	0.99	0.98	0.99
140000	0.96	0.99	0.99	0.99	0.98	0.99
160000	0.96	0.99	0.99	0.99	0.98	0.98
180000	0.95	0.99	0.99	0.98	0.98	0.98
200000	0.95	0.99	0.99	0.98	0.98	0.98
99%						
20000	0.97	0.97	0.97	0.99	0.98	0.99
40000	0.98	0.99	0.98	0.99	0.98	0.99
60000	0.97	0.99	0.98	0.98	0.98	0.98
80000	0.97	0.99	0.98	0.97	0.97	0.96
100000	0.96	0.98	0.98	0.96	0.96	0.95
120000	0.96	0.99	0.98	0.99	0.98	0.99
140000	0.96	0.99	0.98	0.99	0.98	0.99
160000	0.96	0.99	0.99	0.99	0.98	0.98
180000	0.95	0.99	0.99	0.98	0.98	0.98
200000	0.95	0.99	0.99	0.98	0.98	0.98

Table C6 Coefficient of correlations for the STA DBM-2 with VG40 bitumen

Passes	$\eta_{0(S)}$	η_{TV}	$\eta_{0(L)}$	$\|G^*\|/\sin\delta$	J_{nr} *at 3.2 kPa*	$\|G^*\|/(1-(1/\tan\delta\sin\delta))$
50%						
20000	0.98	0.99	0.98	0.97	0.98	0.98
40000	1.00	1.00	1.00	0.99	0.99	0.99
60000	1.00	0.99	1.00	1.00	0.98	1.00
80000	0.99	0.99	0.99	1.00	0.98	0.99
100000	0.98	0.98	0.99	0.99	0.96	0.99
120000	0.98	0.98	0.98	0.99	0.95	0.98
140000	0.97	0.97	0.98	0.98	0.95	0.98
160000	0.97	0.97	0.97	0.98	0.95	0.98
180000	0.97	0.97	0.97	0.98	0.95	0.98
200000	0.97	0.97	0.97	0.98	0.95	0.98
80%						
20000	0.98	0.98	0.97	0.96	0.97	0.97
40000	0.99	0.99	0.99	0.99	0.98	0.99
60000	1.00	1.00	1.00	1.00	0.99	1.00
80000	0.99	0.99	1.00	1.00	0.98	1.00
100000	0.98	0.98	0.98	0.99	0.95	0.98
120000	0.98	0.98	0.98	0.98	0.95	0.98
140000	0.97	0.97	0.98	0.98	0.94	0.98
160000	0.97	0.97	0.97	0.98	0.94	0.98
180000	0.97	0.97	0.97	0.98	0.94	0.97
200000	0.97	0.97	0.97	0.98	0.94	0.97
90%						
20000	0.97	0.97	0.97	0.96	0.97	0.96
40000	0.99	0.99	0.99	0.98	0.98	0.99
60000	1.00	1.00	1.00	0.99	0.99	0.99
80000	0.99	0.99	1.00	1.00	0.98	0.99
100000	0.98	0.98	0.98	0.98	0.95	0.98
120000	0.98	0.97	0.98	0.98	0.95	0.98
140000	0.97	0.97	0.97	0.98	0.94	0.98
160000	0.97	0.97	0.97	0.98	0.94	0.97
180000	0.97	0.97	0.97	0.98	0.94	0.97
200000	0.97	0.97	0.97	0.98	0.94	0.97
99%						
20000	0.96	0.97	0.96	0.95	0.96	0.95
40000	0.98	0.99	0.98	0.97	0.98	0.98
60000	0.99	0.99	0.99	0.99	0.98	0.99
80000	0.99	0.99	0.99	0.99	0.98	0.99
100000	0.98	0.98	0.98	0.98	0.95	0.98
120000	0.97	0.97	0.98	0.98	0.94	0.98
140000	0.97	0.97	0.97	0.98	0.94	0.97
160000	0.97	0.97	0.97	0.98	0.94	0.97
180000	0.97	0.97	0.97	0.97	0.94	0.97
200000	0.97	0.97	0.97	0.97	0.94	0.97

Table C7 Coefficient of correlations for the LTA DBM-2 with VG40 bitumen

Passes	$\eta_{0(S)}$	η_{TV}	$\eta_{0(L)}$	$\|G^*\|/\sin\delta$	J_{nr} *at 3.2 kPa*	$\|G^*\|/(1-(1/\tan\delta\sin\delta))$
50%						
20000	0.97	0.99	0.99	0.99	0.99	0.99
40000	0.97	0.99	1.00	0.99	0.99	0.99
60000	0.97	0.98	0.99	0.99	0.98	0.99
80000	0.96	0.98	0.99	0.99	0.98	0.98
100000	0.95	0.97	0.98	0.98	0.97	0.98
120000	0.95	0.96	0.98	0.98	0.97	0.98
140000	0.94	0.96	0.97	0.97	0.96	0.97
160000	0.94	0.96	0.97	0.97	0.96	0.97
180000	0.94	0.95	0.97	0.97	0.96	0.96
200000	0.93	0.95	0.96	0.96	0.95	0.96
80%						
20000	0.96	0.99	0.99	0.99	0.98	0.99
40000	0.96	0.99	0.99	0.99	0.98	0.99
60000	0.96	0.98	0.99	0.99	0.98	0.99
80000	0.95	0.97	0.98	0.98	0.97	0.98
100000	0.95	0.97	0.98	0.98	0.97	0.98
120000	0.95	0.96	0.97	0.98	0.97	0.97
140000	0.94	0.96	0.97	0.97	0.96	0.97
160000	0.94	0.95	0.97	0.97	0.96	0.97
180000	0.93	0.95	0.96	0.96	0.95	0.96
200000	0.93	0.94	0.96	0.96	0.95	0.96
90%						
20000	0.95	0.98	0.99	0.99	0.98	0.99
40000	0.96	0.98	0.99	0.99	0.98	0.99
60000	0.96	0.98	0.99	0.98	0.98	0.98
80000	0.95	0.97	0.98	0.98	0.97	0.98
100000	0.95	0.96	0.98	0.98	0.97	0.98
120000	0.94	0.96	0.97	0.97	0.97	0.97
140000	0.94	0.95	0.97	0.97	0.96	0.97
160000	0.93	0.95	0.96	0.97	0.96	0.96
180000	0.93	0.94	0.96	0.96	0.95	0.96
200000	0.92	0.94	0.95	0.96	0.95	0.95
99%						
20000	0.94	0.97	0.98	0.98	0.97	0.98
40000	0.95	0.97	0.98	0.98	0.97	0.98
60000	0.95	0.97	0.98	0.98	0.97	0.98
80000	0.95	0.96	0.98	0.98	0.97	0.98
100000	0.94	0.96	0.97	0.97	0.97	0.97
120000	0.94	0.96	0.97	0.97	0.96	0.97
140000	0.94	0.95	0.96	0.97	0.96	0.96
160000	0.93	0.94	0.96	0.96	0.95	0.96
180000	0.92	0.94	0.95	0.96	0.95	0.95
200000	0.92	0.93	0.94	0.95	0.94	0.95

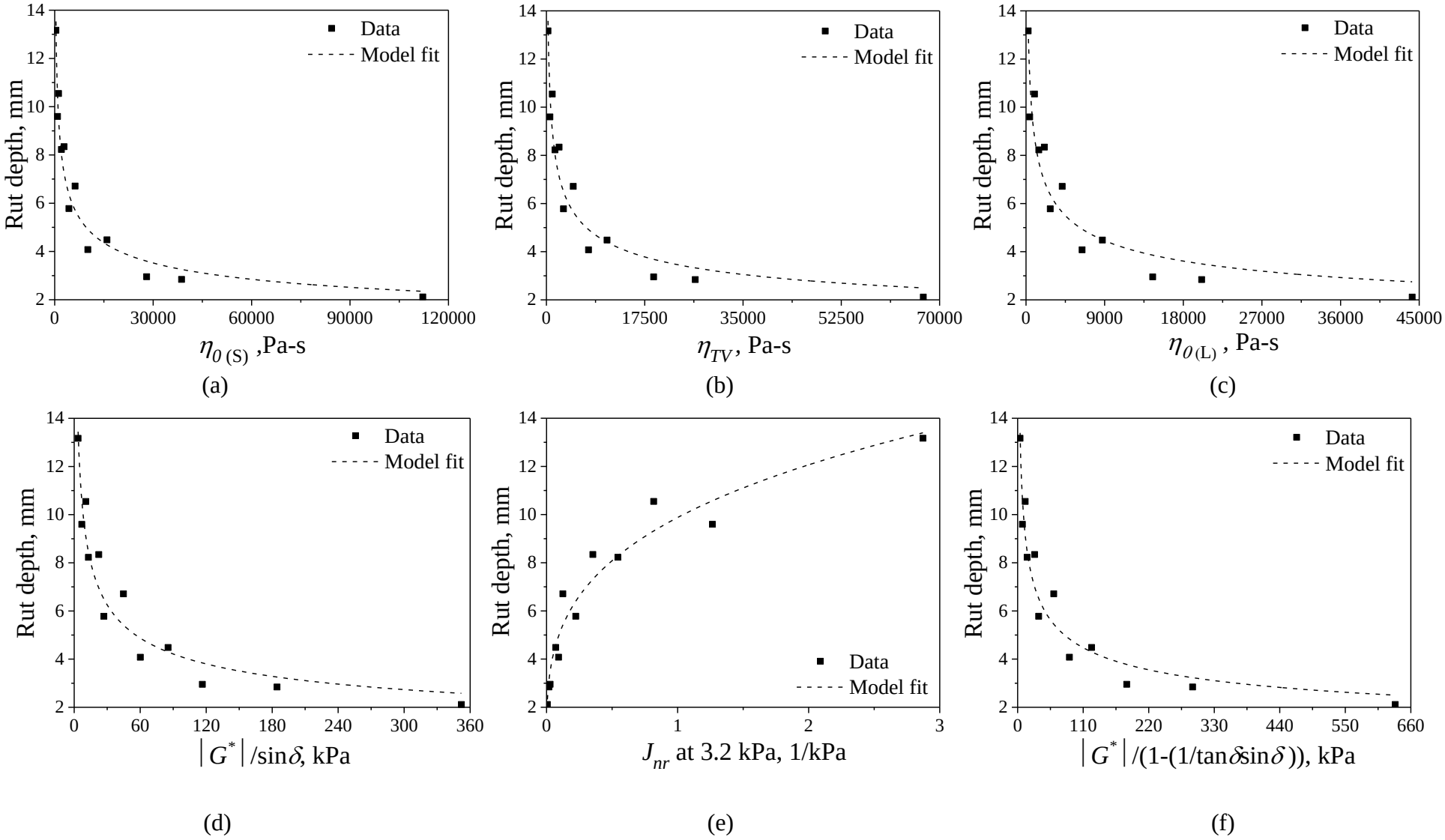

Fig. C1 Rut depth of the STA DBM-2 mixtures versus the six rutting parameters at 20,000 passes at 50% reliability

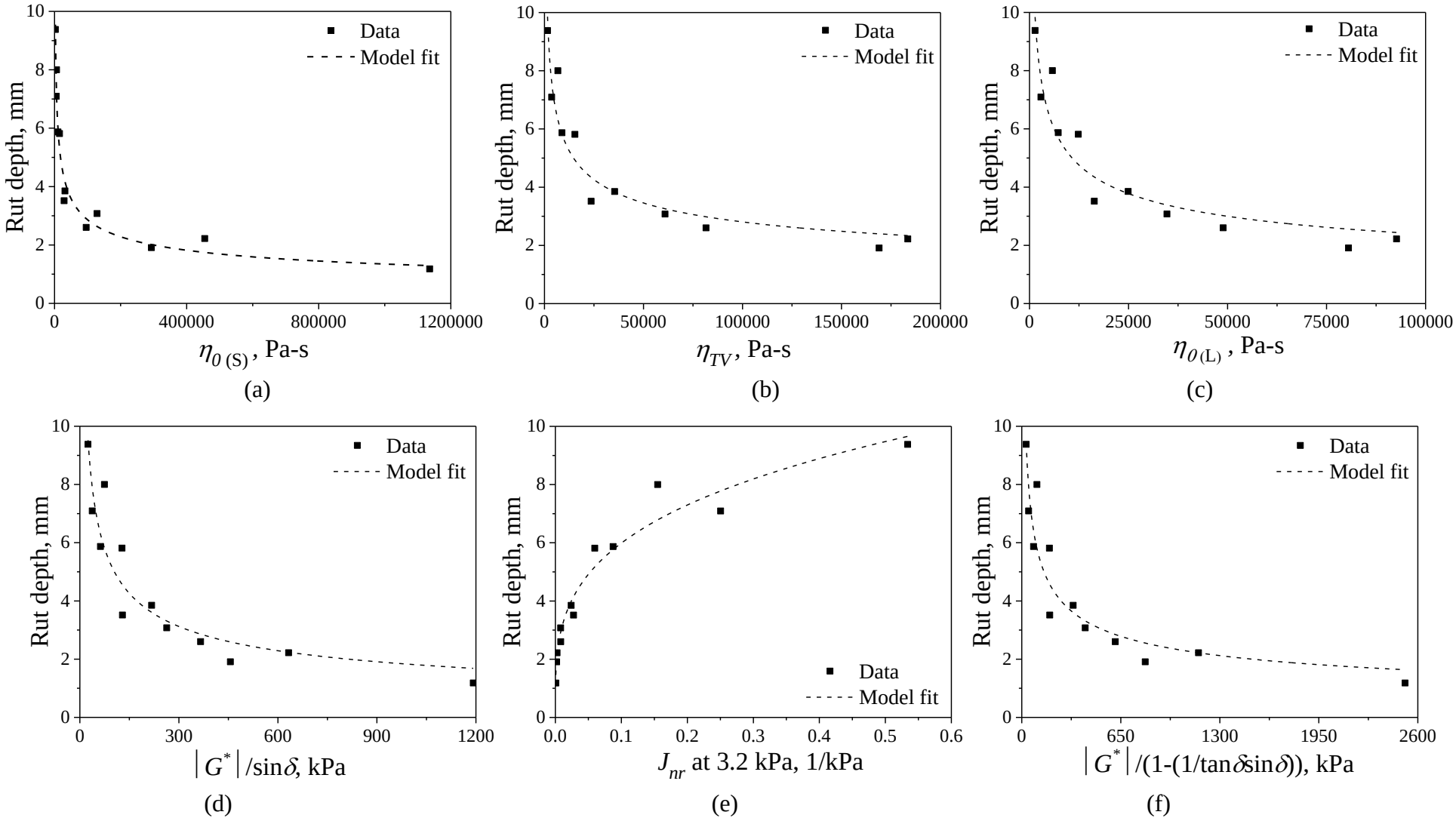

Fig. C2: Rut depth of the LTA DBM-2 mixtures versus the six rutting parameters at 20,000 passes at 50% reliability

Table C8 Coefficient of correlation for STA BC-2 mixture

Passes	$\eta_{0(S)}$	η_{TV}	$\eta_{0(L)}$	$\lvert G^* \rvert / \sin\delta$	J_{nr} at 3.2 kPa	$\lvert G^* \rvert / (1-(1/\tan\delta \sin\delta))$
80%						
20000	0.93	0.90	0.85	0.87	0.92	0.89
40000	0.92	0.89	0.84	0.86	0.91	0.89
60000	0.87	0.83	0.77	0.80	0.85	0.83
80000	0.97	0.97	0.94	0.96	0.98	0.97
100000	0.97	0.96	0.94	0.96	0.97	0.97
120000	0.96	0.96	0.94	0.96	0.97	0.97
140000	0.96	0.96	0.93	0.96	0.96	0.97
160000	0.95	0.95	0.93	0.96	0.96	0.97
180000	0.95	0.95	0.93	0.95	0.95	0.96
200000	0.94	0.94	0.92	0.95	0.95	0.96
90%						
20000	0.94	0.91	0.85	0.89	0.92	0.90
40000	0.93	0.90	0.85	0.89	0.92	0.90
60000	0.88	0.84	0.79	0.84	0.86	0.84
80000	0.97	0.97	0.95	0.98	0.98	0.98
100000	0.97	0.97	0.95	0.97	0.97	0.98
120000	0.96	0.96	0.94	0.97	0.97	0.97
140000	0.96	0.96	0.94	0.97	0.96	0.97
160000	0.95	0.96	0.94	0.97	0.96	0.97
180000	0.95	0.95	0.93	0.97	0.96	0.97
200000	0.94	0.95	0.93	0.96	0.95	0.96
99%						
20000	0.94	0.91	0.86	0.90	0.93	0.90
40000	0.94	0.91	0.86	0.91	0.93	0.91
60000	0.90	0.86	0.81	0.86	0.88	0.86
80000	0.97	0.97	0.96	0.98	0.98	0.98
100000	0.97	0.97	0.96	0.98	0.97	0.98
120000	0.96	0.97	0.95	0.98	0.97	0.98
140000	0.96	0.96	0.95	0.98	0.97	0.97
160000	0.96	0.96	0.95	0.97	0.96	0.97
180000	0.95	0.96	0.94	0.97	0.96	0.97
200000	0.95	0.95	0.94	0.97	0.96	0.97

Table C9 Coefficient of correlation for LTA BC-2 mixture

Passes	$\eta_{0(S)}$	η_{TV}	$\eta_{0(L)}$	$\|G^*\|/\sin\delta$	J_{nr} *at 3.2 kPa*	$\|G^*\|/(1-(1/\tan\delta\sin\delta))$
80%						
20000	0.96	0.95	0.93	0.90	0.96	0.89
40000	0.92	0.92	0.91	0.86	0.92	0.85
60000	0.92	0.83	0.80	0.75	0.90	0.75
80000	0.89	0.79	0.76	0.72	0.88	0.71
100000	0.86	0.76	0.73	0.68	0.85	0.68
120000	0.84	0.74	0.71	0.66	0.83	0.65
140000	0.95	0.93	0.92	0.89	0.97	0.88
160000	0.94	0.93	0.92	0.88	0.97	0.87
180000	0.93	0.92	0.91	0.87	0.96	0.87
200000	0.93	0.92	0.91	0.87	0.96	0.86
90%						
20000	0.96	0.94	0.93	0.89	0.96	0.89
40000	0.91	0.92	0.91	0.86	0.92	0.85
60000	0.91	0.82	0.79	0.75	0.90	0.74
80000	0.88	0.78	0.76	0.71	0.87	0.70
100000	0.85	0.75	0.72	0.68	0.84	0.67
120000	0.83	0.73	0.70	0.65	0.82	0.64
140000	0.94	0.93	0.92	0.89	0.97	0.88
160000	0.94	0.93	0.92	0.88	0.96	0.87
180000	0.93	0.92	0.91	0.87	0.96	0.87
200000	0.92	0.92	0.91	0.87	0.95	0.86
99%						
20000	0.94	0.94	0.93	0.89	0.94	0.88
40000	0.91	0.92	0.91	0.86	0.92	0.85
60000	0.89	0.81	0.78	0.73	0.89	0.73
80000	0.86	0.77	0.74	0.69	0.85	0.68
100000	0.84	0.74	0.71	0.66	0.83	0.65
120000	0.81	0.71	0.68	0.63	0.80	0.62
140000	0.93	0.93	0.93	0.88	0.96	0.88
160000	0.92	0.92	0.92	0.88	0.95	0.87
180000	0.91	0.92	0.91	0.87	0.95	0.86
200000	0.91	0.91	0.91	0.86	0.94	0.86

Table C10 Coefficient of correlation for STA DBM-2 mixture

Passes	$\eta_{0(S)}$	η_{TV}	$\eta_{0(L)}$	$\|G^*\|/\sin\delta$	J_{nr} *at 3.2 kPa*	$\|G^*\|/(1-(1/\tan\delta\sin\delta))$
50%						
20000	0.95	0.93	0.90	0.92	0.94	0.93
40000	0.96	0.95	0.92	0.94	0.96	0.94
60000	0.93	0.90	0.86	0.90	0.92	0.90
80000	0.92	0.89	0.84	0.89	0.91	0.89
100000	0.94	0.93	0.91	0.93	0.94	0.93
120000	0.94	0.93	0.90	0.93	0.94	0.93
140000	0.94	0.93	0.90	0.92	0.93	0.93
160000	0.93	0.93	0.90	0.92	0.93	0.93
180000	0.93	0.92	0.90	0.92	0.93	0.93
200000	0.93	0.92	0.89	0.92	0.93	0.92
80%						
20000	0.95	0.93	0.90	0.92	0.94	0.93
40000	0.96	0.94	0.91	0.94	0.95	0.94
60000	0.93	0.90	0.84	0.89	0.91	0.89
80000	0.92	0.88	0.83	0.88	0.90	0.88
100000	0.93	0.91	0.88	0.91	0.92	0.91
120000	0.92	0.91	0.87	0.90	0.92	0.91
140000	0.92	0.91	0.87	0.90	0.92	0.91
160000	0.92	0.90	0.87	0.90	0.91	0.90
180000	0.91	0.90	0.86	0.90	0.91	0.90
200000	0.91	0.90	0.86	0.89	0.91	0.90
90%						
20000	0.95	0.93	0.89	0.92	0.94	0.92
40000	0.96	0.94	0.91	0.93	0.95	0.94
60000	0.92	0.89	0.83	0.88	0.91	0.89
80000	0.91	0.88	0.82	0.87	0.90	0.88
100000	0.92	0.90	0.86	0.90	0.91	0.90
120000	0.91	0.90	0.86	0.89	0.91	0.90
140000	0.91	0.89	0.85	0.89	0.90	0.89
160000	0.91	0.89	0.85	0.89	0.90	0.89
180000	0.90	0.89	0.85	0.88	0.90	0.89
200000	0.90	0.88	0.84	0.88	0.89	0.88
99%						
20000	0.94	0.92	0.89	0.91	0.94	0.92
40000	0.95	0.93	0.90	0.93	0.94	0.93
60000	0.91	0.88	0.82	0.87	0.90	0.88
80000	0.90	0.87	0.80	0.86	0.89	0.87
100000	0.90	0.88	0.83	0.87	0.89	0.88
120000	0.89	0.87	0.82	0.86	0.88	0.87
140000	0.89	0.87	0.82	0.86	0.88	0.86
160000	0.88	0.86	0.81	0.85	0.87	0.86
180000	0.88	0.86	0.81	0.85	0.87	0.85
200000	0.87	0.85	0.80	0.84	0.86	0.85

Table C11 Coefficient of correlation for LTA DBM-2 mixture

Passes	$\eta_{0(S)}$	η_{TV}	$\eta_{0(L)}$	$\|G^*\|/\sin\delta$	J_{nr} *at 3.2 kPa*	$\|G^*\|/(1-(1/\tan\delta\sin\delta))$
50%						
20000	0.96	0.91	0.89	0.87	0.96	0.87
40000	0.98	0.95	0.93	0.91	0.98	0.91
60000	0.97	0.96	0.95	0.92	0.98	0.91
80000	0.97	0.97	0.95	0.92	0.98	0.92
100000	0.96	0.97	0.96	0.92	0.97	0.92
120000	0.96	0.93	0.91	0.87	0.97	0.86
140000	0.95	0.93	0.91	0.86	0.97	0.86
160000	0.95	0.93	0.91	0.86	0.97	0.86
180000	0.95	0.93	0.91	0.86	0.96	0.86
200000	0.94	0.93	0.91	0.86	0.96	0.86
80%						
20000	0.96	0.90	0.87	0.86	0.95	0.86
40000	0.98	0.95	0.93	0.91	0.97	0.90
60000	0.97	0.96	0.94	0.92	0.98	0.91
80000	0.97	0.96	0.95	0.92	0.98	0.91
100000	0.96	0.96	0.95	0.92	0.97	0.91
120000	0.96	0.93	0.91	0.86	0.97	0.86
140000	0.95	0.93	0.91	0.86	0.96	0.86
160000	0.95	0.93	0.91	0.86	0.96	0.86
180000	0.94	0.92	0.91	0.86	0.96	0.85
200000	0.94	0.92	0.91	0.86	0.96	0.85
90%						
20000	0.95	0.89	0.87	0.86	0.94	0.86
40000	0.97	0.94	0.92	0.90	0.97	0.90
60000	0.97	0.96	0.94	0.92	0.98	0.91
80000	0.97	0.96	0.95	0.92	0.97	0.91
100000	0.96	0.96	0.95	0.92	0.97	0.91
120000	0.95	0.93	0.90	0.86	0.96	0.86
140000	0.95	0.92	0.90	0.86	0.96	0.86
160000	0.95	0.92	0.90	0.86	0.96	0.85
180000	0.94	0.92	0.90	0.86	0.96	0.85
200000	0.94	0.92	0.90	0.85	0.95	0.85
99%						
20000	0.94	0.87	0.85	0.85	0.93	0.85
40000	0.97	0.93	0.92	0.90	0.97	0.90
60000	0.97	0.95	0.94	0.91	0.97	0.91
80000	0.96	0.96	0.95	0.92	0.97	0.91
100000	0.96	0.96	0.95	0.91	0.97	0.91
120000	0.95	0.92	0.90	0.86	0.96	0.85
140000	0.95	0.92	0.90	0.85	0.96	0.85
160000	0.94	0.92	0.89	0.85	0.95	0.85
180000	0.94	0.91	0.89	0.85	0.95	0.84
200000	0.93	0.91	0.89	0.84	0.95	0.84

Table C12 Ratio of increase in $\eta_{0(L)}$ and η_{TV} due to short term aging

Temp., °C	VG20				VG40			
	$\eta_{0(L)}$, Pa-s							
	Unaged	Short-term aged	Long-term aged	Ratio	Unaged	Short-term aged	Long-term aged	Ratio
	a	b	c	b/a	d	e	f	e/d
40	6005	14500	80550	2.4	11600	44200	-	3.8
45	2663	6420	34720	2.4	5610	20100	92670	3.6
50	1340	2780	16380	2.1	2840	8750	48890	3.1
55	528	1462	7266	2.8	1197	4150	24910	3.5
60	*	425	2902	*	612	2100	12330	3.4
65	*	247	1405	*	292	974	5790	3.3
				2.4				***3.5***
η_{TV}, Pa-s								
40	6903	19100	169000	2.8	14100	67100	-	4.8
45	2963	7500	60910	2.5	6400	26500	183500	4.1
50	1600	3040	23560	1.9	3080	10800	81610	3.5
55	580	1534	8849	2.6	1237	4780	35450	3.9
60	*	629	3628	*	627	2270	15400	3.6
65	*	281	1535	*	313	1050	6769	3.4
				2.5				***4.1***

Table C13 Ratio of increase in $\eta_{0(L)}$ in due to long-term aging

Temp., °C	VG20				VG40			
	$\eta_{0(L)}$, Pa-s							
	Unaged	Short-term aged	Long-term aged	Ratio	Unaged	Short-term aged	Long-term aged	Ratio
	a	b	c	c/a	d	e	f	f/d
40	6005	14500	80550	13.4	11600	44200	-	
45	2663	6420	34720	13.0	5610	20100	92670	16.5
50	1340	2780	16380	12.2	2840	8750	48890	17.2
55	528	1462	7266	13.8	1197	4150	24910	20.8
60	*	425	2902		612	2100	12330	20.1
65	*	247	1405		292	974	5790	19.8
				13.1				***18.2***
η_{TV}, Pa-s								
40	6903	19100	169000	24.5	14100	67100	-	
45	2963	7500	60910	20.6	6400	26500	183500	28.7
50	1600	3040	23560	14.7	3080	10800	81610	26.5
55	580	1534	8849	15.3	1237	4780	35450	28.7
60	*	629	3628		627	2270	15400	24.6
65	*	281	1535		313	1050	6769	21.6
				18.8				***27.9***

REFERENCES

1. **AASHTO**. (2014). "Standard method of test for multiple stress creep recovery (MSCR) test of asphalt binder using a dynamic shear rheometer (DSR)". *AASHTO T 350*, American Association of State Highway and Transportation Officials, Washington, DC.

2. **AASHTO**. (2015). "Standard practice for mixture conditioning of hot-mix asphalt (HMA)." *AASHTO R 30-02*, American Association of State Highway and Transportation Officials, Washington, DC.

3. **AASHTO**. (2017). "Standard method of test for Hamburg wheel-track testing of compacted asphalt mixtures." *AASHTO T 324*, American Association of State Highway and Transportation Officials, Washington, DC.

4. **Abo-Qudais, S**. (2004). "Time-temperature and time-aggregate gradation superposition in asphalt mixes". *Road Materials and Pavement Design*, *5* (2), 145-167.

5. **AHD**. (2019). "Thermal equilibrium, The American Heritage Dictionary". Website: https://www.ahdictionary.com/word/search.html?q=thermal+equilibrium. Last accessed- 30/07/2019

6. **Ali, B., Sadek, M.,** and **Shahrour, I**. (2009). "Finite-element model for urban pavement rutting: Analysis of pavement rehabilitation methods." *Journal of Transportation Engineering*, *135* (4), 235-239.

7. **Al-Khateeb, G.**, and **Basheer, I.** (2009). "A three-stage rutting model utilising rutting performance data from the Hamburg Wheel-Tracking Device (WTD)". *Road & Transport Research: A Journal of Australian and New Zealand Research and Practice*, *18* (3), 12-25.

8. **Anderson, D. A.**, and **Kennedy, T. W.** (1993). "Development of SHRP binder specification (with discussion)." *Journal of the Association of Asphalt Paving Technologists*, *62*, 481-507.

9. **Anderson, D. A., Christensen, D. W.**, and **Bahia, H.** (1991). "Physical properties of asphalt cement and the development of performance-related specifications." *Journal of the Association of Asphalt Paving Technologists*, *60*, 437-475.

10. **Anderson, D. A.**, **Le Hir, Y. M.**, **Planche, J. P.**, **Martin, D.**, and **Shenoy, A.** (2002). "Zero shear viscosity of asphalt binders." *Transportation Research Record 1810*, Transportation Research Board, Washington, DC, 54-62.

11. **Annable, T.**, **Buscall, R.**, **Ettelaie, R.**, and **Whittlestone, D.** (1993). "The rheology of solutions of associating polymers: Comparison of experimental behavior with transient network theory". *Journal of Rheology*, *37* (4), 695-726.

12. **Archilla, A. R.**, and **Diaz, L. G.** (2011). "Effects of asphalt mixture properties on permanent deformation response." *Transportation Research Record 2210*, Transportation Research Board, Washington, DC, 1-8.

13. **Asphalt Institute.** (2014). "*Asphalt mix design methods*". *MS-2*, Asphalt Institute, Lexington, KY, USA.

14. **ASTM.** (2003). "History of ASTM committee D04 on road and paving materials, 1903-2003." Website: https://www.astm.org/SNEWS/SEPTEMBER_2003/kandhal_sep03.html, Last accessed – 27/07/2019.

15. **ASTM.** (2015*a*). "Standard test method for multiple stress creep and recovery (MSCR) of asphalt binder using a dynamic shear rheometer." *ASTM D7405-15*, ASTM International, 100 Barr Harbor Drive, West Conshohocken, PA, USA.

16. **ASTM.** (2015*b*). "Standard test method for viscosity determination of asphalt at elevated temperatures using a rotational viscometer." *ASTM D4402M – 15*, ASTM International, 100 Barr Harbor Drive, West Conshohocken, PA, USA.

17. **ASTM.** (2015*c*), "Standard test method for determining the rheological properties of asphalt binder using a dynamic shear rheometer", *ASTM D7175–15*, ASTM International, West Conshohocken, PA, USA.

18. **ASTM.** (2016*a*). "Standard practice for preparation of asphalt mixture specimens using Marshall apparatus." *ASTM D6926-16*, ASTM International.100 Barr Harbor Drive, West Conshohocken, PA, USA.

19. **ASTM.** (2016*b*). "Standard specification for performance graded asphalt binder." *ASTM D6373 – 16*, ASTM International, 100 Barr Harbor Drive, West Conshohocken, PA, USA.

20. **ASTM.** (2018*a*). "Standard practice for accelerated aging of asphalt binder using a pressurized aging vessel (PAV)." *ASTM D6521-18*, ASTM International, 100 Barr Harbor Drive, West Conshohocken, PA, USA.

21. **ASTM.** (2018*b*). "Standard test method for maximum specific gravity and density of asphalt mixtures using automatic vacuum sealing method." *ASTM D6857 / D6857M-18*, ASTM International, 100 Barr Harbor Drive, West Conshohocken, PA, USA.

22. **ASTM.** (2018*c*). "Standard test method for bulk specific gravity and density of compacted asphalt mixtures using automatic vacuum sealing method." *ASTM D6752 / D6752M-18*, ASTM International, 100 Barr Harbor Drive, West Conshohocken, PA, USA.

23. **ASTM.** (2019). "Standard test method for effect of heat and air on a moving film of asphalt (rolling thin-film oven test)". *ASTM D2872 -19*, ASTM International, West Conshohocken, PA, USA.

24. **Austroads.** (2006). "Commissioning a cooper wheel tracking device". *AP-T56/06*, Austroads Technical Report, Sydney, NSW, Australia.

25. **Azari, H.**, and **Mohseni, A.** (2013). "Effect of short-term conditioning and long-term ageing on permanent deformation characteristics of asphalt mixtures". *Road Materials and Pavement Design*, *14* (sup2), 79-91.

26. **Bahia, H. U.**, **Hanson, D. I.**, **Zeng, M.**, **Zhai, H.**, **Khatri, M. A.**, and **Anderson, R. M.** (2001). "Characterization of modified asphalt binders in superpave mix design." *NCHRP Report 459*, National Research Council, Transportation Research Board. Washington, DC.

27. **Behiry, A. E. A. E. M.** (2012). "Fatigue and rutting lives in flexible pavement." *Ain Shams Engineering Journal*, *3* (4), 367-374.

28. **Bell, C. A.**, **AbWahab, Y.**, **Cristi, M. E.**, and **Sosnovske, D.** (1994). "Selection of laboratory aging procedures for asphalt-aggregate mixtures". *SHRP-A-383*, Strategic Highway Research Program, Washington, DC.

29. **Biro, S.**, **Gandhi, T**. and **Amirkhanian, S.** (2009). "Determination of zero shear viscosity of warm asphalt binders." *Construction and Building Materials*, *23*, 2080–2086.

30. **BIS.** (1978). "Methods for Testing Tar and Bituminous Materials: Determination of viscosity - Part II Absolute Viscosity, *IS 1206 Part-II*, Bureau of Indian Standards. Manak Bhavan, 9 Bahadur Shah Zafar Marg, New Delhi.

31. **BIS.** (2013). "Paving bitumen – Specifications". *IS 73*, Bureau of Indian Standards, Fourth revision. Manak Bhavan, 9 Bahadur Shah Zafar Marg, New Delhi.

32. **Boodihal, M. A.**, **Chethan, A.**, **Swamy, R.**, **Sahu, R.**, and **Biligiri, K. P.** (2014). "Development of tyre/road noise assessment methodology in India." *Case Studies in Construction Materials*, *1*, 115-124.

33. **Brookfield Ametek.** (2017). "*More solutions to sticky problems*". AMETEK Brookfield, Inc., USA.

34. **Brown, E.R.**, and **Cross, S.A.** (1989). "A study of in-place rutting of asphalt pavements." *NCAT report, 89-02*, National Center for Asphalt Technology, Auburn University, Alabama, USA.

35. **BS-EN.** (2003). "Bituminous mixtures - Test methods for hot mix asphalt - Part 22: Wheel tracking." *BS EN 12697-22*.

36. **Cardone, F.**, **Ferrotti, G.**, **Frigio, F.**, and **Canestrari, F**. (2014). "Influence of polymer modification on asphalt binder dynamic and steady flow viscosities". *Construction and Building Materials*, *71*, 435-443.

37. **CDOT.** (2014). "Standard method of test for Hamburg wheel-track testing of compacted bituminous mixtures". *CP-L 5112-14*, Colorado Department of Transportation, Denver, Colorado, USA.

38. **CEN.** (2014). "Bitumen and bituminous binders - Preparation of test samples." *EN 12594*, Comite Europeen de Normalisation.

39. **Chen, J. S.**, and **Lin, C. H.** (2000). "Construction of test road to evaluate engineering properties of polymer-modified asphalt binders." *International Journal of Pavement Engineering*, *1* (4), 285-295.

40. **Chen, J. S.**, **Lin, C. H.**, **Stein, E.**, and **Hothan, J.** (2004). "Development of a mechanistic-empirical model to characterize rutting in flexible pavements." *Journal of transportation engineering*, *130* (4), 519-525.

41. **Chowdary, V.**, **Thushara, V. T.**, **Asif, K. A.**, and **Krishnan, J. M.** (2007). "Experimental verification of the evolution of internal structure of asphalt and modified asphalt." *In: 4th International SIIV Congress*, 12-14 September, Palermo, Italy.

42. **CRRI.** (2019). "Flexible Pavements." *Central Road Research Institute*. Website: http://www.crridom.gov.in/content/flexible-pavements. Last accessed – 30/07/2019

43. **D'Angelo, J.A.**, **Kluttz, R.**, **Dongre, R. N.**, **Stephens, K.**, and **Zanzotto, L.** (2007). "Revision of the superpave high temperature binder specification: the multiple stress creep recovery test (with discussion)". *Journal of the Association of Asphalt Paving Technologists*, *76*, 123-162.

44. **D'Angelo, J. A.** (2009). "The relationship of the MSCR test to rutting." *Road Materials and Pavement Design*, *10* (sup1), 61-80.

45. **De Visscher J.**, and **Vanelstraete A.** (2004). "Practical test methods for measuring the zero shear viscosity of bitumi-nous binders". *Materials and Structures*, *37*, 360–364.

46. **De Visscher, J.**, **Paez-Dueñas, A.**, **Cabanillas, P.**, **Carrera, V.**, **Cerny, R.**, **Durand, G.**, and **Lancaster, I.** (2016). "European round robin tests for the multiple stress creep recovery test and contribution to the development of the European standard test method". *6th Eurobitumen and Euraspahlt Congress*, 1-3 June, Prague, Czech Republic.

47. **Delgadillo, R.**, **Cho, D. W.**, and **Bahia, H.** (2006*a*). "Nonlinearity of repeated creep and recovery binder test and relationship with mixture permanent deformation." *Transportation Research Record 1962*, Transportation Research Board, Washington, DC, 2-11.

48. **Delgadillo, R.**, **Nam, K.**, and **Bahia, H.** (2006*b*). "Why do we need to change $G^*/\sin\delta$ and how?". *Road Materials and Pavement Design*, *7* (1), 7-27.

49. **Desmazes C.**, **Lecomte M.**, **Lesueur D.**, and **Phillips, M.** (2000) "A protocol for reliable measurement of zero-shear-viscosity in order to evaluate the anti-rutting performance of binders". *Proceedings of the 2nd Euras-phalt Eurobitume Congress*, 203–11.

50. **Dongre, R.** and **D'Angelo, J.A.** (2003) "Refinement of superpave high-temperature binder specification based on pavement performance in the accelerated loading facility". *Transportation Research Record 1839*, Transportation Research Board, Washington, DC, 39-46.

51. **Dongre, R.**, **D'Angelo, J.A.**, **Reinke, G.**, and **Shenoy, A.** (2004). "New criterion for Superpave high-temperature binder specification". *Transportation Research Board 1875*, Transportation Research Board, Washington, DC, 22-32.

52. **Douglas, R. A.** (1997). "Heavy load, low tire pressure rutting of unbound granular pavements". *Journal of Transportation Engineering*, *123* (5), 357-363.

53. **Fernando, E. G.**, **Button, J. W.**, and **Crockford, W. W.** (1997). "Rut susceptibility of large stone mixtures". *Journal of Transportation Engineering*, *123* (1), 51-59.

54. **Garba, R.** (2002). "*Permanent deformation properties of asphalt concrete mixtures*". Ph.D. thesis. Norwegian University of Science and Technology, Trondheim, Norway.

55. **Ghica, M.V.**, **Hirjau, M.**, **Lupuleasa, D.**, and **Dinu-Pirvu, C.E.** (2016) "Flow and thixotropic parameters for rheological characterization of hydrogels". *Molecules*, 2016; *21* (6):786.

56. **Golalipour, A.**, **Bahia, H. U.**, and **Tabatabaee, H. A.** (2016). "Critical considerations toward better implementation of the multiple stress creep and recovery test". *Journal of Materials in Civil Engineering*, *29* (5), 04016295.

57. **Grebenschikov, S.**, and **Prozzi, J. A.** (2011). "Enhancing mechanistic–empirical pavement design guide rutting-performance predictions with Hamburg wheel-tracking results". *Transportation Research Record 2226*, Transportation Research Board, Washington, DC, 111-118.

58. **Guo, R.**, and **Prozzi, J.A.** (2009). "A statistical analysis of Hamburg wheel tracking device testing results". *Road Materials and Pavement Design*, *10* (sup1), 327-335.

59. **Hafeez, I.**, and **Kamal, M. A.** (2014). "Creep compliance: a parameter to predict rut performance of asphalt binders and mixtures". *Arabian Journal for Science and Engineering*, *39* (8), 5971-5978.

60. **Hicks, R. G.**, **Finn, F. N.**, **Monismith, C. L.**, and **Leahy, R. B.** (1993). "Validation of SHRP binder specification through mix testing (with discussion)". *Journal of the Association of Asphalt Paving Technologists*, *62*, 565-614.

61. **Hoffman, R. L.** (1998). "Explanations for the cause of shear thickening in concentrated colloidal suspensions". *Journal of Rheology*, *42* (1), 111-123.

62. **Hossain, K.**, **Das, P.**, and **Karakas, A.S.** (2018). "Effect of ultraviolet aging on rheological properties of asphalt cement". *Canadian Technical Asphalt Association (CTAA) Conference*, Regina, SK, Canada.

63. **Hussain, J.**, **Wilson, D. J.**, **Henning, T. F.**, and **Alabaster, D.** (2013). "Comparing results between the repeated load triaxial test and accelerated pavement test on unbound aggregate". *Journal of Materials in Civil Engineering*, *26* (3), 476-483.

64. **IAT.** (2000). "India: An asphalt roads country". The Institute of Asphalt Technology. Website:https://www.instituteofasphalt.org/index.php?id=yearbook, Website:https://trid.trb.org/Results?q=&serial=%22THE%20ASPHALT%20YEARBOOK%202000%22. Last accessed – 30/07/2019.

65. **IRC.** (2009). "Specifications for Dense Graded Bituminous Mixes". *IRC 111*, Indian Roads Congress, New Delhi.

66. **IRC.** (2018). "Guidelines for design of flexible pavements". *IRC 37*, Fourth Revision, Indian Roads Congress, New Delhi.

67. **Jeong, S.**, **Kim, J. M.**, and **Baig, C.** (2017). "Molecular characteristics of stress overshoot for polymer melts under start-up shear flow". *The Journal of Chemical Physics*, *147* (23), 234901.

68. **Kakade, V. B.**, **Reddy, I. S.**, and **Reddy, M. A.** (2013). "Identification of rheological parameters of modified binders to predict rutting behavior of bituminous concrete mixes". *Indian Highways*, *41* (11), 9-18.

69. **Kandhal, P. S.**, and **Cooley Jr, L.** (2002). "Coarse-versus fine-graded superpave mixtures: Comparative evaluation of resistance to rutting". *NCAT Report 02-02*, National Center for Asphalt Technology, Auburn University, Alabama, USA.

70. **Kim, O. K.**, **Bell, C. A.**, and **Wilson, J. E.** (1989). "Effect of increased truck tire pressure on asphalt concrete pavement". *Journal of Transportation Engineering*, *115* (4), 329-350.

71. **Krishnan, J.M.** and **Rajagopal, K.R.** (2003). "A review of the uses and modelling of bitumen from ancient to modern times". *ASME Applied Mechanics Review*, *56* (2), 149-214.

72. **Li, B. Q.**, **Mills, L.**, and **McNeil, S.** (2011). "The implications of climate change on pavement performance and design". *UDUTC Report*, University Transportation Center, University of Delaware, Newark, USA.

73. **Liu, C. H.**, **Wu, S. P.**, **Liu, Q. T.**, and **Zhu, G. J.** (2008). "Rheological characteristics of aged asphalt binder". *Journal of Central South University of Technology*, *15* (1), 298-301.

74. **Liu, G.**, **Yang, T.**, **Li, J.**, **Jia, Y.**, **Zhao, Y.**, and **Zhang, J.** (2018). "Effects of aging on rheological properties of asphalt materials and asphalt-filler interaction ability". *Construction and Building Materials*, *168*, 501-511.

75. **Lu, X.**, and **Isacsson, U.** (2002). "Effect of ageing on bitumen chemistry and rheology". *Construction and Building materials*, *16* (1), 15-22.

76. **Mohammad, L. N.**, **Elseifi, M.**, **Cao, W.**, **Raghavendra, A.**, and **Ye, M.** (2017). "Evaluation of various Hamburg wheel-tracking devices and AASHTO T 324 specification for rutting testing of asphalt mixtures". *Road Materials and Pavement Design*, *18* (sup4), 128-143.

77. **Morea, F.**, **Agnusdei, J.O.**, and **Zerbino, R.** (2010). "Comparison of methods for measuring zero shear viscosity in asphalts". *Materials and Structures*, *43*, 499–507.

78. **Morea, F.**, **Agnusdei, J.O.**, and **Zerbino, R.** (2011). "The use of asphalt low shear viscosity to predict permanent deformation performance of asphalt concrete". *Materials and Structures*, *44*, 1241–1248.

79. **Morea, F.**, **Zerbino, R.**, and **Agnusdei, J.** (2012). "Improvements on asphalt mixtures rutting performance characterization by the use of low shear viscosity". *Materials and Structures*, *46*, 267–276.

80. **Morea, F.**, **Zerbino, R.**, and **Agnusdei, J.** (2013). "Wheel tracking rutting performance estimation based on bitumen Low Shear Viscosity (LSV), loading and temperature conditions". *Materials and Structures*, *47*, 683–692.

81. **Morian, N.**, **Hajj, E. Y.**, **Glover, C. J.**, and **Sebaaly, P. E.** (2011). "Oxidative aging of asphalt binders in hot-mix asphalt mixtures". *Transportation Research Record, 2207*, Transportation Research Board, Washington, DC, 107-116.

82. **MoRTH.** (2013). "Specifications for road and bridge works". Indian Roads Congress, New Delhi.

83. **NAPA** and **EAPA**. (2011). "The asphalt paving industry: A global perspective." *Global Series Third Edition*, National Asphalt Pavement Association and European Asphalt Pavement Association.

84. **NCAT.** (2018). "Aging: Avoiding the Inevitable". Website:http://www.eng.auburn.edu/research/centers/ncat/newsroom/2018-spring/aging.html, Last accessed – 30/07/2019.

85. **Nivitha, M. R.**, and **Krishnan, J.M.** (2018). "Rheological characterisation of unmodified and modified bitumen in the 90–200 °C temperature regime". *Road Materials and Pavement Design*, 1-18.

86. **Owende, P. M.**, **Hartman, A. M.**, **Ward, S. M.**, **Gilchrist, M. D.**, and **O'Mahony, M. J.** (2001). "Minimizing distress on flexible pavements using variable tire pressure". *Journal of Transportation Engineering*, *127* (3), 254-262.

87. **Pan, T.**, **Tutumluer, E.**, and **Carpenter, S. H.** (2006). "Effect of coarse aggregate morphology on permanent deformation behavior of hot mix asphalt". *Journal of Transportation Engineering*, *132* (7), 580-589.

88. **Petersen, J. C.**, **Robertson, R. E.**, **Branthaver, J. F.**, **Harnsberger, P. M.**, **Duvall, J. J.**, **Kim, S. S.**, **Anderson, D.A.**, **Christiansen, D.W.** and **Bahia, H. U.** (1994). "Binder characterization and evaluation: Volume I". *SHRP-A-367*, Strategic Highway Research Program, Washington, DC.

89. **Planche, J. P.**, **Martin, D.**, **Lesueur, D.**, and **King, G. N.** (1996). "Evaluation of elastomer modified bitumens using SHRP binder specifications". *1st Eurasphalt and Eurobitume Congress*, 7-10 May, Strasbourg (France).

90. **Polacco, G.**, **Stastna, J.**, **Vlachovicova, Z.**, **Biondi, D.**, and **Zanzotto, L.** (2004). "Temporary networks in polymer-modified asphalts". *Polymer Engineering and Science*, *44* (12), 2185-2193.

91. **Polacco, G.**, **Filippi, S.**, **Merusi, F.**, and **Stastna, G.** (2015). "A review of the fundamentals of polymer-modified asphalts: Asphalt/polymer interactions and principles of compatibility". *Advances in Colloid and Interface Science*, *224*, 72-112.

92. **Poulikakos, L. D.**, **Dos Santos, S.**, **Bueno, M.**, **Kuentzel, S.**, **Hugener, M.**, and **Partl, M. N.** (2014). "Influence of short and long term aging on chemical, microstructural and macro-mechanical properties of recycled asphalt mixtures". *Construction and Building Materials*, *51*, 414-423.

93. **Radhakrishnan, V.**, **Sri, M. R.**, and **Reddy, K. S.** (2018). "Evaluation of asphalt binder rutting parameters". *Construction and Building Materials*, *173*, 298-307.

94. **Rajan, N. K.**, **Selvavathi, V.**, **Sairam, B.**, and **Krishnan, J. M.** (2008). "Rheological characterization of blended paving asphalt". *Road Materials and Pavement Design*, *9* (sup1), 67-86.

95. **Saboo, N.**, and **Kumar, P.** (2016). "Analysis of different test methods for quantifying rutting susceptibility of asphalt binders". *Journal of Materials in Civil Engineering*, *28* (7), 04016024.

96. **Salama, H. K.**, **Chatti, K.**, and **Lyles, R. W.** (2006). "Effect of heavy multiple axle trucks on flexible pavement damage using in-service pavement performance data". *Journal of Transportation Engineering*, *132* (10), 763-770.

97. **Santagata, E.**, **Baglieri, O.**, **Alam, M.**, and **Dalmazzo, D.** (2015). "A novel procedure for the evaluation of anti-rutting potential of asphalt binders". *International Journal of Pavement Engineering*, *16* (4), 287-296.

98. **Schram, S.**, **Williams, R.**, and **Buss, A.** (2014). "Reporting results from the Hamburg wheel tracking device". *Transportation research record 2446*, Transportation research board, Washington, DC, 89-98.

99. **Sefidmazgi, N. R.**, **Tashman, L.**, and **Bahia, H.** (2012). "Internal structure characterization of asphalt mixtures for rutting performance using imaging analysis". *Road Materials and Pavement Design*, *13* (sup1), 21-37.

100. **Shenoy, A.** (2001). "Refinement of the Superpave specification parameter for performance grading of asphalt". *Journal of Transportation Engineering*, *127* (5), 357-362.

101. **Shenoy, A.** (2004). "High temperature performance grading of asphalts through a specification criterion that could capture field performance". *Journal of Transportation Engineering*, *130* (1), 132-137.

102. **Singh, D.**, and **Kataware, A. V.** (2016). "Comparison of different rheological parameters for rutting susceptibility of SBS+ WMA modified binders". *Innovative Infrastructure Solutions*, *1* (1), 28.

103. **Singh, P.**, and **Swamy, A. K.** (2018). "Probabilistic approach to characterise laboratory rutting behaviour of asphalt concrete mixtures". *International Journal of Pavement Engineering*, 1-13.

104. **Sirin, O.**, **Paul, D. K.** and **Kassem, E.** (2018). "State of the art study on aging of asphalt mixtures and use of antioxidant additives". *Advances in Civil Engineering*, 3428961.

105. **Sorensen, A.**, and **Wichert, B.** (2012). "Asphalt and Bitumen", Wiley-VCH Verlag GmbH & Co., KGaA, Weinheim, Germany.

106. **Souraki, Y.**, **Ashrafi, M.**, **Karimaie, H.**, and **Torsaeter, O.** (2012). "Experimental analyses of Athabasca bitumen properties and field scale numerical simulation study of effective parameters on SAGD performance". *Energy and Environment Research*, *2* (1), 140.

107. **Stuart, K. D.**, **Mogawer, W. S.**, and **Romero, P.** (2000). "Validation of asphalt binder and mixture tests that measure rutting susceptibility using the accelerated loading facility". *Report No. FHWA-RD-99-204*, Federal Highway Administration, U.S. Department of Transportation.

108. **Sybilski, D.** (1993). "Non-newtonian viscosity of polymer-modified bitumens." *Materials and Structures*, *26*, 15–23.

109. **Sybilski, D.** (1994). "Relationship between absolute viscosity of polymer-modified bitumens and rutting resistance of pavement". *Materials and Structures*, *27*, 110–120.

110. **Sybilski, D.** (1996). "Zero-shear viscosity of bituminous binder and its relation to bituminous mixture's rutting resistance". *Transportation Research Record* 1535, Transportation Research Board, Washington, DC, 15–21.

111. **Tarbox, S.**, and **Daniel, J. S.** (2012). "Effects of long-term oven aging on reclaimed asphalt pavement mixtures". *Transportation Research Record, 2294*, Transportation Research Board, Washington, DC, 1-15.

112. **Tielking, J. T.**, and **Roberts, F. L.** (1987). "Tire contact pressure and its effect on pavement strain". *Journal of Transportation Engineering*. *113* (1), 56-71.

113. **Tran, N.**, **Turner, P.**, and **Shambley, J.** (2016). "Enhanced compaction to improve durability and extend pavement service life: A literature review." *NCAT Report No. 16-02*, National Center for Asphalt Technology, Auburn University, Alabama, USA.

114. **TxDOT.** (2014). "Test procedure for Hamburg wheel-tracking test". *Tex-242-F*, Texas Department of Transportation, Austin, Texas, USA.

115. **UDOT.** (2015). "Method of test for Hamburg wheel-track testing of compacted hot-mix asphalt (HMA)". *Materials Manual of Instruction – Part 8 Section 990*, Utah Department of Transportation, Taylorsville, Utah, USA.

116. **Viola, G.G.**, and **Baird, D.G.** (1986) "Studies on the transient shear flow behavior of liquid crystalline polymers". *Journal of Rheology*, *30* (3):601-628.

117. **Wang, C.**, and **Zhang, J.** (2014). "Evaluation of rutting parameters of asphalt binder based on rheological test". *International Journal of Engineering and Technology*, *6* (1), 30.

118. **WAPA.** (2019). "Pavement facts". Washington Asphalt Pavement Association. Website: http://www.asphaltwa.com/welcome-facts/. Last accessed- 30/07/2019.

119. **Weidong, L.**, **Zheng, C.**, **Shaopeng, W.**, **Liantong, M.**, and **Gang, L.** (2006). "Rutting resistance of asphalt overlay with multilayer wheel tracking test". *Journal of Wuhan University of Technology -Materials and Science Edition*, *21* (3), 142-145.

120. **Whittle, M.**, and **Dickinson, E.** (1997). "Stress overshoot in a model particle gel". *The Journal of Chemical Physics*, *107* (23), 10191-10200.

121. **Wineman, A. S.**, and **Rajagopal, K. R.** (2000). "Mechanical response of polymers: An introduction". Cambridge University Press, UK.

122. **Witczak, M.W.**, **Kaloush, K.**, **Pellinen T.**, and **El-Basyouny, M.** (2002). "Simple performance test for superpave mix design". *NCHRP Report 465*, National Research Council, Transportation Research Board, Washington, DC.

123. **Wong, W. G.**, **Han, H. F.**, **He, G. P.**, **Qiu, X.**, **Wang, K. C. P.**, and **Lu, W.** (2004). "Effects of water on permanent deformation potential of asphalt concrete mixtures". *Materials and Structures*, *37* (8), 532-538.

124. **Xu, T.**, and **Huang, X.** (2012). "Investigation into causes of in-place rutting in asphalt pavement". *Construction and Building Materials*, *28* (1), 525-530.

125. **Yang, J.**, **Shi, X.**, **Wan, J.**, **Qian, G.**, **Pan, W.**, and **Yang, Y.** (2006). "Evaluation of rutting resistance of double-layered asphalt mixes". *Road Materials and Pavement Design*, *7* (4), 533-542.

126. **Yin, F.**, **Arámbula-Mercado, E.**, **Epps Martin, A.**, **Newcomb, D.**, and **Tran, N.** (2017). "Long-term ageing of asphalt mixtures". *Road Materials and Pavement Design*, *18* (sup1), 2-27.

127. **Zhang, X.**, **Zou, G.**, and **Xu, J.** (2009) "Measurement of zero-shear viscosity in asphalt", *International Journal of Pavement Research and Technology*, *2* (1), 33-36.

128. **Zhao, W.**, **Xiao, F.**, **Amirkhanian, S. N.**, and **Putman, B. J.** (2012). "Characterization of rutting performance of warm additive modified asphalt mixtures". *Construction and Building Materials*, *31*, 265-272.

129. **Zhou, F.**, **Scullion, T.**, and **Sun, L.** (2004). "Verification and modelling of three-stage permanent deformation behaviour of asphalt mixes." *Journal of Transportation Engineering*, *130* (4), 486-494.

LIST OF PUBLICATIONS

1. Mubashirhussain, S., and Chowdary, V. (2019). "Establishing a correlation between absolute viscosity and apparent viscosity for a viscosity grade unmodified bitumen used for road construction in India". *International Journal for Traffic and Transport Engineering*, *9* (1), 8-21.

2. Mubashirhussain, S., and Chowdary, V. (2019). "Influence of short-term ageing and long-term ageing on the thermal equilibrium time for two different viscosity grades of bitumen used for road construction*". International Journal for Traffic and Transport Engineering*, *9* (2), 198-209.

3. A novel steady shear rate sweep protocol to determine zero shear viscosity of unmodified bituminous binders. [Submitted to IJPRT]

4. Response of unmodified bitumen subjected to linear shear rate sweep at different temperatures and aging conditions. [Under Preparation]

5. Development of a representative rut curve by taking into account the rut depth variability along the wheel traverse using a probabilistic approach. [Under Preparation]

6. Influence of aging on the rutting resistance of two different bituminous mixtures. [Under Preparation]

7. Rheological studies on identification of a non-Newtonian rutting parameter for unmodified bitumen. [Under Preparation]